

# Automation Technology for Off-Road Equipment 2006





# **Automation Technology for Off-road Equipment 2006**

Proceedings of the  
1-2 September 2006  
International Conference  
Bonn, Germany

## **Editors**

Matthias Rothmund  
Markus Ehrl  
Hermann Auernhammer

## **Published by**

Landtechnik Weihenstephan

**Copyright © 2006 by**

Landtechnik Weihenstephan,  
Vöttinger Str. 36, D-85354 Freising.

All rights reserved.

International Standard Book Number (ISBN) 3-9808234-2-3

Nothing from this publication may be reproduced, stored in a computerized system or published in any form or in any manner, including electronic, mechanical, reprographic or photographic, without prior written permission from the publishers.

The publisher is not responsible for statements and opinions advanced in its meeting or printed in its publications. They represent the views of the individual to whom they are credited and are not binding to the publishers as a whole.

Printed in Germany

Cover pictures: Markus Ehrl, TU München

Typesetting: camera ready by editors

Printed by: Bode Druck GmbH, Schwalbenweg 1, D-85356 Freising, [www.bode-druck.de](http://www.bode-druck.de)

Sponsored by:



## ATOE 2006 Conference

### OFFICERS

CONFERENCE CHAIR

**Prof. Dr. Hermann Auernhammer**  
Technische Universitaet Muenchen  
Freising, Germany

PAST CONFERENCE CHAIR

**Prof. Dr. Mikio Umeda**  
Kyoto University  
Kyoto, Japan

PROGRAM CHAIR

**Prof. Dr. Simon Blackmore**  
UniBots Ltd.  
UK

PROCEEDINGS CHAIR

**Dr. Matthias Rothmund, Markus Ehrl**  
Technische Universitaet Muenchen  
Freising, Germany

### CONFERENCE ORGANIZING COMMITTEE

**Prof. Dr. H. Auernhammer**  
Technische Universitaet Muenchen  
Germany

**Prof. Dr. S. Blackmore**  
UniBots Ltd.  
UK

**Dr. M. Demmel**  
Bavarian Research Institute for Agriculture  
Germany

**M.Sc. M. Ehrl**  
Technische Universitaet Muenchen  
Germany

**Dr. Th. Engel**  
John Deere AMS Europe  
Germany

**Prof. Dr. N. Noguchi**  
Hokkaido University  
Japan

**Prof. Dr. J. Reid**  
John Deere Technology Center  
USA

**Dr. H. Reiter**  
AGCO  
Germany

**Dr. M. Rothmund**  
Technische Universitaet Muenchen  
Germany

**Dr. C. G. Sørensen**  
Danish Institute of Agricultural Sciences  
Denmark

**Prof. Dr. M. Umeda**  
Kyoto University  
Japan

**Dr. Q. Zhang**  
University of Illinois  
USA

## SCIENTIFIC REVIEW COMMITTEE

**Dr. M. Baldinger**

Pöttinger  
Austria

**Prof. Dr. S. Blackmore**

UniBots Ltd.  
UK

**Dipl.-Ing. R. Buschmeier**

Müller-Elektronik  
Germany

**Dr. Th. Engel**

John Deere AMS Europe  
Germany

**Dr. M. Geyer**

Leibniz Institute for Ag Eng, ATB  
Germany

**Dr. H.W. Griepentrog**

Royal Veterinary and Agricultural University  
Denmark

**Prof. Dr. M. Iida**

Kyoto University  
Japan

**Prof. Dr. N. Noguchi**

Hokkaido University  
Japan

**Dr. M. Quinkhardt**

Agrocom  
Germany

**Prof. Dr. J. Reid**

John Deere Technology Center  
USA

**Dipl.-Ing.(FH) B. Schniederbruns**

Krone  
Germany

**Dr. K.G. Sørensen**

Danish Institute of Agricultural Sciences  
Denmark

**Prof. Dr. A. Visala**

Helsinki University of Technology  
Finland

**Prof. Dr. Q. Zhang**

University of Illinois  
USA

**Dr. W.D. Batchelor**

Mississippi State University  
USA

**Dr. J. Bosch**

PC-Agrar  
Germany

**Dr. M. Demmel**

Bavarian Research Institute for  
Agriculture, Germany

**Prof. T. Gemtos**

University of Thessaly Volos  
Greece

**Prof. G. Grenier**

National School for Ag Eng ENITA  
France

**Dipl.-Ing. P. Hieronymus**

Claas  
Germany

**Prof. Dr. F. Morari**

University of Padua  
Italy

**Dipl.-Ing. R. Ostermeier**

Technische Universität München  
Germany

**Prof. H. Ramon**

Catholic University Leuven  
Belgium

**Dr. H. Reiter**

AGCO  
Germany

**Prof. Dr. J. Schueller**

University of Florida  
USA

**Prof. Dr. G. Vellidis**

University of Georgia  
USA

**Prof. Dr. M. Wang**

China Agricultural University  
China

## PREFACE

Welcome to ATOE 2006 in Bonn, Germany!

After Chicago 2002 and Kyoto 2004, the third ATOE conference is held in Bonn. According to the custom, again it is a pre-conference of a large CIGR event, the CIGR World Congress 2006. This allows to contain the additional expenditures for participants, but also places appropriate emphasis on automation in the off-road area as this is a major topic for land use and agricultural technology today and in future.

In the meantime, the understanding of automation has changed. Guidance technology is state of the art and rejoice in growing popularity and acceptance. Headland management systems supplement the automation. Teleservice is available. Brave persons even speak of "Robot Farming". But to achieve this, a lot of new ideas must be born and a lot of open questions need to be answered.

Hence, please let us introduce and discuss further bricks for the automation of off-road equipment at the ATOE 2006. And let us work, that as in the accustomed two-year-cycle, ATOE 2008 can be realized in order to strengthen and continue the already achieved.

Weihenstephan, July 2006



Prof. Dr. Hermann Auernhammer  
Conference Chair of ATOE 20006



# Table of Contents

Sponsors, Officers and Conference Organization Committee .....	iii
Scientific Review Committee.....	iv
Preface .....	v
Author Index .....	xiii

## *Keynote*

### **Autonomous Systems for European Agriculture**

Blackmore, S., UniBots Ltd.

Griepentrog, W., The Royal Veterinary and Agricultural University, Denmark ..... **Oral Only**

## ***SESSION 01: AUTOMATION STRATEGIES***

Moderator: John F. Reid, John Deere Technology Center

### **Low Cost GPS-based System for Site Specific Farming at Flat**

#### **Terrains - Case Study**

Gavrić, M., Institute of Field and Vegetable Crops, Novi Sad, Serbia (M. L. Martinov).....1

### **Development of Crawler Robot using VRS-RTK-GPS and INS**

Inoue, T., Hokkaido University, Japan (T. Matusi, K. Ishii, and N. Nouguchi).....7

### **HORTIBOT: A System Design of a Robotic Tool Carrier for High-tech**

#### **Plant Nursing**

Sørensen, C. G., Danish Institute of Agricultural Sciences, Denmark

(R. N. Jørgensen, J. M. Pedersen, I. Havn, K. Jensen, H. T. Søgaaard, and L. B. Sørensen).....13

### **Application Potentials of Mobile Fieldscouts**

Langner, H. R., Leibniz Institute for Agricultural Engineering Bornim (ATB), Germany

(D. Ehlert, A. Falke, and G. Duscher).....23

### **Optimal Dynamic Motion Sequence Generation for Multiple Harvesters**

Bochtis, D., Aristotle University of Thessaloniki, Greece

(S. Vougioukas, C. Tsatsarelis, and Y. Ampatzidis).....33

## ***SESSION 02: GUIDANCE AND HEADLAND AUTOMATION I***

Moderator: Thomas Engel, John Deere AMS Europe

### **Multilayer controller for outdoor vehicle**

Reske-Nielsen, A., Technical University Denmark, Denmark

(A. Mejnertsen, N. Andersen, O. Ravn, M. Nørremark, and H. W. Griepentrog).....41

### **Autonomous Navigation with a Weeding Robot**

Bakker, T., Wageningen University, The Netherlands

(C. J. van Asselt, J. Bontsema, J. Müller, and G. van Straten).....51

### **Development of an Autonomous Navigation System Using 2-Dimensional Laser Scanner in an Orchard Real-Time Application**

Barawid Jr., O. C., Hokkaido University, Japan (A. Mizushima, K. Ishii, and N. Noguchi).....59

<b>Mobile Data Repeaters Enhancing the Availability of RTK Correction Data in the Field</b>	
Muhr, T., geo-konzept GmbH, Germany (P. O. Noack).....	65
<b>Greenhouse Robot Navigation using KLT Feature Tracking for Visual Odometry</b>	
Burks, T. F., University of Florida, USA (P. J. Younse).....	71

**SESSION 03: INFORMATION SYSTEMS I**

Moderator: Simon Blackmore, UniBots Ltd.

<b>Study of the Stability of Self Propelled Hydrodynamic Irrigating Machine in Different Operative Conditions</b>	
Formato, A., University of Naples, Italy (S. Faugno, and G. Paolillo).....	91
<b>Enhancement of Information from Satellite Imagery by Integrating an Unmanned Helicopter</b>	
Han-ya, I., Hokkaido University, Japan (K. Ishii, N. Nouguchi, K. Niwa, and J. Yokobori).....	97
<b>Perception-based Autonomy for a Tree-Fruit Production System</b>	
Reid, J. F., John Deere Moline Technology Center, USA .....	<b>Oral Only</b>
<b>Development of Surveying System for Grassland using a Laser Scanner Mounted on a Robot Tractor</b>	
Kang, T. H., Hokkaido University, Japan (K. Siramizu, K. Ishii, and N. Noguchi) .....	103

**SESSION 04: GUIDANCE AND HEADLAND AUTOMATION II**

Moderator: Markus Ehrl, Technische Universitaet Muenchen

<b>A Triplet-Application of a Stereovision-Based Field Recognition System</b>	
Kise, M., University of Illinois at Urbana-Champaign, USA (Q. Zhang, and Y. Yu) .....	109
<b>Autonomous Inter-row Hoeing using GPS Based Side-shift Control</b>	
Griepentrog, H.W., The Royal Veterinary and Agricultural University, Denmark (N. Noerremark, J. Nielsen, and J. S. Ibarra) .....	117
<b>Rice Harvesting Operation by an Autonomous Combine with a GPS and a FOG</b>	
Iida, M., Kyoto University, Japan (Y. Yamada).....	125
<b>Full Automated Rice Transplanting Operation Using GPS Guided Rice Transplanter with long Mat Type Hydroponic Rice Seedlings</b>	
Nagasaka, Y., National Agricultural Research Center, Japan (H. Kitagawa, A. Mizushima, N. Noguchi, Y. Kanetani, N. Umeda, and T. Kokuryu).....	133

**SESSION 05: INFORMATION SYSTEMS II**

Moderator: Matthias Rothmund, Technische Universitaet Muenchen

<b>GI and GPS Systems Enhancing Plot Parcel Creation</b>	
Noack, P. O., geo-konzept GmbH, Germany (T. Muhr, and M. Demmel).....	139
<b>Remote Assisted Task Management for ISOBUS Equipped Tractor-Implement Combination</b>	
Pesonen, L., MTT Agrifood Research Finland, Finland (V. Virolainen, J. Kaivosoja, J. Oittinen, and J. Kivipelto) .....	145

**Supply of Agricultural Process Data with ISOBUS and agroXML**  
 Spietz, C., University of Applied Sciences Bingen, Germany.  
 Steinberger, G., Technische Universitaet Muenchen, Germany ..... **Oral Only**

**New Devices for Automatic Irrigation Based on GSM Network and Radio Communication**  
 Yang, G., China Agricultural University, China ..... **Oral Only**

***SESSION 06: GUIDANCE AND HEADLAND AUTOMATION III***

Moderator: Hans W. Griepentrog,  
 The Royal Veterinary and Agricultural University at Copenhagen

**Split and Merge Based Path Planning for Agricultural Machines**  
 Oksanen, T., Helsinki University of Technology (TKK), Finland (A. Visala).....151

**Recursive Online Path Planning for Agricultural Machines**  
 Oksanen, T., Helsinki University of Technology (TKK), Finland (A. Visala).....161

**Edge Detection for Autonomous Guidance of a Corn Harvester Using Stereo Vision**  
 Rovira-Más, F., Polytechnic University of Valencia, Spain (S. Han, J. Wei, and J. F. Reid).....171

**Reactive Path Tracking for Increased Safety and Robustness during Automatic Guidance**  
 Vougioukas, S., Aristotle University of Thessaloniki, Greece .....183

***SESSION 07: SENSORS AND SENSOR FUSION I***

Moderator: Qin Zhang, University of Illinois at Urbana-Champaign

**Fault Diagnostics in Agricultural Machines**  
 Miettinen, M., Helsinki University of Technology (TKK), Finland  
 (T. Oksanen, M. Öhman, P. Suomi, and A. Visala) .....191

**Texture Feature Extraction for Weed Detection in Organic Farming**  
 Jafari, A., Shiraz University, Iran (J. Bontsema, G. van Straten, and K. van Asselt) .....201

**Using Artificial Neural Networks in Color Image Segmentation for Weed Detection**  
 Jafari, L., Shiraz University, Iran (S. S. Mohtasebi, H. Eghbali, and M. Omid).....209

**Multisensor Data Fusion Implementation for a Sensor based Fertilizer Application System**  
 Ostermeier, R., Technische Universitaet Muenchen, Germany  
 (H. I. Rogge, and H. Auernhammer) .....215

***SESSION 08: X-BY-WIRE***

Moderator: George Vellidis, University of Georgia

**X-By-Wire via ISOBUS Communication Network**  
 Ehrl, M., Technische Universitaet Muenchen, Germany (H. Auernhammer) .....227

**Automatic Velocity Control of a Hydrostatic Vehicle**  
 Foster, C. A., CNH America LLC, USA (R. P. Strosser, J. D. Peters, and J. Q. Sun) .....237

**Autonomous Utility Mower**  
Zeitew, M. A., NavCom Technology, A John Deere Company, USA .....247

**A Basic Approach to Implement Guided Tractor Control  
(With two Executed Examples)**  
Freimann, R., IAV GmbH, Germany.....257

***SESSION 09: SENSORS AND SENSOR FUSION II***  
Moderator: Ralph Ostermeier, Technische Universitaet Muenchen

**Near Infrared Spectroscopy for Quality Measurement on Forage Swathes -  
First Test Bed Experiments**  
Rothmund, M., Technische Universitaet Muenchen, Germany (M. Strobl) .....267

**Research on the Agricultural Drainage Design Using Thermal Remote  
Sensing Attached on Unmanned Helicopter**  
Usami, T., Hokkaido University, Japan (K. Ishii, and N. Noguchi).....273

**A Real-Time Smart Sensor Array for Scheduling Irrigation**  
Vellidis, G., University of Georgia, USA (M. Tucker, and C. Bednarz).....281

**A new approach of Boundary Following for Mobile Robots  
with only 180°-Vision**  
Zhao, Z., College of Engineering, South China Agricultural University, China ..... **Oral Only**

***SESSION 10: SOFTWARE AND CONTROLLERS***  
Moderator: Kazunobu Ishii, Hokkaido University

**A Comparison of Three Steering Controllers for Off-road Vehicles**  
Gao, Y., Yanshan University, China (Q. Zhang).....289

**Software Quality in Distributed Embedded Systems**  
Lenz, J. E., John Deere and Company, USA (R. Landman).....303

**Vehicle Path Planning for Complete Field Coverage Using Genetic Algorithms**  
Ryerson, A. E. F., University of Illinois at Urbana-Champaign, USA (Q. Zhang) .....309

***SESSION 11: COMMUNICATION PROTOCOLS***  
Moderator: John Schueller, University of Florida

**Be ready for the ISOBUS (ISO 11783) - The New Standard  
for Agricultural Machinery**  
Buschmeier, R., Müller-Elektronik GmbH & Co., Germany.....319

**TTA-Group Steer-by-Wire Working Group**  
Seethaler, C., TT Control S.r.l., Brixen, Italy  
(M. Plankensteiner, L. Silberbauer, K. Buus-Jensen, and T. Lovric).....325

**Latest Trends in Automotive Electronic Systems - Highway meets Off-Highway?**  
Rathmann, S., Bosch Engineering GmbH, Germany (R. Fischerkeller).....337

**A Method of Evaluating the Performance of RTK GPS Receivers  
Used in Agriculture**  
Ehsani, R., University of Florida, USA  
(H. Chaoui, D. Grejner-Brzezinska, and M. Sullivan)..... **Paper Only**....345

*Plenary Lectures*

**International Field Robot Event** ..... **Oral Only**

**Wireless Farming**

Mitchell, C., Mitchell Farm, Iowa, USA ..... **Oral Only**

**Off-road Robotics – Reality and Vision**

Zoller, F., Bittner, G., BASE TEN SYSTEMS Electronics GmbH, Germany ..... **Oral Only**



# LOW COST GPS-BASED SYSTEM FOR SITE-SPECIFIC FARMING AT FLAT TERRAINS – CASE STUDY

M. M. Gavrić<sup>1</sup> and M. L. Martinov<sup>2</sup>

## ABSTRACT

Site-Specific Farming has been developed to the level that enables profitable use. The problem of its application in developing countries is high costs of needed equipment. The objective of research was to develop a low-cost system for application of precision farming.

The system consists of low-cost receiver connected to the PLC. The test of the system applicability for local specific spraying of herbicides, following previously defined weed spots was done.

The encouraging results have been obtained. The precision of spraying could be enhanced using new generation of receivers with higher frequency rate and accuracy and including additional parameters for the PLC calculations.

**KEYWORDS.** GPS, IEC 61131-3, PLC, Site-Specific Farming.

## INTRODUCTION

After the removal of Selective Availability (SA), GPS accuracy was increased about ten times – from about 100 m to about 10 m. Using free of charge, satellite-based differential GPS systems (DGPS), e.g., EGNOS in Europe, WAAS in North America and MSAS in Asia, it is possible to achieve accuracies less than 5 m with a stand-alone unit. The requirements for positioning in agriculture are specific. Fields at flat terrains, like Vojvodina – Northern Province of Serbia, are the most appropriate for GPS applications, because of the good satellite.

This paper describes a system which consists of GPS device that uses a free of charge, satellite-based differential GPS signal (EGNOS) and a programmable logic controller (PLC) programmed on the basis of IEC 61131-3 standard. The basic requirement set before the system is that it can be shared among several tractors. The requirements set before the PLC program are that its development and maintenance are simple and transferable to other PLC devices, it is done with the IEC 61131-3 language choice, and that it permits complex calculations using floating point arithmetic. Preliminary results have shown that this system enables the application of site specific farming on tractors equipped with implements without ISOBUS support.

Functioning of the system was tested for application of fixed amounts and concentrations of herbicides in previously identified field spots containing population of weeds.

## MATERIAL AND METHODS

Garmin Etrex Legend, which is commercially available, was selected for use as GPS device. It is capable of receiving EGNOS DGPS signal. PLC device was mounted in tractor cabin and connected, via serial cable, to the GPS device which sends NMEA messages. From the set of NMEA messages, GPRMC was selected because it contains information about all important parameters – GPS position, current speed and direction.

The activity diagram presents PLC program logic.

---

<sup>1</sup> Institute of Field and Vegetable Crops, M. Gorkog 30, Novi Sad, Serbia, gavric@ifvcns.ns.ac.yu

<sup>2</sup> Faculty of Engineering, Trg Dositeja Obradovica 6, Novi Sad, Serbia

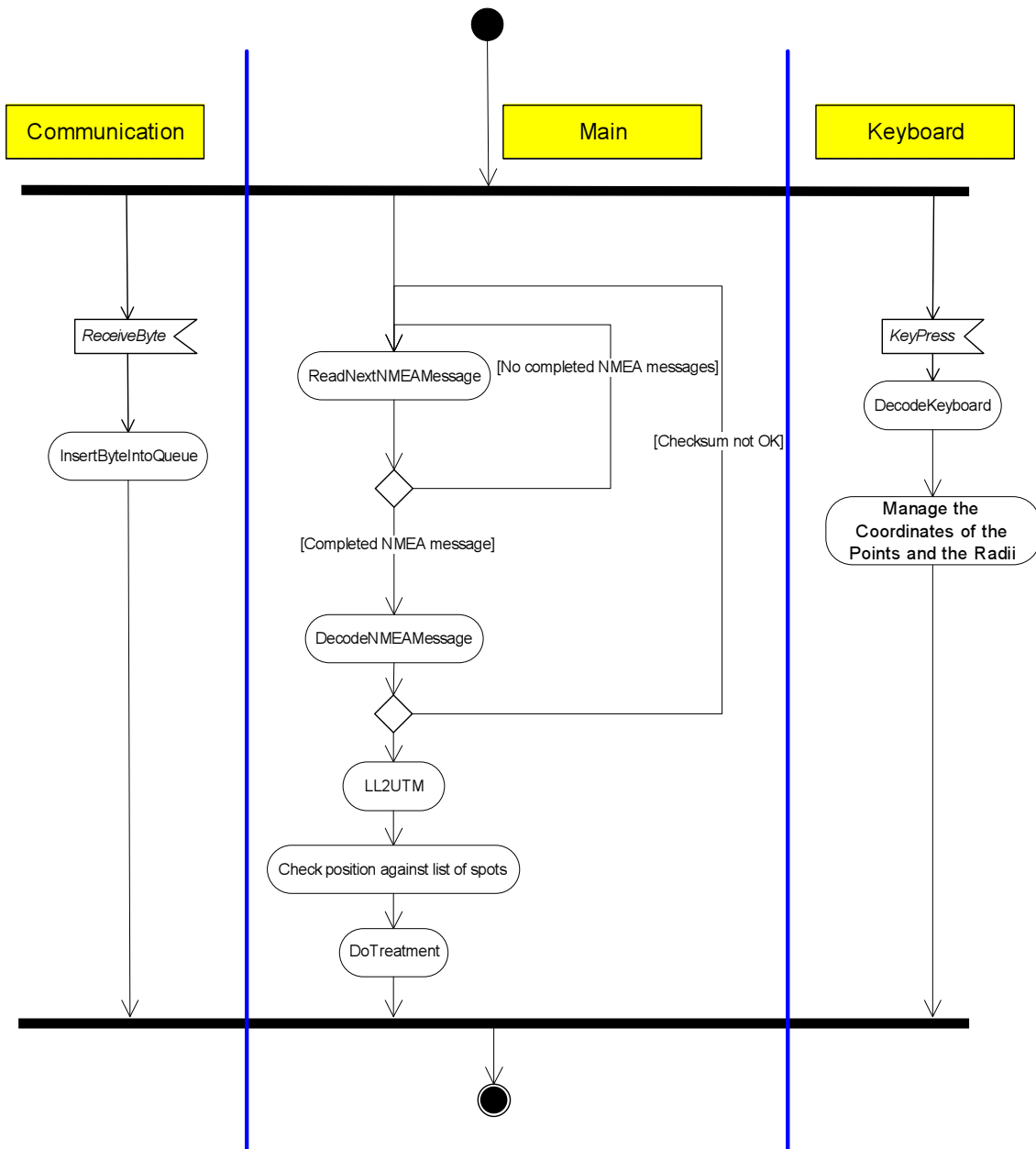


**Figure 1. Activity diagram of PLC program in UML notation. Communication, Main and Keyboard are separate segments of the program which interact through queues. LL2UTM converts coordinates from Latitude-Longitude to UTM projection.**

The selected PLC device is EMC 320, manufactured by NEURON. It uses the programming package CoDeSys, which supports the IEC 61131-3 standard for PLC programming. CoDeSys is manufactured by 3S-Smart Software Solutions GmbH. In this study, programming language Structured Text (ST) is used. The PLC has 16 digital inputs and 16 digital outputs with corresponding LEDs.

The PLC program consists of four basic parts:

**Receiving receipt for application** – there are two ways of preparing the receipt. One way is to download already prepared points and radii to PLC (this could be done on the basis of aerial images or scouting with GPS device). The other way is to define points and radii using the keyboard when tractor is in the field e.g. during an earlier operation.

**Receiving NMEA message** – NMEA messages received from the GPS device are entered into a queue. All messages from the queue are sequentially processed and messages different from GPRMC are discarded. After processing, a single GPRMC message is prepared for decoding.

**Decoding NMEA message** – consists of two stages. The first is checksum validation and the second is decoding. If the checksum is correct then the received NMEA message is decoded. After the decoding, current position, speed, direction, time and date are further processed.

**Calculations based on current position, speed, direction, application receipt, current internal PLC state and state of its inputs** – Current position data are transformed from Geographic Coordinate System (latitude-longitude format) into Projected Coordinate System (UTM format). Speed data is transformed from knots into m/s. In this test, Amazone UF 80 sprayer was used for herbicide application. The sprayer consisted of five sprayer units. Position of each unit was approximated by a point placed in its middle. Calculation for each point was based on the sprayer unit length and the distance between the GPS device and the sprayer.

For example, the calculation for the center unit of the sprayer ( $X_{spr}$ ,  $Y_{spr}$ ) is:

$$X_{spr} = X_{GPS} - 3.1 \cdot \sin \alpha$$

$$Y_{spr} = Y_{GPS} - 3.1 \cdot \cos \alpha$$

The calculation for the first unit to the left is:

$$X_{1L} = X_{spr} - 2.5 \cdot \cos \alpha$$

$$Y_{1L} = Y_{spr} + 2.5 \cdot \sin \alpha$$

The calculation for the second unit to the right is:

$$X_{2R} = X_{spr} - 5 \cdot \sin \alpha$$

$$Y_{2R} = Y_{spr} - 5 \cdot \cos \alpha$$

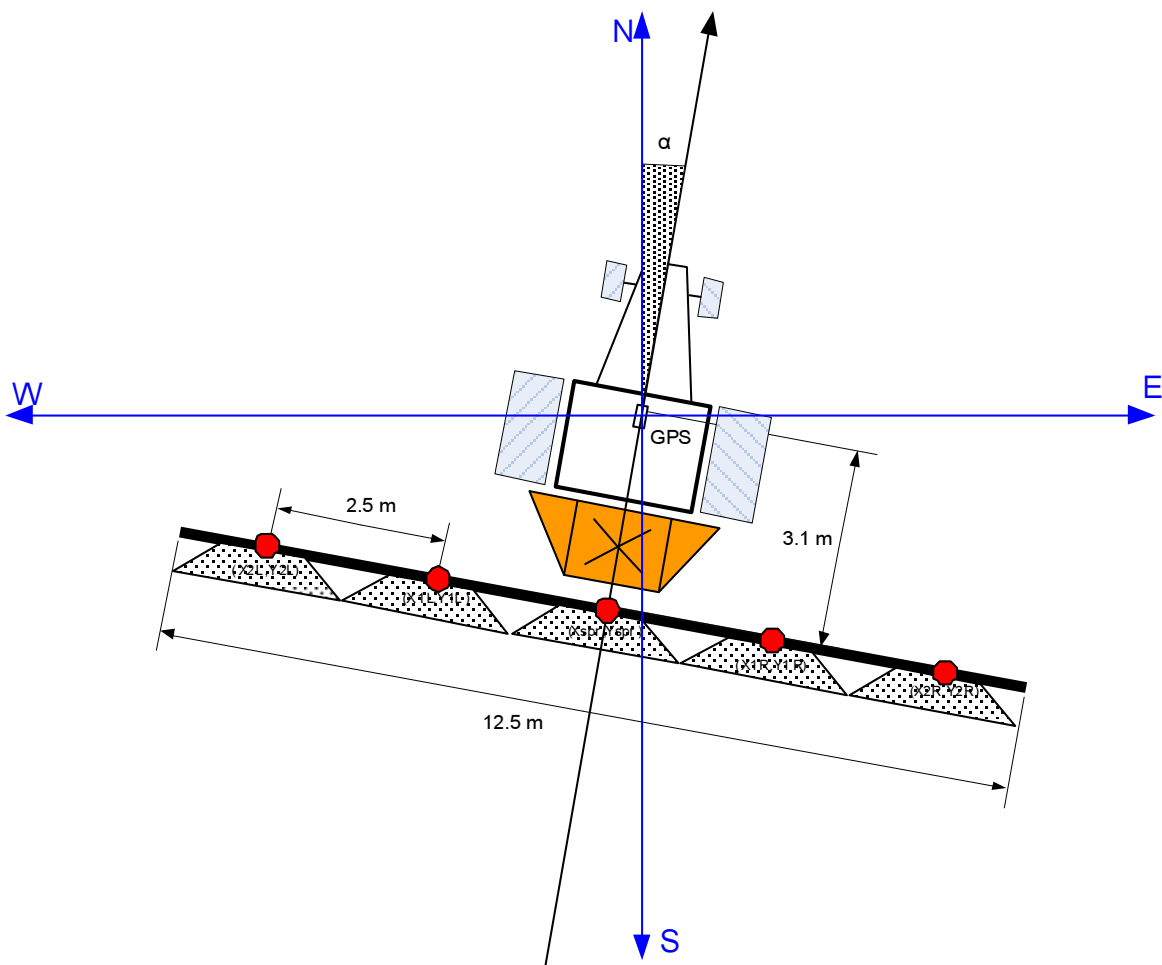


**Figure 2. Scheme of tractor mounted sprayer.  $\alpha$  is the angle between the direction of tractor movement and true north. Red dots are positions of the units. The points are spaced 2.5 meters apart. The distance between the GPS device and the central point of the sprayer is 3.1 meters.**

PLC controls the work of the sprayer units. Each unit is controlled by one digital output. PLC turns the units off or on depending on their calculated position. The operation of the system is shown in the figure 3.

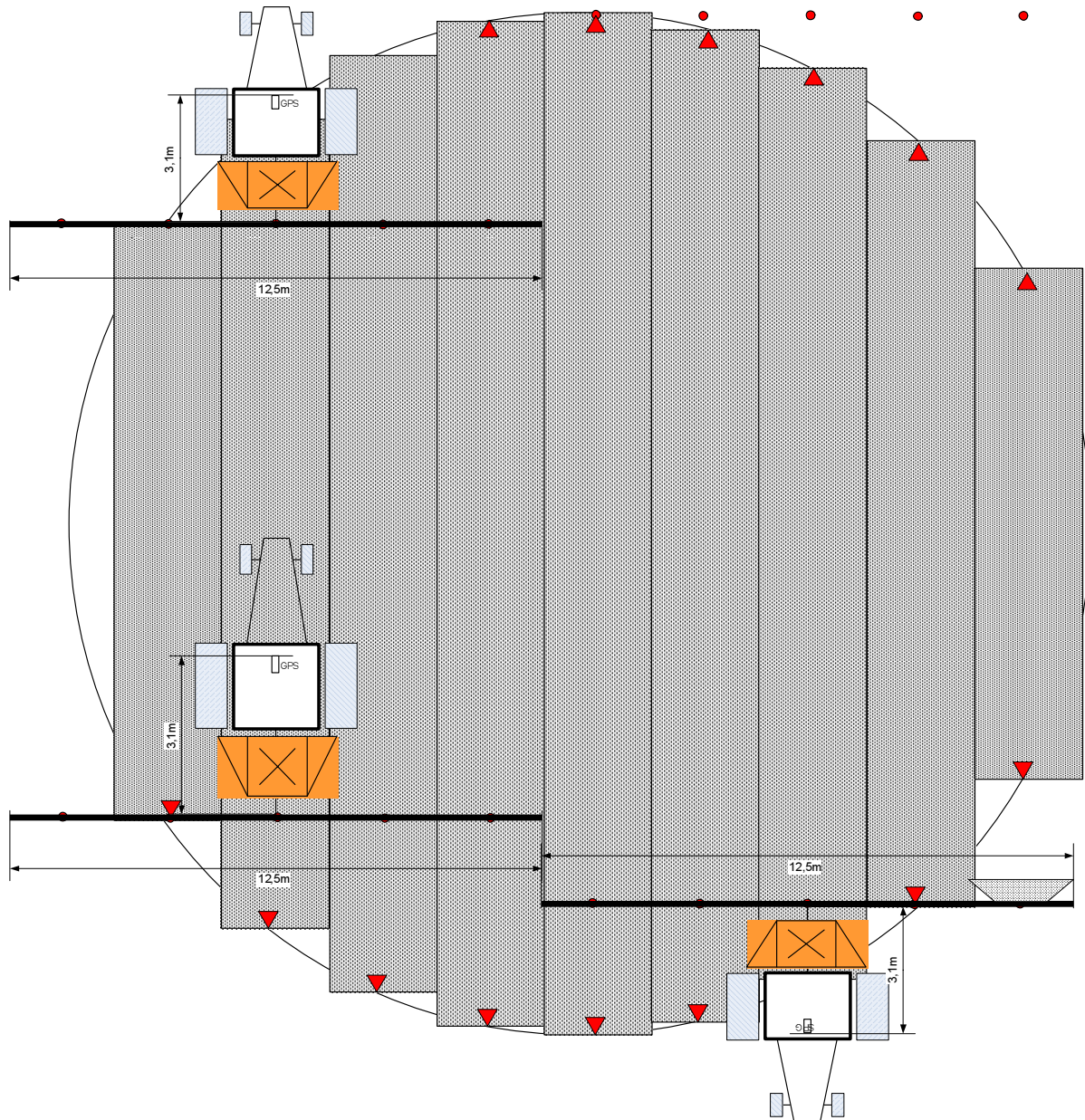


**Figure 3. Start/stop spray points (triangles). Shaded rectangles are the treated area.**

The order of operations for the testing of the system:

- weed scouting using the selected GPS device,
- receipt preparation,
- downloading receipt,
- online testing.

## RESULTS

The tests showed that the frequency of 0.5 Hz, the device sending a NMEA GPRMC message every 2 seconds, was not satisfactory. For example, at tractor speed of 10 km/h, disregarding positioning error and tractor position predicted on the basis of the received speed and direction, the maximum spraying start/stop position error is 5.55 m. Such error occurs when the message is

received immediately before the tractor reaches the start/stop spray point. To reduce the error, position prediction was adjusted to simulate a GPS messaging at 1 Hz (based on the current tractor speed and direction received from GPS). In that way the maximum error was reduced to 2.78 m, at operating speed of 10 km/h. The PLC program calculates spray start/stop delay on the basis of current distance from the sprayer unit to the start/stop point and tractor speed only if the distance is less than 2.78 m, in other case there is no sense to calculate the delay because the unit will not reach the start/stop point in the next second. In practice, the error in herbicide application start/stop point was less than 1 m.

The analysis of the performed herbicide application indicated that the operation was performed with satisfactory accuracy.

## CONCLUSION

The price of device is the basic limiting factor in new technology application in developing countries. In our case, the overall cost of the system in 2005 was 550 €. It should be mentioned here that the handheld GPS device could also be used for other purposes. The tests were performed at a flat terrain, free of disturbances such as electrical lines, large structures, etc.

The initial results obtained with the system are encouraging. The system demonstrated stability and reliability in work and high adaptability to various program changes. The satellite differential correction service provided sufficient accuracy for the performance of individual field operations such as herbicide application. Introduction of additional parameters such as wind speed and direction could improve operation accuracy.

To extend the system's capabilities, it is necessary to use a PLC with analogous inputs and outputs and a GPS device with higher accuracy and frequency rate.

## REFERENCES

1. Sekulić, P., M. Gavrić, M. Martinov, and M. Konstantinović. 2004. GIS and GPS for Sustainable Agriculture and Traceability. EE&AE 2004, *International Scientific Conference, Rousse*, Bulgaria: 362-368.
2. Steede – Terry, K. 2000. Integrating GIS and the Global Positioning System: ESRI Press, ISBN: 1879102811.
3. Upadhyaya, S. K., G. S. Pettygrove, J.W. Oliveira, and B. R. Jahn. 2005. An Introduction – Global Positioning System, Available at: [calspace.ucdavis.edu/Docs/Intro-GPS-Final.pdf](http://calspace.ucdavis.edu/Docs/Intro-GPS-Final.pdf). Accessed December 2005.
4. Gavrić, M., M. Martinov. 2006. Procedures and Accuracy of GPS Use in Agriculture, *Cont. Agr. Engng. Vol 32, No 1-2, Novi Sad*: 96-102.
5. Omnistar 2005. Fugro, Available at: [www.omnistar.com](http://www.omnistar.com) Accessed December 2005.
6. Rizos, C. 2001. How can my position on the paddock help my future direction? *Geospatial Information & Agriculture Conference*, Sydney, Australia, 16-19 July, CD-ROM proc.: 557-572.
7. Sharpe, T., R. Hatch, and F. Nelson. 2005. John Deere's StarFire System: WADGPS for Precision Agriculture Available at: [www.navcomtech.com/docs/StarFireSystem.pdf](http://www.navcomtech.com/docs/StarFireSystem.pdf) Accessed December 2005.
8. Gavrić, M., P. Sekulić. 2004. GIS and GPS Applications in Agriculture (in Serbian), *Zbornik radova*, Sveska 40, Naučni institut za ratarstvo i povrtarstvo, Novi Sad, UDK 631/635(05), YU ISSN 0351-4781: 171-178.
9. Sullivan, M., R. Ehsani, J. Walker, P. Levison, and L. Lang. 2001. Accuracy and Availability of WAAS for Precision Agriculture, *ASAE Meeting Paper*, No: 01-1155.
10. CoDeSys. 2003. CoDeSys. Ver 2.3.1.10. Kempten, Germany, 3S - Smart Software Solutions GmbH.



# DEVELOPMENT OF CRAWLER ROBOT USING SENSOR-FUSION

T. Inoue<sup>1</sup>, T. Matusi<sup>1</sup>, K. Ishii<sup>1</sup> and N. Noguchi<sup>1</sup>

## ABSTRACT

A crawler tractor is a vehicle with tracks instead of wheels. It is very suited for use on soft ground and mud. Nowadays crawler tractors are widely used in agriculture and industry due to their lower ground pressure and high traction efficiency. The laboratory has already developed the necessary controller and algorithm for a wheel-type robot tractor. The objective of this research is to apply the developed controller and developed steering controller to modify the crawler-type tractor into a crawler robot tractor. The platform of the crawler-type tractor is a 59-kW YANMAR CT 801 standard tractor with a built-in controller and actuators in the tractor cabin and for the wheel-type tractor is a 56-kW KUBOTA MD77 standard tractor that was modified into a robot tractor. Primarily, the steering behavior of crawler and wheel type tractor were compared at various speed settings. The navigation system for crawler tractor is based on sensor-fusion of the real-time kinematic global positioning system (RTK-GPS) and inertial measurement unit (IMU). The commands (speed and steering angle) were directly sent to the controller through a controller area network (CAN) bus. The results of the field tests showed that wheel-type tractor's turning radius is not affected by speed; however crawler tractor's turning radius increased while speed increase. It is concluded that the differential steering behavior of the crawler tractor was based on angular velocity, instead of turning angle. Finally, these findings were used to develop an appropriate steering controller for the efficient conversion of crawler type tractor into robot tractor.

**KEYWORDS.** CAN, Crawler Robot, GPS, IMU, Sensor Fusion.

## INTRODUCTION

Japan has 1.7 million ha rice-field (2004). Ninety-nine percent of this is cultivated with wet-rice. Hokkaido, the northernmost island of Japan, does not have long period for cultivating wet-rice due to its long winter season and the amount of accumulated snow which usually reaches to about 1 meter. Negative temperatures do not bode well for plant cultivation. It requires over 10 degrees to germinate rice seeds, over 20 degrees to make it bloom, and over 15 degrees to make them grain-filling. Hokkaido has only 5 months to cultivate wet-rice.

At present, crawler tractors are widely used in Hokkaido because they have lower ground pressure and high traction efficiency which made them adaptable to run smoothly on paddy fields. Their various functions range from the task of cultivating to snow dispersal.

## OBJECTIVE

The objective of this research is to develop the system of running a crawler robot tractor in many situations. The researcher's laboratory has been already successful in developing the necessary controller and algorithm for a wheel-type robot tractor (Kise 2001). Thus, this developed algorithm is applied to a crawler-type tractor in order to efficiently convert it into a robot.

---

<sup>1</sup> Graduate School of Agriculture, Hokkaido University, Sapporo, Japan, [tetsuo@bpe.agr.hokudai.ac.jp](mailto:tetsuo@bpe.agr.hokudai.ac.jp)

## SYSTEM COMPONENTS

### Crawler Tractor

The platform of the crawler-type tractor is a 59-kW YANMAR CT 801 standard tractor. Table 1 shows its specification. The tractor was modified to be able to control some functions or to get some condition data from it electrically. It has a switch that can change manual mode to automatic mode. When the switch is on automatic mode, it can control steering, switching, running direction, changing throttle using analog signal, changing transmission, turning on or off a power take-off (PTO), emergency engine stop switch, using digital signal, up or down 3-point hitch link using analog and digital signal, determining the speed of the tractor, engine rpm using pulse signal, and the position of 3 point hitch link using analog signal. Tractor controller which includes these functions communicates with given electric control unit (ECU).

**Table 1. Specifications of Crawler Tractor.**

Model	CT801	
Drive System	Crawler	
Dimensions	Overall length (mm)	3750
	Overall width (mm)	1950
	Overall height (mm)	2635
	Ground clearance (mm)	380
Weight kg	3990	
Engine	Model	4TNV98T
	Type	4-cycle, water-cooled diesel
	Output(kw(ps))	58.8(80)
	Displacement (cc)	3318
	Fuel Tank Capacity (lit.)	150
Crawler Track	Length(mm)	2165
	Width(mm)	450
	Tread(mm)	1500
	Brake	Wet Disc
	Max. travel speed (km/hr.)	
	Front	18
	Rear	18

### ECU

In order to build an implement electronic control unit (ECU) suitable for ISOBUS communication with low cost and easy implementation, an 8 bit microcontroller PIC18F258, Microchip Co., Ltd. was used. This ECU has 10bit I/O, 5ch A/D and 2ch D/A interfaces that were used for measurement and control of implement frequently, and it can easily be accessed using a CAN message. It also has an I2C bus to correspond for the difference in implements and for flexibility. Thus, this research connected the circuit which uses an 8 bit microcontroller PIC16F876, Microchip Co., Ltd for function enhancement. This circuit has 16bit I/O and 4ch D/A interfaces. This I/O gets pulse data. Additionally, these setting could change easily through RS-232C terminal console. A photo and schematic diagram of ECU were shown in figure 1.

### CAN-BUS

The ISO 11783 standard, currently called ISOBUS, is based on CAN-BUS system in physical layer and intermediate layer for bus management. In this standard, each electric device such as tractor, implement, and terminal for user interface, task management controller, positioning devices and file server contain one or more ECUs and communicate with each other.

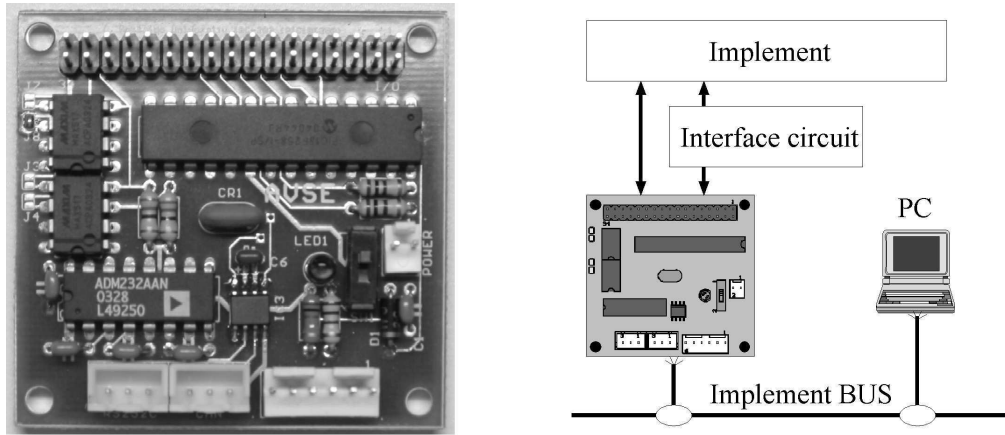


Figure 1. Photograph and schematic diagram of developed ECU.

Figure 2 shows the functions of tractor ECU, tractor PC and their connections using CAN bus system. Tractor ECU controls tractor according to CAN signal. RTK-GPS outputs CAN messages according to SAE J1939 standard, but it does not include GPS status that is necessary for robot tractor safety. For this reason, the RTK-GPS was connected to tractor PC using RS232C, and tractor PC emulates J1939 GPS messages for other ECUs on BUS line.

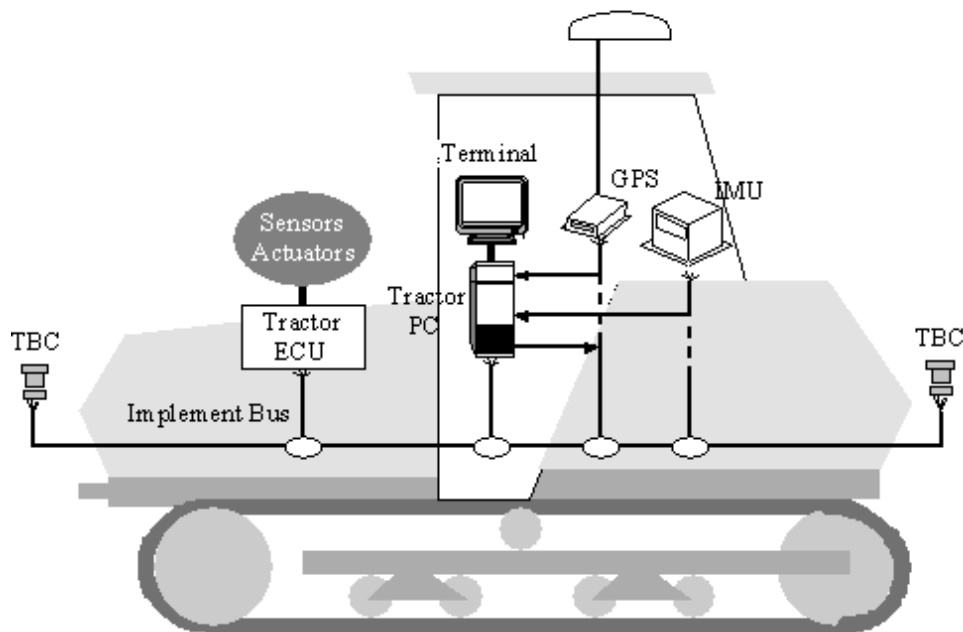


Figure 2. Schematic diagram of developed ECU.

### Sensors

In this research 2 sensors were used as the navigation sensors. A RTK-GPS Legacy-e, Topcon Co., Ltd. which was used to measure the position within 2cm error at 10Hz frequency output and IMU JCS-7402, Japan Aviation Electronics Industry Co., Ltd. which was also used to measure the heading angle with in 2°/min drift errors. The laptop PC was used to get the data and estimate how to go using a sensor fusion technique.

### **METHODS**

First, the difference of movement characteristic between crawler-type and wheel-type tractor MD77, Kubota Co., Ltd. was distinguished because the algorithm of autonomous system is considered for this tractor. There is big difference in turning between these two-type tractors. Wheel-type tractors can control turning by the value of steering angle while the crawler tractor is dependent on the value of voltage from 0V to 5V. Both tractors designated with turning values were given a test run and try to consider conversion equation from steering angle to voltage with

constant engine rpm on flat road. The RTK-GPS data like the given in figure 3 was used to analyze the length of the turning radius. Usually an appropriate turning velocity is needed in agricultural application.

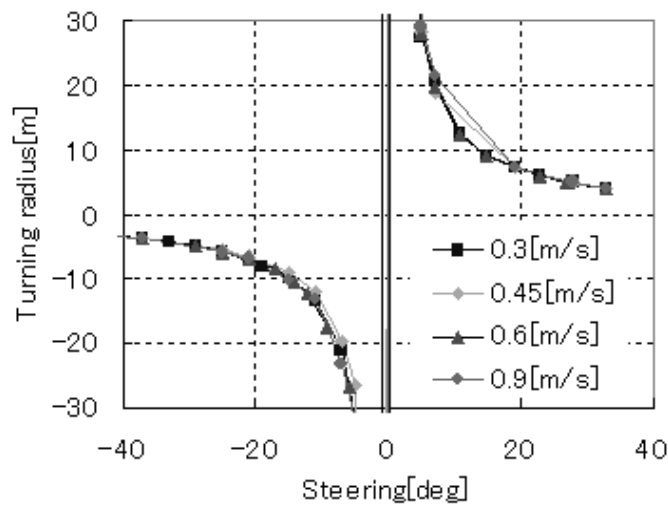


Figure 3. Control steering angle of wheel-type tractor.

Second, the algorithm of autonomous system was modified using this conclusion. Third, an autonomous test run was conducted using modified algorithm.

## RESULTS AND DISCUSSION

### (1) Comparison of wheel-type and crawler-type turning radius

Four different of speed were used 0.3m/s, 0.45m/s, 0.6m/s, 0.9m/s to both tractors. The steering angle of wheel-type tractor was controlled from  $-40^{\circ}$  and  $30^{\circ}$  in each speed and shows the results in figure 4. When the steering angle is negative, the tractor turns left and when it is positive, it turns right. This shows that turning radius depends on steering angle. The data which has the same steering angle is on same curve.

Next, the voltage of turning command of crawler-type was controlled between 0V and 5V in each speed and shows the result in figure 4. When the voltage is between 0V and 2.5V, the tractor turns right and when it is between 2.5V and 5V, it turns left. This shows that turning radius is affected by the angular velocity, not by the voltage. Speed of crawler-tractor is decided by motors for each track and when tractor turns right or left, it controls the speed-ratio of left track's speed to right track's speed and it can turn. The radius increases as the speed increases as shown in figure 4 and figure 5. Looking at angular velocity (Fig. 5), the result of radius is found on same curve in every speed.

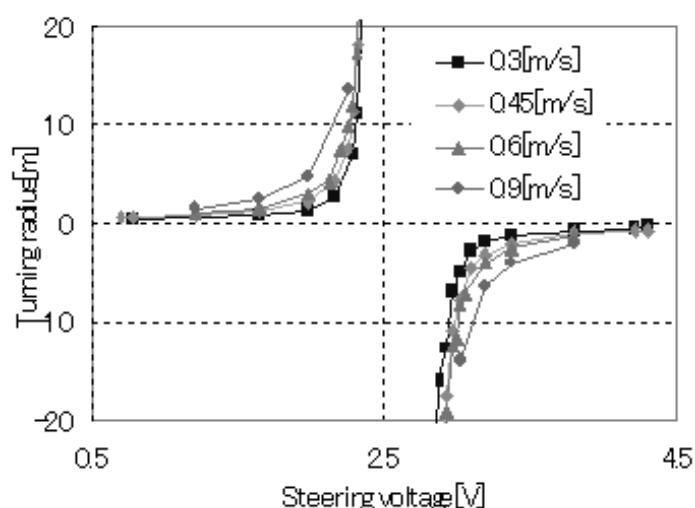


Figure 4. Control steering voltage of crawler-type tractor in turning radius.

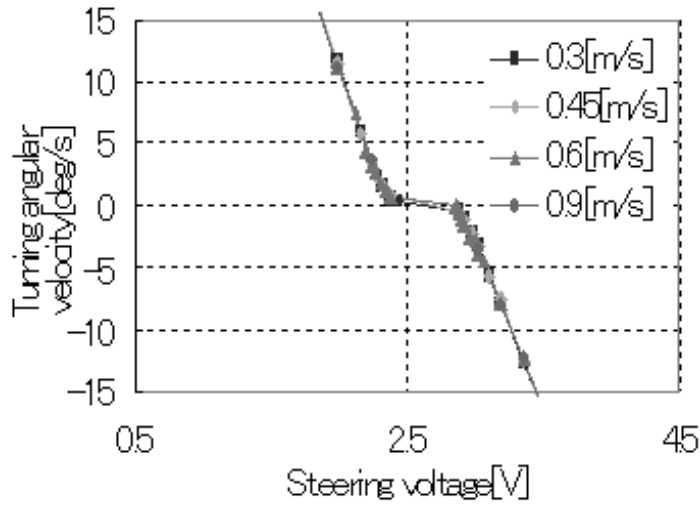


Figure 5. Control steering voltage of crawler-type tractor in angular velocity.

## (2) Steering algorithm for crawler-type

Wheel-type tractor used steering angle for turning, while in the crawler-type tractor used angular velocity. In wheel-type tractor angular velocity is expressed in equation (1) and in crawler-type tractor is expressed in equation (2) where engine rpm is constant.

$$\text{AngularVelocity}(\text{wheel} - \text{type}) = f(\text{speed}, \text{steering}) \quad (1)$$

$$\text{AngularVelocity}(\text{crawler} - \text{type}) = f(\text{voltage}) \quad (2)$$

Assume 0.6m/s speed in agriculture application and derive conversion equation. Firstly, the tractor turns to the right direction. The angular velocity of wheel-tractor is expressed in equation (3) and of crawler-tractor is in equation (4) and the voltage can be calculated in equation (5).

$$\omega = a_{wl} \times \text{Steer} + b_{wl} \quad (3)$$

$$\omega = a_{cl} \times \text{Voltage} + b_{cl} \quad (4)$$

$$\text{Voltage} = \frac{a_{wl}}{a_{cl}} \times \text{Steer} + \frac{1}{a_{cl}} \times (b_{wl} - b_{cl}) \quad (5)$$

Next, turn the tractor to the left direction. Equation (6) is for wheel-type angular velocity and equation (7) is for crawler-type angular velocity. The voltage can be calculated in equation (8).

$$\omega = a_{wr} \times \text{Steer} + b_{wr} \quad (6)$$

$$\omega = a_{cr} \times \text{Voltage} + b_{cr} \quad (7)$$

$$\text{Voltage} = \frac{a_{wr}}{a_{cr}} \times \text{Steer} + \frac{1}{a_{cr}} \times (b_{wr} - b_{cr}) \quad (8)$$

These formulas converted the steering angle output into angular velocity. The result of conversion equation is shown in figure 6. The gray line represents the wheel-type data using the conversion equation and the black line represents the crawler-type data. The figure shows the results were good using the conversion equation.

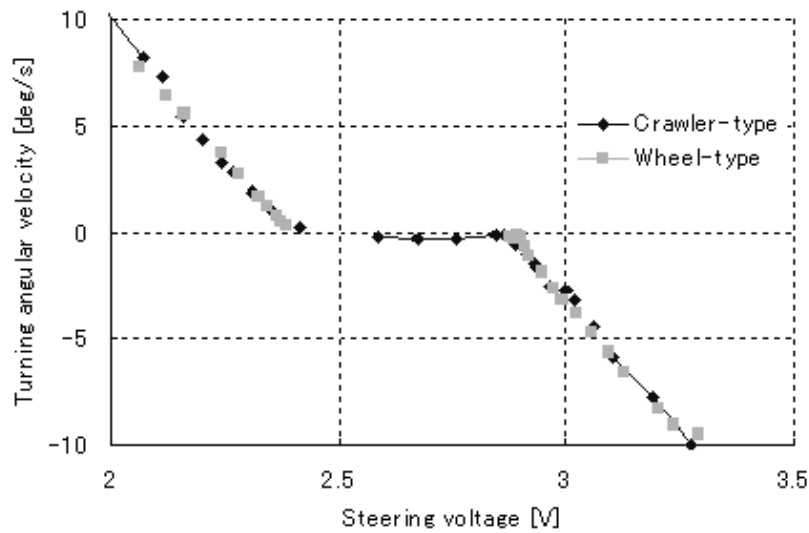


**Figure 6. The result using conversion equation to wheel-type data.**

### (3) Field test

Modifying the wheel-type steering algorithm using the conversion equation, different field test runs were conducted using the developed steering algorithm by the crawler-type tractor in autonomous run.

## CONCLUSION

The elements affecting the turning radius of each tractor were determined by conducting various experiments in different speeds. The data obtained from the wheel type and crawler-type tractor were analyzed. In a wheel-type tractor, steering angle affects the turning radius and in a crawler-type tractor, speed and voltage affects the turning radius. The differential steering behavior of the crawler tractor was based on angular velocity, instead of turning angle. These findings were used to develop an appropriate steering controller using the conversion equation. The developed steering controller was used to modify the crawler tractor into a crawler robot.

Appropriate angular velocity in turning was also determined as 0.6 m/s both in wheel-type and crawler-type tractor. The test runs showed good results in autonomous navigation.

## REFERENCES

1. Kise M., N. Noguchi, K. Ishii, and H. Terao. 2000. Development of the Agricultural Autonomous Tractor with DGPS. Japanese Society of Agricultural Machinery. 62(6): 145-153.
2. Gokan T. 2002. PIC Programming using C language. 1st ed.
3. Gokan T. 2002. Advanced PIC programming for Electronic control. 1st ed.
4. Seo Y., and T. Okamoto. 1998. Agricultural machinery system study. 3rd ed.

# HORTIBOT: A SYSTEM DESIGN OF A ROBOTIC TOOL CARRIER FOR HIGH-TECH PLANT NURSING

R. N. Jørgensen<sup>1</sup>, C. G. Sørensen<sup>1</sup>, J. M. Pedersen<sup>2</sup>, I. Havn<sup>2</sup>, K. Jensen<sup>1</sup>,  
H. T. Søgaard<sup>1</sup> and L. B. Sørensen<sup>2</sup>

## ABSTRACT

Danish organic outdoor gardeners today use 50-300 hours per hectare for manual weeding. Through automatic controlling of an existing commercial machine this often heavy and cost-consuming weeding will be eliminated. At the same time, a fully-automatic registration of field activities will contribute to the efficient implementation of EU directive 178/2002 concerning traceability in the primary production and thereby enhance the food-safety in the production chain.

A radio controlled slope mower is equipped with a new robotic accessory kit. This transforms it into a tool carrier (HortiBot) for high-tech plant nursing for e.g. organic grown vegetables.

The HortiBot is capable of passing over several parcels with visible rows autonomously based on a new commercial row detection system from Eco-Dan a/s, Denmark.

This paper presents the solutions chosen for the HortiBot with regard to hardware mechanical-electrical interfaces and software.

Further, the principles from a Quality Function Deployment (QFD) analysis is used to carry out the solicitation, evaluation and selection of most qualified design parameters and specifications attained to a horticultural robotic tool carrier. The QFD analysis provided a specific measure to evaluate each selected parameter in terms of satisfying user requirements and operational performance aspects.

Based on a combination of importance rating and competitive priority rating important user requirements include easy adaptation to field conditions in terms of row distance and parcel size, profitability, minimum crop damage during operation, and reliability. Lesser importance was attributed to affection value, attractive look, the possibility of out of season usage, and the use of renewable energy.

**KEYWORDS.** Machine, Machine Design, Quality Function Deployment (QFD), Robotics, Specifications, Tool Carrier.

## INTRODUCTION

Within outdoor gardening, weeds are today a major problem, especially for early sown or transplanted crops with a slow growth rate, like carrots and onions. Weed control can be either mechanical inter row combined with intra row pesticide application (90 % of the total outdoor gardening area in Denmark) or mechanical inter row combined with manual intra row weeding (10 % of the total outdoor gardening area in Denmark). There is however, an increasing demand from the consumers and the society to reduce the pesticide use in order to minimize the impact on flora, fauna, aquatic system, and working environment.

Depending on the weed intensity, Danish outdoor gardeners use 50-300 hours per hectare for manual weeding in onions and carrots (Ørum and Christensen, 2001; Melander and Rasmussen, 2001). This is cost-intensive not only in direct labor costs but also in form of labour

---

<sup>1</sup> Ministry of Food, Agriculture and Fisheries. Danish Institute of Agricultural Sciences. Department of Agricultural Engineering, Research Centre Bygholm, Schüttesvej 17, DK-8700 Horsens, Denmark, Rasmus.Joergensen@agrsci.dk

<sup>2</sup> Vitus Bering, University College, Chr. M. Østergårdsvej 4 C, DK - 8700 Horsens, Denmark

allocated to this one operation relative to other urgent tasks within the growing season. Further, there are often difficulties associated with procuring the necessary labour.

### Robots within Plant Production and Outdoor Gardening for Weed Control Today

With regards to relevant weeding robots, worldwide, there exists only a few today. In Denmark there is a prototype called GreenTrac, which is designed as an environmentally sound tool carrier for organic outdoor gardeners. The GreenTrac is not matured for production and is unnecessary big for most tasks (Sørensen and Frederiksen, 2002). In Sweden there is a robot for intra row weeding in sugar beets (Åstrand and Baerveldt, 2002). Israel has a multi-functional prototype robot for transplanting and spraying (Edan and Bechar, 1998). In England an outdoor gardening robot has been developed which is capable of passing over parcels of row crops (e.g. Hague, 1997). However, it cannot perform proper field work.

### Today's Technological Barriers

The majority of agricultural prototype robots base its navigation on high precision satellite position systems, and on field and crop maps. Hence, it is relatively information demanding and complex to work with. From the operator viewpoint, commercialization of a field robot requires that it is significantly simpler to operate (Callaghan et al., 1997; Jørgensen, 2005).

A technological development of weeding robots depends, apart from the market situation, to a great extent on technological barriers and comparability with the existing technological stage. Kassler (2001) lists barriers that have retarded the exploitation of computer-controlled machines in agriculture, e.g.: Insufficiently robust mechanical technology; Costly mechanical technology; Limited capability; Basic knowledge to create technology as dexterous or as skilful as that of a trained worker is currently unavailable.

### The voice of the customer

Within the concept of Total Quality Management (TQM), a number of tools have been adapted to assist the process of customer driven planning and engineering for product development (Cohen, 1995). One such tool is the Quality Function Deployment (QFD), which has as its primary goal the translation of customer requirements into technical requirements of each stage of the product design and production (Chan & Wu, 2001; Crowe & Cheng, 1996). The process involves identifying customers' requirements for a product (WHATs), customers' view on the relative importance of these requirements and the relative performance of the intended product and the main competitors on these requirements. Also, the complete QFD process includes translating the customer requirements into measurable engineering requirements (HOWs) through careful evaluations performed by technicians recognizing the relationships between customer requirements and engineering characteristics.

### Aim and Deliverables

The consumer driven demands to reduce the pesticide usage increase the demand for mechanical weed control as a way to avoid costly hand weeding. Within a few years, new environmentally sound technologies are expected to replace hand weeding. However, this creates a demand for a mechanical unit which will be able to carry future high precision weeding tools with a low constant speed and high precision.

The aim of this paper is to describe a developed robust horticultural robot called Hortibot, which will have the following main characteristics:

- Capable of passing over several parcels with visible rows autonomously based on a commercial row detection system with no or minimal use of Global Positioning Systems (GPS)
- Unskilled workers will be able to operate the basic functions of the Hortibot attending one hour of training
- All operational data is automatically send to an internet based database
- The operation of the Hortibot is documented in terms of feasibility, operational capacity, and economy

Further, the objective is to identify qualified user requirements for the design of a robotic tool carrier to be used carrying various implements for plant nursing.

### Safety Emphasis

Through automatic regulation of an existing commercial machine heavy and cost-consuming weeding is eliminated. Further, fully-automatic controlling will contribute to the efficient implementation of EU directive 178/2002 concerning traceability in the primary production and thereby enhance the food-safety in the production chain.

## **METHODOLOGY**

The project is coordinated by The Danish Institute of Agricultural Sciences, Department of Agricultural Engineering, Denmark, with expertise within technologies for precision weeding, robot technology for agricultural purposes, and machinery management.

The additional partners in the project are Vitus Bering, Denmark, with competences within hydraulics, electrical control, and software development; Special Maskiner, Denmark, with many years experience within specialized machinery to nurse green areas; Eco-Dan a/s, Denmark, which is the leading supplier of vision based solutions for automatic tool guidance within row crops; The horticultural enterprise Inge-Marielund, Denmark, which is the largest producer in Denmark of garden lettuce, china cabbage, and organic onions, grown as a part of the approximately 170 hectare farmed according to organic principles.

### Hardware

The hardware design is modular and will to the largest extent be based on standard components, making tailored components the last resort.

### Software

The software is based on open source and open standard principles. Further, the developer's kits for the software environments should be easy available and inexpensive acquire.

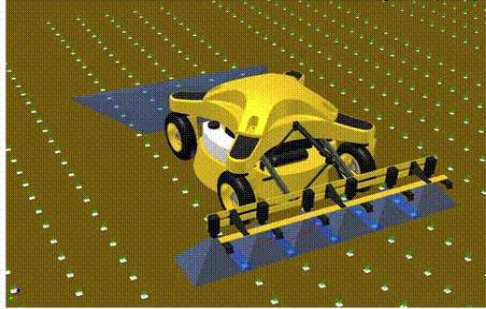
### The voice of the customer

The overall QFD approach involves the ranking of technical specifications in relation to their degree of contribution to the fulfillment of customer or user requirements. In other words, the requirements of various interested parties are transformed into a description of the technical specifications. Akao (1990) defined QFD as "a method for developing a design quality aimed at satisfying the consumer and then translating the consumer's demands into design targets and major quality assurance points to be used throughout the production phase". The analysis steps in this paper focus on: 1) determining customer requirements, 2) ranking the requirements, and 3) competition benchmarking. For further details see Sørensen *et al.* (2006).

### *Selected Competitive Tool Carrier Systems for Weed Control*

The Hortibot tool carrier – see also Jørgensen *et al.* (2006) - was compared with possible competitive tool carriers, here the GreenTrac tool carrier (Sørensen and Frederiksen, 2002) and the tractor equipped with Auto Guidance (AutoFarm, 2006) – see table 1.

**Table 1. Competitive tool carrier systems.**

<p>Petrol engine 12,5 kW    Weight 250 kg    150 kg lift capacity</p>  <p>Height clearance 15 cm    Track gauge 90 cm</p>	<p>HortiBot is a future commercial produced and robust tool carrier. It will enable an automatic execution of one-sided repetitive weeding for outdoor gardening. The HortiBot will be able to carry light weeding tools for parcels of 5–6 rows. No prior planning is needed before starting a weeding job, as the steering is primarily based on a computer-vision-based guidance system. Typically, the operator is an unskilled worker, whose primary job is to monitor one or several weeding robots instead of performing the labour-intensive work manually</p>
<p>Speed 50 m/h – 20 km/h    Weight 1500 kg</p>  <p>Height clearance 60 cm    Lift capacity 400 kg 4 Electric motors 16 kW    Track gauge 1.7 – 2.4 m</p>	<p>GreenTrac is a future tool carrier to be used in the growing season with light tools such as an inter-row cultivator for row crops. Without human assistance, it operates performing light work. The GreenTrac navigates within the field by use of high-precision satellite navigation, requiring that the exact parcel positions and each crop row position must be known beforehand. Each job is planned at the office and then transferred to the GreenTrac's computer. For safety reasons some sort of monitoring will be necessary. However, several vehicles can easily be surveyed by the same person</p>
<p>Weight 4500 kg</p> <p>Diesel engine 80 kW    Lift capacity 5000 kg</p>  <p>Speed 160 m/h – 40 km/h    Track gauge 16-2 m</p>	<p>The tractor is equipped with AutoFarm RTK AutoSteer, which enables machine control for repetitive treatments in the field with an accuracy of 3 cm. With this system, the parcels can be placed in the same locations year after year, reducing the soil compaction of the growth media. AutoFarm RTK AutoSteer is easy to learn and to use for most operators familiar with tractors. The job is planned at the office on an ordinary computer and then transferred to the tractor. A driver is required to perform turns at the headlands and to control the tools on the tractor.</p>

## RESULTS

The best platform identified as offset for a serial produced, reliable, and robust robot for horticultural weeding was found in Spider ILD01. Spider ILD01 is a slope mower for maintenance of uneven terrain with slopes up to 40 degrees and is developed and produced by Dvořák Machine Division, Czech Republic. The propulsion of the 4 wheels is driven by a central hydraulic motor and the steering by a central electrical DC motor. The Spider is remotely controlled by an operator and is changing its heading by turning all 4 wheels in parallel. Hence, the orientation of the vehicle is not controllable, which will be a necessity for future operation within row crops. This transformation of the conventional Spider slope mower into a tool carrying and autonomous robot for horticulture is detailed in the following.

Visually, the changes to the original Spider ILD01 slope mower are minimal as a result of transforming it into the Hortibot as illustrated in figure 1.

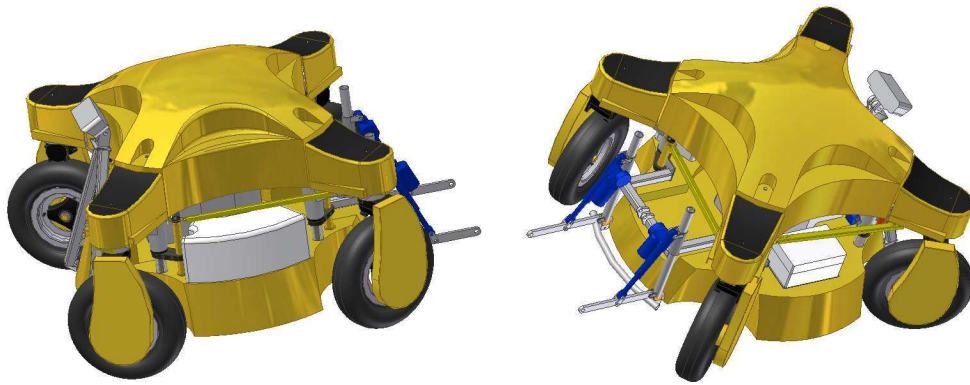


Figure 1. Illustration of the Hortibot with individual wheel control, 3D row vision system, and lift arms.

## Hardware

Overall, the main change to the Spider slope mower has been from common wheel control to individual controllable wheel modules. Each wheel module consist of a hydraulic motor for propulsion, a DC motor for steering, speed and wheel angle sensor, and a control module. The engine is also controlled by a control module, a lift arm with a control module is mounted, and a central Hortibot Control Computer (HCC) has been mounted. The communication between all units is based on a proprietary high speed CANbus. A common control module based on a 16 bit Atmel AVR microprocessor has been developed for the 4 wheel modules, the engine control module, and the lift arm module. The overall mechanical setup and electrical interfaces of the Hortibot can be seen in figure 2.

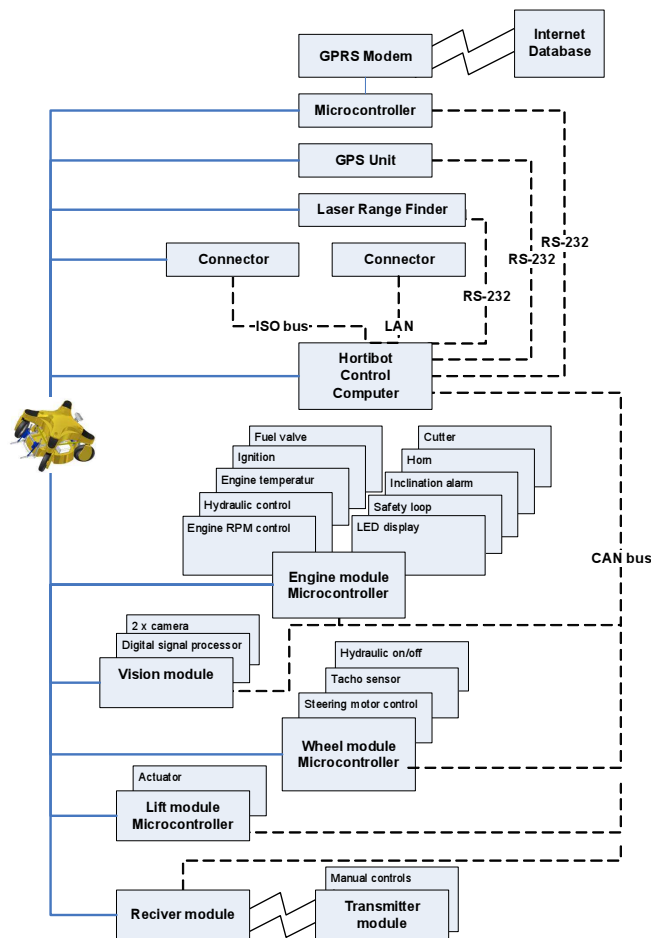


Figure 2. Hardware mechanical-electrical interfaces. The full lines indicate hardware units mounted on the Hortibot. The punctuated lines indicate electrical connections for communication.

The HCC is responsible for performing the Hortibot basic tasks such as position estimation, path following control, payload handling, emergency response, etc. The HCC is an embedded computer based on the industrial standard PC/104 architecture.

The vision module from Eco-Dan A/S, Denmark, is a new stereo vision system which captures color and 3D information from horticultural and agricultural scenes. The output from the latter system is expected to be adequate for the Hortibot navigating within transplanted onion parcels.

The standard transmitter or manual control unit for the Spider ILD01 slope mower is used as remote control for the Hortibot. However, the Spider receiver unit, which also functions as the Spider main control units, has been exchanged with a tailored CANbus enabled receiver, Receiver-R-CAN NANO-L/A2, from NBB Germany.

### Software

The main software solutions with concern to the HCC and the AVR based function modules will briefly be presented in the following.

The operating system of the HCC is an embedded Linux distribution, iComLinux developed by Cetus, Denmark ([www.cetus.dk](http://www.cetus.dk)). The iComLinux mounts the Compact Flash card read-only, and during normal operations all writing operations are performed on a RAM-disk. This has the advantage that the HCC can be switched off at any time without causing file system errors.

The HCC is connected to the sensors, actuators and communication interfaces via external modules interfacing to the HCC via a Controller Area Network (CAN) bus or via serial ports.

The software architecture of the HCC is structured as a set of software modules interfacing to each other via a shared data structure. Each software module is compiled as a Linux program, and it uses the built in Linux shared memory and semaphore features to access the shared data structure. Hence, the software modules can be started, stopped, added and upgraded independently.

### *AVR Based Function Modules*

#### *Design principals of the Function Modules:*

In order to insure a functional and stable design adaptable to future changes and functionalities, the Hortibot design has been inspired by the automobile industry, which has a long experience in doing stable and modulated designs.

This design provides the following benefits:

- Each function module handles all the detailed control of the individual functions
- Each function module can be designed and tested independently of each other and the HCC
- Function modules can easily be reused in future applications. It is easy to make special versions of modules to meet specific needs
- It is possible to select the best computer/controller hardware in each module to obtain the specific functions of the module
- The total functionality of the Hortibot can be extended without being limited by the capacity of the HCC
- The benefit of a structured modularised design include that the demand for special hardware for the HCC is dramatically reduced and a module can easily be changed without any influence on other modules

#### *Shared design of the Function modules*

All function modules require the following components as a minimum:

- *CAN-Protocol Handler* handles the CAN-bus protocol
- *Command Handler* is a component built to interpret the commands sent from the HCC via the CAN-Protocol Handler and control the functions in the module
- *Module Function x* are components handling the specific functionality of the module and handles the interface to sensors and actuators used in the module
- *Utility Package* is a package containing a number of general utility components. These utilities will be available in all function modules, and be based on common source code

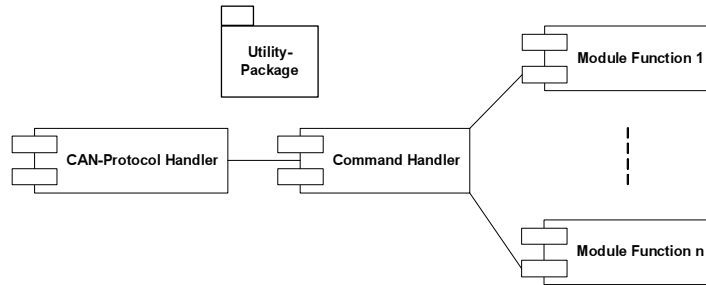


Figure 3. The components in Function modules.

### The voice of the customer

Possible customer requirements were identified using various information sources like literature review, current research activities in the robotic area, existing product screening, etc. Also, semi-structured interviews with progressive horticulturists were used to consolidate the preliminary requirement identifications. See also Sørensen *et al.* (2006).

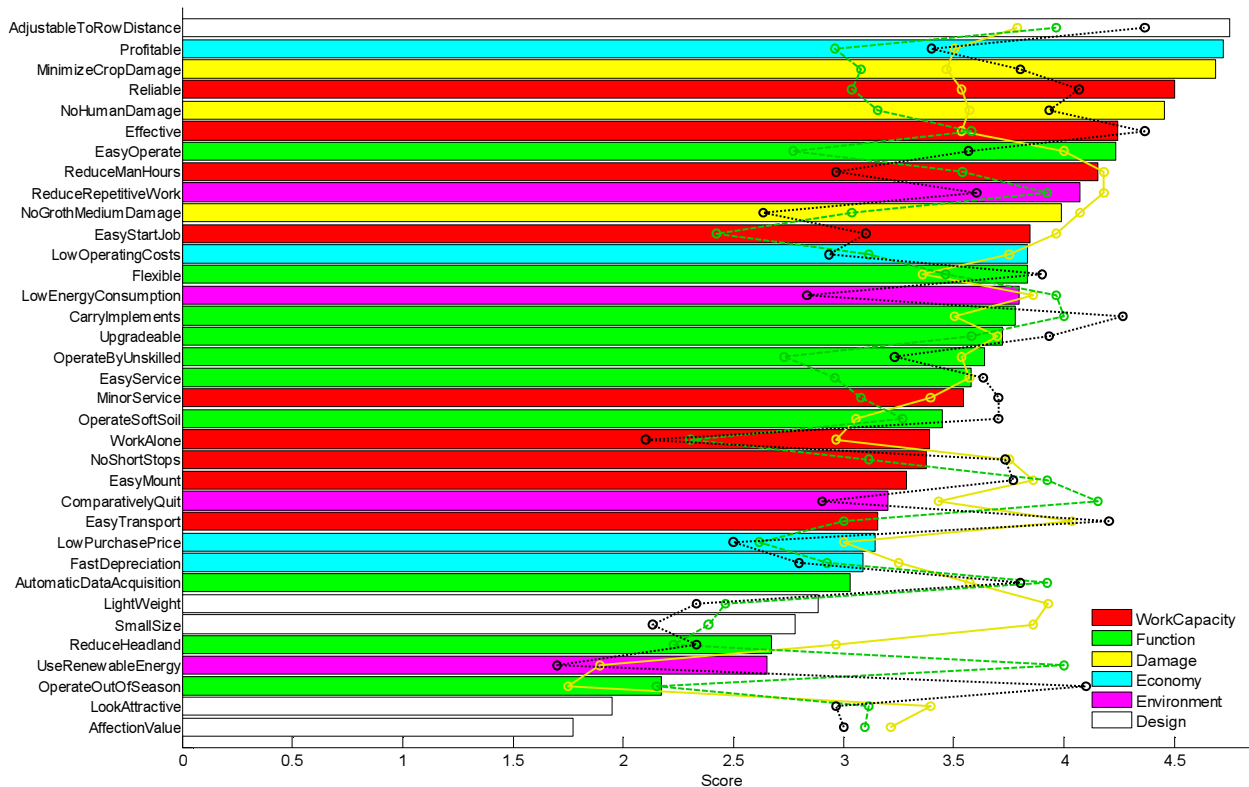


Figure 4. Average importance ratings for the  $R$  requirements shown in the horizontal bars. The yellow full line represents the performance ratings of the Hortibot, the green line punctuation represents the importance ratings of the GreenTrac, and the black dotted punctuation represents the tractor with AutoFarm AutoSteer. Score 0 equals to *not important* and score 5 equals to *very important*. The result is based on 35 interviews from Denmark, Germany, and Switzerland.

Based on the modified importance ratings and the resulting importance ratings the overall range of requirements were sorted in descending order in figure 4. Important user requirements include *adjustable to row distance and parcel size; profitable; minimize damage to crops; and reliable*. Lower ratings are attributed to requirements like *affection value, prestige; attractive look; out of season operations; and use of renewable energy*.

### Competitive Tool Carrier Systems for Weed Control

In order to evaluate the market for Horticultural tool carriers in terms of identifying out the relative position of the proposed product (Hortibot) in the market and specifically, assign priorities for further improvement, the already identified customers rated the relative performance of the three competitive products using a 5 point score scale.

The overall performance ratings of the three competing products in figure 4 show that, for example, the tractor with auto steering scores high on requirements like reliability, adjustability to field conditions, effectiveness, flexibility, etc., while the GreenTrac scores high on requirements like low energy consumption, automatic data acquisition, noiseless operation, use of renewable energy, etc. The Hortibot gets high performance ratings on requirements like reduced man-hours, minimized crop damage, profitability, reduced repetitive work, low operating costs, easy to operate, etc. It is characteristic that, for example, the GreenTrac gets relatively high performance ratings on requirements, which, on the other hand, the users deems less important.

## DISCUSSION

By modifying a remote controlled slope mower it has been shown that it is possible to produce a robust horticultural tool carrier. Weeding is the most profitable operation to automate within outdoors horticulture. Nørremark *et al.* (2006) concluded that most promising weeding tools were laser, rotary steel rods or L-tines and mower. All these tools are relatively light in their construction. Hence, the Hortibot, which can only be able to carry relatively light implements, seems a suitable carrier.

It was shown that the most important user requirements attained to a robotic weeding tool carrier include easy adaptation of the carrier to field conditions in terms of row distance and parcel size. The Hortibot does not fulfill these demands entirely. However, the modular construction makes it relatively simple to adapt the Hortibot. Still, this will demand a redesign of the Spider ILD01 slope mower.

Due to the open source principles with concern to the HCC and the AVR based function modules the Hortibot may be of value for educational institutions and universities in need for a simple and robust tool carrier.

## CONCLUSION

By modifying a remote controlled slope mower it is possible to produce a robust horticultural tool carrier for outdoor horticultural weeding. Due to the open source principles used, the Hortibot may be developed further by other institutions.

QFD is a valuable tool that can be used when developing a new product. It is a structured method where customer requirements can be analyzed and built in during the design stage. In this paper, it was demonstrated how a selected part of the QFD process was carried out for a robotic tool carrier to be used in horticulture.

Based on a combination of importance ratings and competitive priority ratings important user requirements include easy adaptation to field conditions in terms of row distance and parcel size, profitability, minimum crop damage during operation, and reliability. Lesser importance was attributed to affection value, attractive look, the possibility of out of season usage, and the use of renewable energy.

The study has demonstrated the feasibility of applying a systematic planning technique for translation of the “voice of the customer” into the specific design and technical specifications of a robotic tool carrier to be used in horticulture.

Further research will comprise identifying technical specification which best match the identified customer requirements.

### Acknowledgements

This research was supported by The Directorate for Food, Fisheries and Agri Business, Denmark (DFFE). We are grateful to Director Lennart Ahlefeldt-Laurvig, Special Maskiner, Denmark; Dr. Frank Hemmerich, KomTek, Germany; and Sales manager Jan Formánek, Dvořák Machine Devision, Czech Republic, for technical assistance with concern to the Spider ILD01 slope mower. The authors want to thank the participating horticultural users and also, the Swiss Federal Research Station for Agricultural Economics and Engineering and the German Association for

Technology and Structures in Agriculture (KTBL), which have facilitated the contact to users in these countries.

## REFERENCES

1. Akao, Y. and G. H. Mazur. 2003. The leading edge in QFD: past, present and future. *International Journal of Quality & Reliability Management* 20(1): 20-35.
2. Åstrand, B. and A. J. Baerveldt. An agricultural mobile robot with vision-based perception for mechanical weed control. *Autonomous Robots* 13(1): 21-35.
3. AutoFarm. 2006. AutoFarm<sup>®</sup> - Agriculture. Available at: <http://www.novariant.com/agriculture/>. Accessed 15 May 2006.
4. Callaghan, V., P. Chernet, M. Colley, T. Lawson, J. Standeven, M. C. West and M. Ragget 1997. Automating agricultural vehicles. *Industrial Robots* 4(5): 364-369.
5. Chan, L. K., and M. L. Wu. 2005. A systematic approach to quality function deployment with a full illustrative example. *Omega* 33: 119-139.
6. Cohen, L. 1995. Quality Function Deployment. How to Make QFD Work for You. Engineering process improvement series. Addison-Wesley Publishing Company.
7. Crowe, T. J., and C. C. Cheng 1996. Using quality function deployment in manufacturing strategic planning. *International Journal of Operations & Production Management* 16: p. 35ff.
8. Edan, Y and A. Bechar. 1998. Multi-purpose agricultural robot. In: *Proceeding of The Sixth IASTED International Conference, Robotics And Manufacturing*, 205-212. Banff, Canada.
9. Hague T., J. A. Marchant, and N. D. Tillett. 1997. Autonomous robot navigation for precision horticulture. In: *IEEE Int. Conf. On Robotics and Automation*. 1880-1885. Albuquerque, New Mexico.
10. Jørgensen, R. N. 2005. Præcisionsjordbrug – hvor svært kan det være?. In: *Plantekongres 2005*, 74-75, ISBN 87-984996-6-1. (In Danish).
11. Jørgensen, R.N., C.G. Sørensen, K. Jensen, H.T. Søgaard, J.M. Pedersen, L.B. Sørensen, and I. Havn, S. Sibbesen, and J. Nielsen 2006. Hortibot: An Accessory Kit Transforming a Slope Mower into a Robotic Tool Carrier for High-Tech Plant Nursing - Part I. 2006 ASABE Annual International Meeting, Portland Convention Center, Portland, Oregon, 9 - 12 July 2006.
12. Kassler, M. 2001. Agricultural Automation in the new Millennium. *Computers and Electronics in Agriculture*. 30(1-3): 237-240.
13. Melander B, and G. Rasmussen. 2001. Effects of cultural methods and physical weed control on intrarow weed numbers, manual weeding and marketable yield in direct-sown leek and bulb onion. *Weed Research*, 41: 491-508.
14. Nørremark, M., C.G. Sørensen, R.N. Jørgensen 2006. Hortibot: Comparison of present and future phyto-technologies for weed control. 2006 ASABE Annual International Meeting, Portland Convention Center, Portland, Oregon, 9 - 12 July 2006.
15. Ørum, J.E., and J. Christensen. 2001. Produktionsøkonomiske analyser af mulighederne for en reduceret pesticidanvendelse i dansk gartneri. Institute of Food and Resource Economics, Denmark. Report no. 128.
16. Sørensen, C.G., R.N. Jørgensen, J.M. Pedersen, M. Nørremark 2006. Hortibot: Application of Quality Function Deployment (QFD) Method for Horticultural Robotic Tool Carrier Design Planning - Part II. 2006 ASABE Annual International Meeting, Portland Convention Center, Portland, Oregon, 9 - 12 July 2006.
17. Sørensen, M., and T. Frederiksen. 2002. Greentrac – Et miljørigtigt alternativ? Unpublished B.Sc. (Hons) Vitus Bering, CVU, Denmark. Hovedrapport PRO M2. (In Danish).



# APPLICATION POTENTIALS OF FIELDSCOUTS

H. R. Langner<sup>1</sup>, D. Ehlert<sup>1</sup>, A. Falke<sup>2</sup> and G. Duscher<sup>2</sup>

## ABSTRACT

Operational fields for Fieldscouts exist where particular savings in production costs or in manpower may be achieved. The information-guided crop production considers parameters, which have to be recorded site-specifically and are used to control the information-guided crop production. Weeding and selective pest control (mechanical weeding/patch spraying) are such application fields which are in the focus of the article. Design requirements and performance parameters of the modular systems of a Fieldscout are defined on the basis of operation scenarios related to practice.

A Fieldscout scenario for weed/pest ratings should include a subsequent use of mobile platforms for spraying or other weeding acting to reduce the additional costs of the sensing task. The article presents two flexible real-time weed assessment systems as examples for a highly capable Fieldscout application. The first weed assessment system with Inspector-camera and the second system with a three CCD sensor channels are discussed as promising Fieldscout sensor technologies. Additional recording and documentary hardware as well as a concept for the data transfer between autonomous Fieldscouts and its remote control station are proposed.

**KEYWORDS:** Application Technique, CCD Camera, Control Station, Fieldscout, ImSpector, Mobile Platform, Operational Field, Weed Assessment.

## INTRODUCTION

There are several well-known possibilities to capture information such as remote sensing or the use of vehicle based sensors for surveying the ground truth. Fieldscouts for precision agriculture e.g. for out-door agricultural and horticultural applications are anticipated to work precisely and in a smaller scale than high-capacity machines, even enabling individual plant care (Blackmore et al. 2001), (Pedersen et al. 2002). Many advances have been obtained just in the past decade. A multitude of results has been published for a range of potential applications such as

- weeding (Fontaine 2004), (Lee et al. 1999), (Have 2002),
- harvesting (Pilarski et al. 2002), (Henten et al. 2002), (Tillett 1989) or
- tillage (Yukumoto et al. 2000).

Besides the ongoing technological progress qualitative requirements for such developments have been described even more precise (Hagras et al. 2002). Although a high performance level has been obtained for a number of essential subsystems, commercially spread Fieldscout systems are still under research and development so far. It should be expected that for both safety and legal reasons even potentially 'fully' autonomous machines would have to be operated in an semi-autonomous mode, supervised and controlled by at least a remote control and command station, operated by humans (Keicher et al. 2000). Such control stations are needed to stop and restart the system in the case of errors or to shut it down if hazards occur. However, the today's progress has already led to a decreased specific effort for control, enabling a simultaneous supervision of several autonomous machines by one human (Slaughter et al. 1989). From the technical and economic view autonomous Fieldscouts shall grab the farmer attention if they achieve at least the

---

<sup>1</sup> Leibniz-Institute for Agricultural Engineering Potsdam-Bornim, Max-Eyth-Allee 100, Potsdam, Germany, hlangner@atb-potsdam.de

<sup>2</sup> University of Applied Science Brandenburg, Magdeburger Strasse 50, Brandenburg/Havel, Germany

performance parameters of current machinery at similar specific costs, and carry out additional tasks i.e. for management assistance. Previous assumption that small autonomous machines which work round 24h the day at a slower performance would be more efficient than traditional systems may sustain if the total area-related costs for a certain mission would not essentially exceed current expenses.

## **OPERATIONAL FIELDS OF PORTABLE PLATFORMS**

On these assumptions, operational fields would be of interest where particular savings in i.e. crop protection products or manpower may be achieved, or if substantial contribution to sustainability is given. Weeding and pest control (mechanical weeding/patch spraying) and harvesting (selective harvesting or yield estimation) are such fields which are in the focus of both the research and farmers community (Griepentrog et al. 2003), (Keicher & Seufert 2000). The increased awareness for effective production as well as the rising share of technological and machinery development exist and contribute to this.

A less-capacity autonomous Fieldscout would perform immediate weed/pest control on a given farmland in a quasi-continuous mode. This way, the available time frame for performing the task is larger than for conventional systems where high-performing machinery is employed if a weed/pest occupancy threshold is exceeded (Langner et al. 2004). However, the autonomous system must carry out a plurality of driving performance for this quasi-continuous control. Further justification for the use of autonomous Fieldscouts for these tasks might be given by the expenditure of human labor for harvesting and pruning, the reduction of crop protection substances as well as the high consumption and drifting of pesticides in line with the exposure of workers to spray drift. The latter implication on workers safety alone is massive since such technologies can reduce their exposure to potentially harmful substances.

The farmer interests in autonomous Fieldscouts may be increased if the systems are capable to undertake additional recording and documentation tasks. Corresponding requirements arise from recent EU legislation (Regulation 2002), (Regulation 2003), (Regulation 2004a), (Regulation 2004b) as well as from food quality and safety programs. To comply with appropriate legislative provisions relating to the control of hazards in primary production and associated operations the systems should be designed to supply, record-keeping and document information for purposes such as:

- reduced exposure to potentially harmful substances during pest and weed control,
- quality tests and field mapping for selectively harvesting different qualities of grain, fruits or other agricultural products and
- quality tests, traceability and labeling.

The system should be capable to perform many different tasks due to the high-level of sensing and computing equipment of both, the Fieldscout machine and the remote command & control station. The following task list should be carried out:

- site-referenced records of crop protection applications i.e. crop name, location, date, product's active ingredient(s), applied quantity,
- application of post-harvest biocides, waxes and crop protection products during selective harvesting, including generation of documented application records about i.e. produce identity, date, product name and quantity, justification for application,
- documented site management recording system for each field or orchard, with generating and retaining records on occurrence of pests or diseases and control measures,
- surveillance of operation environment to prevent hazardous contamination, i.e. by unauthorised waste disposal and evidence that no substances have been used that are banned in line with up-to-date farm inventory,
- affixing of stickers/labels on harvested produce/containers, to identify its origin (site/farm), and generation of information reports in particular for genetically modified products.

Such autonomously generated information would be easily available for the farm management to comply with its management duties. Own analyses for the design of an autonomous sensing and acting system for weed/pest control in a field have shown that a travel speed of approx. 20 km/h in line with an operating speed higher than 10 km/h, without stopping for carrying out an operation would be the key data for sufficient performance. The components and sub-systems should be designed to assure this. Because of the required drive power and load capacity for sub-systems and i.e. pesticides, mid-sized platforms are preferred as described in (Blackmore et al. 2001), (Pedersen et al. 2002) and (Yukumoto et al. 2000) are preferred. Thereby, both the speed and resulting mechanical stresses of the sub-systems are outstanding challenges. The three-dimensional accelerations which occur with manoeuvring in rough terrain are likely to heavily affect the sub-systems, even causing malfunction. Therefore, the development and implementation of controlled active suspensions for both the entire Fieldscout and selected sub-systems such as for machine vision (navigation, detection) and actuators is considered as an essential precondition for successful operation. Such active suspensions aim to minimise accelerations or even relative ground speed within a certain time slice needed for accurate performance of the task. Moreover, the Fieldscouts should be designed in a crop-saving manner to prevent canopy damages when driving out off the tramlines.

The mid-term design and development of successful autonomous Fieldscouts would be possible if the recent results and know-how of agricultural, industrial and automotive engineering and robotics get merged in an interdisciplinary team. It is therefore proposed to redefine the operational requirements, behaviour characteristics and related tasks for both a weeding/spraying and a selective harvesting system in such a team. A case study would lead to a modular system of a number of sub-units which partially may be used for both applications. It is recommended to define both quantitative and qualitative key characteristics for each task and corresponding sub-system according to the method proposed in (Blackmore et al. 2001). As an economical scenario would underlie this procedure the findings will help to assess the performance of available sub-systems, and to identify further R&D needs. The next section presents potential sub-systems for weed assessment and for pre-harvest mapping, as well as a concept for the information and data transfer between a Fieldscout and the remote control base.

### **SYSTEMS FOR REAL-TIME WEED ASSESSMENT**

Today, herbicides are used on agricultural fields with nearly uniform doses; a site specific spatial treatment of field parts is performed only in singular cases. The common uniform treatment can cause an over dosage in sparse crop stands of a field. This can result in environmental impacts. The hard- and software solution described in the article is one contribution for a better treatment of herbicides in agriculture. The aim of a BMBF funded project at ATB was to develop a high performing system for real-time weed rating, capable to detect weeds at earliest possible stage (cotyledon), between crop rows, at high ground speeds, at varying soil and lighting conditions, not impacted by dying-off plant parts. Due to ground speeds of about 12 km/h, the very short measuring and aperture intervals implicate high demands on the sensor equipment.

The development of the automatic weed rating system was a cooperative work between University of Applied Science Osnabrück, the Comp. Symacon Bildverarbeitung Magdeburg, Comp. Müller Elektronik and the Leibniz-Institute of Agricultural Engineering Potsdam-Bornim (ATB). Some sub-systems like drivers and dynamic link libraries used in the project were part of the hardware package, delivered by company Laser2000. During the project, the University of Applied Science Osnabrueck developed a spectral image processing system based on the ImSpector (Langner et al. 2005). As shown in figure 1, a CMOS camera was used in line with a special lens of ImSpector.

The control unit in the center of figure 1 ensures a precise activation of spraying nozzles by means of an incremental encoder. The two following approaches have been realized with the ImSpector:

- PC-based linear CMOS camera PixelLink. Development of the electronic environment with self-developed software WeedControl and training of the system;
- Micro-controller based, logarithmical CMOS camera Fuga 1000 with CAN bus connection. This system works independent from PC.

The software WeedControl has been developed to control data exchange between PC and camera, to control camera settings and image processing, and to calculate the activation of the nozzles in dependence of the incremental encoder. All parameters such as camera resolution, or used wavelengths for analysis can be comfortably changed by means of the graphic user interface. Further, an On The Screen Display (OSD) unit has been implemented for the synchronization between video and measuring data.

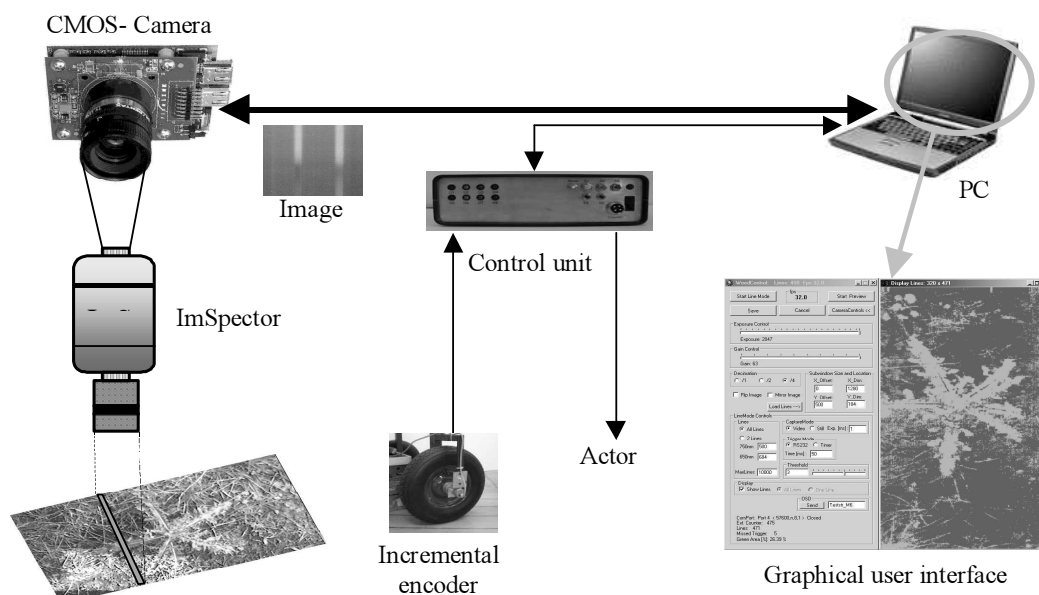


**Figure 1. Layout of the ImSpector system.**

An example of soil-plant-discrimination is given in figure 2 whereas video information is shown in the upper part, the data calculated by the WeedControl software are displayed in the center, and the calculated surface occupancy by weed is given on the bottom. The trigger signal for the actor (nozzle) is generated by setting a threshold value for maximum occupancy level, taking into account the signal of the incremental encoder, the spatial offset between sensor and actor, and of further information.

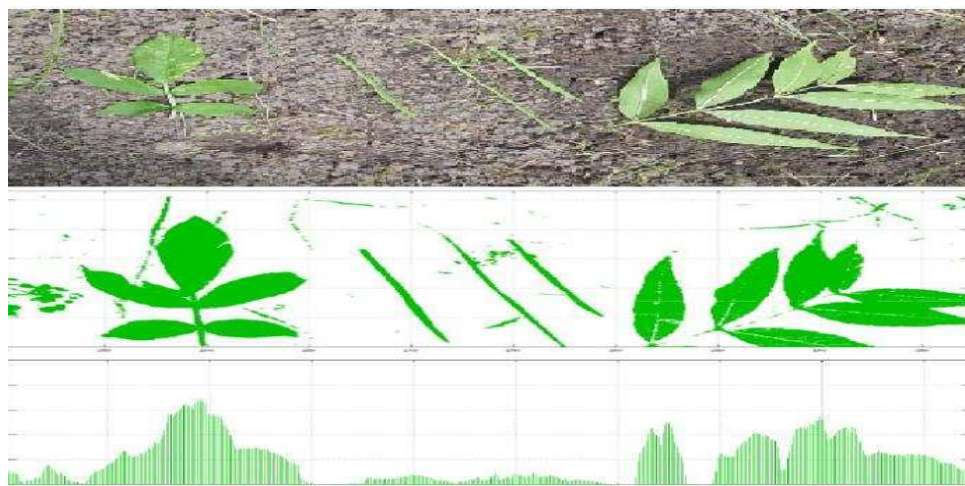


**Figure 2. Soil-plant-discrimination (top: video image, center: processed by the ImSpector system, bottom: calculated surface occupancy).**

A second solution for automatic weed ratings was developed around the special camera MS 2100 CIR, distributed by Laser 2000 company. The frame grabber hardware Meteor2 (Matrox Imaging) and the measurement card DAS-6025 (Measurement Computing Corp.) are designed for the Meteor2/Digital card and delivers a huge number of image processing functions. The camera

application software “Beikraut” is a modular designed system and has interfaces for software improvements (communication modules, GPS data interface, message transfer).

Figure 3 presents the camera MS 2100 mounted for a weed rating application. The camera is installed in 40 cm height, resulting in object size is 20cm x 15 cm when using the whole area of the image chip. The camera is oriented face down to the surface. The camera can shot image series that is like a gap free digital film with binary images (Fig. 4). The image frequency is 5 images per meter and the drive speed can be 3 meter per second or 10,8 km/h. During a measurement the weed count and weed size are related over a path length of 5m, but can be averaged to mean values of weed count and weed sizes with up to a length of 25 images.



**Figure 3. Automatic weed rating detecting with MS 2100 camera.**

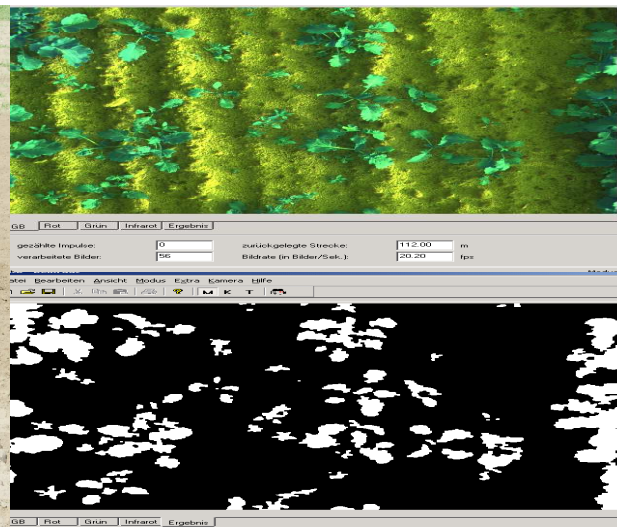


**Figure 4. Image example and binary result.**

## CONCEPTS FOR FIELDSCOUT DESIGN

Data acquisition with a remote-controlled, semi-autonomous platform is a promising solution to meet the requirements above. The presented concept of a complete Fieldscout system for gathering and applying weed information in agriculture consists of three main components: mobile platform, farm machinery and control station. The realization of this concept will include the features:

- Installation of sensor techniques on the Fieldscout and the possibility to shift tasks from the farm machinery via control station to Fieldscouts;
- Remote controlled and (semi-)autonomous data acquisition on with the platform;
- Transfer of data from the platform to the control station in real time;
- Working out of tasks for the farm machinery by using external and internal databases;
- Confirmation signal from the farm machinery when the task has been completed.

The following discussion focuses on potential design variations for a Fieldscout, which has flexible design variations. In the first section it was pointed out, that low costs are a decisive prerequisite for the effectiveness of information acquisition. Therefore, design concepts for Fieldscouts have to concentrate on simple solutions, which will nevertheless have to meet the specific requirements. Driverless platforms need to have all-terrain properties that are comparable to tractors or cross-country vehicles. That is the issue why platforms with too small dimensions are not adequate.

When Fieldscouts with tractor-like dimensions are to be used, fields covered by an established crop plant population are not passable at all or only in tram-lines. For driving along the tram-lines the driverless Fieldscouts require a perfectly working navigation system based on data of the respective lines, as e.g. was presented for the first time at the fair Agritechnica 1997 by GEOTEC, or they will need appropriate image recognition systems (Steckmann et al. 2004), (Schraut 2000).

Another approach for a platform solution is the use of a chassis that has only little influence on crops when driving outside the tram-lines. A chassis with three open spoke wheels was designed and developed for a grain Fieldscout with special consideration on limited costs. Field tests revealed that the small contact points of the spokes on the ground cause only little damage to the crops (Fig. 5). A ground clearance of 1.6 m for the frame in the platform is realized in order to allow driving through established cereal fields. With a wheel diameter of 1.40 m and a total of 12 spokes the desired all-terrain properties and platform running quality could be achieved.



**Figure 5. Fieldscout with spoke wheels.**



**Figure 6. Fieldscout with rubber wheels.**

At the current stage of development, the Fieldscout according figure 6 drives without a combustion engine. Two 12 V batteries with a capacity of 260 Ah supply power to a direct current motor with 430 W nominal power. The torque is 1.0 Nm by nominal power and a revolution speed of  $3000 \text{ min}^{-1}$ . The chassis of the Fieldscout has a total weight of 259 kg including 80 kg battery weight. By using light materials like aluminum or carbon fiber, an optimized design and by using improved modern drive concepts the total mass could be significantly reduced.

The actual Fieldscout versions are only front wheel driven. Other solution could be driven the two wheels at the backside. Driving tests with 1,5 m/s speed on soils with different consistency showed that the spoke wheels cave into ground under wet soil conditions. To counteract this effect, the spoke wheels are equipped with additional thrust rings. The implementation of the thrust rings limits the unwanted sinking of the spokes to an acceptable level. Spoke wheels and their contact areas form a dodecagon and not a circle. That is why on solid ground the spoke wheels introduce a vertical movement and the amplitude  $\Delta h$  can be calculated according to the following equation:

$$\Delta h = \frac{1.40 \text{ m}}{2} \left( 1 - \cos \frac{360^\circ}{2 \cdot 12} \right) = 0.024 \text{ m}$$

For the present geometrical relations of the Field Scout the amplitude  $\Delta h$  is 0,024 m. The value  $\Delta h$  is reduced on compliant drive lanes. Due to the inherent vertical movement the components on the chassis like batteries, devices and sensors, are exposed to acceleration load depending on drive speed and ground properties. This can generate problems when shock sensitive devices are used or sensors are installed which need smooth guiding (e.g. video monitoring cameras). Yet at the moment, the possibilities to diminish the acceleration are not practiced because the additionally surplus mass later has to be taken into consideration.

### CONCEPTS FOR CONTROL AND DATA STORAGE

The first mobile Fieldscout is approached as a prototype at ATB. Prototype is designed in a crop-saving manner (Fig. 5) and is remote controlled. The basic demands on functionality of the remote control equipment are described as follows:

- Information and data capturing, self sensing for obstacle detection,
- bi-directional wireless data and command transfer,
- data storage mailbox system, if the connection to the control station is not established.

The computing environment of the Fieldscout is modular (Falke, 2004). The computing environment uses a serial interfaces (CAN bus, RS232) to connect a central processing unit. central processing consists the embedded micro controller for motor control, steering and communicating to the command station. The permanent connection between Field Scout and remote control station is defined as high-priority task. A communication scheduler for the dynamic control of data transfer is the basic concept of the electronic development to ensure this. The underlying command design and the implementation in software are explained in the following part, containing

- unite software service,
- client for the data acquisition,
- database design and a web server.

The software service is used by the control station is installed on a normal PC hardware. The service receives data through the UMTS net and copies the data into the tables of a relational database system (tables of the MySQL database in the control station). All data analysis are been implemented into the Demon software: Mathematical calculations like mean average value, variance or frequency distributions implemented into the Demons. The Demon interface is open for further improvements. The developments doesn't have to care about the internal structures of the Demon. The access through the interfaces is free of this effort. The data access is fine-grained and will guarantee confidentiality of relevant data from the Fieldscout. The data acquisition client is installed on the PC of the measuring Fieldscout. The data acquisition client gets the measurements over a UMTS card and the radio communications network.

## DISCUSSION

Fieldscouts and mobile platforms will gain the farmers recognition in the future if equivalent performance and expenses may be achieved with respect to current machinery. Fieldscouts will carry out additional tasks for management support in information-guided crop production or in precision livestock farming. Even though the development of commercial Fieldscouts may be achieved in a mid-term scale, we believe they will be operated in semi-autonomous mode for continuous improvements and to create field maps or other legal prerequisites. A transition to fully autonomous operation may be expected after a longer successful operation period of such systems in semi-autonomous mode where the gained experiences are used for continuous improvements, and for creating the required legal prerequisites.

In order to achieve high recognition, Fieldscouts have to fulfill four major demands:

- Fieldscouts should be user friendly designed for operation, attendance and supervision because farmers usually cannot afford to employ a robotics specialist.
- Fieldscouts should be capable of self programming and life-time online learning, of navigating continuously for long periods, and should adapt themselves to any environmental or robot kinematics (Hagras et al. 2002).
- Information captured by Fieldscouts has to be relevant for the method design, since irrelevant information only causes expenses and are without of any benefit.
- Costs for capturing the information have to be low. This implies that the investigation and the manpower have to be minimized (especially the labor costs).

On these assumptions, operational fields for Fieldscouts exist where particular savings in production costs or in manpower may be achieved. Weeding and pest control (mechanical weeding/patch spraying) and selective harvesting or harvest estimation are such fields. Oppose it a Fieldscout scenario for weed/pest ratings should include a subsequent use of mobile platforms for spraying or other weeding acting, because just doing a sensing task would be associated with additional costs and would contradict the cost saving conditions stated above.

## REFERENCES

1. Blackmore, S., Have, H. and S. Fountas. 2001. Autonomous machinery in horticulture: a specification of requirements. In *Proc. of 6th International Symposium on Fruit, Nut and Vegetable Production Engineering*, 25-36. Potsdam.
2. Griepentrog, H.W., Nørremark, M., Nielsen, H. and S. Blackmore. 2003. Individual plant care in cropping systems. In *Proc. 4th European Conference on Precision Agriculture*, 247-251. Stafford, J. and A. Werner, eds. Wageningen, The Netherlands.
3. Hagaras, H., Colley, M., Callaghan, V. and M. Carr-West. 2002. Online learning and adaptation of autonomous mobile robots for sustainable agriculture. *Autonomous Robots* (13) : 37–52.
4. Have H. 2002. Autonomous weeders for christmas tree plantations - a feasibility study. *Pesticide Research* ( 59). Danish Env. Prot. Agency, Copenhagen.
5. Henten van, E.J., Hemming, J., Tuijl van, B.A.J, Kornet, J.G, Meuleman, J., Bontsema, J. and E.A. van Os. 2002. An autonomous robot for harvesting cucumbers in greenhouses. *Autonomous Robots* (13): 241–258.
6. Keicher, R. and H. Seufert. 2000. Automatic guidance for agricultural vehicles in Europe. *Journal Computer and Electronics in Agriculture* 35 (2000): 169-194.
7. Lee, W.S., Slaughter, D.C. and D.K. Giles. 1999. Robotic weed control systems for tomatoes. *Precision Agriculture* (1): 95-13.
8. Pedersen, T.S., Nielsen, K.M., Andersen, P., Bak, T. and J.D. Nielsen. 2002. Development of an autonomous vehicle for weed and crop registration. In *Proc. of AgEng Conference on Agricultural Engineering*, 22-23. Budapest.
9. Pilarski, T., Happold, M., Pangels, H., Ollis, M., Fitzpatrick, K. and A. Stentz. 2002. The Demeter system for automated harvesting. *Autonomous Robots* (13): 9–20.
10. Slaughter, D.C. and R.C. Harrell. 1989. Discriminating fruit robotic harvest using color in natural outdoor scenes. *Transactions of ASAE* (32) 2: 757-763.
11. Steckmann, K., Wulf, O. and Wagner, B. 2004. 3D Laserscanner zur Bereichsüberwachung und Lagebestimmung. In *Proc. DGR Robotics Conf.*, 469-476. Düsseldorf, Germany: VDI-Berichte 1841.
12. Tillett, R.D. 1989. A calibration system for vision-guided agricultural robots. *Journal of Agricultural Engineering Research* (42): 267-267.
13. Yukumoto, O., Matsuo, Y. and N. Noguchi. 2000. Robotization of agricultural vehicles (part 2): Description of the tilling robot. *Japan Agricultural Research Quarterly* (34) 2: 107-114.
14. Falke A. 2004. Funknetzbasierete Strukturierung von mobil gewonnenen Daten aus dem agrartechnischen Bereich und Speicherung in einer Datenbank einschließlich der Entwicklung eines Nutzungskonzepts. Diplomarbeit, Brandenburg: Brandenburg FH - FB Informatik und Medien.
15. Fontaine, V. 2004. Development of a vision-based local positioning system for weed detection. Thesis. Saskatoon: University of Saskatchewan.
16. Langner, H.R., Wartenberg, G., Böttger, H., Ruckelshausen, A., In der Stroth, S., Linz and A. Ramler. 2005. *Messsystem zur Bewertung des Unkrautvorkommens - Bornimer Agrartechnische Berichte*, Heft 44. ed. Leibniz-Institut für Agrartechnik (ATB), Germany.
17. Schraut M. 2000. Umgebungserfassung auf Basis lernender digitaler Karten zur vorausschauenden Konditionierung von Fahrerassistenzsystemen. Dissertation am Lehrstuhl für Realzeit-Computersysteme, München: TU München.
18. Langner, H.R., Ehlert, D. and E. Kramer. 2004. Autonomous robots for field data acquisition in farm management. In *Proc. DGR Robotics Conf.*: 615-624. Düsseldorf, Germany: VDI-Berichte 1841.

19. Regulation (EC). 2002. Laying down the general principles and requirements of food law, establishing the European Food Safety Authority and laying down procedures in matters of food safety. No. 178. Official Journal of the EU L31: 1-24.
20. Regulation (EC). 2003. Concerning the traceability and labelling of genetically modified organisms and the traceability of food and feed products produced from genetically modified organisms. No 1830. Official Journal of the EU L268: 24-28.
21. Regulation (EC). 2004a. On persistent organic pollutants and amending Directive 79/117/EEC. No 850. Official Journal of the EU L158: 7-49.
22. Regulation (EC). 2004b. On the hygiene of foodstuffs (corrigendum). No 852. Official Journal of the EU L139: 3-21.



# OPTIMAL DYNAMIC MOTION SEQUENCE GENERATION FOR MULTIPLE HARVESTERS

D. Bochtis<sup>1</sup>, S. G. Vougioukas<sup>1</sup>, C. Tsatsarelis<sup>1</sup> and Y. Ampatzidis<sup>1</sup>

## ABSTRACT

Harvesting efficiency could be improved significantly by computing optimal harvesting patterns which minimize turning time. Hence, the execution of harvesting operations, especially in case of cooperating harvesters, needs to be carefully planned. In this paper, the operation planning for a fleet of harvesters is formulated as a discrete optimization, multi-Traveling Salesman Problem (m-TSP). Given the number of “cities” and the cost traveling between every pair of them, the m-TSP searches for m round trips (one for every of m salesmen) in a way that every “city” is visited exactly once and the total cost is minimized. In our proposed formulation, the “cities” of the m-TSP correspond to the operating rows of the field. The cost is the nonproductive time, which is spent during the turnings at the headlands. This cost is computed based on the kinematics constraints of the vehicles and on the geometrical space constraints of the field.

An existing heuristic algorithm with low computational requirements (in the order of a few seconds) was adopted for the solution of the m-TSP. The advantage of low computational time makes it feasible to re-plan an optimal fieldwork pattern when it is necessary for the remaining non-harvested field, while the harvesting procedure is being executed. Simulations of scenarios of planning and re-planning optimal harvesting operations are presented.

**KEYWORDS.** Autonomous Machines, Fieldwork Pattern, Harvesting, Mission Planning.

## INTRODUCTION

Recently, efficiency studies have been carried out based on collection of time-stamped position data while the machines were traveling in the field. Positioning data was gathered by accurate GPS-based systems (Global Positioning System). The conclusion of all these studies is that machinery efficiency could be improved significantly by computing optimal fieldwork patterns for the agricultural machines which minimize turning time. According to Hansen et al. (2003), optimization of the combine harvesting pattern in corn fields can increase harvesting efficiency substantially. Pre-planning of combine movement in the field and the use of vehicle position indicators via GPS will contribute to a major improvement in overall efficiency. Furthermore, controlled traffic in the field will also reduce soil compaction. Taylor et al. (2002) have used DGPS data obtained during yield mapping operations to evaluate the potential for improving harvest efficiency. They concluded that harvest efficiency depends more upon turning time rather than unloading time. Hence, farm managers could improve harvest efficiency first by modifying harvest patterns to minimize turning and secondly by unloading grain on-the-go. Benson et al. (2002) supported these conclusions by simulation studies of the in-field harvest operations in the ARENA manufacturing language.

Field efficiency can be mathematically expressed as (Tsatsarelis 2006, Hunt 2001):

$$E_f = \frac{F(t_T)}{t_T + \sum t_i}$$

---

<sup>1</sup> School of Agriculture, Department of Agricultural Engineering, Aristotle University of Thessaloniki, Greece, dionmpo@agro.auth.gr

where  $F(t_T)$  is a function of the theoretical field time (the time the machine is operating in the crop at an optimum travel speed and over its full width of action) and  $t_i$ , are the time losses due to “interruptions”. A significant type of interruption is the time a harvester spends for maneuvering at the headlands. The resulting optimization problem is the minimization of the total maneuvering time. Furthermore, because of the problem’s dynamic nature the implemented algorithm must generate solutions relatively fast.

In this paper, the problem of motion sequence generation for a fleet of  $m$  harvesters is formulated as a discrete optimization, multi-Traveling Salesman Problem (m-TSP). Given a weighted graph with vertices and edges, the m-TSP searches for  $m$  paths (sequences of edges), which - combined - contain all graph vertices. Each vertex must be visited only once by any path, and the total cost of all traversed edges must be minimized. In our proposed formulation, the vertices of the m-TSP correspond to the operating rows of the field. The cost is the nonproductive time, which is spent during the turnings at the headlands. This cost is computed based on the kinematics constraints of the vehicles and on the geometrical space constraints of the field.

An existing heuristic algorithm with low computational requirements (in the order of a few seconds) was adopted for the solution of the m-TSP. The advantage of low computational time makes it feasible to re-plan an optimal fieldwork pattern for the remaining non-harvested field, while the harvesting procedure is being executed. This may be required in case of unexpected changes in the fleet size (e.g., harvester blockage or restarting), or in cases of significant variation in some harvesters’ working rates. Simulations of scenarios like the ones mentioned above were executed, and the corresponding optimal harvesting patterns were computed for various-size teams of harvesters.

### PROBLEM STATEMENT

A fleet of identical harvesters  $h_k \in H$ , where  $0 < k \leq \|H\|$  operate in a field using the alternation pattern, i.e., they travel from one end of the field to the other, in parallel rows, which are not necessarily straight. The number of rows is given by:  $n = \lfloor w/l + 1 \rfloor$ , where  $w$  is the effective operation width of the harvester and  $l$  is the length of the field face. For each harvester  $k$  two geographical field-points (not necessary different) are given: a starting point ( $s_k$ ) end an ending point ( $e_k$ ). These points may be the desirable initial and final row for the harvester operation, or may be some out-of-the-field points; however, they must always lie inside the area in which the harvester is moving on an open area. For example, if the next destination for a harvester is a silo which is connected with the field by a fixed road, then the ending point for the harvester operation is the beginning of the road. Let  $P$  be the set of these points  $P = \{s_k, e_k / 0 < k \leq \|H\|\}$ , let  $L$  be the set of the rows ( $n = \|L\|$ ) and  $N$  be their union:  $N = P \cup L$ ,  $\|N\| = 2\|H\| + \|L\|$ . All the elements of the set  $N$  will be referred to as *nodes*. These sets are in general time-dependent. For example, in case of a harvester blockage the fleet size is decreased and when the harvester restarts the fleet size is increased. Moreover, the ending point of a harvester may have to be changed, if for some reason another new destination is given. For such reasons, the field alternation pattern may have to be re-planned while harvesting the operation is being executed. After the beginning of a plan’s execution the starting point for re-planning is the current harvester positions and the set  $L$  is the set of the remaining un-harvested rows.

The solution results in a permutation  $\pi_k \subset L$  for every harvester  $k$  that contains the sequence of the rows that the harvester must operate in, where  $\pi_k(i)$  is the row that the harvester  $k$  operates at the step  $i$ .

Formally the next summation has to be minimized:

$$\sum_{k=1}^{\|H\|} \left( c_{s_k, \pi_k(1)} + \sum_{i=1}^{\|\pi_k\|} c_{\pi_k(i), \pi_k(i+1)} + c_{\pi_k(\|\pi_k\|), e_k} \right)$$

where  $c_{a,b}$  is the cost for the harvester transition from node  $a$  to node  $b$ .

## Inter-row Cost Matrix

For our planning problem the optimization criterion is the minimization of the nonworking traveled distance (a harvester is traveling without harvesting), which is equivalent to the nonworking time. We categorize nonworking distance to *out-field* and to *in-field* nonworking traveled distance. The first category refers to the length of the paths that connect the harvesters' starting and ending points with their initial and final operating rows. This length includes only the off-road traveled distances. For the calculation of these distances there are two cases. In the first case the starting and ending points are significantly far away from the rows' vertices and we can consider the distances like a set of straight lines that connect these points to these vertices. In the cases where the starting and ending points are close enough to the field, or there are obstacles or other field restrictions, a path planning program is used (Vougioukas et al., 2005) to calculate the traveled distances, because the vehicles kinematics cannot be neglected.

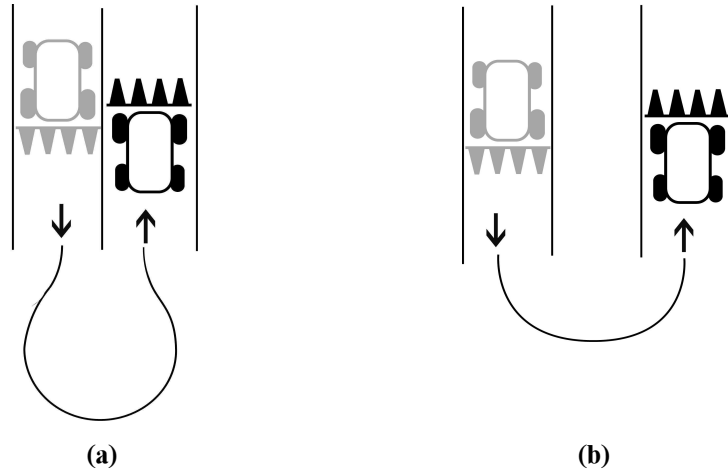


Figure 1. Headland maneuvers (a) loop turn, (b) double corner turn.

The in-field nonworking distances refer to the total length of the maneuvers at the headlands. These distances depend on the harvesters' related characteristics (minimum turning radius, effective operating width) and the harvesters' maneuverability constraints due to field geometry (e.g., presence of obstacles, restricted areas). For the calculation of the distances that the harvester travels at the headlands we consider two types of harvester's maneuvers, the loop turn and the double corner turn (Figure 1). For these types we can assume that the harvester is a vehicle which moves forward on an empty plane. In this case, according to Dubins' Theorem (Dubins, 1957), the shortest path between any two harvester's configurations is a sequence of straight line segments (S) and circular arcs (C) of radius  $R_{min}$  of the form CSC, CCC or a subsequence of one of these, where  $R_{min}$  is the operative lower limit on the turn radius. More specifically,  $R_{min} = \max(R_{dmin}, R_{kmin})$ , where  $R_{dmin}$  is the minimum dynamic turn radius, which generates the maximum permissible lateral acceleration  $\alpha_{max}$  for the vehicle for a given velocity  $v$  ( $R_{dmin} = v / \alpha_{max}^2$ ). Finally,  $R_{kmin}$  is the minimum kinematic turn radius which is imposed by the machine's steering mechanism. For typical working velocities of agricultural machines we can neglect the dynamic limitation.

We consider that the harvester's configuration space (C-space) comprises of three degrees of freedom ( $x, y, \theta$ ) and its actuation space (A-space) is the space of the turning radius. The integral and differential equations, which map A-space to C-space in a flat 2D world, are given below:

$$\begin{aligned} \dot{x} &= v \cos(\theta) & x &= x_0 + v \int_0^t \cos(\theta(t)) dt \\ \dot{y} &= v \sin(\theta) & y &= y_0 + v \int_0^t \sin(\theta(t)) dt \\ \dot{\theta} &= v \frac{1}{R} & \theta &= \theta_0 + \frac{vt}{R} \end{aligned}$$

where  $v$  is the machine's linear velocity,  $(x,y)$  are the coordinates of the rear-wheels axis center,  $\theta$  is the machine's orientation, and  $R$  is the turning radius. We assume that the actuation space is the discrete space  $A = \{R_{\min}, -R_{\min}, \infty\}$  (right turn:  $R=R_{\min}$ , left turn:  $R = -R_{\min}$ , strait route:  $R = \infty$ ). The usual maneuvers of an agricultural machine at the headlands are completed in three stages. For example, for the execution of a loop turn the three stages are: 1) right turn 2) left turn 3) right turn. We assume that during every stage the velocity and the steering angle are constants ( $\dot{v} = \dot{\phi} = 0$ ). Let  $\psi = [x, y, \theta]^T$  represents the state vector and  $\Psi$  the indefinite integral of the state vector. If we integrate the differential equations (2) for any stage the result is:

$$\psi_k = \psi_{k-1} + \Psi_k(t_k) \quad k \in \{1, 2, 3\}$$

Adding the previous equations we get an algebraic system of three equations:

$$\psi_3 = \psi_0 + \sum_{k=1}^3 \Psi_k(t_k)$$

where  $\psi_3, \psi_0$  are the known final and initial state vectors. The duration of each of the three stages is computed by solving the above system. Next, the total path length of the maneuver is computed by adding the corresponding line integrals:

$$\mu = \sum_k s(t_k) \quad \text{where} \quad s(t_k) = \int_c^{t_k} ds = \int_0^{t_k} |\dot{r}(t)| dt = \int_0^{t_k} \sqrt{[\dot{x}(t)]^2 + [\dot{y}(t)]^2} dt$$

By applying the previous method we get:

$$\forall i, j \in L \quad c_{ij} = \begin{cases} R_{\min} \left( 3\pi - 4 \operatorname{asin} \left( \frac{2R_{\min} + |i-j| \cdot w}{4R_{\min}} \right) \right) & \text{if } 2R_{\min} \leq |i-j| \cdot w \\ |i-j| \cdot w + (\pi - 2)R_{\min} & \text{if } 2R_{\min} > |i-j| \cdot w \end{cases}$$

## SIMULATION RESULTS

The algorithm used in this paper is the Clarke-Wright savings algorithm, a well-known algorithm in vehicle routing (Clarke et al., 1964). The algorithm operates in two stages: i) the randomization phase, where an initial solution is computed ii) the improvement phase, where various improvement heuristics are performed based on the use of local search algorithms. These heuristics include: a) the Or-opt operation, which works by deleting a group of nodes from a tour and re-inserting it at another position in the tour (the group sizes may be of 1, 2, and 3 nodes), b) the 2-opt, which deletes two edges, thus breaking the tour into two paths, and then reconnects the paths in the other possible way, c) the swap operation in which two nodes on different routes may be removed from their routes and inserted into the opposite route (Snyder et al., 2004).

Small-sized problems (concerning the number of the rows and the number of the harvesters) are presented for illustration purposes. For the same reason we assume that the harvesters are unloading on-the-go. The difference in the case when the harvesters have to unload at a predetermined place (e.g., a silo, or at the field side) is that in the second case for each harvester more than one route are generated. All harvesters' minimum turning radius is  $R_{\min} = 4m$  and the effective operating width is  $w = 3m$ . We consider this relation between the harvesters characteristics ( $w < R_{\min} < 2w$ ) to reduce their maneuverability. By doing so, the problem difficulty - and the necessity for an optimal plan - is increased. At the first scenario three identical harvesters are going to operate at the same field. The field is divided into 30 operating rows. The total work is distributed equally to the three of them. The destination for all the harvesters after their operation is completed is a point at the left side of the field. This point may be a silo for harvester unloading,

a station for their parking or maintenance, the entry to a new field for harvesting, or the road that drives to other destinations. From the solution of the initial planning we get the three permutations:  $\pi_1 = \langle 1, 4, 7, 10, 13, 16, 12, 9, 5, 2 \rangle$ ,  $\pi_2 = \langle 3, 8, 15, 19, 23, 20, 17, 14, 11, 6 \rangle$ ,  $\pi_3 = \langle 22, 26, 29, 25, 28, 30, 27, 24, 21, 18 \rangle$ . Figures 2a, 2b, 2c illustrate this initial plan for the corresponding harvesters 1, 2 and 3. While at work, we suppose that a mechanical damage causes harvester 1 to reduce its working rate and eventually stop at the row  $\pi_1(4) = 10$ . Re-planning must be performed for the remaining harvesters 2 and 3 ( $\|H'\| = 2$ ) for the un-harvested rows ( $\|L'\| = 16$ ) with new starting points  $s'_2 = \pi_2(5)$  and  $s'_3 = \pi_3(5)$ . The new plan is illustrated in figures 2d, 2e and 2f. The next destination remains the same and this is the reason why the harvesters exit the field as close to the left side of the field as possible. The computational time for the initial planning was 1.9 sec and for the re-planning 0.88 sec.

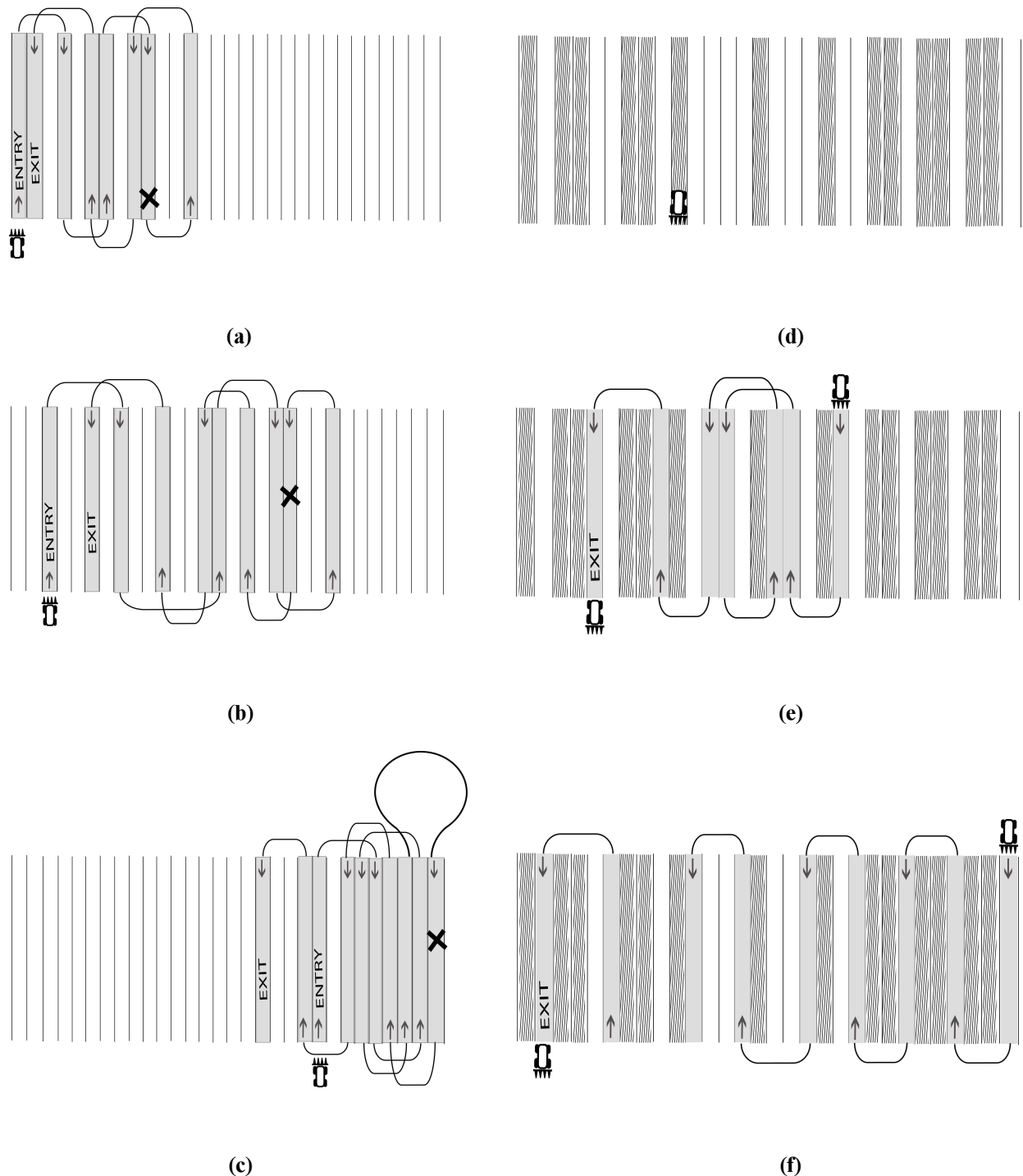


**Figure 2. Motion sequence planning for three harvesters (a, b, c) and re-planning due to the blockage of one of them (d, e, f).**

In the second scenario there are two harvesters with the same characteristics as the previous ones which are going to operate in a 20-row field. As the initial plan is executed (Figures 3a, 3b) the ending point for harvester 2 is changed, and the harvester - after its operation is completed - has to travel to a destination at the right side of the field (e.g., another silo must be used, or harvesting must continue to a field from this side, etc.) (Figures 3c, 3d). The solution time for the initial planning was 1.04 sec and for the re-planning 0.65 sec.

The proposed algorithm can easily handle problem instances with hundred of rows and with a large number of operating harvesters. Figure 4 illustrates the solution progress for a problem instance of 100 rows and a fleet of four harvesters. It shows that near-optimal solutions are generated in a few seconds. Even the first solution, which is generated in 0.06 second, reduces the in-field nonworking traveled distance more than 500m from the case of the typical straight alternation pattern (2,715.2m). If the planning includes the out-field paths, the improvement is even bigger. For these calculations a 2.8 GHz Pentium-4 processor (Windows XP) was used. The details (solution time and number of iterations) for two solutions (the best and the worst) are presented at table 1.

**Table 1. Solution details.**

Solution time (s)		Number of iterations				
Phase 1 Build	Phase 2 Improve	Swap	2- Opt	Or- opt(1)	Or- opt(2)	Or- opt(3)
0.02	0.04	0	0	1	4	12
0.12	5.87	4	1	1	399	167

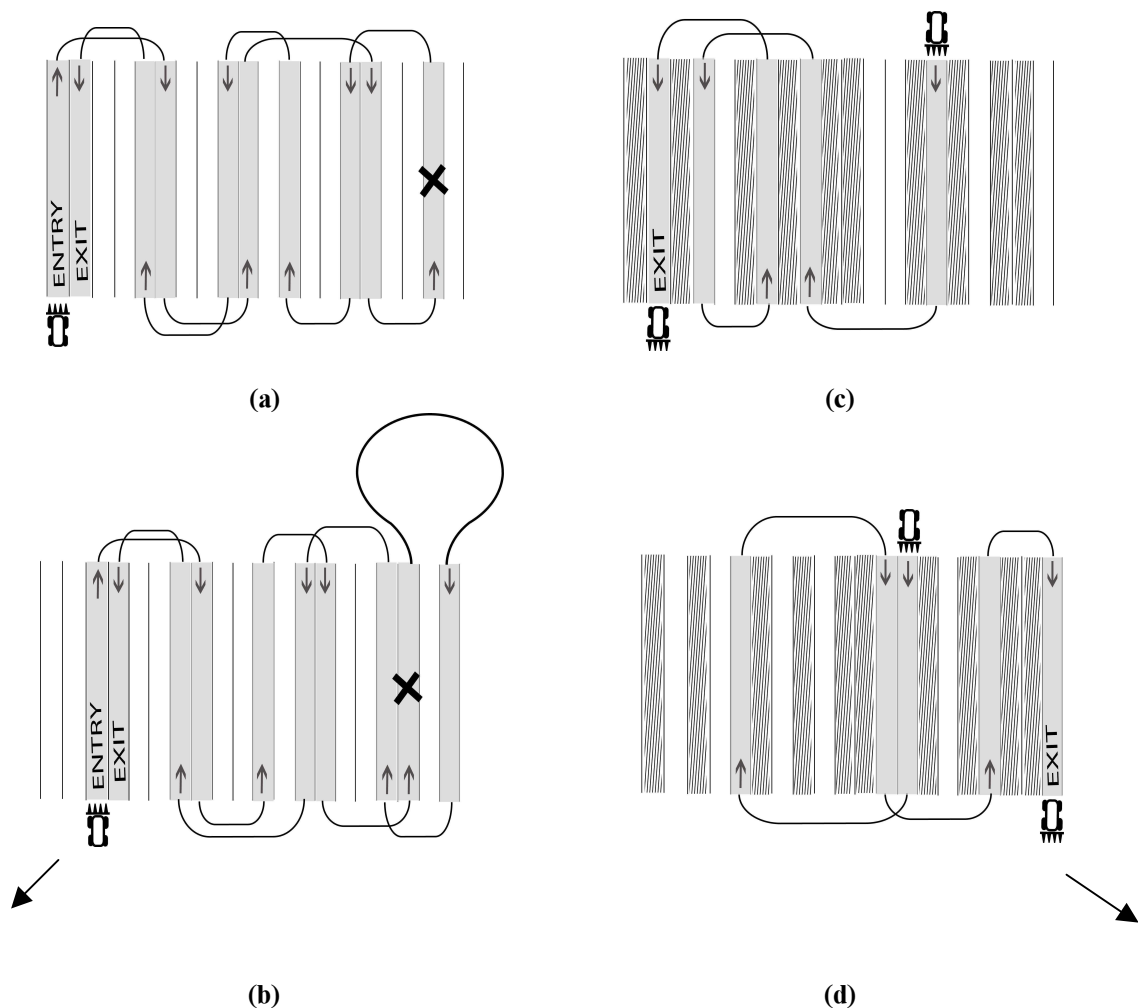


**Figure 3. Motion sequence planning for two harvesters (a, b) and re-planning due to the change of the after operation destination of one of them (c, d).**

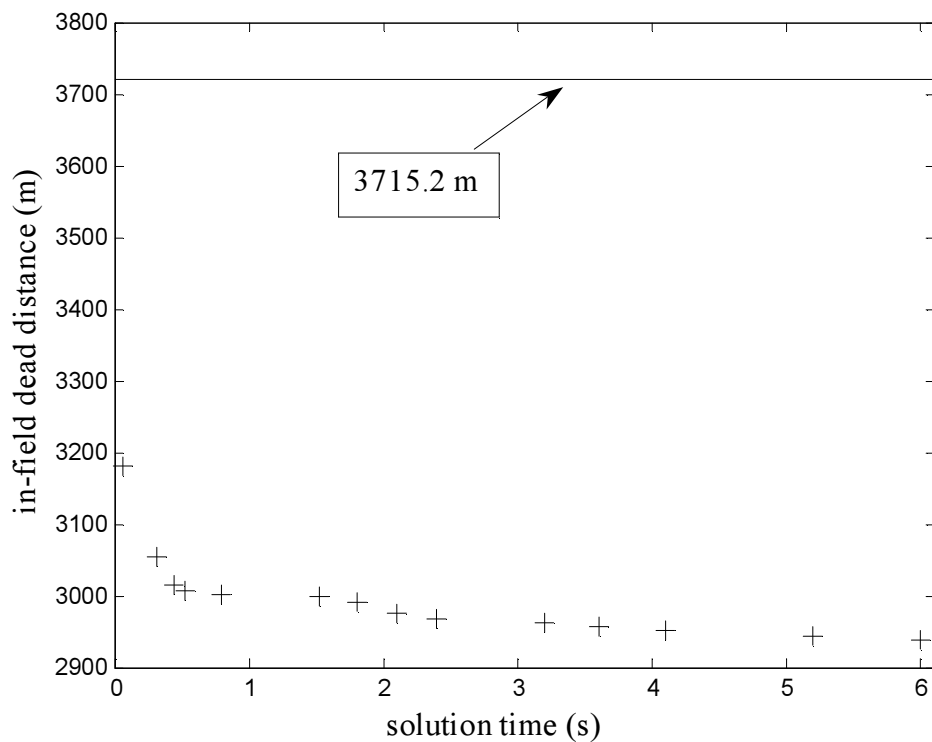


**Figure 4. Solution progress for a problem instance of 100 rows and 4 harvesters.**

## CONCLUSION

In this paper the problem of motion sequence generation for a fleet of harvesters operating according to the alternation pattern, was formulated as a routing problem. Two typical problem instances were solved using an existing heuristic algorithm. The advantage of this algorithm is its low computational requirements. Fast computation of solutions is extremely useful in dynamic problems, where some problem parameters may change during execution, or may be partially known before the execution.

Of course, for the complete adoption of routing algorithms for operations planning like this, modifications must be done which are related to the nature of agricultural operations. For example, the constraint that two harvesters must not move in adjacent rows in reverse directions must be added to the problem formulation. Even so, the planning improvement seems clear, especially when we have to deal with reduced maneuverability.

## REFERENCES

1. Benson, E. R., A. C. Hansen, J. F. Reid, B.L. Warman, and M.A. Brand. 2002. Development of an in-field grain handling simulation in ARENA. ASAE Paper. 02- 3104. St. Joseph, MI. 18pp.
2. Clarke, G., and J. Wright. 1964. Scheduling of vehicles from a central depot to a number of delivery points. *Operations Research*, 12 #4, pp.568-581.
3. Dubins, L.E. 1957. On curves of minimal length with a constraint on average curvature and with prescribed initial and terminal positions and tangents. *American Journal of Mathematics*, 79, pp. 497– 516.
4. Hunt, D. 2001. *Farm Power and Machinery Management*. 10th Ed. Iowa State Press. Ames, Iowa.
5. Snyder, L., and M. Daskin. 2004. A Random-Key Genetic Algorithm for the Generalized Traveling Salesman Problem. Technical Report #04T-018 Dept. of Industrial & Systems Engineering, Lehigh University.

6. Taylor, R.K., M.D. Schrock, and S.A. Staggenborg. 2002. Extracting machinery management information from GPS data. Paper No. 02-10008. St. Joseph, Michigan: ASAE.
7. Tsatsarelis, C. 2006. *Farm Machinery Management*. (In Greek). Thessaloniki.
8. Hansen, A. C., R. H. Hornbaker, and Q. Zhang. 2003. Monitoring and analysis of in-field grain handling operations. *Proceedings of the International Conference on Crop Harvesting*, Louisville, Kentucky USA. ASEA Publication No 701P1103e.
9. Vougioukas, S., S. Blackmore, J. Nielsen, and S. Fountas. 2005. A Two-Stage Route Planning System for Autonomous Agricultural Vehicles. *5th European Conference on Precision Agriculture*, pp. 597-604, Uppsala, Sweden.

# MULTILAYER CONTROLLER FOR OUTDOOR VEHICLE

A. Reske-Nielsen<sup>1</sup>, A. Mejnertsen<sup>1</sup>, N. Andersen<sup>1</sup>, O. Ravn<sup>1</sup>,  
M. Nørremark<sup>2</sup> and H.W. Griepentrog<sup>2</sup>

## ABSTRACT

A full software and hardware solution has been designed, implemented and tested for control of a small agricultural automatic tractor. The objective was to realise a user-friendly, multi-layer controller architecture for an outdoor platform. The collaborative research work was done as a part of a research project within the field of automated agriculture and precision farming.

**KEYWORDS.** Autonomous Tractor, GPS Navigation, Kalman Filter, Mobile Robot.

## INTRODUCTION

Industries where hard physical, repetitive and intensive labour is used have in recent years been subject to automation. Technology has made it feasible to build systems that are more economical, efficient and reliable than human labour. Robotics in agriculture is, however, still in an early state of development, since outdoor automation presents a wide range of complex challenges, including the safety issues that may affect the immediate surroundings. However, agricultural automation bears great promise for the future both economically and environmentally.

Tractors are the backbone of modern agriculture, by providing a versatile platform it can be used to perform many different tasks. This makes the tractor a suitable target for automation.

There exists a great deal of research on the topic of automation of mobile equipment in agriculture. There are two main approaches to agricultural navigation (Stentz et al., 2002). The first approach uses absolute positioning sensors, such as the global positioning system (GPS), magnetic compass, or visual markers. A research project at Stanford University has developed a closed loop system, with GPS and steer angle as feedbacks for an automatic tractor (O'Conner et al. 1996). This research shows that it is entirely possible to navigate a tractor in a field using only GPS, with a very high degree of accuracy.

The second approach uses local data to calculate a position. The routes are determined by a relative frame of reference. Reference points are based on local information, such as individual plants or crop rows derived from a camera image or dead reckoning information, such as odometry, gyroscopes and accelerometers. Based on the local information, a coverage pattern can be calculated. An example of a system that only uses local information for navigation is the combine harvester developed at University of Delaware (Benson et al. 2001). This combine harvester is navigated using machine vision to allow the vehicle to harvest corn with a statistical accuracy that matches even the best GPS based systems.

The two methods have both strength and drawbacks, but neither can be considered a perfect solution. To get a precise and redundant system the two approaches can be combined, thus harvesting the strengths of both and reducing their drawbacks. This paper will describe a system that fuses information from a precision RTK-GPS and local odometry to get precise and redundant navigation.

---

<sup>1</sup> Automation, Ørsted\*DTU, Technical University of Denmark, Building 326, DK-2800 Lyngby, Denmark, anders@crashandburn.dk

<sup>2</sup> The Royal Veterinary and Agricultural University Dept. of Agricultural Sciences Environment, Resources and Technology Højbakkegaard Alle 2, DK-2630 Taastrup, Denmark

The system presented in this paper is more than a mere navigation system, but is a full tractor control system. This includes an easy to use graphical interface, implement control and the possibility make off line simulations of the entire system.

The next section will describe the hardware of the tractor system. Section 3 will contain an overview of the different components in navigation system. The user interface will be explained in section 4. Finally experimental results and a conclusion is given in sections 5 and 6 respectively.

## AUTOMATIC TRACTOR

The project described in this paper is based on the Hako Hakotrac 3000 (Fig. 1) retrofitted with sensors for measuring relevant physical data that is needed for calculating the odometry of the tractor first described in (Blackmore et al. 2004). Magnetic pulse counter has been fitted on the drive shaft to measure the driven distance. A similar magnetic counter has been fitted to the engine shaft to measure the rotation of the engine. A couple of potentiometers have been fitted to the front wheels to give the ability to measure the steering angle.



**Figure 1. Picture of the tractor modified for automatic use.**

In order to steer the tractor a hydraulic power steering has been added. Linear electrical actuators have been added to control the diesel pump and the pedals. The tractor uses a Hydrostatic Continues Variable Transmission (CVT). This means that the diesel engine in front acts as a variable displacement pump and a hydraulic motor is mounted directly to the wheel hub. This allows the power to be controlled by pedals.

An industrial microcontroller, ESX, from Sensor-Technik Wiedemann GmbH has been fitted to the system. The ESX is responsible for reading the tractors sensors and controlling the linear actuators. The ESX provides speed, wheel angle, engine RPM control, control and simple control for raising and lowering of the tool attachment at the rear of the tractor. The ESX has a CAN-bus interface allowing for external control of parameters along with sensor readouts. The connectivity is shown in figure 2.

A hardwired safety loop is connected directly to the actuators and is able to stop the tractor independently of the ESX if an emergency stop is activated. This is currently the only safety system implemented on the tractor.

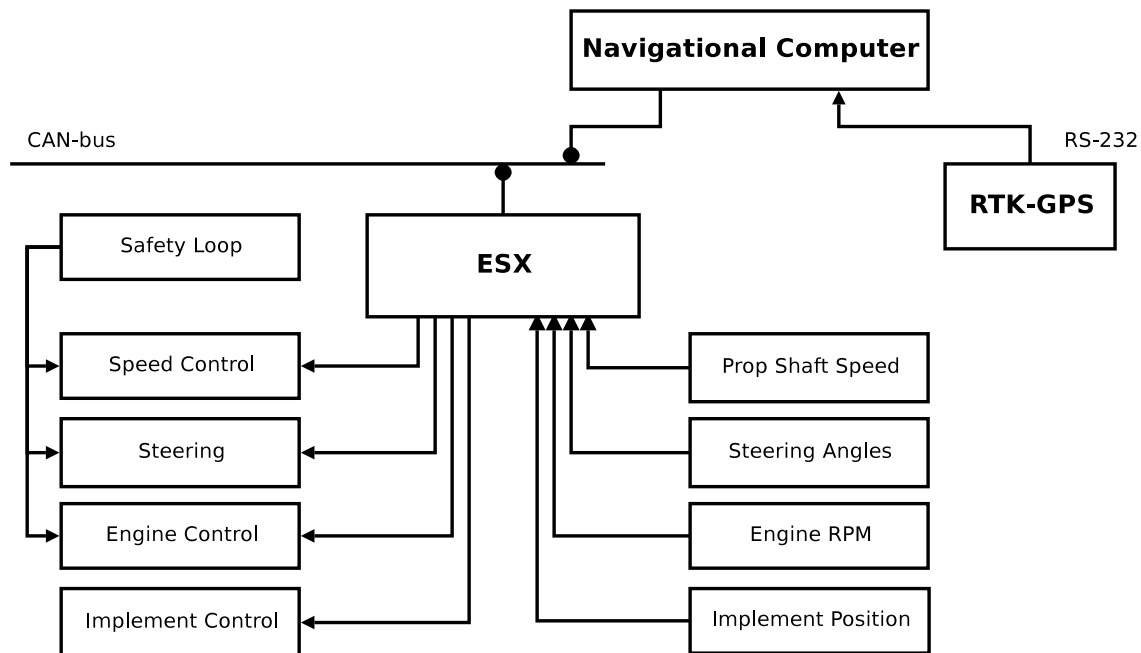


**Figure 2. Diagram of the tractor system and its connectivity.**

The GPS system is a Trimble AgGPS high precision RTK GPS receiver giving a centimetre level accuracy. This receiver can provide a much higher temporal resolution ( $20\text{Hz}$ ) as opposed to GPS receivers normally used in automotive navigation ( $1\text{Hz}$ ). This provides a very good basis for using the GPS measurement directly in a navigational control loop.

The navigational computer is an industrial PC motherboard with an Intel Celeron 400Mhz CPU and 512MB RAM. The storage is a 4GB solid-state compact flash card. The PC has a 16bit ISA PC/104 connector used to attach a CAN-bus controller and a multi-RS232/422/485 interface board. A Debian Linux system is installed on the PC with an Apache web server along with the LinCAN open-source CAN-bus driver. The computer is encased in a custom made aluminium case with an automotive power supply capable of operating off the tractors 12V power supply. The PC is connected to the ESX through CAN port and the GPS on a RS232 port. A client PC can connect to a graphical user interface on the web server on either of the Ethernet ports or through a wireless access point.

## AUTONOMOUS NAVIGATION SYSTEM

This section will present the practical solution to the autonomous navigation system for the tractor.

### System Architecture

The multi layer structure used in the implementation of the system serves primarily to lessen the complexity of each element. This creates independent modules that can be reused in other mobile robot systems, meaning that system specific code is kept to a minimum. The system is structured in five layers as shown in figure 3, on the bottom layer is the ESX hardware controller. This is connected to the next layer, the hardware server, through a CAN bus interface.

The hardware server is the entry level software in the navigation computer. This is responsible for communication to all external equipment, e.g. the GPS on a RS-232 port. The different software layers inside the PC communicate by using TCP socket connections through the system kernel. This is a simple method of sending data between applications that has proven very stable; it is fast and reliable enough for real-time communication.

The low-level mobile robot controller provides all necessary navigation features this also includes an extended Kalman filter for fusing sensor information.

A high-level mission controller has been placed on top of the low-level controller to provide mission overview and to instruct the low level controller as to how the mission should be executed.

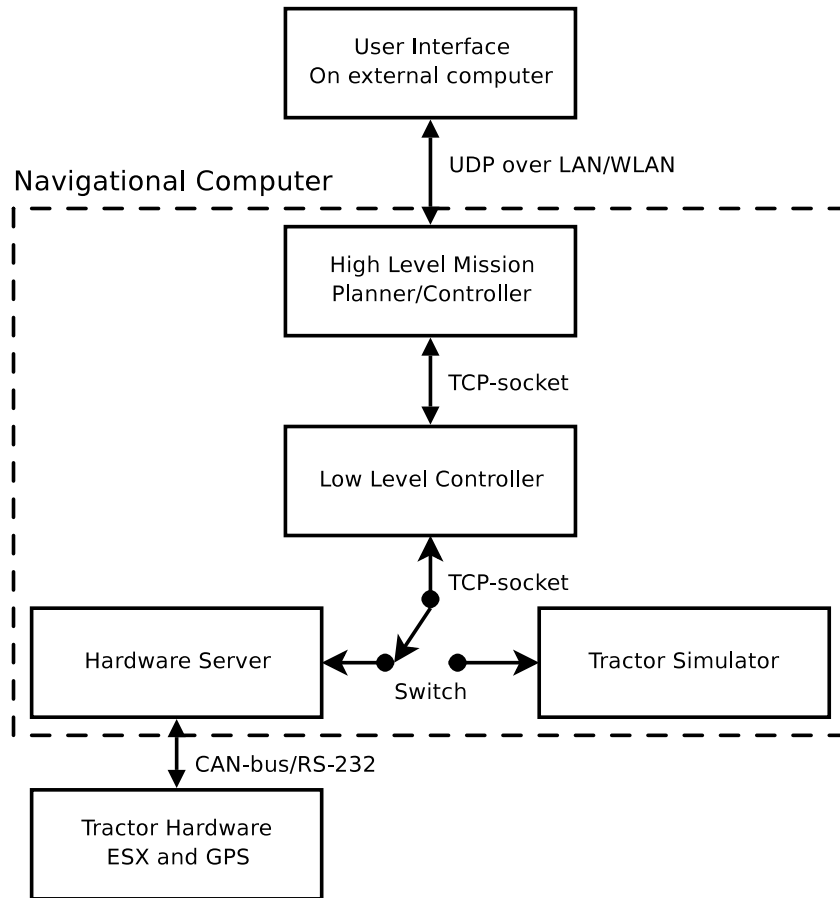


**Figure 3. Block diagram of the elements of the control system.**

The Graphical User Interface (GUI) is a detached part of the system. It is running on the user's computer. The GUI is communicating with the mission planner through datagrams (UDP) over any network connection capable of TCP/IP communication, e.g. wireless Ethernet (WiFi) or even mobile connections like GPRS or UMTS. The GUI is designed to work on a lossy connection and is running as a Java-applet inside the user's normal web browser.

#### Hardware Server

The purpose of the hardware server is to bridge communication between the physical hardware and the upper layers. This server is responsible for getting sensor values from the sensors attached on the physical ports. The data is then parsed and combined into messages according to a structured data protocol and is made available for the low level controller on request. This server is also responsible for maintaining the 100ms sample time assumed by the upper layers. This is done by delaying the acceptance of the next poll.

The program is running multi-threaded to make it possible for simultaneous data exchange between the hardware, the hardware server and the client. E.g. the GPS receiver streams the data, meaning that whenever data is available it is instantaneous transmitted over RS-232 connection to the hardware server. The consequence of this is that if nobody is listening, the data will be lost. Since this is not a wanted scenario a multi-threaded architecture is needed.

#### Low Level Control

The low level control software was originally created for a set of Small Mobil Robots (SMR) used in teaching exercises. The low level controller accepts mobile robot scripting language called SMR-CL as described in (Andersen et al., 2004).

The low-level control is considered low-level in a mobile robot perspective, since the controller is used to handle individual movements of the vehicle. It contains the necessary data management and is used for keeping track of the vehicles local and global position. The overall mission execution is handled on a higher level. The low level controller is only told how to navigate the next few steps and is unaware of anything beyond these few steps.

Some modifications were required in controlling the tractor instead of a SMR. The first addition is an interface library responsible for receiving the data from the hardware server. This is passed on to the low level control program to allow the usage of its functionality. The library provides a real time socket connection to the hardware server. The command interface to the low level controller executes the orders asynchronous as opposed to the real time control algorithms.

When dealing with mobile robots, a local sensor based odometry will always tend to drift. The odometry on the tractor is based upon measurement of the steering angle and movements of the drive shaft. This makes it virtually impossible to navigate precisely over an extended period of time. The GPS provides a measurement of the global position. Using these two sets of information any errors in the odometry can be corrected. The common way of fusing several sensors is by using a Kalman filter. An extended Kalman filter has been designed according to (Larsen, 1998) and adapted to the Ackerman steering principle. The odometric Kalman filter provides sensor fusion between the local odometry and the GPS to achieve a corrected and very precise absolute odometry.

The primary navigation feature used in the low-level controller is the virtual line-follower. This line-follower makes a mobile robot follow a virtual line defined by a point and an angle. The virtual line-follower function uses a weighed combination of distance and angle error for following the line. This gives the ability to navigate precisely between two GPS waypoints in a straight line.

### Multi Robot Simulator

The multi-robot simulator is designed to provide a realistic simulation of a number of different robots. This is used in offline testing and debugging of different control algorithms, software etc. Furthermore the simulator is designed to give the user a graphical representation of the robots' progress. The simulator has been engineered to provide a generic and easy-to-configure simulation environment. Practically this means that a robot in the simulator can have any kinematic design, sensor types, communication interface etc., as long as the robot's control program follows one simple rule: The control program must interface with its sensors and actuators through a socket interface. Besides this the control program can run on any computer, with any kind of operating system and can be written in any programming language.

That the control program uses a "sensor server" to connect to the sensors ensures that the interface to the control program is on a non-physical level. This means that the interface is on a level that easily can be controlled. The simulator simply replaces the hardware server's role in providing sensor data. By doing this, the control program will not notice the difference between the real world and the simulator. The control program is exactly the same when running the simulation and when running in the real world; and this is an important feature. This provides a powerful debugging tool, where not only algorithms but entire systems can be tested.

### High Level Control

The High-level mission controller is created in order to drive complex and dynamic missions, get mission overview and add the possibility to define a XML-based mission file. A mission consists of a number of way-points and a list of actions that should take place once at the point. This includes controlling the tools and different types of turn manoeuvres in order to get to the next way-point. Depending on the size of the headlands available, the type of turn can be chosen. The additional system, mission and sensor overview gives, as opposed to the lower layer controller, a better opportunity to build a higher level of intelligence and foresight. This serves as a link between the user's mission file and the control system.

The high level controller is structured primarily as a client that connects directly to the low-level controller. Communication is done by feeding SMR-CL commands and read relevant information such as sensor and odometry data.

**Program execution:** Once the high-level controller is started it connects to the low-level controller and initialises it to run in "tractor mode". Threads are spawned that are responsible for receiving commands from the GUI and sending data back. Data updates to the GUI are performed at one second intervals. Once the *start* command is received a specified XML file is opened and

the mission is parsed into an internal format. All missing information in the mission is calculated and filled in. The high-level controller implements an open-source XML parser called Expat for reading and extracting data from the XML-format. The Kalman filter is initialised in the way requested by the mission file. Finally the actual mission begins.

**Mission Execution:** The *internal* mission format derived from the XML mission file contains coordinates to all mission points including angle between points. Tasks at a given point are also specified, this includes turning, changing tool position or driving speed. Driving to a mission point is fairly simple using the low level controller's line following function.

When a way-point is reached, the tasks requested at the point are carried out. A turn action is executed as the last action before driving to the next point. The parameters required for the turn algorithms are automatically calculated using the data available. There are two turn types defined, the omega and the fishtail. Once the mission is completed a log file is saved and the system is reset allowing a new mission to be loaded.

**XML-format:** The XML mission file contains all the information for a mission. Giving the nature of the XML-data format further information can easily be added with no consequences for the existing programs (Fig. 4).

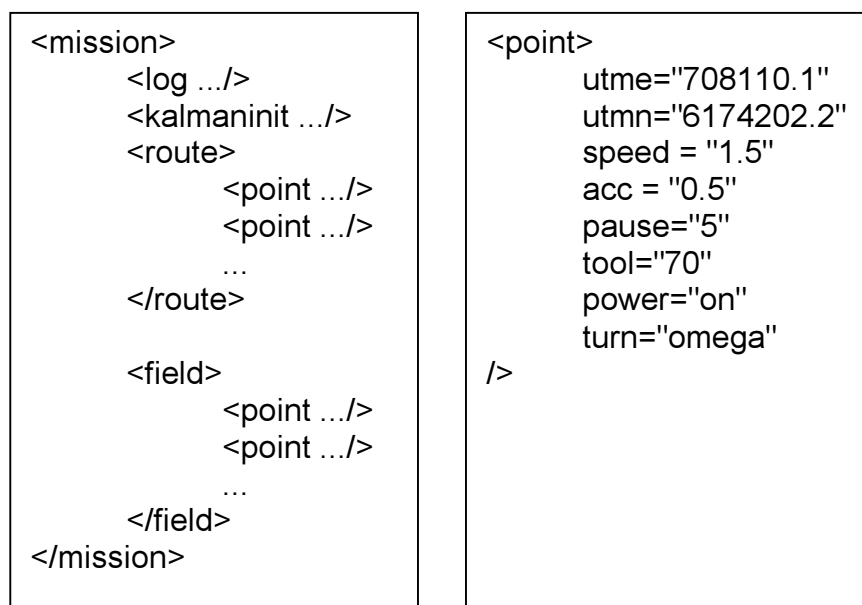


**Figure 4. Structure of the XML mission file and available attributes for the *point* tag.**

The first tags of the mission files concerns initialisation of the system before the actual mission. Such as the data that should be logged in this mission and how the Kalman filter should be initialised. The actual mission points are within the *route* tag and have a number of attributes. The attributes of each point contain the coordinates in UTM-GPS format along with speed and accelerations parameters which used in driving to the point. The rest of the attributes concern what action should be taken once at the wanted point. Most of these attributes are not mandatory to set; only changes in states must be defined.

This makes it possible to plan a mission with very few points and little information, e.g. only the start and stop points are needed for each crop row. This lightens the burden of mission planning for the users of the system.

The level of "intelligence" build into this application is limited to perform certain manoeuvres. The program has been designed to allow easy implantation of further features and intelligence without the need for restructuring. The ability to pause and resume a mission while running is a feature already implemented and can directly be used in case of emergency, obstacle avoidance or other events where deviation from the mission is required.

## USER INTERFACE

The user interface (UI) is designed to give the user a high level interface to the tractor system. Combined with XML mission files, the user can start, monitor and stop various tasks on the tractor. There were some requirements to the interface that had to be fulfilled. First, the UI had to be intuitive to use, the options that are used most frequently should have easy access. There are many considerations, both practical and psychological, that should be taken into account to make a user interface work well. The guidelines given in (Crow et al. 1998) have been used to a great extent in the design of the UI. To summarise the design guidelines, it concerns the limitation and grouping of data and decisions. Second, the UI has to be able to run on an external computer. It was decided to make the UI web based, which gives the possibility for any computer to connect to the system. The only requirement to the connecting computer is that it needs a web browser with a Java virtual machine installed. All modern PCs have a web browser and Java is a common plug-in to web browsers. This has the nice side effect that the UI is inherently cross-platform. One can even imagine that a PDA can be used to control the tractor, making the mobility even greater compared to e.g. a laptop. Furthermore, a web browser is a common tool for any computer user, which means that the user is already accustomed to working with part of the application.

The first thing the user will see when opening the application is a normal looking web page, which includes user guides and different simple mission planning tools. By clicking on a hyperlink the user is redirected to the UI.

The UI has primarily been designed to provide a nice overview of the tractor's current actions. This includes position, different sensor data and status of different subsystems. The reason why this much data is being shown is that the tractor primarily is a research vehicle, not a commercial product. As a research vehicle, "debugging" information is of high value. This means that a large amount of data have to be presented to the user, this is contrary to the original design principles. To combine these opposites, the information has to be present without affecting the ease of use. This problem has been solved, partly by grouping information rationally and partly by representing data in an intuitive graphical manner. An example of the graphic representation is the direction of the tractor which is presented as a blend of a compass and an arrow. This gives an excellent sense of the direction of the tractor (Fig. 5).



Figure 5. Screenshot of the User Interface during mission execution.

The main components of the UI are:

**Map** displays a number of things. The tractor's position, the driven path, the field and the mission. The driven path is represented in two different ways, the Kalman filter's position and the GPS position. The GPS path is a yellow line, while the Kalman position is drawn as a thicker red line. The colours of the map have been chosen to have sharp contrasts, to make it visible even in bright sunlight. The size and focus of the map automatically scales and moves, according to the mission and the driven path.

**Status bar** displays different information about the tractor's current state and status of the subsystems. This information is not crucial but nice to have, especially in a debugging situation.

**Bottom buttons** represents the possibilities the user have to influence the tractor system. The multifunction starting button that starts, pauses and resumes missions, a "load mission" button that requests a mission-file, a "save log" button that saves the current log to a local file, a "clear view" button that clears the driven path, a "reset" button that resets the mission and reconnects to the tractor and finally a "stop" button that terminates the lower level control systems.

This combined, gives a full system and mission overview, with the needed controls to start and stop missions.

## RESULTS

The primary way of testing this system, has been to first run a simulation of the desired mission, to locate bugs or logical errors, then to validate the result in the actual field.

To measure navigational performance of the system, the formalised cross track error has been utilised. The cross track error is defined as the perpendicular distance from the actual position of the vehicle to the desired path. Field measurements show that the tractor drives with a cross track error with a standard deviation of 5-8 cm, depending on the terrain, speed etc.

The intended use of the system, in an end product sense, is that the tractor is fully autonomous in operation. This means the tractor should be able to navigate to the field where a task needs to be done, complete the task and return home. To test this scenario a mission was defined, that would drive the tractor onto a field, cover the field in a sensible manner and return home to the farm. The results of this mission can be seen in figure 6. The results show that the system is able to navigate precisely even on an uneven stubble field. Further investigation shows that the controllers of the tractor are very stable in terms of control signals, e.g. the steering angle of the front wheels are held in more or less the same position when driving in a straight line. This gives the appearance of a tractor that runs "nice" and smooth.

Since completion of this project, the system has been in regular use as part of research projects on precision farming. Different users have utilised the system with satisfactory results, thus proving both the usability and stability of the system.

## CONCLUSION

A complete solution for an autonomous tractor has been implemented and tested. The end product is an easy-to-use autonomous tractor system that implements enhanced control by using high level missions. The system uses a multi-layer structure spanning from a hardware control server, over a low-level mobile robot controller, a high-level mission planner to a graphical user interface. The graphical user interface runs inside a user web browser allowing control and monitoring of the tractor. The GUI offers a one-click interface for starting and controlling the system. Missions are defined using an XML formatted file that can be uploaded to the tractor through the GUI to the tractor. The XML mission file contains structured information relevant for the mission, including special tasks such as controlling the mounted implement. The system has been designed to as usable as possible while maintaining room for extensions. To improve effectiveness of mobile robot development, including the development of the tractor, a test-bench has been created. The heterogeneous multi-robot simulator is capable of emulating the kinematics and electronics of a number of mobile robots in a simulated environment. The system has been tested and verified

through a number of different tests. Comparison between tests done in the simulator and in the field, show almost similar results. Thereby, validating the realism of the simulation.

Field tests show that the system is able to navigate with a high degree of accuracy and control. A complete control and simulation environment has been engineered and tested. Thereby, making the tractor system an easy-to-use and versatile research vehicle for autonomous use. The tractor is used on regular basis for agricultural research at the Royal Veterinary and Agricultural University's research farm.

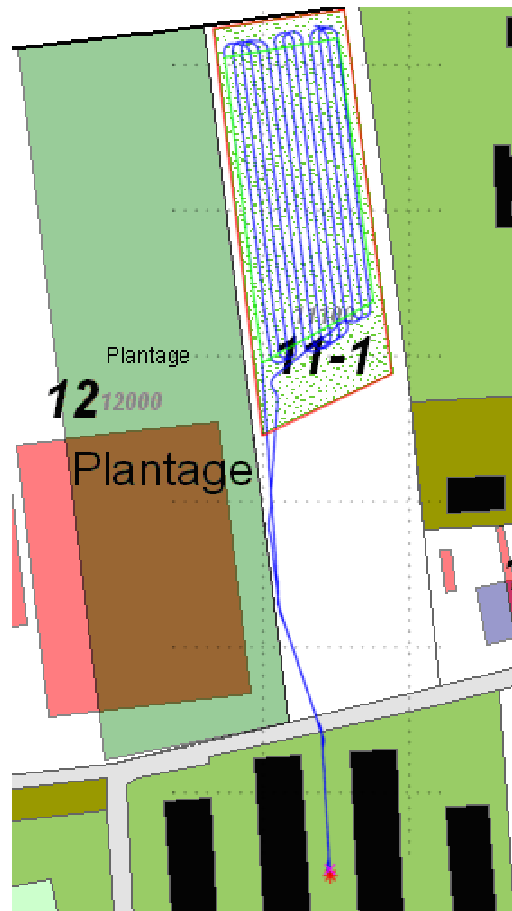


Figure 6. Plot of autonomous test, the tractor starts and ends in the court yard.

## REFERENCES

1. Andersen, N. A., and O. Ravn, 2004, SMR-CL: A Real-time Control Language for Mobile Robots. In *CIGR International conference*, Beijing.
2. Benson, E. R. and J.F. Reid. And Q. Zhang., 2001, *Machine Vision Based Steering System for Agricultural Combines*, ASAE Annual International Meeting 2001.
3. Blackmore, B. S. and Griepentrog, H. W. and Nielsen, H. and Nørremark, M. and Resting-Jeppesen, J., 2004, Development of a Deterministic Autonomous Tractor, The Royal Veterinary and Agricultural University (KVL), Dept. of Agricultural Sciences.
4. Crow, D. and B. J. Jansen, 1998, *The Graphical User Interface: An Introduction*, In Seminal works in computer human interaction. SIGCHI Bulletin, 1998.
5. Larsen, T. D., 1998, Optimal Fusion of Sensors, Department of Automation, Technical University of Denmark.
6. O'Connor, M and T. Bell and G. Elkaim and Dr. B. Parkinson, 1996, *Automatic Steering of Farm Vehicles Using GPS*, Stanford University.
7. Stentz, A. and D. Cristian and C. Wellington and H. Herman and D. Stager, 2002, A System for Semi-Autonomous Tractor Operations. In *Autonomous Robot*, 13(1):87\_103, July 2002.



# AUTONOMOUS NAVIGATION WITH A WEEDING ROBOT

T. Bakker<sup>1</sup>, K. van Asselt<sup>1</sup>, J. Bontsema<sup>2</sup>, J. Müller<sup>3</sup> and G. van Straten<sup>1</sup>

## ABSTRACT

A navigation system for a weeding robot has been designed to navigate autonomously in a field. The vehicle used for the experiments is a specially designed robotic platform for performing autonomous weed control. The platform is four-wheel steered and four-wheel driven. A diesel engine powers the wheels via a hydraulic transmission. The autonomous navigation system uses DGPS, a compass and a camera. The robot uses DGPS to determine in which part of the field it is located: on one of the headlands, or in the middle part of the field. In the middle part of the field it navigates along the rows using the machine vision system. The deviation of the robot is calculated from both the orientation error and the distance from the crop row in front of the robot as supplied by the vision system. When the robot arrives on one of the headlands, it starts to plan a route over the headland to a position in front of the next rows to be weeded. It then follows the planned route using both DGPS and the compass. The deviation is calculated by a specially designed orthogonal projection. The deviation is supplied to a high level controller that determines the set points of the wheel angles. At low level each wheel angle is controlled by a P controller combined with a Smith predictor. Results are presented of preliminary navigation tests in the field.

**KEYWORDS.** Automatic Guidance, Automatic Steering, GPS, Machine Vision, Robots, Robotic Weeding.

## INTRODUCTION

In organic farming there is a need for weeding robots that can replace manual weeding. The required labor for hand weeding is expensive and often difficult to obtain. In 1998 in the Netherlands on average 73 hours hand weeding were spend on one hectare of sugar beet.

In this paper a navigation system for a weeding robot is presented enabling the robot to navigate autonomously over a whole field.

## ROBOTIC PLATFORM

### Platform

The vehicle used for the experiments is a specially designed robotic platform for performing autonomous weed control (Fig. 1). The design of the platform was described earlier by Bakker et al. (2005). The platform is four-wheel steered and four-wheel driven. There is no constraint on the maximum turning angle of a wheel around its vertical axis. Power is provided by a diesel engine that powers the wheels via a hydraulic transmission. The hydraulic transmission consists of a pump supplying oil to eight proportional valves, each connected to one fixed displacement hydraulic motor. Four hydraulic motors are used to drive the wheels, the other four to steer the wheels. The pump/valves combination is a 'load sensing' system: the displacement of the pump is controlled by the maximum oil pressure needed in the system. Computer control of the valves is achieved using pulse width modulation via two micro-controllers connected to a CAN bus.

---

<sup>1</sup> Wageningen University, Systems and Control Group, P.O. Box 17, 6700 AA Wageningen, The Netherlands, [tijmen.bakker@wur.nl](mailto:tijmen.bakker@wur.nl)

<sup>2</sup> Plant Research International BV, P.O. Box 17, 6700 AA Wageningen, The Netherlands

<sup>3</sup> Wageningen University, Farm Technology Group, P.O. Box 17, 6700 AA Wageningen, The Netherlands. Currently working at Institute of Agricultural Engineering, University of Hohenheim, Germany



**Figure 1. The robotic platform in a sugar beet field.**

### Electronics

The weeding robot electronics consists of 7 embedded controllers connected by a CAN bus using the ISO 11783 protocol. In the inside of every wheel rim a cogwheel is mounted for wheel speed measurement. The two magneto resistive sensors per cogwheel are placed in such a way that the direction of rotation can be resolved. The rotation of the wheels is measured by these sensors with a resolution of 100 pulses per wheel revolution. The wheel angle of each wheel is measured by a Kverneland 180 degree sensor with an accuracy of one degree. Per wheel a micro controller is mounted transmitting wheel speed and wheel angles via the CAN bus.

A Basler 301fc color camera with a resolution of 640 x 480 pixels is used to acquire the images needed for row detection. The camera is mounted at 1.11 meters above the ground looking forward and down at an angle of 37 degrees to the vertical. A laptop computer connected to the CAN bus processes the images of the camera connected via fire wire. The Omnistar HP GPS receiver is able to detect the position of the robot with a specified accuracy of 10 cm. The GPS antenna is mounted on a metal plate to prevent multipath errors. An Xsens MTi sensor integrating a magnetometer, 3 gyros and 3 accelerometers is used to measure the vehicle orientation.

One embedded controller running a real time operating system (National Instruments PXI system) also connected to the CAN bus does the vehicle control. The GPS receiver, the Xsens MTi sensor and a radio modem are connected with the PXI via RS232. The radio modem interfaces the remote control used for manual control of the weeding robot. The manual control is used for guaranteeing safety during field trials and for transportation to and from the field. The PXI system gathers wheel angles, wheel speeds, crop row location data, GPS data and remote control data and controls the vehicle by sending messages to the two micro controllers connected to the hydraulic valves.

## NAVIGATION METHODS

### Field description

Before navigating over the field first the boundaries of the headlands and the boundary of the main field area are established. In an initial trial the polygons of the two headlands and the main field area were build from eight coordinates set manually (Fig. 2).

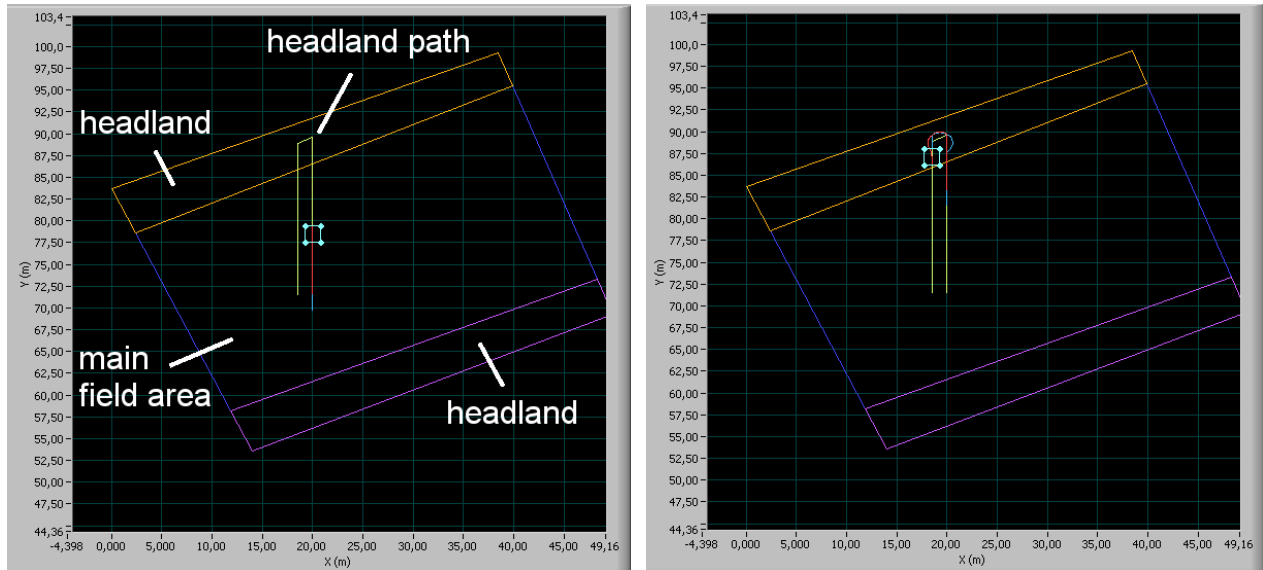


**Figure 2. The polygons indicate the headlands and the main field area. Also the headland path determined from the current robot location is visible. In the right figure the robot follows the headland path in simulation.**

### Point in polygon algorithm

During driving over the field, the robot constantly determines if it is located in one of the polygons using a point in polygon algorithm (Burrough and MacDonnell, 1998). To check if a point is located inside a polygon, a line is extended from the point. If the number of intersections of this line with the polygon envelope (in either direction) is odd, the point is inside the polygon.

The point in polygon software constantly informs the vehicle control software in which of the polygons the robot is located, so this knowledge is used both for security and navigation. Any time the robot is not in the main field area polygon and not in one of the headland polygons, the robot is outside the field and is stopped immediately.

### Crop relative navigation

For navigating along the row, machine vision is used to detect the position of the crop rows relative to the robot. The machine vision algorithm was developed and tested on a sugar beet field prepared in a greenhouse (Bakker et al, 2004). Three complete rows are visible in the image. The first step in the row recognition algorithm, is transforming the RGB image to a grey scale image with enhanced contrast between green plants and soil background. The next step is to correct the images for perspective by an inverse perspective transformation. In the resulting corrected image three rectangular sections of crop row spacing are selected. The first section is selected in the middle of the image. The other two are selected on both sides of the first section. The sections are combined by summing up the grey values of the sections to a combined image. To the resulting combined image grey scale Hough transform is applied. Pixels with a pixel value equal to zero are not processed by the Hough transform. The output of the algorithm is the position of the platform with respect to the crop rows expressed in an offset ( $\epsilon_{\delta}$ ) and an orientation error ( $\epsilon_{\theta}$ ).

Because the camera is mounted at the robot at 1.11 meters from the ground instead of 1.74 meters from the ground in the greenhouse trial, another lens was used to keep the three rows in view of the camera. The area covered by one image was 2.4 meters long in row direction and 1.6 meters wide at the side closest to the camera. The new lens lead to much more lens distortion, which had to be corrected by a non-linear inverse perspective transformation. The build-in function available

in Labview needed about 4.5 seconds per image to perform the inverse non-linear perspective transformation, which is too slow to use for navigation in real-time. Therefore a software routine was written to calculate the pixel displacement by the Labview non-linear perspective transformation for each pixel at the current camera setup. The pixel displacements were stored in a table and while navigating along the rows, each pixel of the incoming images is displaced accordingly.

The time needed to process one image by the algorithm depends on the amount of weed. The image processing time per image needed for the algorithm including the pixel displacement correction, was measured running on a 1.86 GHz laptop using the same image series as in the greenhouse trial. The measured processing time per image was reduced from a range of 0.5 to 1.4 seconds per image (greenhouse trial) to a range of 0.1 to 0.4 seconds per image.

### Navigation on the headland

While driving along the rows in the main field area the robot measures continually its position and orientation and by that its distance to the headland. If the distance of the robot to the headland is less than 3 meters, the robot plans a path to the start of the next row to be followed.

The path consists of three vectors. The first vector is the vector indicating the robot position and its orientation, extended to a length so that it crosses the main field/headland boundary by a distance of 2 meters. The third vector is a vector parallel to the first one at an offset of plus or minus the working width, in this case 1.5 meters. This vector is also extended to a length so that it crosses the headland boundary by a distance of 2 meters. The second vector connects the ends of the first and the third vector.

After the robot has planned the headland path, it starts to follow the path immediately until the robot arrives in the middle part of the field again. Then it switches to crop row following again.

The whole navigation is performed autonomously. The only information needed before navigating over the field are the field and headland boundaries and the turning direction of the robot on the first headland to arrive at. If the robot is brought to the field the user indicates the first turning direction so that the sign of the offset of the third headland path vector to the first headland path vector is known. For the other headland the turning direction is opposite to the first one.

## **VEHICLE CONTROL**

### High level control

The vehicle control consists of two levels. At high level the wheel angle set points and wheel speed set points are determined in order to decrease the deviation from the path and the error in orientation. At low level, controllers are used to realize the wheel angles and wheel speeds determined by the high level control.

The deviation and the orientation error of the robot from a path are determined in two ways. In case of navigation by camera the orientation error and the distance from the crop row in front of the vehicle are supplied by the vision system. In case of navigating along a line of positions (x, y) when driving along the headland path, the deviation and orientation error are calculated by a specially designed orthogonal projection on the path using the measured orientation and the GPS position.

Imagine a virtual front wheel positioned on the robot frame exactly in between the two real front wheels and a virtual rear wheel positioned exactly in between the real rear wheels. From the deviation and the orientation error both the deviation of the virtual front wheel and the deviation of the virtual rear wheel from the path can be determined.

In case of crop row following, the high level controller minimizes the deviation of the virtual front wheel by a PI controller, while the rear wheel angle set point is set to zero (front-wheel steering). In case of headland path following both the deviation of the virtual front wheel and the deviation of a rear wheel are controlled by PI controllers. The PI controllers determine the set points for the wheel angles of a virtual front wheel and a virtual rear wheel. From these set points and a speed set point the angle and speed set points of all the four wheels are calculated using a kinematic

model. The vehicle model used is derived from earlier work from Campion et al. (1996) and Bendtsen et al. (2002).

#### Low level control

At low level for each wheel the wheel angle and wheel speed are controlled. The hydraulic valves used for steering the wheels of the weeding robot have a certain reaction time, resulting in a time delay of the steering. Furthermore, if a valve has an open time of less than a dead time, a control does not have any effect. So the wheel angle process can be represented by:

$$\dot{\beta} = 0 \quad \text{for } t_{open} < t_{dead}$$

$$\dot{\beta} = Kp \cdot u(t - t_d) \quad \text{for } t_{open} > t_{dead}$$

and:

$$u(t) = U - 4495 \quad \text{if } 2500 < U < 4000$$

$$u(t) = 0 \quad \text{if } 4000 < U < 6000$$

$$u(t) = U - 5405 \quad \text{if } 6000 < U < 7500$$

Where:

$\dot{\beta}$  is wheel angle steering speed [°/s].

$Kp$  is the gain of the process and equals 0.0712.

$u$  is the control corrected for the dead band.

$U$  is the control [% $U_{DC}$ ·100].

$U_{DC}$  is the power supply voltage and equals about 12 [V].

$t_d$  is the delay of the system and equals 0.25 [s].

$t_{open}$  is the total time where  $U < 4000$  or the total time where  $U > 6000$ .

$t_{dead}$  is the dead zone of the system and equals 0.15 [s].

$K_p$  is determined from step responses of the system. To compensate for the time delay a P controller with Smith predictor is used for the wheel steering control (Stephanopoulos, 1984). The average error of a series of 96 measurements on a set point change of 10 degrees decreased within one second to zero plus or minus 2 degrees (Fig. 3).

The wheel speeds are controlled by PI controllers.

## **RESULTS FROM FIELD TRIALS**

### Path following on the headland

A field trial was carried out on a field with no crop rows, but with field boundary and headlands defined. In the middle part of the field where normally the crop rows are, deviation of the crop rows was set to zero, causing the robot to drive straight in this part. The algorithm was first tested in simulation (Fig. 2b). Both in simulation and on the real field, the robot was planning a headland path successfully. Also the robot was able to follow the headland path. However, until now the accuracy of path following, especially the accuracy of the orientation, was clearly not good enough to function well in a real field. This was mainly caused by limited accuracy of the compass output. In a stationary test in which the robot was turned 90 degrees according to the compass the real orientation change was about 85 degrees.

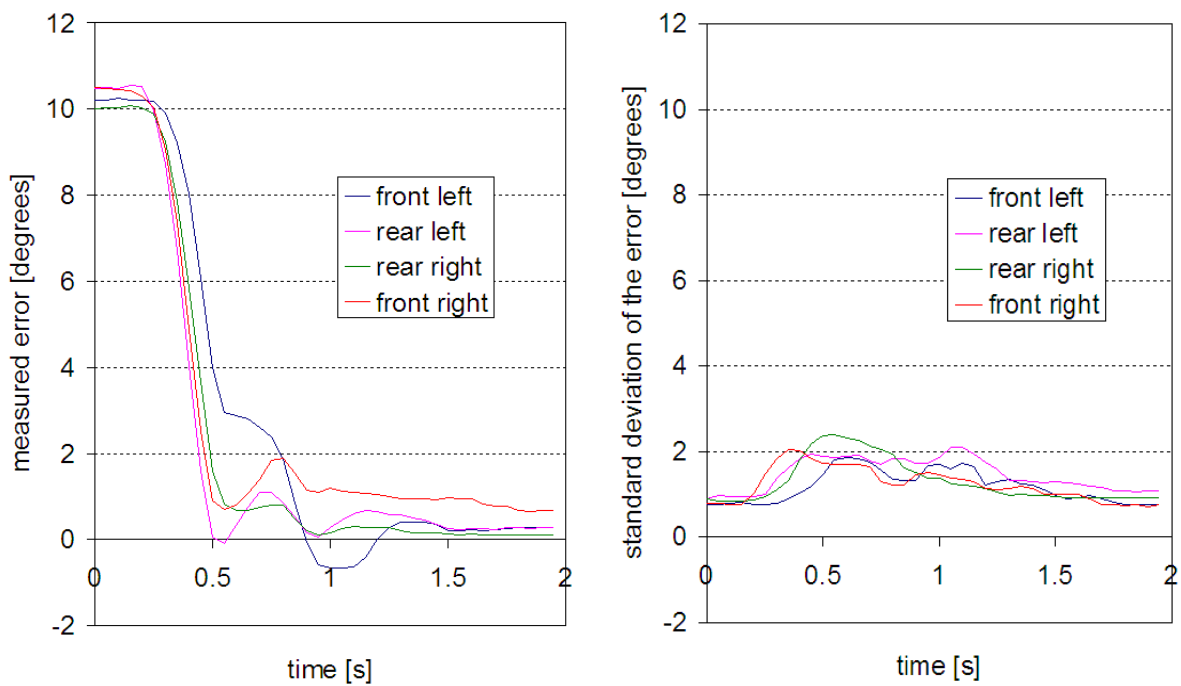


**Figure 3. Wheel angle error after a set point change of 10 degrees at  $t = 0$  (left). The standard deviation is plot in the right figure.**

### Crop row following

In a sugar beet field the crop row following was tested. In two trials the weeding robot followed the crop rows successfully over distance of about 9 m. The deviation from the crop rows increased over the distance and the weeding robot did not stay within two crop rows in the end. A pin was attached making a track within the crop rows (Fig. 4).



**Figure 4. Measuring the accuracy of crop row following.**

After the trials a cord was placed along the crop rows and pulled tight. The deviation of the track from the cord was measured at regular intervals of about 0.5 meters in the row direction. The results are visualized in figure 5. As the figure shows instable behavior, it is obvious that more work is needed.

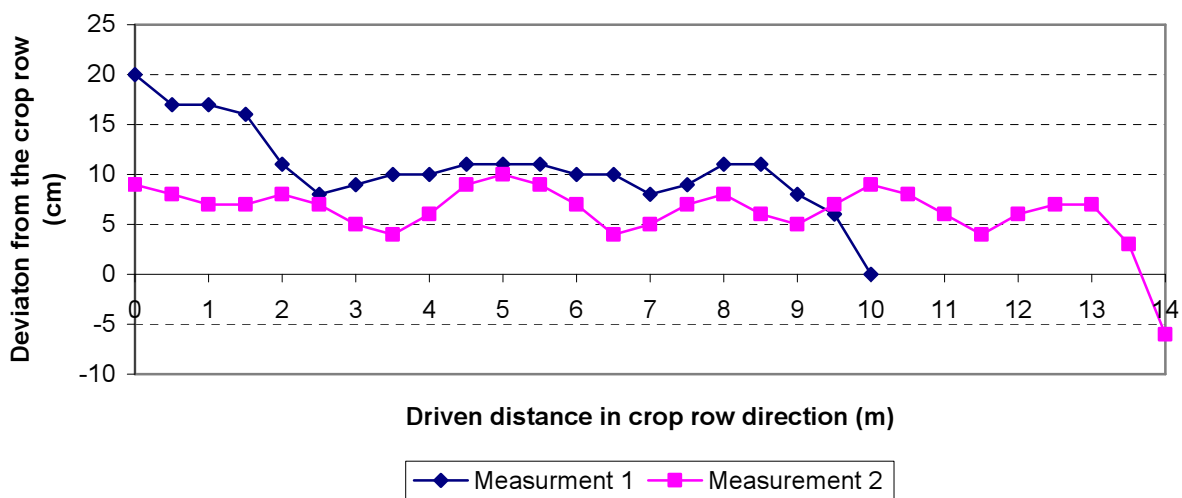


Figure 5. Deviation of the robot from the crop row.

## CONCLUSION

Determining if the robot is inside the field by the applied point in polygon algorithm on the field boundary is a robust method for safety, preventing the robot from leaving the field. Separating a field into polygons of the headlands and the main field area and application of a point in polygon algorithm is a robust method for headland detection. Online path planning of a headland path to be followed works successfully. While the robot was able to follow the headland path, the accuracy of the orientation of the robot during path following needs to be increased. With the current instrumentation and controller settings the robot is able to navigate along the crop rows over a limited distance. The increasing deviation from the crop rows indicates that the high level controller must be improved. Currently simulation studies are performed with a new high level controller.

## REFERENCES

1. Bakker, T., H. Wouters, C.J. van Asselt, J. Bontsema, J. Müller, G. van Straten and L. Tang. 2004. A vision based row detection system for sugar beet. In *Computer-Bildanalyse in der Landwirtschaft. Workshop 2004. Bornimer Agrartechnische Berichte. Heft 37.*, 42-55. Potsdam-Bornim / Braunschweig.
2. Bakker, T., H. Wouters, C.J. van Asselt, J. Bontsema, J. Müller and G. van Straten. 2005. An autonomous weeding robot for organic farming. In *Preprints of the International Conference on Field and Service Robotics.*, 580-591. Port Douglas, Australia.
3. Bendtsen, J.D., P. Andersen and S. Pedersen. 2002. Robust feedback-linearisation-based control design for a wheeled mobile robot; Hiroshima, Japan 9-13 September: 6th International Symposium on Advanced Vehicle Control (AVEC '02).
4. Burrough, P.A. and MacDonnell, R.A. 1998. Principles of Geographical Information systems. Oxford: Oxford University Press.
5. Campion, G., G. Bastin and B. D'Andréa-Novel. 1996. Structural properties and classification of kinematic and dynamic models of wheeled mobile robots. *IEEE Transactions on Robotics and Automation*, 12(1): 47-62.
6. Stephanopoulos, G. 1984. Chemical process control: An introduction to theory and practice. London: Prentice-Hall International.



# DEVELOPMENT OF AN AUTONOMOUS NAVIGATION SYSTEM USING 2-DIMENSIONAL LASER SCANNER IN AN ORCHARD REAL-TIME APPLICATION

O. C. Barawid Jr.<sup>1</sup>, A. Mizushima<sup>2</sup>, K. Ishii<sup>1</sup> and N. Noguchi<sup>1</sup>

## ABSTRACT

The objective of this study is to develop an automatic guidance system for autonomous vehicle that can navigate between row crops, such as in an orchard, in real time application. The study focused solely on straight line recognition of the tree rows using a laser scanner instead of global positioning system as a navigation sensor. Hough transform was used as the algorithm to recognize the tree rows as straight line. Auto-regression method eliminated the white Gaussian noise in the laser scanner data. Calibration method was used to get the offset position of the laser scanner to correct the heading and lateral error evaluation. An appropriate speed for tractor was also determined. The entire program for this research was written using C++ programming. By obtaining the minimum 0.11 m lateral and 1.50 degrees heading mean errors, it was possible to navigate the robot tractor autonomously between the orchard tree rows.

**KEYWORDS.** 2-D Laser Scanner, Auto-regression, Hough Transform, Orchard, Robot Tractor.

## INTRODUCTION

The application of the autonomous navigation in an orchard is an ideal task because the same operations are just being repeatedly performed over the years. Usually in an orchard autonomous navigation, path planning is one of the most important tasks. The autonomous vehicle needs a path navigation to follow to perform its task. Most of the developed research about path planning navigation in an orchard is a map based application wherein the autonomous vehicle can only be used in a specific orchard site.

Applying autonomous navigation in a map-based application requires path planning first before the vehicle can perform its task. Path planning basically refers to map generation where a thorough survey of the orchard is the utmost priority. In a map-based application, the surveyed area is the only place where the tractor can be used. Another map needs to be provided for the next area and so on. This task of surveying and map generation will prove to be time consuming for the farmer or the owner of the orchard. Commonly used navigation sensors include real-time kinematic global positioning system (RTK-GPS), laser radar, an inertial sensor unit, a laser scanner, a geomagnetic direction sensor, a posture sensor and a CCD camera.

The four methods applied in this research were tree rows detection algorithm method, laser scanner calibration method, noise removal using auto-regression (AR) method, and determination of the appropriate speed of the robot tractor that has the minimum guidance error. Tree rows detection algorithm extracted straight lines out from the orchard crop rows image. Auto regression eliminated the Gaussian noise present in lateral error and heading error. Calibration method determined the equipped position and angle of the laser scanner. And appropriate speed for autonomous navigation was determined by conducting different autonomous field runs in various speeds.

---

<sup>1</sup> Vehicle Robotics Laboratory, Bio-production Engineering, Graduate School of Agriculture, Hokkaido University, Kita 9, Nishi 9, Kita Ku, Sapporo, Japan, oscar@bpe.agr.hokudai.ac.jp

<sup>2</sup> Deere & Company, Moline, Illinois 61265, USA.

## SYSTEM COMPONENTS

This research used a 56-kW standard tractor, which was modified into a robot tractor. The robot tractor controlled steering, transmission (forward, neutral and backward), power take-off (PTO), engine speed, brake system and three-point hitches (up and down). The navigation sensor was a 2-dimensional laser scanner which was mounted on the front of the robot tractor. The laser scanner can detect a maximum distance and angle of the surrounding environment of 80 m and 180 degrees, respectively. The laser range has two adjustable modes of 8 m and 80 m and has an average error of 35 mm and 5 cm, respectively. The angle resolution has 3 adjustable modes of 0.25, 0.5, and 1 degree and has a response time of 53 ms, 26 ms, and 13 ms, respectively. The distance range of the laser scanner was set to 80 m mode. The angle range was set to 1 degree mode and response time was set to 13 ms mode. The distance error of the laser scanner is +/- 5 cm. For the calibration of the laser scanner mounted on the front of the robot tractor, RTK-GPS was used as the positioning sensor with an accuracy of +/- 2 cm, a fiber optical gyroscope (FOG) was used as the heading sensor with a heading accuracy of +/- 0.05 degree/hour and a total station was used which is a transit (surveying instrument) to get the relative position of the perpendicular wall (x, y and z axes) with an accuracy of +/- 3 mm for fine mode and +/- 10 mm for course mode. The total station was set to fine mode setting. The RTK-GPS and FOG were connected to the laptop PC with RS-232 cable.

## METHODS

### Orchard rows detection algorithm

The Hough transform used in this research as orchard row detection algorithm. The main advantage of using Hough transform compared to commonly used method like least squared error method of fitting lines to image data, is that even if group points varies to some extent, asking for a straight line is possible.

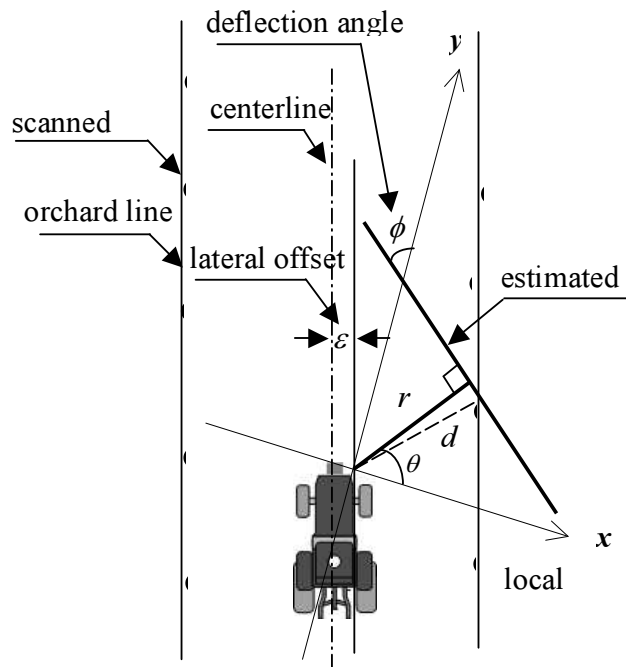


**Figure 1. An outline on how to recognize the orchard rows using Hough transform as algorithm.**

Hough transform extracted a straight line in an orchard rows from the data obtained by the laser scanner in a real time circumference environment. The shortest distance ( $r$ ) can be calculated in equation (1).

$$r_{i,j} = d_i \cos(\phi_j - \theta_i) \quad (0 \leq i \leq 180, 0 \leq j \leq 180) \quad (1)$$

Figure 2 shows the actual captured points of the laser scanner. The black line in the middle of the orchard was recognized as the main target course of the robot tractor. It served as the lateral offset for the robot tractor navigation to follow. In plotting these captured points into sine wave  $r-\theta$

space shown in figure 3, a cluster of intersections of sinusoids can be seen. The majority of intersection of these sinusoids which estimated the equation of the line would become the orchard row lines. These points of majority intersections were served as the solution for recognizing the orchard rows.

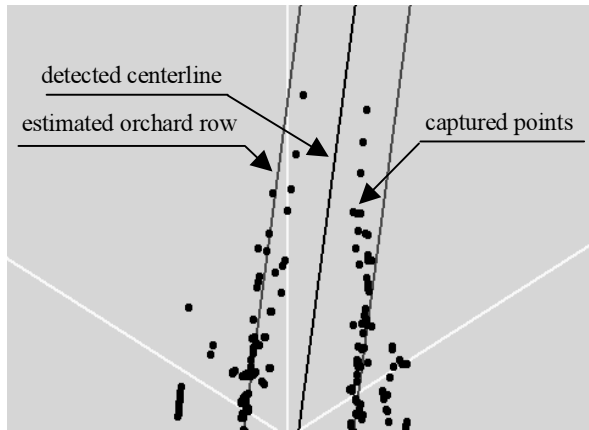


Figure 2. Actual captured points by the laser scanner in a computer window of the orchard tree rows.

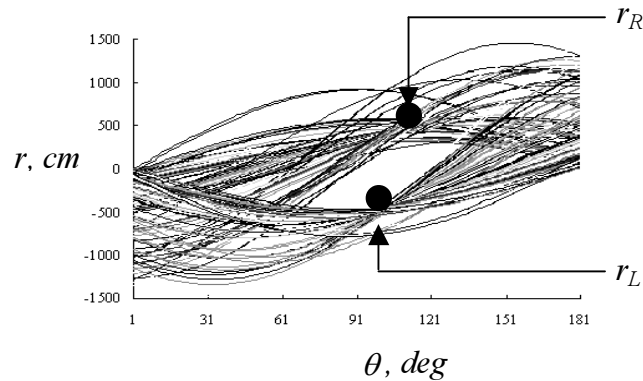


Figure 3. Illustration of the captured points of the laser scanner transform to sinusoids in r- space.

#### Calibration method of the mounted sensor

It is necessary to evaluate the exact attachment position of the laser scanner because it will affect the accuracy evaluation of the robot tractor such as the lateral error and heading error outputs. The values of the offset position of the laser scanner were  $a = - 0.056$  m,  $b = 2.57$  m and  $\delta = 2.8$  deg from the northing UTM coordinates. Figure 4 shows the outline for calibrating the laser scanner.

#### Noise removal and time series analysis using an auto-regression (AR) method

The results obtained in the Hough transform have a noise data. The noise data is contained in the lateral offset and heading error. In order to get the minimum error in lateral and heading error, noise removal method using linear time series general auto-regression (AR) analysis was used to refine the output data which does not have a time delay. Defining the general auto-regressive model of order  $k$ , denoted AR( $k$ ) as

$$\varepsilon_t = x_t + a_1x_{t-1} + \dots + a_kx_{t-k}, \quad t = k + 1, \dots, n, \quad (2)$$

The problem in auto-regression analysis (Bourke et al., 1998) is to derive the best values for  $a_1, \dots, a_k$  or the auto-regressive coefficients given a series  $x_t$ . The majority of methods assume the series  $x_t$  is linear and stationary. The case of conditional maximum likelihood estimates of the parameters (Priestley et al., 1981) is identical with the least square estimates. Thus, solving for the values of auto-regressive coefficients ( $a_1, \dots, a_k$ ) in matrix form

$$\mathbf{a}_p = \mathbf{R}_k^{-1} \mathbf{A}_k \quad (3)$$

There is no straightforward way to determine the correct model order. An order just after the point at which the RMS error flattens out is usually an appropriate order (Bourke et al., 1998). But there is a formal technique for AR model order determination. The more refined version of "residual variance plot" is the Akaike's final prediction error ( $F_{pe(k)}$ ). This method starts by fitting AR models of increasing order,  $k$ , and for each  $k$  one computes the expression,

$$F_{pe(k)} = \frac{n+k}{n-k} \sigma_\varepsilon^2 \quad (4)$$

Solving for  $\sigma_\varepsilon^2$  in equation (5);

$$\sigma_\varepsilon^2 = R(0) + a_1 R(1) + \dots + a_k R(k) \quad (5)$$

Plotting  $F_{pe(k)}$  values against  $k$  shows the value of the final prediction error for increasing numbers of order of the model ( $k$ ). The value of  $k$  obtained the minimum value was four as the appropriate order of the model or auto-regression (AR4).

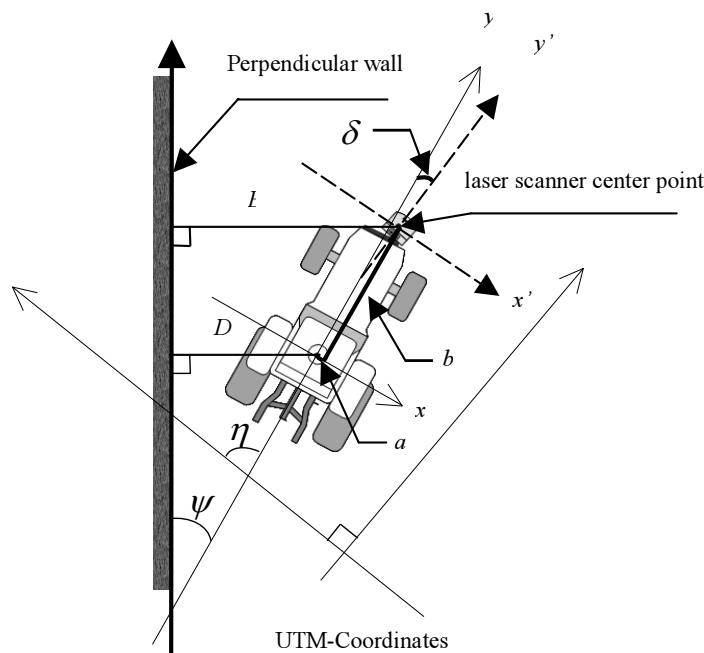


**Figure 4. Calibration method outline using a perpendicular wall as the reference line for getting the laser scanner exact position.**

#### Determination of the appropriate speed of the robot tractor

Determination of the appropriate speed is one of the important tasks to do in real-time application of autonomous vehicle. The aim of determining the appropriate speed of the robot tractor is to get the minimum guidance error. The tractor speed in autonomous navigation will affect the accuracy of the robot tractor's performance such as increase in heading error and lateral error. Six different runs were conducted at 0.36 m/s, 0.48 m/s, 0.62 m/s, 0.86 m/s, 1.23 m/s and 1.43 m/s. The appropriate speed for the autonomous navigation was determined as 0.36 m/s.

## **RESULTS AND DISCUSSION**

#### Evaluating the accuracy of the autonomous run

The developed automatic navigation system was tested in the Hokkaido University, Sapporo, Japan. Since the test area was not an actual orchard, there were some parts in the experiment site

where trees were sparse. Hence, irregularities in the form of gaps between trees were given due considerations in the study. Different test runs were made all throughout the whole expanse of the area notwithstanding the presence of some gaps between the trees. Single course run was referred to as the complete run. The test runs conducted on the area that best resembles an orchard due to the uniformity and alignment of trees was called the specified run. The Gaussian noise was eliminated using the AR analysis with a correct model order of four or AR4. The result of the specified run yielded 0.11 m and 1.5 deg for lateral and heading mean errors, respectively. Figure 5 shows the graphic representation of the evaluated autonomous accuracy.

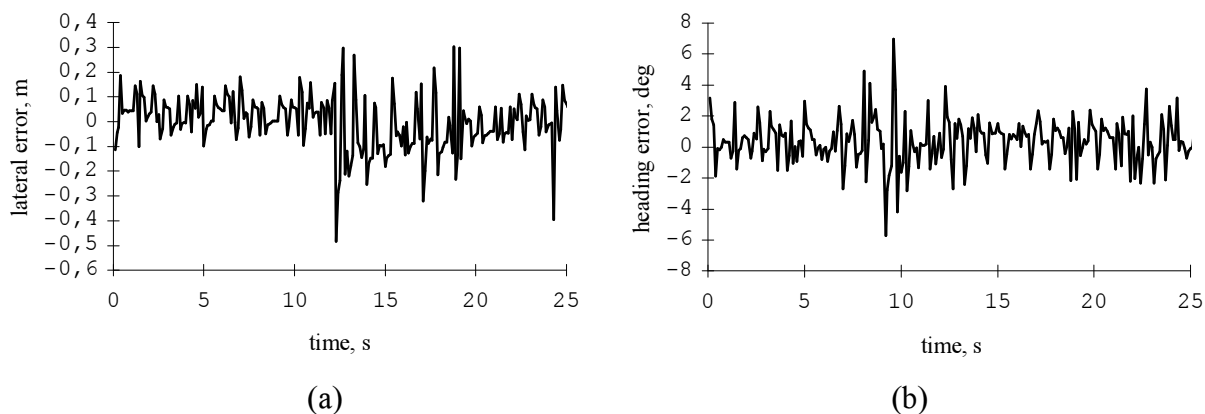


**Figure 5. (a) Evaluated accuracy in lateral error of the autonomous run with a root mean square error of 0.11 m; (b) Evaluated accuracy in heading error of the autonomous run with a root mean square error of 1.5 degrees.**

#### Evaluating the accuracy in various speeds

Autonomous runs in various speeds were conducted and evaluated to know the most appropriate speed needed in this research. The run which yielded the least guidance error was considered the most appropriate speed. Each run calculated the lateral and heading mean errors from actual data to the AR4 application. Table 1 shows the summary of the lateral and heading mean errors of actual data (AR4) in specified run with respect to the various speed runs. In the tables, 0.36 m/s run have the minimum lateral and mean error. This speed was enough and appropriate to navigate the robot tractor between the orchard rows because resulting errors were relatively small and it was the speed used in the evaluation of the autonomous accuracy of this research.

**Table 1. Summary of the root mean square (RMS) errors of lateral and heading mean errors of different speed in specified run.**

Speed, m/s	Auto-regression (AR4) in specified run	
	Lateral error, m	Heading error, deg
0.36	0.11	1.5
0.48	0.14	3.3
0.62	0.19	3.4
0.86	0.36	3.3
1.23	0.21	5.3
1.43	0.36	4.9

### CONCLUSION

This research developed an autonomous navigation system that can be used in a real-time application such as orchard navigation without using GPS. A 2-dimensional laser scanner was used as the navigation sensor to recognize the orchard rows. A calibration method determined the relative position of the laser scanner served as the offset values which in turn were used to get the accuracy of the autonomous navigation of the robot tractor by correcting the lateral and heading mean error outputs. The AR method was used to eliminate Gaussian noise and obtained the

minimum lateral and heading mean error. A total station measured the relative position of the perpendicular wall that was used in the calibration method. FOG measured the heading angle. Conditional maximum likelihood estimates calculated the auto-regression coefficients that were necessary for getting the estimated minimum mean error in auto-regression analysis. An Akaike information criterion (AIC) obtained the correct model order for getting the estimated minimum mean error in the auto-regression analysis. As a result, the evaluated autonomous accuracy was 0.11 m and 1.5 deg in the lateral and in the heading mean error, respectively. To ensure that the evaluated accuracy was adequate enough for the autonomous navigation, a comparison of the stationary and moving data mean error was made. The stationary data or normal Gaussian noise has a heading and lateral mean error of 0.5 deg and 0.05 m, respectively. The results in moving data mean error was sufficient for autonomous navigation in a real-time application.

In this research, the appropriate speed was determined as 0.36 m/s. This speed has the minimum mean error compared to the other test runs' speed.

## REFERENCES

1. Burks, T.F., V. Subramanian, and S. Singh. 2004. Autonomous greenhouse sprayer vehicle using machine vision and ladar for steering control. In Proc. Automation Technology for Off-Road Equipment Conf., 79-90.
2. Erbach D.C., C. H. Choi, and K. Noh. 199. Automated guidance for agricultural tractors. In Proc. ASAE Symposium on Automated Agriculture for the 21st Century. Chicago, 182-191.
3. Gonzales R. C., and R. E. Woods. 1993. Digital Image Processing. USA, Addison-Wesley Publishing.
4. Guo L. S., and Q. Zhang. 2004. A low-cost navigation system for autonomous off-road vehicles. In Proc. Automation Technology for Off-Road Equipment Conf, 107-119.
5. Hakura J., and A. Yoshikazu. 2001. Self-localization based on ego motion detection using optic flow. In Proc. Fourth IFAC Symposium on Intelligent Autonomous Vehicle, 320-331.
6. Kendall S. M., and J. K. Ord. 1990. Time Series. Great Britain, British Library Cataloguing in Publication Data.
7. Kise M., N. Noguchi, K. Ishii, and H. Terao. 2001. Development of the agricultural autonomous tractor with an RTK-GPS and FOG. In Proc. Fourth IFAC Symposium on Intelligent Autonomous Vehicle, 103-108.
8. Kise M., N. Noguchi, K. Ishii, and H. Terao. 2002. Field Mobile Robot Navigated by RTK-GPS and FOG (Part 1). Journal of JSAM 63(5): 74-79.
9. McQuarrie A., and C. L. Tsai. 1998. Regression and Time Series Model Selection. Singapore, World Scientific.

# MOBILE DATA REPEATERS ENHANCING THE AVAILABILITY OF RTK CORRECTION DATA IN THE FIELD

T. Muhr<sup>1</sup> and P.O. Noack<sup>1</sup>

## ABSTRACT

The effective use of automated steering systems in crop production and plot trials relies on accurate and reliable position sensors. Such sensors are also mandatory for the safe use of autonomous vehicles in agriculture and horticulture.

RTK GPS systems provide position accuracy in the range of centimeters. They require the operation of a local base station. Due to high acquisition costs and the high skill set required to operate these systems, they have until recently exclusively been used for land surveying. Frequencies and the transmission power for broadcasting RTK corrections directly relate to the service coverage and are subject to limitations by federal regulations and laws.

Mobile Data Repeaters are able to receive GPS correction data via wireless internet (e.g. GPRS) using the Ntrip protocol and retransmitting the data on a licensed frequency via low power radios. This helps to overcome the limitations intrinsic in the use of only one of either transmission technology and allows for the flexible use of different correction data sources. Thus operation and maintenance costs for base stations are reduced while adding flexibility for the data recipient with respect to changes in technology and cost structure.

**KEYWORDS.** Correction Data, Data Repeater, GPS Mobile, NTrip, RTK.

## INTRODUCTION

**GPS.** The Global Navigation Satellite System (GNSS) GPS has become an integral part of all kinds of different applications. GPS sensors provide position measurements and may be used globally. The accuracy of position measurements depends on the quality of hardware and software as well as on the quality of differential correction data which accounts for errors in signal range measurements due to signal interference in the atmosphere.

**RTK.** RTK GPS systems use pseudo range as well as carrier phase measurements from both GPS frequencies (L1 and L2) to calculate a position (Leick 2004). When provided with differential corrections from a base station, RTK GPS receivers achieve a dynamic position accuracy in the range of centimeters and below. In order to correctly resolve the carrier phase ambiguity, the base station must be located within a 40 km range (base line) from the roving GPS receiver. Using a single base station, the accuracy of the rover position degrades with increasing the base line (1 to 2 ppm or 1 to 2 cm per 10 km).

**RTK Networks.** Data from different base stations may be gathered to create a RTK network. This helps overcome the limitations of single base stations by extending the maximum base line length for resolving the carrier phase ambiguity and by decreasing the degradation of accuracy with increasing base lines. Networked RTK base stations may be up to 100 km apart still providing valid and accurate correction data for the area covered by the network.

**Telemetry.** In order to provide roving RTK GPS receivers with differential corrections from single base stations or a RTK network the correction messages need to be broadcasted by terrestrial telemetry. The frequencies assigned for the transmission of RTK correction data and the maximum

---

<sup>1</sup> geo-konzept GmbH, Gut Wittenfeld, D-85111 Adelschlag, Germany, [tmuhr@geo-konzept.de](mailto:tmuhr@geo-konzept.de), [pnoack@geo-konzept.de](mailto:pnoack@geo-konzept.de)



Ntrip server may also compute corrections for a virtual reference station (VRS) using different correction sources from within a base station network.

3. **Ntrip client.** Ntrip clients can connect to Ntrip casters, obtain information on all correction sources available from this caster (source table) and retrieve correction data providing a mount point and user access information (login and password). The Ntrip client also needs to provide information on his approximate position. This is necessary in order to assign a data stream from the nearest base station or to compute virtual correction data generated from different data streams.

Figure 3 shows the relationship between Ntrip casters, Ntrip servers and Ntrip clients.

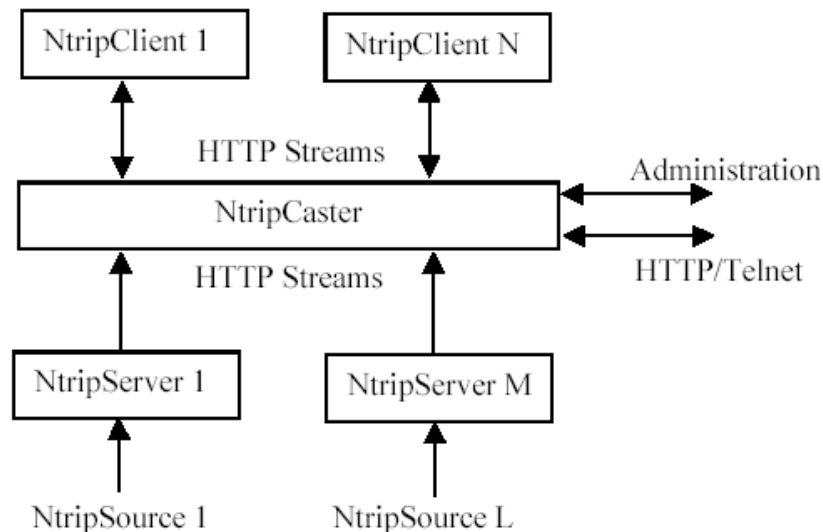


**Figure 3. Ntrip streaming system.**

### THE CONCEPT OF MOBILE DATA REPEATERS

Acquiring and maintaining local base stations demands a high financial input and may eventually require high skill sets. As per definition a local base station can only cover a limited area with differential correction data. This is due to legal regulations for broadcasting and the degradation of rover performance with increasing distance from base stations. Therefore the costs for the generation and transmission of differential RTK corrections per rover are substantial.

The concept of a single service provider setting up base stations to cover a large area and providing the correction data from single base stations or virtual base stations as a payed service via radio modems or GSM has already been adopted in the 1990s by SAPOS (cooperation of german survey authorities). This service is mainly being used by professional surveyors. High prices for decoders and high service fees have prevented the adoption of this service in other market segments.

ASCOS (commercial correction data service provided by EON Ruhrgas) is following a similar concept. The ASCOS service is providing differential corrections mainly focussed on Ntrip using GPRS and GSM based serial data transmission. The use of ASCOS corrections relies on the GSM/GPRS coverage in the area of use.

High precision GPS RTK applications in rural areas with poor GSM/GPRS coverage (e.g. agriculture) still rely on the use radio modems for transmitting correction data from locally managed base stations. In other areas of the world similar services are in operation.

Mobile Data Repeaters can overcome the necessity to operate local base stations in areas with poor GSM/GPRS coverage (Fig. 4). They consist to three components:

1. Ntrip client with GPRS/UMTS modem. The Ntrip client is activated every time the Mobile Data Repeater is switched on. It uses a GPRS or UMTS modem to connect to Ntrip data

sources through a Ntrip caster. Mount points and user access information may be preconfigured and changed through a serial connection or with SMS messages.

2. Radio modem. The radio modem transmits the correction data received by the Ntrip client in order to cover areas where GSM/GPRS is not available.
3. Low cost GPS receiver. OEM GPS receivers with a standard accuracy of less than 10 m are available at less than 100 US \$. The position information from this receiver is frequently being sent to the Ntrip caster . The Ntrip caster uses this information to either compute corrections for a virtual reference station or to assign the corrections from the nearest base station to the Ntrip data stream.

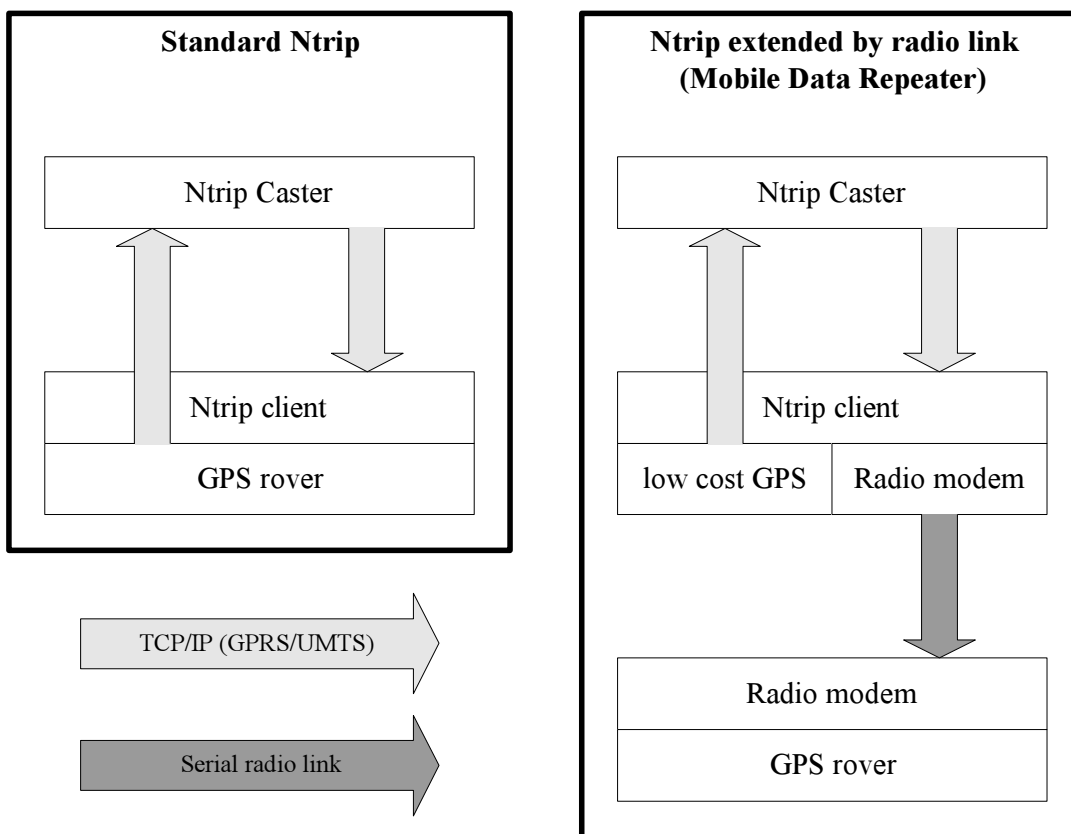


Figure 4. Comparing standard Ntrip with Mobile Data Repeaters.

## DISCUSSION

Using Ntrip provides the user with the flexibility to access different Ntrip sources. Currently only a few sources for Ntrip data streams are available, most of them being commercial (e.g. ASCOS). When more service providers enter the market, the prices for service fees are likely to drop substantially due to competition and a growing number of users. Mobile Data Repeaters using Ntrip can be instantly reconfigured to access Ntrip data streams from competing and more attractive services.

The charges on the use of GPRS and UMTS services are based on the volume of data transfer rather than the connection time based charges of GSM. Differential corrections only require small bandwidths so that the cost for data transfer between the Ntrip caster and Ntrip client can be substantially cut down with increasing GPRS/UMTS coverage.

The use of GPRS and UMTS also enables rovers to access data from local base stations which would be out of reach of a radio link. Due to legal regulations of transmission power, the maximum range that can be covered with a local base station using a radio modem link is approximately 20 km depending on topology and the regulations in the country of use. GPRS and UMTS allow to extend the range to the maximum of 40 km or more depending on whether the

data is provided by a single base station or a network of base stations (virtual base station). So using Mobile Data Repeaters and Ntrip may even help users using a single base station to extend their coverage by setting up an Ntrip server and connecting it to their local base station. This effectively is an alternative to using radio repeaters.

In standard Ntrip applications the position of the rover is directly provided by the roving GPS receiver. Within the concept of Mobile Data Repeaters this would require a bidirectional communication between the rover the Mobile Data Repeater. Using a low cost GPS receiver as part of the Mobile Data repeater saves hardware costs and minimises the overhead for acquiring radio licenses for additional transmitters from the regulation authorities. However, when using correction data from a base station network providing the position of the Mobile Data Repeater instead of the true rover position accuracy may degrade in the range of millimeters depending on the distance between the rover and the Mobile Data Repeater.

Preliminary tests have proven the feasibility of the concept. Ntrip data received with a Ntrip PC client has been broadcasted with a UHF radio. A GPS based automated steering systems on a tractor using the correction data was performing as expected. However, during some time periods the age of correction data was well exceeding the age of correction data received from a local base station using a radio link.

The concept of Mobile Data Repeaters is comprising a MCU which is automatically coping with the problems arising of connection drop outs and excessively delayed data packets. Because there is a multitude of standards being actively used for transmitting RTK correction data (RTCM 2.x, RTCM 3,x, RTCA, CMR, CMR+), intelligent format conversion is certainly among the tasks for this MCU.

Provided that further tests during 2006 are successful the authors expect a finished product to be available by early 2007.

## CONCLUSION

The concept of Mobile Data Repeaters enhances the use of high precision GPS systems without operating a local base station in rural or remote areas with sparse GSM/GPRS coverage. Mobile Data Repeaters have been designed to fully cover such areas with GPS correction data received from a point with stable GSM/GPRS reception.

Mobile Data Repeaters also help to extend the range of local base stations which normally use radio modems for data propagation the signal power of which is regulated by law. Mobile Data Repeaters provide maximum flexibility with respect to service fees as they may use data streams from any commercial or private Ntrip source.

Preliminary tests have successfully proved that the concept of Mobile Data Repeaters is feasible. However, further tests and improvements are necessary until a market ready product can be made available.

## REFERENCES

1. Leick, A. 2004. GPS Satellite Surveying, John Wiley and Sons.
2. Networked Transport of RTCM via Internet Protocol (Ntrip). 2005. Bundesamt für Kartographie und Geodäsie, [http://igs.ifag.de/index\\_ntrip.htm](http://igs.ifag.de/index_ntrip.htm)



# GREENHOUSE ROBOT NAVIGATION USING KLT FEATURE TRACKING FOR VISUAL ODOMETRY

P. J. Younse<sup>1</sup> and T. F. Burks<sup>1</sup>

## ABSTRACT

A visual odometer was developed for an autonomous greenhouse sprayer to estimate vehicle translation and rotation relative to the world coordinate system during navigation. Digital images were taken from a CCD camera mounted on the robot. 7 x 7 pixel features were selected in the image using the KLT algorithm (Csetverikov, 2004). Features were tracked from image to image by finding the best 7 x 7 pixel match of the feature within a 25 x 25 pixel search box. By analyzing the movement of these features, vehicle rotation and translation were estimated. Five features were tracked with the odometer.

Tests were run to verify the visual odometer's accuracy during translation, rotation, and on various surfaces. The visual odometer ran at an average of 10 Hz during experimentation. Translation tests of the odometer in a lab environment gave an average error of 4.85 cm for a 30.5 cm forward translation and 12.4 cm average error for a 305 cm translation. Rotation tests of the odometer in a lab environment gave an average error of 1° for a 45° rotation and an 8° error for a 180° rotation about the vehicle z-axis. Tests completed on concrete, sand, and gravel demonstrated adaptability of the odometer on different ground surfaces that are common in greenhouses. The visual odometer was successfully integrated into a visual navigation system for intersection navigation of an autonomous greenhouse sprayer.

**KEYWORDS.** Feature Tracking, KLT Algorithm, Machine Vision, Vehicle Navigation, Visual Odometry.

## INTRODUCTION

Vehicle automation is a growing interest among the agricultural community. Many feasibility studies were made on autonomous agricultural vehicles. Have et al. (2002) investigated the development of autonomous weeders for Christmas tree plantations. Design requirements for such a vehicle were explored, specific behaviors for navigation and operation defined, and a system architecture proposed. Hellström (2002) performed a similar study for autonomous forest machines as part of a project to develop unmanned vehicles that transport timber.

Another application of autonomous agricultural vehicles is autonomous greenhouse spraying. Benefits of an autonomous greenhouse sprayer include increased accuracy and precision with spraying, which would contribute to more efficient use of resources, capability to operate 24-hours a day, and decreased health risks associated with human exposure to dangerous chemicals.

Singh (2004) designed an 81 x 41 cm autonomous greenhouse sprayer. The vehicle was designed to navigate through 46, 51, and 61 cm aisles. Two 560-watt DC motors with 20:1 gear reducers powered two separate three-wheel drive trains. Turning was accomplished with differential steering. Vehicle control down the center of test paths was carried out independently using ultrasonic range sensors, ladar, and machine vision with a fuzzy PD controller (Singh, 2004; Singh and Subramanian, 2004). The navigation system developed in Younse (2005) performed intersection detection and navigation using machine vision. Visual odometry was utilized in this navigation system during the intersection navigation algorithm.

---

<sup>1</sup> Agricultural & Biological Engineering Department, University of Florida, Gainesville, FL, USA, [pyounse@ufl.edu](mailto:pyounse@ufl.edu)

Visual odometry allows estimation of vehicle translation and rotation relative to the world coordinate system during navigation solely based on images from a camera. The advantage of visual odometry over conventional odometry techniques is that it bases vehicle movement on the movement of the path relative to the vehicle and is not affected by wheel slippage or turning. Also, if the vehicle is already equipped with a camera for navigation, no additional instruments are required, reducing vehicle cost and complexity.

Visual odometry has been accomplished by tracking feature points from one image to the next and then computing the vehicle translation and rotation from these points. Nistér et al., 2003, detected Harris corners, tracked these features between image frames, and used a combination of the 5-point algorithm, 3-point algorithm, and triangulation to estimate 3D camera pose, and in turn, vehicle movement. Pollefeys, 2004, also discussed and compared techniques to calculate 3D information and camera motion by tracking sets of feature points through image sequences using structure and motion.

The visual odometry technique discussed in this paper differs from traditional visual odometry and structure and motion approaches in that it takes advantage of a flat ground plane assumption made for a vehicle with a fixed camera traveling on relatively flat ground. From this assumption, the visual odometry described only requires tracking a minimum two feature points (though five points were used for testing to make the system more robust and help eliminate error). Also, algorithms used to calculate vehicle rotation and translation between frames in a 3D-environment, such as the 8-point algorithm (Chojnacki et al., 2003), are not required, which allows faster processing and the ability to more easily run navigation software with the visual odometry on a single camera system in real-time.

### SYSTEM COMPONENTS

A Sony FCB-EX7805 CCD camera was mounted onto the robotic sprayer developed by Singh (2004), as shown in Figure 1. A single camera was chosen as opposed to a multiple camera setup or stereovision to reduce costs that come with additional equipment and reduce complexity associated with calibrating multiple cameras. An Integral Technologies Flashbus MV Pro frame grabber was used to capture 640 x 480 pixel color images from the camera. A PC with a 2.4 GHz processor acquired images from the camera and performed the visual odometry routine for each frame. All programming was implemented in C++. A Sony FCB-EX7805 CCD camera was mounted onto the robotic sprayer developed by Singh (2004), as shown in figure 1.

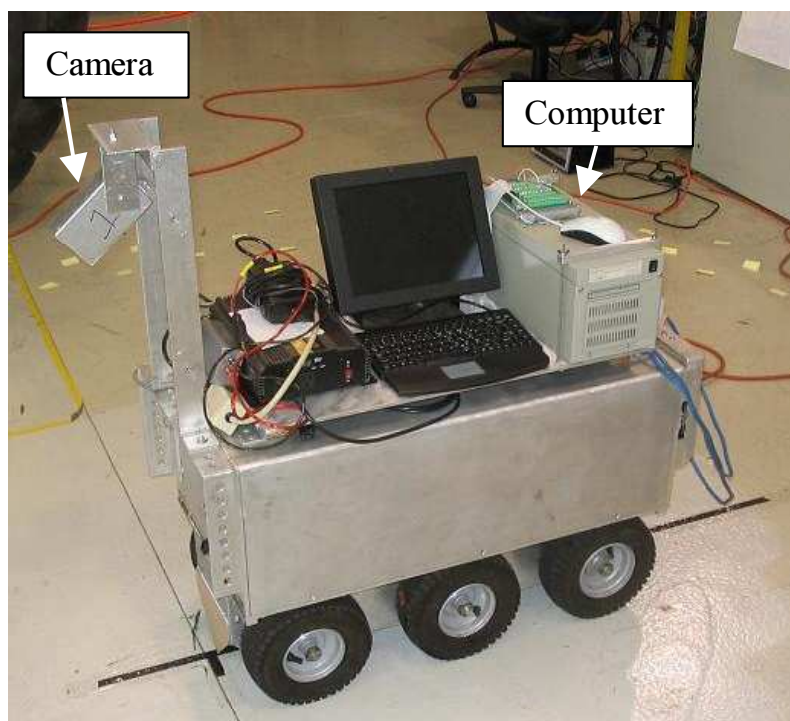


**Figure 1. Camera-mounted robotic sprayer.**

## METHODS

### Camera Model

Sets of intrinsic and extrinsic camera parameters were found to describe the camera. Intrinsic parameters account for the focal length, principal point, skew, and lens distortion. Extrinsic parameters account for the rotation and translation of the camera coordinate system relative to the vehicle coordinate system. Using the intrinsic and extrinsic camera parameters, ground points in the vehicle coordinate system could be transformed into pixel coordinates and vice versa, as shown in figure 2.

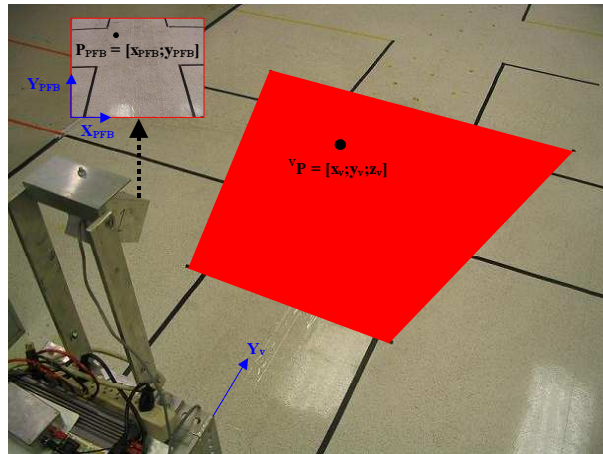


Figure 2. Relationship between a ground point in the vehicle system and image plane.

Intrinsic parameters were calculated using the Camera Calibration Toolbox for Matlab developed by Bouguet (2004). Extrinsic parameters were calculated by measuring the rotation and translation of the camera coordinate system relative to the vehicle coordinate system shown in figure 3. To transform pixel coordinates to points in the vehicle system, the intrinsic and extrinsic parameters were used, along with the assumption that points in the image exist on a fixed ground plane.

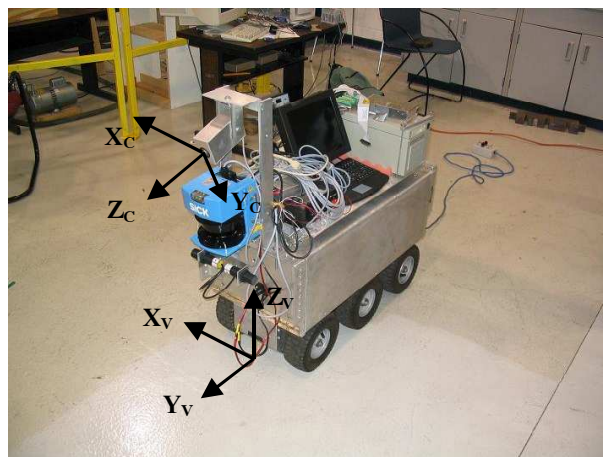


Figure 3. Camera (C) and vehicle (V) coordinate systems.

## VISUAL ODOMETER

The visual odometer was developed to estimate vehicle position and orientation relative to the world coordinate system over time. The odometer determines vehicle movement by tracking features on the ground. The following steps are carried out in this process:

1. Initialize odometer
2. Initial search for features

3. Tracking features
4. Determination of position and orientation change

### *Initialize Odometer*

When the odometer is initialized, the world coordinate system is defined relative to the vehicle coordinate system. All translations and rotations in subsequent images will be relative to this world system

### *Initial Search for Features*

The odometer relies on tracking features through a set of image frames. When starting the odometer, an initial set of features must be found for tracking. The large, rectangular box in the upper-center area of the image in Figure 4A shows where initial features are found. The KLT search box is 151 pixels wide, 31 pixels high, and located at pixel row 380 and column 320. These specifications were chosen to allow pixels to be tracked a large distance when the vehicle is moving forward. The KLT search box size was specified because searching the entire image for features would take too much computation time.

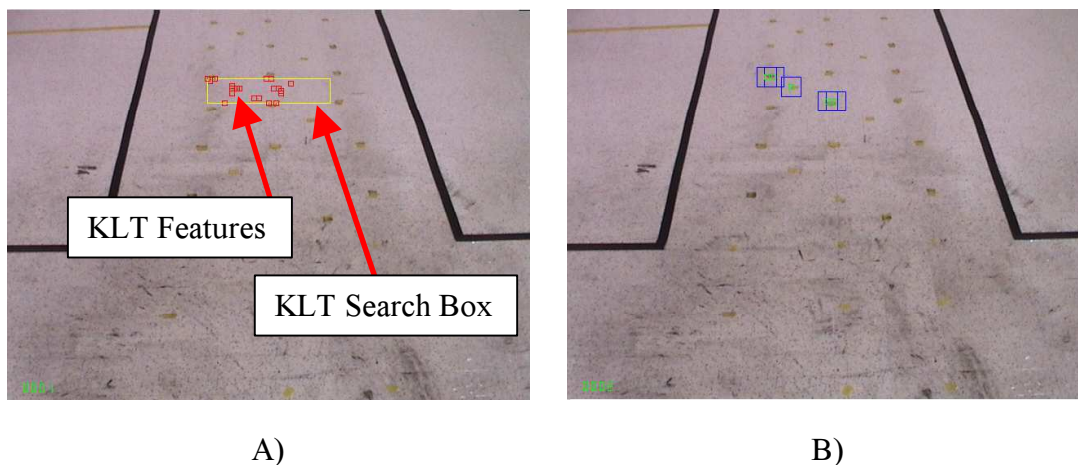


**Figure 4. Initial search for features. A) Good features found in search box. B) Five strongest KLT features selected for tracking.**

Within the search box, good features are defined as corners found using the KLT algorithm (Csetverikov, 2004). 7x7 pixel sizes were chosen as feature sizes, because they are small enough for fast searching and large enough to uniquely define the feature. The strongest corner features found by the KLT algorithm are shown as smaller boxes within the search box in figure 4A. Because tracking features takes significant computation time, the number used in the tracking process is limited to a minimum. A minimum of two features is needed to define the vehicle motion relative to the ground. The five strongest features found with the KLT algorithm, represented by the smaller boxes in Figure 4B, are used for tracking.

### *Tracking Features*

Figure 5 demonstrates feature tracking in two subsequent images. The small boxes mark the five 7x7 pixel features being tracked. Features are tracked by saving the 7x7 pixel feature in the first image and looking for a 7x7 pixel area that best matches it in the second image. Only the area within the larger 25x25 pixel box is searched. The size of the search box was based on the velocity of the vehicle and selected to cover the possible movement of features in the image plane from frame to frame. The location of the feature search box is based on the movement of that feature found in the last frame.

To locate the features defined in image  $I_1$  (Fig. 5A) in image  $I_2$  (Fig. 5B), the sum-of-squared difference (SSD) is calculated for each possible 7x7 pixel area in the search box using the following equation (Barron et al., 1993):

$$SSD_{1,2}(x; d) = \sum_{j=-n}^n \sum_{i=-n}^n W(i, j) [I_1(x + (i, j)) - I_2(x + d + (i, j))]^2$$

where  $W$  is a discrete 2-d window function,  $x$  is the center pixel coordinates of the feature defined in frame 1,  $n = \text{floor}(\text{feature pixel width}/2)$ , and  $d$  is the pixel row and column shift used to move the 7x7 pixel area within the search box in image  $I_2$ . The best match gives the least sum-of-squared difference. Figure 6 shows a larger view of the five features tracked from the first and second frame in figure 5.

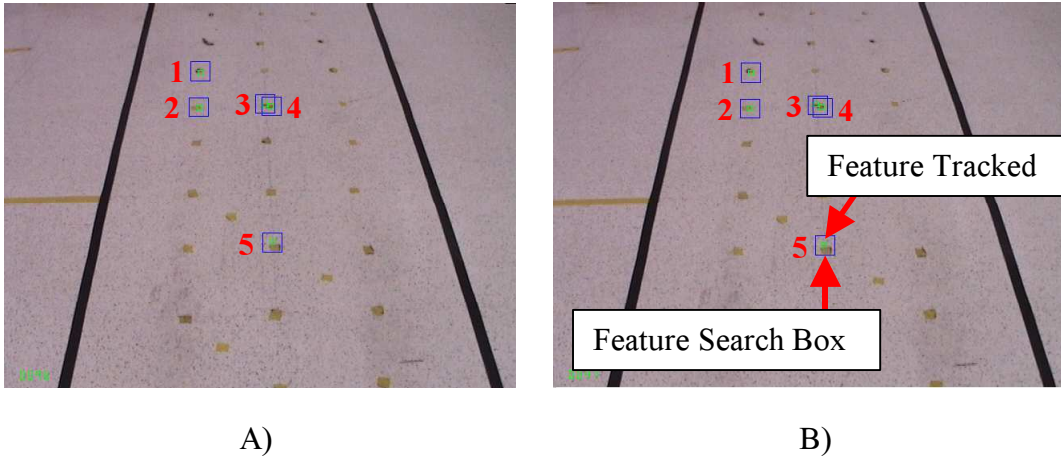


Figure 5. Tracking features. A) First frame. B) Second frame.



Figure 6. Large view of features matched in Figure 5. A) Features 1 through 5 in Figure 5A. B) Features 1 through 5 in Figure 5B. Note the outer feature pixels are not visible due to the box drawn around the feature.

The restraint made on the features for the visual odometer is that they must be fixed on the ground plane. This restraint can be made because most greenhouse floors are relatively flat, and any small variations in the surface will be averaged out by the odometer over the course of the drive. However, certain conditions that must be avoided when tracking features are:

1. The feature tracked is significantly above or below the ground plane (due to features found in a gully, in holes, or on mounds).
2. The feature moves independent of the ground plane (due to features from moving objects or changing shadows on the ground).
3. The feature is lost or not correctly tracked (due to a change in scenery over the feature area or errors from the feature matching process).

To prevent these conditions from occurring during feature tracking, a geometric relationship amongst the features is defined from frame to frame. The distance from each feature to all other

features is measured and recorded. Figure 7 shows the distance calculated between features 1 and 5.  ${}^1F_1$  and  ${}^1F_5$  represent the coordinates of features 1 and 5 in the vehicle coordinate system in image frame 1. Note that these coordinates assume the features exist on the ground plane as defined in the camera model.  ${}^1d_{1,5}$  represents the distance between features 1 and 5 in image frame 1. Table 1 shows the complete distance measurements between features from frame 1 in figure 5A.

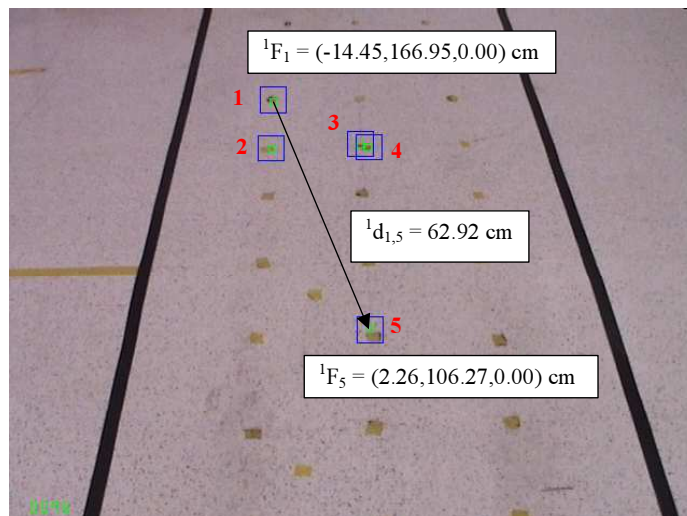


Figure 7. Distance between features 1 and 5 in image frame 1.

Table 1. Distances between features in frame 1 shown in figure 5A in centimeters.

Feature	1	2	3	4	5
1	${}^1d_{1,1} = 0.00$	${}^1d_{1,2} = 16.36$	${}^1d_{1,3} = 21.82$	${}^1d_{1,4} = 23.44$	${}^1d_{1,5} = 62.92$
2	${}^1d_{2,1} = 16.36$	${}^1d_{2,2} = 0.00$	${}^1d_{2,3} = 14.91$	${}^1d_{2,4} = 16.13$	${}^1d_{2,5} = 47.04$
3	${}^1d_{3,1} = 21.82$	${}^1d_{3,2} = 14.91$	${}^1d_{3,3} = 0.00$	${}^1d_{3,4} = 1.63$	${}^1d_{3,5} = 45.62$
4	${}^1d_{4,1} = 23.44$	${}^1d_{4,2} = 16.13$	${}^1d_{4,3} = 1.63$	${}^1d_{4,4} = 0.00$	${}^1d_{4,5} = 44.58$
5	${}^1d_{5,1} = 62.92$	${}^1d_{5,2} = 47.04$	${}^1d_{5,3} = 45.62$	${}^1d_{5,4} = 44.58$	${}^1d_{5,5} = 0.00$

Table 2. Distances between features in frame 2 shown in figure 5B in centimeters.

Feature	1	2	3	4	5
1	${}^2d_{1,1} = 0.00$	${}^2d_{1,2} = 16.59$	${}^2d_{1,3} = 21.69$	${}^2d_{1,4} = 23.55$	${}^2d_{1,5} = 62.92$
2	${}^2d_{2,1} = 16.59$	${}^2d_{2,2} = 0.00$	${}^2d_{2,3} = 14.86$	${}^2d_{2,4} = 16.03$	${}^2d_{2,5} = 46.84$
3	${}^2d_{3,1} = 21.69$	${}^2d_{3,2} = 14.86$	${}^2d_{3,3} = 0.00$	${}^2d_{3,4} = 1.85$	${}^2d_{3,5} = 45.75$
4	${}^2d_{4,1} = 23.55$	${}^2d_{4,2} = 16.03$	${}^2d_{4,3} = 1.85$	${}^2d_{4,4} = 0.00$	${}^2d_{4,5} = 44.37$
5	${}^2d_{5,1} = 62.92$	${}^2d_{5,2} = 46.84$	${}^2d_{5,3} = 45.75$	${}^2d_{5,4} = 44.37$	${}^2d_{5,5} = 0.00$

When the features from the first frame are found in the second frame, the distance relationship calculations are repeated. Table 2 shows the complete distance measurements between features from frame 2 in figure 5B. Next, the difference between the distance measurements from frame 1 to frame 2 are calculated and shown in table 3. Note that this difference in distances between points is not dependent on how far the features are from one another, but based on how accurate the feature matching algorithm can estimate the position of each feature at the particular distance it is from the camera (closer features have higher pixel resolution and therefore their position can be calculated more accurately).

**Table 3. Difference in feature distance in frame 1 (Tab. 1) and frame 2 (Tab. 2) in centimeters.**

Feature	1	2	3	4	5
1	0.00	0.23	0.13	0.10	0.00
2	0.23	0.00	0.05	0.10	0.20
3	0.13	0.05	0.00	0.23	0.13
4	0.10	0.10	0.23	0.00	0.20
5	0.00	0.20	0.13	0.20	0.00

If all features were fixed to the ground and tracked accurately, the distance relationships between each of the features should remain the same. Analyzing the change in distances between the two frames compared in table 3 show little change, proving all five of the tracked features are valid.

If any of the features being tracked falls into the three conditions described above (they existed above or below the ground plane, were on a moving object, or not correctly matched), they can be identified by looking at the difference in feature distances between frames as described above. Figure 8 demonstrates a case when a feature was not tracked correctly between two consecutive frames. A close-up of the five features being tracked is shown in figure 8C and figure 8D. In figure 8B, all features were successfully tracked in frame 2 except for feature 1. Feature 1 was determined to be non-valid by performing the distance relationship analysis between features in each of the two frames. Table 4 and table 5 show the complete distance measurements between features from frame 1 in figure 8A and frame 2 in figure 8B. The difference between the distance measurements from frame 1 to frame 2 are calculated and shown in table 6.

**Table 4. Distances between features in frame 1 shown in figure 8A in centimeters.**

Feature	1	2	3	4	5
1	${}^1d_{1,1} = 0.00$	${}^1d_{1,2} = 2.34$	${}^1d_{1,3} = 9.32$	${}^1d_{1,4} = 19.71$	${}^1d_{1,5} = 20.42$
2	${}^1d_{2,1} = 2.34$	${}^1d_{2,2} = 0.00$	${}^1d_{2,3} = 7.21$	${}^1d_{2,4} = 17.48$	${}^1d_{2,5} = 18.14$
3	${}^1d_{3,1} = 9.32$	${}^1d_{3,2} = 7.21$	${}^1d_{3,3} = 0.00$	${}^1d_{3,4} = 10.54$	${}^1d_{3,5} = 11.35$
4	${}^1d_{4,1} = 19.71$	${}^1d_{4,2} = 17.48$	${}^1d_{4,3} = 10.54$	${}^1d_{4,4} = 0.00$	${}^1d_{4,5} = 1.24$
5	${}^1d_{5,1} = 20.42$	${}^1d_{5,2} = 18.14$	${}^1d_{5,3} = 11.35$	${}^1d_{5,4} = 1.24$	${}^1d_{5,5} = 0.00$

**Table 5. Distances between features in frame 2 shown in figure 8B in centimeters.**

Feature	1	2	3	4	5
1	${}^2d_{1,1} = 0.00$	${}^2d_{1,2} = 2.08$	${}^2d_{1,3} = 9.17$	${}^2d_{1,4} = 19.43$	${}^2d_{1,5} = 20.09$
2	${}^2d_{2,1} = 2.08$	${}^2d_{2,2} = 0.00$	${}^2d_{2,3} = 7.14$	${}^2d_{2,4} = 17.32$	${}^2d_{2,5} = 17.98$
3	${}^2d_{3,1} = 9.17$	${}^2d_{3,2} = 7.14$	${}^2d_{3,3} = 0.00$	${}^2d_{3,4} = 10.46$	${}^2d_{3,5} = 11.28$
4	${}^2d_{4,1} = 19.43$	${}^2d_{4,2} = 17.32$	${}^2d_{4,3} = 10.46$	${}^2d_{4,4} = 0.00$	${}^2d_{4,5} = 1.22$
5	${}^2d_{5,1} = 20.09$	${}^2d_{5,2} = 17.98$	${}^2d_{5,3} = 11.28$	${}^2d_{5,4} = 1.22$	${}^2d_{5,5} = 0.00$

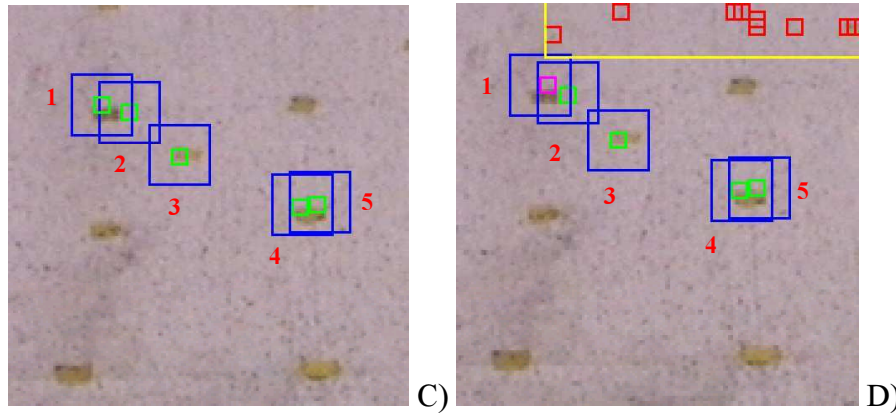
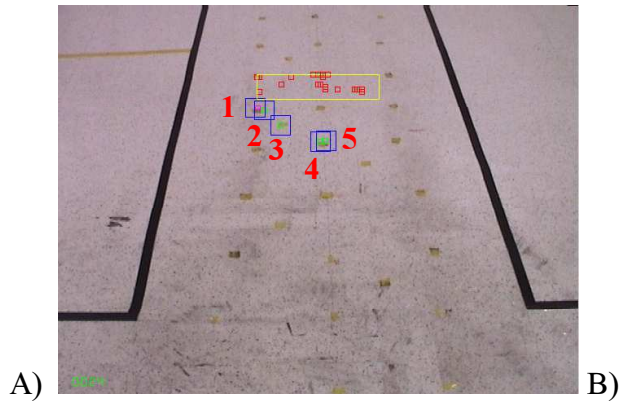


**Figure 8. Mistracked feature. A) First frame. B) Second frame. C) Close-up of features from first frame. D) Close-up of features from second frame.**

**Table 6. Difference in feature distance in frame 1 (Tab. 4) and frame 2 (Tab. 5) in centimeters.**

Feature	1	2	3	4	5
1	0.00	<b>0.25</b>	0.15	<b>0.28</b>	<b>0.33</b>
2	<b>0.25</b>	0.00	0.08	0.15	0.15
3	0.15	0.08	0.00	0.08	0.08
4	<b>0.28</b>	0.15	0.08	0.00	0.03
5	<b>0.33</b>	0.15	0.08	0.03	0.00

As seen in table 6, many of the changes of distances measured from feature 1 (the highlighted row) changed significantly more than those for the other four features. A threshold value of 0.25 cm was set to pick out change in feature distances that indicated significant change. Any change of distance  $\geq 0.25$  cm is labeled as a significant change. These are marked in bold in table 6. If the number of high changes is  $\geq (n/2)$ , where  $n$  is the number of features, then the feature is labeled as invalid. For the case in Table 6,  $n/2 = 5/2 = 2.5$ . The number of significant changes for feature 1 is 3. Since  $3 > 2.5$ , the feature is classified as invalid. When a feature is classified as invalid, it is removed from the tracking list and not used in the visual odometer calculations, and a new search is run on the current image to find a new feature to replace it (seen by the new rectangular KLT search box in figure 8B).

All features whose search area has moved outside the image are also removed from the tracking list. A new feature search is calculated to find new features to replace them. Figure 9 demonstrates a three-frame sequence in which a feature is lost, replaced, and tracked.

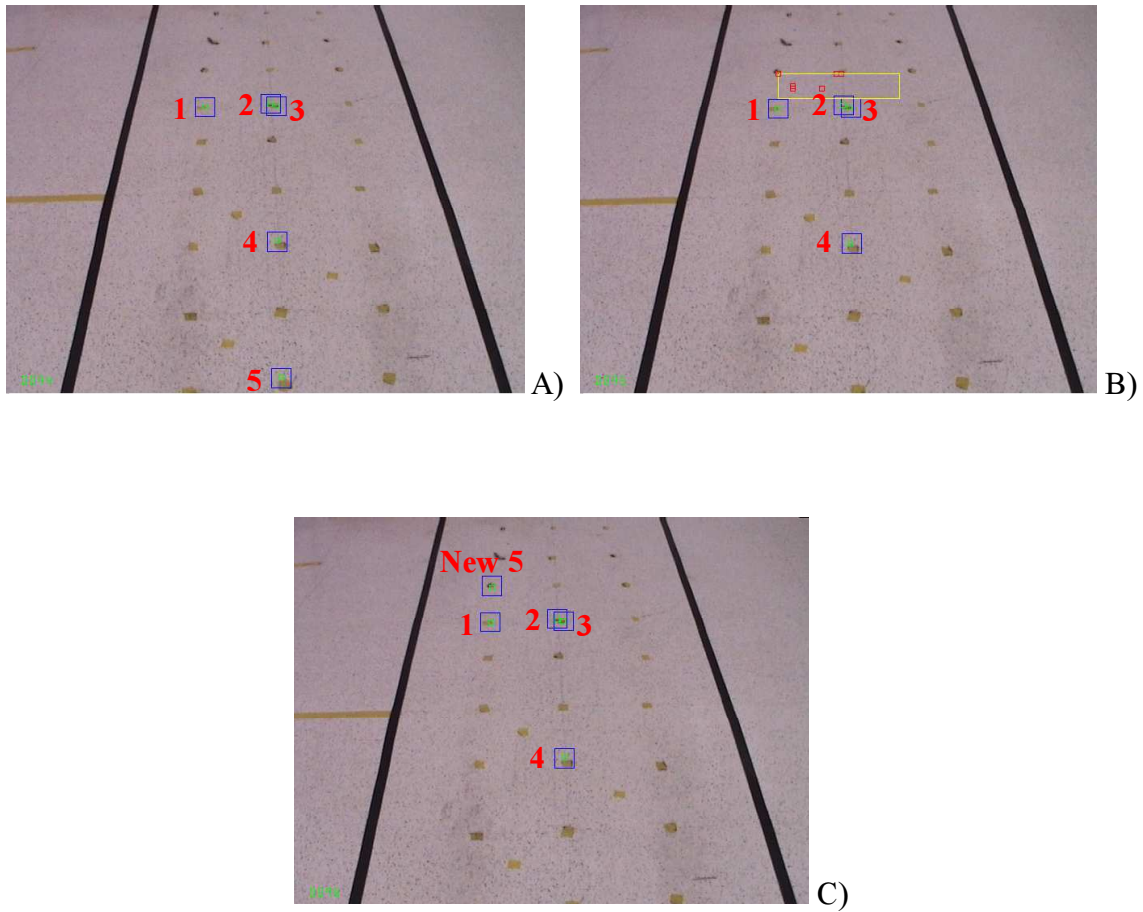


**Figure 9. Feature leaving image and replaced. A) Frame 1: Five features tracked. B) Frame 2: feature 5 moved off image and replacement feature search. C) Frame 3: New feature 5 tracked.**

#### *Determination of Position and Orientation Change*

Based on the movement of the tracked features, the change in vehicle position and orientation is calculated between frames. Given two features tracked successfully from frame 1 to frame 2, the translation of the vehicle and the rotation of the vehicle about the world z-axis are found. The first calculation performed is the rotation of the features in frame 2 relative to the features in frame 1. Since the features are fixed in the world coordinate system, this is equivalent to finding the rotation for the world system in frame 2 relative to the world system in frame 1. Figure 10 shows the calculations of two consecutive frames using the coordinates of two features.

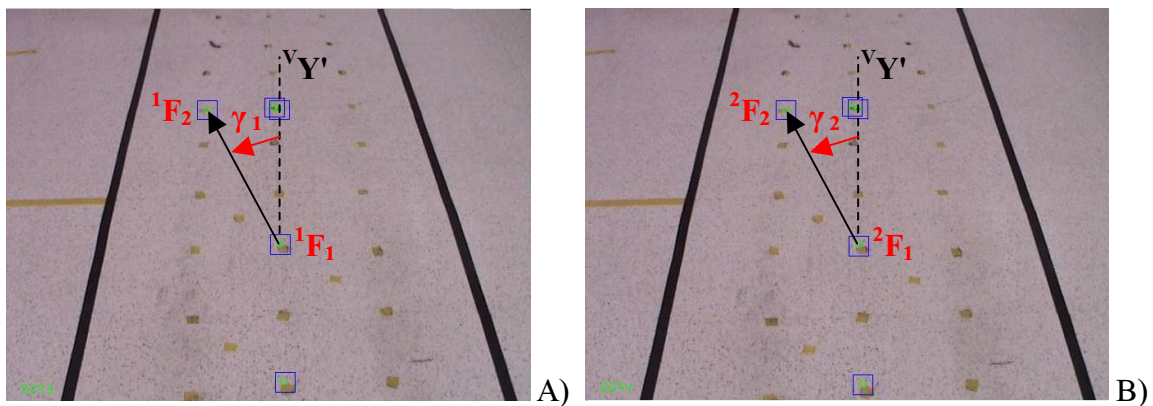


**Figure 10. Calculation of rotation between two consecutive frames. A) Frame 1. B) Frame 2.**

$^1F_1$  and  $^1F_2$  represents the coordinates of features 1 and 2 from frame 1 in the vehicle coordinate system.  $^2F_1$  and  $^2F_2$  represents the coordinates of features 1 and 2 from frame 2 in the vehicle coordinate system.  $^vY'$  represents a line drawn through feature 1 parallel to the y-axis of the vehicle coordinate system.  $\gamma_1$  and  $\gamma_2$  represent the angles between  $^vY'$  and a ray drawn from

feature 1 to feature 2 in the two frames. The rotation of the world system in frame 2 relative to the world system in frame 1,  $\gamma$ , is calculated:

$$\gamma = \gamma_2 - \gamma_1$$

Given the vehicle system coordinates of feature 1 in frame 1,  ${}^1F_1 = ({}^1F_{1,x}, {}^1F_{1,y}, {}^1F_{1,z})$ , and feature 1 in frame 2,  ${}^2F_1 = ({}^2F_{1,x}, {}^2F_{1,y}, {}^2F_{1,z})$ , the translation of the world system in frame 2 relative to the world system frame 1 is calculated next. Let  ${}^1T_2$  represent the transformation matrix relating the world system in frame 2 to the world system frame 1. The relationship between the coordinates of feature 1 in frame 1 and frame 2 is given by:

$${}^1F_1 = {}^1T_2 \cdot {}^2F_1$$

Expanding this matrix and assuming vehicle rotation only occurs about its z-axis (which is sufficient on a level floor),

$$\begin{bmatrix} {}^1F_{1,x} \\ {}^1F_{1,y} \\ {}^1F_{1,z} \\ 1 \end{bmatrix} = \begin{bmatrix} \cos(\gamma) & -\sin(\gamma) & 0 & T_x \\ \sin(\gamma) & \cos(\gamma) & 0 & T_y \\ 0 & 0 & 1 & T_z \\ 0 & 0 & 0 & 1 \end{bmatrix} \cdot \begin{bmatrix} {}^2F_{1,x} \\ {}^2F_{1,y} \\ {}^2F_{1,z} \\ 1 \end{bmatrix}$$

With the assumption that all points are on the ground ( ${}^1F_{1,z}, {}^2F_{1,z} = 0$ ), the translation of the world frame in the vehicle coordinate system in the x, y, and z directions,  $T_x$ ,  $T_y$  and  $T_z$ , are solved:

$$\begin{aligned} T_x &= {}^1F_{1,x} - (\cos(\gamma) \cdot {}^2F_{1,x} - \sin(\gamma) \cdot {}^2F_{1,y}) \\ T_y &= {}^1F_{1,y} - (\sin(\gamma) \cdot {}^2F_{1,x} + \cos(\gamma) \cdot {}^2F_{1,y}) \\ T_z &= 0 \end{aligned}$$

To find the best estimates for the rotation,  $\gamma$ , and translation,  $T_x$ ,  $T_y$ , and  $T_z$ , between frames, these values are calculated for all combinations of the valid tracked features. For each set of rotation and translation values calculated,  ${}^1T_2$  is composed and multiplied with the coordinates of each of the features,  ${}^2F_i$ , to calculate  ${}^1F'_i$ .

$${}^1F'_i = {}^1T_2 \cdot {}^2F_i$$

An error for the estimated set of rotation and translation values is

$$error = \sum_{i=1}^n ({}^1F'_i - {}^1F_i)^2$$

where n is the number of valid tracked features available. The set of rotation and translation values yielding the least error is used as the best estimate for  $\gamma$ ,  $T_x$ ,  $T_y$  and  $T_z$ . As demonstrated before, this set of values is used to develop  ${}^1T_2$ , which represents the transformation matrix relating the world system in frame 2 to the world system frame 1:

$${}^1T_2 = \begin{bmatrix} \cos(\gamma) & -\sin(\gamma) & 0 & T_x \\ \sin(\gamma) & \cos(\gamma) & 0 & T_y \\ 0 & 0 & 1 & T_z \\ 0 & 0 & 0 & 1 \end{bmatrix}$$

If  ${}^wT_{V,old}$  represents the last calculated transformation matrix relating the vehicle coordinate system to the world system, a new  ${}^wT_V$  is calculated using the latest  ${}^1T_2$ :

$${}^wT_V = {}^wT_{V,old} \cdot {}^1T_2$$

The final location of the vehicle in the world coordinate system is  ${}^wP_V = ({}^w x_V, {}^w y_V, {}^w z_V)$ . The final orientation of the vehicle about the world z-axis is  ${}^w \gamma_V$ . Both are extracted from  ${}^wT_V$ :

$${}^wT_V = \begin{bmatrix} \cos({}^w \gamma_V) & -\sin({}^w \gamma_V) & 0 & {}^w x_V \\ \sin({}^w \gamma_V) & \cos({}^w \gamma_V) & 0 & {}^w y_V \\ 0 & 0 & 1 & {}^w z_V \\ 0 & 0 & 0 & 1 \end{bmatrix}$$

$${}^w \gamma_V = a \tan 2(\sin({}^w \gamma_V), \cos({}^w \gamma_V))$$

${}^vT_w$ , representing the transformation matrix relating the world system to the vehicle coordinate system, can also be calculated from  ${}^wT_V$  (Crane and Duffy, 1998):

$${}^wT_V = \begin{bmatrix} \cos({}^w \gamma_V) & -\sin({}^w \gamma_V) & 0 & {}^w x_V \\ \sin({}^w \gamma_V) & \cos({}^w \gamma_V) & 0 & {}^w y_V \\ 0 & 0 & 1 & {}^w z_V \\ 0 & 0 & 0 & 1 \end{bmatrix} = \begin{bmatrix} R_w & & T_w \\ 0 & 0 & 0 & 1 \end{bmatrix}$$

$${}^vT_w = \begin{bmatrix} R_w^T & & -R_w^T \cdot T_w \\ 0 & 0 & 0 & 1 \end{bmatrix}$$

## EXPERIMENTAL SETUP

Three experiments were run to test the visual odometer accuracy and its utilization on various level surfaces:

- Translation Test
- Rotation Test
- Verification Tests on Various Surfaces

### Translation Test

Vehicle translation estimation is used during intersection navigation to determine when the vehicle has traveled far enough into the intersection to start its turn. The position must be accurate to ensure proper alignment of the vehicle with the next path after turning. Since the vehicle is

commanded to drive a specified distance forward along a straight line, the odometer translation test is run on a straight line along the vehicle y-axis. Small squares of tape were placed 15.24 cm apart along the vehicle x- and y-coordinate plane on the ground along the path to provide adequate features for the visual odometer to track (Fig. 11). Figure 12 shows the tape marks as seen from the camera image.

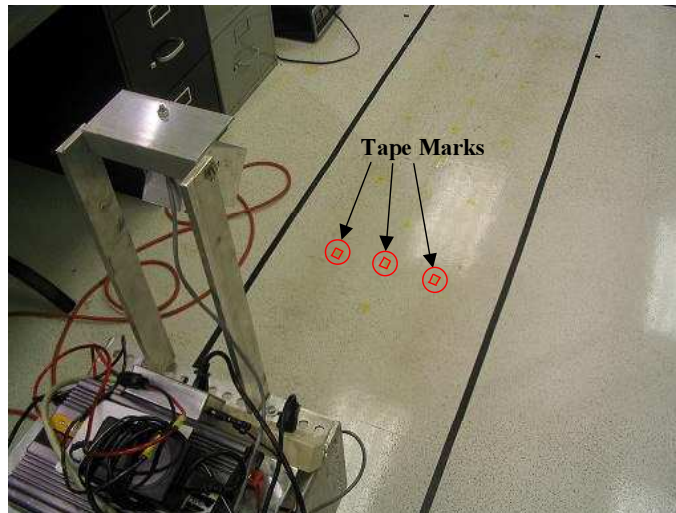


**Figure 11. Yellow tape marks used for features during odometer test.**

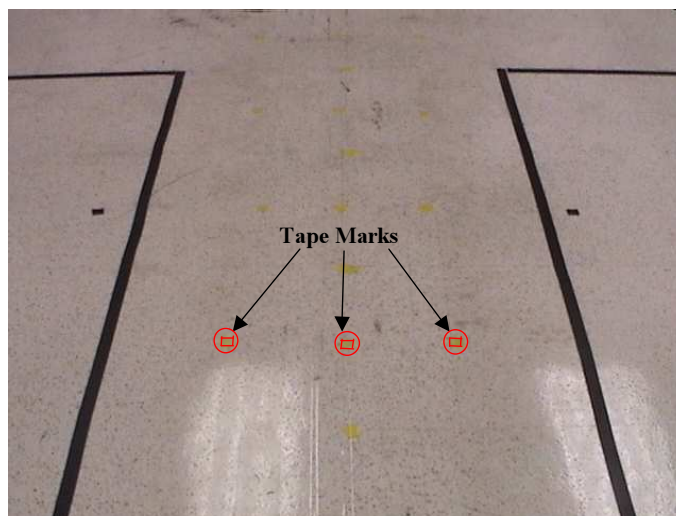


**Figure 12. Camera view of path with tape marks.**

For each test, the vehicle was lined up with a reference line and set up at a starting position, and the world coordinate system was initialized as the starting vehicle coordinate system. The vehicle was instructed to drive straight for a specified distance along the world y-axis direction and stop when the visual odometer read a distance greater than the specified distance. Distances of 15.24 cm to 304.8 cm in 15.24 cm increments were tested. The largest distance, 304.8 cm, was selected as the maximum range a vehicle would have to travel to reach the end of a 152.4 cm wide intersection if the visual odometer was started when the beginning of the intersection was 114.3 cm from the vehicle. Three runs were performed for each distance. The vehicle was driven forward at approximately 11 cm per second.

The x and y translations from the visual odometer were recorded at the end of each run. The origin of the vehicle coordinate system at the end was marked and its translation in the x- and y-directions were measured relative to the world coordinate system at the start. Measurements were made to the nearest 0.3 cm using a ruler. The measured vehicle translation was compared to the odometer estimation and an error was calculated.

## ROTATION TEST

A similar test was conducted for rotation. Instead of tape marks on the floor, paper marks were used. The marks were placed in a circle approximately 150 cm in front of the vehicle so they only appear in the portion of the image where new features are searched for by the visual odometer (Fig. 13).

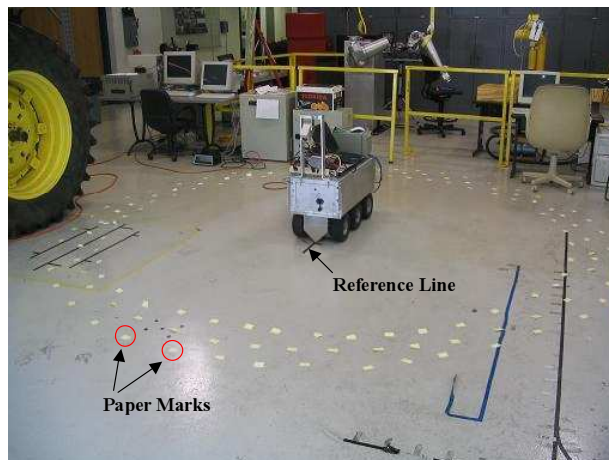


**Figure 13. Experimental setup for visual odometer rotation test.**

For each test, the vehicle was lined up with a reference line (Fig. 13) and set up at a starting position. The world coordinate system was initialized as the starting vehicle coordinate system. The vehicle was instructed to rotate a specified angle clockwise about the vehicle z-axis and stop when the visual odometer read a distance equal to or greater than that angle. Angles of  $45^\circ$  to  $180^\circ$  in  $45^\circ$  increments were used. Three runs were performed for each angle. The vehicle was rotated clockwise at approximately  $3^\circ$  per second.

The angle of rotation from the visual odometer was recorded at the end of each run. The front and back of the vehicle were marked on the ground, and a line was drawn between the two to measure vehicle rotation relative to the starting reference line. The angle was measured to the nearest degree. The measured vehicle rotation was compared to the odometer estimation and an error was calculated.

## VERIFICATION TESTS ON VARIOUS SURFACES

To prove that the visual odometer can work in a greenhouse environment, tests were also run on various surfaces that may be found in a greenhouse. These included concrete, sand, and gravel. All three tests were performed outdoors. The experimental setups for each surface and the view of the surface as seen by the camera are shown in figure 14, figure 15, and figure 16. Sand and gravel were placed along the driving path with a width large enough to cover the area of the image where feature tracking occurs. The material was placed on a tarp for ease of cleanup and did not affect results.

For each test, the vehicle was lined up with a reference line and set up at a starting position, and the world coordinate system was initialized as the starting vehicle coordinate system. The vehicle was instructed to drive straight for a 152.4 cm distance along the world y-axis direction and stop when the visual odometer read a distance greater than that distance. Three runs were made for each surface. The vehicle was driven forward at approximately 11 cm per second, as in the earlier translation test.

The x and y translations from the visual odometer were recorded at the end of each run. The origin of the vehicle coordinate system at the end was marked, and its translation in the x- and y-directions was measured relative to the vehicle coordinate system at the start. Measurements were made to the nearest 0.3 cm using a ruler. A string was laid down the center of the path along the initial vehicle y-axis at the end of each run as a reference to measure translation. The measured vehicle translation was compared to the odometer estimation and an error was calculated.

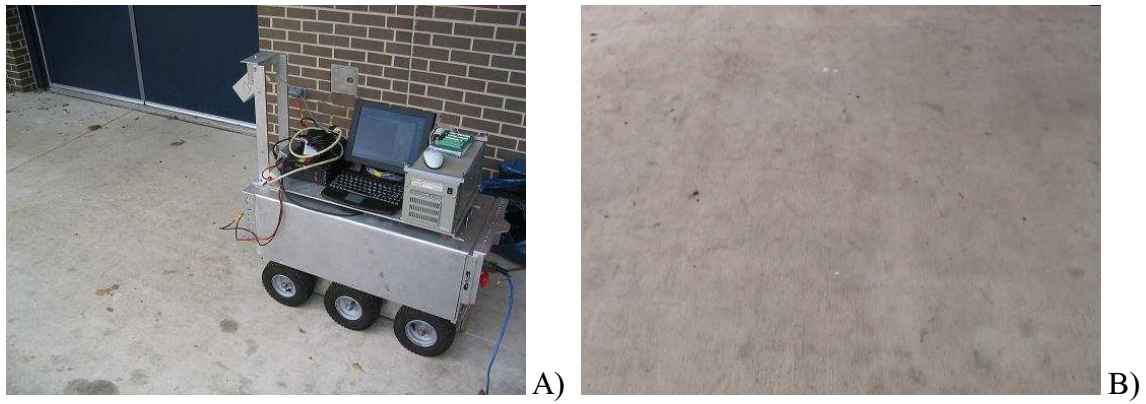


**Figure 14. Concrete test setup. A) Concrete surface. B) Camera view.**

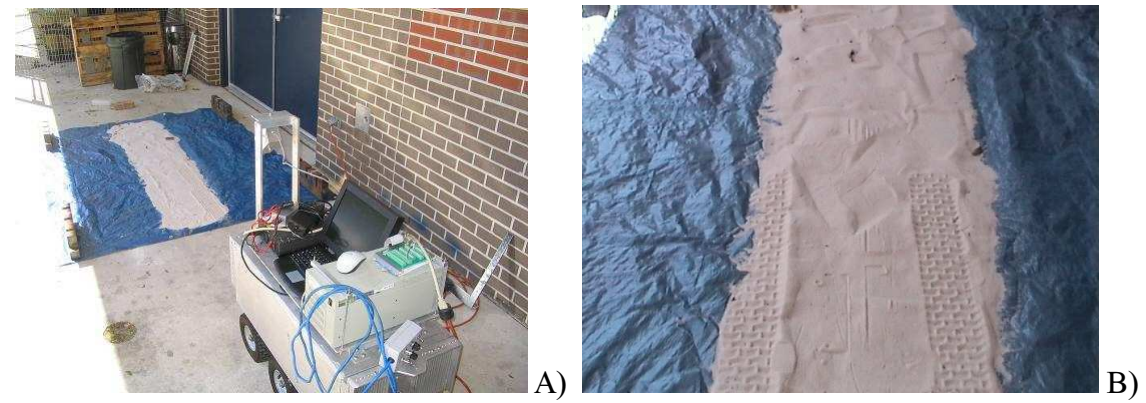


**Figure 15. Sand test setup. A) Sand surface. B) Camera view.**

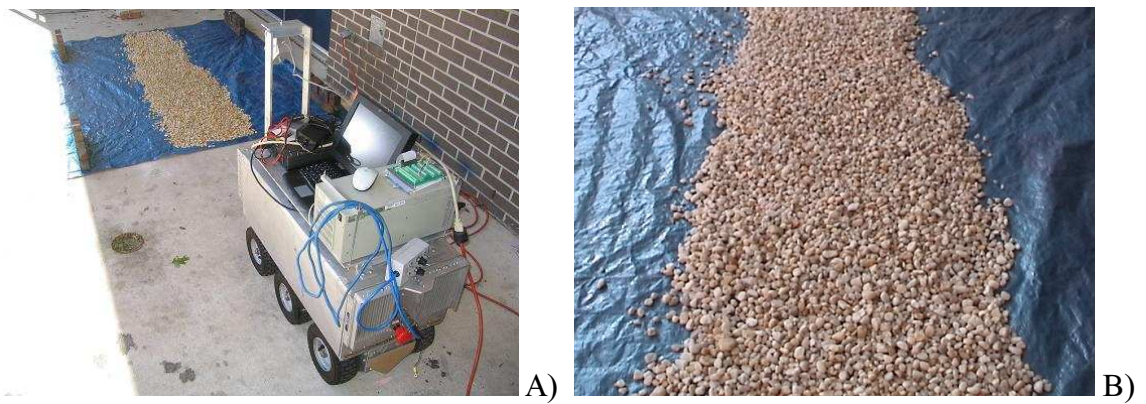


**Figure 16. Gravel test setup. A) Gravel surface. B) Camera view.**

## RESULTS

Results were obtained for the translation tests, rotation tests, and verification tests on various surfaces. The visual odometer ran at an average of 10 Hz during experimentation.

### TRANSLATION TEST

Results obtained from the three translation test runs are shown in table 7, table 8, and table 9.

**Table 7. Translation test Run 1.**

Command Distance (cm)	Odometer $x_v$ (cm)	Odometer $y_v$ (cm)	Measured $x_v$ (cm)	Measured $y_v$ (cm)	Error (cm)
30.48	4.22	32.44	-0.64	33.02	4.88
60.96	0.66	62.89	0.00	65.10	2.29
91.44	-3.28	92.61	0.33	95.25	4.47
121.92	-10.92	123.95	0.33	124.46	11.25
152.40	-3.23	154.25	0.97	156.85	4.93
182.88	1.24	184.73	-1.60	185.12	2.87
213.36	5.54	215.62	0.00	214.63	5.61
243.84	-6.27	246.10	-4.45	243.21	3.43
274.32	12.01	276.15	-3.81	276.86	15.85
304.80	-29.49	307.14	-1.60	306.07	27.91

**Table 8. Translation test Run 2.**

Command Distance (cm)	Odometer $x_v$ (cm)	Odometer $y_v$ (cm)	Measured $x_v$ (cm)	Measured $y_v$ (cm)	Error (cm)
30.48	1.57	32.49	-0.33	33.66	2.24
60.96	10.41	64.29	0.33	67.31	10.52
91.44	0.74	93.68	0.64	96.52	2.84
121.92	3.58	123.49	0.00	125.73	4.22
152.40	-4.93	154.33	0.00	154.31	4.93
182.88	9.37	184.28	-1.27	184.15	10.64
213.36	-1.04	214.83	-1.91	211.46	3.48
243.84	-0.30	245.03	-3.51	244.48	3.25
274.32	-6.71	275.74	-0.64	272.11	7.09
304.80	0.18	305.94	-2.54	300.69	5.92

**Table 9. Translation test Run 3.**

Command Distance (cm)	Odometer $x_v$ (cm)	Odometer $y_v$ (cm)	Measured $x_v$ (cm)	Measured $y_v$ (cm)	Error (cm)
30.48	7.26	33.20	0.00	34.93	7.47
60.96	-7.21	62.97	0.00	64.77	7.44
91.44	0.84	92.74	0.33	95.25	2.57
121.92	-1.22	123.60	0.33	126.37	3.15
152.40	-7.80	154.69	0.33	153.04	8.28
182.88	3.51	185.22	0.97	182.25	3.91
213.36	-5.08	215.19	0.97	215.60	6.05
243.84	-9.50	246.35	-3.51	246.08	6.02
274.32	7.16	275.97	-2.54	274.65	9.78
304.80	-0.76	307.06	-3.18	304.80	3.30

The errors listed in the tables represent the difference in distance between the measured vehicle position and the position estimated by the visual odometer. Table 10 shows the average, minimum, maximum errors and standard deviations from the three runs. The general error range remained consistent throughout the range of distances tested. These odometer errors are the result of the camera model errors relating pixels to points in the vehicle coordinate system as discussed in the previous experiment. Even though a ground feature may have been tracked successfully from the top of the image to the bottom, its perceived coordinates by the camera model could be off by several centimeters by the time it reaches the bottom of the image. Depending on where in the

image a feature was originally found and how far it was tracked down the path determined the error contribution it made.

**Table 10. Average error over the three translation test runs.**

Command Distance (cm)	Average Error (cm)	Minimum Error (cm)	Maximum Error (cm)	Standard Deviation (cm)
30.48	4.85	2.24	7.47	2.62
60.96	6.76	2.29	10.52	4.16
91.44	3.30	2.57	4.47	1.02
121.92	6.22	3.15	11.25	4.40
152.40	6.05	4.93	8.28	1.94
182.88	5.82	2.87	10.64	4.22
213.36	5.05	3.48	6.05	1.37
243.84	4.22	3.25	6.02	1.55
274.32	10.90	7.09	15.85	4.48
304.80	12.40	3.30	27.91	13.52

Several runs gave very high errors above 10 cm, with the largest occurring during Run 1 at the 304.80 cm distance with a 27.91 cm error. The main contributions to these errors were poor estimation of the vehicle translation along its x-axis. Since the error remains relatively low out to 243 cm, it is possible that vision distortion on the far horizon may contribute to the significant jump in error beyond 243 cm. However, it is clear that at moderate command distances, the average error is less than 7 cm with relatively small variation. In practice, this accuracy has proven adequate for navigating corners in greenhouse simulation tests.

## ROTATION TEST

Results obtained from the three rotation test runs are shown in table 11, table 12, and table 13.

**Table 11. Rotation test Run 1.**

Command Angle (deg)	Odometer Angle (deg)	Measured Angle (deg)	Error (deg)
45	45	45	0
90	90	90	0
135	136	145	9
180	182	190	8

**Table 12. Rotation test Run 2.**

Command Angle (deg)	Odometer Angle (deg)	Measured Angle (deg)	Error (deg)
45	46	48	2
90	90	88	2
135	136	150	14
180	182	166	16

**Table 13. Rotation test Run 3.**

Command Angle (deg)	Odometer Angle (deg)	Measured Angle (deg)	Error (deg)
45	46	44	2
90	90	91	1
135	135	155	20
180	181	182	1

The errors listed in the tables represent the difference in rotation between the measured vehicle orientation and the orientation estimated by the visual odometer. Table 14 shows the average, minimum, maximum errors and standard deviations from the three runs. There is a general trend that the farther the command distance, the larger the error. The maximum error during experimentation was 20°, which occurred during a 135° turn. It would be interesting to evaluate whether the turning rate and dynamics of the vehicle influenced the error at larger command angles. The accuracy of the 45° and 90° turn angles are extremely good and suggest that it may be possible to improve the performance at larger turn angles.

**Table 14. Average error over the three rotation test runs.**

Command Angle (deg)	Average Error (deg)	Minimum Error (deg)	Maximum Error (deg)	Standard Deviation (deg)
45	1	0	2	1
90	1	0	2	1
135	14	9	20	5
180	8	1	16	8

### VERIFICATION TESTS ON VARIOUS SURFACES

The results obtained for a commanded vehicle translation of 152.4 cm on concrete, sand, and gravel are shown in table 15, table 16, and table 17.

**Table 15. Translation test for concrete.**

Run	Odometer $x_v$ (cm)	Odometer $y_v$ (cm)	Measured $x_v$ (cm)	Measured $y_v$ (cm)	Error (cm)
1	-19.84	154.69	-0.33	150.50	19.96
2	-10.44	154.08	-0.33	150.50	10.74
3	-6.30	154.53	-0.33	152.10	6.45

**Table 16. Translation test for sand.**

Run	Odometer $x_v$ (cm)	Odometer $y_v$ (cm)	Measured $x_v$ (cm)	Measured $y_v$ (cm)	Error (cm)
1	-5.97	154.03	-3.51	150.83	4.06
2	-7.32	153.97	-2.54	148.59	7.19
3	-7.19	154.23	-4.45	152.40	2.97

**Table 17. Translation test for gravel.**

Run	Odometer $x_v$ (cm)	Odometer $y_v$ (cm)	Measured $x_v$ (cm)	Measured $y_v$ (cm)	Error (cm)
1	-11.30	152.83	-5.08	146.05	9.19
2	-7.09	154.36	-5.08	147.32	7.32
3	-6.78	154.00	-3.81	144.78	9.68

The errors listed in the tables represent the difference in distance between the measured vehicle position and the position estimated by the visual odometer. Table 18 shows the average, minimum, maximum errors, and standard deviations from the three runs for each surface. The errors acquired from the testing on the lab floor at 152.4 cm as reported in table 10 are also shown in table 18 for comparison. The error results for sand and gravel compare favorably with that found on the lab floor. In these cases, the availability of distinct surface features provide a good basis for visual odometry. However, the concrete surface demonstrates significantly higher errors, which may be attributed to the less distinct image features.

**Table 18. Average error over the three test runs for concrete, sand, and gravel.**

Surface	Average Error (cm)	Minimum Error (cm)	Maximum Error (cm)	Standard Deviation (cm)
Concrete	12.40	6.45	19.96	6.91
Sand	4.75	2.97	7.19	2.19
Gravel	8.74	7.32	9.68	1.25
Lab	6.05	4.93	8.28	1.94

## CONCLUSION

The visual odometer gave accurate estimation of vehicle translation and rotation. Translation tests of the odometer in a lab environment gave an average error of 4.85 cm for a 30.5 cm forward translation and 12.4 cm average error for a 305 cm translation. This increased error may be due to far horizon image distortion. Rotation tests of the odometer in a lab environment gave an average error of 1° for a 45° rotation about the vehicle z-axis and 8° error for a 180° rotation. These were within an acceptable range, as demonstrated in the intersection navigation tests for turning in Younse (2005), allowing the visual odometer to guide the vehicle to a position in the intersection suitable for the turn. Any positional errors in the location of the vehicle turning center were dealt with successfully by the path following algorithm after the turn, which corrected any offset error and guided the vehicle towards the center of the second path. Finally, tests completed on concrete, sand, and gravel demonstrated adaptability of the odometer on different ground surfaces that are common in greenhouses.

The visual odometer can be improved by averaging vehicle translation and rotation over multiple points from several frames, as opposed to using just two features per frame. Utilization of techniques researched by Nistér et al. (2004) can allow the visual odometer to track features that aren't restricted to the ground plane.

## ACKNOWLEDGEMENTS

This research was conducted at the University of Florida, Institute of Food and Agricultural Sciences, through funding provided by the National Foliage Foundation.

## REFERENCES

1. Bouguet, J. 2004. Camera Calibration Toolbox for Matlab. Available at: [http://www.vision.caltech.edu/bouguetj/calib\\_doc](http://www.vision.caltech.edu/bouguetj/calib_doc). Accessed Aug. 2004.
2. Chojnacki, W., M. Brooks, A. Hengel, D. Gawley. 2003. Revisiting Hartley's Normalized Eight-Point Algorithm. *IEEE Transactions on Pattern Analysis and Machine Intelligence*, Vol. 25, No. 9.
3. Crane, C. & Duffy, J. 1998. Kinematic Analysis of Robot Manipulators. New York, New York: Cambridge University Press, 9.
4. Csetverikov, D. 2004. Basic Algorithms for Digital Image Analysis: a course. Budapest, Hungary: Institute of Informatics Eötvös Loránd University. Aug. 2004. Available WWW: <http://visual.ipan.sztaki.hu>
5. Have, H., S. Blackmore, B. Keller, H. Fountas, S. Nielsen, and F. Theilby. 2002. Autonomous Weeders for Christmas Tree Plantations- A Feasibility Study. *Pesticide Research 59*. Denmark: Danish Environmental Protection Agency, Danish Ministry of the Environment.
6. Hellström, T. 2002. Autonomous Navigation for Forest Machines: A Pre-Study. Umeå, Sweden: Department of Computing Science, Umeå University.
7. Nistér, D., O. Naroditsky, & J. Bergen. 2004. Visual Odometry. *Proceedings of the 2004 IEEE Computer Society Conference on Computer Vision and Pattern Recognition*, Vol. 1, 652-659.

8. Pollefeys, M. 2004, Spring. Visual 3D Modeling from Images. Tutorial Notes. Chapel Hill, NC: University of North Carolina.
9. Singh, S. 2004. Autonomous Robotic Vehicle for Greenhouse Spraying. ME thesis. Gainesville, Fla.: University of Florida, Department of Agricultural and Biological Engineering.
10. Singh, S., & V. Subramanian. 2004. Autonomous Greenhouse Sprayer Vehicle using Machine Vision and Ladar for Steering Control. *Proceedings of the 2004 ASAE Automation Technology for Off-road Equipment*, St. Joseph, Mich., 79-90.
11. Younse, P. 2005. Intersection Detection and Navigation for an Autonomous Greenhouse Sprayer using Machine Vision. ME thesis. Gainesville, Fla.: University of Florida, Department of Agricultural and Biological Engineering.



# STUDY OF THE STABILITY OF SELF PROPELLED HYDRODYNAMIC IRRIGATING MACHINE IN DIFFERENT OPERATIVE CONDITIONS

A. Formato<sup>1</sup>, S. Faugno<sup>1</sup> and G. Paolillo<sup>1</sup>

## ABSTRACT

This research program has concerned in the theoretical- experimental - numerical- analysis of the dynamic overturn of self propelled hydrodynamic irrigating machineries. Different stability conditions have been analyzed and the limit draught force has been evaluated in function of the soil slope, machine weight, rafter slope, friction coefficients and soil reaction forces and reported in table, which can easily be applied, make it possible for builders to evaluate the effect of each of these factors on the machine stability.

**KEYWORDS.** Hydrodynamic Irrigation Machine, Numerical Analysis.

## INTRODUCTION

Although the technological development has determined an evolution of the agricultural machineries, so much to be guaranteed comfort conditions for the operators, nevertheless operational conditions subsist for still some typologies of machineries that don't succeed in guaranteeing the safety of the operators, despite is present on the agricultural machineries safety devices that prevent even the occasional contact with the parts in movement of the machineries (carter, life belts, safety bonnets). Nevertheless the scientific contributions are still few for the evaluation of the parameters mechanical, operational and environmental useful to define the safety limit conditions, often increased by the fatigue of the drivers in relationship to other physical agents. Limited they are also the studies of the dynamics of the overthrow of the system formed of operative machine - tractor and of some operative machine in particular how the irrigating machines, used besides under very different operational conditions. Generally to avoid the turnover of the self propelled hydrodynamic irrigating machine caused by an excessive draught force, these machines have 3 stabilizers denominated rafter opportunely tilted respect to the vertical direction. Besides, this machine has a sensor that points out the machine slope during the operative phase of the machine to avoid its turnover. However despite all these regulations, during the operative phase of the machine, some unexpected critical conditions have happened, that have caused serious damages to the users.

## MATERIALS AND METHODS

In this research, a theoretical-numerical-experimental study of the dynamics of the overturn of the self propelled hydrodynamic irrigating machine has been performed. To better understanding the dynamics of the turnover and to determine the limit operative conditions dependent on machine-crop-soil interaction, the equilibrium conditions of the considered machine are considered, taking into account the friction conditions and the operative conditions of the considered system. Insofar a draft scheme has been performed for the considered machine and stability has been considered to the turnover during the working phase. Operative Machine is illustrated in figure 1 and in figure 2, the forces scheme is reported denoting with:  $T$  = draught force applied to 0.5 of the spool ray; parallel to the support plane;  $W$  = weight, applied in the barycentre G of the spool;  $T_w$  = resultant of the weight  $W$  and of the draught  $T$ , and it forms an angle  $\delta$  with the support plan;  $R_p$  = rafter

---

<sup>1</sup> Department of Agricultural Engineering and Agronomy, University of Naples "Federico II", Naples, Italy, formato@unina.it

reaction;  $R_a$  = support reaction;  $\alpha$  = Rafter Slope angle;  $\Psi$  = angle formed by the support plane with the horizontal plane;  $f_a$  = friction coefficient with the soil;  $f_b$  = friction coefficient between rafter and soil. Then in the point G of the spool will be applied the strength  $T'=T$ ; the force  $W$  and the moment  $M$  owed to the transport of  $T$  in G; such moment is

$$M = T * R$$

Besides, it has been evaluated the  $T$  value in function of  $\Psi, W, \alpha, f_a, f_b$ , and  $R_a$  considering an operative machine with the following characteristic data:  $\alpha = 33^\circ$ ;  $f_a = 0.3$ ;  $f_b = 0.6$ ;  $b_l = 1.2\text{m}$ ;  $W = 1300\text{ Kg}$  with unrolled pipe;  $W = 2000\text{ Kg}$  with rolled pipe;  $r = 0.6\text{m}$ ;  $m = 2\text{m}$ ;  $\Psi$  = ranging between  $0 - 30$ ;  $R_a = 0 - 100 - 200\text{ daN}$ . The draught forces have been calculated by a program code, and the values are reported in table.

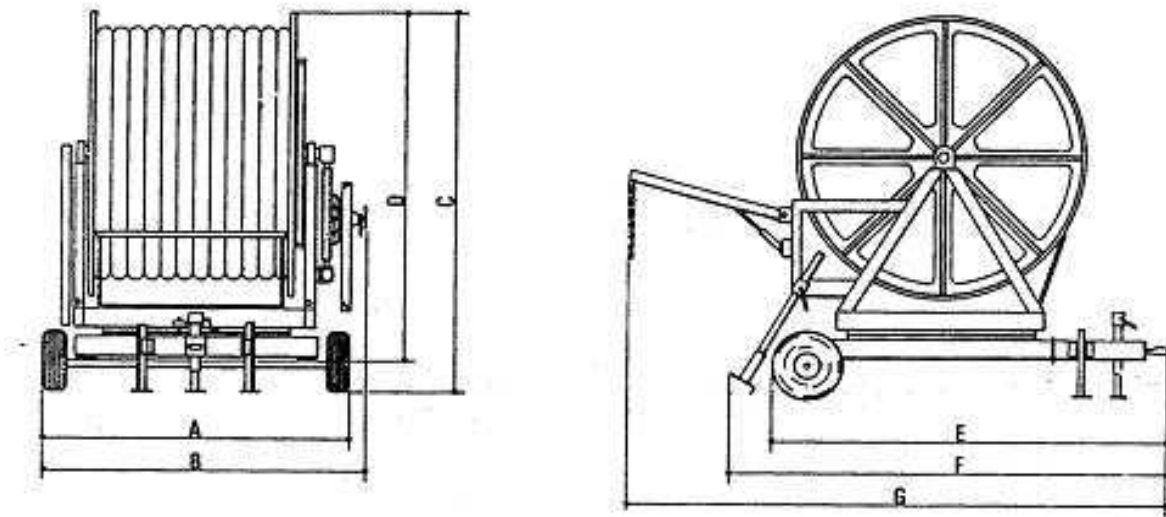


Figure 1. Self propelled hydrodynamic irrigating machine.

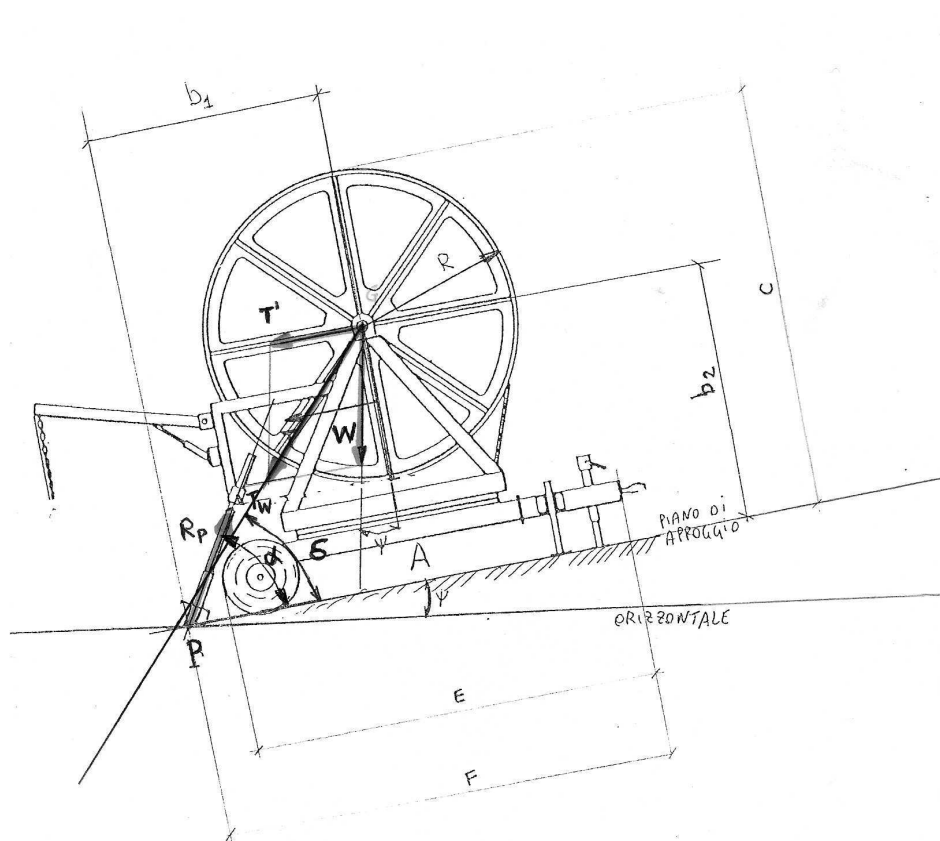


Figure 2. Force acting scheme.

**Table 1. Overall machine dimensions.**

	A	C	D	E	F	G	weight [kg]
dimension [mm]	2500	3900	3470	4200	4500	6500	4180

### Experimental tests

The followings critical conditions that happen during the phase of the rolling of the pipeline have to be considered: - water fill pipe and empty pipe; - dry and wet soil; - resistance to the wrapping of the pipe; - geometric parameters (barycentre position, masses etc.). Besides some experimental tests have been performed on an irrigating machine, in way to be able to compare the theoretical results with those experimental. Insofar a self propelled hydrodynamic irrigating machine has been considered and whose characteristic parameters are reported in table 1 , and the draught force value (T) necessary to wind the pipe was measured in different operative conditions (pipe length m. 250) of which about 240 m. in contact with the soil. As it regards the necessary draught force there is to observe that it is formed of:

- 1) a friction resistance of the pipe on the soil (that is function in turn of the pipe length),
- 2) a resistance to the advancement of the irrigator and
- 3) a resistance to the pipe wrapping depending in turn by the material characteristics, by the diameter of the wound coil and by the water pressure.

Three different operative conditions were considered:

- a) empty pipe, unrolled on the soil with an only coil wound on the spool,
- b) fill water pipe full, unrolled on the soil with an only coil wound on the spool,
- c) fill water pipe with pressure  $p = 8 \cdot 10^5$  Pa, unrolled on the soil with an only coil wound on the spool.

Besides with the purpose to evaluate the wrapping resistance of the considered pipe an experimental test has been performed preparing a device that allows to wind the empty pipeline (having inside diameter of 73 mm, external diameter of 90 mm, thickness of 8.5 mm) on a wheel with diameter of 1200 mm, and measuring the necessary tangential force to the wrapping (wrapping resistance). In this test a constant tangential force equal around 90 daN has been detected.

### Numerical tests

Besides, for a better understanding of the problem object of the present study, some simplified models to perform numerical simulations have been considered, by finite elements method and the obtained results have been compared with the experimental data. A 3-D geometric model has been performed of the considered machine (Fig.1) and different critical limit conditions have been considered and simulated by a program code, subsequently a combination among the different critical conditions have been performed determining other critical conditions that have been compared with those experimental ones.

## **DATA RESULTS AND DISCUSSION**

As it regards the experimental test a) considering 240 m. of empty pipe with weight of 432 daN, it has been detected experimentally a total draught equal to around 240 daN. Because the detected resistance to the pipe wrapping has been of 90 daN and that the resistance of the irrigator has been of around 20 daN, we can deduce that the friction resistance has to be equal to 129.6 daN that reported to the pipe weight of 432 daN implies that the friction coefficient is equal to 0.3. As it regards the experimental test b) considering 240 m of fill water pipe with weight of 1488 daN, a total draught has been detected equal around 550 daN. Because the pipe wrapping resistance is 90 daN, and that the irrigator resistance is around 20 daN, a friction resistance results equal to 446.4 daN. As it regards the experimental test c) considering 240 ms. of fill water pipe with weight of 1488 Kg, with water pressure of  $8 \cdot 10^5$  Pa, it has been detected a total draught of 650 daN with a

friction resistance of the irrigator of around 20 daN, with a friction resistance equal to 446.4 daN, it can be deduced a wrapping resistance of 190 daN. These values allow to deduce that in this case the increase of the only pressure in the pipe inside has involved an increase of the value of the pipe wrapping resistance of around 100 daN. That is the pipe is more rigid for which the wrapping resistance is increased. As it concerns the numerical results, by the obtained results we can deduce that with the friction coefficients used, during the dynamic analysis performed, the machine considered before overturns and after crawls because, at the same  $\gamma$  values, the  $T_t$  values that determine the crawling are all greater than the  $T_r$  values that determine the turnover and the obtained values are reported in table.2.

**Table 2. Slope angle Values  $\gamma$  in function of the draught force that provokes the turnover ( $T_r$ ) and the crawling ( $T_t$ ) for the considered machine.**

Ra [daN]	PSI [gradi]	$T_r$ [daN]	$T_t$ [daN]	W [daN]	Ra [daN]	PSI [gradi]	$T_r$ [daN]	$T_t$ [daN]	W [daN]
0	30	36	1770	1300	0	30	57	2708	2000
0	25	225	1987	1300	0	25	345	3040	2000
0	20	411	2184	1300	0	20	632	3341	2000
0	15	596	2364	1300	0	15	917	3616	2000
0	10	775	2531	1300	0	10	1197	3872	2000
0	5	948	2680	1300	0	5	1457	4100	2000
0	0	1114	2795	1300	0	0	1714	4376	2000
100	30	0	1585	1300	100	30	0	2523	2000
100	25	139	1802	1300	100	25	259	2855	2000
100	20	325	1999	1300	100	20	546	3161	2000
100	15	510	2179	1300	100	15	831	3431	2000
100	10	689	2346	1300	100	10	1111	3687	2000
100	5	862	2495	1300	100	5	1371	3915	2000
100	0	1028	2610	1300	100	0	1628	4091	2000
200	30	0	1400	1300	200	30	0	2338	2000
200	25	53	1617	1300	200	25	173	2670	2000
200	20	239	1814	1300	200	20	460	2981	2000
200	15	424	1994	1300	200	15	745	3246	2000
200	10	603	2162	1300	200	10	1025	3502	2000
200	5	776	2310	1300	200	5	1285	3730	2000
200	0	942	2425	1300	200	0	1542	3906	2000

## CONCLUSIONS

They have been considered critical limit conditions for the stability of self propelled hydrodynamic irrigating machine in different operative conditions, and experimental and numerical tests have been performed for their determination. The draught force values in different conditions have been evaluated through experimental tests:

- a) empty pipe, unrolled on the soil with an only coil wound on the spool,
- b) fill water pipe full, unrolled on the soil with an only coil wound on the spool,
- c) fill water pipe with pressure  $p = 8 \cdot 10^5$  Pa, unrolled on the soil with an only coil wound on the spool.

In the first case considered a draught force value has been found equal to around 240 daN, in the second case a draught force value has been found equal to around 550 daN, in the third case a draught force value has been found equal to around 650 daN. By the data analysis of the detected data in full field, on a machine spool with diameter of 127 cm, it is possible to deduce immediately that varying in the last two tests only the water pressure value, the total draught force value is

increased of 100 daN, which is to evidently attribute to the pressure changing which increases the polyethylene pipe rigidity. Besides through the numerical tests other limit conditions very dangerous have been determined during the pipe rewinding phase on clayey soil very water flooded (also for rain), with pipe entirely developed on the soil and sunk in it. In such critical conditions, it has been seen that a very high T value can be reached, that can provoke the turnover of the machine also for  $Y = 0$  (horizontal case).

## REFERENCES

1. Arndt J.F. (1971). Roll-over protective structure for farm and construction tractors – A 50 years review. ASAE Technical Paper Series 710508; Warrendale, PA.
2. Ayers P. D., Liu J. (1999). Off-road vehicle rollover and field testing of stability index. *Journal of Agricultural Safety and Health*, 5(1),59-71.
3. Conama. (1992). La tutela della sicurezza nell'uso delle macchine agricole. Ed. Clueb, Bologna,61-92.
4. Devis D., Rehkuger G. (1974). Agricultural Wheel-Tractor Overturns. *Transactions of the ASAE*. 17(3),477-483 e 484-488.
5. Gasparetto E. (1974). Rassegna Informativa. *Rivista di Ingegneria Agraria*, 5,79-100.
6. Harris J. R., Mucino V. H., Etherton J. R., Snyder K., Means K. H. (2000). Finite element modelling of ROPS in static testing and rear overturn. *Journal of Agricultural Safety and Health*, 6(3), 215-225.
7. Maresca A.(1994). Infortuni agricoli. *Macchine e Motori agricoli*, 7-8.
8. Martini P., Taglioli L. (1983). Prove funzionali su irrigatore semovente a pivot - L'irrigazione. *Luglio-Dicembre 1983*.
9. Myers J. R. (2000) Prevention Effectiveness of Rollover protective structure, parts 1,2,3, *Journal of agricultural Safety and Health*, 6 (1), 29-70.
10. Pana-Cryan R., Myers M. L. (2000). Prevention Effectiveness of Rollover Structures-Part III: Economic Analysis. *Journal of Agricultural Safety and Health*, 6(1), 57-70.
11. Romano F., Formato A. (1997). Caratteristiche funzionali e costruttive delle irrigatrici idrodinamiche semoventi e loro influenza sulla sicurezza degli addetti all'utilizzazione. *Atti del VI Convegno Nazionale AIIA*, 9-12 settembre, Ancona, 4, 207-216.
12. Romano F., Formato A., Capaldo A. (2002). Considerazioni sulla sicurezza delle macchine agricole in particolari condizioni di impiego. *Atti del Convegno Nazionale AIIA*, 11-15 settembre, Alghero (SS), 1, 119-125.



# ENHANCEMENT OF INFORMATION FROM SATELLITE IMAGERY BY INTEGRATING AN UNMANNED HELICOPTER

I. Han-Ya<sup>1</sup>, K. Ishii<sup>1</sup>, N. Noguchi<sup>1</sup>, K. Niwa<sup>2</sup> and J. Yokobori<sup>2</sup>

## ABSTRACT

Precision farming (PF) was begun in the latter 20th century. In Japan and other countries, there are many researches on remote sensing use different kinds of sensors and platforms. One of the applications of the remote sensing in agriculture is to obtain crop status. Recently, field images can be obtained by QuickBird-2, SPOT and other satellites. However, these satellites are affected by the atmospheric conditions, and also the spatial resolution is fairly low. In addition, the images taken by these satellites have large position errors. And generally, the large number of ground truth reference points must be set to make image calibration to be successful.

The objective of this study is to develop a reliable field monitoring system combining helicopter-base and satellite-base remote-sensing. Since an ambient illumination (AI) sensor is attached on the unmanned helicopter, an effect of atmospheric condition to a satellite image can be compensated. The normalized difference vegetation index (NDVI) of satellite was transformed to reflectance value through image by the unmanned helicopter. In addition, the images taken by the helicopter were also used for calibration of satellite imagery. Therefore, the helicopter-base system will contribute to enhance the satellite-base remote-sensing.

**KEYWORDS.** Limit of Resolution, NDVI, Precision Farming, QuickBird-2, SPOT5.

## INTRODUCTION

Remote sensing is used not only for agricultural environment monitoring but also for many cases such as detecting forest fires, observing disaster circumstances and making a plan for the urban development. Large information is needed for these kinds of cases. To get large information, sensing platforms are necessary to use such as helicopter, airplane and satellite. These sensing platforms can easily get large information.

Recently, researchers are studying on the remote sensing for various fields. In Japan and other countries, different kinds of sensors and platforms are used on studying remote sensing. Crop information status is one of the applications of remote sensing. Usually QuickBird-2, SPOT5 and other satellites obtain field images and using different methods crop information status can be determined from these field images.

In Hokkaido, Japan satellite image is used for rice and wheat fields (Okuno et al., 2005). It is used for monitoring the crop and soil status. However, these satellite images are affected by the atmospheric conditions, and also the spatial resolution is low. And generally, the large number of ground truth reference points must be set to make image calibration success. It requires much labor and time to get the ground truth data. In order to resolve these problems, combining helicopter image and satellite image is a useful method (Noguchi, 2003) (Niwa, 2004). The goal of this research is to normalize and enhance the information on the satellite image such as green, red, near infrared and normalized different vegetation index (NDVI).

---

<sup>1</sup> Bio-production Engineering, Graduate School of Agriculture, Hokkaido University, Kita 9, Nishi 9, Kita Ku, Sapporo, Japan, issei@bpe.agr.hokudai.ac.jp

<sup>2</sup> Zukosha Co.,Ltd., Kita 1, Nishi 18, Obihiro, Japan

## SYSTEM SENSING PLATFORM

In this research, unmanned helicopter was used equipped with machine vision. It flies at a low altitude and the machine vision has high resolution. Figure 1 shows the sensing platform. The helicopter's machine vision used in this research was Duncan tech MS2100. It has 640 x 480 pixels and its diagonal angle of view is 26.51 [°]. Accordingly its resolution depends on the altitudes of the helicopter. The altitudes were 5 [m] and 25 [m] when imageries were acquired. The area of imageries was 1.4x1.9 [m] and 7.1x9.4 [m]. Table 1 shows the specification of different sensors. Figure 2 shows the filter characteristic of MS2100.

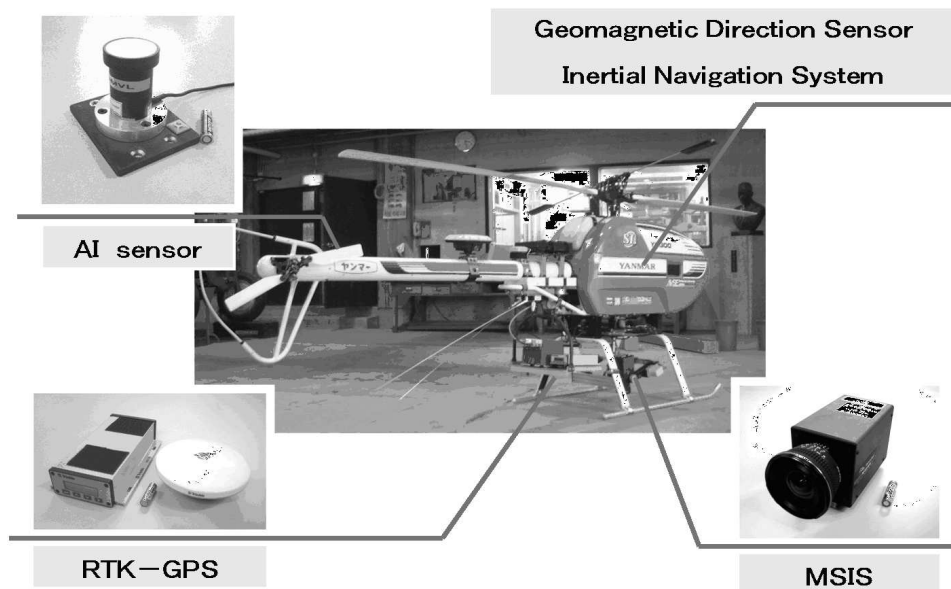


Figure 1. Helicopter-base sensing system.

## METHODS

The helicopter images are affected by various factors such as sun light. But the effects can be removed by a correcting equation. Therefore, helicopter image can get the absolute color of the object. The satellite imageries can take the imagery of the wavelength range of blue, green, red and NIR. Corrected color information of satellite imagery was written as  $B$ . SPOT5 images are corrected by equation 1, and QuickBird-2's are by equation 2:

$$B_{SPOT5} = GL/C \quad (1)$$

$$B_{QuickBird-2} = C GL \quad (2)$$

where  $GL$  is gray level,  $C$  is given every imagery.

Corrected color information of helicopter imagery was written as  $Ref$ . This is the information removed the effects of the ambient illumination ( $AI$ ), exposure time ( $Exp$ ) and CCD gain ( $Gain$ ) shown in equation 3.

$$Ref = \frac{C_0 GL + C_1}{(AI + C_2)(Exp + C_3)(e^{C_{gain}} + C_5)} \quad (3)$$

These parameters are explained in following:

$$AI = C_{AI} (E_{AI} + BL)$$

$$GL \propto a_{AI} AI + b_{AI} \quad (4)$$

where  $AI$  is the ambient illumination [ $\mu\text{mol}/\text{cm}^2$ ],  $C_{AI}$  is a scale factor [ $\mu\text{mol}/\text{cm}^2/\text{mV}$ ],  $E_{AI}$  is measured voltage [V] and  $BL$  is black level voltage [V].

$$t_{Exp} = C_{Exp} \cdot Pixels \cdot Exp$$

$$GL \propto a_{Exp} Exp + b_{Exp} \quad (5)$$

$t_{Exp}$  is exposure time [ms],  $C_{Exp}$  is a scale factor[ms/line](In the case of MS2100 is 0.065.),  $Pixels$  is number of pixels in every each line (In the case of MS2100 is 640) and  $Exp$  is a digital value indicating exposure time of MS2100.

$$r = \log_{10}(V_o/V_I) = \ln(V_o/V_I)/\ln 10 = 0.094Gain - 4$$

$$V_o/V_I = e^{0.021644 Gain - 0.921034}$$

$$GL \propto e^{a_{Gain}Gain - b_{Gain} + c_{Gain}} \quad (6)$$

$r$  is a input-output gain [db],  $Gain$  is a digital value indicating a gain of MS2100.

$$GL = s \cdot GL_{out} - GL_0 \quad (7)$$

$GL$  is a real gray level,  $GL_{out}$  is a gray level acquired from MS2100 and  $GL_0$  is an offset of gray level.

To acquire coefficients ( $C_0 - C_5$ ), the basic test was performed using a color scale. Using this data, nonlinear regression analysis was used with least square.

Positioning data of the helicopter were measured by real-time kinematic global positioning system (RTK-GPS). Attitude angle of helicopter were measured by inertial measurement unit (IMU). Positioning data of the helicopter imageries were calculated from these data (Sugiura et al., 2003).

Both satellite imageries were taken on July 18th in 2004. The helicopter imageries were taken on July 15th in 2004.

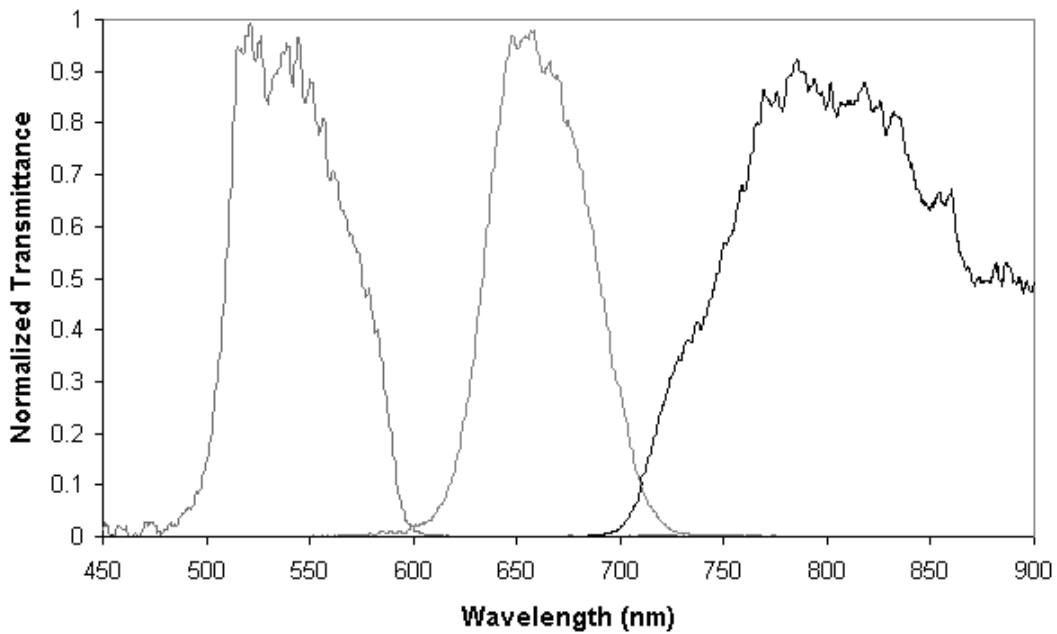


Figure 2. The filter characteristic of MS2100.

**Table 1. Specification of the sensors.**

		SPOT5	QuickBird-2	Helicopter
Altitude	[m]	$822 \times 10^3$	$450 \times 10^3$	5 - 10
Resolution	[m]	10	2.5	$3 - 15 \times 10^{-3}$
Multi spectral wave range [ $\times 10^{-9}$ m]	Blue	-	450 - 520	-
	Green	500 - 590	520 - 600	540
	Red	610 - 680	630 - 690	660
	NIR	780 - 890	760 - 900	810
	SWIR	1580 - 1750	-	-

## RESULTS AND DISCUSSION

### Relationship between satellite and helicopter

In this research, we used the multi-spectral imageries taken by SPOT5, QuickBird-2 and helicopter. These imageries were synchronously taken. As every vision covers the same wavelength range and takes same objects, the color information of the satellite and helicopter images will be integrated. At first, the relation of the information on green, red and NIR were examined. Figures 3 and 4 shows the relationship between the sensors.

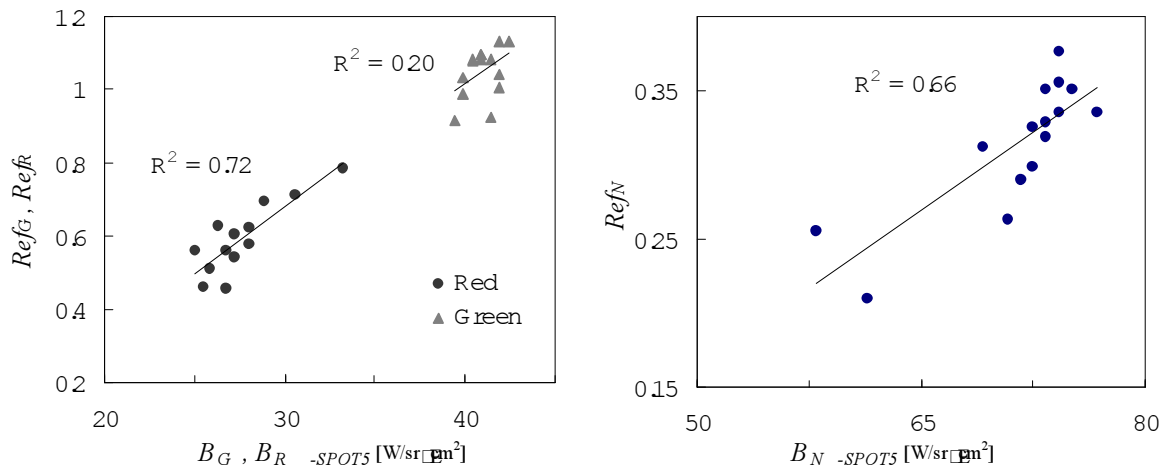


**Figure 3. The relationship between SPOT5 imageries and helicopter imageries.**

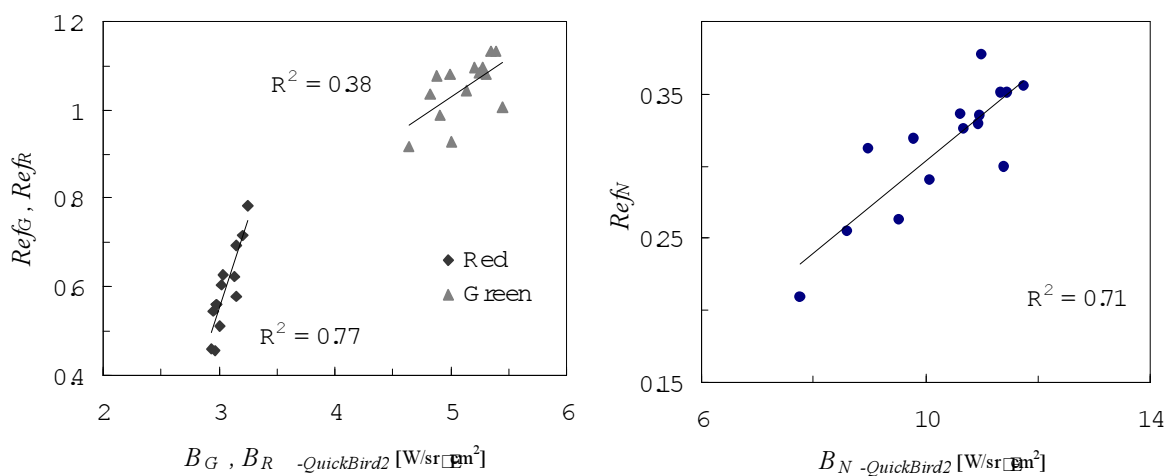


**Figure 4. The relationship between QuickBird-2 imageries and helicopter imageries.**

In the figures, there is high correlation in the information about the red and NIR, but there is low correlation about green. The cause is Rayleigh scattering. Rayleigh scattering is the scattering of light, or other electromagnetic radiation, by particles much smaller than the wavelength of the light. It occurs when light travels in transparent solids and liquids, but is most prominently seen in gases. The wavelength of green is short. Therefore, it is easy for green to be scattered.

Next, the relation of the information on NDVI was examined. NDVI is the value which used red and NIR. The leaf of the plant absorbs red and reflects NIR (Fig. 5). So NDVI is used when estimating the plant growth.

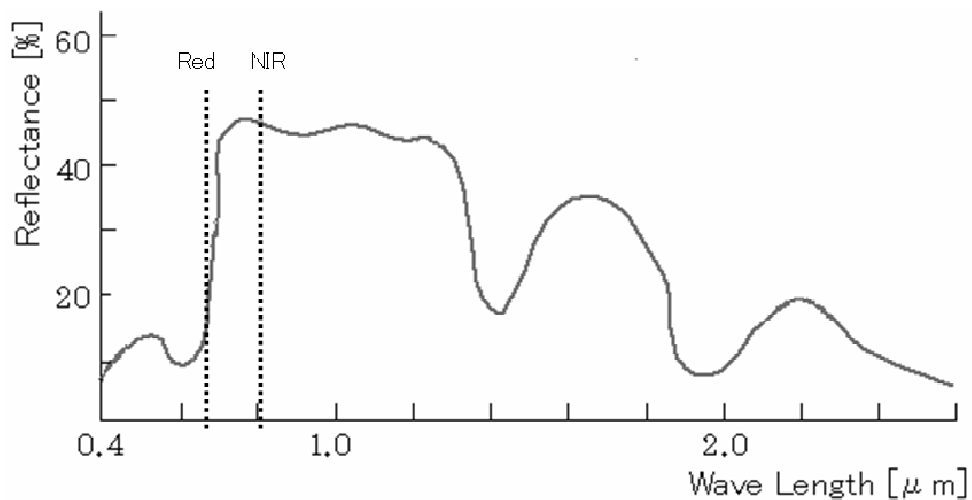
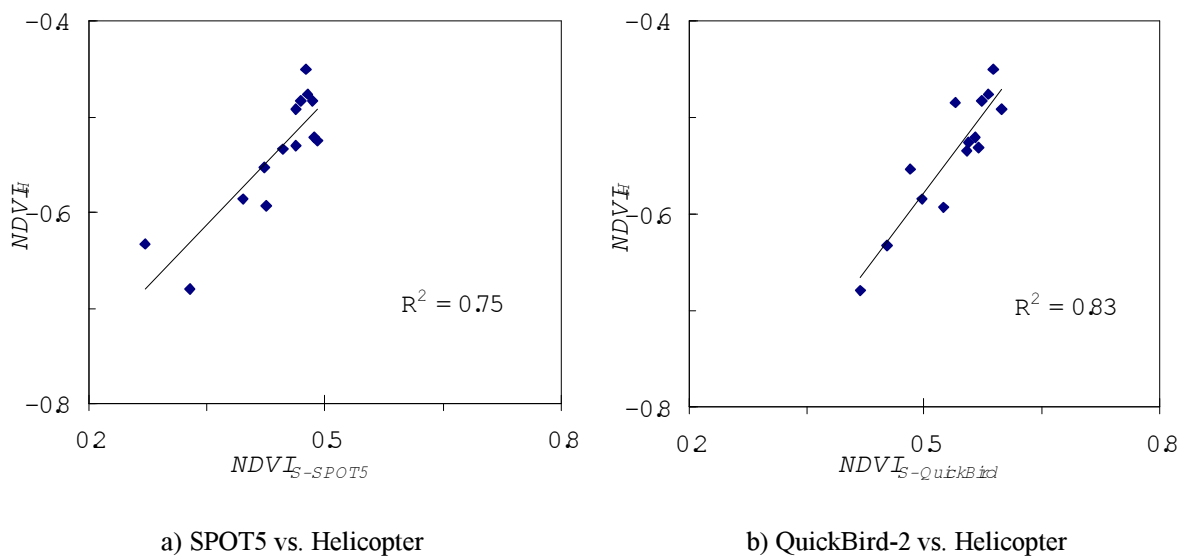


Figure 5. The spectral reflectance of the leaf.

$NDVI_S$  is the satellite-base NDVI given by the equation 8, and  $NDVI_H$  is helicopter-base NDVI given by the equation 9.

$$NDVI_S = \frac{B_N - B_R}{B_N + B_R} \quad (8)$$

$$NDVI_H = \frac{Ref_N - Ref_R}{Ref_N + Ref_R} \quad (9)$$



a) SPOT5 vs. Helicopter

b) QuickBird-2 vs. Helicopter

Figure 6. The relationship between  $NDVI_S$  and  $NDVI_H$ .

There is high correlation between satellite-base NDVI and helicopter-base NDVI (Fig. 6). It is possible for helicopter imageries to do luminous environment revision. Therefore, it is possible to do revision of the color information on the relative satellite imageries in using helicopter imageries.

## CONCLUSION

The research developed a reliable field monitoring system by normalizing and enhancing the information on the satellite imagery and the helicopter imagery that can do luminous environment revision and with high resolution such as green, red, NIR and NDVI. On the color of red and NIR, there is high correlation between satellite imagery and helicopter imagery. Figure 6 suggests that there is also high correlation between satellite-base NDVI and helicopter-base NDVI. Therefore, it is possible to do revision of the color information on the relative satellite imageries in using helicopter imageries. Using these color information, the field status can be estimated without ground truth data.

## REFERENCES

1. Okuno, R. and Hongou, C. 2005. Remote Sensing Using Satellite Imageries (in Japanese). Journal of Hokkaido Branch of the Japanese Society of Agricultural Machinery. Vol.45. 119-125.
2. Noguchi, N. 2003. Field Monitoring Based on Unmanned Helicopter. ENVIRONMENT CONTROL IN BIOLOGY [Biological monitoring and control under the outdoor environment] 41-47.
3. Niwa, K. 2004. The Conditions of Precision Farming in the United States of America and That Introduction to Tokachi District. Journal of Hokkaido Branch of the Japanese Society of Agricultural Machinery. Vol.44. 101-105.
4. Sugiura, R., Noguchi, N., Ishii, K. and Terao, H. 2002. Remote Sensing Technology for Field Information Using Unmanned Helicopter. ATOE. 120-128.
5. Waladi, W., B. Partek, and J. Manoosh. 1999. Regulating ammonia concentration in swine housing: Part II. Application examples. *Trans. ASAE* 43(4): 540-547.

# DEVELOPMENT OF SURVEYING SYSTEM FOR GRASSLAND USING A LASER SCANNER MOUNTED ON A ROBOT TRACTOR

T. H. Kang<sup>1</sup>, K. Siramizu<sup>1</sup>, K. Ishii<sup>1</sup> and N. Noguchi<sup>1</sup>

## ABSTRACT

Recently, large machinery is introduced for the grass harvesting in dairy farming. To improve the working efficiency of the large machinery, it is necessary to modify the irregularities of the field terrain, but there are no effective criteria for modification of irregularities of the grassland. One of the important factors to consider in modification of irregularities is inclination angle of the grassland which is calculated from the geographical features. The objective of this research is to develop a surveying system using a laser scanner attached on the robot tractor. The scope of the study is to get a terrain and vehicle dynamics during operation on a grassland. The research used a 56-kW tractor that was modified into a robot tractor and a 2-dimensional laser scanner which gathers environment information such as distance and angle of the object in front of the sensor. The measured terrain by the laser scanner and vehicle dynamic information such as accelerations and vehicle inclinations by an inertial measurement unit (IMU) during grass harvest were used to generate GIS maps. Since measurement of a vehicle location is essential to make a geographical information system (GIS) map, a real-time kinematic global positioning system (RTK-GPS) provided the vehicle absolute positions. The results of the field test showed a root mean squared (RMS) error of 2.9 cm when the laser was scanning directly below the robot tractor. The R.M.S. error of the laser scanning at 2 m and 4 m with respect to robot tractor centerline were 4.6 cm and 4.4 cm respectively. Finally, the generated GIS maps were used to modify the irregularities of the field terrain.

**KEYWORDS.** GIS, Grassland, IMU, Laser Scanner, Robot Tractor, Surveying System.

## INTRODUCTION

Japan agriculture is confronted with the labor shortage, the aging of the farmers, and the decrease of numbers of the farmers. One possible solution to these problems is the use of advanced production management information which might be promoted a labor saving and lowering the cost of the agricultural outputs. Advanced information management can be achieved by applying information technology (IT), such as geographic information system (GIS). Hokkaido Development Bureau in Japan performed a development plan investigation project in 2003 entitled "Using of the new land and the investigation of the farm village creation business by the IT agriculture" (Chiba, 2005). The project investigated remote sensing of the ground by using low altitude sensing and satellite sensing. And it also gathered various viewpoints of the information management by using the GIS in different private and public sectors. The result of the project suggested that the need of land improvement is necessary from the various information of the GIS, and it was confirmed that the development of new farming by efficient field management is attainable, such as variable fertilization (Hara, 2005; Ishii, 2005; Okuno and Hongo, 2005; Niwa and Yokobori, 2005). Moreover, other studies used satellite image and unmanned helicopter for acquiring environmental information. The relationship among the geographical features, soil moisture and humus content rate of the soil was determined (Inoue, 1997; Sugaira et al., 2003; Yokobori et al., 2004).

---

<sup>1</sup> Graduate School of Agriculture, Hokkaido University, Sapporo, Japan, lamokthk@avse.bpe.agr.hokudai.ac.jp

The objective of this research is to develop a surveying system using a laser scanner mounted on front of the robot tractor. The robot tractor autonomously ran 2 m mesh in the field. Then, selected geographical feature data were collected. From these data the accuracy of the geographical features were evaluated.

## MATERIALS

Figure 1 illustrates the configuration of the surveying system. The research used a standard 56-kW tractor (MD77, Kubota ltd.) that was modified into a robot tractor as the sensing platform. It controlled most of its functions by a computer connected to control area network (CAN) communication, such as steering angle, engine speed, throttle position, three-point hitches (up and down), etc. To gather spatial information, a laser scanner (SICK LMS291) was used. This sensor radially scanned in a plane over 180 degrees with an angular resolution of 1 degree. It measured the relative position such as distance and angle of existing objects in front of it with a set maximum range of 80 m and a measurement error of  $\pm 5$  cm. The laser scanner was installed in the counter weight part of the robot tractor facing the ground. To generate a GIS map based on spatial information, vehicle location is essential; RTK-GPS, Trimble MS750 provided vehicle positions, and an IMU (JCS7401A, Japan Aviation Electronics Industry) provided direction and inclination angles.

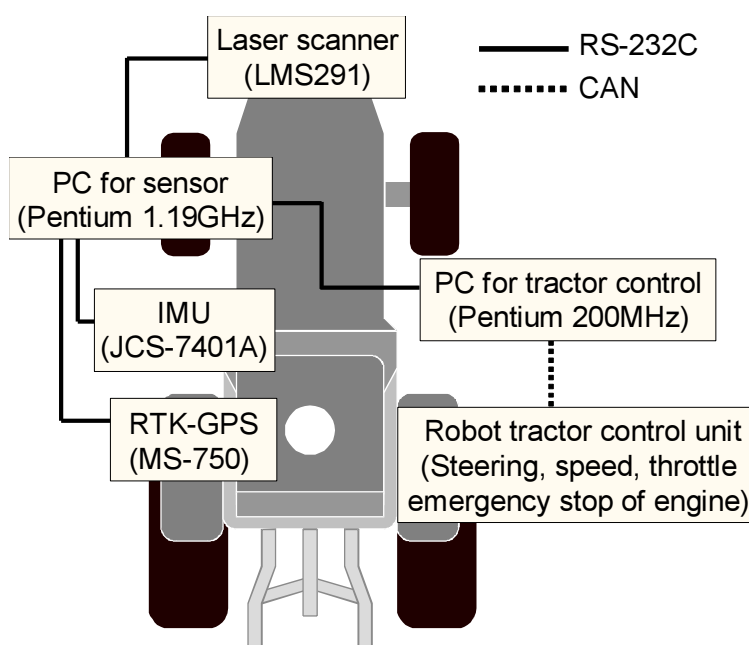


Figure 1. Schematic diagram of field information sensing system.

## METHODS

### Evaluation of geographical features data

Field tests were conducted at the grassland of Nakafurano in Japan. The area was 1.2 ha. The robot tractor was autonomously driven following the navigation paths with 2-m space mesh, while vehicle locations and terrain information were simultaneously measured and recorded to the PC. To evaluate the change of geographical features, irregularity modification is needed before and after measurement of the data. The robot tractor entire running speed was set to 1.2 m/s, and measured about 47 running trajectory for a period 74 minutes.

### Extraction of geographical features data

The accuracy of the developed terrain surveying system was evaluated. The reference terrain data was calculated from robot tractor's position. However, obtained position data was corrected by using the inclination angle of the robot tractor measured by IMU (Mizushima, 2000). As for the laser scanner, 181 measurement points can acquire in a single scan measurement. It is necessary to

extract data according to the sampling interval of the geographical features data that becomes the reference data. Figure 2 shows the extraction concept of the geographical features data with the laser scanner. The base line was derived from a vehicle position and the direction. The equation of the base line is given by equation (1).

$$(X - X_i)\cos\phi - (Y - Y_i)\sin\phi = 0 \quad (1)$$

$(X_i \ Y_i)^T$  is a plane position of the irradiation point, and  $\phi$  is direction of the vehicle. When the sampling interval of standard data is assumed to be  $L$ , the point where the distance from this base point line is the shortest to  $L$  have been extracted. The point to assume  $D$  to be minimal derived an equation (2).

$$D = \left| (X - X_i)\cos\phi - (Y - Y_i)\sin\phi - L \right| \quad (2)$$

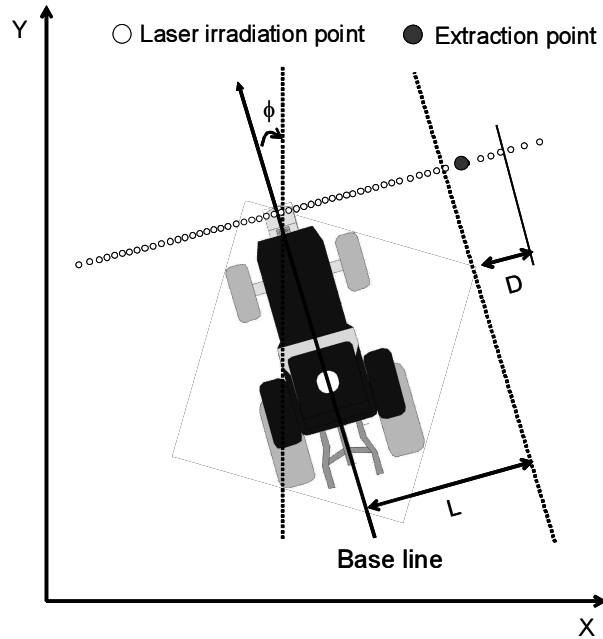


**Figure 2. Topographical data extraction by laser scanner.**

Figure 3 shows the concept of calculating the error of the laser irradiation point. Altitude  $Z_r$  as the reference point corresponding to the position of the laser irradiation point was used the position and altitude of two sampling points expressed in equation (3).

$$Z_r = (1-t)Z_i + tZ_{i+1} \quad (3)$$

However,  $t = \frac{l_{i,j}}{l_j}$ ,  $l_j = l_{i,j} + l_{i+1,j}$

$Z_i, Z_{i+1}$  is an altitude measured by GPS.  $l_j$  is distance deflection of two sampling points.  $l_{i,j}, l_{i+1,j}$  is distance deflection between the laser irradiation point and each sampling point. Therefore, if the altitude of the laser irradiation point is assumed to be  $Z_l$ , the error  $\varepsilon_z$  can be calculated in equation (4).

$$\varepsilon_z = Z_l - Z_r \quad (4)$$

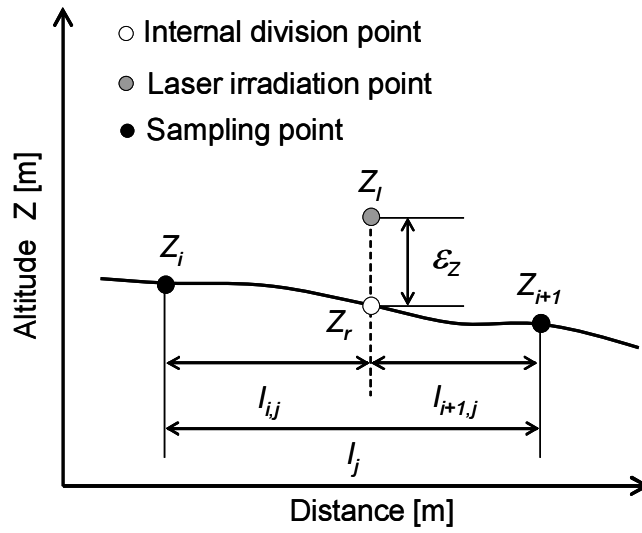


Figure 3. Calculation of error using topographical data measured by laser scanner and robot tractor.

## RESULTS AND DISCUSSION

### Accuracy evaluation

Figure 4 shows three conditions of evaluating the accuracy. Three point-data of 0 m, 2 m and 4 m with respect to the centerline of the tractor obtained by the laser scanner were used to generate the topographical map. If the two position data, 0 m and 2 m from the center can be applied, the map can be generated by 6-m space navigation paths. That means a required time was reduced up to 1/3 of the original working time. Table 2 shows the relationship between the result of the accuracy evaluation and working time. The mean error of maps generated by spaces of 0 m, 2 m and 4 m were 5.2 cm, 16.6 cm, and 21.4 cm, respectively.

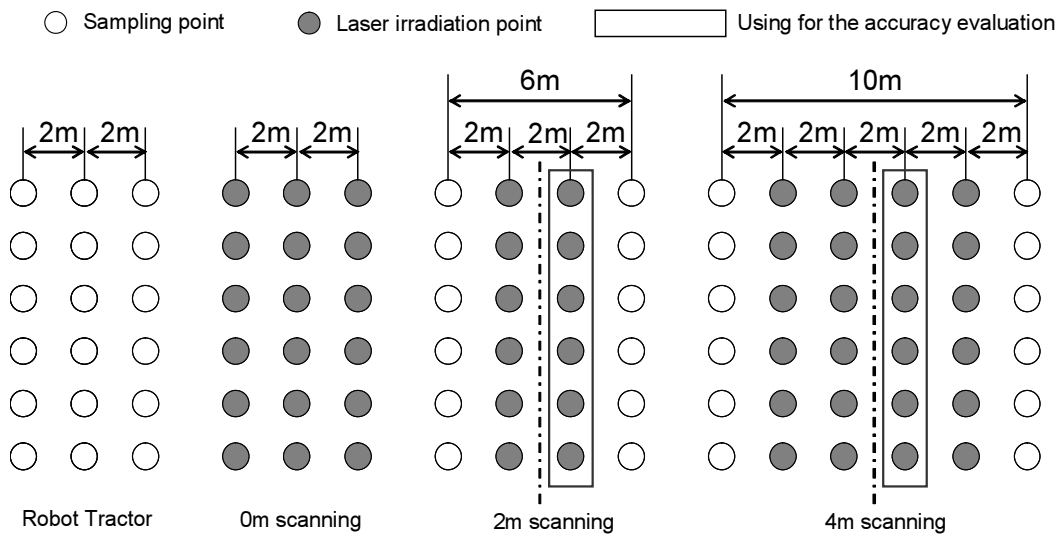


Figure 4. Accuracy evaluation model of laser scanner.

Table 1. Error and working time by the scanning conditions.

Width of scanning	Error [cm]	Working time [min]
0 m	5.2	74
2 m	16.6	25
4 m	21.4	15

## GIS maps of geographical features information

Figure 5 shows the geographical features map using the data obtained by the laser scanner and standard geographical features map using the robot tractor data. When standard geographical features map (Fig. 5a) is compared with 0 m scanning condition (Fig. 5b), the part that corresponds to the contour line is smoothed, but the tendency as the whole looks similar. Figure 5c and figure 5d show the geographical features map was made by scanning distance 2 m and 4 m, respectively. The part on the northeast side shows the tendency of a little uneven compared with the topographical map (Fig. 5a) that becomes a standard. However, a similar result is seen overall the field.

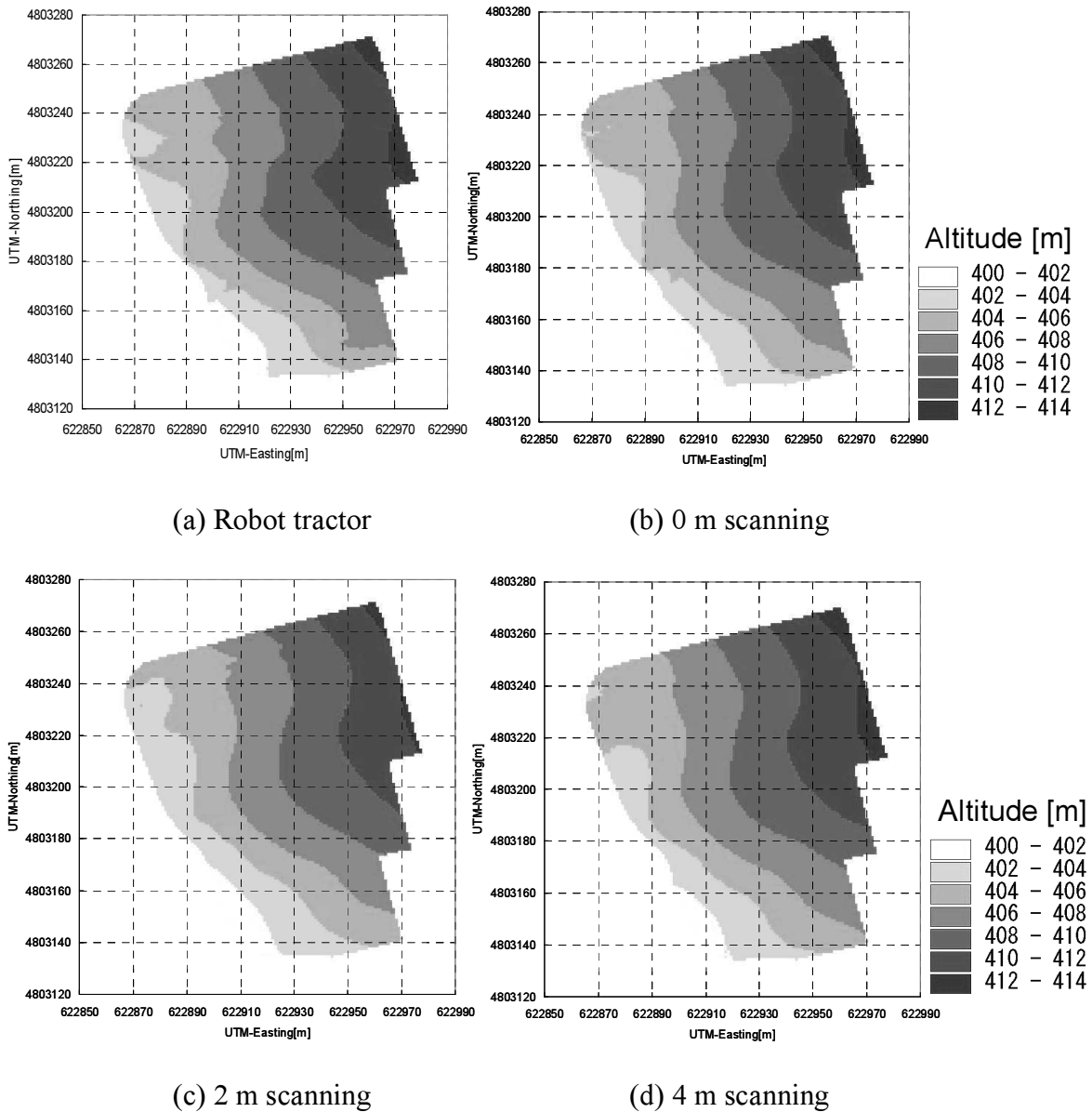


Figure 5. Topographical maps measured by robot tractor and laser scanner.

## CONCLUSIONS

This research uses the laser scanner mounted on the robot tractor to gather terrain information of a field, to make management decisions both efficient and precise. The GIS map was also generated using the obtained data. The laser scanner was scanning on the front of the robot tractor facing the ground, at 0 m, 2 m and 4 m from the tractor's centerline, and it was autonomously driven by navigation paths with 2 m space mesh in the field. The vehicle locations and terrain information were simultaneously measured and recorded. As a result, when the laser was scanning at the beneath of the robot tractor, average error of 5.2 cm. At 2 m, average error was 16.6 cm; at 4 m, the average error was 21.4 cm.

## REFERENCES

1. Chiba, Y. 2005. The development of investigation on IT Agriculture by Hokkaido Regional Development Bureau and the actual state of IT agriculture in USA (in Japanese). Journal of Hokkaido branch of JSAM, 45, 103-107.
2. Hara, K. 2005. Precision agriculture applying ground base remote sensing (in Japanese). Journal of Hokkaido branch of JSAM, 45, 109-112.
3. Inoue, Y. 1997. Remote sensing of crop and vegetative environment (Part2). Journal of Japan remote sensing society, 17(4), 57-67.
4. Ishii, K. 2005. Field Environment monitoring using an unmanned helicopter (in Japanese). Journal of Hokkaido branch of JSAM, 45, 113-117.
5. Mizushima, A., Noguchi, N., Ishii, I., Terao, H. 2000. Correction of GPS position by vehicle inclinations for agricultural vehicle guidance, Journal of JSAM, 62(4), 146-153.
6. Niwa, K., Yokobori, J. 2005. Field Management applying information technology in Tokachi District of Hokkaido (in Japanese). Journal of Hokkaido branch of JSAM, 45, 131-135.
7. Okuno, R., Hongo, C. 2005. The application of satellite remote sensing (in Japanese). Journal of Hokkaido branch of JSAM, 45, 119-125.
8. Sugiura, R., Noguchi, N., Ishii, K., Terao, H. 2003. Development of remote sensing system using an unmanned helicopter (Part1). Journal of JSAM, 65(1), 53-61.
9. Yokobori, J., Niwa, K., Sugiura, R., Noguchi, N., Chiba, Y. 2004. Variable management for uniform potato yield using remote sensing Images with unmanned helicopter. Proceedings of the 2004 ASAE International Conference on Automation Technology for Off-road Equipment, 447-454.

# A TRIPLET-APPLICATION OF A STEREOVISION-BASED FIELD RECOGNITION SYSTEM

M. Kise<sup>1</sup>, Q. Zhang<sup>2</sup> and Y. Yu<sup>2</sup>

## ABSTRACT

This research aims to develop a stereovision-based field recognition system capable of detecting crop row in 3D for tractor guidance, assessing crop growth conditions via 3D field mapping, and providing real-time tractor stability prediction for preventing rollover accident. The vehicle guidance application detects the relative position of the vehicle with respect to the crop rows in a 3D crop elevation map then creates a navigate control signal to guide the vehicle following crop rows. Meanwhile, the same stereovision sensor can be used to make a direct measurement of plant biophysical parameters, such as the height, canopy area and volume of crops, to support real-time crop growth assessment. In addition, by integrating with a vehicle attitude sensing unit, this stereovision system can also perform an on-line prediction to assess the possibility of tractor rollover in terms of detected look-ahead terrain and motion status of the vehicle. A series of field validation tests indicated that this stereovision system can accomplish all three functions by navigating a tractor following crop rows with a trajectory tracking accuracy of 0.10 m, creating a 3D field map to measure crop heights within an RMS error of 0.04 m, and predicting tractor postures approximately 8.0 m ahead of its actual position with consistent accuracy.

**KEYWORDS.** 3D Field Map, Stereo Vision, Tractor Automation, Tractor Rollover, Vehicle Motion Simulator.

## INTRODUCTION

Three machine vision-based applications, consisting of tractor automation guidance in rowed crop field, 3D field mapping for crop growth assessment, and online tractor motion simulation for rollover precautions, are integrated based on one stereo camera and implemented on agricultural machinery. The motivation of creating the three-in-one technology is very simple — to improve operation efficiency by increasing the productivity and safety. Automated guidance can greatly reduce driver fatigue and therefore increase both productivity and safety of the operation. By understanding the status of crop growth, in-season site-specific nutrient management can be practiced without sacrificing productivity. Not only are their driving forces in common; the information obtained from either application carries additional information for supporting the other application. However, even though three applications have such a similarity, numerous researchers have developed these applications separately (Tsai and Huang, 1984; Adiv, 1985; Tomasi and Kanade, 1991; He et al., 2003; Rovira-Más et al., 2005; Lines et al., 2001).

## 3D FIELD RECOGNITION SYSTEM

### 3D Elevation Map Construction

A stereovision camera consists of two identical cameras with their optical axis being geometrically arranged in parallel. A stereo image attains the 3D field scene information by means of recording the same field scene from slightly offset viewpoints using the two constructing cameras. The 3D elevation map created from a stereo image of the scene is baseline data of the triplet application in this research. In guidance application, the relative position of vehicle to crop rows is measured

---

<sup>1</sup> U.S. Department of Agriculture, Agricultural Research Service, Athens, GA30605, USA, mkise@saa.ars.usda.gov

<sup>2</sup> University of Illinois at Urbana-Champaign, Urbana, IL 61801, USA

based on the elevation difference between crop rows and the ground in the 3D elevation map. An elevation map created from each stereo image is integrated to form the map of entire field as crop growth assessing carrier. For a tractor rollover prediction, a vehicle motion described by vehicle postures is dynamically simulated as a hypothetical vehicle travels on a reconstructed virtual 3D terrain map.

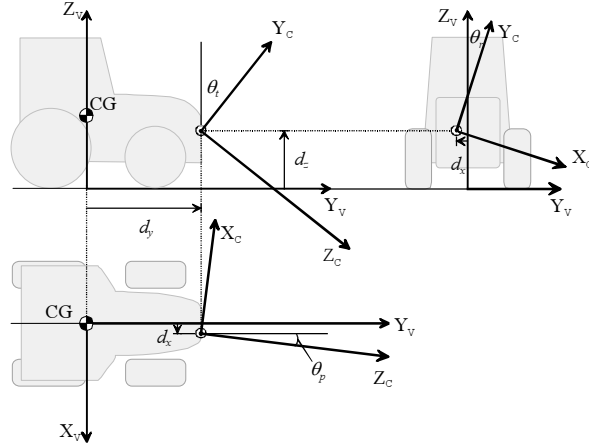


**Figure 1. Coordinates systems for the 3D field mapping system.**

The ground coordinates  $X_G Y_G Z_G$  of the elevation map is defined by setting its origin at the vehicle CG as shown in figure 1. The  $X_G$  and  $Y_G$  axes are defined as the vehicle longitudinal and lateral directions and the  $Z_G$  axis is defined in parallel to the gravity direction, respectively. Similarly, the camera coordinates  $X_c Y_c Z_c$  is defined by setting its origin at the center of the left camera focal point, with its  $X$ ,  $Y$  and  $Z$  axis arbitrarily defined. To create a 3D virtual terrain in front of the vehicle, it is necessary to convert the locations of 3D points in the stereo image from the camera coordinates into the ground coordinates. This transformation is expressed as follows:

$$\begin{pmatrix} x_g \\ y_g \\ z_g \end{pmatrix} = \begin{pmatrix} 0 & 0 & 1 \\ -1 & 0 & 0 \\ 0 & -1 & 0 \end{pmatrix} R_Y(\sigma_y) R_X(\sigma_x) R_Z(\sigma_z) \begin{pmatrix} x_c \\ y_c \\ z_c \end{pmatrix} + \begin{pmatrix} x_d \\ y_d \\ z_d \end{pmatrix} \quad (1)$$

Where,  $\sigma_x$ ,  $\sigma_y$ , and  $\sigma_z$  are the tilt, pan and roll angles of the camera mount,  $(x_d, y_d, z_d)$  is the camera position offset to the tractor CG.  $R_X$ ,  $R_Y$  and  $R_Z$  are rotation matrices around  $X_c$ ,  $Y_c$ , and  $Z_c$  axes as defined below:

$$R_X(\theta) = \begin{pmatrix} 1 & 0 & 0 \\ 0 & \cos \theta & \sin \theta \\ 0 & -\sin \theta & \cos \theta \end{pmatrix}, R_Y(\theta) = \begin{pmatrix} \cos \theta & 0 & -\sin \theta \\ 0 & 1 & 0 \\ \sin \theta & 0 & \cos \theta \end{pmatrix}, R_Z(\theta) = \begin{pmatrix} \cos \theta & \sin \theta & 0 \\ -\sin \theta & \cos \theta & 0 \\ 0 & 0 & 1 \end{pmatrix}$$

Where  $\theta$  is a rotational angle.

Figure 2 shows the example of 3D elevation map based on a stereo image taken at soybean field. As shown in figure 2a, the original field scene image represents the soybean rows with crop height approximately 0.40 m and row spacing of 0.75 m. The disparity map of stereo image (Figure 2b) encodes the depth of a scene, therefore, is the baseline data for the 3D elevation map creation. The elevation map is then created using the method described above. A gray level of the map indicates the height at the corresponding location in the field as a brighter pixel represents higher elevation.

#### Platform Setup

The stereo camera used in this research (STH-MD1-W (VidereDesign, CA)) for 3D field scene recognition has 230 mm baseline with 12 mm lenses. The camera was installed in front of the research platform tractor (John Deere 7700) 2.2 m above the ground level with tilting downward. With the introduced configuration, this camera was capable of capturing a field scene between approximately 2 m and 10 m in front of the tractor. The tractor platform was modified by installing

an electro-hydraulic steering system in parallel to existing hydraulic steering mechanism for implementing automated steering.

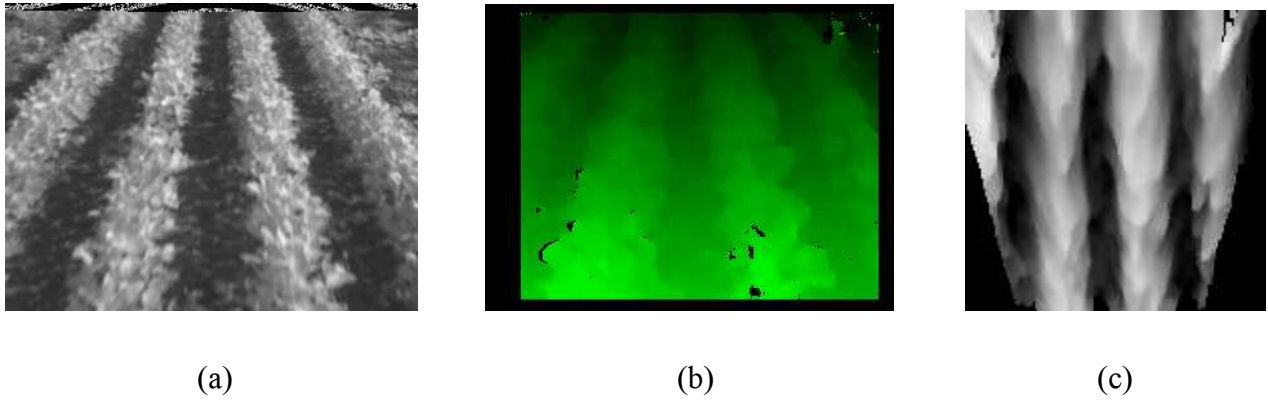


Figure 2. Example of 3D elevation map creation; (a) an original image (left camera); (b) its disparity image; (c) an elevation map.

## TRACTOR AUTOMATION

### Guidance Algorithm

The core of machine vision-based vehicle guidance is the ability to identify the pathway from the acquired images of the fields. The major challenge for such a system in agriculture applications is the difficulty in finding crop row features reliably from field images under varying ambient light conditions. The stereo 3D image, reconstructed based on the difference between the two images, is less sensitive to ambient light changes, so provide a practical means to solve the problem.

The basic idea on navigating a tractor automatically following crop rows using an elevation map is to determine the relative position of the tractor with respect to crop rows using the elevation difference between crop rows and the ground. To identify such a point (aka navigation point) in an elevation map, a cross correlation-based algorithm was developed in this research. Based on this algorithm, a crop model function is designed to represent the cross-section of crop rows. This crop model, defined by a three-cycle cosine function, has a period equal to the inter-row spacing of the actual crop rows and thus expressed as follows:

$$g(i) = \cos(2\pi ri/w) \quad (0 \leq i \leq 3 \frac{w}{r}) \quad (2)$$

where:  $g(i)$  is crop model function;  $r$  is the pixel resolution of the elevation map and  $w$  is the inter-row spacing.

Using the crop model function, a cross correlation matching method was applied to determine the navigation point. Based on this method, the horizontal line in the crop elevation map was used as one data series and the crop model function as the other series. Simply, a navigation point has to be found at the point maximizing the correction index  $c(\tau)$  between the two data series:

$$c(\tau) = \frac{\sum_{i=0}^{m-1} (h(i+\tau) - \bar{h})(g(i) - \bar{g})}{\sqrt{\sum_{i=0}^{m-1} (h(i+\tau) - \bar{h})^2 \sum_{i=0}^{m-1} (g(i) - \bar{g})^2}} \quad (3)$$

where:  $h(i)$  is the data series from the crop elevation map;  $g(i)$  is the crop model function;  $\bar{h}$  and  $\bar{g}$  are the means of corresponding series; and  $m$  is the number of data points in  $g$  series.

Equation (3) is repeatedly computed with delays  $\tau$  from 0 to one complete cycle. The  $\tau$  resulting in the maximum value for  $c(\tau)$  is selected as the navigation point. As illustrated in figure 3, a

maximum correlation value (0.81) was reached at a point in between two center crop rows. After the navigation point is determined, the steering angle for correcting the offset can be determined using the following equations.

$$\delta = a\phi, \phi = \tan^{-1}\left(\frac{y_n}{x_n}\right) \quad (4)$$

where:  $(x_n, y_n)$  is a navigation point with respect to vehicle coordinates;  $\phi$  is a heading angle of a tractor with respect to target crop rows; and  $a$  is a proportional steering control gain.

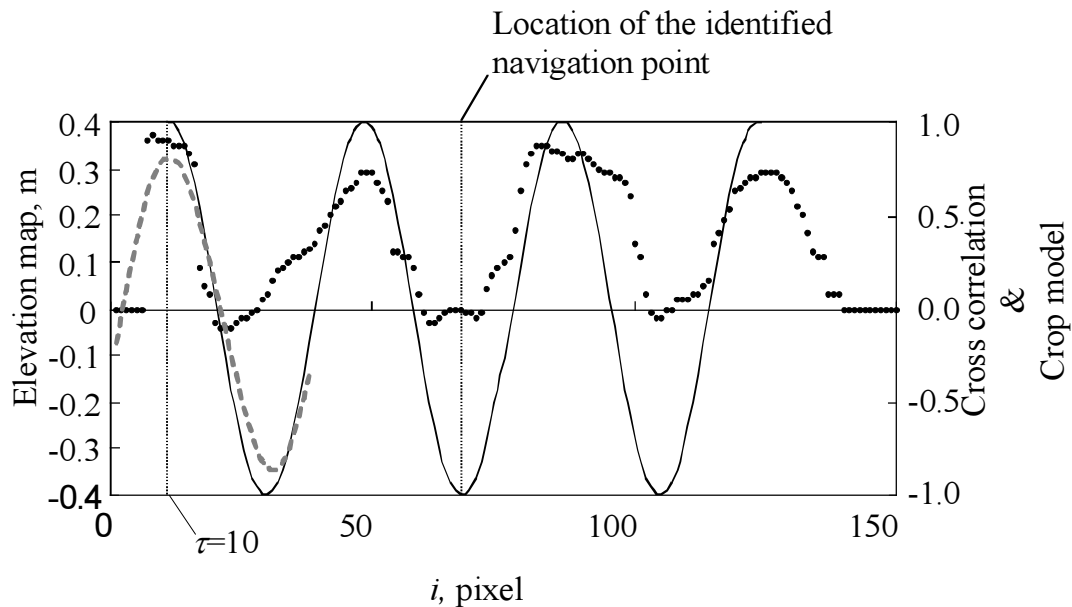


**Figure 3. Illustration of navigation point determination by means of cross correlation analysis.**  
 ..... elevation map, — crop model ( $\tau=10$ ), --- cross correlation

#### Result of Field Test

A series of automated tractor guidance tests were conducted in rowed, either straight or curved, soybean fields to validate the performance of the navigation system. To provide the reference data for evaluating the navigation performance, the crop row positions were measured using an RTK-GPS (accuracy of 0.02 m) mounted on the cabin directly over the CG while the tractor was traveled over the rows carefully driven by a human driver. Figure 4 shows the tracking result conducted on a near straight row at 2.5 m/s.

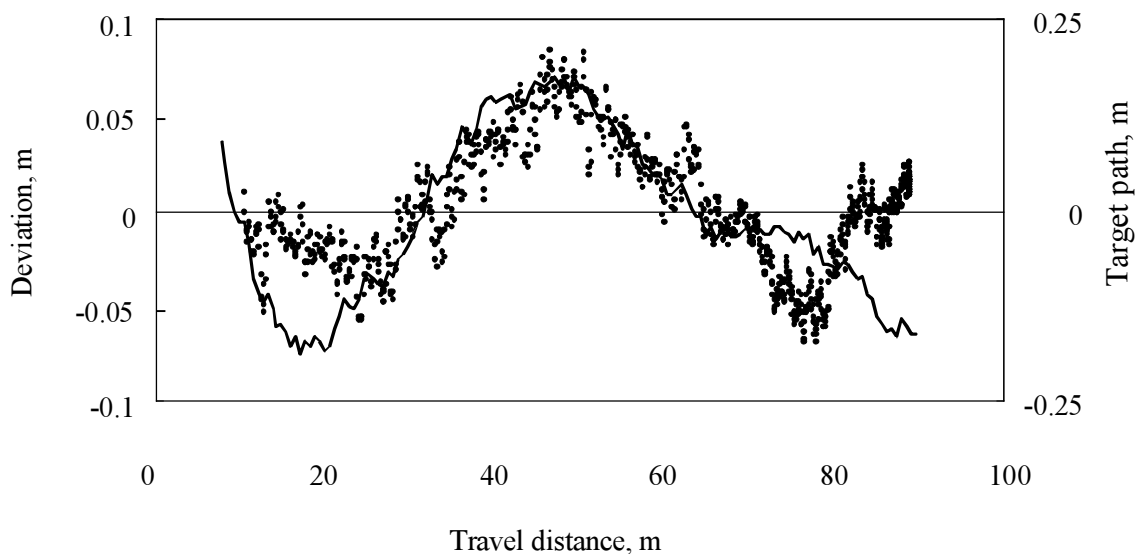


**Figure 4. Row tracking result of an auto-guided tractor following a straight path at 2.5 m/s.**  
 ..... lateral deviation of the guidance path to the target path, — reference path

A total of 333 stereovision images were collected and processed during this test. Field observation indicated that the tractor did not run over any soybean plants. The RMS of the lateral deviation between the guidance path and the reference path was 0.03 m. Similar results were obtained from field tests when the automatically guided tractor was following the curved paths at a travel speed of 2.0 m/s. In all field tests, the auto-guided tractor did not run over any crop rows. The path following tolerant was 0.10 m in tests having an inter-row spacing width between adjacent rows of 0.55 m and a tire width of 0.45 m.

### Field Elevation Map

In navigation application, an elevation map of the entire field was created from the stereo images used for the tractor guidance. This elevation map can also be used for crop growth assessment. For example, a test field was divided into three plots in terms of the day of planting. The crops in different plots were at 44, 52, and 65 days after planting (DAP), and the approximate crop heights were 0.55, 0.70, and 0.80 m, respectively, at the day of the image collection. Figure 5 shows a field elevation map created based on the stereo image stream acquired at the test field. In the elevation map, a gray level indicates the height at the corresponding location in the field as a brighter pixel represents higher elevation. The resolution of the elevation map is 0.015m/pixel. The plot 1 is the darkest region in the map which suggests that its average elevation is the lowest among three plots, while the plot 3 shows the highest gray level suggesting that the average plants height at the plot 3 are the highest in the field. This result matches the actual crop growth status in the field.

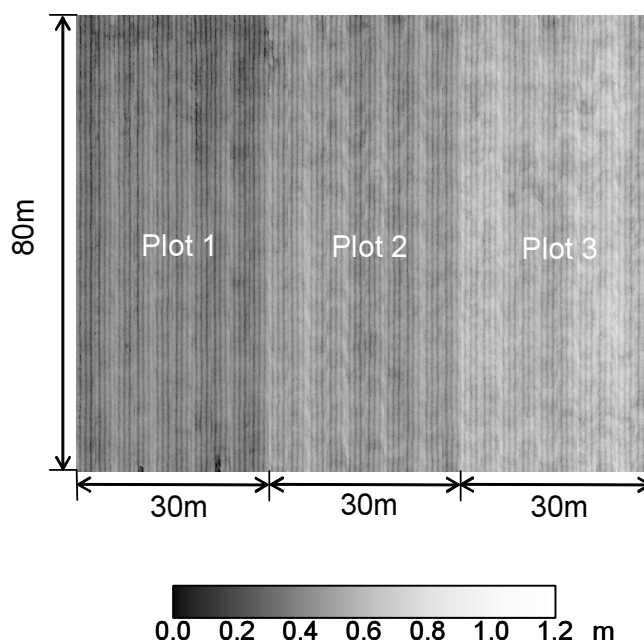


**Figure 5. 3D field elevation map created by stereovision-based mapping system; 90m x 80m entire 3D map consisting of three plots of 44, 52, and 65 DAPs.**

## **ONLINE TRACTOR MOTION SIMULATOR FOR ROLLOVER PRECAUTIONS**

### Online Simulation Algorithm

Because a vehicle-mounted stereovision camera can detect the immediate terrain in front of the moving vehicle, and then uses this terrain information to create a 3D terrain map on which a virtual vehicle will travel to estimate the future roll and pitch angles and/or rates. One of the dominant factors of tractor rollover is tractor stability while traveling on a slope. Such a stability can be determined by tractor postures expressed by roll and pitch angles. For a more reliable prediction of a tractor rollover, the dynamic postures of the vehicle need to be considered in terms of terrain changes. Such a terrain change can be represented using a plane, and this plane on which the vehicle is being placed can be expressed by the following equation:

$$a_p x_g + b_p y_g + c_p z_g + 1 = 0 \quad (5)$$

where,  $[a_p, b_p, c_p]^T$  is a vector perpendicular to the plane, and hence represents the attitude of the vehicle.

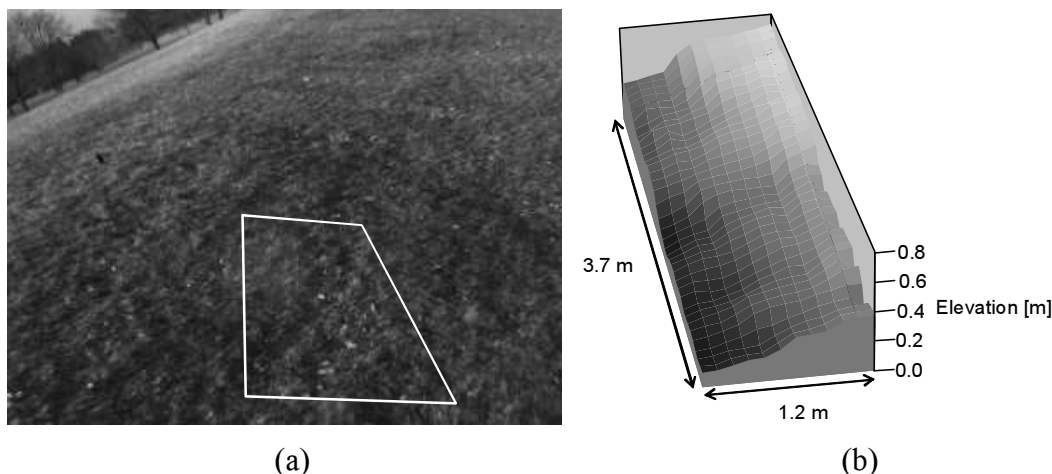
Because  $[a_p, b_p, c_p]^T$  is perpendicular to the plane on which the vehicle is traveling, this vector can be defined as the gravitational vector that rotates  $\theta_r$  around the  $X_G$  axis first, then rotates  $\theta_p$  around the  $Y_G$  axis.  $\theta_r$  and  $\theta_p$  are defined as the pitch and roll angles of the virtual vehicle on the field terrain, and therefore, can be represented by the following equation:

$$R_Y(-\theta_p)R_X(-\theta_r) \begin{pmatrix} 0 \\ 0 \\ h \end{pmatrix} = \begin{pmatrix} a_p \\ b_p \\ c_p \end{pmatrix}, \quad h = \sqrt{a_p^2 + b_p^2 + c_p^2} \quad (6)$$

It should be noted that the roll and pitch angles are measured using a vehicle-mounted inertial measurement unit (JCS-7401A, JAE, Tokyo, Japan). This unit can measure roll and pitch angles and angular rates of the vehicle platform dynamically with an accuracy of  $\pm 2^\circ$  for the angles, and  $\pm 5^\circ \text{ s}^{-1}$  for the angular rates. IMU data is also used as the reference signal in the field test

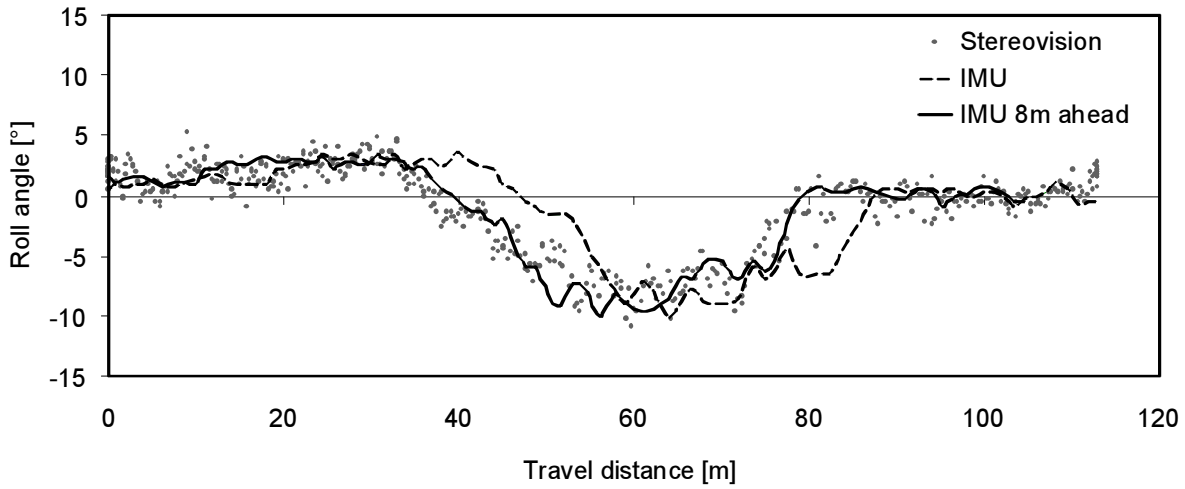
### Result and Field Test

A series of field tests on various terrains were conducted in an actual field environment. The vehicle was traveling in the field on a predetermined straight path at a constant speed (1.2m/s). Creation of a 3D virtual field based on an acquired stereo image from the test site is illustrated in figure 6. The white quadrangle in the original left image (Fig. 6(a)) indicates the ROI of the 3D terrain map as shown in figure 6(b). This path includes not only side-banks, but also up-hill and down-hill slopes with a 5.2 m elevation difference.



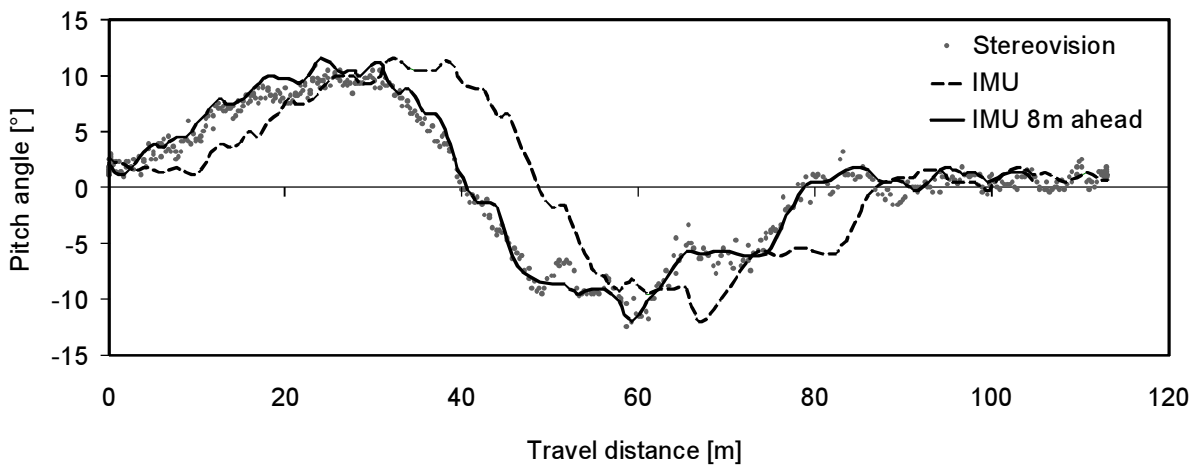
**Figure 6. Tested terrain and created 3D terrain map; (a) Original left image with a white quadrangle indicating the ROI of the terrain map; (b) 3D terrain map.**

Figure 7 compares the roll angle predicted by the motion simulator with the reference values measured using the IMU when the vehicle platform traveled on the path shown in figure 6. Both the predicted and measured results indicate that the roll angle varies between  $-11^\circ$  and  $4^\circ$  while traveling on the path. There is a constant offset between the predicted roll angle and the reference value. This offsets correspond to the look-ahead distance: while the sensor provides the measured values at the position the vehicle is located, the estimator predicts values about 8.0 m ahead of the current position. When shifting the data by 8.0 m ahead of the current position, the reference data fits the predicted data well. This result shows that the motion simulator could accurately predict the vehicle roll angle 8.0 m ahead of the vehicle current position. The RMS error of the predicted roll angle referenced to the IMU data is less than  $1.5^\circ$  after shifting 8.0 m ahead.



**Figure 7. predicted roll angle comparing to IMU data.**

Figure 8 shows the comparison between the predicted pitch angles and the measured values on the same path. Similar to the result shown in figure 7, the motion simulator can accurately predict the pitch angle 8.0 m ahead of the moving vehicle. Both the predicted and the IMU pitch angles vary between  $-12^{\circ}$  and  $12^{\circ}$  on this test path. After realigning the predicted and IMU pitch angles, the RMS error is less than  $1.0^{\circ}$ .



**Figure 8. Predicted pitch angle comparing to IMU data.**

## CONCLUSION

This research investigated the fundamental technology for a “triplet applications” of stereovision-systems a tractor, including 3D crop row detection for navigation, 3D field mapping for crop growth assessment, and online tractor motion simulation for rollover precautions. Those triplet applications are based on a 3D field scene created in terms of stereo images captured by tractor-mounted stereo camera. A series of field tests were conducted separately to verify each function of those applications. The tractor guidance application was tested at several types of crop rows including straight, curved and weedy rows. The result indicated that the guidance system could navigate the tractor at a speed up to 3.0 m/s without damaging plants in all tests conducted at different type of rows. The validation test for 3D field mapping application was conducted at a soybean field consisting of three different plots with crops planted at different days. Crops at each plot had different heights at the day of validation test. The validation results proved that the stereovision-based 3D field mapping system could generate a field elevation map with the RMS error of 0.04 m in terms of the plant height, which was favorable accuracy as the field sensing information. The validation test was conducted at a field with various slopes in order to evaluate ability of the vehicle stability estimation in terms of tractor posture in a look-ahead location. This system was capable of predicting the posture parameters of a moving vehicle 8.0 m ahead of the vehicle based on acquired stereo images with favorable and consistent accuracy.

## REFERENCES

1. Adiv, G. 1985. Determining three-dimensional motion and structure from optical flow generated by several moving objects. *IEEE Transactions on Pattern Analysis and Machine Intelligence* 7(4): 384-401.
2. He, D.X, Y. Matsuura , T. Kozai, K.C. Ting. 2003. A binocular stereovision system for transplant growth variables analysis. *Applied Eng in Agriculture* 19(5), 611–617.
3. Rovira Más, F., Q. Zhang, J. F. Reid. 2005. Creation of three-dimensional crop maps based on aerial stereo images. *Biosystems Engineering*, 90(3): 251-259.
4. Tomasi, C. and T. Kanade. 1991. Shape and motion from image streams: a factorization method. Technical report CMU-CS-91-172, Carnegie Mellon University, Pittsburgh, Penn.
5. Tsai, R.Y. and T.S. Huang. 1984. Uniqueness and estimation of three-dimensional motion parameters of rigid objects with curved surfaces. *IEEE Transactions on Pattern Analysis and Machine Intelligence* 6(1): 13-27.

# AUTONOMOUS INTER-ROW HOEING USING GPS BASED SIDE-SHIFT CONTROL

H. W. Griepentrog<sup>1</sup>, M. Noerremark<sup>1</sup>, J. Nielsen<sup>1</sup> and J. S. Ibarra<sup>2</sup>

## ABSTRACT

Several developments and investigations have been done to automate the lateral control of hoes with the aim to achieve higher weeding efficiency and decreased labor costs. The aim of this project was to investigate the accuracy and limitations for a computer controlled hoeing operation based on a GPS system. A conventional hoe and an electro-hydraulic side shift frame was used and attached to a small automatic tractor. The main task of the controller systems was to minimize the lateral deviations between current GPS positions of the hoe related to a predefined route. The range of the cross track errors (standard deviations) altered between 0.009 m and 0.028 m for the hoe (ground measurements). The hoe system enables hoeing up to 83 % of a field surface area with a speed of 2 km h<sup>-1</sup> and up to 79 % by driving with 4 km h<sup>-1</sup>. The GPS based system showed its potential to be used for high accurate crop row guidance e.g. with an inter-row hoe. Further research should be carried out to investigate sensor fusion systems consisting of GPS and other sensors e.g. based on computer vision.

**KEYWORDS.** Automation, Autonomous Tractor, GPS, Hoeing, Weed Control.

## INTRODUCTION

In order to reduce herbicide input or completely substitute chemical inputs and minimize labor costs mechanical weed control operations are an increasingly important option. Hoeing is one of oldest, highly matured and most common non-chemical weeding operation. Its weed control principle can be defined as (Laber 1999):

- Operational: Soil engaged treatment (tillage) between crop rows
- Physical: Soil coverage of weeds, weed root / stem cutting and uprooting of weeds (whole plant or partly)
- Physiological: Reduction of photosynthesis and reduction of water transpiration

Hoeing is at least 120 years old and still a standard weed control operation today. The first hoes were horse pulled and the ones today are tractor mounted or still tractor pulled. Currently often a second operator is controlling the hoe laterally by hand and based on operator's vision. Tines or rotating discs (rotary hoes) are fixed to a frame and penetrate the upper crust of the soil. The treatment is effective on dry, compact soil and a stable working depth is maintained by ground wheels.

As for most mechanical weeding operations crop plant losses always occur. Especially if high weed control efficiencies are aimed at. Crop losses result from soil coverage, crop leaf damage, root damage and disturbance. The standard hoe setting for the untreated crop row strips is 10 cm which gives approximately a maximum of 80 % area treatment e.g. in sugar beet. This row band width is measured as a row clearance between the hoe unit tools e.g. shares. Most crop losses are due to soil disturbance close to crop plants. A conflict of aims appears between i) maximizing treated area to increase weeding efficiency and ii) minimizing crop losses by keeping a sufficient

---

<sup>1</sup> The Royal Veterinary and Agricultural University, Department of Agricultural Sciences, Højbakkegaard Alle 2, 2630 Taastrup, Denmark, hwg@kvl.dk

<sup>2</sup> University of Navarre, Faculty of Agricultural Engineering, Campus de Arrosadia, 31006 Pamplona, Spain

distance to crop rows. Therefore the adjustment of the hoe unit working width becomes an important factor for achieving an acceptable cultivation result.

Several developments and investigations have been done to automate the lateral control of hoes (Tillett, 1991; Home, 2003). Today the most promising automation principles are based on GPS (Van Zuydam et al., 1995; Dijksterhuis et al., 1998) and computer vision (Tillett et al., 2002; Soegaard & Olsen, 2003; Astrand & Baerveldt, 2005). A fusion of both is seen today as the most promising strategy, because advantages and disadvantages of absolute and relative referencing principles compensate each other (Pilarski, 2002; Downey et al., 2003).

The aim of this project was to investigate the accuracy and limitations for a computer controlled hoeing operation based on an RTKGPS system. The objectives were i) to design and optimize a side-shift system for lateral control of a conventional inter-row hoe, ii) to quantify the accuracy of the performance (cross track errors) and iii) to determine an optimum hoe unit working width (Ibarra, 2005). For all field tests an unmanned and fully automatic tractor was used to provide mechanical, hydraulic and electric power. The tractor's navigation controller was also based on RTKGPS.

## MATERIALS AND METHODS

### Inter-row Hoe

A conventional inter-row hoe was used (Baertschi-Fobro, Switzerland) consisting of five units to treat four crop rows. The hoe units including toolbar are light to be operational for a small automatic tractor. Each unit had a parallelogram for height compensation and a ground wheel for controlling the working depth. Three hoe units had each three standard A-blade cultivators as the outer ones had only two.

For determining an optimal hoe unit working width an untreated band or safety band for the crop rows had to be defined. Furthermore a failure tolerance for hoeing into the safety band around crop rows (5 %) and the standard deviations of lateral errors from the field experiments were used.

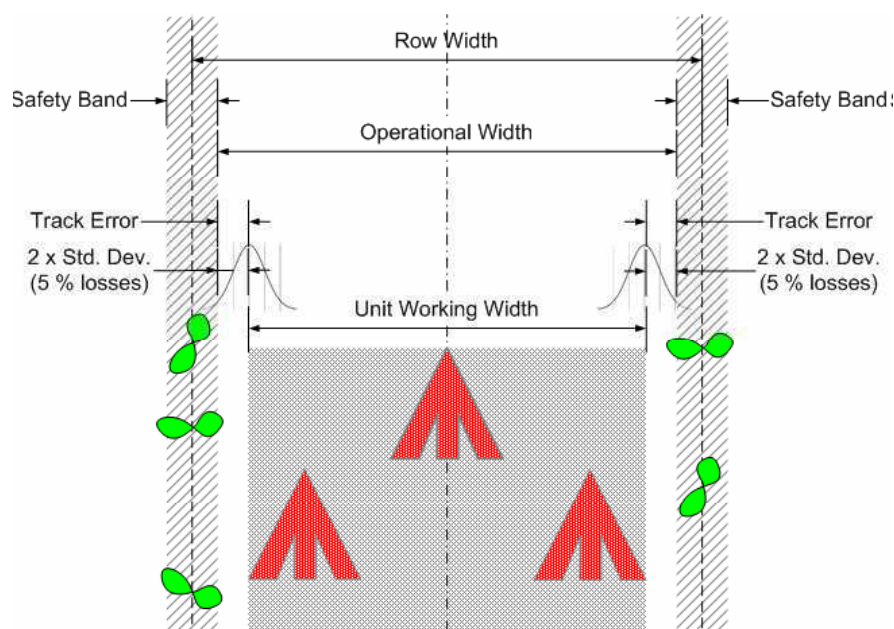


**Figure 1. Unit working width setting by considering cross track errors, crop losses and an untreated band (safety band).**

According to figure 1 the unit working width was determined and set by using the following equation:

$$X_{\text{unit working width}} = X_{\text{row width}} - (X_{\text{untreated}} + 4 S_{\text{standard deviation}})$$

## Side-shift Toolbar System

The aim of the side-shift system as displayed in figure 2 was to center the hoe units between the rows and parallel to the crop rows with a minimum of lateral deviations (cross track error). Furthermore, the idea was to keep the side-shift somehow independent from the motion behavior of the pulling tractor.

The side-shift controller was configured to keep the GPS antenna of the hoe on the same planned route as the automatic tractor was using for its navigation. This setup enables a somehow independency of the implement from the pulling tractor.

A double toolbar side-shift system carried five hoe units to cover four crop rows. The system was attached to the tractor using the rear three point linkage. The tractor only pulled the hoe system via loose linkages as the hoe had two carrying ground wheels. A soil engaging disc (diameter 0.47 m) was mounted in the center of the first toolbar which was connected to the tractor. The disc functioned as a counterpart to compensate for lateral reaction forces resulting from the side-shift's lateral movements (2nd toolbar).

The lateral position of the 2nd toolbar was altered by controlling the oil flow rate to a double acting hydraulic cylinder with a stroke length of 0.2 m. A 2-way solenoid valve allowed a left / right switching and a proportional valve regulated the oil flow rate to vary the piston velocity. The different flow rates to ensure the same piston speeds for left and right directions were achieved by using individual calibration settings.

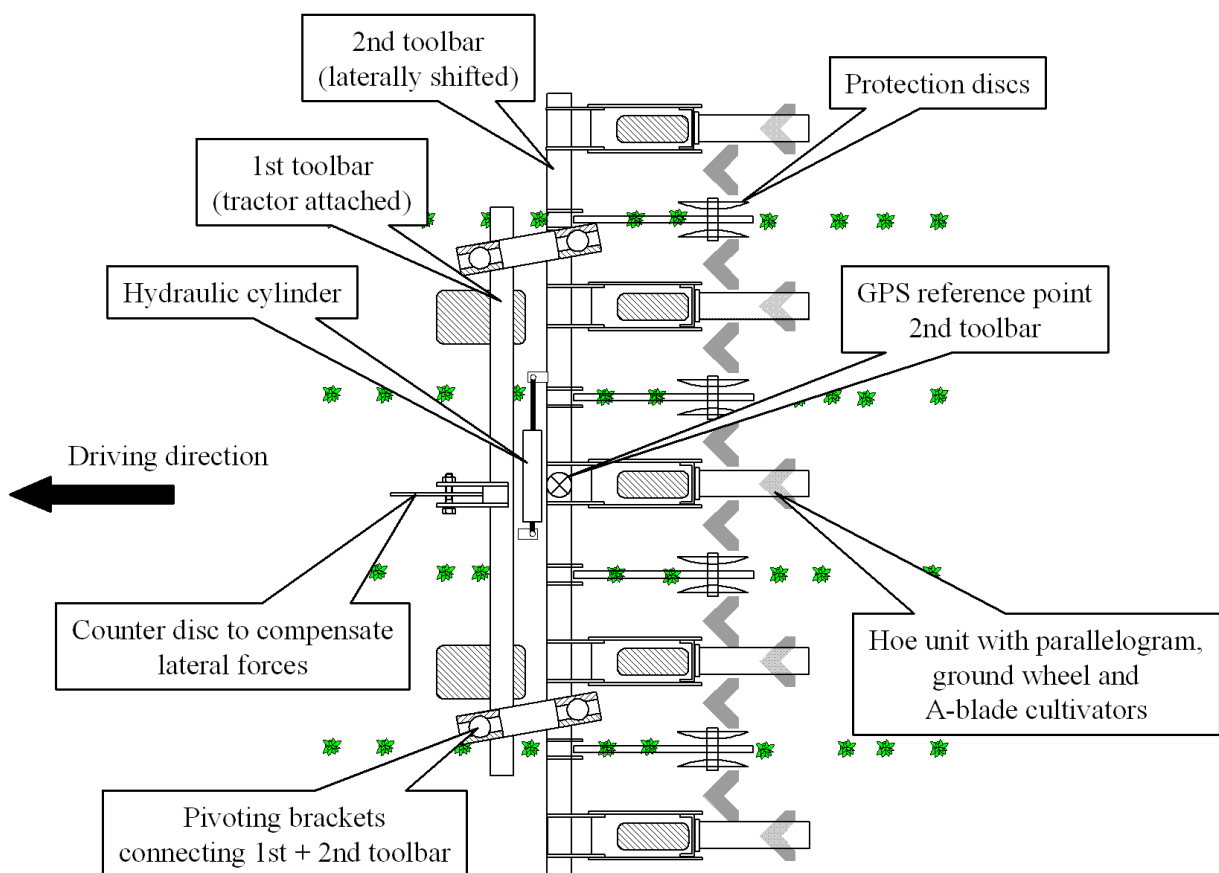


**Figure 2. Conventional inter-row hoe and the toolbar side-shift system.**

## Controller

### *Hardware*

The lateral control of the inter-row hoe was based on an RTKGPS (Trimble MS750) and a dual axis tilt sensor (Applied Geomechanics, MD900). The GPS was connected to a local reference station via an FM radio modem (Satel 3ASd). The GPS antenna was mounted at a height of 1.3 m

in the middle of the 2nd toolbar and functioned as a closed-loop feedback for keeping the hoe on the planned route.

A PC/104-based computing platform was used. It comprised a 400 MHz Via Eden processor (Pentium class). Additional boards were connected to allow digital, analog and PWM I/O connections. The analog voltage and power to control and operate the hydraulic valves respectively was provided directly from the amplifier board via three-pole standard valve connectors.

### Software

The controller software was developed in the programming tool MATLAB Simulink from MathWorks. It allows modeling and simulating of system functionality prior to actual tests. The software comprised, i) a route tracking, ii) hydraulic cylinder velocity control and iii) a left / right direction switching of the hydraulic cylinder.

The software used a standard PID controller to minimize the route tracking errors (cross track errors). When starting the route tracking - a route is defined by waypoints - the "next waypoint" is selected when the Euclidean distance becomes less than 0.5 m (Fig. 3 and Fig. 4). When following a route the hoe position is translated to the coordinate system with waypoint  $P_2$  as Origo and waypoint  $P_1$  on the negative x-axis. When the y-axis is crossed, the waypoints are shifted and the next segment between waypoints is chosen as the reference from which the cross track error is calculated.

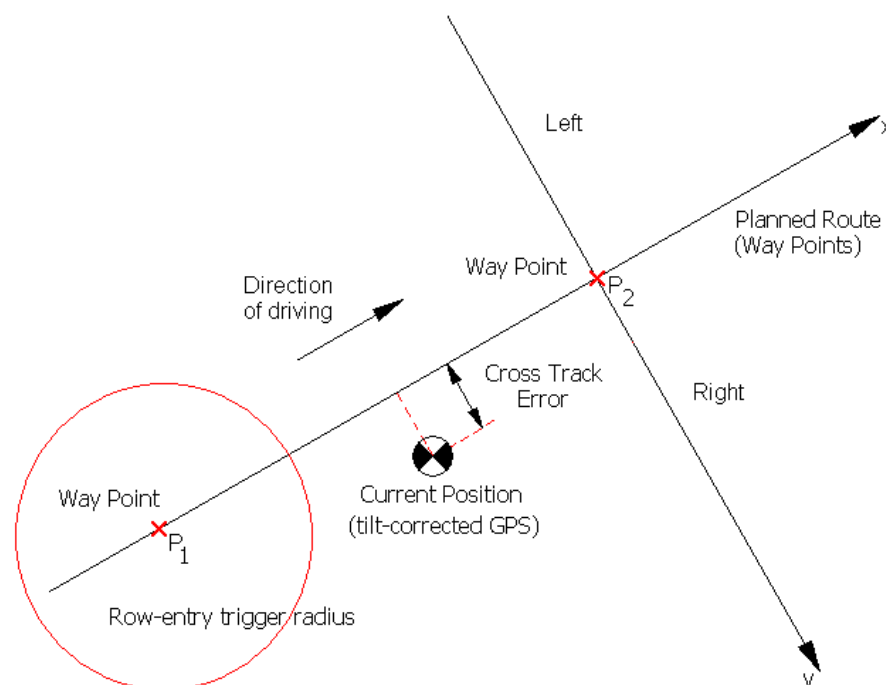


**Figure 3. Determination of cross track errors from GPS positions and planned route defined by waypoints.**

The hoe operation had to be planned prior to the weeding cultivation. The route waypoints were generated from geo-referenced seed positions. The geo-referenced seed positions were determined from the seeding operation of the cultivated crop plants by logging and processing GPS and seeder attitude data (Griepentrog et al., 2005).

### Autonomous Tractor

An automatic tractor was used to operate the hoe. This conventional 20 kW tractor (Hakotrac 3000) was retrofitted with an RTKGPS (Trimble MS750) and a controller system for navigation. The steering control, engine speed, vehicle speed, PTO and three point linkage was achieved by using an electronic controller unit (ESX). Two electro-hydraulic valves (Sauer Danfoss EHP) actuate the steering and electric linear motors (Linak) control engine rpm and continuously variable transmission (CVT). The safety interlocks and emergency shutdown was achieved by a combination of stamp computers (with PIC microcontrollers), radio links and hardwired relays.

The tractor navigation controller was designed to follow a predetermined route plan accurately and repeatable e.g. across a field with planned action points for implement control (Blackmore et al., 2004).

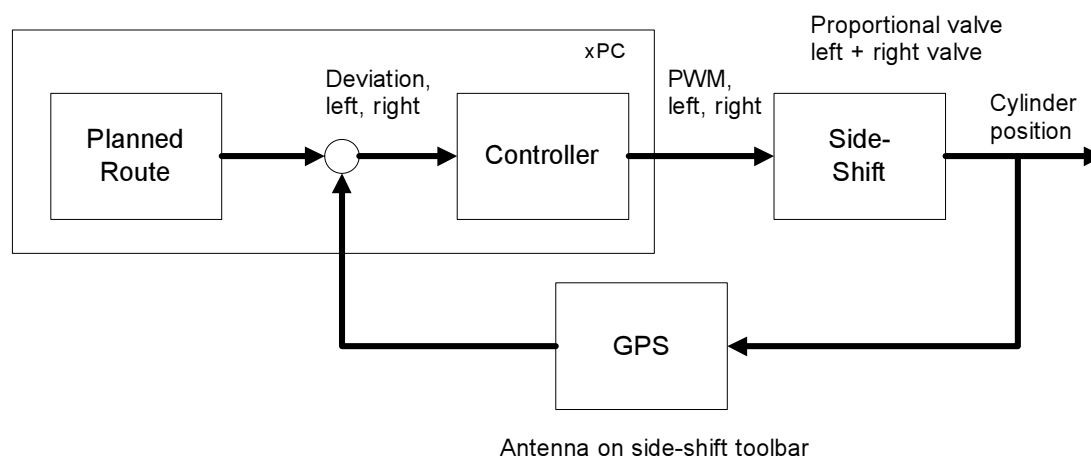


**Figure 4. Lateral control system for a hoe (side-shift).**

### Field Experiment

The field trial was carried out at the KVL research farm, Denmark, on 7<sup>th</sup> and 8<sup>th</sup> July 2005 (55°40.16726'N, 12°18.52900'E). The experiments included driving along eight straight trajectories. The length of each straight line trajectory was 45 m.

The field experiments were carried out by using varying forward speeds and driving directions. The system was tested with 4 tracks in each orientation East-West (1.1 to 1.4) and North-South (2.1 to 2.4). The testing was conducted by driving with two speeds: 2 km/h for tracks 1.1, 1.2, 2.1 and 2.2 and 4 km h<sup>-1</sup> for tracks 1.3, 1.4, 2.3 and 2.4. Compared to a standard hoeing operation with a standard tractor the speeds are low. The reason is that the performance of the small automatic tractor limited the speeds.

Virtual crop plant rows were set up by using small white plastic sticks. Two complete repetitions were made. The working depth of the hoe was set to as shallow as possible (0.010 to 0.020 m).

### Data acquisition and analysis

A rigid disc was attached to one hoe unit parallelogram to create a small furrow to indicate the hoe trajectory as it passed across the field. Ground distances between this furrow and the crop rows were measured by a hand ruler to describe the lateral hoe movement. Furthermore the side-shift GPS output string was also logged.

The performance of the hoe was assessed i) by analyzing data from lateral ground measurements between hoe trajectory and plant rows and ii) by analyzing tilt corrected GPS position data as they were used for the control system.

## **RESULTS AND DISCUSSION**

The cross track errors can be divided up into bias (mean deviation) and variability (standard deviation). A summary of the results for all trial variants are presented in figure 5 and 6.

The range of the mean values altered quite low between – 0.016 m to 0.011 m (Fig. 5). The ground measurements (ruler) showed higher mean values than calculated from the GPS data, means the repeatability was not as high as for the GPS data. The range of the mean values from the GPS altered only  $\pm 0.003$  m. This could be due to the use of different measurement techniques or due to the controller's characteristic to minimize the lateral deviations of GPS positions from the planned route. Home (2003) analyzed the cross track errors for different row guidance systems as with a tractor driver, a second operator and a computer vision system. The investigations included no GPS system. The author observed a similar small range of the bias (– 0.017 m and 0.009 m).

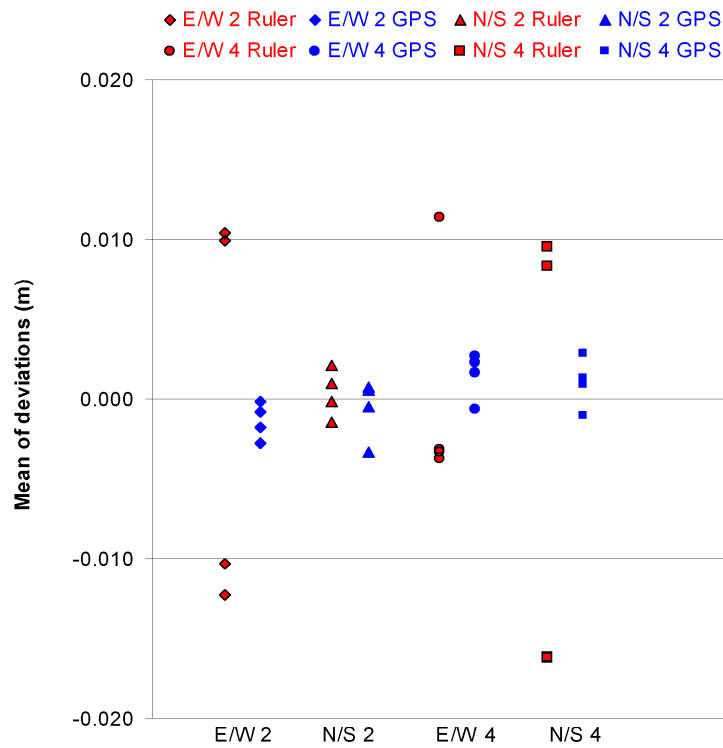


**Figure 5. Mean lateral deviations versus ground measurements and GPS position logging and versus heading directions and forward speed (E/W east-west, N/S north-south, 2 and 4 km h<sup>-1</sup>).**

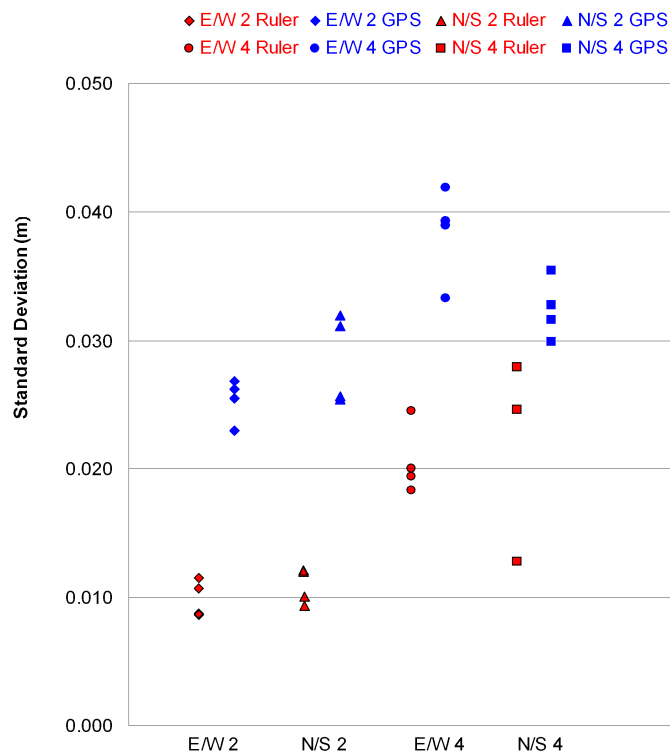


**Figure 6. Mean standard deviations of lateral errors versus ground measurements and GPS position logging and versus heading directions and forward speed (E/W east-west, N/S north-south, 2 and 4 km h<sup>-1</sup>).**

The variability of the cross track error can be described by using the standard deviation (Fig. 6). There are three obvious trends in the graph i) the values from the GPS logging are much higher compared to the ground measurements, ii) the values increase from lower to higher driving speeds for both observations and iii) the repeatability for the lower speeds seems higher.

The range of the standard deviations altered between 0.009 m and 0.028 m for the hoe (ground measurements) and between 0.023 m and 0.042 m for the GPS logging. The smaller lateral variations of the hoe occur probably due to the inertial forces which is system intrinsic. These forces suppress high frequency movements (low pass filter). Home (2003) published a range for the standard deviation of 0.009 m to 0.022 m for a tractor driver, a second operator and a computer vision system. The best results were obtained by using a computer vision system as a row guidance (0.009 m).

The experiments were carried out by using a small automatic tractor. Due to the tractor design the track width was much smaller than from a standard tractor. The tractor size reduced the maximum forward speed for hoeing to 4 km h<sup>-1</sup> due to too dynamic vehicle performances.

Due to the lower dynamic vehicle behaviors at slow speeds it seems that the repeatability was higher.

**Table 1. Hoe unit working width and treated area versus forward speed and cross track errors (row width 0.5 m, untreated row band 0.010 m and failure tolerance 5 %).**

Forward speed [km h <sup>-1</sup> ]	Standard deviation of cross track errors [mm]	Hoe unit working width [m]	Treated area [%]
2.0	9 – 12	0.404 – 0.415	81 – 83
4.3	13 – 28	0.338 – 0.399	68 – 79

Table 1 presents the treated or hoed surface areas based on the analysis of the cross track errors acquired from the field experiments. The setting of the optimum hoe unit working width is also displayed based on the field results. Small standard deviations of the track errors resulted in wider width of the hoeing units and in high effected field surface areas. The hoe system enables hoeing up to 83 % of a field surface area with a speed of 2 km h<sup>-1</sup> and up to 79 % by driving with 4.3 km h<sup>-1</sup>.

## CONCLUSION

A row guidance method consisting of an electro-hydraulic side shift system for implement attachment was developed and tested. The GPS based system showed its potential to be used for high accurate crop row guidance e.g. with an inter-row hoe. The mean as well as the standard deviations of the cross track errors were comparable with other row guidance systems as traditional tractor mounted and computer vision systems. Further research should be carried out to investigate sensor fusion systems consisting of GPS and other sensors e.g. based on computer vision.

## REFERENCES

1. Astrand, B.; Baerveldt, A. J. 2005. A vision based row-following system for agricultural field machinery. *Mechatronics* 15(2) p.251-269.
2. Blackmore, B. S.; Griepentrog, H. W.; Nielsen, H.; Nørremark, M.; Resting-Jeppesen, J. 2004. Development of a deterministic autonomous tractor. In: *Proceedings CIGR*, 11.11.2004 Beijing, China.
3. Dijksterhuis, H. L.; Van Willigenburg, L. G.; Van Zuydam, R. P. 1998. Centimetre-precision guidance of moving implements in the open field: a simulation based on GPS measurements. *Computers and Electronics in Agriculture* 20 p.185-197.
4. Downey, D.; Giles, D.; Slaughter, D. C. 2003. Ground based vision identification for weed mapping using DGPS. In: *Proceedings ASAE Annual International Meeting Las Vegas, Nevada, USA, ASAE*, paper no. 03-1005.

5. Griepentrog, H. W.; Nørremark, M.; Nielsen, H.; Blackmore, B. S. 2005. Seed mapping of sugar beet. *Precision Agriculture* 6(2) p.157-165.
6. Home, M. 2003. An investigation into the design of cultivation systems for inter- and intra-row weed control. Unpublished PhD diss. Silsoe, UK: Cranfield University, National Soil Resources Institute, Engineering Group.
7. Ibarra, J.S. 2005. Assessment of the performance of a GPS and side-shift controlled inter-row hoe. MSc thesis. Copenhagen, Denmark: The Royal Veterinary and Agricultural University, Department of Agricultural Sciences.
8. Laber H. 1999. Effizienz mechanischer Unkrautregulationsmaßnahmen im Freilandgemüsebau. Unpublished PhD diss. Hanover, Germany: University of Hanover, Faculty of Horticulture.
9. Pilarski, T.; Happold, M.; Pangels, H.; Ollis, M.; Fitzpatrick, K.; Stentz, A. 2002. The Demeter System for Automated Harvesting. *Autonomous Robots* 13 p.9-20.
10. Soegaard, H. T.; Olsen, H. J. 2003. Determination of crop rows by image analysis without segmentation. *Computers and Electronics in Agriculture* 38(2) p.141-158.
11. Tillett, N. D. 1991. Automatic guidance sensors for agricultural field machines - a review. *Journal of Agricultural Engineering Research* 50(3) p.167-187.
12. Tillett, N. D.; Hague, T.; Miles, S. J. 2002. Inter-row vision guidance for mechanical weed control in sugar beet. *Computers and Electronics in Agriculture* 33 p.163-177.
13. Van Zuydam, R. P.; Sonneveld, C.; Naber, H. 1995. Weed control in sugar beet by precision guided implements. *Crop Protection* 14(4) p.335-340.

# RICE HARVESTING OPERATIONS USING AN AUTONOMOUS COMBINE WITH A GPS AND A FOG

M. Iida<sup>1</sup> and Y. Yamada<sup>2</sup>

## ABSTRACT

In this study, an autonomous combine harvester has been developed to harvest rice in a rice paddy field. This combine was equipped with an RTK-GPS and a fiber optic gyro (FOG) sensor to detect its posture.

Field tests were carried out to estimate the performance of this autonomous combine, and a desired path for harvesting rice was planned using the GPS position data of rice stalks measured previously. The desired path consisted of straight paths to harvest, and turning paths to change the direction of the combine. Specifically, the turning path was a combination with the left turning as a move forward and the right turning as a move backward.

In the field test, the combine harvested rice successfully three laps within the R.M.S. there was 95mm of lateral deviation from the desired straight path and R.M.S. 1.3° of yaw angle error. After turning at the headland, the maximums of lateral deviation and yaw angle error from the next desired path were 140mm and 2.2°, respectively.

**KEYWORDS.** Autonomous Vehicle, Head-feeding Combine, Planning of Desired Path, Straight Running Control, Turning Control.

## INTRODUCTION

An automatic control and navigation for agricultural vehicles is an important technology to enhance production efficiency and safety of operations. In Japan, Kanetoh (1977) reported the first study on an unmanned head-feeding combine harvesting rice automatically. In this study, the unmanned combine detected the position of rice stalks using tactile type sensors, and followed the rice rows to harvest them. If the sensors detected them at the end of rice rows, the combine changed its direction by about 90°. The developed combine also had an automatic packing mechanism for harvested rice. In order to change the direction of combine precisely at the headland, Kito et al., (1991a and 1991b) studied the turning control of the combine using a gyro sensor to minimize the error of turning angle at the headland. In addition, there were reports on the autonomous combines equipped with machine vision systems and/or a GPS harvesting alfalfa and corn (Ollis et al., 1997; Benson et al., 2003).

In fact, there are a numerous studies on automated and autonomous tractors. The automatic guidance tractor developed at Stanford University employed four RTK-GPS receivers to provide the tractor posture information (Bell, 2000). The robot tractor developed at Hokkaido University used an RTK-GPS to provide tractor position information and an IMU (inertia measurement unit) to provide tractor heading information (Kise et al., 2002).

In these studies to develop automatic and autonomous vehicles in agriculture, the vehicles are able to follow crop rows and operate more precisely than human operators. The important sensing device supporting these navigations was an RTK-GPS. It was possible to enhance the accuracy of automatic operation by a combination of the RTK-GPS and a gyro sensor in some research. While

---

<sup>1</sup> Laboratory of Field Robotics, Division of Environmental Science and Technology, Graduate School of Agriculture, Kyoto University, Sakyo-ku, Kyoto 606-8502, Japan, iida@elam.kais.kyoto-u.ac.jp.

<sup>2</sup> Nomura Research Institute, 1-6-5 Marunouchi, Chiyoda-ku, Tokyo 100-0005, Japan. This work had been done when he was a graduate student at Kyoto University

the RTK-GPS is still expensive, it is frequently used for precision agriculture and is an indispensable tool in agriculture.

In this paper, an autonomous head-feeding combine equipped with an RTK-GPS and a FOG (fiber optic gyro) sensor was developed for harvesting rice. The desired path for the harvesting operation was planned using the GPS data of rice positions measured previously. In order to change the direction of the combine efficiently at the headland, a turning control method is proposed in this paper.

## MATERIAL AND METHOD

### Autonomous Combine

Figure 1 shows the autonomous combine developed in this study. The base machine is a 2-row head-feeding combine (*Mitsubishi Agricultural Machinery Co., Ltd.*, model VM3G, 9.6kW) with a small grain tank. This combine was the crawler type vehicle, and it has an HST (Hydrostatic transmission) to change the speed continuously. In the case of steering, it also changes the speed of the left or right crawler by operating the clutches and brakes in the transmission.



**Figure 1. Autonomous combine developed.**

The control system of the combine was designed as shown in figure 2. The main components of the control system were a note PC (*IBM*, model ThinkPad X390) and a microcomputer (*Renesas Technology Corp.*, model H8S/2612, 20MHz). The note PC was connected with RTK-GPS (*Nikon-Trimble Co., Ltd.*, MS750) and a FOG (*JAE*, JCS-7401A) through serial ports to measure the position and yaw angle of the combine. The RTK-GPS receiver obtained the correction data using a VRS (Virtual Reference Station) service with a mobile phone. The position and yaw angle of the combine were updated at the rate of 5Hz and 50Hz, respectively. The note PC calculated the lateral deviation and yaw angle error between the desired path and the actual posture of the combine, and then sent the control commands for steering and speed control into the microcomputer through the serial port at the rate of 5Hz.

The microcomputer controlled the traveling speed and steering of the combine according to the control commands sent from the note PC. In addition, it operated the height of the cutting platform. Since the base machine could change the traveling speed continuously by the HST, a DC motor operated the main lever connected with the swash plate of the HST to change the traveling speed. The position of main lever was detected by a potentiometer as a feedback signal. Furthermore, two ways of steering control were adopted to maintain the straight path and left turn at the headland.

For the straight traveling, the microcomputer operated the transmission clutches with the hydraulic solenoid valves. When the combine turned at the headland, an AC servomotor operated the clutch and brake in the transmission to change the direction rapidly. The microcomputer sent the data of the main lever position and steering control to the note PC at the rate of 5 Hz.

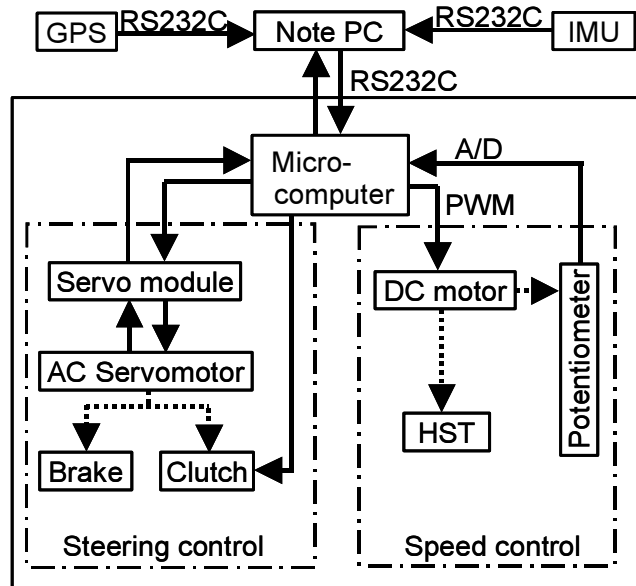


Figure 2. Steering and speed control system.

### Desired Path for Harvesting

In this study, the rice area in the test field was assumed to be rectangular. The note PC planned the desired path for harvesting rice using the GPS data of rice positions measured previously. In order to harvest rice with the autonomous combine, the desired path was planned with a combination of straight traveling and left turning. When a human operator harvests rice using the head-feeding combine, he operates the combine to travel along the rectangle shape path counterclockwise. It was, therefore, thought that planning the spiral rectangular shape path was useful and efficient.

Figure 3 shows a concrete example of the desired path for harvest. In this figure, the solid lines represent the straight path to harvest rice, and six solid lines in total mean six times to harvest. In addition, the break lines represent that the combine moves toward the next straight path after changing direction. The left turns at the headland total 10 times. Consequently, the combine will harvest rice three laps counterclockwise.

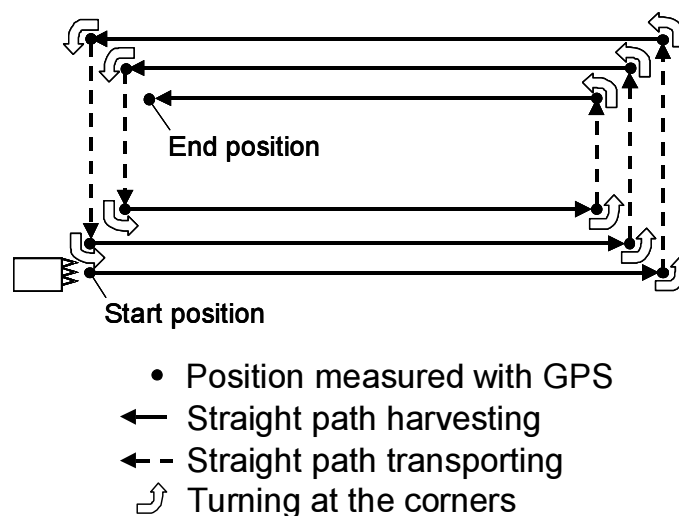


Figure 3. Desired path planned for the harvesting operation using the positions of rice measured with the GPS.

### Straight Traveling Control

It was assumed that the rice rows were straight in this control mode. At first, the desired path was represented with the start position, the length, and the direction in the field coordinate. The note PC calculated the lateral deviation  $d$  and the yaw angle error  $\theta$  from the desired straight path and the traveling distance  $s$  from the start position using the posture information from the GPS and the FOG. The speed of the combine was considered as a constant speed while traveling along the straight path. The input  $u$  of the steering control was determined with the lateral deviation  $d$  and the yaw angle error  $\theta$  as the following equation.

$$u = \alpha d + \beta \theta \quad (1)$$

where  $\alpha$  and  $\beta$  are gains, depending on the speed. In the straight traveling control, as it is not necessary for the combine to change its direction at the high yaw rate, the left or right clutch of the transmission was operated by the On-Off control according to the following conditions:

- i)  $u \geq 0$ , the right clutch is off, then the combine turns to the right.
- ii)  $u < 0$ , the left clutch is off, then the combine turns to the left.

When the combine arrives at the end of desired straight path, the combine stops immediately and then it changes from straight traveling control to turning control.

### Turning Control

Turning control means that the combine changes its direction to harvest other rice rows. In this control, an AC servomotor operated both clutch and brake driven the left or right crawler. As the test combine could not spin turn, it turned while moving forward or backward. If it turns to the desired yaw angle  $\psi$  [deg] suddenly, it causes a large lateral error between the next desired path and the position of combine. In order to minimize the lateral error, the combine changed its direction by a combination of left and right turns as shown in figure 5. It was assumed that the combine moved on the arcs while turning at a constant speed. This turning combination mimics the turning operation pattern by a human operator. Therefore, it was expected that the combine could change direction efficiently and experimentally in small spaces such as headlands by this turning control method.

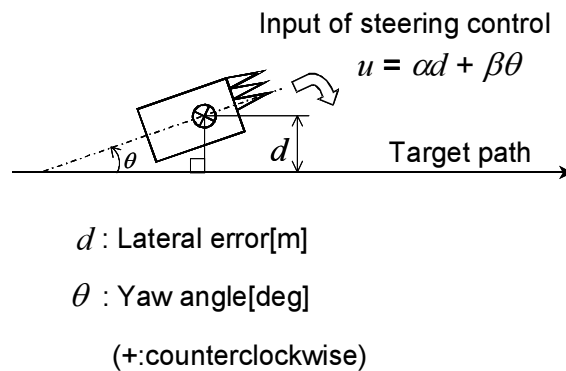


**Figure 4. Steering control for straight traveling.**

The turning control method consists of 1) left turns at the angle  $\psi/2$  [deg] while traveling forward, 2) reversing at a constant interval  $a$ , and 3) right turns at the angle  $\psi/2$  [deg] while moving backward. The yaw angle of the combine was measured with the FOG. After changing the direction of the yaw angle  $\psi$  [deg], the combine stopped immediately and reset the yaw angle of the FOG before traveling the next straight path.

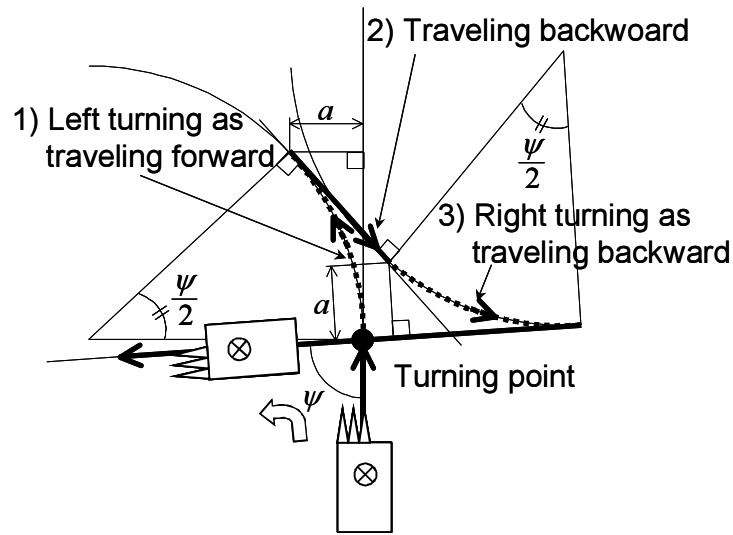


Figure 5. Turning method to change direction.

**Field Test**

Field tests were carried out in a paddy field (135° 31' 55" E, 35° 5' 29" N) in Yagi, Nantan, Kyoto, Japan in October, 2005. Figure 6 shows the shape of the field and the harvest rice area. In this figure, the origin represents the northwest point of the field. Although the total area of the field was 16a, the rice area was a rectangle of 22m x 11m.

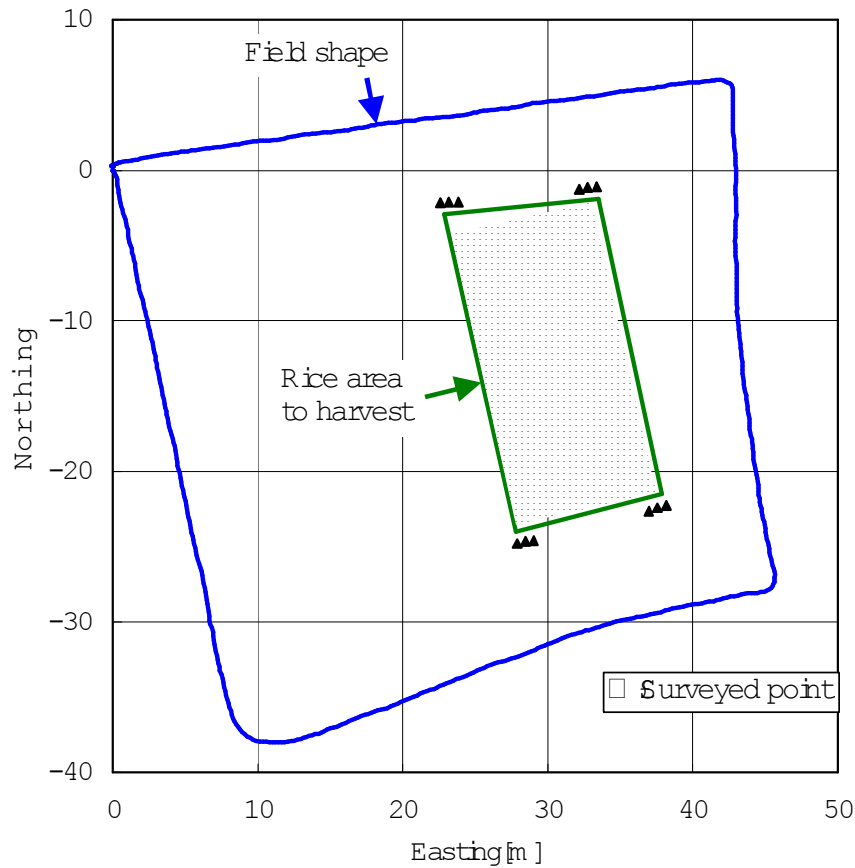
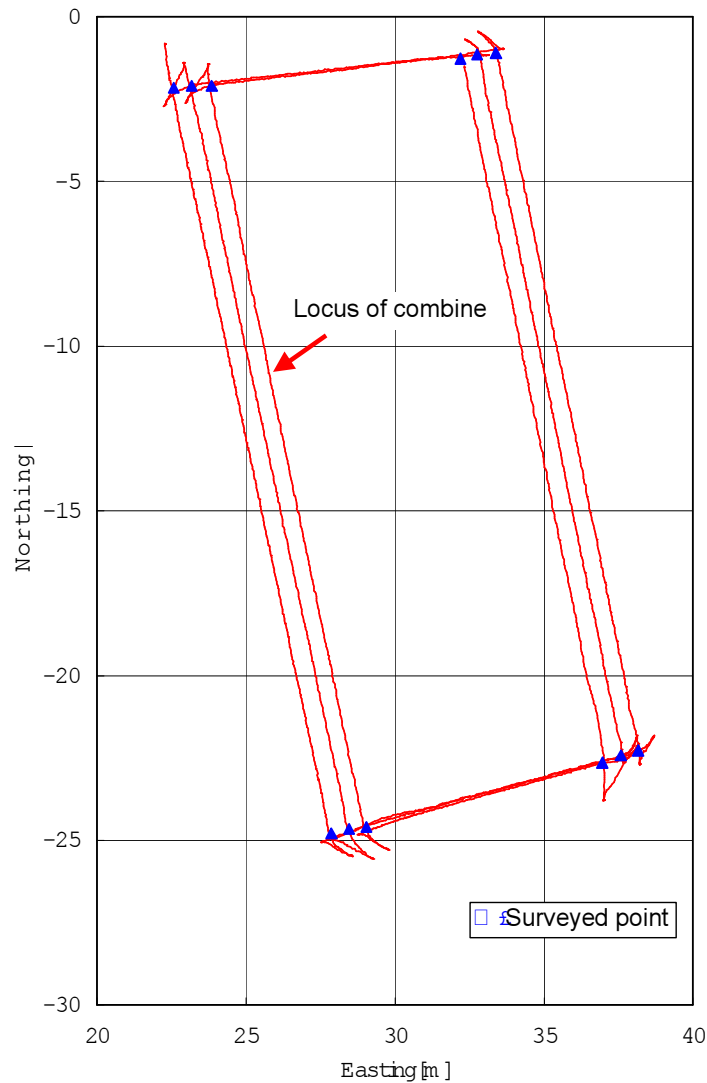


Figure 6. Test field shape and rice area to harvest.

In the experiment, the autonomous combine harvested rice three laps in consideration of the grain tank capacity. Twelve positions of rice stalks were surveyed to plan the desired path with RTK-GPS. These positions are represented by marks ▲ in the figure 6. The combine harvested two rice rows according to this desired path. The data from the GPS and the FOG were stored in the hard disk of the note PC.

## RESULTS AND DISCUSSION

Figure 7 shows the experimental result for traveling locus of the combine. The coordinate system is the same in figure 6. The combine harvested twelve rice rows in total counterclockwise. It took thirty minutes and twenty-five seconds for the combine to harvest at an average speed of 0.3m/s. The combine worked well without problems such as clogging with stalks during harvesting. In addition, there was no rice left after the combine had harvested.



**Figure 7. Traveling locus of combine when harvesting rice.**

Table 1 shows the lateral deviations and the yaw angle error of the combine in the straight path tracking. The maximum and R.M.S. of the lateral deviation were 156mm and 95mm, respectively. The maximum and R.M.S. of the yaw angle error were  $-13.2^\circ$  and  $8.60^\circ$ , respectively. The bias of the yaw angle of the FOG caused the error. However, if the combine traveled more than 2m, the lateral error converged within the clearance 30cm between rice rows. It will be important to correct the bias of the yaw angle in order to minimize the lateral error and the yaw angle error in the future, although these errors were not significant for harvesting operations.

Table 2 shows the lateral errors between the next straight path and the combine position and the turning angle errors in the left turning mode at the headland. The maximum and R.M.S. of the turning angle error were  $2.2^\circ$  and  $1.3^\circ$ , respectively. The maximum and R.M.S. of the lateral error were 140mm and 100mm, respectively. The experimental results indicated that the turning control method proposed was efficient.

**Table 1. Lateral deviations and yaw angle errors while traveling straight.**

No.	Lateral deviation [m]					Yaw angle error [°]				
	Means	Max.	Min.	Std. dev.	RMS	Means	Max.	Min.	Std. dev.	RMS
1	0.038	0.064	0.002	0.010	0.039	-3.48	1.59	-6.40	1.44	3.76
2	0.055	0.099	-0.045	0.021	0.059	-5.08	3.95	-7.93	2.21	5.54
3	0.065	0.121	0.040	0.011	0.066	-6.69	-2.47	-11.65	1.74	6.91
4	0.056	0.089	-0.018	0.018	0.059	-5.75	0.23	-8.98	1.98	6.08
5	0.063	0.100	0.015	0.012	0.064	-6.00	0.92	-9.67	1.55	6.20
6	0.091	0.156	-0.020	0.028	0.095	-8.06	2.87	-13.22	3.00	8.60
7	0.047	0.083	0.005	0.012	0.049	-4.58	3.28	-9.04	1.71	4.89
8	0.074	0.139	0.034	0.018	0.076	-7.56	-4.16	-12.52	1.68	7.75
9	0.026	0.063	-0.005	0.011	0.028	-2.47	1.21	-5.95	1.52	2.90
10	0.060	0.096	-0.030	0.028	0.066	-5.41	2.64	-9.13	2.80	6.09
11	0.024	0.069	-0.040	0.017	0.030	-2.49	2.62	-9.90	2.07	3.24

**Table 2. Lateral errors and yaw angle errors of the combine after turning.**

No.		1	2	3	4	5	6	7	8	9	10	RMS
Yaw angle	Desired	90.6	89.0	82.9	97.6	90.6	89.0	83.3	96.9	90.9	88.7	
	Error	-0.6	1.7	0.8	1.7	1.1	-0.1	-1.0	-0.3	2.0	2.2	1.3
Lateral error [m]		-0.07	0.08	-0.02	0.02	-0.02	0.05	0.14	0.03	-0.03	0.03	0.1

## CONCLUSION

An autonomous combine equipped with the GPS and the IMU was developed to harvest rice automatically. The desired path for the harvesting operation was planned using the position data of the rice measured with GPS previously. The combine harvested rice successfully three laps within the R.M.S. 95mm of the lateral deviation from the desired straight path and the R.M.S. 1.3° of the yaw angle error. The way of turning control at the headland was planned as a combination with the left turn moving forward and the right turn moving backward. After turning, the maximum of the lateral deviation and the yaw angle error from the next desired path were 140mm and 2.2°, respectively. The result indicate that controlled turning was effective and precise to change direction at the headland.

## REFERENCES

1. Benson, E. R., Reid, J. F., Zhang, Q., 2003. Machine vision-based guidance system for an agricultural small-grain harvester, *Trans. ASAE*, 46(4), 1255-1264.
2. Iida, M., Kudo, M., Ono, K., Umeda, M., 2001. Autonomous follow-up vehicle system for agriculture (Part 3)(in Japanese), *Journal of JSAM*, 63(4), 80-84.
3. Kanetoh, Y., 1977. Driverless Combine Harvester, *Proc. Int. Grain and Forage Harvesting Conf.*, 38-42.
4. Kito, K., Nishimura, I., Kawamura, T., 1991. Optimum running control of head-feeding combine (Part1) (in Japanese). *Journal of JSAM*, 53(2), 63-70.
5. Kito, K., Nishimura, I., Kawamura, T., 1991. Optimum running control of head-feeding combine (Part2) (in Japanese). *Journal of JSAM*, 53(6), 59-66.
6. Kise, M., Noguchi, N., Ishii, K., Terao, H., 2002. Field mobile robot navigated by RTK-GPS and FOG (Part3), *Journal of JSAM*, 64(2), 102-110.
7. Nagasaka, Y., Taniwaki, K., Otani, R., Shigeta, K., Sasaki, Y., 1999. The development of autonomous rice transplanter (Part 1) (in Japanese), *Journal of JSAM*, 61(6), 179-186.
8. Ollis, M., Stentz, A., 1997. Vision-based perception for an autonomous harvester, *Proc. IROS'97*, 3, 1838-1844.
9. Yukumoto, O., Matsuo, Y., Noguchi, N., Suzuki, M., 1998. Development of tilling robot using position sensing system and geomagnetic direction sensor, *Journal of JSAM*, 60(5), 53-61.



# FULL AUTOMATED RICE TRANSPLANTING OPERATION USING GPS GUIDED RICE TRANSPLANTER WITH LONG MAT TYPE HYDROPONIC RICE SEEDLINGS

Y. Nagasaka<sup>1</sup>, H. Kitagawa<sup>1</sup>, A. Mizushima<sup>2</sup>, N. Noguchi<sup>2</sup>, Y. Kanetani<sup>1</sup>,  
N. Umeda<sup>1</sup> and T. Kokuryu<sup>1</sup>

## ABSTRACT

We have developed an RTK-GPS guided autonomous rice transplanter. We have already report about that autonomous rice transplanter in ATOE 2002 meeting (Nagasaka et al., 2002). In 2005, we modified the rice transplanter to carry long mat type hydroponic rice seedlings (Tasaka et al., 1998) and attach the herbicide dripping machine. Because of using long mat type hydroponic rice seedlings, we don't need to supply the seedlings during rice transplanting operation in 0.3ha Japanese standard size field. So we can make full autonomous rice transplanting operation with a new modified rice transplanter.

We improve the sensor to reduce the vehicle cost. We remove expensive FOG posture sensor and we use low cost posture sensor which was developed in Hokkaido University to measure the azimuth and inclination (Mizushima et al., 2002). We modified processing program of this sensor to adapt rice transplanting operation. We use network RTKGPS instead of establishing reference station.

We had an experiment of our modified rice transplanter in farmer's field. It took about one hour from entering to going out of the field. The experiment was almost succeeded.

**KEYWORDS.** Automatic Guidance, GPS, Long Mat Type Hydroponic Rice Seedlings, Paddy Field, Rice Transplanter.

## INTRODUCTION

The objective of this study is to develop an automated operating system in paddy fields. The goal of this research is that one operator controls multiple machines and makes a highly efficient operation. In Japan, operating area for one farmer is going to increase, but it is not enough consolidated. Probably they are dispersed. It is necessary to develop an automated operation technology that one operator drives multiple machine at several dispersed fields. It is possible when operators use automated control system.

We developed an automated rice transplanter and made a 6-row automated rice transplanting operation (Nagasaka et al., 2000). Then we modified this rice transplanter to make more precise operation. We also used RTKGPS and FOG sensors and replaced a vehicle control system. A programmable logic controller (PLC) is used to make a precise actuator Control. All data is sent with digital signal (Nagasaka et al., 2004).

Until year 2004, we use conventional type rice seedlings for an autonomous rice transplanter. At that time, we need to supply the seedlings during operation and it is the problem for a full automated rice transplanting operation. Tasaka et al. (1998) developed long mat type hydroponic rice seedlings and a several dozens of farmers use these seedlings in present (Kitagawa et al., 2004). We modified operating attachment of autonomous rice transplanter to carry these seedlings.

---

<sup>1</sup> National Agricultural Research Center, 3-1-1 Kannondai, Tsukuba, Ibaraki 3058666 Japan, zentei@affrc.go.jp

<sup>2</sup> Hokkaido University, Kita-ku, Sapporo, 0608589 Japan

In this study, we also aim to develop lower cost system. First, we remove expensive FOG posture sensor and we use low cost posture sensor which was developed in Hokkaido University (Mizushima et al., 2002). This sensor consists of two inclination sensors and three rate gyro sensors. Then we used network-based RTKGPS. (Rizos, 2002). In Japan, Geographical Survey Institute has established about 1,200 GPS-based control stations throughout the country.

We report about modified rice transplanter and discuss about results of the full automated operation experiment in farmer's paddy field.

## MATERIALS AND METHODS

### Automated Rice Transplanter

We modified a 6-row rice transplanter. Figure 1 shows the modification of the rice transplanter for control by a computer whose CPU is 486 compatible 66 MHz. Figure 2 shows the automated rice transplanting system. GPS data is sent to posture sensor, and then posture sensor sends corrected position and direction data to the main computer. The main computer calculates the control parameters and sends them to a PLC (Programmable Logic Controller) through parallel output port every 200 milliseconds. The PLC received control parameters from main computer through parallel input unit, then control actuators. All actuators are connected to relays, so the moving direction and speed could be controlled with pulse width from PLC. The steering angle was sensed with an absolute rotary encoder and it was controlled by DC-motor. The clutch and brakes positions were sensed with proximity sensors and they were controlled by electrical linear cylinders. The positions of transplanting instruments control lever, of engine throttle and of HST lever were measured with absolute rotary encoders and they were controlled by electrical linear cylinders. The PLC control loop was 2 milliseconds.

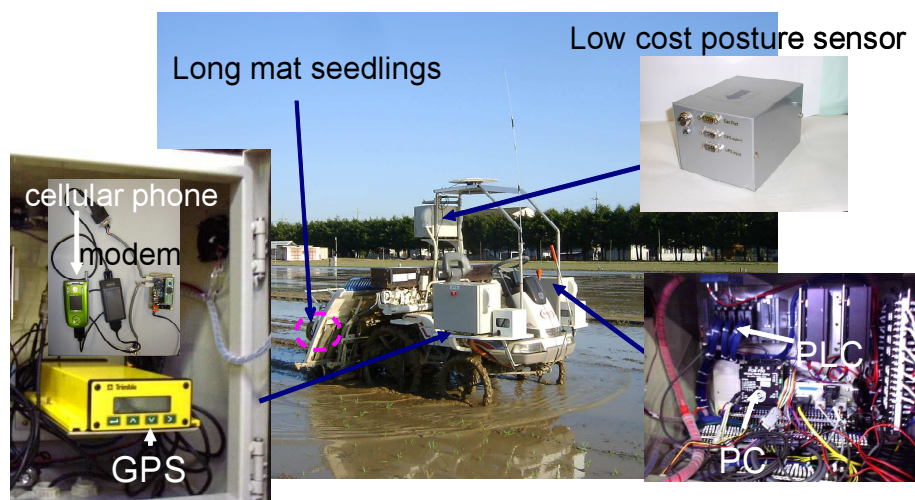


**Figure 1. Automated rice transplanter.**

### Sensors

A network-based RTKGPS was used to locate the position of the rice transplanter. In this study, we use network RTKGPS reference stations which have been established by Geographical Survey Institute. These reference stations were established as GPS based control stations to monitor daily movement of the land of Japan. Observation data thus obtained are made available for actual survey works and for studies of earthquakes and volcanic activities (Geographical Survey Institute, 2006). When we use them as GPS reference stations, we don't need to establish our own reference station. We can reduce the number of expensive GPS receiver. For the communication between the reference station network and the rover station, cellular phone and modem were used. The baud rate was set at 38,400 bps.

A low cost posture sensor was used to measure the yaw, roll and the pitch angles. It costs one tenth compare with expensive FOG sensor. This sensor consists of two inclination sensors, three rate

gyro sensors and 16 bit micro-controller. It receives GPS position data and output inclination corrected position data and azimuth.

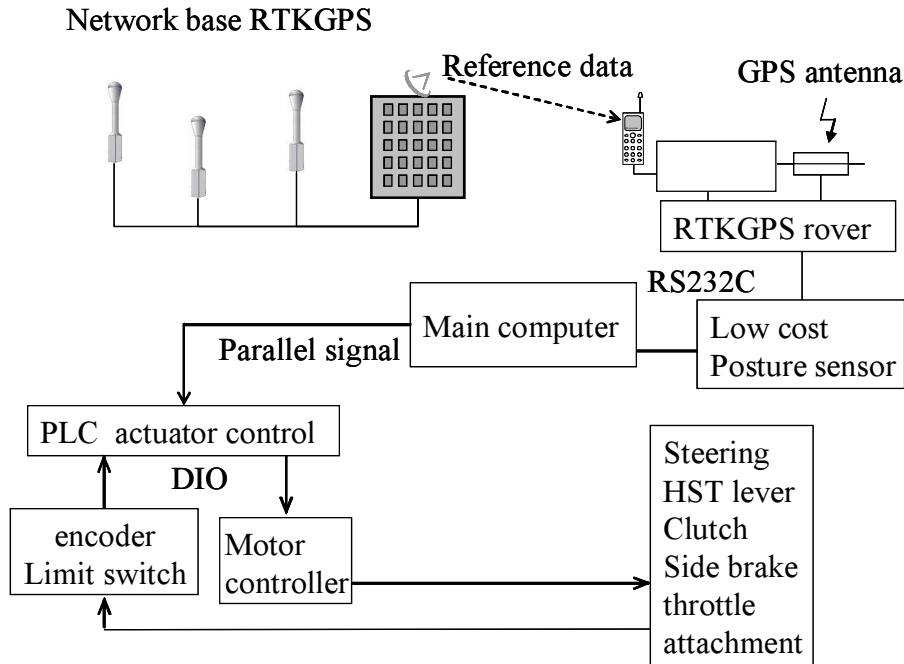


Figure 2. Automated rice transplanting system.

Roll and pitch angles are measured by inclination sensor and rate gyro. Usually, inclination sensor has delay and rate gyro has drift. A micro-controller receives both analog data and calculates real time data. Yaw angle is measured by only rate gyro. The drift is too large when we use the data as it is. Micro-controller receives GPS position data and calculates the path of the vehicle, and then it compares the rate gyro sensor data with vehicle direction, and cancels rate gyro drift.

This low cost sensor was developed for the tractor operation for speed more than 1 m/s. The operation speed of our rice transplanter is slower than tractor operation. Usually it is 0.7 m/s and at the turning it is slower than this. Turning radius at the headland is around 2 m. It is smaller than tractor. So we modify the software of this low cost sensor to adapt to rice transplanting operation.

### Control Method

The desired traveling path was calculated with four corner points of the square field measured by RTKGPS before operation. With four corner position data, we calculated and made desired operation path. We programmed the width of headland is 3.9 m. It means two path of operation. The rice transplanter must be driven along the desired path. The steering is controlled to get back close to the desired path. When it is supposed that the deviation from the target line is  $d$  and the yaw angle is  $\psi$ , the aiming steering angle  $d_{aim}$  is given as the following equation.  $K_{p1}$ ,  $K_{p2}$  are decided by the vehicle speed.

$$d_{aim} = K_{p1}d + K_{p2}\psi \quad (1)$$

The GPS data quality indicator was monitored while the rice transplanter travels automatically, and if the radio link between GPS base station and GPS rover station is disconnected, the clutch is released and the operation is interrupted.

At the headland, the rice transplanter moves forward and backward to turn so as to minimize the headland space. The width of headland is 3.9 m. Figure 3 shows the way of turning at the headland. When the rice transplanter reaches the edge of the field, it stops and reset posture sensor. While the rice transplanter is turning, the rice transplanter obtains only yaw angle gyro sensor data. Because turning radius is so small, drift-corrected yaw angle data is not effective at the turning and it is enough short to use non drift-corrected yaw angle data during around 30 seconds turning.

Until the yaw angle is over 160 degrees, the steering angle is kept 40 degrees and one side brake is applied. When the yaw angle becomes more than 160 degrees, the rice transplanter is controlled to

get back close to next desired path. Then rice transplanter resets posture sensor again and starts next operation. If the rice transplanter does not get close the new desired path enough after turning, the steering is controlled to get close to the desired path when it moves to backward.

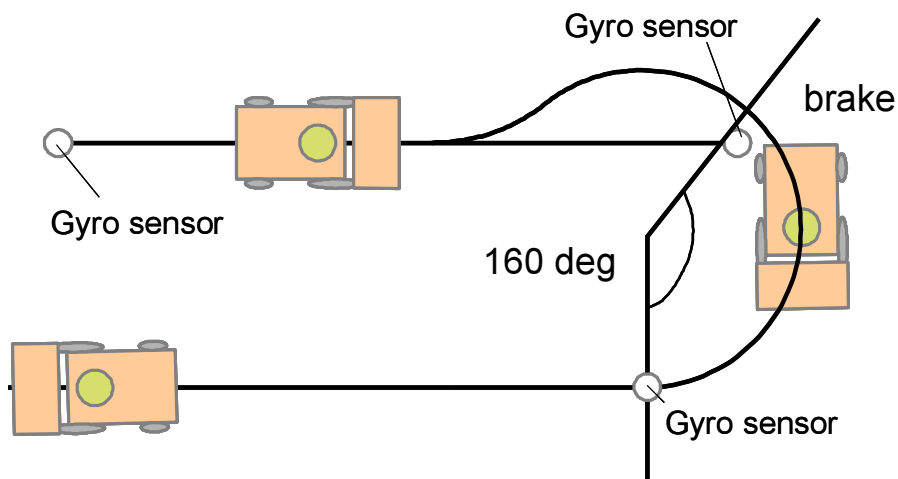


**Figure 3. Turning at the headland.**

### RESULTS AND DISCUSSION

The experiment was conducted 3 days after puddling. We set this rice transplanter at the entrance of the field. When Program started, it entered to the field and after transplanting at the whole headland, it went out from the field.

Figure 4 shows the rice transplanter in operation. The depth of the paddy was about 15 cm. The rice transplanter went for and back in a 30 m \* 100 m square field. It took almost one hour for 0.3 ha Japanese standard size field.



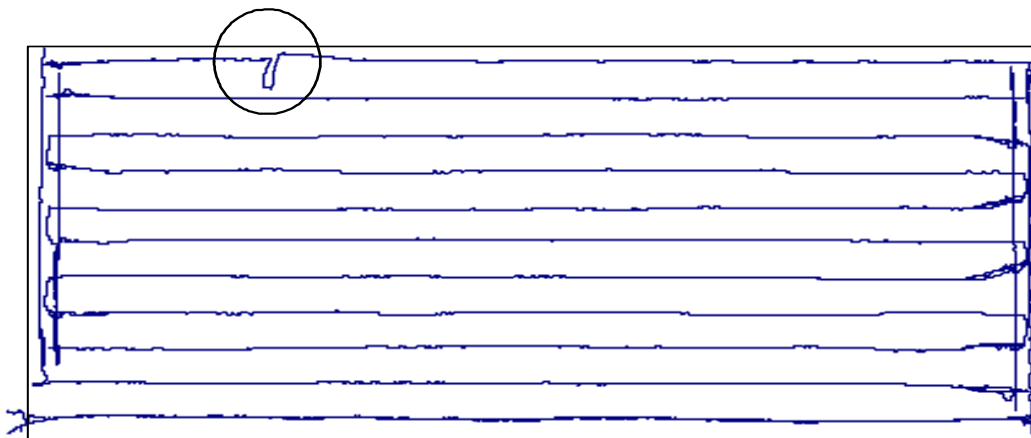
**Figure 4. The rice transplanter in operation.**

Figure 5 shows the path of the rice transplanter. In this data, the influence of the vehicle inclination was corrected. The deviation from the desired straight path was less than 12 cm at 0.7 m/s of travel speed during the operation. Around the part highlighted with a circle, the path is

distorted 70 cm. At this part, posture sensor outputs abnormal roll and pitch angle. We try to fix the reason in present.

After turning at headland, when the deviation from the next desired path was more than 30 cm or direction at the start point was not enough close to aiming direction, the path became meander. In those cases, though the direction of the rice transplanter was not enough close to aiming direction, the rice transplanter reset low cost sensor and recognized it to be as correct direction at the start point. The low cost sensor yaw angle output could not recognize an absolute direction after reset. A micro-controller in the sensor referenced GPS position path and corrected the direction output. Until the low cost sensor received enough number of GPS position data, the path was meander. So every operation path, when the rice transplanter traveled more than 30 m, the path leveled off.

For puddling, we used 37.3 kW output tractor and it made wheel track in the field because of its weight. The tread of the tractor and that of the rice transplanter are different. So the rice transplanter sometimes followed tractor wheel track and couldn't get back close to the desired path. Even the deviation was more than 15 cm and the steering angle was set to 5 degrees, it was hard to get out of the tractor wheel track.



**Figure 5. The path of the automatic operation.**

When the reference data communication link was disconnected, the clutch was released and operation was interrupted. Then as soon as the radio link was connected, it started operation again.

## CONCLUSION

In this study, we made full automated rice transplanting operation and aimed to develop lower cost system. To make full automated rice transplanting operation, we carry long mat type hydroponic seedlings. To reduce the machine cost, we used low cost posture sensor instead of expensive FOG sensor and also used network based RTKGPS.

Though the operation accuracy has not been enough yet, the full automated transplanting experiment almost succeeded from entering into the paddy field to going outside.

## REFERENCES

1. GSI, 2006. Geographical Survey Institute, Geodetic Survey. Available at: <http://www.gsi.go.jp/ENGLISH/index.html>. Accessed 10 June 2006.
2. Kitagawa, H. Ogura, A., Tasaka, K., Shiratsuchi, H. and Yashiro, M. 2004. One-man rice transplanting technology of long-mat seedling culture system. *Proc. World rice research conference 2004*, 456. Tsukuba, Japan. MAFF.
3. Mizushima, A., Noguchi, N. and Ishii, K. 2004. Automatic navigation of agricultural vehicle using low cost attitude sensor, In *Proc. Automation technology for off-road equipment 2004*, 98-106, ASAE.

4. Nagasaka, Y., Otani, R., Shigeta, K. and Taniwaki, K. 2000. A Study about an Automated Rice Transplanter with GPS and FOG. ASAE Paper No. 00-1045. Milwaukee, WI., ASAE.
5. Nagasaka, Y., Umeda, N. Kanetai, Y. 2002. Automated rice transplanter with GPS and FOG, In *Proc. Automation technology for off-road equipment 2002*, 190-195, ASAE.
6. Nagasaka, Y. Umeda, N. Kanetai, Y., Taniwaki, K. and Sasaki, Y. 2004. Autonomous guidance for rice transplanting using global positioning and gyroscopes, *Computers and Electronics in Agriculture* 43 223-234.
7. Rizos, C. 2002. Network RTK research and implementation - A Geodetic Perspective, *J. of Global Positioning Systems* 1( 2) 144-150.
8. Tasaka, K. 1998. Outline of raising and transplanting technology for long mat type hydroponic rice seedlings., Ag. Eng. Paper 98-A-061, Oslo, EurAgEng.

# GI AND GPS SYSTEMS ENHANCING PLOT PARCEL CREATION

P. O. Noack<sup>1</sup>, T. Muhr<sup>1</sup> and M. Demmel<sup>2</sup>

## ABSTRACT

Parcel plot trials are a standard method in scientific and commercial research. Comparing quantity and quality of yield from different parcels helps to determine how different breeds of plants perform in *ceteris paribus* conditions and under standardized treatment. Parcel plot trials are also used for comparing the effect of different intensities of treatment with herbicides, insecticides and fertilizer on the growth of plants of the same breed.

Creating parcel plots is labour and cost intensive. Marking the relative distances between the parcel boundaries involves the use of traditional land survey methods. The Bavarian State Research Center for Agriculture and geo-konzept GmbH have refined existing GPS and GI systems to cut down the costs involved in seed plot trials and extend their reliability.

An extension for a standard GIS software package has been developed to support the computer aided creation of parcel plot blocks. The software provides an import interface to standard parcel plot management databases and an export interface to a mobile computer device used for controlling a commercial automated steering system.

The automated steering system uses a RTK-GPS sensor and gyroscopes to control the driving direction during the creation of plot parcels. A mobile computer device triggers the sowing machine when the tractor enters a plot parcel. This allows to locate newly created parcels and to recover existing parcels with a longitudinal accuracy of 10 cm and a lateral accuracy of 2 cm.

**KEYWORDS.** Automated Steering System, GIS, GPS, Parcel Plot Trials.

## INTRODUCTION

**Parcel plot trials.** Parcels are small rectangular plots covered with crops having a dimension in the range of a few meters. They are being arranged in rectangular parcel blocks in a field with pathways separating the parcels in longitudinal direction. Parcels within a parcel block are

- covered with the same breed of a plant but treated differently with respect to herbicide or fertilizer application and
- covered with different breeds of a plant with all parcels being treated the same.

Parcel plot trials are a standard method in commercial and scientific research for determining the effects of different treatments on plants. They are also extensively undertaken to identify superior plant breeds under defined conditions (soil, climate, treatment).

Parcel blocks are established by marking the edges of the parcel block and the pathways with stakes or chalk. This is commonly accomplished by using standard survey methods. This process is very labour and cost intensive. For seeding, special sowing machines are being used. They are usually triggered manually when passing a mark at the edge of a parcel.

Some parcel plot sowing machines can be automated to remove the remaining seeds from the seeding system of the sowing machine at the end of the parcel. Other sowing machines require that the amount of seed applied, the seeding density and the length of the parcels match to finish the application of seeds at the end of parcel.

---

<sup>1</sup> geo-konzept GmbH, Gut Wittenfeld, D-85111 Adelschlag, Germany, pnoack@geo-konzept.de

<sup>2</sup> Bavarian State Research Center for Agriculture (LfL), D-85354 Freising, Germany

**GIS.** Geographic Information Systems (GIS) allow to view and to edit objects in real world coordinates. They can handle vector objects (and their attributes) in the form of points, lines and polygons. Similar to Computer Aided Design (CAD) systems, GI systems may be used or adapted to construct, move and rotate complex objects. Creating a rectangular agglomeration of rectangular blocks like a parcel block trial to be moved and rotated according the users needs can be achieved in substantially less time than with standard surveying methods on site.

**GPS and automated steering systems.** GPS is a satellite based navigation system. GPS receivers using information from both GPS frequencies (L1 and L2) and receiving corrections from a local base station can determine their position with an accuracy in the range of a few centimeters (RTK GPS). Several manufacturers have combined RTK GPS receivers with accelerometers and gyroscopes to exactly determine position, heading, roll, pitch and yaw of a moving vehicle. The values measured allow to manipulate the vehicle steering system through electro hydraulic valves and keep the vehicle on predefined tracks with a very high accuracy.

### SOFTWARE FOR DESIGNING PLOT PARCEL BLOCKS

The software for creating parcel block trials has been derived from an existing GI system which had originally been developed for other purposes. The software requires a field boundary to be loaded before creating parcel blocks. The field boundary may be loaded as an ESRI Shape file and must contain WGS 84 coordinates.

After loading the field boundary the first step is to define the number of rows and columns of the parcel block as well as the width of the pathways. This process is facilitated by a parcel block editor (Fig. 1). The number of parcels in longitudinal direction (rows) within the parcel block can be manually entered. The number of columns (number of parcels in latitudinal direction) can be defined for the whole parcel block or individually for each row. The width of the pathways may also be entered for all pathways or for each pathway individually.

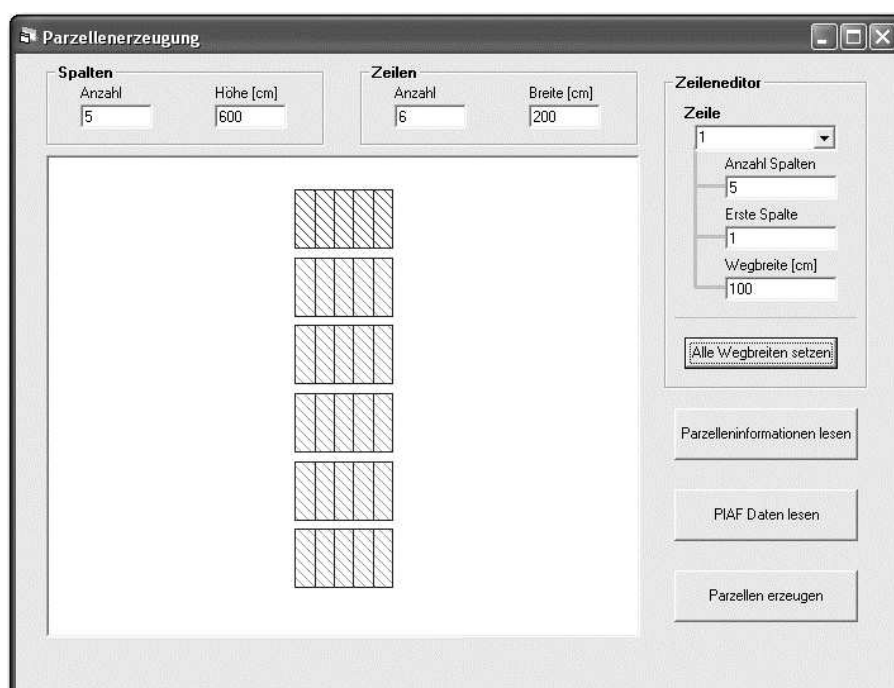


**Figure 1. Creating parcel blocks.**

After the parcel block has been created it will be placed in the center of gravity of the field boundary. It may then be freely moved and rotated until the parcel block is located in the desired position. When the parcel block location has been adjusted, the trigger points for the seeding machine and reference line for the automated steering system can be created with a single mouse click (Fig. 2). The user is prompted for the offset between the GPS antenna and the sowing machine because this offset has to be accounted for when creating the trigger points. The reference

line and the trigger points as well the parcel outlines are automatically saved in ESRI Shape file format to hard disk.

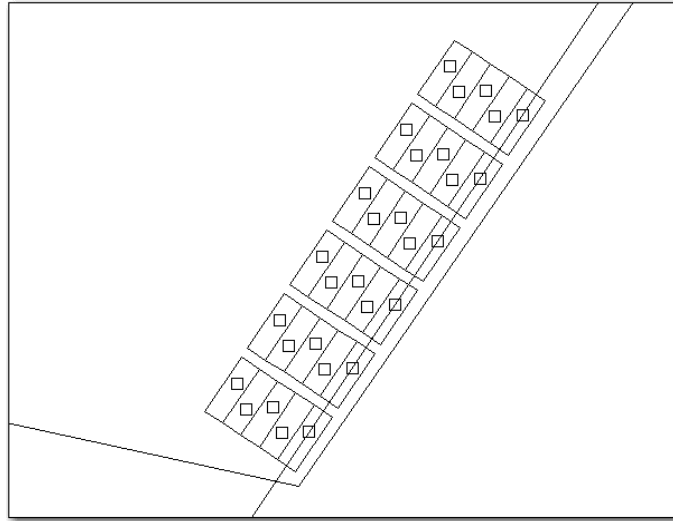


**Figure 2. Parcel blocks with trigger points and guidance line.**

After creating the trigger points and the reference line, the data can be exported to a CF data card. This data card contains files arranged in certain directory structure and can be inserted into a mobile field computer (Trimble AgGPS 170). This device acts as an interface between the tractor driver, the automated steering system and the sowing machine.

### **MOBILE COMPUTER DEVICE FOR AUTOMATED STEERING AND APPLICATION CONTROL**

The Trimble AgGPS 170 is a very rugged mobile field computer which has been designed to control a Trimble AgGPS Autopilot system as well as other external devices (Fig. 3). It also allows for logging attributed spatial data. Attributes may be entered manually or with a barcode scanner.



**Figure 3. Trimble AgGPS 170 mobile field computer.**

The integrated software FieldManager reads data from a CF card. The data is structured by client, farm and field. All data created by the above described desktop GI system are stored in a field directory. Once this field is opened with FieldManager software, the field boundary and all data prepared with the software for parcel plot creation are visible on the screen (Fig. 4).

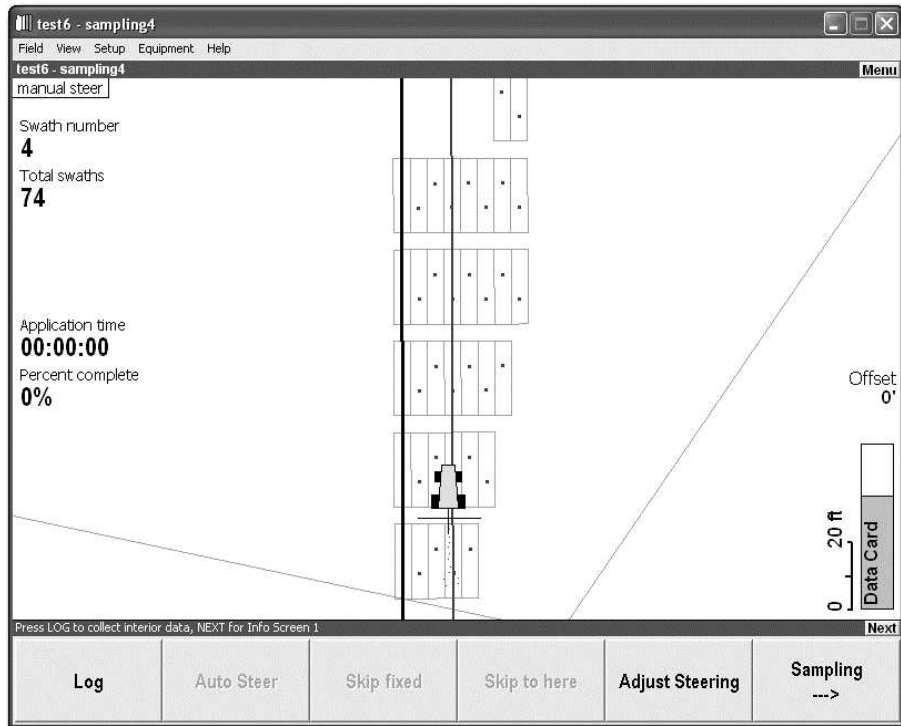


**Figure 4. Parcel blocks on AgGPS 170.**

The automated steering systems on the tractor will keep the vehicle automatically on the reference line with an accuracy of 2 cm. Once the tractor moves to next column of parcels the reference line is shifted by the working width of the sowing machine which is to be entered in the configuration settings of the FieldManager software. The driver of the tractor will only have to take care of turning the machine at the end of each parcel column.

When the GPS antenna on the tractor passes over one of the trigger points the AgGPS 170 provides an electric signal. This signal is fed into a relay box on the seeding machine. The relay box generates a switch signal which is routed to a solenoid connected to the seed bin on top of the seeding machine (Fig. 5). The seeds are then released into the seeding system.



**Figure 5. Seeding machine with seed bin and solenoid switch (picture by Konrad Fink, LfL).**

The offset between the GPS antenna and the sowing machine has been accounted for during the process of creating the trigger points in the parcel plot creation software. However, there will be some delay until the seeds are released into the soil. This delay time depends on the sowing machine and on the kind of seed. In trials with a Hege sowing machine and barley seeds the delay

was found to be approximately one second. The FieldManager software on the AgGPS 170 mobile field computer allows to set a delay time. It will trigger an event by sending the electric signal ahead of the time reaching the trigger point according to the delay time set in the configuration menu.

## RESULTS AND DISCUSSION

First trials with a 40 hp Deutz tractor and a Hege sowing machine (Fig. 6) have been undertaken at the Bavarian State Research Center for Agriculture in Freising (Germany) in spring 2005. The Trimble AgGPS Autopilot system being a standard component that has been commercially available since 2000 has been keeping the tractor on the reference line with an accuracy of two centimeters as expected.



**Figure 6. Tractor sowing parcel block trial (picture by Konrad Fink, LfL).**

During several consecutive trials the delay time between triggering the solenoid and the seeds reaching the seed shares had to be determined. Parcels were sown with barley on parallel tracks driving in opposite directions. After the crop had germinated the offset between the beginning and the end of neighboring parcels was measured with a band tape. This procedure was repeated with different delay times until a delay time of one second had been determined for this model of sowing machine and barley seeds. After this value had been applied, the system was creating the parcel boundaries with a longitudinal accuracy of approximately 10 cm. This value is in the same range which is achieved when the seeding process is triggered manually by the operator of the seeding machine. However, the operator is also in charge of refilling the seeding bin at the beginning of each parcel. Triggering the seeding process automatically increases the potential working speed and reduces the likelihood that the wrong seed is filled into the seeding bin.

The above described procedure for determining the delay times has proven to be too labour and time intensive. It is therefore suggested to determine the point in time when the seeds leave the sowing machine with an optical device or a microphone. This would allow to assemble a setup that triggers the solenoid and measures the time until the first seeds are detected at the seed shares.

## CONCLUSION

The concept of a system for the automated creation of seed plot trials has proven to be viable. Designing the plot trials with the help of software has helped to substantially save input in terms of time and labour. The automated steering system automatically keeps the tractor on the predefined tracks with a very high accuracy, relieves the driver and minimises errors during long working hours. The settings of the system components for triggering the seeding machine may be further refined.

### Acknowledgements

The authors would like to thank Dr. Zeltner, Mr. Fink and Mr. Schmidt (all Bavarian State Research Center for Agriculture (LfL), Freising, Germany) for their kind collaboration during the development of the above described system for the automated creation of seed plot trials.

# REMOTE ASSISTED TASK MANAGEMENT FOR ISOBUS EQUIPPED TRACTOR-IMPLEMENT COMBINATION

V. Virolainen<sup>1</sup>, L. Pesonen<sup>1</sup>, J. Kaivosoja<sup>1</sup>, J. Oittinen<sup>2</sup> and J. Kivipelto<sup>2</sup>

## ABSTRACT

Efficient task management is a key to profitable use of an automated tractor-implement combination in the field. The information management system which is used to operate automation of the tractor-implement combination can be used to manage the external information such as to the task or surrounded environment related information, as well. User-friendly open operation environment that provides possibilities for intelligent on-line functions in the field and remote support via internet connections is introduced. The system utilizes open system interfaces and ICT standards, such as ISOBUS, to enable compatibility between different system parts. Wireless communication enables information exchange between off-road automation machines and external operators like support services, databases or clients. Maintaining the wireless internet based remote support system is cost efficient, since it can be used for communication between several parties. Disadvantage is that internet connection exposes the system to malicious programs and variable quality of service. The experiences from the case study concerning remote assisted task management of ISOBUS compatible tractor-implement combination were encouraging. The importance and possibilities of internet will increase further. Still there is a need for further research and development work in the areas of openness, dependability as well as user and task specific optimization of the calculation and data transfer capacity. Additional, but unavoidable challenge will be the integration of site-specific data and GIS to the other information systems.

**KEYWORDS.** Agriculture, Database, GIS, ICT, Information, Internet, ISOBUS, Management, Mobile, Openness, Usability, Wireless.

## INTRODUCTION

Sophisticated automation systems require advanced information management. Intelligent functions such as fault diagnostics, assisted user interfaces and location dependent control are typical for a novel automation also in off-road machinery like tractor-implement combinations (Suomi et al 2006). The information management system, which is used to operate automation, can be used to manage the external information like to the task or surrounded environment related information, as well. Efficient task management is a key to profitable use of an automated tractor-implement combination in the field. Wireless communication enables information exchange between off-road automation machines and external operators like support services, databases or clients. This brings great possibilities to improve quality and profitability of businesses like machinery contracting. However, there are several challenges to meet before all benefits of information management of off-road automation systems are gained. The main challenges are discussed in this study.

## CASE STUDY

The aim of the case study was to investigate remote assisted task management of a tractor-  
implement combination. The system consisted of the ISOBUS compatible AGRIX system (Fig. 1) as a platform and an information management system provided by Bitcomp Oy (Fig. 2) that was attached to it.

---

<sup>1</sup> MTT Agrifood Research Finland, Vakolantie 55, FI-03400 Vihti, Finland, liisa.pesonen@mtt.fi

<sup>2</sup> Bitcomp Oy, Yliopistonkatu 36 / Torikeskus, FI-40100 Jyväskylä, Finland

The system utilizes open system interfaces and ICT standards, such as ISOBUS, to enable compatibility between different system parts. ISOBUS compatible Agrix system, a plant production automation system (Oksanen et al 2005), consists of five operational parts, connected together with ISOBUS CAN. The parts are: Virtual Terminal (VT), Tractor Electronic Control Unit (T-ECU), Implement Electronic Control Unit (Implement ECU), Task Controller (TC) and external sensors like GPS. VT is used to provide a user interface. A virtual terminal has a graphic display, soft keys and some means to enter data. An implement ECU uploads its user interface to the terminal. T-ECU is responsible for transmitting the tractor's status information to the ISO 11783 network. All the controllers on a single implement (Implement ECUs) form a working set. In a working set, one controller functions as a working set master. The working set master is responsible for transmitting the user interface to the VT. The communication between modules, e.g. VT and TC, is standardized.

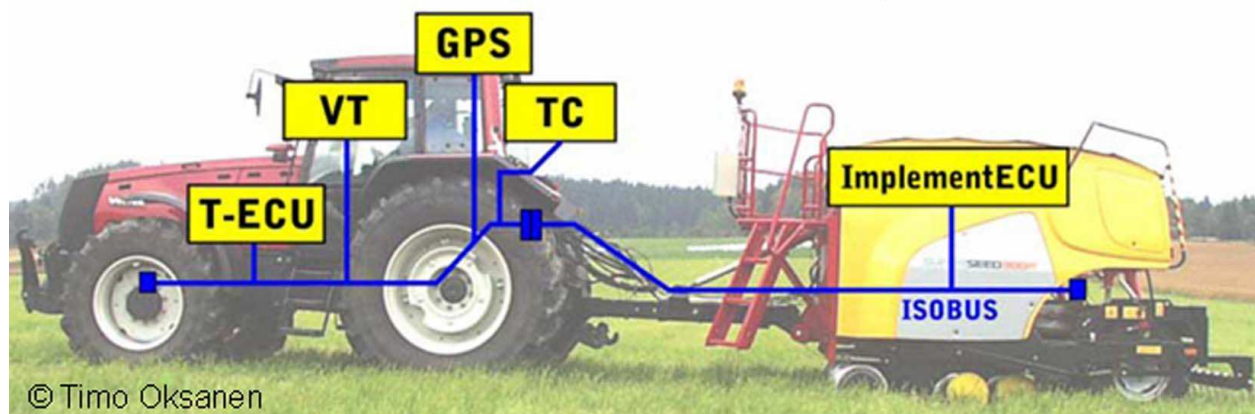


**Figure 1. ISOBUS compatible Agrix system, a plant production automation system.**

The planned tasks are imported to the TC. The TC is used for the execution of work tasks and the results of the tasks are sent back to a Farm Management Information System (FMIS), e.g. a stationary farm computer of the farmer or the contractor. A FMIS computer is used for planning and evaluation of field work. Interaction between user and TC may be realized through a VT or other interface.

The task management can be supported by several actors joining the system. The system developed by Bitcomp Oy is devised open so that it can be easily connected with other systems using XML (eXtensible Markup Language) or SMS alerts. It is possible to log in to the system from internet via authentication mechanism. Two kinds of user interfaces are offered, one for the farmers and one for the advisors. The system is based on WebWisu Farm Management Information system (FMIS) so, that when the normal cultivation plans are done in the office application of the WebWisu, the task files are created automatically by adding only the positioning data.

The task can be downloaded and updated in the field, and realized task can be reported straight to the customer via wireless internet connection. It is possible to send recorded field data files immediately after work to a centralized database, where it is stored and saved, thus being available for authorized re-users. Farmer's data is placed straight to the book keeping system the office WebWisu. The Agrix system operates with site-specific data. External site-specific task data such as application maps are imported to the system's database from farmer's PC as shape files. The tasks can be downloaded from the database to the Agrix TC via GPRS connection as an XML. Pocket PC acts as Agrix TC, which offers benefits of portability. Data format in the TC is adapted to follow the draft of ISO 11783-10 standard. Tasks can be created or imported with PC. Mobile phone can be used to supply SMS alerts with the system.

Centralized task management provides better quality control and traceability. Finnish agricultural advisory organization ProAgria, implements data warehouse services and makes necessary reports from the data. Food industry, administration, GIS-providers, forecast services etc. can connect to the Bitcomp's system using XML.

Wireless internet connection provides possibility to on-line support during the task. The updated task plan can be downloaded to the TC just before executing the task from the support service or from the client. And when adjustment or advice are needed during the work, e.g. changed weather conditions, new instructions can be downloaded rapidly, thus avoiding long downtimes. When the task is done, to the TC recorded document of realized work can be uploaded to support service (central database) or to the client immediately from the field. In this way the client can check and accept the done work at the time the machinery is still located on the working site, in case there is something in performed task that requires still additional attention.

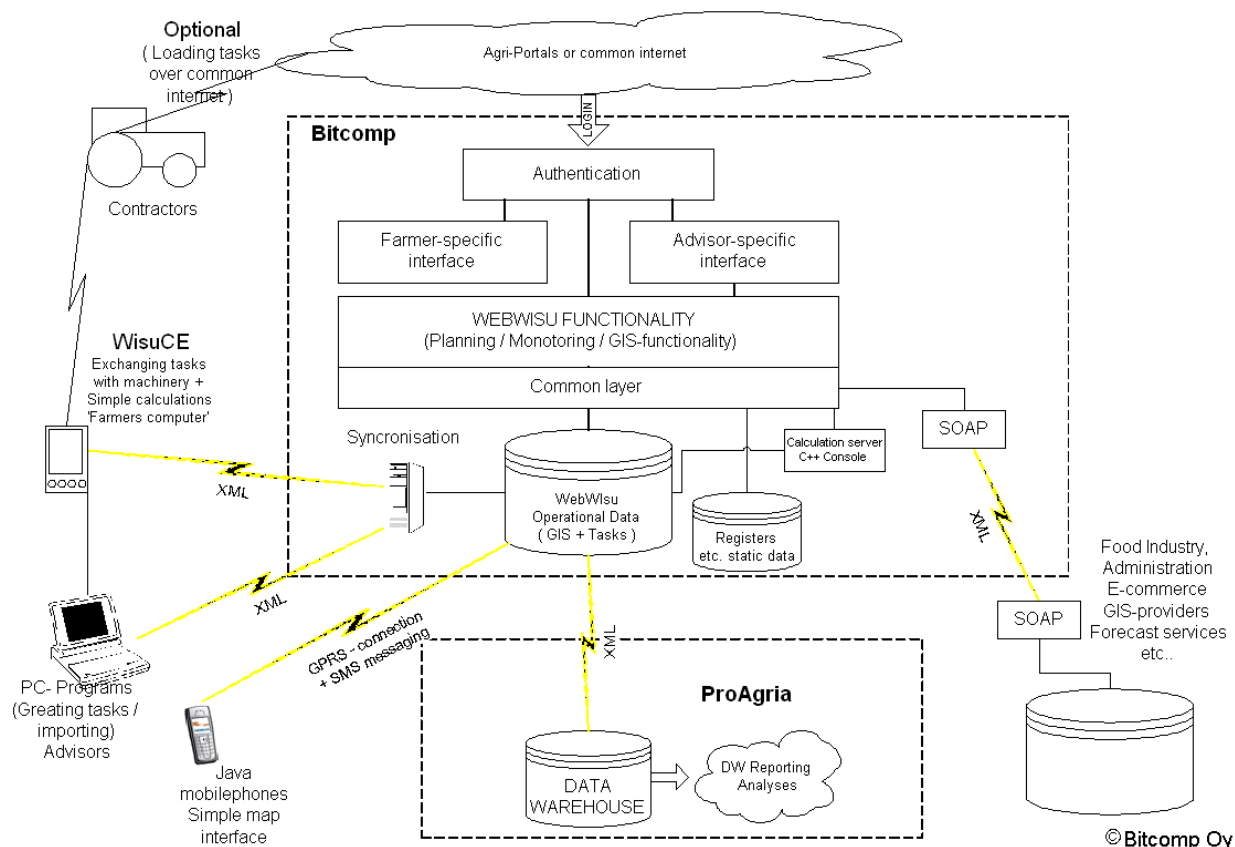


Figure 2. Open interface centralized data management system by Bitcomp Oy.

## REQUIREMENTS AND CONCERNS

Wireless remote assistance is an important feature when system usability of mobile working unit is considered. It enables availability of information just on time independent on the location. Controlled open interfaces of the systems enable compatibility between different information systems. This creates possibilities for new kinds of services, where several information producers may provide support to the same user. Utilizing common internet makes it possible for working unit to connect to the information society and its' services. However, there are several concerns and requirements to consider when applying remote support systems to mobile working units.

### Openness

Openness in the above mentioned case study means data transfer through controlled open interface, which is determined by the software provider. However, it is not always the case, that software providers are willing to offer the open interfaces. Also, there is a lack of common practices how to obey the mentioned controlled open interfaces. The development of internet technology together with the rapid adoption of the XML standard is revolutionizing data exchange within and between organizations (Meneghello 2001). Thus, XML based systems seems most promising also in agricultural applications. However, there is no reason which prevents the use of both an optimized native application specific format, and interchange format like XML (Shrestha 2004). For agricultural use aimed XMLs such as ISOBUS-XML, AgroXML and FODM™ (Field Operation Data Model) are under development at the moment.

The meaning for XML grammar is to bring the independence of data and programs to the information exchange. Information from different sources could be brought to the system in a same format. XML itself is not a file format. It doesn't describe set of logical descriptions, instead the file formats could be build on top of XML. Software can access to the data through various data models built by the parser where items of interest are defined by the associated XML schema. This means that such software is independent of the physical arrangement of the data.

More challenge is faced when site-specific data is in question. Within identical GIS platforms and database paradigm, the systems might have different conceptual database schema, different data collection schemes, or different quality parameters (Bishr 1997). Among others, to improve data exchange and to enable interoperability of independently developed applications, OGC (Open Geospatial Consortium, Inc.) has established the XML-based standard known as GML (Geography Markup Language). GML is an XML grammar written in XML schema. It is for the modeling, transport, and storage of geographic information. GML is defined as an XML encoding of geographic information, including both spatial and non-spatial properties of geographic features and it is designed to represent arbitrary data structures. This induces a lot of extra work when converting data between GML and other formats.

A question about sharing information sets a challenge for the data management. The transferred data can have parallel but differently authorized users. For example, data that are essential for a support service provider may be desired to protect from competitors. Finding reasonable limits for the information allowance and still keeping the system open and avoiding confrontation needs effort.

#### Data transfer capacity, distributed calculation and backup

The amount of collected sensor data a can vary from few kB/ha to GB/ha (machine vision). It may not be feasible to send all the data to central databases through wireless internet or GPRS connection. Average transfer speed of GPRS is as low as 30-80 kbit/s, and also wireless internet may be slow. Only urgent data, such as data used for remote fault diagnoses, are reasonable to send straight from the field to central databases, where data are available to for example remote support providers. Also the data that are supposed to be stored centralized, like refined documentation data for FMIS, are usable to upload straight from the tractor. However, it is necessary to record all the logged data in order to be able to trace possible fault functions afterwards. Even tough there are fault diagnostics built in to the system it would not cover all possible malfunction cases. The faulty functions can become visible after a certain time, and in that case backup data would be valuable when improving the system. Backup data bring also legal support in cases where the quality of a contractor's work is under speculation. The backup data can be saved to memory cards or hard drives in the tractor and be uploaded to the backup system for instance during the breaks at office yard via WLAN.

Remote support service can execute most of demanding, to the task related, calculations and send them to mobile unit. Especially, semantic web provide assisted help to find needed information easier. Automation system in mobile working unit such as tractor-implement combination can provide sensor data that can be used to provide to a sensor fusion based intelligent assistance for the driver. Intelligent functions can be intensified by external, via internet received up-to-date data, like weather data. However, sensor fusion based assistive functions and automated task updates require on-board calculation capacity. If only filtered and refined data are sent to be stored and maintained, the refining process needs calculation capacity, as well.

Present technology enables high precision site-specific data collection in crop production. This set new requirement also to FMIS. Managing into field specific accuracy refined originally site-specific output data reduces the benefits that could be achieved from intelligent implements. The larger the fields and the in-field variations are the bigger is the benefit from the more precise data management. More precise data can also improve data analysis, online support, implement calibration and reliability.

#### Dependability

There are also to dependability related concerns like availability, reliability, safety, integrity and maintainability of the support data or service. Security is composition of integrity, availability and

confidentiality which means the absence of unauthorized disclosure of information (Avizienis et al. 2004). In rural areas, especially the availability of the internet connection may be a problem. The tendency is to provide fast internet connections to all users. In Finland the goal is to cover the whole country with wireless broadband network by the end of year 2009.

The situation in telecommunications is changing rapidly. NGN (Next Generation Network) concept has been developed (ITU 2004), and it is assumed to become to common use in the near future. NGN is a packet-based network, which is able to provide services including telecommunication services, and it is able to make use of multiple broadband, QoS-enabled transport technologies and in which service-related functions are independent from underlying transport-related technologies. It offers unrestricted access by users to different service providers. It supports generalized mobility which will allow consistent and ubiquitous provision of services to users.

Mobile unit with unprotected wireless communication may cause safety problems by interfering to other wireless networks. Disabling the SSID broadcast, using WEP and configuring the network to allow only known IP and MAC address usage make more difficult to disturb the network (Dunham 2005). If the system is not protected with virus protection and other specific programs, malicious programs may cause malfunctions in operation of the working unit. Thus, unprotected networks and systems will create a risk of severe environmental and economical damages.

#### Awareness of the user over the information flow

It is important that the driver is aware of data and information flows that are taking place. Simple and natural dialogue in this case between ISOBUS VT and the user is needed. The system has to speak the user's language and the system status has to be visible providing necessary feedback data (Haapala et al. 2006). The driver has to be able to control the data flow. In case of remote service by automation or equipment manufacturers to guarantee optimal working efficiency, the driver has to be aware of when connection to support service is active.

Availability and timing of information and data has to be fitted to drivers working habits, working culture and to the working process defined by the task. The system interface has to be pleasant and easy to use, and the driver has to be able to trust the reliability of the information received and produced by the system.

Saliba et al. (2005) have studied user-perceived quality of service (QoS) in wireless data networks. Network engineers have been trying to dimension wireless networks to run in most efficient way by concentrating in QoS. Nowadays user perceptions are used in dimensioning. Reliability, efficiency, predictability and satisfaction are the main factors in users view. The main result of Saliba et al. (2005) was, that QoS is application specific. Various applications require different level of network performance to satisfy users.

## CONCLUSION

Remote just-on-time support intensifies task management and working efficiency of mobile working units like tractor-implement combinations. Use of centralized databases as data storages, enables a data management system where data is saved only once, but it is yet available to different re-users. Maintaining the wireless internet based remote support system is cost efficient, since it can be used for communication between several parties. Disadvantage is that internet connection exposes the system to malicious programs and variable quality of service. The experiences from the case study concerning remote assisted task management of ISOBUS compatible tractor-implement combination were encouraging. The importance and possibilities of internet will increase further. Especially, NGN is a very promising new technology. Still there is a need for further research and development work in the areas of openness, dependability as well as user and task specific optimization of the calculation and data transfer capacity. Additional, but unavoidable challenge will be the integration of site-specific data and GIS to the other information systems.

## REFERENCES

1. Ahvenainen, M. 2003. Wireless LAN security. MS thesis. Helsinki University of Technology. Department of electrical and communications engineering.
2. Avizienis, A., J.-C. Laprie, B. Randell and C. Landwehr. 2004. Basic concepts and taxonomy of dependable and secure computing. *IEEE Trans. Dependable and Secure Computing* 1(1), 11-33.
3. Bishr, Y. 1997. Semantic Aspect of Interoperable GIS. PhD thesis, Wageningen Agricultural University and ITC.
4. ITU. 2006. Definition of Next Generation Network. Available at: [http://www.itu.int/ITU-T/studygroups/com13/ngn2004/working\\_definition.html](http://www.itu.int/ITU-T/studygroups/com13/ngn2004/working_definition.html). Accessed 31.5.2006.
5. Dunham, K. 2005. Wireless Worries and Wisdom. *Information Systems Security*. 14(3): 5-8.
6. Haapala, H., L. Pesonen, and P. Nurkka. 2006. Usability as a Challenge in Precision Agriculture – case study: an ISOBUS VT. *Agricultural Engineering International: the CIGR Ejournal*. 9 p.
7. Meneghello, M. 2001. XML (eXtensible Markup Language) - The New Language of Data Exchange. *Cartography*, 30(1): 51-57.
8. Next Generation Network Standards to be Defined at ITU. Available at: [http://www.itu.int/newsarchive/press\\_releases/2004/05.html](http://www.itu.int/newsarchive/press_releases/2004/05.html). Accessed 31.5.2006.
9. OGC. 2003. The Importance of Going “Open”, an Open GIS Consortium (OGC) White Paper. Available at: [http://portal.opengeospatial.org/files/index.php?artifact\\_id=6211&version=2&format=htm#\\_ftn1](http://portal.opengeospatial.org/files/index.php?artifact_id=6211&version=2&format=htm#_ftn1). Accessed 31.5.2006.
10. Oksanen, T., P. Suomi, A. Visala, H. Haapala. 2005. ISOBUS compatible implements in the project AGRIX. In: (edit.) J.V. Stafford. *Precision Agriculture '05*. 565-572.
11. QEDS. 2006 TC 56 — IEC Dependability Standards — FAQs. Available at: <http://standardsgroup.asq.org/dependability/tc56/faq.html>. Accessed 31.5.2006.
12. Saliba, A. J., M. A. Beresford, M. Ivanovich, and P. Fitzpatrick. 2005. *Pers Ubiquit Comput* 9: 413-422.
13. Shrestha, B. 2004. XML Database Technology and its use for GML. Available at: [http://www.itc.nl/library/Papers\\_2004/msc/gfm/shrestha.pdf](http://www.itc.nl/library/Papers_2004/msc/gfm/shrestha.pdf). Accessed 31.5.2006.
14. Suomi, P., T. Oksanen, L. Pesonen, J. Kaivosoja, H. Haapala, and A. Visala. 2006. Intelligent functions for crop production automation. *Proc. of XVI CIGR World Congress 2006, Bonn*.

# SPLIT AND MERGE BASED PATH PLANNING FOR AGRICULTURAL MACHINES

T. Oksanen<sup>1</sup> and A. Visala<sup>1</sup>

## ABSTRACT

If the field plot shape is not rectangular and if it contains obstacles, the coverage path planning problem is hard to solve for a non-omni directional machine. Scientists have developed several algorithms to solve this coverage path planning problem, but all of them have pros and cons. If the machines were omni directional and turning times were decreased to insignificant, the problem would be quite easy to solve using known robotic path planning methods. Traditional agricultural machines, like tractors, tractor-trailer combinations, self-propelled harvesters and other man-driven machines are slow to turn at headlands. This is the most differentiating property of the problem formulation compared to traditional robotic coverage path planning, which has dealt mainly with omni directional kinematics.

In this paper a higher level algorithm to split a complex shaped field plot to smaller parts is presented. The higher level splitting algorithm is presented in detail in this paper. The algorithm can handle any field, including obstacles. The algorithm is based on trapezoidal split, merge and search. The algorithm is suited to any kind of vehicle, which is described with a few parameters, like working width and turning time function. In the latest version, the required headlands are generated automatically and there is also a possibility to define regional restrictions as forbidden driving directions. With this formulation it is possible to take into consideration the previous operations, under drains and steep gradients.

**KEYWORDS.** Agricultural Machines, Agricultural Robotics, Coverage, Field, Field Robots, Guidance, Mission Planning, Motion Control, Path Planning, Plots, Tractors.

## INTRODUCTION

Tractors and self propelled farming machines moving on the fields are traditionally driven by a human driver. The human driver has designed the driving strategy of a single field by himself, without any assistance. He/she has chosen the strategy on the basis of type of task, working machine and especially on experience. In family size farms the strategy is based mostly on experience and the driving strategy remains the same over the years. If the field shape is not rectangular or if there are obstacles, the generation of the strategy is not so simple. Usually the most optimal solution is not even the goal, a nearly optimal feasible solution is sufficient.

Autonomous field machines or robots will come, sooner or later. The new issues for autonomous operation are safety, detection of failures, recovering after failures, and automatic refilling or emptying. As a human driver no longer operates the machine, automatic path planning is also needed, the robot has to find a route to execute the task. An optimal solution would be perfect, but a valid solution near optimal would be sufficient in most cases.

In order to be autonomous, a mobile robot has to know or solve four things: what is the task to do, what is the way to complete it, what is already known and what is the position related to known (Murphy, 2000). In agricultural applications the task is usually given by a human operator. Also the last two are more or less solved, because fields are mapped environment and accurate positioning devices are on the market. So the most difficult part in agricultural robot applications

---

<sup>1</sup> TKK Helsinki University of Technology, Automation Technology Laboratory, FIN-02150 ESPOO, Finland, timo.oksanen@tkk.fi

to be solved by artificial intelligence is mission planning. Path planning is one of the key tasks in mission planning. (Reid, 2004).

Roboticians understand path planning as an algorithm that has to find a path from place A to place B so that no collisions with obstacles occur and the path is optimal with respect to a certain measure, for example traveling in minimum time or using minimum energy. In robotics path planning has been divided into two classes, to qualitative and quantitative navigation. In qualitative navigation the environment is structured so that the robot can identify landmarks and navigate using them to follow a route. In quantitative or metric navigation an exact map describes the world and it is not dependent on viewpoint (Murphy, 2000).

In agricultural robotics the task is usually to cover the whole field, not only going from point A to point B. This kind of path planning is so different from traditional robot path planning that the algorithms are not directly suitable. Similar applications are demining, painting, mowing, mapping unknown environments etc. This kind of autonomous applications are so new (or coming) that need for this kind of path planning has appeared lately.

In Gray (2001), the orchard tractor navigation development was reported. Orchards are not open fields, trees form blocks in which the navigation is one problem to be solved and the whole mission is another. In Sorensen et al. (2004) a method for optimizing the vehicle route by defining the field nodes as a graph and formulating it as the Chinese Postman Problem. In Stoll (2003) the idea of dividing the field into subfields based on the longest side of the field or the longest segment of a field polygon. Acar et al. (2002) have introduced the use of cellular decompositions not only for path planning between two points, but also for coverage of free space, various patterns for decomposition are presented. Choset (2001) makes a survey of coverage path planning algorithms and classifies the algorithms to three classes: approximate, semi-approximate and exact. As a conclusion it may be said that the path planning of coverage type task is still under research and a general usable optimal and provable algorithm has not been developed yet, so there is space and need for further research of path planning. In this paper, an enhanced version of split and merge approach using straight driving lines is presented. Earlier version was presented by Oksanen et al. (2005).

## PLANNING

The shape and size of fields varies a lot, especially in Finland fields are usually bounded by other terrain types, like forests, lakes, rocky terrain etc., and shapes are far from orthogonal and convex. If the field is convex and it does not contain any obstacles, path planning for agricultural tasks is quite simple, and only the main driving direction has to be found. The whole field is driven in that direction except headlands if needed. The selection of the main driving direction on the basis the longest edge of field has been a rule of thumb for farmers. Here this rule of thumb based on common sense has been dismissed and it will be checked if the result is still the same.

If the field is nonconvex which means that it has "bays", finding the optimal solution is hard. One possibility to solve the problem is to use split and merge approach for segmentation used in computer vision. The field is split into simple shaped subfields which are convex or near convex, an optimal solution is found for driving in the subfields and finally the solutions are combined. If the shape of a subfield is for example rectangular, finding the optimal driving strategy is pretty simple, even if not trivial. The drawback of this method is that the output, the driving route, is not necessarily a globally optimal solution, but suboptimal.

For some environment and some operations there are limitations for driving direction. For example the under drainage system made based on height variation limits the ploughing directions, for certain soil types. Also the driving direction in previous operation may limit the driving direction, or more generally the chain of field operations. For example in tilling it may be suggested not to drive in the same direction as the field is ploughed. Another case when driving directions may be wanted to limit is a series of small permanent obstacles and wide working machine, like electric poles and sprayer. Then in the surroundings of electric line it may not be suitable to drive in directions that differ from the direction of electric line only a little bit.

Here it is assumed that the layout of the environment (field) is known. This can be assumed because fields are not changing over the years and the mapping is made, at least in Finland. The requirements for a good coverage path planning algorithm are: suitability for all kind of fields, for all kind of machines, and efficient enough in order to be solved in reasonable time.

This paper concentrates on the higher level algorithm to divide a complex shaped field into simple subfields in which the route planning is easy to do. The algorithm is suitable for all kind of crop farming machines where the task is to do some action in all places in the field exactly once.

### Definitions

Certain type definitions have been set. The field is considered as an uniform 2D region which may contain obstacles. An *exterior polygon* describes the field outer boundaries and *interior polygons* describe the obstacles. *Vertices* are corner points of the polygon. *Edges* are line segments that connect vertices.

A *trapezoid* is an quadrangle which has two opposite parallel sides. A *triangle* is a special case of a trapezoid. A *block* is a polygon which is constructed by merging two or more trapezoids in their parallel and equal sides – in block two edges are parallel. *Headland* is a region in which the machine is to be turned. *Prohibited region* is a region which is a part of field where certain driving directions are prohibited.

### Objective

The objective is to divide a complicated field into subfields. The algorithm searches first largest or most efficiently driven subfields, removes them from the original field and keeps finding subfields until the whole field is computed. In search of each subfield, the optimal driving direction is determined. In each step the field is split into trapezoids, the trapezoids are merged to larger blocks and the selection is made using certain criterion which takes into consideration the area and the route length of block and the efficiency of driving.

## **ALGORITHM**

### Splitting

Crop farming machines have certain working width, which usually remains constant. The requirements for best efficiency and quality are: the driving lines are exactly side by side, no gaps, no overlapping and the turning in headlands is made in minimum time. Parallel swathing assistants or light bars or autopilots help human driver to keep the machine in lane.

It has been assumed that the driving lines should be side by side and parallel to each other in order to be a good strategy. Due to that assumption, trapezoid has been selected as a prototype of the shape. Trapezoid has two opposite sides parallel corresponding to the driving direction and the other sides correspond to the edge of the field or the headland.

In this algorithm the field is split into trapezoids, this belongs to the set of exact cellular decompositions (Latombe, 1991). All vertices of the exterior polygon are projected at given direction to all sides and trapezoids are detected. If the field contains obstacles, the interior polygon nodes are also projected to all sides of the polygons. An example of triangulation is presented in figure 1. In the field on the left the number of trapezoids is 11 and in the field on the right the number is 18.

### Merging

After splitting the field into trapezoids, the next step is to combine them as far as possible. The requirement is that two trapezoids have to have exactly matching sides and the angle of ending sides is not too steep. The second requirement prevents combining trapezoids which are far from rectangular shape and should be handled in later phases separately. The minimum angle between matching side and ending side is set to 20 degrees (90 degrees means right angle). The example of merging trapezoids is presented in figure 2.

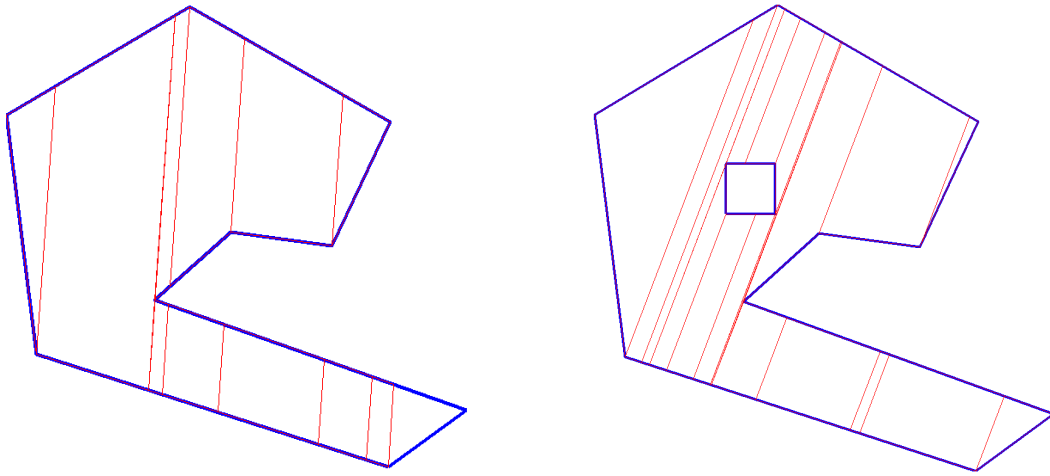


**Figure 1. Two examples of triangulation.**

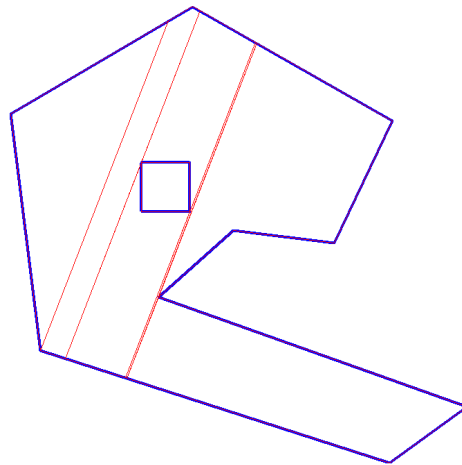


**Figure 2. Merged trapezoids.**

### Selection criterion

The idea is that the regions which are most efficient to handle are driven first and the same algorithm is applied iteratively for the rest until the whole field is handled. The region to be selected in each step is a block, the best one of them has to be selected.

The area of the block, the distance of route fitting inside the block and the efficiency of driving are variables in selection criterion. The area is simply the area of the block. The distance is calculated using the working width information and the headland width is subtracted from that. The distance corresponds to the distance that can be driven at normal driving speed with operational part of machine working. The time consumed in the block is estimated from the distance calculated previously and the time spent in headlands is added. The estimate of turning time in certain headland angle can be calculated for example using optimal control techniques (Oksanen et al., 2004) or by splines (Noguchi et al., 2001). In perpendicular headlands (compared to driving direction) the quality is best (minimum overlapping in headlands).

In practice efficiency is the primary variable which should be maximized, but this leads easily to a situation where narrow and long blocks are selected first. That leads to an unwanted combined solution. Therefore the other two measures are needed too. All the measures (area, distance, efficiency) are normalized and the cost is a weighted sum of these. Currently the tuned weights are: efficiency 65 %, area 15 % and distance 20 % and these are used in the results below.

If some subfields are already selected, a bonus is added to the calculated cost in the directions of them. This prevents adjacent subfield directions not to differ from each other by small angles only.

With most cropping machines, a small correction in direction leads to inefficiency and to quality loss.

#### Search of the driving direction

Splitting into trapezoids and merging them to blocks is made in certain direction. However, the direction is not known and it has to be solved. The characteristics of the blocks are not changing smoothly when the direction is changed in infinitesimal steps, so the cost function of search is not smooth. This means that all possible directions should be gone through (between 0 and 180 degrees) and it takes a lot of calculation time. The following heuristics have been used.

The search algorithm is as follows:

1. Cost is calculated in 6 directions: 0, 30, 60, 90, 120 and 150 degrees.
2. The three best directions are selected, others are dropped.
3. The step size in direction angle of search is divided by two.
4. New search directions are added to the both sides of the three best directions.
5. Cost is calculated in directions which are not yet calculated.
6. If the goal resolution is reached, exit, otherwise go to step 2.

After 5 iterations, the resolution is below one degree which has been found to be sufficient.

This heuristic search algorithm was tested with a random set of real fields and the solution was compared to brute-force solution with the same resolution. The result was that over 97 percent of the solutions matched and only less than one percent of the solutions were far from the global maximum.

#### Headlands

As described above, the headland width is reduced from the main driving lines when calculating the efficiency. In this way the solution will be correct, but in some cases a headland is not needed. If the direction of blocks after first iteration vary from each other, it is evident that one end of block is common to the parallel side of the other block and generally then the headland is not needed. The other case when headland is not needed is a block which has very steep headland angle e.g. below 15 degrees (90 degrees means again right angle), then the headland can be driven by bending the driving line. The number of swaths needed in headland is input variable for algorithm.

#### Prohibited driving directions

As mentioned above, for some environments and some operations there are limitations for the driving direction. This can be formulated to this path planning algorithm by defining a prohibited region, in which range of prohibited driving directions are set in degrees. If the set of prohibited driving directions is not uniform, multiple prohibited regions may be used.

In the algorithm the prohibited regions are taken into account in split phase. If the current search angle is in the angle range of the prohibited region, the prohibited region is handled as an obstacle or interior polygon. After selection, in removing phase, the prohibited regions are cropped if needed. It is required that prohibited regions are inside the field region.

## **TEST RESULTS**

Previously (Oksanen et al., 2005) the test results with 1500 real fields were presented. The conclusion from those tests is that this algorithm works nicely for fields with straight edges. The solutions for fields with curved edges are valid, but not so efficient. Here is presented latest results.

Automatic determination of headlands was developed. In the figures below, the headlands are drawn with blue color, and the main swaths are drawn with green. In figure 3, a H-shaped field is presented with the solution. At first the algorithm has found two long vertical blocks on each side

and finally the horizontal block between vertical blocks is handled. The headlands are needed only at the end of vertical blocks and they are automatically generated.

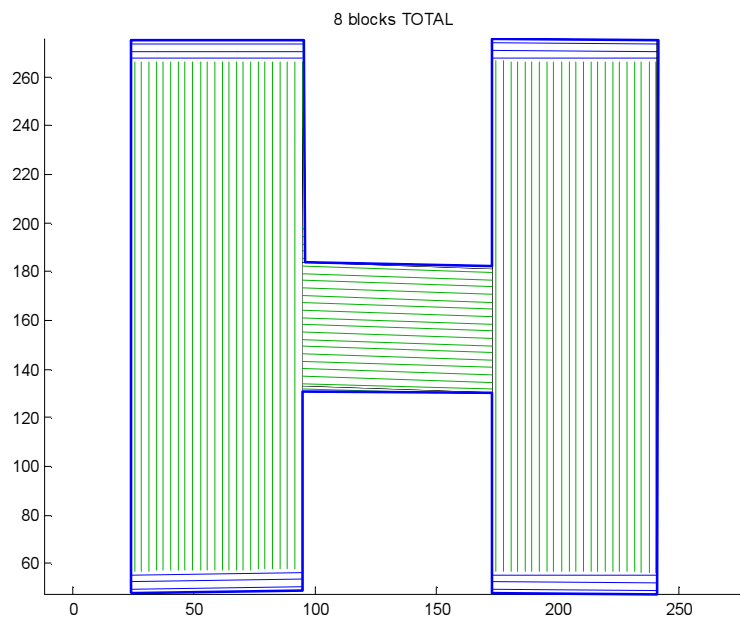


**Figure 3. H-shaped field with headlands.**

In figure 4, a field with many bays is shown. As it can be seen, the main driving direction was determined on the largest block in the middle. For three of four bays the same driving direction is found to be top-rated (NB: a small bonus is given to direction of neighboring blocks). The headlands are needed in most edges, but if the direction of edges is near enough to the direction of swaths (in these tests 5 degrees), the headland is not laid.

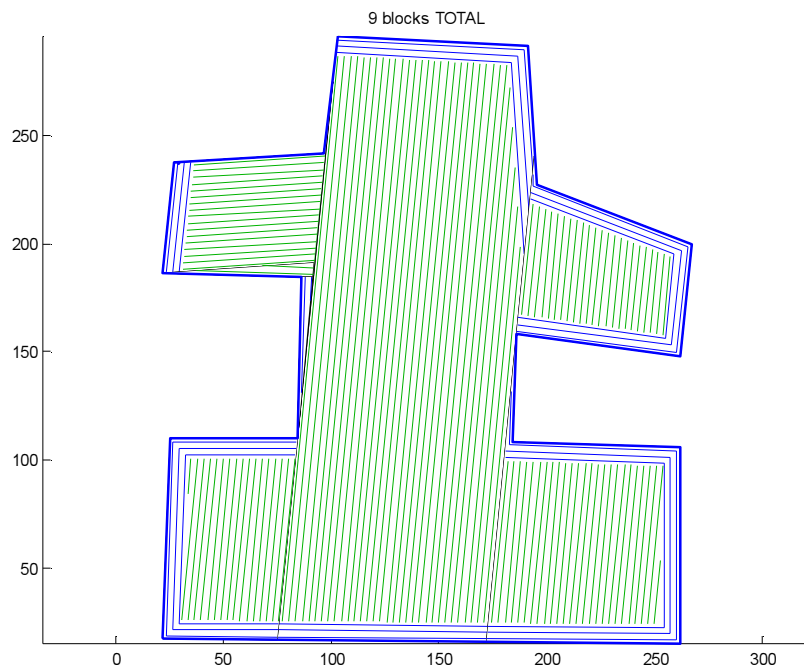


**Figure 4. Field with many bays.**

### Prohibited regions

As described, with the prohibited regions it is possible to define impossible driving directions due to height variation and machine properties or to define unwanted, inefficient driving directions.

In figure 5, a C-shaped field is shown. On the left is a solution without any prohibited regions. The final solution consists of 5 blocks, saving two headlands. On the right a fictional escarpment (steep

slope) is inserted on one corner, this is marked with dashed line and a small red triangles, "bow", represent the forbidden driving directions. This means that the driver does not want to drive the escarpment up-down-up, but diagonal driving is allowed. Maybe his/her tractor does not have enough horsepower to drive it uphill. However it can be seen that the solution found without the prohibited region has changed dramatically. The driving direction is changed all around the field plot and headlands are required all around the field.

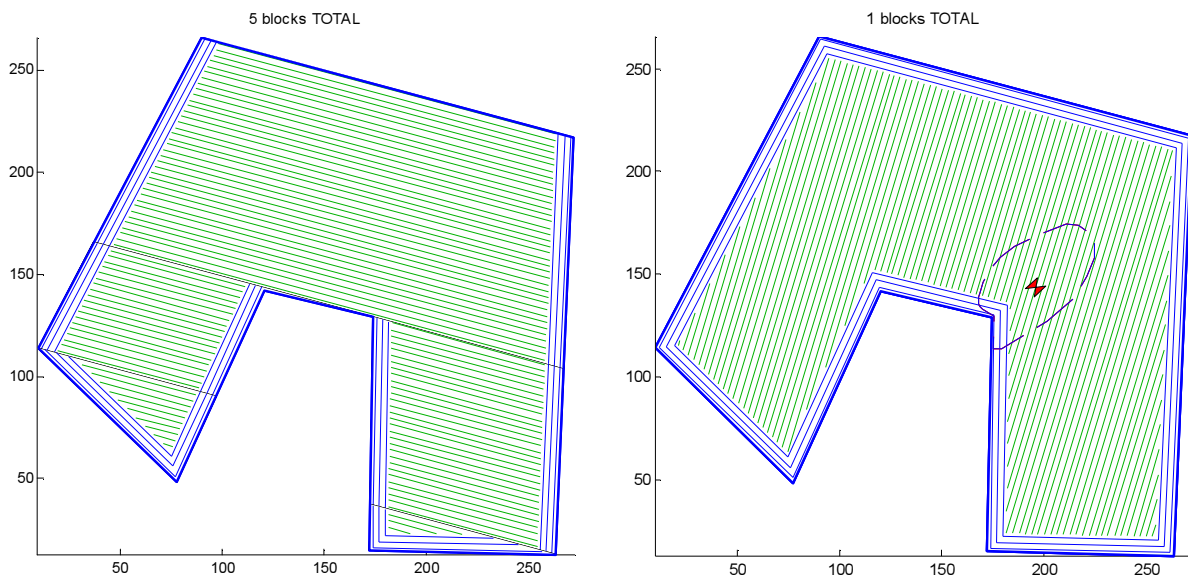


**Figure 5. C-shaped field without and with prohibited regions.**

Lets consider another example. In Northern Europe most of the field plots are underdrained. Underdrainage is important especially in soil types which are not transmitting water easily. In certain field operations, like in ploughing it is not recommended to drive in the same direction as the pipes are laid; ploughed furrow is also kind of "pipe". When the furrows and pipes cross, the effect of drainage is at its best. In figure 6, a field with underdrainage system is presented. A bold blue dashed line represent the collector pipe in the drainage system and blue lines are lateral pipes. Two prohibited regions are marked with red dashed lines and red "bows" are marking the forbidden driving direction range.

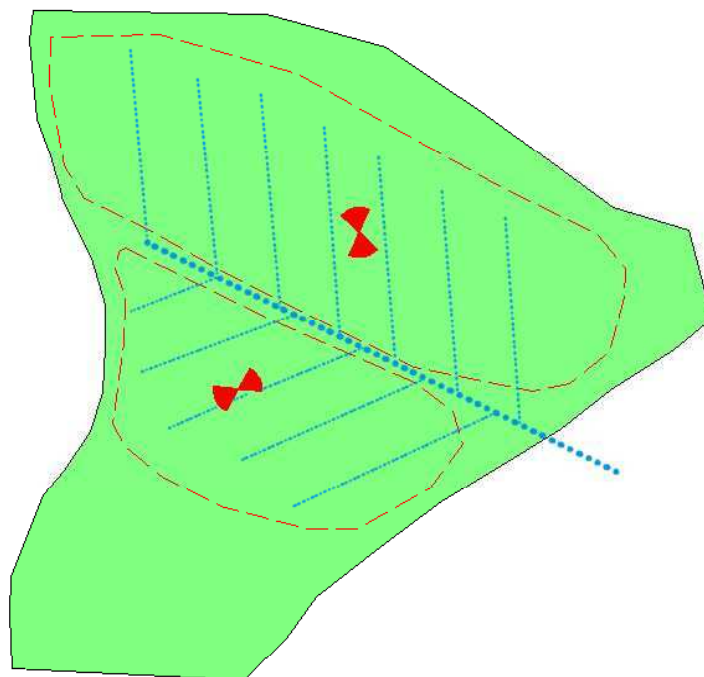


**Figure 6. Field with underdrainage system.**

In figure 7, on the left the solution of algorithm without taking underdrainage into account is presented and on the right it is considered. In both cases one dominant driving direction exists, but the right one fulfills the requirement of prohibited region. Actually the efficiency is almost the same in both cases, in simulation the right one is only 0,2% worse than the left one, if using total driving time as a measure. Naturally this fact applies only for this particular field.

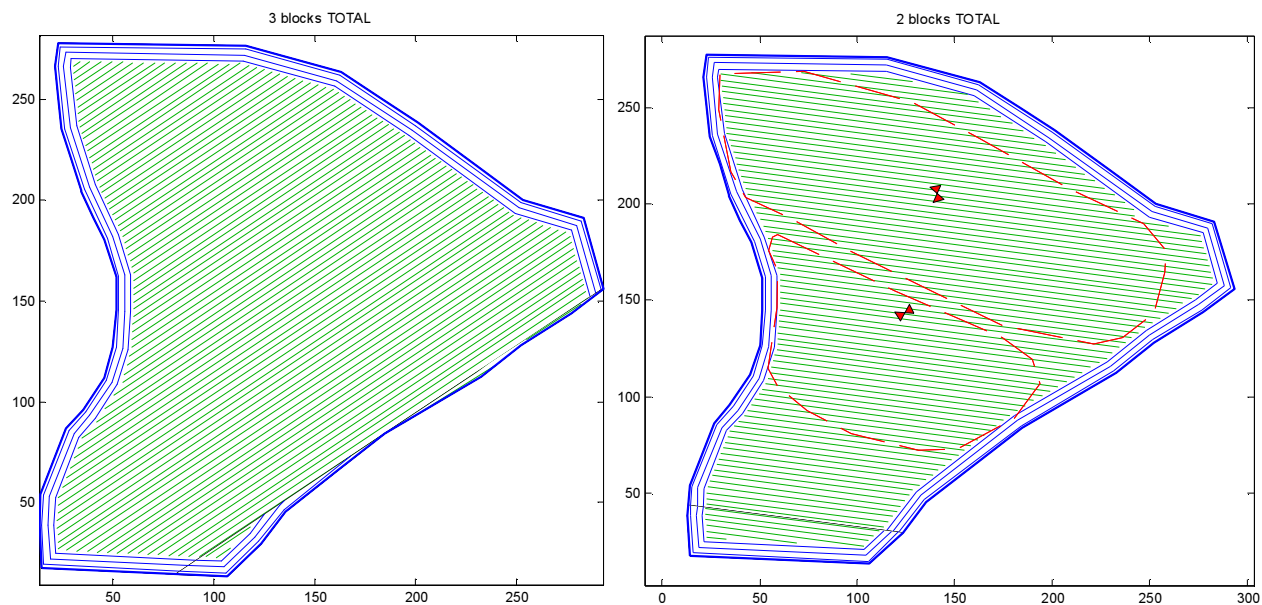


Figure 7. Solution without and with underdrainage.

## CONCLUSION

Path planning for robots working in fields is not yet solved. Various algorithms for path planning have been introduced, but they are still more like a collection of algorithms.

In this paper an algorithm for dividing a field into subfields is presented. The shape of a subfield is simple, so it can be driven using parallel swathing techniques. The algorithm relies on splitting the field into trapezoids, merging them to larger blocks, using search algorithm select the best driving direction and recursing the search until the whole field has been divided. The algorithm belongs to the set of exact cellular decompositions. Trapezoidal decomposition has been utilized as a part in the algorithm. Algorithm can solve the routes for any field, with any number of obstacles and any kind of shape.

In the latest version the headlands are automatically generated where needed. With prohibited regions the previous operations, underdrains and steep gradients can be taken into account. In prohibited regions certain driving directions are marked prohibited.

One drawback of the algorithm is that it only can use straight driving lines. Some fields do not have straight boundaries. Especially in fields which are narrow, long and curved, the solution is far from optimal. Refilling or emptying of the machine should be included in path planning. A general usable coverage path planning algorithm should be able to adapt to agricultural task specific requirements.

## REFERENCES

1. Acar, E. U., Choset H., Rizzi A. A., Atkar P. N., Hull D. 2002. Morse decompositions for coverage tasks. *The International Journal of Robotics Research*. 21(4): 331-344.
2. Choset, H. 2001. Coverage for robotics - A survey of recent results. *Annals of Mathematics and Artificial Intelligence*. 31:113-126.
3. Gray, S. A. 2001. Planning and replanning events for autonomous orchard tractors. Master's thesis, Utah State University, Logan, Utah.

4. Latombe, J.C. 1991. *Robot Motion Planning*. Boston, MA.: Kluwer Academic Publishers.
5. Murphy, R. R. 2000. *Introduction to AI Robotics*. A Bradford Book, The MIT Press.
6. Noguchi, N., Reid, J. F., Zhang Q. and Will, J. D. 2001. Turning Function for Robot Tractor Based on Spline Function. *ASAE Annual Meeting 2001*. ASAE Paper No. 011196.
7. Oksanen, T., Visala, A. 2004. Optimal control of tractor-trailer system in headlands. *ASAE International Conference on Automation Technology for Off-road Equipment*, Kyoto. Japan, pp. 255-263.
8. Oksanen, T., Kosonen, S., Visala, A. 2005. Path planning algorithm for field traffic. *ASAE Annual Meeting 2005*. ASAE Paper No. 053087.
9. Palmer, R., Wild, D., Runtz, K. 1988. Efficient path generation for field operations. Dept. of Computer Science, University of Regina.
10. Reid, J.F. 2004. Mobile Intelligent Equipment for Off-road Environments. *ASAE International Conference on Automation Technology for Off-road Equipment*, Kyoto. Japan, pp. 1-9.
11. Sørensen, C. G., Bak, T., Jørgensen, R. N. 2004. Mission planner for agricultural robotics. *AgEng 2004*, Leuven, Belgium. 8pp.



# RECURSIVE ONLINE PATH PLANNING FOR AGRICULTURAL MACHINES

T. Oksanen<sup>1</sup> and A. Visala<sup>1</sup>

## ABSTRACT

If the shape of field plot is not rectangular and if it contains obstacles, the coverage path planning problem is hard to solve for a non-omnidirectional machine. Scientists have developed several algorithms to solve this coverage path planning problem, but all of them have pros and cons. If the machines were omnidirectional and turning times were decreased to insignificant, the problem would be quite easy to solve using known robotic path planning methods. In this paper a new algorithm to solve the path planning problem is presented. This algorithm is designed for real-time usage and it solves the problem recursively: the operated area is removed from the field and the algorithm is repeated until the whole field plot is completed. In the development phase of algorithm, a simulator has been utilized. The underlying idea is to calculate the efficiency for all possibilities to make one trip around the field and to select the best one. It is assumed that every new swath is side-by-side to the some previous one or to the boundary of the field plot. However, even if the underlying idea is simple, the search space explodes when the number of corners of the field plot raises and heuristics is needed in order to restrict the number of possibilities without losing optimality. The algorithm is suited to any kind of vehicle, which is described with a few parameters, like working width and minimum turning radius. Preliminary results are very promising and are presented in the paper.

**KEYWORDS.** Algorithms, Field Machines, Field Operations, Field Robots, Field Traffic, Mission Planning, Optimization, Path Planning, Simulation.

## INTRODUCTION

Agricultural field robots need automatic mission planning, and path planning is one of the key tasks in mission planning, see Oksanen et al. 2006.

In Gray (2001), the orchard tractor navigation development was reported. Orchards are not open fields, trees form blocks in which the navigation is one problem to be solved and the whole mission is another. In Sorensen et al. (2004) a method for optimizing vehicle route by defining the field nodes as a graph and formulating it as the Chinese Postman Problem. In Stoll (2003) the idea of dividing the field into subfields based on the longest side of the field or the longest segment of a field polygon. Acar et al. (2002) have introduced the use of cellular decompositions not only for path planning between two points, but also for coverage of free space, various patterns for decomposition are presented. Choset (2001) makes a survey of coverage path planning algorithms and classifies the algorithms to three classes: approximate, semi-approximate and exact. Oksanen et al. (2005) presented a split and merge based algorithm to solve higher level planning problem for complex shaped fields. As the conclusion it may be said that the path planning of coverage type task is still under research and a general usable optimal and provable algorithm has not been developed yet, so there is space and need for further research of path planning.

## DEFINITIONS

*Online path planning algorithm* means that it may be used online in the vehicle, so that the planning calculation runs in the computer so fast that the vehicle does not need to limit its speed in

---

<sup>1</sup> TKK Helsinki University of Technology, Automation Technology Laboratory, FIN-02150 ESPOO, Finland, timo.oksanen@tkk.fi

order to wait for the solution. *Offline path planning algorithm* is a precalculated path. The online algorithm has better adaptivity, but offline algorithm may lead to better total solution.

*Polyline* is a continuous line composed of one or more line segments, the line segments. A *closed polyline* is a polyline where the starting point and ending point is common. *Vertex* is the point where polyline segments end. *Edge* is a line segment in closed polyline. One vertex is shared by exactly two edges. *Polygon* is a synonym for closed polyline. *Critical vertex* is a vertex where the vehicle must stop the operation and make a turn.

Here *Field* is a uniform 2D-region, made by exactly one exterior closed polyline and free number of interior closed polylines representing obstacles.

## THE ALGORITHM

### Assumptions and limitations

Some assumptions and limitations are first set:

1. all the swaths must be side-by-side,
2. the turning times and path lengths are know a priori for all headland turnings for the machine being used, or they are very quick to calculate
3. the working width is constant

For assumption 2, a precalculation and sampling may be used, see e.g. Oksanen et al. (2004) or Noguchi et al. (2001). This precalculation applies until the machine properties remain the same. The algorithm has to solve the turning time so many times, that look-up table is needed in order to keep the computing time reasonable.

At this phase of development the refilling/emptying the machine is not considered, but it may and will be added to the algorithm later.

### Required sub algorithms

The most important sub algorithm is so called *polygon offsetting*. The aim is to move each edge of region inwards (or in some cases outwards) so that the perpendicular distance is between subtracted region and original is wanted. This problem is analog to the field operation where one round is driven around the field once, doing some operation, and the inner boundary of operated area is to be identified. This is a well known problem in computational geometry. There are several methods to solve this, see e.g. Yang et al. (1993), Choi et al. (2001a) and Choi et al. (2001b). Here it is used a *straight skeleton* method, (Aichholzer et al. 1995) and (Felkel et al. 1998). The algorithm can handle convex regions as well as holes in the region.

### The basic idea

Lets consider a simple field, shape of rectangle, see figure 1. Let the initial state of machine be I, both the location and the direction. The A-B-C-D polygon represents a region which interior needs to be operated and these points may be considered also as a critical vertices. As the limitation 1 was set, a restricted set of movements exists. The problem is to search the best route.

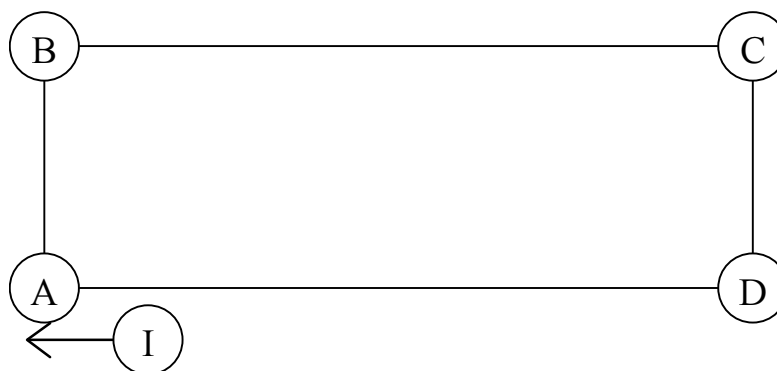


Figure 1. A simple field.

In order to find the global optimum, according to certain cost, all possible routes to the end have to be compared, e.g. I-A-B-C-D-A'-B'-C'-D'-A"-... until the whole region has been operated. The computational cost of this problem will increase exponentially when the number of corner points increase and/or area/working width ratio increases.

In control engineering, a similar problem arises in optimal control. Search from all possible control functions is impossible, generally. Optimal control methods that minimize certain criterion exists but in real time operation and for nonlinear systems those are not practical. Model predictive control is a way to improve feedback control: in certain time step and control, the system behavior is analytically predicted over the *prediction horizon*. The control law can be solved using predicted behavior and by minimizing the criterion over the *control horizon*. Only the first action of the solved control function is applied in each step, and in the next time step all the computations are repeated. (Maciejowski 2002).

Here the same analogy is applied to path action search. The "control horizon" and "prediction horizon" are actually equal in tests later, but "prediction horizon" could be longer, roughly it should be multiple of "control horizon". Let the "control horizon" be defined as *search horizon* later in this paper.

The search horizon is defined as:

- start point is the nearest vertex to current position (or initial point at the startup)
- starting direction is free, clockwise (CW) or counter-clockwise (CCW)
- stop when near start point (A', offsetted A)
- zero or one reversion in direction
- some segments may be skipped
- if the segment is skipped in one direction it must be skipped also in the other direction

Lets get back to our simple field, figure 1. The possible routes could be I-A-B-C-D-A' ; I-A-D-C-B-A' rounding the whole field, the subsets of those with skipping edges. The routes with single reversion in direction in CW would be I-A-B-C-D-C'-B'-A' ; I-A-B-C-B'-A' ; I-A-B-A', plus the subsets. And the same in CCW direction. This will lead to

$$2 \cdot \left( 2^N + \sum_{i=1}^{N-1} 2^{N-i} \right) \quad (1)$$

upper limit of choices, where N is the number of critical vertices. The multiplier 2 is the number of directions, the first part is for circular driving and the second part for reversing in different points. There is some redundancy, because some sub solutions (with skipping) in circular driving versus reversible driving are congruent; therefore this equation gives only the upper limit of choices.

For N=4 (in our case), the upper limit of choices will be 96. For N=7, it is 1152 and for N=10 it is 12288 and for N=20 it is over 23 million. So the reasonable number of critical vertices is around 10, naturally depending on computing resources and efficiency function.

### Generating routes

In order to generate all possible routes in search horizon, the polygon offsetting algorithm is utilized. The region boundary is offsetted by the half of working width (in a practical application the overlap must be considered), offsetting is made for three times. The first offset gives the first center line for machine, the second is a boundary of first operation swath, and the third is for the reverse center line.

### The efficiency function

All the driving is divided into two groups: working and turning, the latter contains all driving where the implement or some functional part of machine is not in operational state. The efficiency

function is calculated for all possible routes in the search horizon. Let the route lengths be  $s_W, s_T$ , for working and turning, respectively; and  $t_W, t_T$  for route driving times. The driving speed may vary. The cost is

$$\frac{\sum_i s_W^i}{\sum_i t_W^i + \sum_i t_T^i}, \quad (2)$$

where the sum operates over route segments. In other words the cost function measures efficiency of route, operated area divided by operation time.

#### Selection of best route in search horizon

The efficiency function is calculated for all possible routes and the route having maximum efficiency is selected. This phase of algorithm can be speeded up using approximate turning times and turning path lengths, utilizing precalculation and look-up tables. When the best route is selected, a more computationally intensive, more accurate trajectory planning algorithm may be used. As stressed above, only the first segment of selected route is applied at each step of the algorithm.

#### Simulation of driving

In simulation, the route to be applied in each step must be subtracted from the original region, representing field still not operated. This phase turns out to be difficult, because the shape and characteristics of offsetted region may change dramatically. Basically a new boundary of region representing the route to be applied is found by finding the next offset polygon line segments and replacing the previous outer boundary with that and also removing the head and tail line segments of operational area from the original region. Treatment of special cases is needed if the offset method is not working.

#### Simplifying routes

If the original polygon(s) representing the field, has many vertices, there are two ways to speed up the calculation of the algorithms. One is to reduce the number of vertices, by approximating the polygon with other having less vertices, and the other is to use the original polygon but merging line segments to polylines. Here the latter is applied, the former may be added in the future if needed.

In merging line segments, a condition is needed. The natural condition to merge or not to merge is the curvature of polyline representing region boundary. The curvature limit and the maximum turning radius of the machine in operational state have an inverse relation. The problem is that here the region format of polygon was selected and the curvature cannot be calculated (appearing singularly), because the curve should be smooth in order to calculate curvature. If only the change in direction is calculated (traveling along polygon around), it may lead to wrong results, if the line segments are very short and direction change is very small in all cases.

Several different conditions were tested and the following seems to work best. Let  $r$  be the turning radius of machine (note: in operational state). For every vertex in polygon, a circle with radius  $2r$  is drawn, see figure 2. The nearest line segments in both directions of polygon are selected (bold) and the curvature estimate (direction change in certain distance) is calculated. The limit for this value is a tuning variable, in tests thirty degrees was used with  $r=10$  m.

#### Non-convex fields

If the field is not convex (concave) or it contain obstacles, the region representing non-operated area will easily split into separate regions, or the region is not uniform any more. In these cases the route segment generation is similar: the region offsetting is made for all separate regions, separately. The actual problem in these cases is that the number of possible routes will be large, as the "jumps" from one region to the other must be free. This may be limited by limiting the allowed "jump points" in each region, preferably to one. The easiest, but not optimal, way to overcome this problem is to restrict the path planning into single region and squeeze them one at a time. The

other, prima facie better, way is to stop the search horizon also after one jump, see the definition. This part of research is still under work, and no general conclusion is available at this phase.

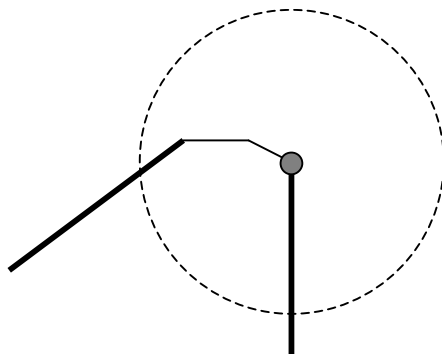


**Figure 2. Merging condition.**

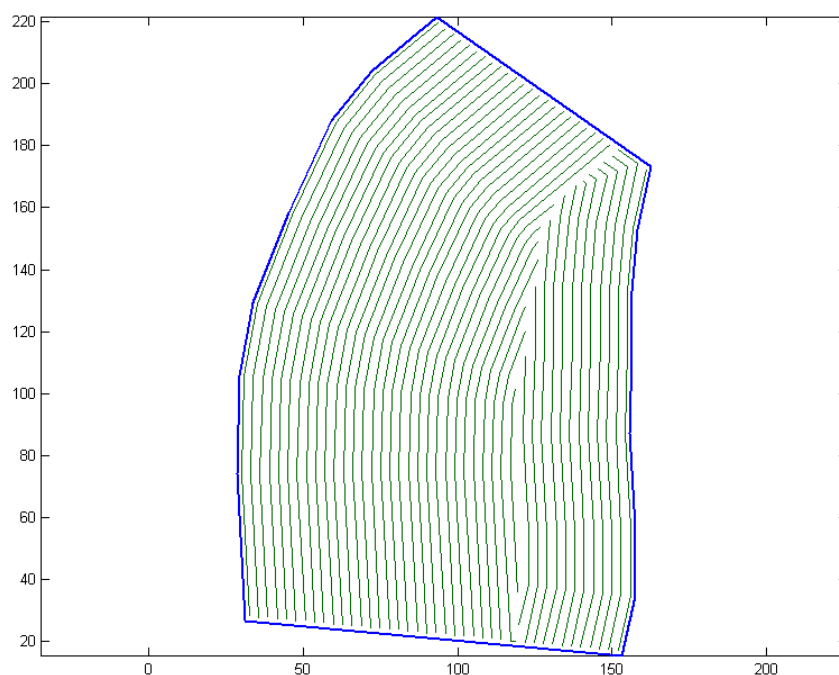
## RESULTS

The algorithm has been tested with some hand-drawn fields. The algorithm works reliably for all convex fields, and for some non-convex fields that do not split into separate regions during simulation. The property to support jumps is still under development and is not functioning reliably.

The machine specific parameters in the results below have been: working width 3 m, driving speed 10 km/h in working phase, 6 km/h in minimum radius turnings, minimum turning radius 6 m at headlands and 10 m at operation. These are the only parameters needed in simulation.

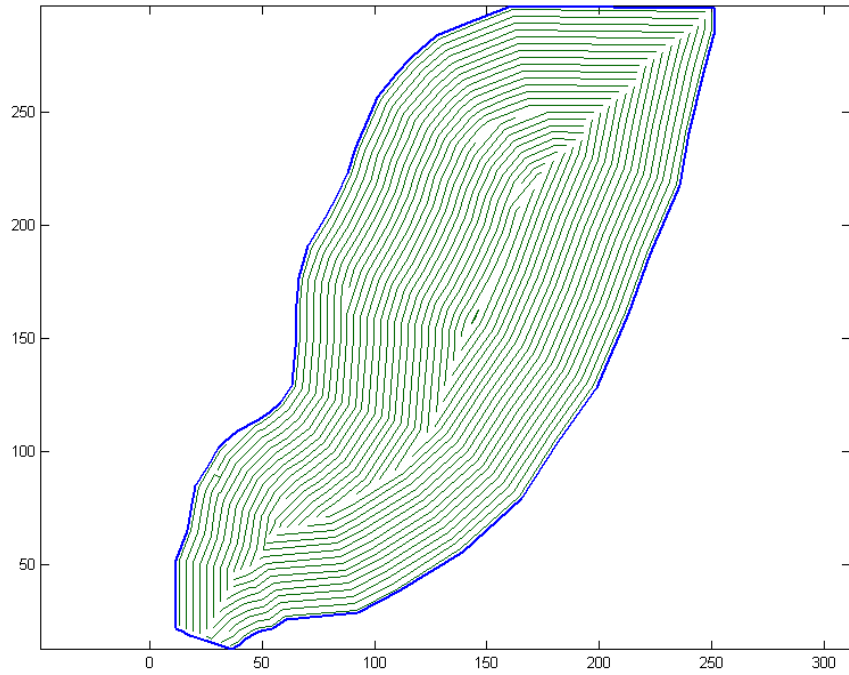
Headland or turning area is not considered yet. However for many operations it is suitable to drive the field around for example three times and after that apply this algorithm.

Figure 3 presents a convex field with one long curved edge. Turning routes or driving order are not shown. The algorithm has first driven the left side (longest) back-and-forth until it is sensible to change to squeeze swathing technique. The result is reasonable.



**Figure 3. Field with one curve edge.**

A field with no straight edges is shown in figure 4. The algorithm first drives the field around but some turnings are made back-and-forth. Also this solution is reasonable.



**Figure 4. Field with curved edges.**

In figure 5, a L-shaped field is presented. For this field the algorithm first behaves so that field is driven around counter-clockwise with skipping to short edges and after nine rounds it starts to drive "wings" separately, because the turning curve length from L-outcorner to L-incorner becomes short, the solution is plausible.

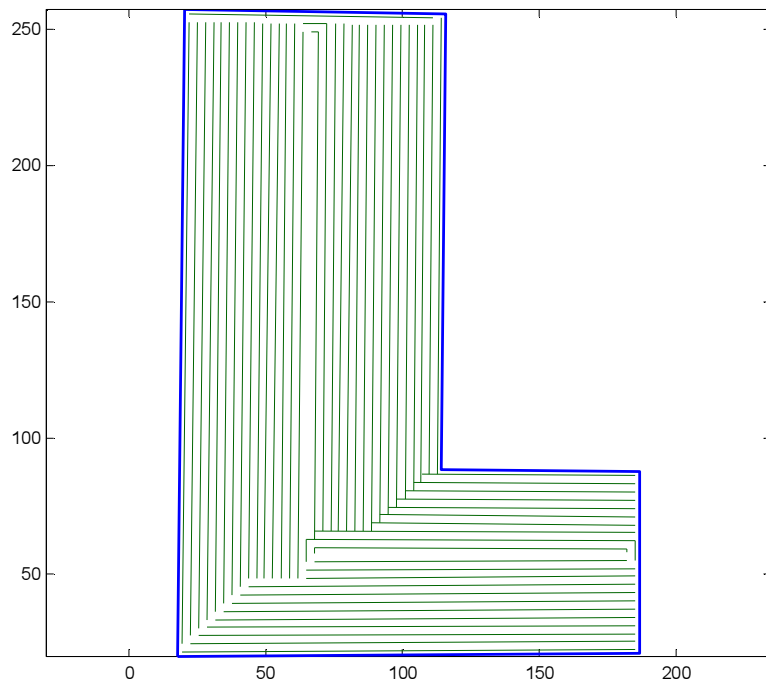


**Figure 5. L-shaped field.**

In figure 6, the field plot has the shape of letter T. At the beginning the simulation drives the longest edge back-and-forth until the turning to short edges parallel to long becomes quicker. Then the longest edge and the two short edges are driven around a couple of times, by skipping the gap between two short edges. After a couple of rounds the turning cost will become more or less the same between these two and simulation goes back to driving the field back-and-forth. Finally the last "bay" is driven. It may be more efficient to operate the area between two short edges instead of skipping it, but in this approach it was set a limitation that each swath must be side-by-side with some earlier one, or the edge of field.

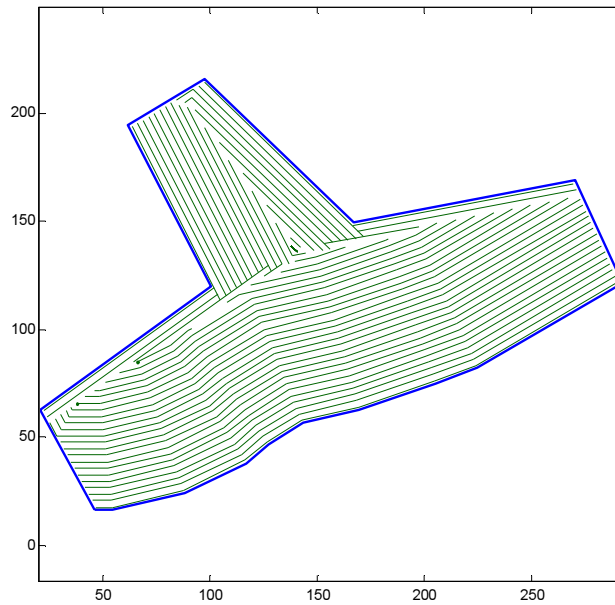


**Figure 6. T-shaped field.**

### Speed of algorithm

With a modern office computer (P4@3.2GHz), the whole calculation of L-shaped field (with 6 critical vertices) takes about 5 minutes, when the field area is 2.7 hectares and the simulated driving in that field takes 88 minutes. With this complexity the algorithm work well in real time but it cannot be guaranteed.

If this algorithm is applied in real time, the edge being driven currently should be simulated to the end, when the driver has decided it, and the search can be made for the next corner. The time to make calculation decreases as the field is operated, at least if driving around-style. For a real-time assisting system it must be noted that there is no guarantee that the calculation is finished in certain time. Therefore some heuristics must be used to either calculate first rough solution or sort the possible solutions based on some pre-known criteria (for example from earlier calculations) and after that calculate as many solution possibilities as there is time.

### Quick comparison of driving techniques

A quick comparison of algorithms is made in this phase. This comparison is not an accurate one, but gives some idea. In figure 7, a boomerang shaped field is presented. On the left is a solution from the algorithm presented in (Oksanen et al. 2005), in the middle is a forced simulation of circular or spiral type driving and on the right is the solution from the algorithm presented in this paper. In case A needed headlands are taken into consideration, in case B the headlands are created automatically, but in case C the headlands are not required so from this is coming a little difference.

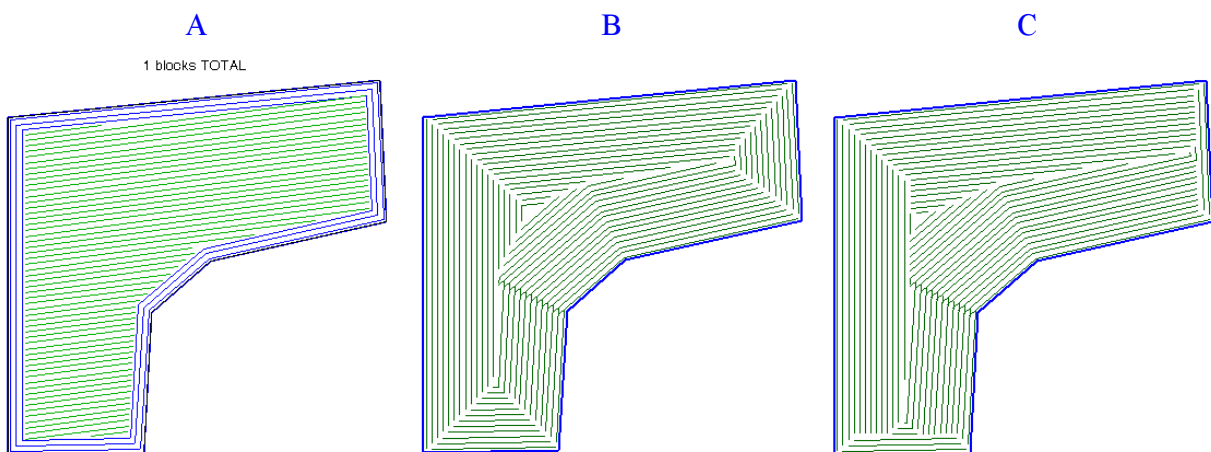


**Figure 7. Comparison of driving techniques: split & merge, forced rounding, this algorithm.**

The statistics of results in figure 7 are compared in table 1. Extra driving means the amount of additional driving distance due to turnings. This is calculated by comparing the total driving distance to the value of field area divided by working width. It can be seen that the solutions A and C will give almost equal efficiency in this field. Together with operation or mission planning, the other requirements will be decisive; for example in row crop farming the parallel lines may be better. A comparison with other simple shaped fields without obstacles give similar results. It seems that algorithm C is a slightly better than A when the edges of field plot are curved.

**Table 1. Comparison of driving techniques.**

	<b>A</b>	<b>B</b>	<b>C</b>
number of turnings	74	85	70
total driving distance	12.2 km	13.5 km	12.0 km
total driving time	1h 25m 39s	1h 42m 41s	1h 28m 03s
extra driving	46.7 %	62.5%	45.0%

## CONCLUSION

In this paper a new algorithm for coverage path planning, especially for field operations, is presented. Due to limitations set, the algorithm is not able to find the global absolute optimal solution, but it is always suboptimal. However the global optimality is not goal itself, if it is hard to find, in most cases suboptimal, suitable solution is sufficient. Because the optimal solution is not available, it is difficult to see how near to optimal the solutions of various algorithms are.

The algorithm works well for convex fields with no obstacles. The algorithm can handle field plot as complex as ten corner points, in which the actual turning is needed. A couple of simplification methods are presented in the paper in order to speed up computing. Still more simplification is needed in order to support strongly non-convex fields. More heuristics is needed to struggle with the curse of dimensionality.

The algorithm works currently in real time with convex and moderate shaped fields, with less than 10 critical vertices. In the future the full support for non-convex fields and obstacles should be developed and there the requirement for real-time usability becomes more important. The headlands or the turning area should be taken into consideration, so that this algorithm would be usable from the beginning of operation.

A quick comparison of driving techniques was presented. Based on this comparison nothing general cannot be concluded. A more comprehensive study is required and probably it will show that one algorithm works better for some field shapes and the other for another kind of shapes. As it is practically impossible to find an absolute optimal route with all kinds of machines and with all kinds of field plots, the problem must be restricted in some direction. In the real world several algorithms for path planning may be tried offline and the best overall solution is applied.

## REFERENCES

1. Acar, E. U., Choset, H., Rizzi, A. A., Atkar, P. N., Hull, D. 2002. Morse decompositions for coverage tasks. *The International Journal of Robotics Research*. 21(4): 331-344.
2. Aichholzer, O., Aurenhammer, F., Alberts, D. and Gärtner, B. 1995. A Novel Type of Skeleton for Polygons. *Journal of Universal Computer Science*, 1 (1995):752-761.
3. Choi, H.I., Han, C.Y., Choi, S.W, Moon, H.P, Roh, K.H. and Wee N.-S. 2001. Two-dimensional O@sets via Medial Axis Transform I: Mathematical Theory. *Preprint*. Available at: [http://newton.kias.re.kr/~swchoi/homepage/offset\\_theory.pdf](http://newton.kias.re.kr/~swchoi/homepage/offset_theory.pdf). Accessed 17 May 2006.
4. Choi, H.I., Han, C.Y., Choi, S.W, Moon, H.P, Roh, K.H. and Wee N.-S. 2001. Two-dimensional O@sets via Medial Axis Transform II: Algorithm. *Preprint*. Available at: [http://newton.kias.re.kr/~swchoi/homepage/offset\\_alg.pdf](http://newton.kias.re.kr/~swchoi/homepage/offset_alg.pdf). Accessed 17 May 2006.

5. Choset, H. 2001. Coverage for robotics - A survey of recent results. *Annals of Mathematics and Artificial Intelligence*. 31:113-126.
6. Felkel, P. and Obdrzalek, S. 1998. Straight Skeleton Implementation. *Proceedings of Spring Conference on Computer Graphics*, Budmerice, Slovakia. pp. 210-218.
7. Gray, S. A., 2001. Planning and replanning events for autonomous orchard tractors. Master's thesis, Utah State University, Logan, Utah.
8. Latombe, J.C. 1991. *Robot Motion Planning*. Boston, MA.: Kluwer Academic Publishers.
9. Maciejowski, J.M. 2002. *Predictive Control with Constraints*, Prentice Hall, England.
10. Murphy, R. R. 2000. *Introduction to AI Robotics*. A Bradford Book, The MIT Press.
11. Oksanen, T., Visala, A. 2004. Optimal control of tractor-trailer system in headlands. *ASAE International Conference on Automation Technology for Off-road Equipment*, Kyoto, Japan, pp. 255-263.
12. Oksanen, T., Kosonen, S., Visala, A. 2005. Path planning algorithm for field traffic. *ASAE Annual Meeting 2005*. ASAE Paper No. 053087.
13. Oksanen, T., Visala, A. 2006. Split and Merge Based Path Planning for Agricultural Machines. *ASABE International Conference on Automation Technology for Off-road Equipment*, Bonn, Germany.
14. Noguchi, N., Reid, J. F., Zhang Q. and Will, J. D. 2001. Turning Function for Robot Tractor Based on Spline Function. *ASAE Annual Meeting 2001*. ASAE Paper No. 011196.
15. Palmer, R., Wild, D., Runtz, K. 1988. Efficient path generation for field operations. Dept. of Computer Science, University of Regina.
16. Sørensen, C. G., Bak, T., Jørgensen, R. N. 2004. Mission planner for agricultural robotics. *AgEng 2004*, Leuven, Belgium. 8pp.
17. Yang, S.-N. and Huang, M.-L. 1993. A new offsetting algorithm based on tracing technique. *Proc. on the second ACM symposium on Solid modeling and applications*. pp. 201-210. ACM Press.



# EDGE DETECTION FOR AUTONOMOUS GUIDANCE OF A CORN HARVESTER USING STEREO VISION

F. Rovira-Más<sup>1</sup>, S. Han<sup>2</sup>, J. Wei<sup>3</sup> and J. F. Reid<sup>4</sup>

## ABSTRACT

The growing demand for applications in Precision Agriculture has been proportional to the emergent interest in automatic guidance of agricultural machines. The difficult, and at the same time strenuous, task of driving a harvester during the prolonged working days of the harvesting season justifies the special attention paid to this technology. The development of Global Navigation Satellite Systems has meant an important push for autonomous navigation, especially in the case of off-road vehicles. However, experience has shown that automatic guidance inside the tight arrangement of crop rows is difficult to achieve unless local positioning sensors take part in the localization unit of auto-steered machines. This research develops a perception engine based on stereoscopic vision to detect the cut-uncut edge of corn during harvesting operations. The stereo camera was mounted on the head of an agricultural combine. The algorithm implemented was capable of finding the edge of corn, allowing the system to automatically guide the combine at regular harvesting speeds.

**KEYWORDS.** Autonomous Navigation, Corn Harvester, Edge Detection, Guidance, Precision Agriculture, Stereoscopic Vision, Visual Perception.

## INTRODUCTION

Among typical agricultural operations, harvesting is one of the most delicate because it usually needs to be carried out in a narrow period of time when ambient conditions are favorable. Total benefits obtained from the crop depend on the yield harvested, which is sensitive to the quality of the harvesting operation. If maize, for example, is the crop to be reaped, a combination of circumstances has to be met: adequate moisture content in the corncob; good weather conditions with absence of rain or snow; dry soil to allow the circulation of the machines; accessible combine and loading truck; and operators' availability. When all these constraints are taken into consideration, it is not rare to request combining from dawn to dusk, even during the night, for several days in a row. Under these demanding conditions, the operator is forced to work under stress and fatigue that can result in poor performance, or what is much worse, in a serious accident. If the ultimate goal of technology is to improve life, harvesting operations bring a breeding ground for its application. A natural and logical use of technology in this case would be through assisting in the vehicle's navigation. There is no need to attain a complete automatic guidance solution in order to be considered a satisfactory outcome; a semi-autonomous result would be helpful in managing the combine since it would relieve the operator from some hours of strenuous work. Furthermore, it would be beneficial for acquiring experience in guidance systems, which, eventually, will lead to fully autonomous prototypes. This research investigates in such direction, trying to bring some light to the challenge of autonomous navigation for agricultural combines.

---

<sup>1</sup> Polytechnic University of Valencia. 46022 Valencia, Spain, frovira@dmta.upv.es

<sup>2</sup> John Deere Agricultural Management Solutions. Urbandale, IA 50322, USA

<sup>3</sup> Kansas State University. Manhattan, KS 66502, USA

<sup>4</sup> John Deere Technology Center. Moline, IL 61265, USA

Since the incorporation of sensors, electronics, and computers to agriculture at the end of the eighties, and more generally after the nineties, many automatic guidance architectures for off-road vehicles have been proposed, both in industry and academia. Machine vision solutions seem to be the most appropriate for the situations faced during harvesting, however, they are not exempt from complexities and challenges. One of such intricacies deals with the camera location, for which there is no definite solution. Benson et al. (2001) studied four camera locations for combine guidance, and arrived to the conclusion that the best position for the camera is above the cabin. One of the positions discarded in that work placed the camera attached to the combine head, pointing at the cut-uncut edge. The main cause for rejecting the low camera position on the combine's head was due to sparse crop and shadows. In spite of the flawed results experienced with such location in previous research projects, the solution proposed in this work places the camera on the head of the combine, but adds two significant changes: first, the camera was mounted on a sliding bar on the combine's head in such a way that a better view of the cut-uncut edge was acquired by rotating the camera towards the crop; and second, stereovision was employed as the main perception method. The advantages of stereo over monocular vision can, to some extent, account for the shadows issue: a change in ambient illumination will affect both stereo sensors simultaneously. Therefore, the texture patterns that allow stereo matching will remain unaltered, as long as there is enough light for the camera to detect distinct features in both images of the stereo pair. This property of stereo vision, together with the fact that stereo provides the range or third coordinate, has motivated the advent of multiple applications for robot perception and autonomous navigation in the last five years. Murray and Jennings (1997) demonstrated that stereo is an alternative to laser and sonar, and built a lab robot that used stereo for localization and mapping of an unknown environment. The scenes found during harvesting present certain structure as corn is planted following regular rows separated evenly a known distance. There is, therefore, an *a priori* knowledge about the scene to be acquired by the stereo camera. If landmarks can be placed in the field of view of the camera, the location of a vehicle can be determined by means of stereo (Wang et al., 2005); and if a solid model of the target object is available, a robotic manipulator will have at its disposal a modeled environment for automatic tasks (Lee et al., 2005). While agricultural applications are still scarce (Rovira-Más and Reid, 2004; Kise et al., 2005; Rovira-Más et al., 2005; Wei et al., 2005), the possibilities of perception via stereo are expanding in all directions; from 3D mapping for underwater autonomous vehicles challenged by limited visibility caused by turbid waters (Khamene and Negahdaripour, 1999) to humanoid robots that walk around unknown home environments (Sabe et al., 2004).

The object of this study is to develop a perception engine based on stereoscopic vision to detect the cut-uncut edge of corn during harvesting operations. Several hardware configurations and different edge detection algorithms were evaluated in the course of the experiments.

## SYSTEM ARCHITECTURE AND TEST PLATFORMS

The perception sensor was a binocular stereo camera (BumbleBee, Point Grey Research Inc., Vancouver, Canada) with a 120 mm baseline, and 6 mm focal length lenses yielding a horizontal field of view of 42 °. The camera communicated with the on-board processing computer (Motion Computing Inc, Austin, TX, USA) via an IEEE 1394 connection. The edge detection algorithm was implemented in the processing computer and the resulting output, namely the vehicle's offset, was sent to the control unit of the combine. The corn harvester selected to perform navigation tests was a John Deere 9660 STS (Deere and Company, Moline, IL, USA) equipped with AutoTrac™, an auto-steering system that provides positioning corrections using a GPS receiver as the principal localization sensor. The offsets (lateral misalignments) calculated by the AutoTrac algorithm were substituted by the offsets sent by the stereo processor, being the steering controller and mechanism those of the original AutoTrac.

One of the key parameters in the system was the camera location. Several options were tested before attempting to guide the combine in the field. The monocular camera approach reported by Benson et al. (2001) found a low position on the head to be problematic, but when a stereo camera was employed as the main perception sensor, the possibility of rendering a 3D view of the scene resulted in several advantages for that placement. Nevertheless, different alternatives were studied

within the head before deciding a permanent mount. Figure 1 illustrates the general layout of the system: (a) side view; (b) top view. The first experiments were conducted in Weslaco, Texas (USA), on July 14, 2005. The objective of that preparatory phase was to scrutinize the potential of stereo for combine guidance. Stereo images were taken with the following parameters, as defined in figure 1:  $h_c = 1.61$  m,  $\theta = 0^\circ$ ,  $L_r = 0.965$  m,  $L_w = 5.842$  m, and  $L_c = 0$ . Difficulties encountered detecting the edge, as explained in the following sections, led to a reformulation of some parameters, being the camera position for the automatic guidance tests, carried out in Des Moines, Iowa, (USA) on October 21, 2005, given by  $h_c = 1.66$  m,  $\theta = 30^\circ$ ,  $L_c = 1.42$  m. The camera was always mounted flat except for one test where it was tilted down  $5^\circ$ .

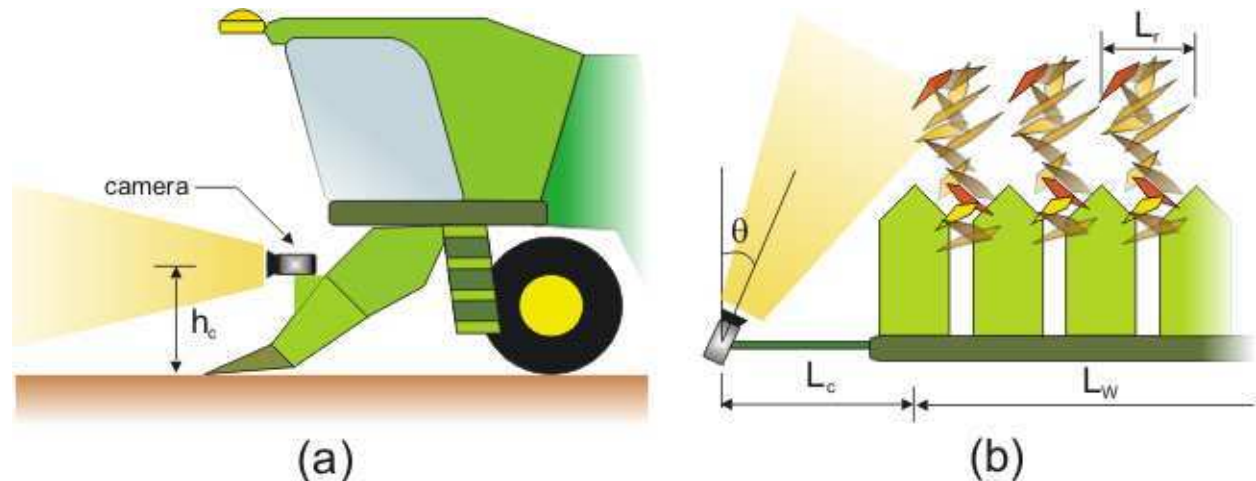


Figure 1. System design for autonomous guidance of a combine using stereo vision: (a) side view; (b) top view.

### FINDING THE EDGE

Before obtaining high quality point clouds, it is necessary to acquire satisfactory stereo images, that is, to get acceptable disparity images. In the first configuration of the system, the camera was mounted just on the head's left side without using the extension arm, and looking ahead ( $\theta = 0^\circ$  and  $L_c = 0$ ) at 1.61 m high. Figure 2 shows a raw left image (a) and its corresponding disparity image (b) where dark intensities represent far objects and black stands for filtered mismatches.

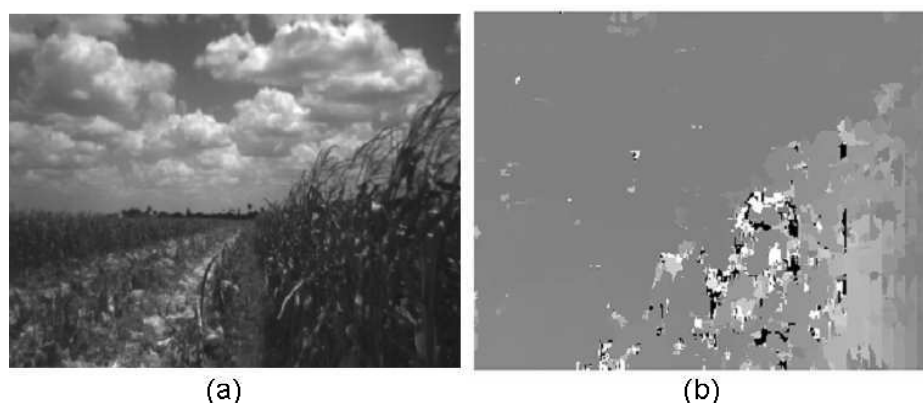
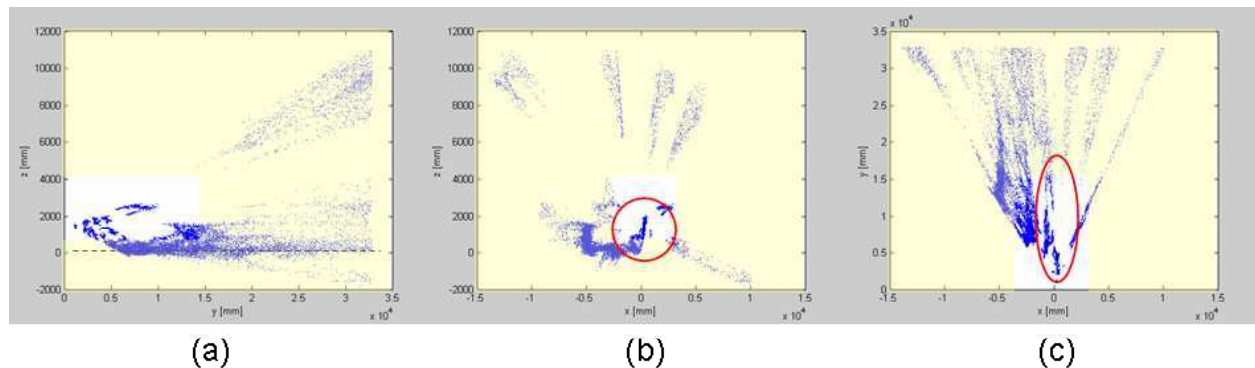


Figure 2. Outputs from the stereo camera: (a) left image; (b) disparity image.

The disparity image stores the 3D information of the sensed scene in camera coordinates. The first step in the data process is a transformation from the original camera coordinates to the ground coordinates as defined by Rovira-Más and Reid (2004). The result of that transformation is a point cloud of the scene given in a more intuitive frame. Figure 3 represents the 3D cloud of the scene given in figure 2: (a) side view YZ; (b) front view XZ; and (c) top view XY. The ground system of coordinates places its origin at ground level right under the optical center of the left lens. The approximate expected position for the cut-uncut edge can be determined beforehand, and therefore

3D information can be restricted to important zones. Apart from reducing the size of the point clouds, reducing the processing time accordingly, this operation has special relevance when noise is taken into account. The side view of the point cloud given in figure 3 (a) shows wrong 3D locations for heights ( $Z$ ) over 4 m caused by the cloudy sky. The representation of the ground level is rather flat, and it is located at  $Z = 0$ , which indicates a good coordinate transformation; however the 3D information close to the ground level is not important to find the edge, and can be neglected for such purpose. The depiction of the edge can be easily identified in the front view of figure 3 (b). An edge remaining from previous passes is also noticeable around 5 m left. As shown in the side view, heights over 4 m rendered incorrect information. The top view of the scene (Fig. 3 (c)) demonstrates the low reliability of data for ranges greater than 15 m. For the scene studied in figure 3, a reasonable three-dimensional space for data processing can be defined by (1).

$$x \in [-2500, 2500] \text{ mm}; \quad y \in [0, 15000] \text{ mm}; \quad z \in [1000, 4000] \text{ mm} \quad (1)$$



**Figure 3.** 3D point cloud of the scene given in figure 2: (a) side view; (b) front view; and (c) top view.

The cloud point represented in figure 3, under spatial restrictions similar to the ones stated in Expression 1, was converted into a *density grid*, as defined in Rovira-Más and Reid (2004). The  $Z$  coordinate was limited to the interval  $[500, 2000]$  mm, yielding the  $37 \times 50$  grid of figure 4 (a). The variation of the 3D density ( $d3d$ ) as a function of the range  $Y$  is plotted in figure 4 (b).

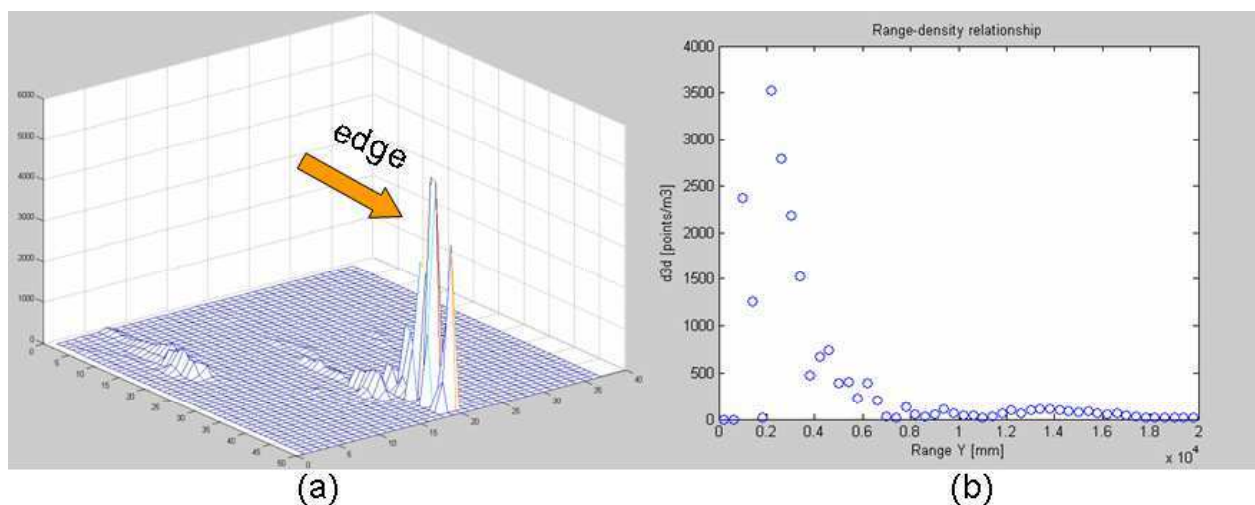


**Figure 4.** Density grid representation: (a) grid; and (b) density-range relationship.

The graphic of figure 4 (b) indicates that the 3D density drops very fast in the first 8 m, being very low beyond 10 m. In spite of this unbalance, the position of the edge is well determined, as indicated in figure 4 (a). In this particular application, where the goal is to detect the cut-uncut edge, since the key information resides in those cells located close to the camera, there is, apparently, no urgent need to range-compensate the 3D density.

## Gradient Operation

With the aim of enhancing the position of the cut-uncut edge so that it can be detected more reliably, the gradient mask ( $V$ ) of equation 2 was applied to a density grid defined around the location of the edge. The resulting graphical representation is plotted in figure 5: (a) gives a three-dimensional view of the value of the gradient for every cell, and (b) provides the same data through a two-dimensional color map.

$$V = \begin{bmatrix} -1 & -2 & 0 & 2 & 1 \end{bmatrix} \quad (2)$$

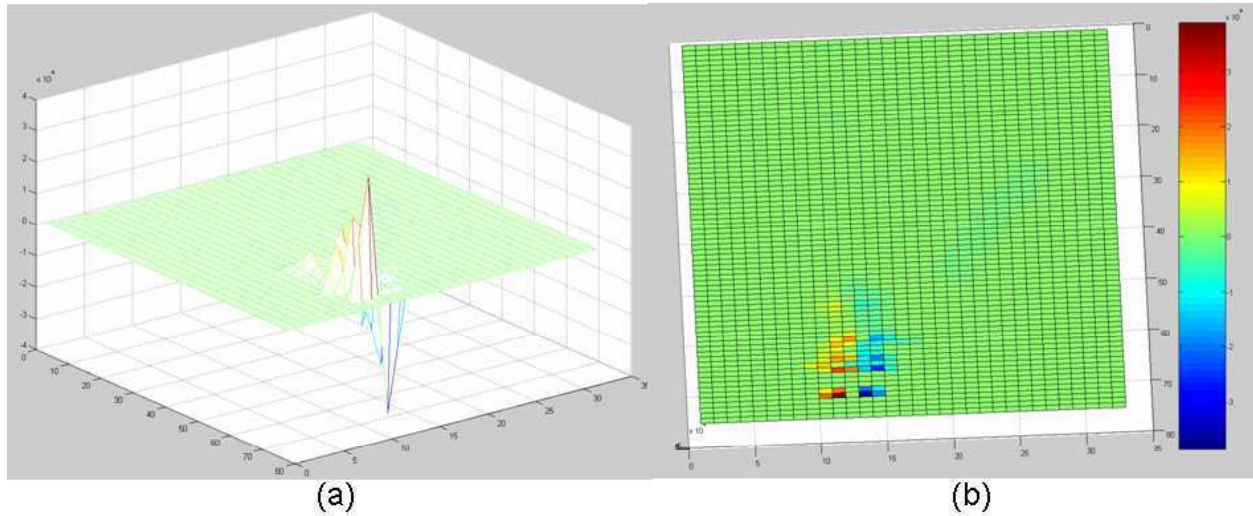


**Figure 5. Application of Gradient Operation: (a) 3D view; and (b) 2D color map.**

The gradient mask marked transitions rather intensely, producing a large increment negative maximum- positive maximum where the edge lays. Once the gradient grid was calculated, the maximum value for each row was registered, as well as its cell location. After the computation of the maximum gradient values, a threshold (5% of the maximum value in the grid) was applied to eliminate low-reliability locations. Finally, the X coordinate of the remaining cells were stored to estimate the vehicle's offset. Figure 6 shows the approximated position for the edge in a 3D visualization (a), and in a 2D graph (b).

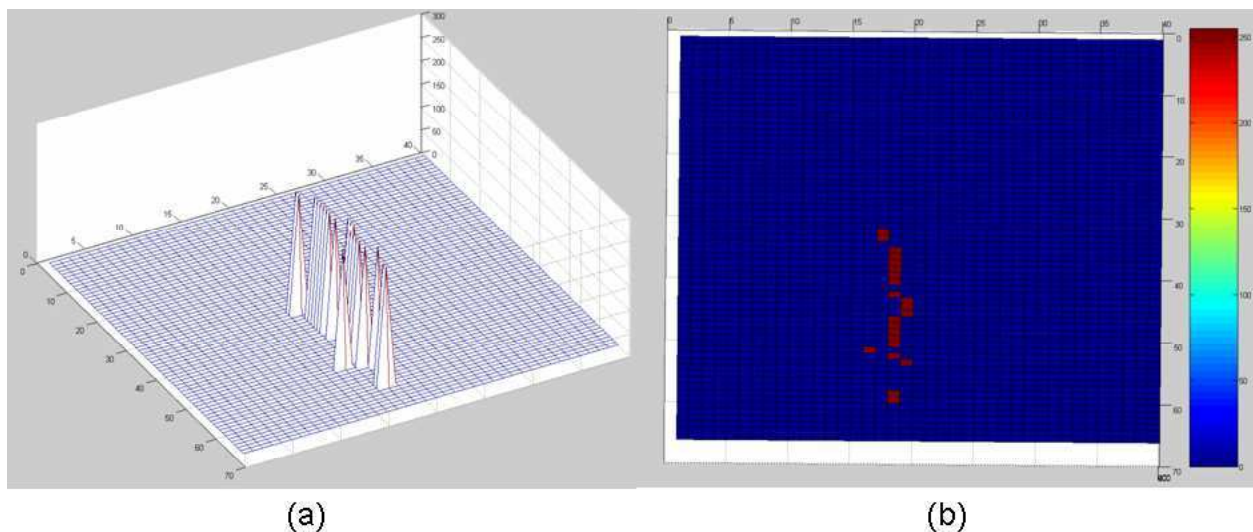


**Figure 6. Estimated edge position through the gradient operation: (a) 3D view; and (b) 2D representation.**

When only the first row was detected (row that signals the position of the cut-uncut edge), the gradient operation yielded similar results to the outcomes obtained after detecting the edge directly from the density grid. However, the gradient became more valuable when special situations

occurred. One such circumstance took place when several rows were detected in the same scene. The gradient procedure marked the largest transition between the maximum and minimum peaks for the edge. Figure 7 (a) represents the gradient response when more than one row is captured in the image. Figure 7 (b) provides the locations of the found rows. The highest peak to peak difference determined the placement of the edge, and the density of those rows detected on the right side of the chosen row were weighted by a reduction coefficient before calculating the final position of the edge.

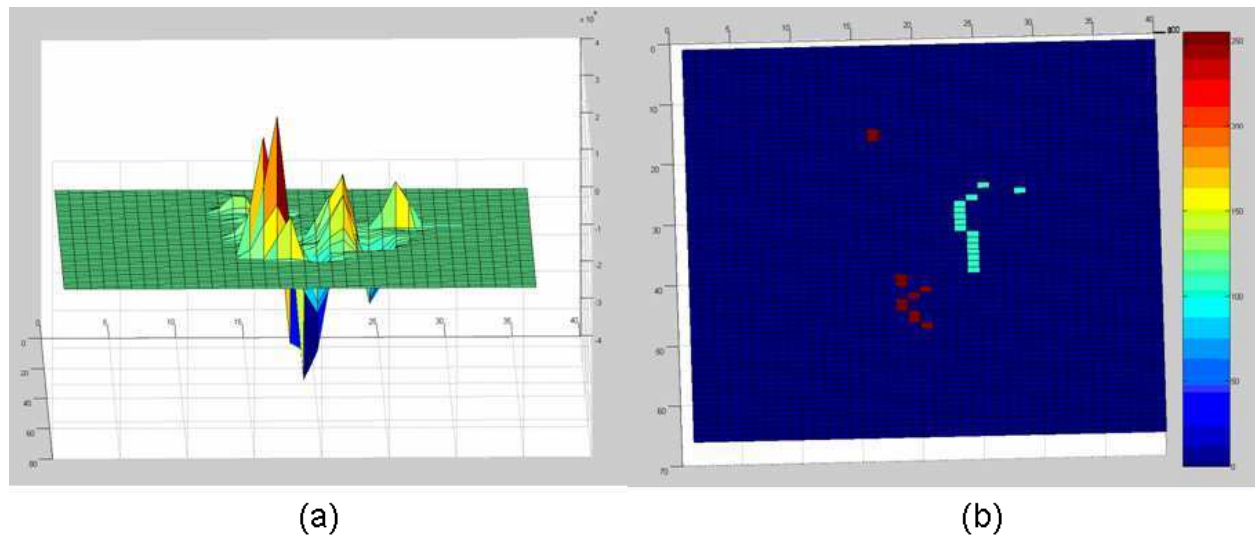


**Figure 7. Edge detection when several rows are captured in the scene: (a) 3D view; and (b) 2D map.**

Even though the camera was initially installed on the left side of the combine head with  $\theta = 0^\circ$  and  $L_c = 0$  (Fig. 1), the navigation tests were performed with a significantly different configuration:  $\theta = 30^\circ$  and  $L_c = 1.42$  m. The reason for such modifications falls on the need to generate more robust stereo images and avoid the detection of multiple rows as shown in figure 7. An even more problematic situation arose when the corn leaves got so near to the camera that they touched the lenses and blocked part of the field of view. In that case, the cut-uncut edge was not always properly detected, causing problems of instability. Figure 8 illustrates the situation of a camera mounted too close to the actual crop: (a) left image of the stereo pair; (b) gradient representation of the scene; and (c) approximate position of the edge after the inner rows have been penalized.

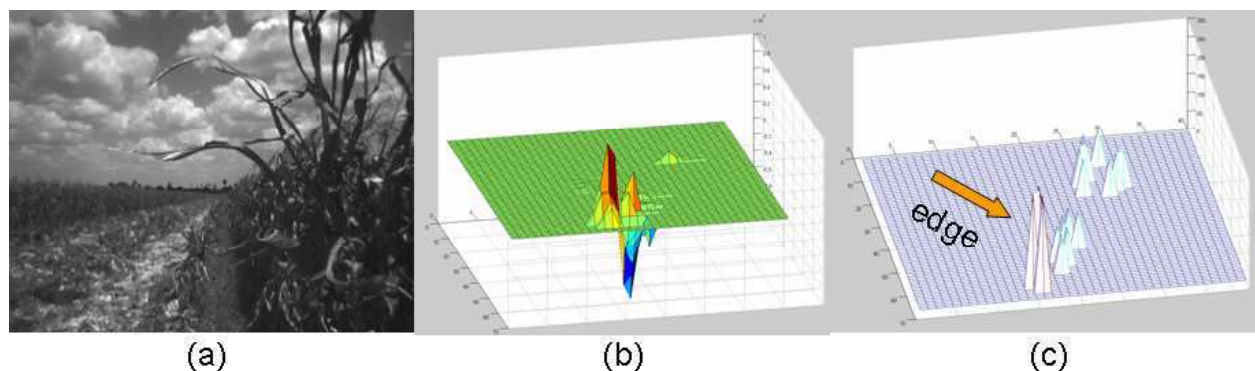


**Figure 8. Inappropriate distance camera-crop: (a) raw image; (b) gradient plot; (c) estimated edge position.**

## CONFIDENCE METRICS

With the second configuration for the camera position ( $h_c = 1.66$  m,  $\theta = 30^\circ$ ,  $L_c = 1.42$  m.), the estimates for the edge's position improved, yet sometimes there were appreciable differences between consecutive estimates. The objective of the *confidence index* is to assess the quality of the edge position estimation, in such a way that every result (estimate) is accompanied by a quality

indicator, representing a confidence value for the solution. The expression for the Confidence Index ( $CI$ ) is defined in (3), where  $M_x$  is the moment index and  $C_x$  is the clustering index, whose definitions are included in the next paragraphs.

$$CI = M_x \cdot C_x \quad (3)$$

### Moment and Moment Index

Figure 9 represents an archetypal output of the edge detection algorithm: a set of cells arranged approximately drawing a line. For every single valid cell, three parameters are known:  $x$  coordinate,  $y$  coordinate, and 3D density. Valid cells are those whose density exceeds certain threshold, determined after the gradient operation. The optimal position of the edge is approximated by a regression line applied to the valid cells.

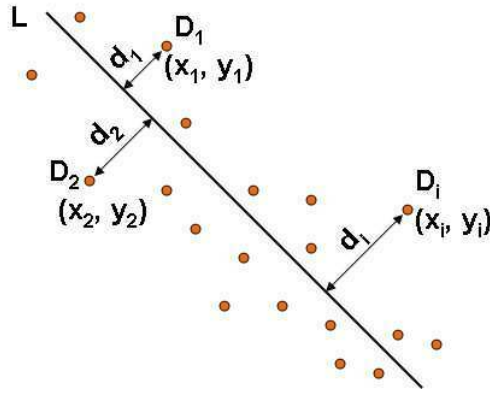


Figure 9. Confidence index calculation: *Moment* definition.

The *Moment* for a particular image  $k$  is defined in equation 4, where  $n$  is the number of valid cells after thresholding,  $d_i$  is the perpendicular distance from valid cell  $i$  to the fit line  $L$ , and  $D_i$  is the density of the cell number  $i$ .

$$M_k = \sum_{i=1}^n \frac{d_i^2}{D_i} \quad (4)$$

If the fit line  $L$  is determined by the equation  $L \equiv ax + by + c = 0$ , the perpendicular distance for the valid cells  $d_i$  can be calculated following the conventional expression of equation 5:

$$d_i = \frac{|a \cdot x_i + b \cdot y_i + c|}{\sqrt{a^2 + b^2}} \quad (5)$$

Due to the fact that the *Moment Index* was intended to range between 0 and 1, a maximum value reachable by the *Moment* had to be deduced. Such value was named the *estimated maximum moment of the image k (MoMax<sub>k</sub>)*, and was defined according to equation 6. Note that an adjustment constant equal to 2 has been arbitrarily added to the denominator in order to obtain more rational values for the *Confidence Index CI*. The other parameters taking part in the equation are  $d_{max}$  as the maximum distance considered in the image  $k$  after the threshold has been applied, and  $D_{min}$ , the non-zero minimum density recorded among the  $n$  valid cells.

$$MoMax_k = \frac{n \cdot d_{max}^2}{2 \cdot D_{min}} ; D_{min} \neq 0 \quad (6)$$

The expression of the *Moment Index* is given in equation 7. It is, by definition, a number comprised in the interval  $[0, 1]$ , and it will decrease when the valid cells are located far from the regression line and having low densities, since that specific combination will enlarge the *Moment*  $M_k$ .

$$M_x = 1 - \frac{M_k}{MoMax_k} \quad (7)$$

### Clustering Index

An alternative way to evaluate the capacity of the valid cells to delimit the cut-uncut edge is by quantifying their tendency to cluster around the optimal line  $L$ . A basic procedure to quantify that clustering ability is by analyzing the distribution of the perpendicular distances  $d_i$  calculated with equation 5. The standard deviation of the perpendicular distances  $d_i$  for a given image is shown in equation 8, where  $\bar{d}$  is the average perpendicular distance:

$$\sigma_d = \sqrt{\frac{\sum_{i=1}^n (d_i - \bar{d})^2}{n-1}} \quad (8)$$

The *Clustering Index*  $C_x$  is finally defined in equation 9a, with the conditional constraint stated in equation 9b, which assures that  $C_x$  is never above 1.

$$C_x = 0.8 + \frac{0.2}{\sigma_d} \quad (9a)$$

$$\text{If } C_x > 1 \Rightarrow C_x = 1 \quad (9b)$$

The ultimate goal of the confidence metrics is to rate the quality of the estimate (offset) and weight its contribution to the final control command accordingly, mainly if sensor fusion is employed for automatic guidance. In the navigation tests performed with the combine, the *Confidence Index* was calculated but no action was taken in the steering based on such index.

The plots represented in figure 10 give three examples of the application of the confidence metrics to the edge detection algorithm: (a) CI = 60%; (b) CI = 80%; and (c) CI = 94%. Table 1 lists the key parameters involved in the calculation of CI for the cases represented in figure 10.

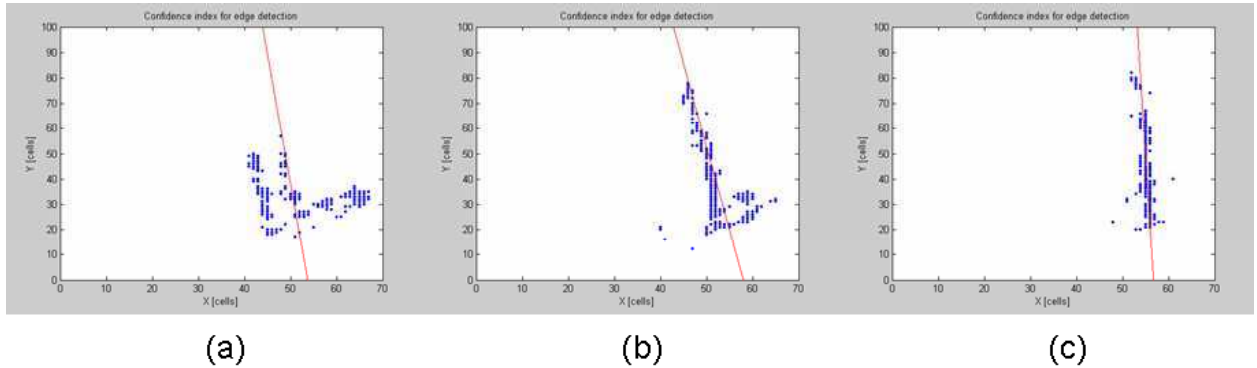


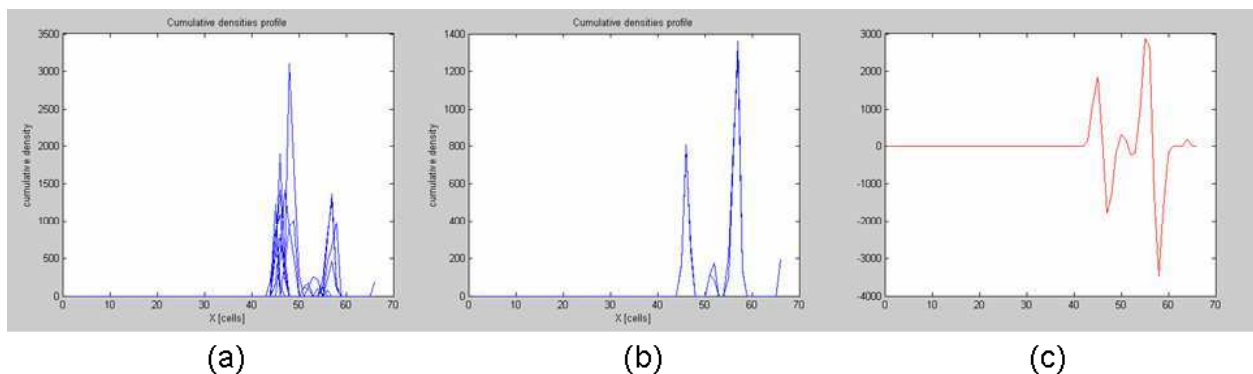
Figure 10. Confidence Metrics for edge detection: (a) CI = 60%; (b) CI = 80%; and (c) CI = 94%.

Table 1. Basic parameters obtained in the calculation of the *Confidence Index* CI for the images of figure 10.

Case	$n$	$M$	$d_{max}$	$D_{min}$	$MoMax$	$M_x$	$\sigma_d$	$\bar{d}$	$C_x$	CI
(a)	154	112	15	45	385	0.71	4.7	5.3	0.84	60 %
(b)	168	33	13	34	417	0.92	2.9	1.5	0.87	80 %
(c)	121	2	6	44	49	0.96	1.1	0.2	0.98	94 %

## OFFSET ESTIMATION

The methodology covered thus far tries to identify the approximate location of the cut-uncut edge and, at the same time, provide an estimate of the quality of the solution found. Once the grid cells that bear the key information have been isolated, the offset of the vehicle is computed from the position of the selected cells. The *offset* can be defined as the lateral distance between the actual position of the combine, and its optimal position determined by the location of the cut-uncut edge. The offset is the output of the edge detection algorithm, and is sent out to the steering control unit of the AutoTrac system. The first step in the calculation of the offset is to generate the profile of cumulative densities by summing up the densities for every column of the grid, eliminating the data stored in the boundaries of the grid (20%). Figure 11 (a) represents the profile of cumulative densities for several images whilst figure 11 (b) plots the profile for a single image. In the former case, it is difficult to decide where the best placement for the edge is. The latter gives a clearer idea of the possible situation for the searched edge, however, there are two distinct peaks separated by 10 cells, and an extra verification would be helpful before making the final decision. The application of the gradient operation, defined in equation 2, to the profile of figure 11 (b) gave the profile of figure 11 (c), where the biggest peak to peak difference provides a redundant value for the approximated position of the edge. The most accurate estimates were obtained with the gradient operation, although most of the times the results from both plots coincided. After the final position for the solution cell has been chosen, the last step consists of transforming the position of that cell to conventional length units, taking into account the extension of the arm  $L_c$  and the width of the combine head fingers.



**Figure 11. Offset estimation: (a) cumulative densities of several images; (b) cumulative densities of a single image; and (c) gradient applied to the profile of cumulative densities of (b).**

## RESULTS

The results obtained during the preparatory tests led to the final configuration camera-vehicle defined by the parameters  $h_c = 1.66$  m,  $\theta = 30^\circ$ , and  $L_c = 1.42$  m (Fig. 1), as well as to the development and tuning of the algorithm. The conclusive experiments to examine the behavior of the entire system were carried out guiding the combine autonomously through a cornfield in central Iowa (USA), on October 21, 2005. Since the auto-steering was executed by the AutoTrac system, it was not possible to introduce modifications in the steering controller or vehicle dynamics model; correct offsets given by the algorithm were supposed to produce stable and precise navigation. The assessment of the quality of the automatic guidance was realized visually, paying attention to possible damage caused to the crop. Corn usually leans as the snouts of the combine head run over the plants laterally, which is easily detected from the cabin. The harvester was automatically guided through the field for several passes at speeds ranging from 2.5 to 4 km/h, a representative velocity interval for corn harvesting operations. The stability of the vehicle greatly depended on the quality of the images and, consequently, the edge detection results. Figure 12 shows two results of the edge detection algorithm when the edge was not the only feature detected: in (a) there were some leaves registered in the grid on the left of the edge; and in (b) there were plants belonging to the inner rows detected on the right side of the cut-uncut edge.

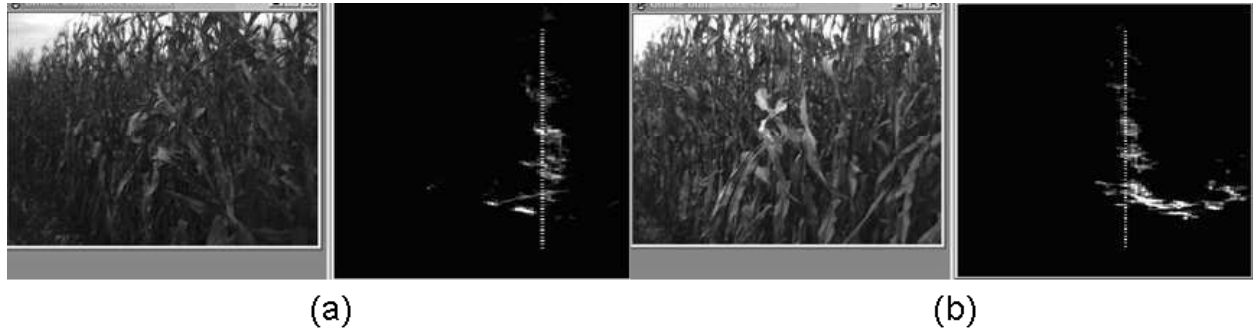


**Figure 12. Edge detection results.**

Figure 13 represents the opposite case, when the edge is basically the unique feature detected in the density grid. Even though there were some cells providing information on the right side of the edge in (b), they had low density values, and basically did not perturb the estimation of the line. In the four cases presented in figures 12 and 13, the position of the estimated edge (marked by a dotted vertical line) gives the impression of being properly situated.

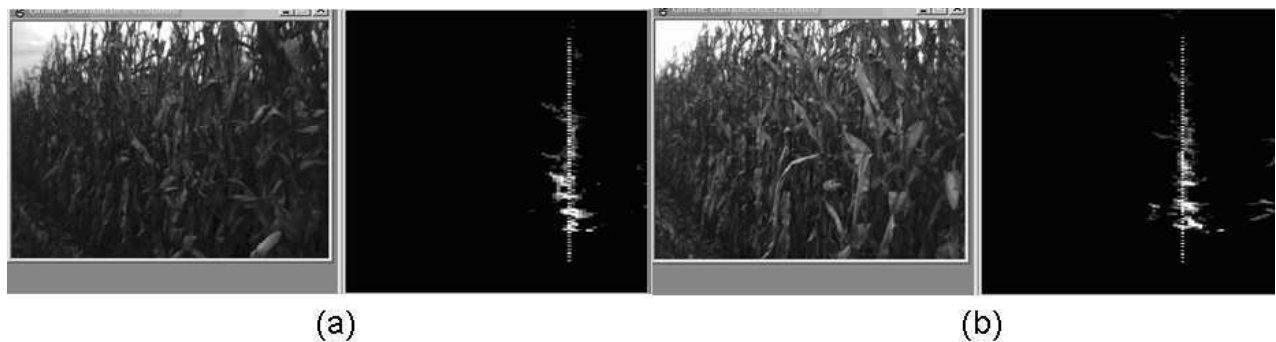


**Figure 13. Edge detection results.**

## CONCLUSION

The numerous benefits of assisting combine drivers in the monotonous task of harvesting motivated the development of an algorithm for autonomous guidance of harvesters. The elaborated methodology was based on the detection of the cut-uncut edge of corn plants using stereoscopic vision. Several operations and techniques such as density grids and gradient profiles turned out to be very helpful in estimating the position of the edge. A confidence index to evaluate the probability of obtaining good results was also developed, although it was not used in the actual control of the vehicle. One of the most sensitive parameters in the configuration of the system was the location of the camera. The best results were achieved with a low camera position on the combine head, and by separating the camera from the cut-uncut edge with an extension arm. Even though this solution turned out to be optimal from the image processing standpoint, it is not the most adequate from the structural point of view: a metal bar with a camera and its cables protruding from the combine head does not seem to be an efficient design. The choice of stereo for the perception of the edge produced good results due to the advantage of having the three dimensions of a scene where the wall created by the edge can be easily detected. The combine was capable of driving autonomously at regular harvesting speeds; however, more guidance tests are necessary to challenge the system and develop a more robust algorithm that can work for a broad variety of conditions. A methodology to evaluate the quality of the automatic task would also be beneficial for comparing the results found with different configurations of the developed system.

### Acknowledgements

The authors would like to express their gratitude to Chenghai Yang and Alfredo Gómez from the USDA Integrated Farming and Natural Resources Research Group (Weslaco, Texas) for their assistance in the image acquisition stage of the research. Appreciation is also conveyed to Deere and Company for the support throughout the entire duration of the project.

## REFERENCES

1. Benson, E. R., J. F. Reid, and Q. Zhang. 2001. Machine vision based steering system for agricultural combines. ASAE Paper No. 011159. St. Joseph, Mich.: ASABE.
2. Khamene, A., and S. Negahdaripour. 1999. Building 3D elevation maps of sea-floor scenes from underwater stereo images. In *Proc. OCEANS '99 MTS/IEEE*, 1: 64- 70.
3. Kise, M., Q. Zhang, and F. Rovira-Más. 2005. A stereovision-based crop row detection method for tractor-automated guidance. *Biosystems Engineering*, 90(4): 357-367.
4. Lee, S., D. Jang, E. Kim, S. Hong, and J. Han. 2005. A real-time 3D workspace modeling with stereo camera. In *Proc. IEEE/RSJ International Conference on Intelligent Robots and Systems (IROS 2005)*, 2140 – 2147.
5. Murray, D., and C. Jennings. 1997. Stereo vision based mapping and navigation for mobile robots. In *Proc. IEEE International Conference on Robotics and Automation*, 2: 1694 – 1699.
6. Rovira-Más, F., and J. F. Reid. 2004. 3D density and density maps for stereo vision-based navigation. In *Proc. Automatic Technology for Off-Road Equipment Conference (ATOE 2004)*, 24 – 35.
7. Rovira-Más, F., Q. Zhang, and J. F. Reid. 2005. Creation of three-dimensional crop maps based on aerial stereoimages. *Biosystems Engineering*, 90(3), 251 – 259.
8. Sabe, K., M. Fukuchi, J.-S. Gutmann, T. Ohashi, K. Kawamoto, and T. Yoshigahara. 2004. Obstacle avoidance and path planning for humanoid robots using stereo vision. In *Proc. IEEE International Conference on Robotics and Automation (ICRA '04)*, 1: 592 – 597.
9. Wang, L. K., S. Hsieh, E. C. Hsueh, F. Hsaio, and K. Huang. 2005. Complete pose determination for low altitude unmanned aerial vehicle using stereo vision. In *Proc. IEEE/RSJ International Conference on Intelligent Robots and Systems (IROS 2005)*, 108 – 113.
10. Wei, J., F. Rovira-Más, J. F. Reid, and S. Han. 2005. Obstacle detection using stereo vision to enhance safety of autonomous machines. *Transactions of the ASABE*, 48(6): 2389 – 2397.



# REACTIVE PATH TRACKING FOR INCREASED SAFETY AND ROBUSTNESS DURING AUTOMATIC GUIDANCE

S. G. Vougioukas<sup>1</sup>

## ABSTRACT

In this paper, a nonlinear model predictive tracking (NMPT) controller is presented for tractor automatic guidance. The basic idea is to use a motion model for the vehicle and compute in real-time, at every time step  $k$ , an optimal  $M$ -step-ahead control sequence, which minimizes the total  $M$ -step tracking error of the projected motion. In the presence of obstacles, the controller deviates from reference trajectories safely and robustly, by incorporating into the optimization obstacle-distance information from range sensors (e.g., laser scanner, ultrasound). Numerous simulations were performed and the NMPT consistently converged to the desired trajectories and followed them accurately, despite large initial errors and discontinuities in the desired velocities and orientations. Reactive path tracking in the presence of a path-interfering obstacle was also tested successfully. The controller's performance depended strongly on parameters such as the optimization horizon  $M$ , and the cost-weights assigned to the various tracking errors. The optimization horizon regulates a trade-off between timely obstacle avoidance and tracking quality (large  $M$ ) vs. consistently fast convergence (small  $M$ ). The cost-weights affect tracking quality and also the shape of the path, by regulating trade-offs among position, orientation, and velocity errors. Overall, NMPT seems to offer a promising approach for advanced precision guidance applications, and deserves further investigation.

**KEYWORDS.** Model Predictive Control, Obstacle Avoidance, Off Road Vehicles, Trajectory Tracking.

## INTRODUCTION

Modern auto-steering systems for tractors can provide accurate and repeatable path tracking of consistently straight or curved rows at an operator-set speed. It is expected that precision farming operations will increasingly rely on more advanced autonomous navigation capabilities of agricultural vehicles. Such capabilities include for example, sharp turns and reverse motions during headland turns, variable speed control, and eventually navigation among field obstacles. The standard approach to autonomous guidance involves two stages. In the first stage, the vehicle's motion trajectory is computed and - if possible - optimized before the actual execution (Vougioukas, et al., 2005). In the second stage, a digital tracking controller controls the vehicle's actuators so that the reference trajectory is followed accurately. A well known theoretical result (Brockett, 1983) for under-actuated non holonomic systems, such as wheeled vehicles under the no-slip constraint, is that linear controllers cannot offer good tracking performance for complex maneuvers, sharp turns and reverse motions. Various techniques have been proposed for tracking paths (Amidi, 1990; Zhang and Qiu, 2004; Witt, et al., 2004) and trajectories (Balluchi, et al., 1996; Divelbiss and Wen, 1997; Wen and Jung, 2004) for wheeled vehicles.

An important problem with the two-stage approach is that long-term autonomous operation in the field cannot be entirely pre-planned, because of imprecision in the field map (e.g., exact locations of trees, fences, ditches, etc). Furthermore, the environment is dynamic because of moving obstacles, such as other vehicles, humans, or animals.

---

<sup>1</sup> Aristotle University of Thessaloniki, Department of Agricultural Engineering, 54124 Thessaloniki, Greece, bougis@agro.auth.gr

In this paper, a nonlinear model predictive tracking (NMPT) controller is presented, which incorporates obstacle-distance information from sensors (e.g., laser scanner, ultrasound), in order to track a reference trajectory safely and robustly. The basic idea behind NMPT is to use a motion model for the vehicle and compute in real-time, at every time step  $k$ , an optimal  $M$ -step-ahead control sequence. This control minimizes the total  $M$ -step tracking error of the projected motion of the vehicle model. In order to avoid any obstacles, the inverse of each obstacle-distance sensor reading is added as a penalty term in the cost function. The first element of the control sequence computed at step  $k$  is applied to the vehicle at sample  $k+1$  because of the nonzero computation time required. At sample  $k+1$  the same problem is solved with updated sensor data, until the vehicle reaches its goal state.

## NON-LINEAR MODEL PREDICTIVE CONTROL THEORY

A brief description of the non linear model predictive control methodology is given next (Kouvaritakis and Cannon, 2001). Let a system's discrete state equation be of the form:

$$\mathbf{x}_{k+1} = \mathbf{f}(\mathbf{x}_k, \mathbf{u}_k), \quad k \geq 0 \quad (1)$$

where  $\mathbf{x}_k \in \mathbb{R}^n$  and  $\mathbf{u}_k \in \mathbb{R}^m$ . The state and control vectors are subject to constraints of the form:

$$\mathbf{x}_{\min} \leq \mathbf{x}_k \leq \mathbf{x}_{\max}, \quad \mathbf{u}_{\min} \leq \mathbf{u}_k \leq \mathbf{u}_{\max} \quad (2)$$

Let  $\mathbf{x}_k^d, k = 0, 1, \dots, N$  be a desired state trajectory and  $\mathbf{e}_k = \mathbf{x}_k - \mathbf{x}_k^d$  be the error between the actual and the desired trajectories. The basic idea behind nonlinear model predictive control (NMPC) is to solve at every time step  $k$  a finite-horizon optimal control problem. Given the actual state  $\mathbf{x}_k$ , an optimal  $M$ -step-ahead control sequence  $\mathbf{u}_{k,M}^*$  is computed, which minimizes a cost function  $J$ :

$$\mathbf{u}_{k,M}^* = [\mathbf{u}_k^* \ \mathbf{u}_{k+1}^* \ \dots \ \mathbf{u}_{k+M}^*] = \arg \min_{\mathbf{u}_k, \mathbf{u}_{k+1}, \dots, \mathbf{u}_{k+M}} J \quad (3)$$

The cost function has the following form:

$$J = \theta(\mathbf{e}_{k+M+1}) + \sum_{j=k}^{\min(N, k+M)} \phi(\mathbf{x}_j, \mathbf{u}_j) \quad (4)$$

where the tracking error of the last state of the finite horizon is penalized by a function  $\theta$  which typically has a quadratic form:

$$\theta(\mathbf{e}_{k+M+1}) = \mathbf{e}_{k+M+1}^T \mathbf{Q}_e \mathbf{e}_{k+M+1} \quad (5)$$

At each step, the state, tracking error and control effort along the optimizing horizon can be penalized also by a quadratic form:

$$\phi(\mathbf{x}_j, \mathbf{u}_j) = \mathbf{x}_j^T \mathbf{Q}_x \mathbf{x}_j + \mathbf{e}_j^T \mathbf{Q}_e \mathbf{e}_j + \mathbf{u}_j^T \mathbf{Q}_u \mathbf{u}_j \quad (6)$$

The control applied to the actual system at sample  $k$  is the first element of  $\mathbf{u}_{k,M}^*$ . At sample  $k+1$  the system has moved to a new state  $\mathbf{x}_{k+1}$  which differs from the predicted state due to disturbances and model errors. However, when NMPC is used for fast dynamic systems, such as moving vehicles, the first element of the control sequence computed at step  $k$  is applied to the vehicle at sample  $k+1$  (at best) because of the nonzero computation time required. At sample  $k+1$  the same problem is solved with updated sensor data, until the system reaches its goal state  $\mathbf{x}_N^d$ .

## NON-LINEAR MODEL PREDICTIVE PATH TRACKING

The proposed approach to path tracking is to use non linear model predictive control as a high-level tracking controller (NMPT), which uses a simple kinematical model for the vehicle motion, and incorporate dynamic models for steering and speed control. This approach avoids the complexities of full dynamic modeling, while retaining the required accuracy for low working-speeds. Of course, simple dynamic models, such as bicycle models (Wong, 1993) could be used

for the NMPT, but still unknown model parameters related to tire-soil interaction need to be identified. A simple kinematical model for a front-wheel steered tractor is given next:

$$\dot{x} = v \cos \theta, \quad \dot{y} = v \sin \theta, \quad \dot{\theta} = v \frac{\tan \phi}{L} \quad (7)$$

The  $x$  and  $y$  coordinates give the position of the tractor's rear-wheel axle midpoint and the tractor's orientation is given by the angle  $\theta$ . The wheelbase length is  $L$ , the steering angle is  $\phi$  and the vehicle speed is  $v$ . At a lower-level, a steering controller model is used to create an "abstraction" of the steering system dynamics (Stombaugh, et al., 1998, Wu, et al., 1998); the same holds for speed controllers. In this work, the combination of the steering controller and steering linkage is modeled as a 1<sup>st</sup> order system with time-lag  $\tau_\phi$ ; an analogous abstraction is used for speed control.

$$\dot{\phi} = -\frac{1}{\tau_\phi} \phi + \frac{1}{\tau_\phi} u_\phi, \quad \dot{v} = -\frac{1}{\tau_v} v + \frac{1}{\tau_v} u_v \quad (8)$$

This means that the NMPT provides a desired steering angle  $u_\phi$  to the steering controller and the actual wheels' steering angle follows the command with first order dynamics. Similarly, velocity commands  $u_v$  are issued by the NMPT to the speed controller. Of course, different models (e.g. second order) could be used, as long as their parameters can be identified. From the NMPT point of view the vehicle is described by equations (7),(8) the system state is  $\mathbf{x} = [x \ y \ \theta \ \phi \ v]^T$  and the control is  $\mathbf{u} = [u_v \ u_\phi]^T$ . The tracking error is defined as the difference between the desired and actual trajectory points at each controller sample.

## NUMERICAL SOLUTION

In the general case, NMPC optimization can only be solved numerically. The system equations must be discretized so that they can be expressed in the form of equation (1) and solved. In this paper the indirect approach was used, which uses gradient descent in order to minimize the problem's Hamiltonian (Kirk, 1970). The Hamiltonian for NMPC optimization is

$$H = \phi(\mathbf{x}_k, \mathbf{u}_k) + \lambda_{k+1}^T \mathbf{f}(\mathbf{x}_k, \mathbf{u}_k) \quad (9)$$

where  $\lambda_k$  is the costate sequence, which must satisfy the following equations

$$\lambda_{k+M} = \frac{\partial \theta}{\partial \mathbf{x}_{k+M}}, \quad \lambda_j = \frac{\partial H}{\partial \mathbf{x}_j} = \frac{\partial \phi}{\partial \mathbf{x}_j} + \frac{\partial \mathbf{f}^T}{\partial \mathbf{x}_j} \lambda_{j+1}, \quad j = k, \dots, k+M-1 \quad (10)$$

The main idea behind the gradient descent algorithm is the following: if we start from a nominal solution  $\mathbf{u}_{k,M}^*$  which is close to the optimum, in order to minimize  $J$ , a variation  $\delta \mathbf{u}_{k,M}^*$  of this control must be computed, such that the variation  $\delta J$  should be always negative:

$$\delta J = \sum_{j=k}^{k+M} \left[ \frac{\partial H}{\partial \mathbf{u}_j} \right]^T \delta \mathbf{u}_j, \quad \text{where} \quad \frac{\partial H}{\partial \mathbf{u}_j} = \frac{\partial \phi}{\partial \mathbf{u}_j} + \frac{\partial \mathbf{f}^T}{\partial \mathbf{u}_j} \lambda_{j+1} \quad (11)$$

This can be achieved by moving the control in the opposite direction of the Hamiltonian's control gradient (steepest descent).

$$\mathbf{u}_j^{i+1} = \mathbf{u}_j^i - K \frac{\partial H}{\partial \mathbf{u}_j^i}, \quad j = k, \dots, k+M \quad (12)$$

where the gain  $K$  is a sufficiently small positive number. The algorithm proceeds as follows: at each step  $k$ , given an initial  $\mathbf{u}_{k,M}^*$  the gradient descent iteration index  $i$  is initialized to zero and equation (1) is used to compute the open-loop trajectory  $\mathbf{x}_{k,M}^* = [\mathbf{x}_k^* \ \mathbf{x}_{k+1}^* \ \dots \ \mathbf{x}_{k+M+1}^*]$ . Next,  $\lambda_j^i$  and  $\partial H / \partial \mathbf{u}_j$  are computed using equations (10) and (11) respectively, and the updated controls  $\mathbf{u}_j^{i+1}$  are computed by equation(12). Finally,  $i$  is incremented and the iterations continue, until a convergence termination criterion is satisfied.

## REACTIVE PATH TRACKING FOR OBSTACLE AVOIDANCE

The desired motion trajectory has been computed by some motion planning algorithm and is assumed to be collision-free. During the actual motion execution it is possible that obstacles appear in the tractor's path, which had not been present in the planning phase (e.g., animals, humans, machines). This may also happen because of imprecision in the field map, or tractor localization errors. If the tractor is equipped with range sensors, such as a laser scanner or arrays of ultrasound sensors, then at any time, the distances of a number of obstacle points from the respective sensor are known. These distances can be incorporated in the cost function, so that the computed control tracks the desired trajectory, while staying away from the obstacles. Let  $T_{sl}$  be the fixed transformation matrix of the  $l$ th sensor frame with respect to the tractor frame, and  $T(\mathbf{x})$  be the transformation matrix of the tractor's frame with respect to the fixed navigation frame. Let  ${}^{S_l} \mathbf{r}_m(\mathbf{x})$  be the  $m$ th range measurement of the  $l$ th sensor, in the sensor frame, at tractor state  $\mathbf{x}$ . The corresponding obstacle-point position expressed in the navigation frame is  $\mathbf{p}_{lm} = T(\mathbf{x})T_{S_l} {}^{S_l} \mathbf{r}_m(\mathbf{x})$  and is independent of the tractor state. The  $l$ th sensor's frame origin expressed in the navigation frame is  $\mathbf{s}_l(\mathbf{x}) = T(\mathbf{x})T_{S_l} {}^{S_l} \mathbf{s}$ , where  ${}^{S_l} \mathbf{s} = [0 \ 0 \ 1]^T$ . Hence, their relative distance vector, expressed in the navigation frame is:

$$\mathbf{a}_{lm}(\mathbf{x}) = \mathbf{p}_{lm} - \mathbf{s}_l(\mathbf{x}) \quad (13)$$

and the scalar distance is  $D_{lm}(\mathbf{x}) = (\mathbf{a}_{lm}^T \mathbf{a}_{lm})^{1/2}$ . The obstacle points contribute to the cost functions  $\theta$  and  $\varphi$  with a term which penalizes states which result in proximity with the obstacles:

$$V(\mathbf{x}) = \sum_{l=1}^L \sum_{m=1}^{M_l} \left( \frac{C}{D_{lm}(\mathbf{x}) + \varepsilon} \right)^\rho \quad (14)$$

where  $L$  is the number of range sensors,  $M_l$  is the number of readings of the  $l$ th sensor,  $\varepsilon$  is a small positive real number,  $C > 0$  and  $\rho > 1$ . In order to solve the system of equations (10), the terms  $\partial\phi/\partial\mathbf{x}_j$ ,  $\partial\theta/\partial\mathbf{x}_j$  are needed. Thus, we need to compute  $dV_{lm}/d\mathbf{x}_j$ , which can be shown to be:

$$\frac{dV_{lm}}{d\mathbf{x}_j} = \frac{-\rho C^\rho}{(D_{lm}(\mathbf{x}_j) + \varepsilon)^{\rho+1}} \frac{dD_{lm}}{d\mathbf{x}_j}, \text{ where } \frac{dD_{lm}}{d\mathbf{x}_j} = \left( \frac{d\mathbf{a}_{lm}}{d\mathbf{x}_j} \right) \frac{dD_{lm}}{d\mathbf{a}_{lm}} = \frac{1}{D_{lm}} \left( \frac{d\mathbf{a}_{lm}}{d\mathbf{x}_j} \right) \mathbf{a}_{lm} \quad (15)$$

Using equation (13) and noticing that the obstacle-point  $\mathbf{p}_{lm}$  is independent of the robot state, the term  $d\mathbf{a}_{lm}/d\mathbf{x}_j$  is found to be equal to  $-d\mathbf{s}_l/d\mathbf{x}_j$ . The derivatives of this term must be computed numerically (e.g., by central differences) because no analytical expressions are known for the obstacles.

## SIMULATION RESULTS

The NMPT was implemented in C++ and numerous simulations were performed. An ideal scenario was assumed for the range sensors, i.e., that a virtual sensor was available, which reported the minimum distance between the vehicle and any obstacles. The tractor's wheelbase was set to 2.4 m, with  $|\varphi|_{max}=60^\circ$  and  $|v|_{max}=1$  m/s. The state equations' integration step was set to 0.01s for increased accuracy, whereas the NMPT sampling period was  $dt=100$  ms. The steering and speed time-lags were  $\tau_\varphi=0.15$  s and  $\tau_v=1$ s respectively. All the elements of all cost matrices were set to zero. The diagonal elements of  $\mathbf{Q}_e$  were set to  $q_e(1,1)=q_e(2,2)=1500$  (distance error costs) and  $q_e(3,3)=1500$  (orientation error cost). The velocity errors were penalized less, with  $q_e(5,5)=500$ , because path accuracy was considered more important. The NMPT gradient descent algorithm was allowed to execute for 100 iterations and the optimization horizon was set to  $M=25$ .

In a first experiment the tractor followed a key-hole shaped path, typical of a headland maneuver at a constant speed of 0.5 m/s. The desired and executed paths for two different starting positions are shown in figure 1a. Both starting positions contained a  $\pm 0.5$  m horizontal initial error, whereas the second position had also a  $20^\circ$  orientation error. Both trajectories converged to the desired one despite the relatively large initial errors. The average and maximum trajectory tracking errors after

convergence were 0.96cm and 1.36cm respectively, i.e., the NMPT followed the trajectory very closely. The average and maximum velocity tracking errors after convergence were 0.48% and 2.02% respectively. Each new control computation required 13.1ms on a Pentium 2.6 GHz single-CPU system, which is adequate for real-time implementation. Next, a rectangular obstacle was introduced in a position which prohibited exact path following and the simulation was executed again.

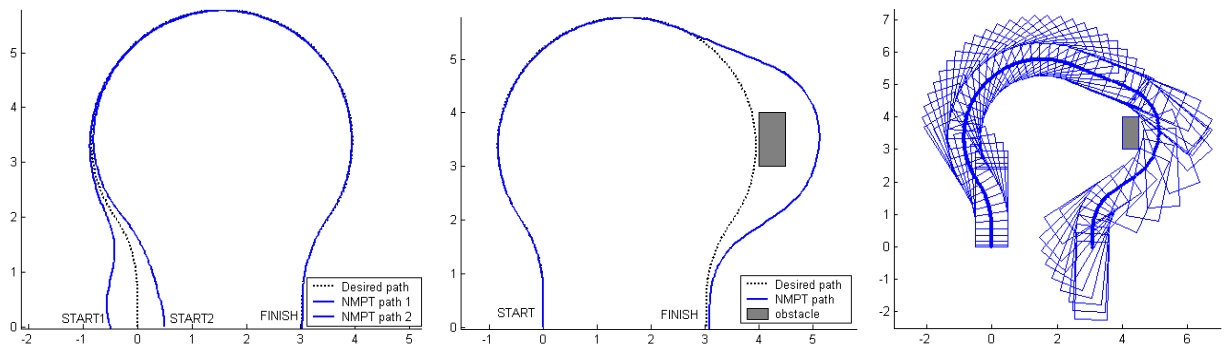


Figure 1. a) Key-hole maneuver, b) path deformation due to obstacle, c) executed vehicle motion trace.

As it is shown in figure 1b, the NMPT deviated from the desired trajectory in order to safely avoid the obstacle. Figure 1c shows a trace of the vehicle's obstacle-avoidance reactive motion. When the obstacle cost was included in the cost function, the required computation for each new control increased to 130ms. However, this number is the result of very expensive minimum distance gradient computations, which would not be necessary in a real scenario with range sensors.

In a second experiment a fish-tail maneuver was executed, which contained large discontinuities in both orientation and velocity. Figure 2a shows three different executed paths for two different starting positions. The first path resulted from an initial horizontal position error of +0.5 m. The second and third paths resulted from an initial error of -0.5m and an orientation error of  $20^\circ$ . The second path converged more slowly to the desired path than the third path, because the orientation penalty term in the  $\mathbf{Q}_e$  matrix was  $q_e(3,3)=1500$ , whereas for the third path a smaller value of  $q_e(3,3)=100$  was used. Hence, a position vs. orientation error trade-off existed. In figure 2b the deviation of the NMPT from the desired trajectory is shown in the presence of an unexpected obstacle. Finally, figure 2c shows a trace of the vehicle's obstacle-avoidance reactive motion.

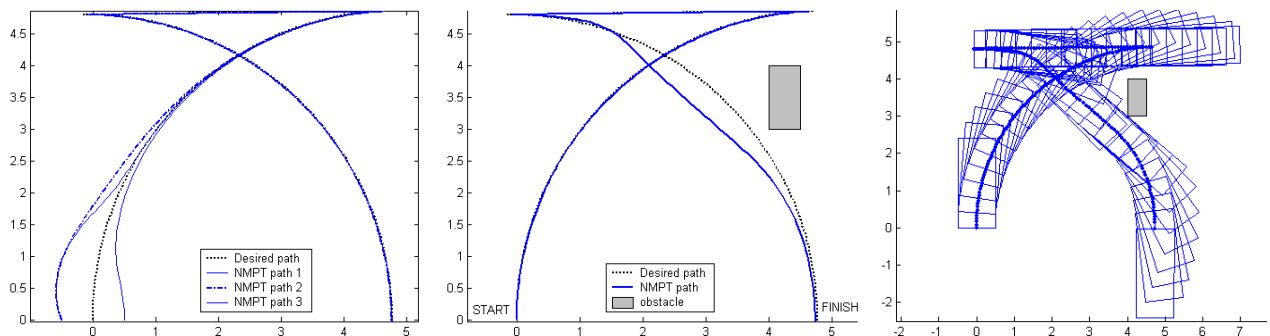


Figure 2. a) Fish-tail manoeuvre, b) path deformation due to obstacle, c) executed vehicle motion trace.

## CONCLUSION

The NMPT consistently converged to the desired trajectories and followed them accurately, despite large initial errors and discontinuities in the desired velocity and orientation. Overall, the computational cost does not seem to be prohibitive for real-time control. The optimization horizon  $M$  is an important parameter, which regulates a trade-off between timely obstacle avoidance and tracking quality (large  $M$ ) vs. fast solution time (small  $M$ ). Also, in the presence of obstacles the convergence rate of the gradient descent numerical procedure varied along the path. The delayed computation of "fresh" NMPT controls, even if it happens intermittently, can create problems

during real-time control. If the NMPT solution time is  $\lambda$  times longer than  $dt$ , then at the next  $\lambda$  steps the optimal control computed at step  $k$  must be used. This is equivalent to open-loop control and the tracker's stability for large  $\lambda$  needs to be investigated further. A partial solution to the speed problem could be the use of more advanced numerical techniques for the NMPT optimization. For example, a direct approach, such as *direct transcription* could be used, which casts the optimal control problem into a constrained Nonlinear Programming Problem (NLP). Such problems can be solved very efficiently using sparse Sequential Quadratic Programming (Betts, 1998).

Another issue is the choice of the cost matrix elements. From our simulations it was clear that they affect tracking quality as well as the shape of the path. This is due to trade-offs among position, orientation, and velocity errors, and appropriate values for different types of motions need to be found. A characteristic of trajectory tracking, which came up during simulations is that obstacle avoidance may lead to significantly longer paths. Given that the desired trajectory is defined by  $N$  points and that the NMPT sampling interval  $dt$  is fixed, longer paths can be traversed with the same  $N$  and  $dt$  parameters, only if the vehicle's velocity is increased; this may lead to increased velocity tracking errors. More importantly, if the path is too long (e.g.,  $N_p$  points, with  $N_p \gg N$ ), the maximum velocity cannot be exceeded and the executed trajectory will not terminate at the goal. A solution to this problem could be the asynchronous advancement of the executed and desired trajectory indices, so that at the end of the motion (after  $N_p$  points) the vehicle's state is  $\mathbf{x}_{N_p} = \mathbf{x}_N^d$ .

Finally, the calculation of the distances between the vehicle and any obstacles - along with the gradient of these distances - based on actual range sensors' measurements needs to be addressed. An important issue is expected to be the noise contained in such measurements (amplified by differentiation) and its effect on NMPT convergence.

Overall, in theory, NMPT offers tracking capabilities for wheeled vehicles, which linear controllers cannot match (Brockett, 1983). Hence, it seems to offer a promising approach for advanced precision guidance applications, and it deserves further investigation.

## REFERENCES

1. Amidi, O. (1990). Integrated Mobile Robot Control. Masters Thesis, Dept. Of Electrical and Computer Engineering, CMU, Pittsburgh, PA.
2. Betts, J. (1998). Survey of Numerical Methods for Trajectory Optimization. *Journal of Guidance, Control, and Dynamics*, v.21(2), 193-207.
3. Brockett, R. 1983. Asymptotic stability and feedback stabilization. In *Differential Geometric Control Theory* (R. Brockett, R. Millman and J. Sussmann. (Ed.)). Birkhauser. 27,181-208.
4. Divelbiss, A., and Wen, J. (1997). Trajectory Tracking Control of a Car-Trailer System. *IEEE Transactions on Control Systems Technology*, v.5(3), 269-278.
5. Kirk, D.E. (1970). *Optimal Control Theory: An Introduction*, Prentice Hall, Englewood Cliffs, New Jersey, U.S.A.
6. Kouvaritakis B., and Cannon, M. eds. (2001). *Non-Linear Predictive Control: Theory and Practice*, IEE Publishing, London.
7. Stombaugh, T., Benson, E., Hummel, J. (1998). Automatic guidance of agricultural vehicles at high field speeds. ASAE Paper 983110. St. Joseph, MI.
8. Vougioukas, S., Blackmore, S., Nielsen, J., and Fountas, S. (2005). A Two-Stage Route Planning System for Autonomous Agricultural Vehicles. *5th European Conference on Precision Agriculture*, pp. 597-604, Uppsala, Sweden.
9. Wen, J., and Jung, Sooyong. (2004). Nonlinear Model Predictive Control based on Predicted State Error Convergence. *Proceeding of the 2004 American Control Conference*. Boston, Massachusetts, 2227-2232.
10. Witt, J., Crane C.D.III, and Armstrong,D. (2004). Autonomous Ground Vehicle Path Tracking. *Journal of Robotic Systems* v.21(8), 439-449.

11. Wu, D., Zhang, Q., Reid, J., Qiu, H., Benson, E. (1998). Model Recognition and Simulation of an E:H Steering Controller on Off-Road Equipment. In: Nair, S., Mistry, S. (Eds). Fluid Power Systems and Technology 1998, ASME, New York, pp. 55–60.
12. Wong, J. (1993). Theory of Ground Vehicles. John Wiley & Sons Ltd, New York, p.50-55.
13. Zhang, Q., and Qiu, H. (2004). A Dynamic Path Search Algorithm for Tractor Automatic Navigation. Transactions of the ASAE, v. 47(2): 639–646.



# FAULT DIAGNOSTICS IN AGRICULTURAL MACHINES

M. Miettinen<sup>1</sup>, T. Oksanen<sup>1</sup>, M. Öhman<sup>1</sup>, P. Suomi<sup>2</sup> and A. Visala<sup>1</sup>

## ABSTRACT

Fault diagnostics in industrial applications has become very popular research topic. In agriculture the time window to complete tasks may be very short. Timing the field operations is critical when machine and human resources are limited. Different kind of dynamic model based fault detection and diagnosis methods have been studied throughout the process automation context.

Here fault diagnostics has been studied with three agricultural implements, two drills and one sprayer. In the first drill, scalar statistical analysis and classification of temporal feature patterns can be applied to analysis of possible faults in the analog measurements. In the second drill fault diagnostics was developed for electrical actuators. The nominal model of actuator was identified with test procedure, and the faults are detected by comparing the measured behavior to the nominal model. In the sprayer the pump is the most critical component with many different failure modes. Frequency domain analysis and fuzzy classifier were utilized to detect faults. Different faults were induced to the pump and the diagnostics were developed based on the collected data.

Remote diagnostics is needed if the failures are hard to detect automatically. For example some actuators change their behavior slowly due to wearing and it may be difficult to know when the fatal failure will appear. By implementing remote diagnostics the manufacturer can centrally collect fault diagnostics data and use statistical methods for improving and fine tuning preventive maintenance programs. Here the remote diagnostics system was developed to one implement, hydraulic actuator condition monitoring in one drill. The remote diagnostics features were implemented in the Task Controller of an ISOBUS compatible machine control system.

In all cases the self diagnostics methods were implemented as software components to the implement controller software and were tested for functionality with real agricultural implements. A good development procedure and tools for fault diagnostics is presented also in the paper.

**KEYWORDS.** Condition Monitoring, Fault Diagnostics, Machines, Mechatronics, Remote Diagnosis, Sensors, Seed Drills, Services, Software Components, Sprayers.

## INTRODUCTION

The general development of engineering and automation has offered new possibilities for agriculture area. New requirements for automation systems in agricultural machines are set and especially reliability of systems has become more important research area. Because fault diagnostic is an important part of reliability of automation systems in agricultural implements a research and a development studies were needed in that area too. Auernhammer (2003) has considered new intelligent technologies in agriculture and role of mechatronics, the combination of mechanics and electronics together with hydraulics makes intelligent components available which can be connected using electronic communication. Also Sigrimis et al. (2000) have discussed widely the incoming information society in their paper. According to them concurrent engineering in biology, mechanics, electronics and other areas gives possibilities to create information and communications services and applications for example to agriculture, and it is an

---

<sup>1</sup> Helsinki University of Technology, Automation Technology Laboratory. PO Box 5500, FIN-02015 TKK, Finland, mikko.miettinen@tkk.fi

<sup>2</sup> MTT Agrifood Research Finland, Plant production research, Vakolantie 55, FIN-03400 Vihti, Finland

unique challenge for Agro-Engineering. ICT technologies of GroupWare, simulation tools, design tools, and in field implementations are the enabling technologies to help the task.

In the AGRIX project (Automation system for agricultural implements) an ISO 11783 compatible prototype system was developed. The system consists of one tractor and four different implements. A generic, configurable, open and smart implement controller was the main goal in the project. Fault diagnostics was developed for one pneumatic combined seed drill, one no-tillage drill and one sprayer. References see e.g. Öhman et al. (2004), Öhman et al. (2005), Oksanen et al. (2004), Oksanen et al. (2005a) and Oksanen et al. (2005b).

Fault diagnostics has become very popular research topic in industrial applications. Fault diagnostics is desired in modern process control, because the processes are commonly linked to each other and if some part of a process fails the whole process is affected and economic losses may be remarkable.

In agriculture the field operations are mostly time critical. Timing the field operations is critical when machine and human resources are limited. It is important to have the machines in proper working condition when they are needed on the field. The failure probability must be low and if the failure happens the down time must be short. Therefore the fault diagnostics function is profitable also in agricultural machines.

Fault diagnostics can be considered as an added value for product. Product life cycle approach is common when developing and marketing new products today. Life cycle management is a business decision-making approach that considers benefits, costs and risks over the full cycle of a product or service. This approach is also known as extended product. Remote diagnosis and telemaintenance are typical examples of such services.

## **METHODS AND TOOLS**

### Fault diagnostic methods

Different kind of dynamic model based fault detection and diagnosis methods have been studied throughout the process automation context, see e.g. Patton et al. (2000) The application of these methods in working machine context is difficult, because the monitored subsystems are usually too simple SISO systems in order to utilize real logical redundancy on the basis of MIMO dynamical models. In the same way another main approach in fault diagnosis, based on multivariate statistics, see e.g. Jong-Min et al (2004), PCA, PLS etc. seems to be too much for this application.

### Methods applied in this paper

Methods used in the AGRIX project vary from model based to time signal processing frequency transforms and fuzzy logic. Also statistical data based methods are studied. Different methods used were determined after an extensive test-program done to each implement. Methods used here are based e.g. Hammouri et al. (2004), Lee et al. (2004), Manabu et al. (2004), Oakland (2003) and Venkatasubramanian (2003). Results are presented in Miettinen (2005).

For example quite simple scalar statistical analysis and classification of temporal feature patterns can be applied on analysis of possible failures. The most important measurement on which one could apply model based dynamical methods is the behavior of oil pressure in main line measured during hydraulic valve control. The behavior of oil pressure is very context dependent but it surely contains information about certain faults. In the position control of hydraulic cylinders the hits on the limits can probably be detected from the oil pressure measurement. These will be studied. Systematic and simple procedures for remote fault diagnosis and maintenance will be developed and tested. The methods should be reliable and there should not be wrong alarms nor undetected faults.

### Traditional development tools

High-level graphical programming tools are widely used in industrial automation. Most embedded systems on the other hand are still programmed with assembler or C languages because of the platform limitations. However, the computational and memory limitations are becoming less

important with every new generation of micro-controllers. The control functions of traditional agricultural machines have been quite simple and low-level languages have been adequate for programming these systems. But the machines are getting bigger and more complex. Large machines require more automation to keep the operator strain at an acceptable level. Emerging production methods, such as precision farming, require positioning systems and feedback control. Automation technology can also be used to produce more accurate farm records. To reach their full potential, separate control systems need to be connected. Creating distributed real-time embedded control systems with low-level languages is slow, error-prone and prohibitively expensive, especially if the production series are small. Platform limitations have also prohibited the wide use of intelligent fault detection algorithms. Also, the more complex the machine is the more it can benefit from a fault diagnostics system.

#### Higher level development tools

Higher level development tools provide graphical programming framework for building control systems and other periodically executable software components with same functionalities that traditional programming tools provide. Code reusability with graphical development tools is easier than with traditional code. In the AGRIX project RTI's Constellation software development system was chosen for building control systems, RTI (2003). Constellation allows that components for processing continuous signals are executed at the specified frequency. The control systems can also be reconfigured on the fly by activating and deactivating components. This kind of mode change is needed e.g. to transition from manual to automatic control. In addition, Constellation provides a framework for processing discrete events. UML-style state machines can be used for event processing. State transitions can be triggered by events or changes in continuous signals. Because time can be handled as a continuous signal, implementing time-dependent state transitions is very easy. Constellation encourages component reuse. The components are loosely coupled by well defined interfaces. Because components are connected using interfaces, it is possible to compose fundamentally different control systems from the same set of components. Creating new interfaces and adding them to new components is easy. New components can be created by combining existing components, drawing state machines or by writing primitive components with C++. Because Constellation is based on C++ programming language, it creates relatively efficient and fast code. Constellation runs in Windows and Linux operating systems. It can also create executables for VxWorks operating system and supports various processor architectures.

MATLAB is a software package for mathematical computing. Several MATLAB extensions, called toolboxes, offer computing tools for special application and method areas. MATLAB/Simulink is a tool with graphical user interface for modeling, simulating and analyzing dynamic systems. Simulink is mainly used to simulate and analyze dynamic systems, both linear and nonlinear, in continuous and discrete time and hybrid of those. Simulink is widely used in control engineering. Constellation has wrappers for Simulink models so that they can be used as easily as C++ components. Most controllers, filters and fault diagnostics were created with Simulink.

In Figure 1, Simulink model has been imported as a Constellation component. Simulink model inside this Constellation Composite Component is shown in figure 4.

## **MACHINES**

In the AGRIX project (Automation system for agricultural implements) an ISO 11783 compatible prototype system was developed. The system consists of one tractor and four different implements. A generic, configurable, open and smart implement controller was the main goal in the project. Fault diagnostics was developed for three of our case implements, one pneumatic combined seed drill, one no-tillage drill and one sprayer.

The system architecture of the AGRIX system is based on ISO 11783 (ISOBUS) network. In the project, commercial Virtual Terminal was used, and also a commercial tractor was equipped with ISOBUS adapter. The developed parts are the implement controller (same platform for all

implements), compatible Task Controller and the adapter to connect GPS to the network. For research purposes the system contains also a separate logging system.

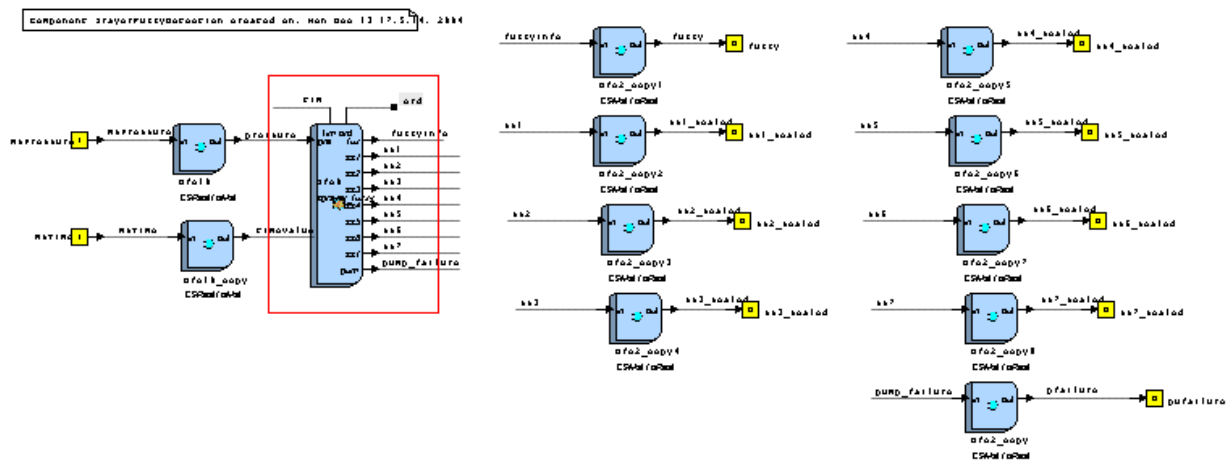


Figure 1. Simulink model inside Constellation.

The hitch connected Junkkari sprayer has PTO powered pump and its boom is divided into five sections. The pump is a fixed volume pump i.e. the liquid flow is proportional to pump's rotation speed. The coarse regulation is done by manual pressure relief valve next to the pump. The continuous control is done by an electrically controlled pressure relief valve just after the coarse regulator. Coarse regulator was tuned to keep the pressure at 7 bars. The pressure sensor and flow meter are located after the valves and that information are used in control system. The section valves are located after those, parallel. The flow goes through selection valves either to sections or back to the tank through tunable choke. In discussions with the sprayer manufacturer it turned out that pump faults are the most common faults in the sprayer.

In the pneumatic combine fertilizer and seed drill (Tume Airmaster, Fig. 2) coulters are located at the rear, containers in the middle and leveling board at the front. This drill has seven hydraulic functions which can be controlled separately using magnetic valves in this prototype. A pressure sensor was installed to the pressure line; this information was considered to have rich information content about the state of machine. For research purposes several limit switches were installed to hydraulic functions, in order to gather sufficient information for the off-line fault diagnostics development phase.



Figure 2. The implements used: Tume Airmaster™, Junkkari™ sprayer, and Junkkari Superseed™.

The no-tillage drill (Junkkari Superseed, Fig. 2) has hydraulic functions, which are directly connected to tractor's ISOBUS valves. The implement controller controls the valves through the ISOBUS network. The used ISOBUS valves are able to transmit the estimated flow, and this was meant to be used in diagnostics. In both drills, electrical linear actuators were used to control feeder device application rates, and these electrical actuators were considered vulnerable.

## RESULTS

Extensive testing of the implements was carried out to recognize normal and abnormal operation of the selected subsystems. Sensors that could help detect failures were added, but main idea was to see if faults could be detected with the sensors already in place. After normal and abnormal operation modes were measured the best way to identify the failure were chosen and the diagnostic component was developed. Varying fault diagnostic components were implemented with Simulink and tested in real machines. Common failures were caused on purpose to test operation of the components in real conditions. MTT Agrifood Research Finland has tested the system with diagnostic components for one season.

### The sprayer

Pressure sensor was situated in the main water line to measure liquid pressure. Liquid pressure was studied in normal and faulty situations of pump operation using different sprayer pressures. First assumption was that cavitation of the pump would increase the standard deviation of the pressure which was confirmed experimentally. It was established that different pump failures such as forcing valve or suction valve failures and cavitation produced high standard deviation to the measured pressure. To differentiate between these failures the frequency domain was used instead of the time domain. Power spectrum was produced and different failures were successfully detected with fuzzy logic rules that were devised from normal operation. Normal and failure functionality analysis was done by deliberately causing usual pump failures and measuring the failure conditions. In figure 3, it is possible to see that cavitation causes abnormal frequencies in the power spectrum when changing pressure.

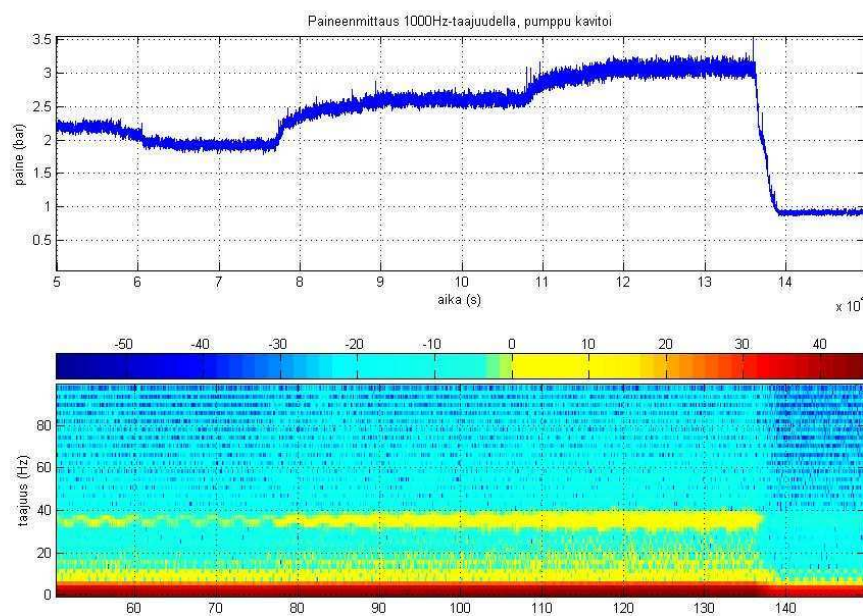


**Figure 3. Power spectrum of pressure measurement when the pump is cavitating.**

The structure of the fault detector is shown in figure 4. The power spectrum is calculated in real time from collected measurement data. The calculated power spectrum is fed into the fuzzy logic classifier. Fuzzy rules calculate fuzzed value which is unfuzzified and fed it into the fault isolator component which decides whether the implement is operating normally or has a failure.

Failure messages are displayed to the user on the Virtual Terminal (ISOBUS) and are saved to Task Controller task file.

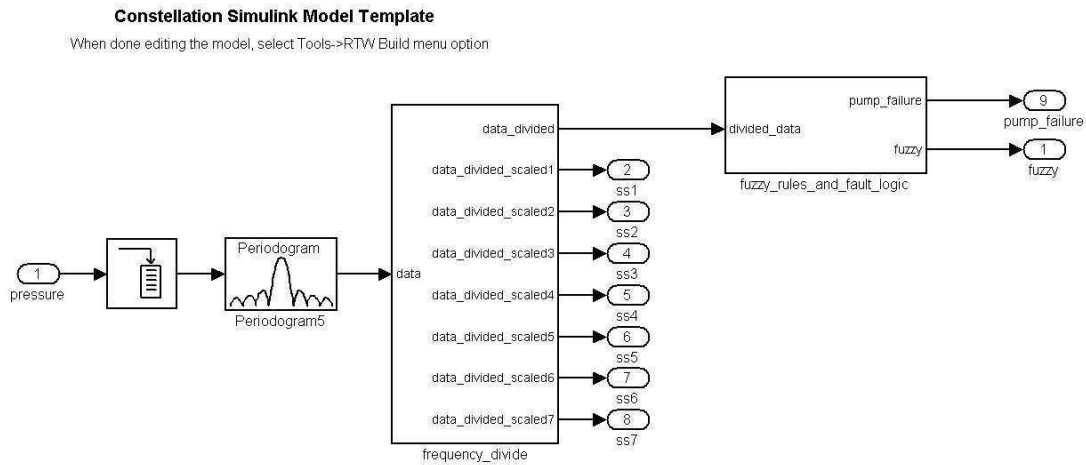


**Figure 4. Simulink model of Sprayer Fault Diagnostics.**

### Hydraulics of the drill

12 limit sensors and one oil pressure sensor were installed. The idea was to use only the oil pressure measurement in the pump line together with controlled on/off valves in the drill to detect behavior of the hydraulic cylinders. The limit sensors were installed only for the data analysis purposes, in order to have numeric data when actions really happened. In the developed diagnostics system component the limit sensor data is not necessary, but it can be used to monitor oil pressure sensor and vice versa.

SPC (Statistical Process Control) was used to detect failures in hydraulic actuators. Variation of individual hydraulic cylinders were calculated and alarm limits and failure borders were established during normal use of the drill hydraulics.

Three independent failure detectors were developed. The main detector calculates individual operation times of the actuators from oil pressure sensor information. Limit sensor detector was first developed to confirm detected behavior of the hydraulic valves from the pressure sensor detector. If both pressure sensor and limit sensors are used in the machine then all cumulated information can be used to detect sensor failures. The third failure model detects sensor failures by comparing statistical values calculated by the two previous detectors.

Variation of one such hydraulic controller in use is shown in figure 5. Alarm borders are shown in red.

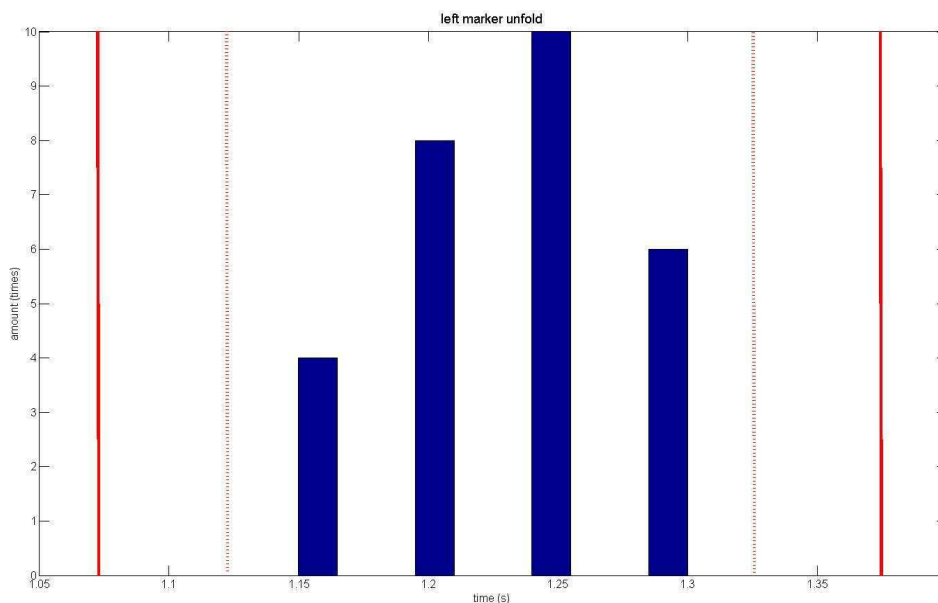


**Figure 5. Example of Statistical process values for controlling state.**

Using the flow estimates from the ISOBUS valves to improve the fault detection was also attempted. However this was not successful because the flow estimates from the ISOBUS-valves used in the project were too inaccurate.

Electrical actuators in the drill

Linear actuator fault detection component used measured current consumption. Basically it monitors if actuator gets stuck (jammed), potentiometer is broken or the motor doesn't get any power. Secondary goal was to monitor individual actuators over time. Linear actuators are monitored by their power consumption and operational speed.

Linear actuators were first tested for power consumption versus resisting force. Results of one such test is shown in figure 6. Then linear actuator speed versus resisting force was tested. Results are shown in figure 7.

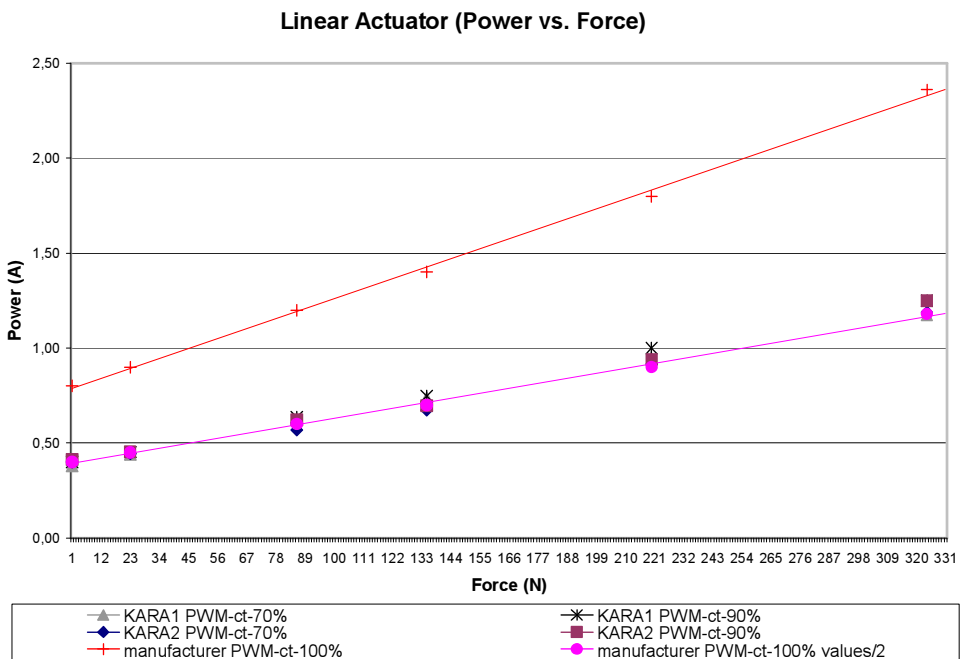


Figure 6. Linear actuators power consumption versus force.

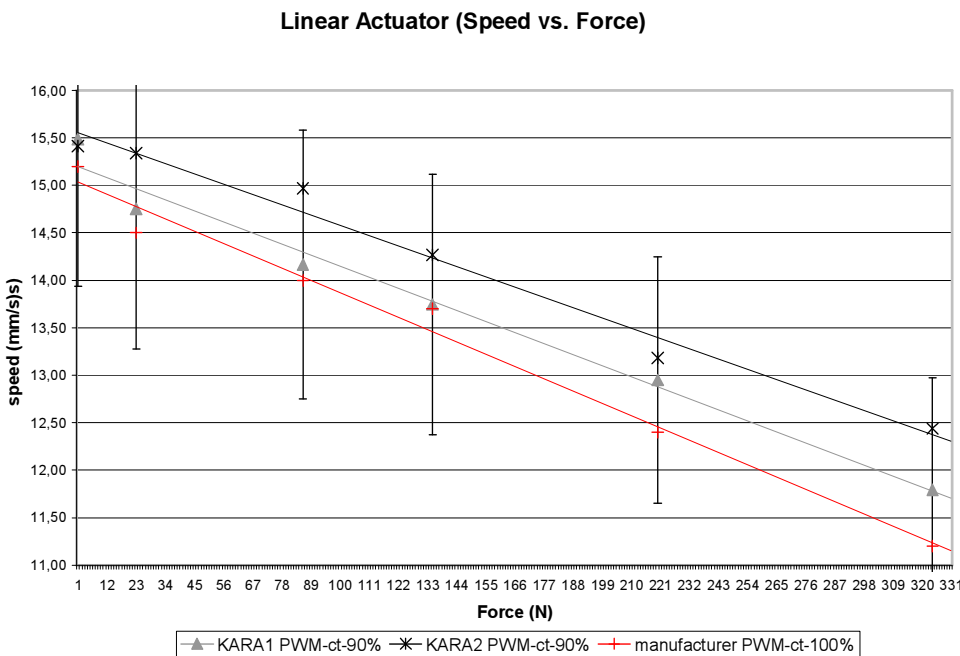


Figure 7. Linear actuators speed versus force.

By combining those two models in force, the power consumption versus actuator speed was defined. Linear actuator fault detector checked power consumption versus speed at run time and compares it to defined value. Calculation is constricted to movement that lasts over two seconds so that start friction doesn't affect measured values too much. This model can follow changes in power consumption and speed. Fault detector has also parts that monitors common failures such as actuator is not moving or responding. These failures could be caused by potentiometer or electric wire failure. Linear actuator component displays failures to the user on the Virtual Terminal (ISOBUS).

Structure of actuator fault detector is shown in figure 8. Simulink model contains StateFlow-component (mean\_calculation) which monitors actuator functions and calculates key ratios, on the left. Errors are reported to the user. Key ratios are then fed into power consumption model which give as model defined speed. The calculated speed is then compared to model speed.

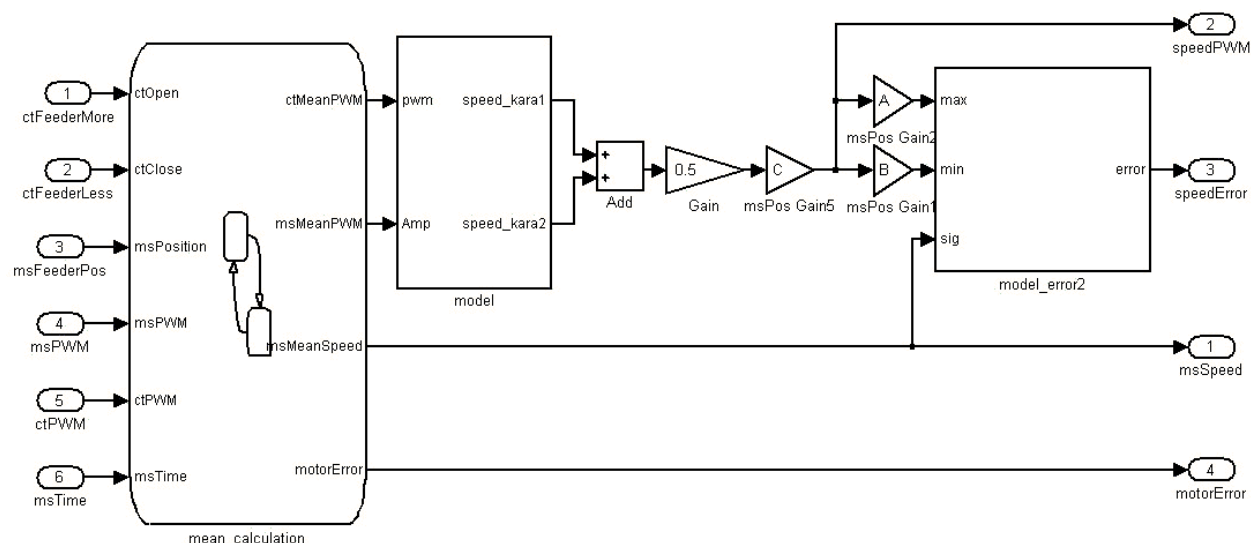


Figure 8. Linear actuators fault detection Simulink component.

### Telemaintenance

Remote diagnosis and telemaintenance was also one of the studied problems in farming implements. All realized fault diagnostic components calculate selected key ratios to be sent to the fictional maintenance service provider. Remote diagnostics were implemented as non-real time because continuous connection was not seen as a real option at the moment. This was also a good way to develop component operation over time. Remote diagnosis was built so that it used basics of ISO 11783 standard, ISO (2004). Diagnosis information is asked from implement by Task Controller which stores fault detection component data and can send it to the service provider through farm management information system (FMIS) or directly over GPRS connection. Both of these ways were tested in the thesis. Task Controller used was also developed in the AGRIX project. Fault diagnostics was not yet defined in the ISO 11783 standard during AGRIX project. Work done shows that remote diagnostics information can be easily mediated through Task Controller. No additional GPRS component was needed because modern mobile phones have built in GPRS and Bluetooth. Bluetooth and GPRS were used to connect Task Controller to service provider.

### CONCLUSION

The commonly known fault diagnostics methods were used in machine control system to detect system failures and the sources for them. The methods were tested with three different implements, one sprayer and two different kinds of combine drills. In sprayer it was concentrated on the pump faults, in one drill for hydraulic actuators and on the other drill for electrical linear actuator. In all cases first the normal operation properties were analyzed and if possible also the failure state properties. The signals were recorded and data based online fault diagnostics system

were developed using data and simulation. Finally the diagnostics system was tested successfully with all the machines in field tests carried out by MTT Agrifood Research Finland.

Technically it is possible to develop fault diagnostic functionality for implement controllers, but it needs time and proper analysis of machine functionality, both in normal and fault states. If the machine behaves differently in different conditions it has to be modeled and the conditional state has to be detected directly or indirectly. A good way to do the analysis is to first plan a set of tests which will produce a rich set of data in normal condition, then cause the faults and do the same. The data should be recorded from all sensors available in machine and also store additional test information. The data should be analyzed using proper tools. And finally the automatic diagnostics system can be developed straight-forwardly based on analysis.

It depends on the machine, the amount of machines produced, and customer needs that how profitable it is to develop fault diagnostics. The generality for fault diagnostics is hard to find if the machines vary from each other. The generality can be found from the components of machine. For example the electrical linear actuator could contain internal fault diagnosis and intelligent protection against external malfunctions. However the proper tools can speed up the development process.

## REFERENCES

1. Auernhammer, H. 2002. The Role of Mechatronics in Crop Product Traceability. *Agricultural Engineering International: the CIGR Journal of Scientific Research and Development*. Invited Overview Paper. Vol. IV. October, 2002.
2. Hammouri H., Kabore P., Othman S., Biston J. 2002. Failure diagnosis and nonlinear observer. Application to a hydraulic process. *Journal of the Franklin Institute* 339. 455-478.
3. ISO 2004. ISO/WD 11783-10. Tractors, machinery for agriculture and forestry – serial control and communication network Part 10: General Standard.
4. Lee J., Kyoo Yoo C., Lee I. 2004. Statistical process monitoring with independent component analysis. *Journal of Process Control* 14. 467-485.
5. Kano M., Hasebe S., Hashimoto I., Ohno H. 2004. Evolution of multivariate statistical process control: application of independent analysis and external analysis. *Computers and Chemical Engineering* 28. 1157-1166.
6. Miettinen M., Liikkuvien työkoneiden vikadiagnostiikka ja etähuolto. Masters thesis (M.Sc. Eng). Helsinki University of Technology. Automation Technology Laboratory. 2005.
7. Oakland J. 2003. *Statistical process control*. Butterworth-Heinemann, 2003. 445 p. ISBN: 0-7506-5766-9.
8. Öhman M., Oksanen T., Miettinen M., Visala A. 2004. Remote Maintenance of Agricultural Machines. *The 1st IFAC Symposium on Telematics Applications in Automation and Robotics*. Helsinki 2004, pp. 149-154.
9. Öhman, M., Visala, A. 2005. Design and Implementation of Machine Control Systems with modern Software development Tools. *The 5th International Conference on Field and Service Robotics*. Port Douglas, Australia, July 29-31 2005. 6 p.
10. Oksanen, T., Öhman, M., Miettinen, M., Visala, A. 2005a. ISOBUS compatible implements in precision farming. *5th European Conference on Precision Agriculture (ECPA)*, Implementation of Precision Agriculture. Uppsala 2005, Sweden.
11. Oksanen, T., Öhman, M., Miettinen, M., Visala, A. 2004. Open configurable control system for precision farming. *Automation Technology for Off-road Equipment Conference*. Kyoto, Japan 2004.
12. Oksanen, T., Öhman, M., Miettinen, M., Visala, A. 2005b. "ISO 11783 - standard and its implementation," Proceeding of *16th IFAC World Conference*, Prague 2005, Czech Republic.

13. Patton R.J., Frank P.M., Clark N.R., (Eds.). 2000. *Issues of Fault Diagnosis for Dynamic Systems*. Springer. 570s. ISBN 3-540-19968-3.
14. RTI 2003. Constellation User's Manual. Real-Time Innovations Inc.
15. Sigrimis. N., Hashimoto. Y., Munack. A. & De Baerdemaeker. J. 1999. Prospects in Agricultural Engineering in the Information Age: Technological Developments for the Producer and the Consumer. *CIGR Journal of Scientific Research and Development*. Invited Overview Paper. Vol. I, December, 1999.
16. Venkatasubramanian V., Rengaswamy R., Yin K., Surya N. Kavuri. 2003. A review of process fault detection and diagnosis Part I: Quantative model-based methods. *Computers and Chemical Engineering*. 27. 2003. 293-311.

# TEXTURE FEATURE EXTRACTION FOR WEED DETECTION IN ORGANIC FARMING

A. Jafari<sup>1</sup>, J. Bontsema<sup>2</sup>, G. van Straten<sup>3</sup> and K. van Asselt<sup>3</sup>

## ABSTRACT

Mechanical weed control and spot spraying with selective herbicides needs a high degree of correct classification rate of weeds against the crop.

Enhancement in segmentation result is expected to be found if different image processing techniques are combined in classification and decision making algorithms.

Texture features provide plenty of information which can be used to detect the weeds based on the differences in texture of plant canopies.

In this study, four texture features from the co-occurrence matrices have been investigated on four weed species and carrot images acquired from the normal condition in the field. Extracted features were energy, inertia, entropy and correlation.

To exclude the effect of surrounding soil texture on plants texture an amendment was exerted on co-occurrence matrix which is described in this paper.

Discriminant analysis was used to classify weeds based on texture features. Overall correct classification rate of carrots and weeds was 91% while 80% of carrots were classified correctly. Increasing image gray level from 8 to 32 didn't improve the correct classification rate.

**KEYWORDS.** Carrot, Feature Extraction, Organic Farming, Texture, Weed.

## INTRODUCTION

Weed detection by means of machine vision has been investigated in different ways. Researchers have tried a wide range of different image processing techniques to segment weeds from the crop while most of them can be categorized in three main groups: shape analysis, color segmentation and texture analysis.

Shape based methods can be successful when leaves don't overlap, like early stages of growing when plants are small (Aitkenhead et al. 2003, Terawaki et al. 2002). Color segmentation methods must be used when significant difference exists between the colors of plants. This condition normally happens when plants are grown up enough. (Jafari et al. 2004). Texture based methods are also useful in the case of leaves occlusion that more often occur in normal field condition.

Texture is an attribute representing the spatial arrangement of the gray levels of the pixels in a region (Haralik et al. 1973). Gray level co-occurrence matrix (GLCOM), which was firstly introduced by Haralik (1973), was used widely for image segmentation.

Shearer and Holmes (1990) extended the idea of using co-occurrence matrices in conjunction to hue, saturation and intensity color attributes. They defined color co-occurrence matrices and 33 color texture features extracted from relative color co-occurrence matrices on 64 gray level basis.

---

<sup>1</sup> Agricultural Machinery Department, Shiraz University, Iran, ajafari@shirazu.ac.ir

<sup>2</sup> Plant Research International, Wageningen, The Netherlands

<sup>3</sup> Systems and Control Group, Wageningen University, The Netherlands

Meyer et al. (1998) proposed the excess green co-occurrence matrix for classification of weeds and four weed species. The method was successful in classifying soil from the plants with a classification rate of 99%. Classification accuracies of individual species ranged from 30 to 77%.

As it has been mentioned in that case and other approaches, an important problem for texture feature classification is that the two sets of pixels i.e. plant and soil pixels should not be mixed in a single co-occurrence matrix.

Plants leaves have special texture that can be used to differentiate between different plants species. However using single leaf texture for different plants classification is not an easy task due to leaves overlapping, curling and surrounding soil texture. Tsheko (2002) used a single leaf texture as a parameter to classify the leaves of different plant species. Correct classification rate of 71% to 93% was attained for 7 types of leaves.

To construct a co-occurrence matrix (COM) for a part of image that represents a special texture, first a block or sub-image must be chosen which relates just to the considered plant and minimum parts of soil present in the block. Background soil texture will affect the texture features extracted from the block selected, so selecting such sub-images is a problem.

Accurate block size selection is very important because it has a direct effect on the extracted features. Therefore different coverage of plant canopy on the soil in the sub-images (plant density), will yield different magnitudes for texture features. To attenuate this problem, researchers tried to choose the block size as close as possible to the size of plant canopy.

But it is almost impossible to reach such conditions in the field where weeds have different ages and size. Weed patches are rarely uniform or predictable with respect to spatial distribution or species composition (Meyer 1998). Therefore in such studies the percentage of soil which is covered by plant (plant density) has been mentioned to show how much of the selected texture features belongs to the target plant.

Some researchers had proposed choosing a block size involving the maximum continuous canopy available in all off the images taken. For example the percentage of plant matter in the sub-image in a texture analysis research reported by Shearer and Holmes (1990) ranged from 53% to 100% for sub-images, while in some cases the block size was considered as an sub-image involving just one leaf of the plant (Kularatna 2005).

In this study a method for extracting texture features which just belongs to plants is described. Also the four texture features energy, inertia, entropy and correlation extracted from excess green co-occurrence matrix have been evaluated for classification of carrot plants and four weed species.

## MATERIAL AND METHODS

To provide the data for texture analysis, 200 images captured from carrot plants and four weed species in carrot fields near Wageningen university i.e. *Stellaria media*, *Lolium perenne L.* *Chenopodium Album*, *Convolvulus arvensis*. For each of the weed species 40 sub-image were cropped to determine the texture features. Excess green co-occurrence matrix has been constructed for each sub-image or block. LabVIEW software ver. 7.1 (National Instruments 2004) was used for coding the co-occurrence matrices.

Co-occurrence matrix introduced by Haralik et al (1973) is normalized as below:

$$p(i, j) = \frac{P(i, j)}{\sum_{i=0}^{N-1} \sum_{j=0}^{N-1} P(i, j)}$$

Here P(i,j) is the relative frequency of pairs of neighboring pixels, one having a gray level value of i and the other j and separated by a distance d. The co-occurrence matrix is a function of both the distance between neighboring pixels (d) and orientation. In this study the distance d=1 pixel was chosen.

Four usual orientations mentioned in literatures are  $\theta = 0, 45, 90$  and  $135$  degree. When the positions of all samples are fixed, some differences might be seen when the considered direction of COM is changed. In such cases the best direction in constructing the COM can be investigated. But in the case of plant recognition, direction can not be expressed as a source of variation because plants can grow in any direction randomly. Therefore even if some differences were seen between different plants in some directions it couldn't be mentioned as a feature. Thus the mean values of the selected features of COM were calculated for four main directions i.e.  $0, 45, 90$  and  $135$ .

The selected features in this study were: energy, inertia, entropy and correlation.

Energy is a measure of image homogeneity. A higher value represents a more homogenous image.

Inertia is a measure for the coarseness of an image. When inertia is high there will be small regions in the texture with the same grey level.

Entropy shows the amount of disorder in the image. So, a homogeneous image has lower entropy than an inhomogeneous image.

Correlation is a measure of linear dependency of intensity values in an image. The correlation feature measures the correlation between the elements of the matrix. When correlation is high the image will be more complex than when correlation is low.

### Resolution

It is obvious that low resolution may fade some details in the image and a resolution higher than the necessary value increases the processing time. Therefore a preliminary study was achieved on the images to choose a reasonable resolution in which small leaves are visible and consist of a sufficient number of pixels in their width. Images were captured at a distance of 1 meter from the soil surface with a resolution of  $1600 \times 1200$  pixel related to an area of  $70 \times 60 \text{ cm}^2$  on the ground.

### Sub-image (block) selection

If a special plant is surrounded by different textures from background or other plants, the selected features will highly dependent to the density of plants in the sub-images. Because the surrounding textures affect the texture features extracted from the COM. In this study a size of  $200 \times 200$  pixel was considered for the selected blocks.

Figure 1 shows two different block sizes of  $200 \times 200$  pixel and  $400 \times 400$  pixel. The first sub-image (block) is chosen so that it has minimum possible surrounding soil to decrease the effect of soil texture on plant texture features. As it can be seen these two blocks have different COM however the target plant is the same in both image. It is due to the fact that a black background which is produced after exerting excess green on image still represents a special texture. This black texture will affect the overall texture extracted from the block.

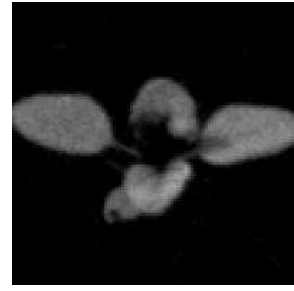
In this study we have described the way to avoid the problem of neighborhood pixels (background soil) on desired plant texture.

Excess green method has demonstrated its ability to differentiate between soil and plants based on their color (Woebbeck 1995, Meyer 1998). In color segmentation we can use this method efficiently to segment plants from the soil by exerting a threshold on excess green images which yields a black image or zero values for the soil. But in texture analysis a black image also has its own texture. Thus every feature extraction from excess green COM is a mixture of features belonging both to plant and the produced black image and it can be said that the block texture is an average of two different textures from which one is the plant canopy and the second one is an almost homogenous black texture.

To solve this problem we should just remove the effects of black background on COM. Black background enters into the COM in two ways. At first, in as much as black background is the frequency of gray level transitions from 0 to 0, it will increase the first element of the COM i.e.  $(0,0)$ . And secondly it will increase the denominators of all elements of COM which is the total summation of elements.



**a**



**b**

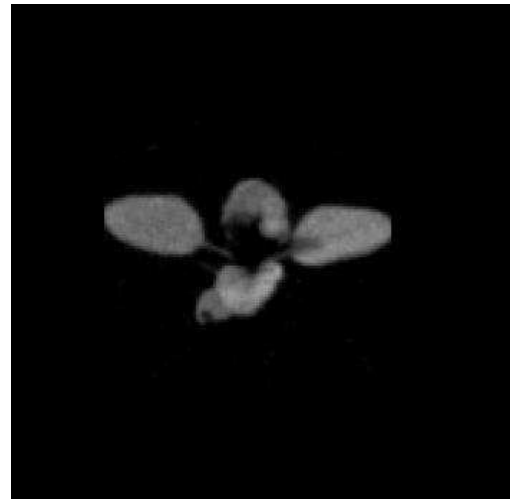
0.7610	0.0065	0.0025	0.0013	0.0004	0.0001	0.0000	0.0000
0.0065	0.0087	0.0023	0.0018	0.0013	0.0006	0.0000	0.0000
0.0025	0.0023	0.0059	0.0016	0.0013	0.0011	0.0001	0.0001
0.0013	0.0018	0.0016	0.0065	0.0020	0.0017	0.0007	0.0001
0.0004	0.0013	0.0013	0.0020	0.0066	0.0029	0.0015	0.0003
0.0001	0.0006	0.0011	0.0017	0.0029	0.0161	0.0063	0.0014
0.0000	0.0000	0.0001	0.0007	0.0015	0.0063	0.0392	0.0092
0.0000	0.0000	0.0001	0.0001	0.0003	0.0014	0.0092	0.0268

→ { Energy = 0.583  
 Inertia= 0.932  
 Entropy= -1.358  
 Correlation= -0.640

**c**



**d**



**e**

0.9220	0.0021	0.0008	0.0004	0.0002	0.0001	0.0000	0.0000
0.0021	0.0028	0.0008	0.0006	0.0004	0.0002	0.0000	0.0000
0.0008	0.0008	0.0019	0.0005	0.0004	0.0004	0.0000	0.0000
0.0004	0.0006	0.0005	0.0021	0.0006	0.0006	0.0002	0.0000
0.0002	0.0004	0.0004	0.0006	0.0022	0.0009	0.0005	0.0001
0.0001	0.0002	0.0004	0.0006	0.0009	0.0052	0.0021	0.0004
0.0000	0.0000	0.0000	0.0002	0.0005	0.0021	0.0127	0.0030
0.0000	0.0000	0.0000	0.0000	0.0001	0.0004	0.0030	0.0087

→ { Energy = 0.850  
 Inertia= 0.978  
 Entropy= -0.539  
 Correlation= -0.702

**f**

**Figure 1. Different block sizes and their corresponding co-occurrence matrix for an image of *Chenopodium Album*; a) block size of 200×200 pixel, b) excess green image 200×200 pixel, c) COM and extracted features of block "b", d) block size of 400×400 pixel, d) excess green image 400×400 pixel f) COM and extracted features of block "e".**

Now it is obvious that for having a COM independent of surrounding black texture, we should just omit these mentioned effects from the COM. This task can be coded so that a new COM can be determined. But it is much easier to add an amendment to traditional COM to make a new COM for this case as described in figure 2. The new COM will be:

$$\text{COM} = [p(i,j)]; \quad p(i,j) = \begin{cases} \frac{P(i,j)}{\sum_{i=0}^{N-1} \sum_{j=0}^{N-1} P(i,j) - P(0,0)} & \\ 0 & i=j=0 \end{cases}$$

This new COM is completely independent with respect to block size and it doesn't matter how much background soil exists in the image. This method determines the COM of the plant without soil. The selected features Energy, Inertia, Entropy and Correlation were extracted from the new COM.

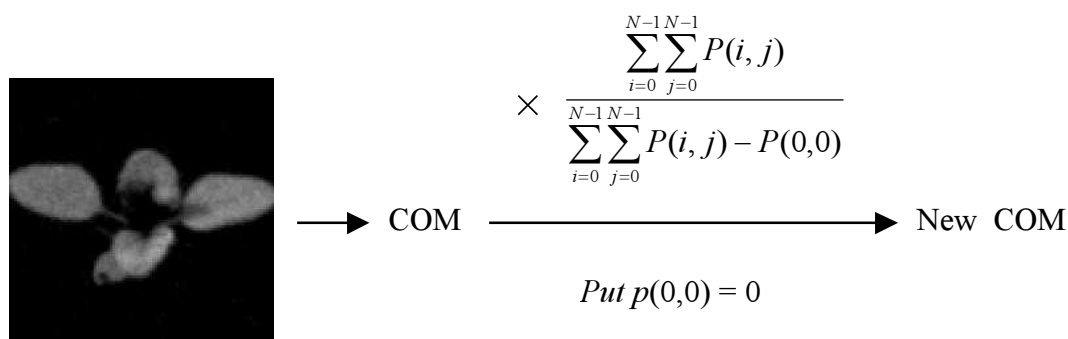


**Figure 2. New co-occurrence matrix construction by exerting an amendment on common co-occurrence matrix to omit the soil effect on plant texture.**

### Gray level

Two gray levels 8 and 32 were considered in determining COM to investigate the effect of image quantization on correct classification rate. Carrot and four weed species were classified using discriminant analysis.

## RESULTS

The effect of the proposed amendment for omitting the surrounding soil texture on the plant features has been shown in figure 3. As it can be seen the COM for both sub-images are the same. Using this new COM one can select different block sizes without any effect from the amount of soil pixels that may appear in the image. Thus the plant density or percentage of plant coverage doesn't affect the COM.

However it doesn't mean different block sizes of a plant have equal values for the features. It must be noted that the block size should be representative of the target texture. For instance a block consisting of plant canopy is different than that consisting of just a part of a leaf.

Table 1 and table 2 show that carrot plants and three weeds *Convolvulus arvensis*, *Stellaria media* and *Chenopodium Album* are similar in texture and couldn't be correctly classified. It might be due to small size of plants which made the texture features to be close.

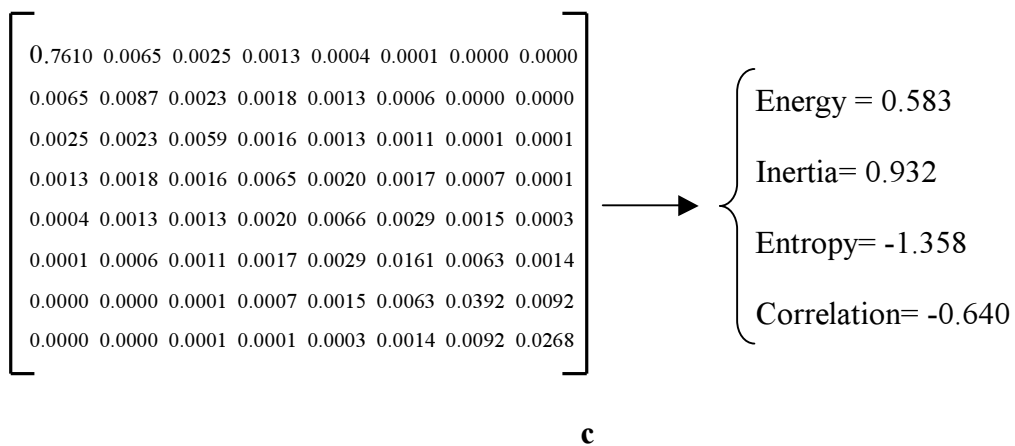
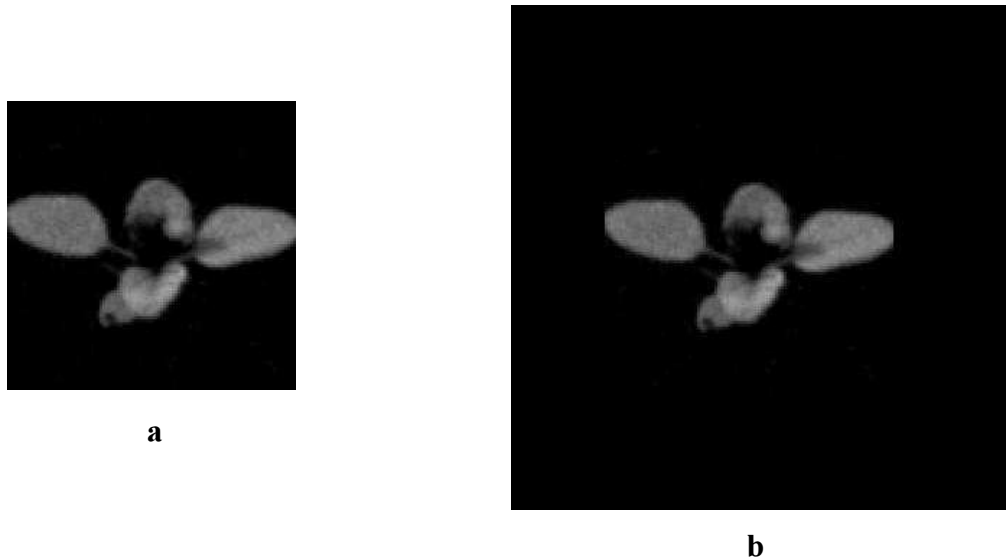


**Figure 3.** New COM proposed to eliminate the effect of surrounding soil texture a) block size of 200×200 pixel, b) block size of 400×400 pixel, c) proposed COM and extracted features which is the same for both sub-images.

**Table 1.** Classification results based on 8 gray levels.

Plants		Predicted Group Membership					Total
		Carrot	Lolium	Convolvulus	Stellaria	Chenopodium	
%	Carrot	80	0	10	5	5	100
	Lolium	0	100	0	0	0	100
	Convolvulus	0	0	100	0	0	100
	Stellaria	10	0	0	90	0	100
	Chenopodium	0	0	15	0	85	100
91% of original grouped cases correctly classified.							

**Table 2.** Classification results based on 32 gray levels.

Plants		Predicted Group Membership					Total
		Carrot	Lolium	Convolvulus	Stellaria	Chenopodium	
%	Carrot	75	0	5	10	10	100
	Lolium	0	90	0	10	0	100
	Convolvulus	0	0	80	0	20	100
	Stellaria	15	0	0	85	0	100
	Chenopodium	0	0	15	0	85	100
83% of original grouped cases correctly classified.							

## CONCLUSION

The proposed method for constructing COM completely solved the problem of block selection. In this method extracted texture features just belong to the plant without the effect of their surrounding soil texture.

Texture methods are useful when plant canopy is big enough to have many leaves to represent their special texture. In cases like as in this study, that plants have different sizes and canopies are small, variances of texture features will be large and the features can not be referred to the special plant texture.

Increasing the gray level yielded a worse result. Knowing that taking lower gray levels fades the details of the leaves, it can be deduced that the differences between plant textures were mostly related to the overall texture of the canopy not to the details of leaf surfaces.

Further work can be done on different resolutions which are more likely to appear due to fluctuations of the image acquisition system during the movement on the rough surface of the field. So the effect of different resolutions on classification rate must be investigated.

## REFERENCES

1. Aitkenhead, M. J., I. A. Dalgetty, C. E. Mullins, A. J. S. McDonald and N. J. C. Strachan. 2003. Weed and crop discrimination using image analysis and artificial intelligence methods. *Computers and Electronics in Agriculture* 39: 157-171.
2. Burks, T. F., S. A. Shearer, J. R. Heath and K. D. Donohue. 2005. Evaluation of Neural-network Classifiers for Weed Species Discrimination. *Biosystems Engineering* 91(3): 293–304.
3. Haralick, R. M., K. Shanmugam and I. Dinstein. 1973. Textural Features for Image Classification. *IEEE Transactions on Systems, Man, and Cybernetics*, SMC-3 610–621.
4. Jafari, A., S. S. Mohtasebi, H. Eghbali and M. Omid. 2004. Color Feature Extraction by Means of Discriminant Analysis for Weed Segmentation. ASAE Paper No. 043059. St. Joseph, Mich. ASAE.
5. Kularatna, D. 2005. Weed Identification System. Available at: [www.ele.auckland.ac.nz/archives/reports2005/pdfs/image%20Processing/proj\\_144\\_dkul002.pdf](http://www.ele.auckland.ac.nz/archives/reports2005/pdfs/image%20Processing/proj_144_dkul002.pdf) . Accessed 10 March 2006.
6. LabVIEW. 2004. *National Instruments*. Ver 7.1.
7. Meyer, G. E., T. Mehta, M. F. Kocher, D. A. Mortensen and A. Samal. 1998. Textural Imaging and Discriminant Analysis for Distinguishing Weeds for Spot Spraying. *Trans. ASAE* 43(4): 540-547 41(4): 1189-1197.
8. Terawaki, M., T. Kataoka, H. Okamoto and S. Hata. 2002. Distinction between sugar beet and weeds for development of automatic thinner and weeding machine of sugar beet. Proceeding of the Automation Technology for Off-Road Equipment Conference (Chicago, Illinois, USA).
9. Tshenko, R. 2002. Discrimination of Plant Species Using Co Occurrence Matrix of Leaves. *Agricultural Engineering International: the CIGR Journal of Scientific Research and Development*. Manuscript IT 01 004. Vol. IV.
10. Woebbecke, D. M., G. E. Meyer, K. Von Bargen, and D. A. Mortensen. 1995. Color indices for weed identification under various soil, residue, and lighting conditions. *Trans. ASAE* 38(1): 259-269.



# USING ARTIFICIAL NEURAL NETWORKS IN COLOR IMAGE SEGMENTATION FOR WEED DETECTION

L. Jafari<sup>1</sup>, S. S. Mohtasebi<sup>2</sup>, H. Eghbali<sup>3</sup> and M. Omid<sup>2</sup>

## ABSTRACT

Artificial neural networks are widely used in conjunction with image processing methods to imitate human perceive in object recognition. By now several approaches have been tried in verification the ability of neural networks in plants recognition based on the extracted features.

In this study multi layer perceptron (MLP) and radial basis function (RBF) neural networks have been examined for weed-crop recognition based on color information. RGB data related to weeds and sugar beet plants were used as input data to the neural networks. It is more probable that in every feature extraction some data loss occur which might have been useful for segmentation. The objective of this research was to investigate the feasibility of classifying weeds and main crop pixels just based on their RGB values, without any feature extraction. So it was tried not to discard any information of RGB images and make the neural network decide which data can be related to which class.

Several network topologies were considered differing by the number of neurons in the first and second hidden layers. One and two hidden layers were used in multi-layer perceptron (MLP) neural networks with fixed learning rate and Levenberg-Marquardt training algorithm. Radial basis function (RBF) networks with 500 neurons in the hidden layer were also used for this classification.

In case of MLP neural networks, the best result was gained from 3-10-10-2 network with a mean CCR of 89%. For radial basis neural network, mean CCR equal to 86% was gained.

**KEYWORDS.** Artificial Neural Networks, Classification, Image processing, Sugar beet, Weed Detection.

## INTRODUCTION

Weed detection is the main pace of designing a weed killing machine capable of recognizing, uprooting or spraying the weeds autonomously. To attain this aim, researches have tried the use of image processing techniques for extracting features which are different between the weeds and main crop.

Astrand and Baerveldt (2003) used some combinations of color and shape features to segment weeds on sugar beet rows. They evaluated shape features for single plants and showed that plant recognition based on color vision is feasible with three features (green mean, compactness and elongation) and a 5-nearest neighbors classifier. Color features could solely have up to 92% success rate in classification. This rate increased to 96% by adding two shape features.

Shape features have been mostly fed to neural networks to distinguish the shape of small canopies or leaves (Cho et al. 2002). Yang *et al.* (2002) used artificial neural networks (ANN) to classify corn and weeds. They used gray level values of each pixel of the cropped images as the inputs for the ANN. Since all pixels including soil and plant pixels were entered to the ANN, it could be said that this method have also used shape features in classification of weeds and crop.

---

<sup>1</sup> Shiraz University, College of Agriculture, Farm Machinery Department, Iran, Jafari@persianmail.com

<sup>2</sup> Tehran University, College of Biosystem engineering, Iran

<sup>3</sup> Computer Engineering Dept., Shiraz University, Iran

Color and texture features are useful especially when plants are grown up enough. Burks et al. (2005) used HSI color spaces and made different combinations of hue, saturation and intensity components as color features for ANN inputs.

Comparison of statistical and neural networks classifiers have shown in some cases statistical classifiers yielded a higher degree of correct classification (Karimi et al. 2005; Marchant and Onyango 2003) while in some cases neural networks had better classification accuracy (Burks et al. 2005) or almost the same result as statistical methods (Pydipati et al. 2005).

In this study no feature extraction has been carried out on images, and RGB values of the pixels related just to weeds and crop were the only inputs of the ANN. Thus color features have been implicitly used in the ANN. Our assumption was that each feature extraction may discard some information of the image which could be correlated to the target classes. So we employ the ANN to make the relation between inputs and outputs. The objectives of this study were:

- To investigate the feasibility of weed-crop classification using ANN without any feature extraction.
- To compare multi layer perceptron (MLP) and radial basis (RB) neural networks for classification weeds and crops.

## MATERIAL AND METHODS

In as much as RGB values of the pixels were considered as inputs of the ANN, sufficient data could be fed to the ANN which yields more reliable result. 300 digital images from several agricultural field of Fars province in Iran were taken under various lighting conditions. Resolution of the images was 1600×1200 pixels concerning to a field of view of about 70×60 cm on the ground. Images were taken at a distance of about 1.2 m from the soil surface having 24-bit data. Neural Networks Toolbox version 4.0.1 for use with MATLAB version 6.5 (Mathworks 2002) was used for algorithm development.

Common weeds in the images included Wild Spinach (*Chenopodium album* L.), Redroot Pigweed (*Amaranthus retroflexus* L.), Chinese Lantern plant (*Physalis alkekengi* L.), Little Hogweed (*Portulaca oleracea* L.), Field Bindweed (*Convolvulus arvensis* L.), Green Foxtail (*Setaria vertidis* L. Beauv) and Barnyardgrass (*Echinochloa crus-gali* (L.) Beauv).

For each plant species 20 pieces (7×7 pixel) of corresponding canopies were cropped. RGB data of the selected pixels were used as inputs for ANNs.

### Multi Layer Perceptron (MLP) networks

Normalization of data was done using the code *prestd* provided by MATLAB based on the following equation:

$$X_i = \frac{x_i - \mu}{\sigma} \quad i = 1, \dots, n$$

Where  $X_i$  represents the  $i$ th data and  $\mu$  and  $\sigma$  are mean and standard deviation of data respectively.

Levenberg-Marquardt back propagation algorithm was used as training function and learning rate of 0.5 was considered in ANNs architecture. In MLP networks, logarithm-sigmoid function was chosen as transfer function (Fig. 1). To avoid ANN overtraining, "early stopping" method was used. Collected data were divided to three sets randomly i.e. training set, validation set and test set. Whenever the mean square error of evaluating set began to rise, the training process of the network would be stopped.

Following states of classification were investigated:

- Classification of sugar beet against all the weeds (Two classes)
- Classification of all weed species and sugar beet (Eight classes)

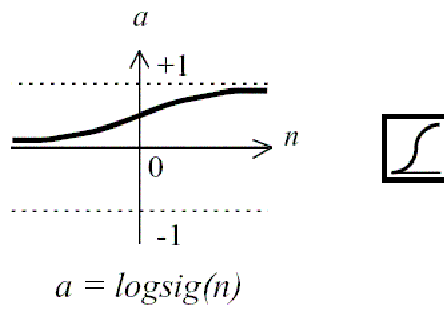


**Figure 1. Logarithm-sigmoid function.**

ANNs had a topology differing by the number of hidden layers and the number of neurons in each layer (Fig. 2, Fig. 3).

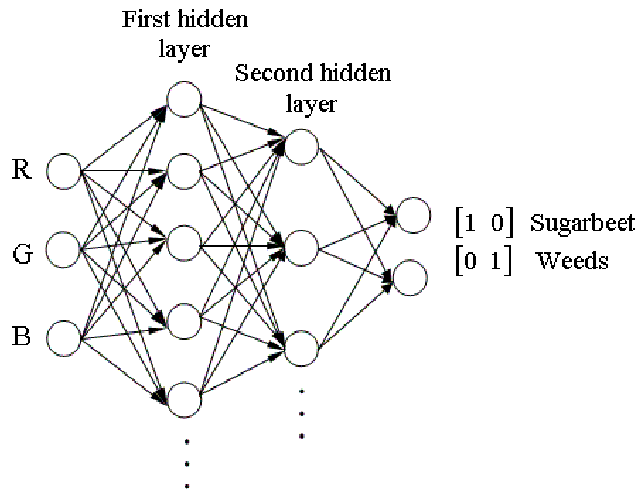


**Figure 2. ANN used to classify plants into two classes.**

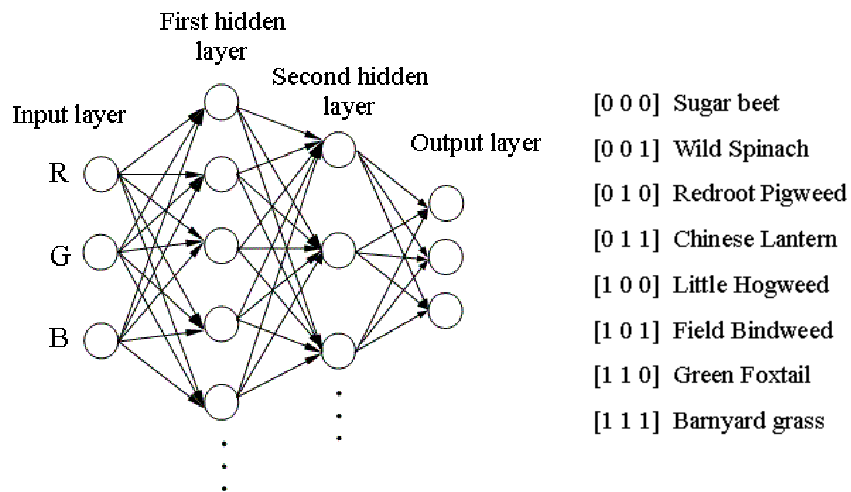


**Figure 3. Distributed representation of ANN used to classify plants into eight classes.**

Using logarithm sigmoid function causes the output not to be exact 1 or 0. Thus the bigger component was set to 1 and the smaller one was set to 0. This correction was coded in MATLAB.

Radial Basis Function (RBF) Networks

Radial-Basis Function Networks used for pattern classification are based on Cover's theorem on the separability of patterns (Manchester University, 2006). This theorem states that nonlinearly

separable patterns can be separated linearly if the pattern is cast nonlinearly into a higher dimensional space. Therefore we are looking for a network that converts the input to a higher dimension after which it can be classified using only one layer of neurons with linear activation functions.

Radial basis networks may require more neurons than standard feed-forward backpropagation networks, but often they can be designed in a fraction of the time it takes to train standard feed-forward networks. They work best when many training vectors are available (MathWorks, 2002).

The transfer function for a radial basis neuron is:

$$radbas(n) = e^{-n^2}$$

Which has a bell ring shape as shown in figure4.

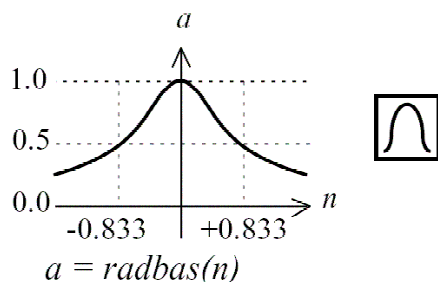


**Figure 4. Radial basis function.**

Since the input vector had a dimension of 3 by 500, the hidden layer of the RBF networks produced up to 500 neurons to simulate the relation between inputs and outputs. Control parameters in this section are SPREAD and GOAL. Different SPREAD constants were examined and a value 0.05 which gave the best result was chosen and Goal was set to  $10^{-4}$ .

## RESULTS

Training process of all MLP networks were stopped by early stopping. It means that validation data stopped the networks training as soon as the validation MSE began to rise. Table 1 represents the mean square error of networks examined.

**Table 1. Mean square error of different network topologies for classification into two classes (weeds against sugar beet).**

Network Topology	MSE	Network Topology	MSE
3-2-2	0.136	3-20-2	0.119
3-3-2	0.135	3-2-2-2	0.114
3-4-2	0.125	3-3-3-3	0.124
3-6-2	0.124	3-4-4-2	0.124
3-8-2	0.123	3-6-6-2	0.120
3-10-2	0.123	3-8-8-2	0.118
3-15-2	0.120	3-10-10-2	0.110

As it can be seen increasing the number of nodes and layers of the networks have had a trivial improvement in the results. The last network which had a topology of 3-10-10-2 was used for simulation the test data.

Correct classification rate was determined by writing a code to count the points correctly classified in their corresponding classes. Similar code was written to determine misclassification rate.

As a result,  $MCR_{sug}$  which was the percent of pixels of sugar beet misclassified as weeds was computed as high as 8% and the percent of pixels of weeds correctly classified as weeds ( $CCR_{weed}$ ) was computed as high as 86% (Tab. 2).

In the second state that eight classes of plants (sugar beet and seven weed species) were considered to be classified, ANNs didn't yielded a better result (Tab. 3 and Tab. 4).

Table 5 and table 6 show the results of classification using RBF neural networks. Comparing the results of MLP networks and RBF networks shows that MLP networks could give a better classification rate than that of RBF networks.

Similar to MLP networks, changing the classification classes from two to eight have decreased the classification accuracies.

**Table 2. Classification result of weeds and sugar beet into two classes using MLPNN.**

	Plants species	Sugar beet	Weeds
%	Sugar beet	92	8
	Weeds	14	86

**Table 3. Mean square error of different network topologies for classification into eight classes (weeds and sugar beet).**

Network Topology	MSE	Network Topology	MSE
3-2-2	0.217	3-20-2	0.199
3-3-2	0.215	3-2-2-2	0.400
3-4-2	0.214	3-3-3-3	0.321
3-6-2	0.212	3-4-4-2	0.205
3-8-2	0.204	3-6-6-2	0.199
3-10-2	0.199	3-8-8-2	0.196
3-15-2	0.198	3-10-10-2	0.196

**Table 4. Classification result of weeds and sugar beet into eight classes using MLPNN.**

Plants species	Sugar beet	Wild Spinach	Redroot Pigweed	Chinese Lantern	Little Hogweed	Field Bindweed	Green Foxtail	Barnyard-grass
CCR%	77	72	53	46	67	72	74	68

**Table 5. Classification result of weeds and sugar beet into two classes using RBFNN.**

	Plants species	Sugar beet	Weeds
%	Sugar beet	88	12
	Weeds	16	84

**Table 6. Correct classification rates for classification of weeds and sugar beet into eight classes using RBFNN.**

Plants species	Sugar beet	Wild Spinach	Redroot Pigweed	Chinese Lantern	Little Hogweed	Field Bindweed	Green Foxtail	Barnyardgrass
CCR%	73	69	51	42	63	68	70	66

## CONCLUSION

MLP and RBF neural networks were used to classify weeds and crop just based on their RGB values of the pixels. Correct classification rates were not high enough to be used solely. But in as much as these results have been just based on color information, it may be useful to combine this method with shape and texture methods to reach higher accuracies.

Classifying the plants in two classes "weeds" and "sugar beet" gave a better result comparing to classifying them to eight classes of different plant species.

MLP and RBF neural networks were compared based on classification accuracies for weed and sugar beet plants. MLP networks achieved a better classification comparing to RBF networks. In addition, MLP networks don't have a limitation for the size of input vectors but it is a problem in case of RBF networks because input vector defines the size of hidden layer of the network.

## REFERENCES

1. Astrand, B., and A. Baerveldt. 2003. A mobile robot for mechanical weed control. *International Sugar Journal* VOL. 105 NO.1250.
2. Burks, T. F., S. A. Shearer, J. R. Heath and K. D. Donohue. 2005. Evaluation of neural network classifiers for weed species discrimination. *Biosystems Engineering* 91(3), 293–304.
3. Cho, S. I., D. S. Lee and J. Y. Jeong. 2002. Weed-plant discrimination by machine vision and artificial neural network. *Biosystems engineering* 83(3), 275–280.
4. Karimi, K., S. O. Prasher, H. McNairn, R. B. Bonnell, P. Dutilleul and P. K. Goel. 2005. Classification accuracy of discriminant analysis, artificial neural networks, and decision trees for weed and nitrogen stress detection in corn. *Trans. ASAE* 48(3): 1261–1268.
5. Manchester University. 2006. Radial Basis Function Networks. Available at: <http://www.eng.man.ac.uk/mech/merg/research/datafusion.org.uk/techniques/rbf.html> Accessed 3 April 2006.
6. Marchant, J. A. and C. M. Onyango. 2003. Comparison of a Bayesian classifier with a multilayer feed-forward neural network using the example of plant/weed/soil discrimination. *Computers and Electronics in Agriculture* 39: 3-22.
7. Mathworks. 2002. MATLAB Neural Network Toolbox. User's Guide version 3.00. The Mathworks, Inc. Natick, MA.
8. Pydipati, R., T. F. Burks and W. S. Lee. 2005. Statistical and neural network classifiers for citrus disease detection using machine vision. *Trans. ASAE* 48(5): 2007–2014.
9. Yang, C. C., S. O. Prasher and J. A. Landry. 2002. Weed recognition in corn fields using back-propagation neural network models. *Canadian Biosystems Engineering* 44:15-22.

# MULTISENSOR DATA FUSION IMPLEMENTATION FOR A SENSOR BASED FERTILIZER APPLICATION SYSTEM

R. Ostermeier<sup>1</sup>, H. I. Rogge<sup>2</sup> and H. Auernhammer<sup>1</sup>

## ABSTRACT

"Mapping systems" ("mapping approach"), real-time sensor-actuator systems ("sensor approach") or the combination of both ("Real-time approach with map overlay") determine the process control in mobile application systems for spatially variable fertilization. Within the integrated research project "Information Systems Precision Farming Duernast" (IKB Duernast) the implementation of the "Real-time approach with map overlay" was done for intensive nitrogen fertilization. The bottom line of this sophisticated approach is a comprehensive situation assessment, a typical multisensor data fusion task. Based on a functional and procedural modeling of the multisensor data fusion and decision making process, it could be pointed out that an expert system is an adequate fusion paradigm and algorithm. Therefore, a software simulation with an expert system as core element was implemented to fuse on-line sensor technology measurements (REIP), maps (yield, EM38, environmental constraints, draft force) and user inputs in order to derive an application set point in real-time. The development of an expert system can be viewed as a structured transformation in five levels from the "specification level", the "task level", the "problem solving level" and the "knowledge base level" to the "tool level". In the "tool level" the hybrid expert system shell JESS (Java Expert System Shell) was selected for implementation due to the results of preceding levels. Knowledge acquisition was done within another IKB-subproject by the means of data mining. Typical and maximal times of 10 ms and 60 ms for one fusion cycle were measured running this application on a 32-bit processor hardware (Intel Pentium III Mobile, 1 GHz).

**KEYWORDS.** Data Fusion, Expert System, Multisensor, Process Control, Real-time Approach with Map Overlay, Sensor, Sensor Fusion, Site-specific Fertilization.

## INTRODUCTION

Three different system approaches determine the process control in mobile application systems for spatially variable fertilization. These are "mapping systems" ("mapping approach"), real-time sensor-actuator systems ("sensor approach") or the combination of both ("Real-time approach with map overlay"). Mapping approach and sensor approach have disadvantages depending on the system, however the "Real-time approach with map overlay" may overcome the disadvantages of both (Auernhammer, 2001). In principle, the basic idea of this approach is to lead a process or system, here plants and their surroundings, to an ecological and economic optimum. This requires information about the current state of the process and its inputs, i.e. "precision farming maps" and on-line sensor technology process data. The possibility for intervention on the process is fertilization. Thereby, the application set point is derived by expert knowledge and the input information at hand. Documentation completes the procedure. In summary, this means the current situation for each local site must be investigated and assessed. Thereupon, action (application set point) has to be derived. From the information technology point of view, this system approach is a topic of multisensor data fusion und requires appropriate methods and terminology. Basically, multisensor data fusion systems can be analyzed and modeled by a functional model and a process

---

<sup>1</sup> Technische Universitaet Muenchen, Crop Production Engineering, Freising, Germany, [ralph.ostermeier@wzw.tum.de](mailto:ralph.ostermeier@wzw.tum.de)

<sup>2</sup> Boehringer Ingelheim, Ingelheim, Germany

model (Steinberg and Bowman, 2001). A functional model should describe at the highest abstraction level what analysis functions or processes need to be performed. While a process model describes at a high level of abstraction how this analysis is accomplished. Based on this abstract view of demands, requirements and problem-solving paradigm, a system architecture (high level abstraction of hardware - software implementation) can be designed. Established and appropriate systems engineering methods have to be applied for further transformation of this system architecture into a concrete technical implementation by hardware and software. Ostermeier and Auernhammer (2004) defined a complete theoretical framework with a functional model, process model and system architecture for the “Real-time approach with map overlay” and applied it to a real-time process control for a sensor based fertilizer application system within the integrated research project “Information Systems Precision Farming Duernast” (IKB Duernast) (Auernhammer et al., 1999). From a functional point of view the “Real-time approach with map overlay” can be completely specified according to the revised JDL data fusion model. This model was specified by the Joint Directors of Laboratories (JDL) and was revised by Steinberg and Bowman (2001) (Fig. 1) in 1998.

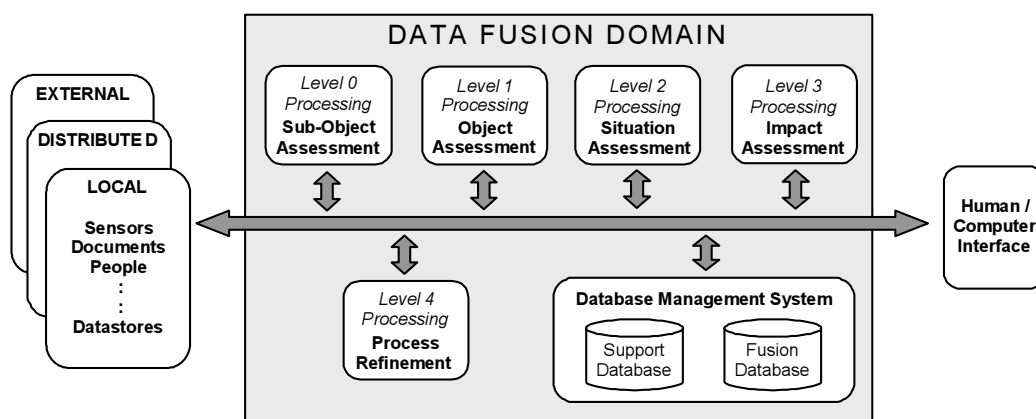


Figure 1. Revised JDL data fusion model (Steinberg and Bowman, 2001).

Due to noncommensurate information sources, there is no fusion at raw data level possible, but fusion at feature/state or decision level is demanded. Although the “Real-time approach with map overlay” comprises all JDL functional levels, main focus is put on Level 2 Processing - Situation Assessment within the IKB Duernast project, since the bottom line is a comprehensive situation assessment, i.e. an assessment of current on-line sensor technology measurements with context-sensitive interpretation. Ostermeier and Auernhammer (2004) derived by the means of Antony’s (1995) process model an appropriate data fusion algorithm for the Level 2 Processing. A conventional expert system with its forward-inference production rule paradigm was determined as a suitable problem solving paradigm. Ostermeier et al. (2003) stated the proposal of an in-field controller in order to integrate this approach into ISO 11783 compliant data communication systems.

## OBJECTIVES

Within the integrated research project IKB Duernast, the “Real-time approach with map overlay” for intensive nitrogen fertilization should be implemented in form of a personal computer (PC) based simulation including an intuitive man machine interface. The PC based simulation should be confined on the second nitrogen application. Therefore data of on-line sensor technology (vegetation index: REIP) and data of “precision farming maps” (historic yield of the year 1998, EM38 measurement, soil draft force and applied fertilizer rate of the first application in the same year), originating from the IKB-Duernast Farm Management Information System (FMIS), and environmental protection restrictions should be fused in real-time. Main focus should be put on the implementation of the basic multisensor data fusion algorithm for JDL level 2 processing “Situation assessment” with resulting derivation of control action. As already stated in the introduction a suitable problem solving paradigm is a conventional expert system with its forward-

inference production rule paradigm. In an effort to implement technical systems efficiently and goal-oriented, an integrated specification and design process is an essential element and plays an important role in successful translation of requirements into physical implementation. This should be especially pointed out for the implementation of the expert system within the simulation development.

## METHODS AND MATERIAL

### Architecture of an Expert System

The architecture of an expert system is well described in several artificial intelligence textbooks, e.g. according to Sriram (1997) an expert system comprises the main elements inference mechanism, knowledge base, context, knowledge acquisition facility, explanation facility and user interface.

### Development Process of an Expert System

According to Luger (2004) it is necessary for the development of an expert system as in the case of many other AI (artificial intelligence) programs to differ from the conventional process and to create a prototype quite early and to work out gradually and to optimize the code. An explorative development cycle is therefore the suitable engineering method. An explorative development process, however, does not absolve the developer from a structured procedure.

The major steps of an evolutionary development process are depicted in figure 2. The identification phase describes what are problem domain characteristics, the scope, who will participate and what the resources are. In the conceptualization step needed information and techniques to solve the problems and tasks are identified. In the formalization phase the concepts should be put in a formalized representation. This involves the selection of a knowledge representing scheme and the appropriate tools for building the expert system.

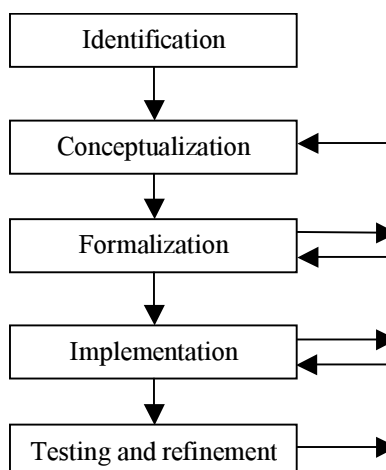


**Figure 2. Explorative development process of an expert system (according to Sriram).**

The implementation step comprises encoding the knowledge obtained in the previous step into software and hardware - a prototype. In the testing and refinement phase the capacity of the prototype is inspected. The problem solving capacity should be analyzed, as well as errors and the weaknesses, so that they could be eliminated.

In order to work straightforward, one part of the identification phase and the whole conceptualization and formalization phases can be supported by an appropriate method described by Sriram (1997). He defines the development of a knowledge based system as a structured transformation from a “specification level” to a “tool level”. So the one part of the identification phase and the whole conceptualization phase can be achieved by the first three steps “specification level”, “task level” and “problem solving level”. The formalization phase can be accomplished through the transformation from the “knowledge base level” to the “tool level”. In the following

section there is a brief description of the five levels, which are necessary to determine the required tool, conducted.

*Specification level:* The problem (derivation of the required nitrogen application rate), its constraints and the solution are described in this level.

*Task level:* The “task level” describes problems, which engineers solve, such as diagnosis planning, simulation, interpretation, control, monitoring, etc. The type of expert system to be chosen will have to cover the aspects of the problems.

*Problem solving level:* In this level a selection of the knowledge evaluation and control mechanisms is conducted. These mechanisms are used to enable and accelerate the problem solving.

*Knowledge base level:* In this level a selection of the possible knowledge representation is conducted.

*Tool level:* In this level the programming paradigm(s) for implementation has to be chosen based on the previous analyses.

### Knowledge Acquisition

Knowledge acquisition is one of the most significant parts for the implementation of an expert system. It is the process of eliciting domain knowledge from experts or textbooks for encoding in an appropriate tool. The spectrum of knowledge acquisition modes ranges from manual techniques to fully automated techniques. For this project, the agricultural engineering knowledge was acquired from textbooks and discussions with colleagues of the TU Muenchen subject group Crop Production Engineering and encoded manually. To elicit the crop production knowledge the following procedure was carried out. The knowledge acquisition was conducted in close cooperation with the IKB subproject 12 “Deriving of Decision Support Rules for Site Specific N-Fertilization” (Weigert and Wagner, 2003). This subproject developed the crop production knowledge by the application of data mining techniques and provided all the necessary field trial test data (on-line sensor technology measurements and overlay maps) for the simulation. Therefore research was conducted at fields located in Freising, Germany.

## RESULTS

According to the presented method, the implementation of the simulation is explained in the following, starting with conceptualization and formalization since identification is mainly important for project management and here technical aspects should be in the focus.

### Conceptualization and Formalization

#### *Specification Level*

The problem, its constraints and the basic solution approach by multisensor data fusion have been already described in the chapters introduction and objectives. So only one main real-time requirement has to be determined. The whole process of gathering, transferring and processing data, plus the reaction time of the actuator (fertilizer spreader), has to be performed within the available time. Therefore the expert system's data processing, i.e. one data fusion and decision cycle, is limited by the time. The total time available for sensing, data processing and adjusting the fertilizer spreader actuator is calculated using the following equation:

$$t_T = \frac{s}{v} \quad (1)$$

where:

- $t_T$  = total available time
- $s$  = total distance from starting point of sensor view to point of fertilizer application
- $v$  = velocity of the tractor-implement combination

Assuming a tractor-implement combination driving with a velocity of 4.0 m/s, using equation 1 and a total distance of 6.5 m the total time available is as shown bellow:

$$t_T = \frac{s}{v} = \frac{6.5 \text{ m}}{4.0 \text{ m/s}} = 1.6 \text{ s}$$

The partial time  $t_p$  required for data communication and signal processing in the sensors ( $\sim 30$  ms) as well as the operating time of the fertilizer spreader ( $\sim 650$  ms; measurements at TU Muenchen subject group Crop Production Engineering in order to determine minimal response times of a fertilizer spreader actuator with modified control) can be determined to 680 ms. To determine the time available to the expert system  $t_{XPS}$ , these 680 ms have to be subtracted from the result of equation 1, as shown below:

$$t_{XPS} = 1.6 \text{ s} - 0.68 \text{ s} = 0.92 \text{ s}$$

### *Task Level*

Sriram (1997) characterizes the “task level” as follows. “The range of expert system applications spans from derivation to formation problems. In derivation problems, the problem conditions are specified as parts of a solution description, i.e. the possible outcomes exist in the knowledge base. So the solution to these problems involves the identification of the solution path. In formation problems, problem conditions are given in the form of properties that a solution must satisfy as a whole. An exact solution(s) does not (normally) exist in the knowledge-base, but the inference mechanism can generate the solution by utilizing knowledge in the knowledge base.”

It is obvious, that the “Real-time approach with map overlay” can be best described by monitoring and control. These tasks tend to be more derivative. In order to enable site specific fertilization, the process control has to be conducted within a given time. For this it is advantageous if main parts of the solution already exist in the knowledge base and guarantee a deterministic behavior in certain limits.

### *Problem Solving Level*

The process of problem solving is a search in a solution realm (Barr and Feigenbaum, 1981). The number of possible derivations from the beginning to the target is the solution realm. Artificial intelligence uses steps of action for the search. In each step a number of solutions is possible. Some facts and rules may lead to a “combinatory explosion” in the steps of action for the search. Conflicts may also occur, when more than one rule is applicable. The objective is to search for the fastest way to get the answer.

Therefore some typical problem solving techniques and architectures have proved to be useful. They can be subdivided into knowledge centered and search centered. A combination of both is appropriate for this task.

### Knowledge Centered Problem Solving Techniques and Architectures

Goal and data:

As stated in the introduction an appropriate problem-solving approach for the data fusion algorithm for the Level 2 Processing was derived by the means of Antony’s (1995) process model. Canonical problem solving form IX with its forward-inference production rule paradigm was determined to be appropriate. This is a generation-based algorithm and supports the selection of forward chaining out of the realm of knowledge-centered problem solving techniques and architectures. Forward chaining is a data driven reasoning, which means that the reasoning starts with known data from the data bases. The search goes from the premises to the conclusions. In the case of the derivation of the application rate by the expert system the symptoms are available (map and sensor data) and the system has to infer from them (data driven) to reach the solution (hypotheses that are the number of all possible application rates).

Inexactness:

Dealing with another knowledge-centered parameter the consideration of inexactness was done according to the following premises. Data coming from the overlay maps were already corrected by mapping correction algorithms like proposed e.g. by Blackmore (1999), Noack et al. (2003) or

Bachmaier and Auernhammer (2005), i.e. some kind of JDL level 1 processing, and therefore do not need a special treatment. On-line sensor technology measurements have to be corrected either by JDL level 1 processing (e.g. default values, simple moving average, Kalman filter) or at JDL level 2 processing using a different rule set when values (attributes) are missing.

Modularization:

The functional modeling showed that the knowledge can be modularized. So it is obvious to structure the knowledge base in four rule set modules: crop production assessment, constraints effects, agricultural engineering assessment and evaluation & decision.

Conflict resolution:

Good rule based system design avoids the use of salience (giving rules a higher priority) and a strict processing control otherwise it would be better to select another problem solving paradigm. One important issue is to design a decision tree with ensured consistency, but there are cases with no or more solutions. To deal with these situations each of the four rule set modules has got a second decision stage of assessment (sum up) where rules were implemented to select the most appropriate solution or to insert a default value. On a more elementary stage, conflict resolution is done by the following search centered problem solving technique and architecture.

#### Search Centered Problem Solving Techniques and Architectures

Two common simple search strategies are the depth-first and breadth-first search. A depth-first search explores a path until the last level, before backtracking and exploring another path. A breadth-first search explores the nodes closest to the root, before exploring the ones in the next level. The depth-first search is more efficient as the breadth-first in situations where the required statement is not close to the root node and the branching factor is not small. For the case at hand it was identified that to represent the relations of premises and conclusions defined by the rules, a tree with deep levels (many input data types) is required. Therefore the depth-first search is recommended as the main search mechanism for the task.

#### *Knowledge Base Level*

Usually expert system applications deal with symbolic knowledge. Typical knowledge representations for this kind of knowledge are: Production rules, semantic networks, frames, scripts, logic and model based representation.

Weigert and Wagner (2003) showed within the IKB research project that decision support for site specific N-fertilization, i.e. defining the application rate, could be represented by production rules. These rules can be depicted as decision trees. All the crop production knowledge is formulated as a decision tree with a deep level of 10 at maximum. The resulting recommendations for an application set point are discrete steps of 10 kg/ha and range from 0 to 100 kg/ha. Also the knowledge about the constraints, like repeated application (overlapping) or limitations due to environmental regulations and user input in order to command a relative adjustment of the set point, are formulated as rules. In the same way the agricultural engineering assessment can be defined for the selection of the operating mode (manually or automatically) and the analysis of the "health state" of the implement and on-line sensor technology.

The facts are also a part of the knowledge base of an expert system and have an influence on the selection of an appropriate tool. Facts (data) should represent "precision farming maps", on-line sensor technology measurements and characteristics and different components and parameters of the tractor implement combination. A well adapted and intuitive representation for these facts is an object-oriented approach.

#### *Tool Level*

The main software tools for the development of expert systems range from conventional programming languages up to hybrid shells. Conventional programming languages, e.g. C or Fortran, can be used for the development of an expert system, but they are not the best choice since they do not support the construction of expert systems. Artificial Intelligence programming languages were developed specifically for the construction of expert systems. They can be classified as rule-based, logic-based, network-based and frame-based, according to the

representation formalism applied. Examples are Prolog and OPS5. Hybrid artificial programming languages were also developed to build expert systems. Their main characteristic is to provide different programming paradigms and several different forms of inference strategies in one framework. Examples are Kappa, KEE, and Nexpert. Shells are expert systems with an empty knowledge base, built for a specific purpose. The programmer simply needs to insert the knowledge into the knowledge base. One disadvantage of using shells is the loss in flexibility, due to the fact that the knowledge engineer has to work with the given characteristics of the tool. Hybrid Shells provide in addition to a simple shell the possibility of using different knowledge representations and inference strategies different in one framework. Since project time and funding was limited it would not be very useful to develop a whole expert system by using conventional or artificial intelligence programming languages if a shell could be found which fulfills all the requirements. The shell has to support forward chaining, depth-first searching, rule based knowledge representation, rule set modularization and object oriented representation of facts. Usually this variety is best fulfilled by a hybrid shell. The “real-time approach with map overlay” requires data processing in real-time according to the specification level, thus an expert system capable of processing the data in real-time is indispensable. Further main criteria for the selection were the development environment, programming interfaces, support and costs.

Based on those premises and especially due to the guaranteed real-time capability G2 (Gensym Corporation, USA) was the ideal candidate but the costs exceeded the research subproject budget. So JESS (Java Expert System Shell) (Sandia National Laboratories) (Friedmann, 2003) was chosen. JESS is free for academic and non commercial use. It is a rule based hybrid expert system shell written in Java™ (Sun Microsystems Inc.), inspired by CLIPS, which can create, manipulate and reason about Java objects. JESS offers bi-directional chaining and uses a very fast matching algorithm (RETE) to process rules. This algorithm uses a data structure, which enables a fast match-recognize-act cycle, but it does not assure a response within a guaranteed time. The performance of a RETE based expert system depends principally on the number of partial matches generated by the rules, rather than on the number of rules and facts.

### Implementation

The implementation was carried out on different notebook computers with the operating systems Microsoft Windows 2000 Professional or Microsoft Windows XP Home. Based on these hardware and operating system combinations a Java 2 SE Virtual Machine and the expert system shell JESS (Version 6.14) were installed. The rough system design of the simulation is depicted in figure 3.

The whole rule set comprises about 160 rules and is organized in four different components (modules). The first component are rules for crop production assessment (Fig. 4). The second component are rules which are processing predefined constraints. The third component are rules for an agricultural engineering assessment, which take e.g. prioritized user inputs or the “health state” of the on-line sensor technology into account. The fourth component sums up the results of the first three components and takes a final recommendation for the application set point. Furthermore some rules are also implemented for control of sequence of operations, cyclic triggering and module focus change.

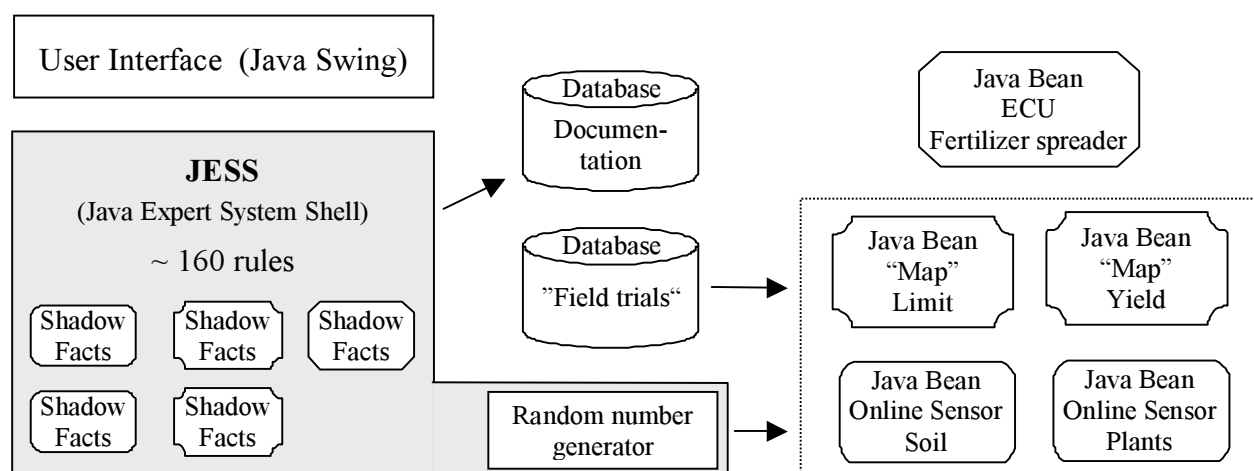


Figure 3. Schematic overview of the simulation.

Use of the object oriented software component technology JavaBeans (Sun Microsystems Inc.) allows to simulate the process surroundings and to get the facts for the expert system at the same time. For this purpose shadow facts are created in JESS, in which the attributes of an on-line sensor technology, overlay map or tractor implement combination component, each imitated by a JavaBean, are mirrored. The test data of the JavaBeans can be simulated by a random number generator or read from a database as real field trial data. The database was implemented using the open source database product MySQL. The read and write access was programmed as Java object, which can be integrated into JESS. The fertilizer spreader is also implemented as a JavaBean, the data flow direction only turns round. The derived application set point is put in the fertilizer spreader shadow fact and reflected to the fertilizer spreader JavaBean. In parallel, this set point is stored in the database for documentation purposes. Time measurement data about the period of an assessment and decision cycle are also stored in the database as well as the database access times. Therewith all relevant multisensor data fusion and documentation processes of the real-time process control for a sensor based fertilizer application system have been implemented.

```
(defrule CROP_PRODUCTION::N40-2 "Recommendation N40 Rule 2"

  (reip2 (plant_attribute ?p1&: (<= ?p1 722.25000)))
  (yield (soil_attribute ?s1&: (> ?s1 8.577623)))
  (tforce (soil_attribute ?s2&: (> ?s2 34.00000)))
  (yield (soil_attribute ?s3&: (<= ?s3 9.462849)))
  (reip2 (plant_attribute ?p2&: (> ?p2 721.82001)))
  (tforce (soil_attribute ?s4&: (> ?s4 30.00000)))
  (n1 (implement_attribute ?i&: (> ?i 50.00000)))
  (reip2 (plant_attribute ?p3&: (> ?p3 721.62000)))
  (reip2 (plant_attribute ?p4&: (<= ?p4 722.45001)))
  (yesREIP)
  (trigger)

=>

(assert (CROP_PRODUCTION::N_recommendation
(setpoint 40)
(explanation "40 kg/ha since rule < N40-2 >"))))
```

Figure 4. Exemplary of a rule in JESS - Code.

Since JESS has got only a command line based I/O (Input/Output) interface an interactive user interface (Fig. 5) was developed using Java's GUI (Graphical User Interface) library Swing.

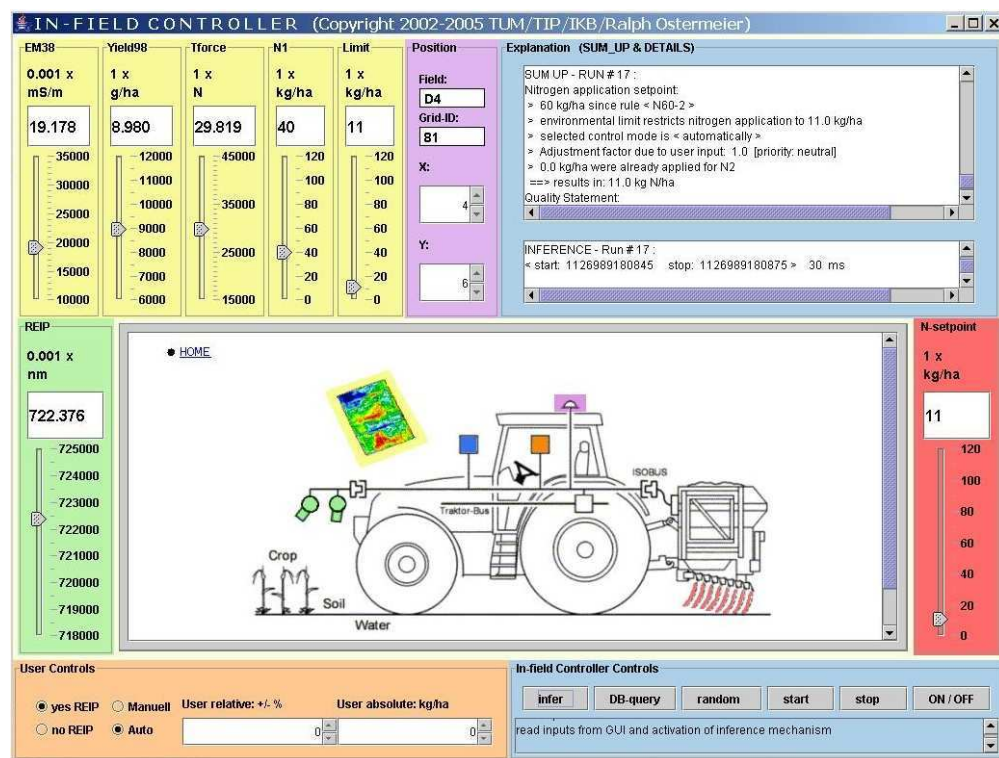


Figure 5. User interface of the simulation.

Both, the overlay map values and the on-line sensor technology values can be adjusted by the sliders. At the same time these sliders have a display function. At the “N-set point” panel this is the only functionality, for all other measurement values the display functionality is important when test data are created by a random number generator or read from the database. At the “User Controls” panel the user can command own decision and over-steering wishes, like e.g. the selection between manual or automatic operation or a proportional set point over-controlling. Furthermore certain adjustments also can be carried out. So the online sensor (REIP) can be switched off (fault simulation and simulation of the mapping approach respectively). The expert system recognizes this new situation and uses an alternative set of rules for the crop production assessment. Without an explanation interface an expert system is incomplete. This interface is implemented by two components, the central panel and the “Explanation” panel. The central panel can interpret and display HTML (HyperText Markup Language) pages. In the currently implemented revision the user can overlook the whole process control and rule set in a graphical form (overview screen, decision trees and mind maps). Furthermore the inference sequence and the therefore needed time of each cycle is listed in the “Explanation” panel.

### Testing and refinement

Testing which means verification and validation is a critical element of expert system development. It is hard to verify these systems since specifications are non-existing or fuzzy and changing due to the evolutionary development process. So validation, i.e. the program performs the functions it is intended for, takes the centre stage. The following two evaluation measures were especially tested and ascertained. Within IKB Duernast subproject 12 the automatically by data mining generated decision trees were discussed with other crop production experts of the research group. So for field trial data the resulting application set point vector could be determined and used as a reference for testing the expert system in an automatic way. In order to cover also extreme value ranges and to test the constraints and the influence of user inputs, interactive examination (manual testing) of the system and an assessment by colleagues was conducted. Finally the system was presented to a broad audience at exhibitions and at the IKB Duernast research group’s final colloquium. Besides testing the correctness of the implemented rule set the computational performance regarding the real-time capability was carried out. Thousands of test data were generated using the random number generator feature of the simulation and were processed by the data fusion and decision functionality of the implemented expert system. The results for the typical (~ 85% of all passes) and maximum processing times for one assessment and decision cycle are listed for different hardware configurations in Table 1. If 40 ms for the database read and write access are added in the worst case of 90 ms then the maximal available time of 0.92 s is only make used by 14 %, i.e. the system is real-time capable within the defined boundary conditions and still offers growth potential.

**Table 1. Processing times for one assessment and decision cycle of the simulation.**

Index	Processor	Memory	Operating System	Processing time typical	Processing time maximal
1	Intel Pentium III Mobile, 1.0 GHz	640 MB RAM	Microsoft Windows 2000 Professional	10 ms	60 ms
2	Intel Pentium III Celeron, 0.8 GHz	256 MB RAM	Microsoft Windows XP Home	20 ms	90 ms
3	Intel Pentium III Celeron, 1.5 GHz	256 MB RAM	Microsoft Windows XP Home	10 ms	60 ms

## CONCLUSION

Within the integrated research project IKB Duernast, the “Real-time approach with map overlay”, a typical multisensor data fusion task, could be implemented in form of a personal computer based simulation including an intuitive man machine interface. Therefore a software simulation with an

expert system as core element was implemented to fuse on-line sensor technology measurements (REIP), maps (yield, EM38, environmental constraints, draft force) and user inputs in order to derive a nitrogen application set point in real-time. An integrated development process could be established and exemplarily shows the implementation of a multisensor data fusion system for an agricultural engineering process control. The explorative development process of the expert system can be viewed as a structured transformation in five levels from the “specification level” to the “tool level”. An analysis according to the five transformation levels, which was based on the functional and procedural modeling of the whole multisensor data fusion process, revealed that the hybrid expert system shell JESS (Java Expert System Shell) is an appropriate programming paradigm for implementation of the simulation. Although JESS possesses no hard real-time capability, carried out performance measurements showed that the simulated process control is soft real-time capable on a 32-bit processor hardware (Intel Pentium III Mobile, 1 GHz) and a Microsoft Windows 2000 or XP operating system. Certainly the quality of the whole process control depends on the quality of the set of rules and of the facts. In this area further interdisciplinary research with colleagues from plant sciences, agricultural economics and ecology should be aspired. Additional further research is necessary for an enhanced inexactness treatment, for performance increase by the use of parallel architectures and a successful transfer to practical application needs techniques for an automatic maintenance of the knowledge base.

#### Acknowledgements

This work was part of the integrated research project “Information Systems Precision Farming Duernast” IKB Duernast (<http://ikb.weihenstephan.de>) which was financially promoted by the “German Research Council DFG”.

#### REFERENCES

1. Antony, R. T. 1995. *Principles of Data Fusion Automation*. Boston: Artech House.
2. Auernhammer, H., M. Demmel, F. X. Maidl, U. Schmidhalter, T. Schneider and P. Wagner. 1999. An On-Farm Communication System for Precision Farming with Nitrogen Real-Time Application. ASAE-Paper No. 991150. St. Joseph, MI, USA: American Society of Agricultural Engineers.
3. Auernhammer, H. 2001. Precision farming - the environmental challenge. *Computers and Electronics in Agriculture* 30: 31-42.
4. Bachmaier, M. and H. Auernhammer. 2005. Yield mapping based on robust fitting paraboloid ones in butterfly and elliptic neighborhoods. In *Precision Agriculture '05*, 741-750. J. V. Stafford, eds. Wageningen: Wageningen Academic Publishers.
5. Barr, A. and E. Feigenbaum. 1981. *The Handbook of Artificial Intelligence*. Volume 1. Los Altos, California: William Kaufmann Inc.
6. Blackmore, S. 1999. Remedial Correction of Yield Map Data. *Precision Agriculture 1/1999*: 53-66.
7. Friedman-Hill, E. 2003. *JESS in Action*. Greenwich: Manning Publications Co.
8. ISO 11783 - International Organization for Standardization: Tractors, machinery for agriculture and forestry - Serial control and communication data network. Part 1 to 11.
9. Luger, G. F. 2004. *Artificial Intelligence: Structures and Strategies for Complex Problem Solving*. 5th. ed. New York: Pearson Education - Addison-Wesley.
10. Noack, P. O., T. Muhr and M. Demmel. 2003. An Algorithm for Automatic Detection of Defective Yield Data. In *Precision Agriculture*, 445-450. J. Stafford and A. Werner, eds. Berlin, Germany: Wageningen Academic Publishers.
11. Ostermeier, R., H. Auernhammer and M. Demmel. 2003. Development of an in-field controller for an agricultural bus-system based on open source program library lbs-lib. In *Precision Agriculture*, 515-520. J. Stafford and A. Werner, eds. Berlin, Germany: Wageningen Academic Publishers.

12. Ostermeier, R. and H. Auernhammer. 2004. Real-time process control for a sensor based fertilizer application system using multisensor data fusion. In *AGENG LEUVEN 2004, Engineering the future*, CD-ROM (full papers), Session 10 -Nr. 352-Ostermeier.pdf, 1-8. Leuven, Belgium.
13. Sriram, R. D. 1997. *Intelligent systems for engineering*. Berlin Heidelberg New York: Springer-Verlag.
14. Steinberg, A. N. and Ch. L. Bowman. 2001. Revisions to the JDL Data Fusion Model. In: *Handbook of multisensor data fusion*, 2-1 - 2-19. Hall D. L. and J. Llinas, eds. Boca Raton: CRC Press LLC.
15. Weigert, G. and P. Wagner. 2003. Development of decision rules for site-specific N fertilization by the application of data mining techniques. In *Precision Agriculture*, 711-715. J. Stafford and A. Werner, eds. Berlin, Germany: Wageningen Academic Publishers.



# X-BY-WIRE VIA ISOBUS COMMUNICATION NETWORK

M. Ehrl<sup>1</sup> and H. Auernhammer<sup>1</sup>

## ABSTRACT

Satellite based guidance technology is a very challenging principle for future automation of agricultural machinery. The first generation type of systems are primarily self-contained solutions and added to the existing system set-up of the tractor. As being an important step towards robotics in agricultural machines, a better integration of this technology into the mechanical, hydraulic and especially the electronic architecture is a major issue. In principle, there are two main strategies for the integration. One is a concept based on a proprietary, manufacturer specific approach. The other one is to map as many functions as possible into the just state of the art becoming open and standardized ISOBUS. Within this paper, the capabilities of ISOBUS to be used for X-by-Wire applications are discussed from different point of views. In consequence, ISOBUS can only be used to create X-by-Wire applications with mechanical or hydraulic backup. Basic real-time capability with a reaction time of 100 ms seems to be achievable. However, some features of time-triggered protocols like determinism should be integrated by simulation on application layer level. Such concepts are the introduction of a heartbeat mechanism to serve as a coarse time synchronization and timeout reference. Additionally, the lack of unique and hard-wired addressing within ISOBUS demands new concepts like encryption algorithms. Based upon this theoretical consideration, a first proposal for a Steer-by-Wire approach via ISOBUS has been derived and implemented. First results are very promising, but further investigations like fault injection trials and extended network set-ups with pre-defined bus load scenarios are necessary.

**KEYWORDS.** Electronic Communication, ISO 11783, ISOBUS, Steer-By-Wire, X-By-Wire.

## INTRODUCTION

The introduction of automatic guidance systems based on satellite navigation within the last few years was a great step towards robotics in agricultural tractors. This emphasizes the general trend of setting up systems, which allow more and more functions to be automated (Auernhammer, 2004; Reid, 2004). This comes, because electronic systems are able to do work better than the human driver. Important parameters are increased and stable accuracy at extended operational times. As the machines become larger for being more efficient, it gets even more important to have dependable and energy efficient systems which are able to operate in a harsh environment over leastwise 10 to 15 years.

A major prerequisite for the automation of functions is the interconnection of all basically self-contained electronic systems in an agricultural working machine in order to realize a distributed electronic system. Since 1991, huge efforts of both industry and science have been undertaken on creating a standard for the interconnection of Electronic Control Units (ECU) in agricultural tractors and self-propelled machines. Therefore, the ISO 11783 (ISOBUS) standard was formed. This standard defines an open communication protocol at physical and application layer level and is based on Controller Area Network (CAN) protocol (ISO 11898-1, 2003).

The standardization of an overall agricultural communication system requires a very complex range of specifications. Major needs are supplying basic signals (e.g. speed, hitch position, ...) to implements, control of implements by a single user interface, automated data acquisition, task control, diagnostics, teleservice, on-line sensor technology, the integration of Tractor-Control-by-

---

<sup>1</sup> Technische Universitaet Muenchen, Agricultural Systems Engineering, D-85354 Freising, Germany, markus.ehrl@wzw.tum.de

Implement scenarios and so forth. Today, the ISO 11783 standard comprises 13 parts with an overall size of several hundred pages. After publication of the Virtual Terminal (ISO 11783-6) in June 2004, various manufacturers have placed ISOBUS conform products on the market, and even more are expected in the near future. Therefore, agricultural equipment manufacturers have invested huge amounts of money for the development of this standard and even more for the design of compatible products. Currently, some manufacturers have set-up their whole electronic product range upon ISOBUS. Accounting these facts, it can be assumed that ISOBUS will be the main communication protocol at least for the next few generations of agricultural machinery and equipment.

X-by-Wire is a concept, where safety critical operations of machines like steering, braking or powertrain control, normally done by mechanical or hydraulic components, are fully implemented by electronic systems. The communication network is therefore the backbone of X-by-Wire applications and has essential requirements like real-time performance, fault-tolerance and high dependability. These requirements are mainly granted for time-triggered protocols (Kopetz, 1997).

## OBJECTIVE

The main objective of this paper are considerations about the integration of X-by-Wire functionality within ISOBUS networks based on CAN. A thorough analysis of the protocol, the interrelation of several parts of the standard and certain protocol mechanisms have to be evaluated in order to estimate the impacts on safety-related issues. For that, basic principles and requirements of safe, fault-tolerant, real-time communication systems need to be analyzed. At further, this should exemplary be pointed out on a real set-up of a Steer-by-Wire application.

## STEERING AND NAVIGATION SYSTEM BASICS

For innovations based on electronic equipment, it is the normal case that these systems are self-contained solutions at first. In the second or third generation, these systems become more and more integrated within the overall system architecture. This can also be assumed for the whole range of automatic guidance systems for agricultural machines. Depending on the manufacturer (Noack, 2004), these systems typically consist of the following components:

- user interface,
- navigation controller,
- on/off or proportional hydraulic valve as actuator,
- Real Time Kinematic Differential (RTK) GPS for high precision position information,
- Inertial Measurement Unit (IMU) for roll/pitch/yaw compensation,
- steering angle sensor(s),
- hydraulic pressure sensor(s),
- activation/deactivation switch,
- dead-man safety system.

Most of these components are added to the tractor with no or just partial interconnection to the major electronic architecture of the tractor (Fig. 1). This first generation of Steer-by-Wire systems still remains with mechanical or hydraulic backup, acting as a redundant backslide layer (Pudszuhn, 2003). Due to IEC 61508 (IEC 61508), those systems are categorized to Safety Integrity Level (SIL) 3 and need to be fail-operational, which means fault-tolerant by redundancy. A Failure Mode Effects Analysis (FMEA) (Martinus, 2005) of the hydraulic valve is therefore required. Additionally, the Steer-by-Wire mode is only allowed up to a maximum speed of 25 km/h. Although, these first generation X-by-Wire systems are fail-safe due to their intrinsic design, determinism of the message transfer, the service of a global network time and redundance at the timing services become already important (Führer, 2000).

Within the original hydraulic steering loop, an additional hydraulic valve with pressure sensors is fitted. Basic operation is to steer the system by steering wheel. The operator is allowed to assign the leadership to an electronic device such as a simple potentiometer, an electronic joystick or an automatic satellite navigation system. As soon as the operator touches the steering wheel which can be sensed by a pressure sensor, the leadership is automatically returned and the electronic input path is deactivated. This is very interesting for different working conditions in the field where the leadership of the steering wheel can be transferred to ergonomically enhanced devices such as a reverse driving facility.

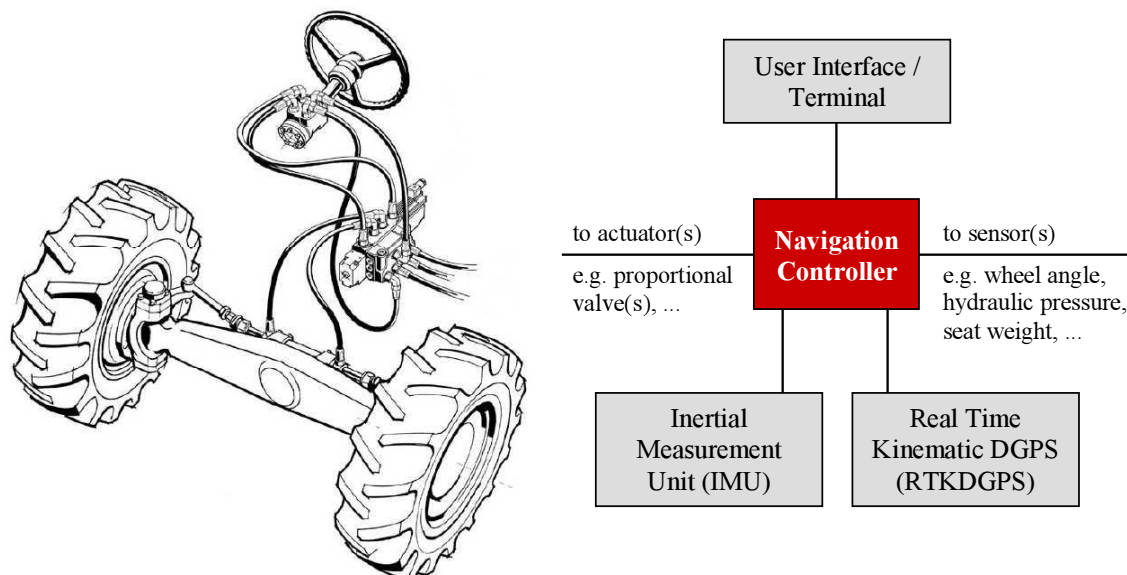


**Figure 1. Typical system set-up of a first generation automatic guidance system for tractors.**

The electronic steering path offers new strategies like the adjustment of

- the steering speed in dependence of driving speed,
- the maximum steering angle in dependence of driving speed,
- steering parameters due to tractor tilt (roll/pitch angle on hillsides).

In future, these systems need to be fully integrated within the overall electronic architecture of the tractor for offering new and optimized functionality. A deep integration of the navigation system allows not only to Steer-by-Wire, but also to additionally control Powertrain-by-Wire like engine speed and the continuous variable gearbox in order to realize optimal strategies for regaining the parallel pathway after turning or the adaptation of driving speed because accuracy constraints can/cannot be met at lower/higher driving speed.

### **ARCHITECTURE FOR STEER-BY-WIRE INTEGRATION**

To fully integrate an automatic navigation system within the electronic system architecture of a modern tractor with ISOBUS capability, there are basically two different strategies possible. The crux of the matter is the location of the navigation controller.

1. A tractor manufacturer with its own navigation controller (or having an exclusive agreement with an external company) has the ability to connect the navigation controller to the tractor internal bus segment. Here, the advantage is to have a much more safe and predictable communication (for both event- or time-triggered protocols) as this segment has a known and fixed number of nodes after fabrication and therefore measurable delays and maximum bus loads under normal operation. This generally requires to implement the (often proprietary) tractor internal application-layer protocol within the navigation controller for acting as a proper network member. Also, there needs to be a user interface which might be an additional unit or requires a second communication channel to the external ISOBUS network for using the available VT.

2. From a third party manufacturer point of view, an integration is optimally realized within the external ISOBUS communication segment, where any communication is standardized and the VT can ideally be used as user interface. Here, the requirements on the communication safety and real-time needs are the crucial points to be considered. As shown in figure 2, the steering angle set-point has to travel thru the ISOBUS segment to the Tractor ECU, acting as a gateway to the tractor internal bus segment before arriving at the steering control ECU and being applied to the electro-hydraulic valve. Because of the gateway, a chaining of several hardly predictable delays is the consequence.

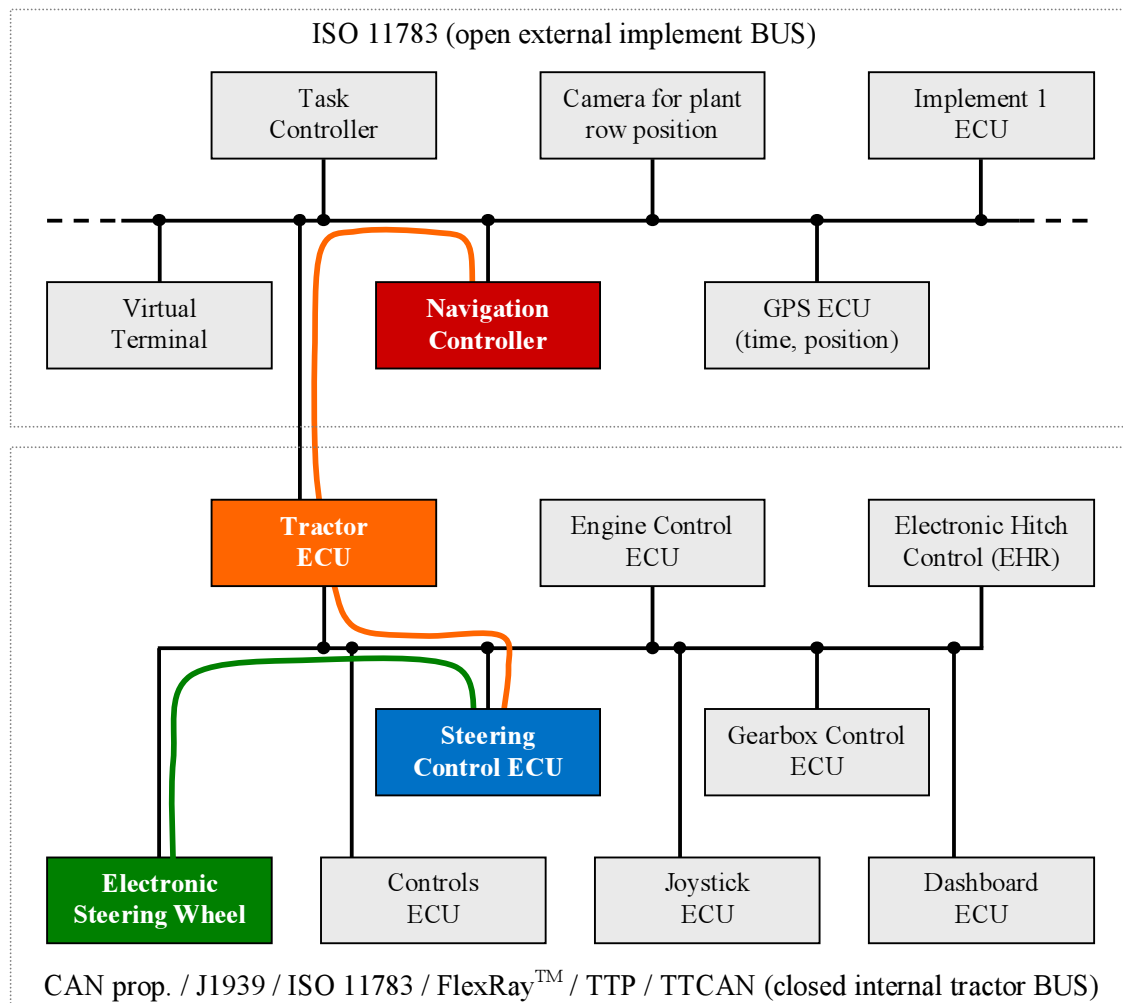


**Figure 2. Network topology with Navigation Controller in external ISOBUS segment.**

The first option is definitely the more safe way for integrating the navigation controller within the network architecture of a tractor, but has great drawbacks concerning flexibility and the realization of the user interface. Due to the actual ISO 11783 definition, the tractor ECU has the only gateway functionality and not support transparent VT message transfer. If the communication protocol of the internal tractor bus is also based upon ISOBUS, a connection to a separate CAN channel of the VT can solve at least one problem. Considering ISOBUS as being an open, plug and play network for the interconnection of ECUs, the second option seems to be ideally suitable. As the number of nodes is not fixed and even runtime-extendable, the communication on this bus-segment is the unknown, unless there are mechanisms which guarantee safe and predictable real-time capabilities.

As automatic guidance systems are taking over the control of the steering functionality for a defined period of time, these systems can well be accounted as a Tractor-Control-By-Implement approach. Within ISOBUS, this concept is covered by Remote Control Messages (RCM) and was profoundly investigated by Freimann (2004). Another example for this approach is that an implement defines set-points for torque, engine speed or gearbox control which is generally a Powertrain-by-Wire approach via ISOBUS. Here, the problems with delays and real-time requirements are of equal character.

## X-BY-WIRE FUNDAMENTALS

X-by-Wire allows to realize and fully perform safety-critical operations of machines by electronic systems. Safe X-by-Wire applications are capable to meet many important parameters like fault-tolerance, real-time performance, dependability, flexibility, scalability and others (Kopetz, 1997, 1998). Within this context, several phrases and terms such as 'redundancy' or 'real-time' are often used and interpreted differently in literature. A comprehensive overview about these terms is given by Ehret (2003).

### Redundancy

As ISOBUS is a very important standard for agricultural equipment, an weighty matter is to what extent ISOBUS can provide X-by-Wire functionality. Several publications already discussed the problems of CAN being used for those kind of applications (Kopetz, 1998; Führer 2000, Wei, 2005). Besides several issues, the main reason is the lack of redundancy of the physical communication layer (hardware redundancy). CAN does not allow to drive two replicated channels, because of the error detection and immediate retry mechanism. The deactivation of this functionality has already been considered, but therefore a very strong mechanism of CAN is lost.

The requirements towards redundancy of a system are depicted in figure 3. When a system is redundant, it is possible to detect and handle errors in some way. Redundancy can be divided in:

- Information redundancy: Such as checksums, acknowledgment, parity checks.
- Hardware redundancy: Replicated components, watchdog timers and other hardware whose purpose is to increase dependability or to detect errors.
- Time redundancy: Such as double- and re-execution.

There has to be a clear distinction between X-by-Wire systems which have still a mechanical or hydraulic backup, as first generation guidance systems, and completely electronically controlled units being pure X-by-Wire systems.

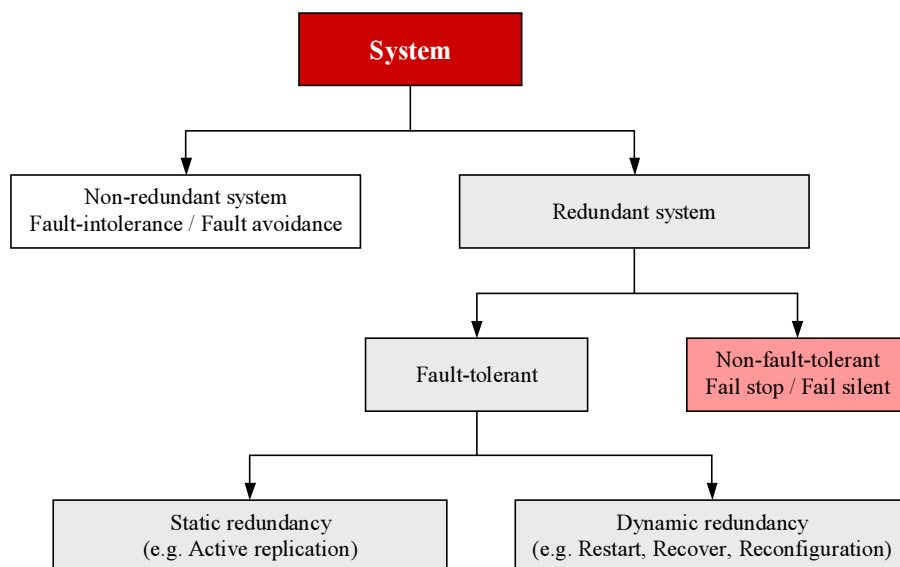


Figure 3. System Redundancy (due to Askerdal et al., 2000).

### Real-Time performance / capability

As real-time performance is claimed for X-by-Wire communication systems, the meaning of this term needs to be clearly defined. An adequate definition was found in Wikipedia.

In computer science, a real-time system has a time critical constraint i.e. operational deadlines from event to system response. Therefore, a non-real-time system is one for which there is no deadline. A real time system may be one, where its application can be considered to be mission critical like an Anti-lock Braking System (ABS). A distinction can be made between those systems which will suffer a critical failure if time constraints are violated (hard real-time), and those which

will not (soft real-time). A system is said to be hard real-time, if the correctness of an operation depends not only upon the logical correctness of the operation but also upon the time at which it is performed. An operation performed after the deadline is, by definition, incorrect, and has no value.

For the definition of a control task, it is insufficient only to declare the task as real-time. The overall requirements are merely complete, after the time within the system has to react was defined. Due to the application, the value of this reaction time can vary within a broad range.

Picking up the example of navigation control of a tractor, the real-time reaction time is considered to be dependent of the driving speed. As faster the tractor drives, as shorter the reaction time needs to be. Actual systems usually calculate the position at 10 Hz interval, which is equal to the position output rate of the utilized RTKDGPS receivers. Furthermore, this type of Steer-by-Wire application is considered to be hard-real time. Also, Freimann (2004, p. 21) states a cycle time of 100 ms for Tractor-Control-by-Implement approaches.

#### Event-triggered vs. time-triggered

ISOBUS is based on CAN being an event-triggered protocol. This means, that a message is only sent when an event occurs. The arbitrating mechanism of CAN ensures, that all messages are transferred according to the priority of their identifiers and the message with the highest priority will not be disturbed. This mechanism makes CAN very robust und provides high flexibility, but is not deterministic. The latency and jitter of a message with a certain priority at a certain time can not be guaranteed whilst dependent of the overall system condition. Even for a message with highest priority and thus always winning the arbitration process, the latency cannot be determined because of the of the error detection and immediate retry mechanism.

For pure X-by-Wire systems, the transmission of safety-critical messages must even be deterministic at the maximum busload. Hence, the concept of Time-Triggered Architecture (TTA) or hybrid protocols (time- and event-triggered) becomes essential. Currently, there are three different time-triggered protocols under discussion and development:

- Time-Triggered Protocol (TTP),
- Time-Triggered CAN (TTCAN) and
- FlexRay™.

Both, TTP and FleyRay are specified for having redundant communication channels and are therefore candidates for pure X-by-Wire applications. Wei (2005) has compared these three protocols from an agricultural point of view and excluded TTCAN for X-by-Wire applications due to single channel design an therefore being non-fault-tolerant. Müller (2002) has proposed mechanisms to synchronize TTCAN networks of any reasonable redundancy level which leads to fault-tolerant systems. Thus, all three types of time-triggered protocols still need to be considered for future X-by-Wire applications in the agricultural area.

Particularly, the extensions of TTCAN compared to CAN are of great interest, because the TTCAN protocol is realized in software in a higher layer on top of CAN. In TTCAN, all participants within the network are synchronized via the identifier of a reference message. As soon as the first bit of the frame, the Start of Frame (SOF) bit is recognized, the local time unit is synchronized and the individual participants know when to send their frames.

In TTP, the synchronization of all network members is done by a shared clock synchronization algorithm, which needs at least four nodes to work with the claimed precision. As true time-triggered systems are working with predefined time slots, the network design has to be defined and be common knowledge to all nodes before runtime. This makes TTA networks highly deterministic, but very inflexible concerning changes or extensions, because each node needs to be reconfigured. Another important property is the possibility to guard the bus against non authorized bus accesses by so called bus guardians. This allows the active prevention of the occurrence of Babbling Idiots on the network.

Comparing event- and time-triggered protocols, a broad range of different characteristics can be found. Table 1 shows a list of fundamental differences between both types of protocols.

**Table 1. Comparison of event-triggered (CAN) and time-triggered(TTP) protocols due to Kopetz (1998).**

Characteristic	CAN	TTP
Application domain	Soft real-time systems with flexibility requirements	Hard real-time systems with composability, timeliness and dependability requirements
Temporal control	Event triggered	Time-triggered
Extensibility	Excellent in non time-critical applications	Only simple, if extension planned for in original design
Membership service	Not provided	Provided
Clock synchronization	Not provided	Provided in $\mu$ s range
Replica determinism	Not provided	Provided
Latency jitter	Variable, load dependent	Constant
Media access	Carrier Sense Multiple Access with Arbitration by Message Priority (CSMA/AMP), collision avoidance	Time Division Multiple Access (TDMA)
Frame types	Data, Remote, Error, Overload	Initialization (I), Normal (N)
Error handling strategy	Immediate retry	Replicated channels, fail-silence
Load	Depends on number of events	Constant
Instant of sending	After event occurrence	Periodically, at a priori known points in time
Handling at receiver	queued and consumed on reading	new version replaces previous version, not consumed on reading
Consequences of message loss	Loss of state synchronization between sender and receiver	Unavailability of current state information for a sampling interval
Babbling idiot avoidance	No provisions	Independent bus guardian

### Consequences for ISOBUS

Consequently, it can be stated, that ISOBUS only allows to create a fail stop/silent system (Fig. 3, right) due to its CAN physical and data link layer. Therefore, ISOBUS can only be used to create X-by-Wire systems with mechanical or hydraulic backup.

Suppositional, using high prioritized messages and a precise timeout detection of the navigation controller, ISOBUS should be able to provide real-time capability with 100 ms reaction time.

Considering the comparison with time-triggered protocols, it can be assumed that deterministic behavior cannot be accomplished by CAN because of in-built error prevention. In order to minimize the delay, the Arbitration by Message Priority (AMP) mechanism can be utilized by using high priority identifiers for safety-critical messages like Steer-by-Wire commands. Another possibility to improve the timing behavior of the overall system and to allow remote detection of failures in other nodes is to implement heartbeat. This is a timed mechanism using coarse synchronization.

The problem that a bubbling idiot blocks the bus and thus prevents other nodes from sending cannot actively be eliminated in CAN networks. For a safety critical application, the only way to tackle this problem is to switch in fail silent mode and activate the redundant backslide layer.

Another safety-relevant issue emerges within the network management of ISOBUS. Each participant has to have its own and network wide unique source address, which forms the native addressing mechanism in CAN. The address must be claimed at startup due to a defined procedure and is afterwards used for the communication with all other nodes. Because the source address is assigned in a dynamic procedure and not hard-wired within the logic of each controller, it is very simple for any node to send messages with another source address. This type of error, intended or unintended can cause severe problems for safety critical applications. One way to handle this problem is, that the real owner of a certain source address reacts, when receiving a message of its own address. If there is no real owner, this is less critical but also needs to be prevented.

## TEST IMPLEMENTATION OF STEER-BY-WIRE VIA ISOBUS

On account of the mentioned considerations, a test implementation of a Steer-by-Wire application via ISOBUS was set-up and evaluated. In contrary to the formerly proposed integrated network architecture, all components of this test implementation were realized as ISOBUS conform devices. The schematic network structure is depicted in figure 4. The system was fitted to a *FENDT Vario 818* which already provides full ISOBUS functionality by means of a Tractor ECU and a Virtual Terminal. The steering control ECU was designed as a closed loop control system by using a wheel angle sensor and a PVG32 proportional hydraulic valve of *SAUER DANFOSS* as actuator. The steering controller provides VT functionality and can fully be operated via the *FENDT Vario Terminal*. Another ISOBUS conform controller, the electronic steering wheel also fitted with VT capability was designed and attached to the network. Here, a potentiometer is used to produce dynamic set-point alternations of the front axel steering angle.

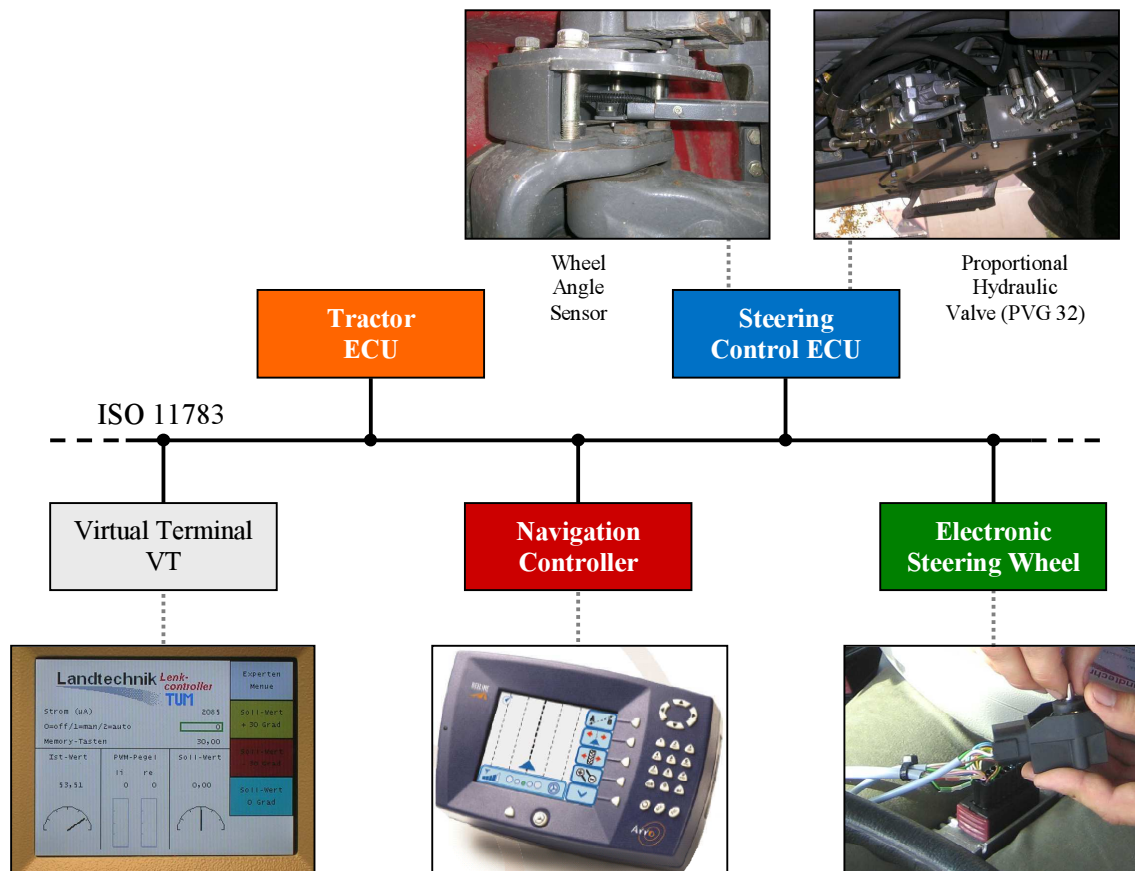


Figure 4. Schematic network structure of Steer-by-Wire application via ISOBUS.

As a first step, set-point changes of the steering angle have been applied via the user interface of the steering control ECU by simply pressing predefined buttons of the VT. Here, the communication messages are only of type ECU-to-VT and vice versa. The same approach is used for the control of implements like fertilizer distributor applications or others.

The first Steer-by-Wire relevant communication was achieved by sending changing wheel angle set-points by means of the electronic steering wheel. In order to address the formerly mentioned safety-related issues, a special communication mechanism was implemented. At first, a set-point sending routine of 10 Hz cycle time was established. In parallel, a special heartbeat mechanism among the steering control ECU and the electronic steering wheel was set-up at 5 Hz. This heartbeat mechanism serves on the one hand as a coarse synchronization and timeout mechanism, and ensures on the other, that both systems are vital and the sender surely uses its own source address. An encryption/decryption algorithm was applied on the values of the eight data bytes of each heartbeat message (DES, 1999). Alternatively, the ISOBUS NAME of both controllers was used for enhancing safety by means of the heartbeat message. After first feasibility tests, the system was comprehensive evaluated in field tests with up to 30 km/h driving speed. The system

proved to stay fully operational without any interruptions under the given conditions. As ISOBUS is an open interconnection network, additional work needs to focus on the conduction of fault injection trials. The system needs to be stressed in a specific way to detect the critical points where the mechanical backslide layer becomes active.

As a second Steer-by-Wire approach via ISOBUS, the system was configured to accept and process steering angle set-points from the navigation controller of the *BEELINE* guidance system (Fig. 4). In this case, it was not possible to introduce software changes on the navigation controller side, whereas the safety mechanism by heartbeat was deactivated. Again, the system was fully operational without any downtimes for a broad range of field tests.

## CONCLUSIONS

With automatic guidance systems, a new category of automated functions of agricultural tractor and implement combinations emerges on the market, which needs to be considered especially from a safety-related point of view. In principle, there are two main strategies for the integration of these systems into the overall machine architecture. One is a concept based on a proprietary, manufacturer specific approach, based on the tractor internal bus. The other one is to map as many functions as possible into the just state of the art becoming open and standardized ISOBUS communication network.

Within this paper, the capabilities of ISOBUS to be used for X-by-Wire applications have been discussed from different point of views. In consequence ISOBUS can only be used to create X-by-Wire applications with mechanical or hydraulic backup. Under certain conditions, a real-time capability with a reaction time of 100 ms seems to be achievable. However, some features of time-triggered protocols like determinism must be simulated on application layer level by software. Such concepts are the introduction of a heartbeat mechanism to serve as a coarse time synchronization and timeout reference. Additionally, as there is a lack of unique and hard-wired addressing within ISOBUS, new concepts like encryption algorithms for cyclic keep alive messages are proposed.

By means of an exemplary implementation of a Steer-by-Wire architecture using ISOBUS, the above mentioned concepts have been realized and tested. First results are very promising, but further investigations are necessary. These are fault injection trials and extended network set-ups with pre-defined bus load scenarios. Future aim could be the establishment of a guideline for X-by-Wire implementations via the open standardized agricultural bus-system ISOBUS.

## REFERENCES

1. Askerdal, Ö., V. Claesson, L.-B. Fredriksson, J. Hedberg, J. Johansson, H. Larsson, C. Sterje (2000). Error detection and handling, PÅLBUS Task 10.5, Revision 4, 15 June 2000.
2. Auernhammer, H. (2004): Off- Road Automation Technology in European Agriculture- State of the Art and expected Trends. In: Proceedings of the 7-8 October 2004 International Conference Kyoto, Japan: Automation Technology for Off- Road Equipment 2004. St.Josef: ASAE 2004, pp.10-23, ISBN: 1-892769-45-x.
3. DES (1999). Data Encryption Standard - DES, Federal Information, Processing Standard Publication 46-3 (FIPS PUB 46-3), Reaffirmed, 1999 October 25.
4. Ehret J. (2003). Validation of Safety-Critical Distributed Real-Time Systems. Dissertation Fakultät für Elektrotechnik und Informationstechnik , Technische Universität München, 2003.
5. Freimann, R. (2004). Automation mobiler Arbeitsmaschinen – Gerät steuert Traktor. Dissertation, Technische Universität München, Institut für Landmaschinen, VDI Verlag GmbH, Düsseldorf 2004, ISBN 3-18-311614-6.
6. Führer, T., B. Müller, W. Dieterle, F. Hartwich, R. Hugel, M. Walther (2000). Time Triggered Communication on CAN (Time Triggered CAN - TTCAN), Robert Bosch GmbH, Proceedings 7th International CAN Conference, 2000, Amsterdam.  
<http://www.can-cia.org/can/ttcan/fuehrer.pdf>

7. IEC 61508. Functional safety of electrical/electronic/programmable electronic safety-related systems – Parts 1-7. International Electrotechnical Commission<sup>3</sup>, Geneva, Switzerland.
8. ISO 11783. Tractors and machinery for agriculture and forestry – Serial control and communications data network, Part 1-13, International Organization for Standardization, Genève, Switzerland.
9. ISO 11898-1 (2003). Road vehicles - Controller area network (CAN), Part 1: Data link layer and physical signalling. International Organization for Standardization, Geneva, Switzerland.
10. ISO 11898-4 (2004). Road vehicles - Controller area network (CAN), Part 4: Time-triggered communication. International Organization for Standardization, Geneva, Switzerland.
11. Kopetz, H. (1997). Real-Time Systems: Design Principles for Distributed Embedded Applications, Kluwer Academic Publishers, 1997, ISBN 0-7923-9894-7.
12. Kopetz, H. (1998). A Comparison of CAN and TTP, Technical Report, Technische Universität Wien, Austria, 1998.
13. Martinus, M. A. (2005). Funktionale Sicherheit von mechatronischen Systemen bei mobilen Arbeitsmaschinen. Dissertation, Technische Universität München, Institut für Landmaschinen, VDI Verlag GmbH, Düsseldorf 2005, ISBN 3-18-358612-6.
14. Müller, B., T. Führer, F. Hartwich, R. Hugel, H. Weiler (2002). Fault tolerant TTCAN Networks. In Proc. 8th International CAN Conference, Las Vegas, 2002.
15. Noack, P. (2004). GPS gestützte automatische Lenksysteme, 59 Landtechnik 5/2004, S. 256-257, ISSN: 0023-8082.
16. Pudszuhn, R. (2003). Entwicklung elektrohydraulischer Lenksysteme in der Landtechnik / Development steer by wire systems for agriculture, In: Tagung Landtechnik, VDI-Verlag, VDI-Berichte 1798, S.231-238.
17. Reid, J. F. (2004). Mobile Intelligent Equipment for Off-road Environments. In: Proceedings of the 7-8 October 2004 International Conference Kyoto, Japan: Automation Technology for Off- Road Equipment 2004. St.Josef: ASAE 2004, pp.1-9, ISBN: 1-892769-45-x.
18. Wei, J., N. Zhang, D. Lenhert, S. Han (2005). An Overview and Comparison of Time-Triggered Protocols For X-By-Wire Applications. ASAE Annual International Meeting, 17-20 July, Tampa, Florida, ASAE.
19. Wikipedia. The free encyclopedia, Keyword: Real-time computing.  
[http://en.wikipedia.org/wiki/Real-time\\_computing](http://en.wikipedia.org/wiki/Real-time_computing)

# AUTOMATIC VELOCITY CONTROL OF A HYDROSTATIC VEHICLE

C. A. Foster<sup>1</sup>, R. P. Strosser<sup>1</sup>, J. D. Peters<sup>1</sup> and J. Q. Sun<sup>2</sup>

## ABSTRACT

The velocity of a vehicle with a hydrostatic drive train can vary considerably when working in environments with varying grades and ground conditions. A velocity control methodology is presented for an agricultural vehicle with a hydrostatic drive train. A cascade control design incorporating a current control, cylinder position control and velocity control is proposed. The cylinder position controller uses a set of gain scheduled lag compensators in series with a sequence of segmented deadzone inversions. The deadzone inversions compensate for nonlinear valve dynamics. The velocity controller consists of a digital feedback control. A stability analysis of the closed loop system is performed. Simulations based on experimental data are used to validate the control designs. Experimental results from a self-propelled windrower are used to demonstrate the effectiveness of the control system.

**KEYWORDS.** Electro-hydraulics, Embedded Control, Segmented Deadzone Inversion, Variable-structure Feedback Control, Velocity Control.

## INTRODUCTION

In the past two decades the use of electronic control systems in vehicles has been steadily increasing. Due to economies of scale the auto industry has lead the way in the application of electronic controls on vehicles. Systems such as cruise-control, electronic engine management, climate control and electronic transmissions are now common in automobiles. In the last ten years manufacturers of agricultural machinery have been developing and releasing more electronic control systems on their equipment. Precision agriculture is an area of research and development making extensive use of control systems (Auernhammer, 2001, Earl et al., 2000, Zhang et al., 2002). Vehicle automation with control systems is an important element of precision agriculture. The material presented in this work demonstrates an automatic velocity control system for a self-propelled windrower.

Automatic velocity control, known as ‘cruise-control’ in automobiles, has been available for quite sometime. Automobile drive-trains exhibit non-linear dynamic behavior, particularly at lower speeds (Fritz, 1996). At higher speeds the behavior becomes more linear. Classical linear controls have been successful in the higher speed ranges. The emerging technology of automated-highway-systems (AHS) calls for speed control systems that work over the full range of speeds (Rajamani et al., 2000, Rajamani et al., 2001, Rajamani et al., 2002). A variety of nonlinear and adaptive systems have been developed to address this issue (Fritz, 1996, Ishida et al., 1992, McMahon et al., 1990, Setlur et al., 2003).

The work presented here documents the development and testing of a cost-effective velocity control system for a self-propelled windrower with a hydrostatic drive-train. The velocity control system is designed to track an operator defined reference and reject disturbances. It is likely that velocity control will become a subsystem of control systems that operate at a higher level in a fully automated windrower.

---

<sup>1</sup> CNH America LLC., 500 Diller Ave, New Holland, PA 17557, USA, [chris.foster@cnh.com](mailto:chris.foster@cnh.com)

<sup>2</sup> Department of Mechanical Engineering, University of Delaware, Newark, DE 19716, USA

## DESCRIPTION OF EXPERIMENTAL HARDWARE

The hydrostatic drive-train of the windrower is composed of two primary components, hydraulic pumps and hydraulic motors. The traditional power source is a diesel engine connected directly to the hydraulic pumps. The propulsion system consists of two independent hydrostatic loops, one driving each of the front wheels. Each hydrostatic loop is powered by a variable displacement axial piston pump.

The pump displacements are controlled through a mechanical linkage. An electro hydraulic system composed of a spring-centered hydraulic cylinder and a proportional flow control valve is used to equally displace the pintle arms. The hydraulic cylinder position therefore correlates with the average vehicle velocity. The measured average velocity will be the feedback signal in the velocity control design. The hydraulic cylinder is spring-centered to a neutral position where the vehicle becomes stationary. Figure 1 shows a diagram of the hardware. If unsafe operation of the system is detected the power to the system can be shut down and the spring will center the cylinder bringing the vehicle to a stop.

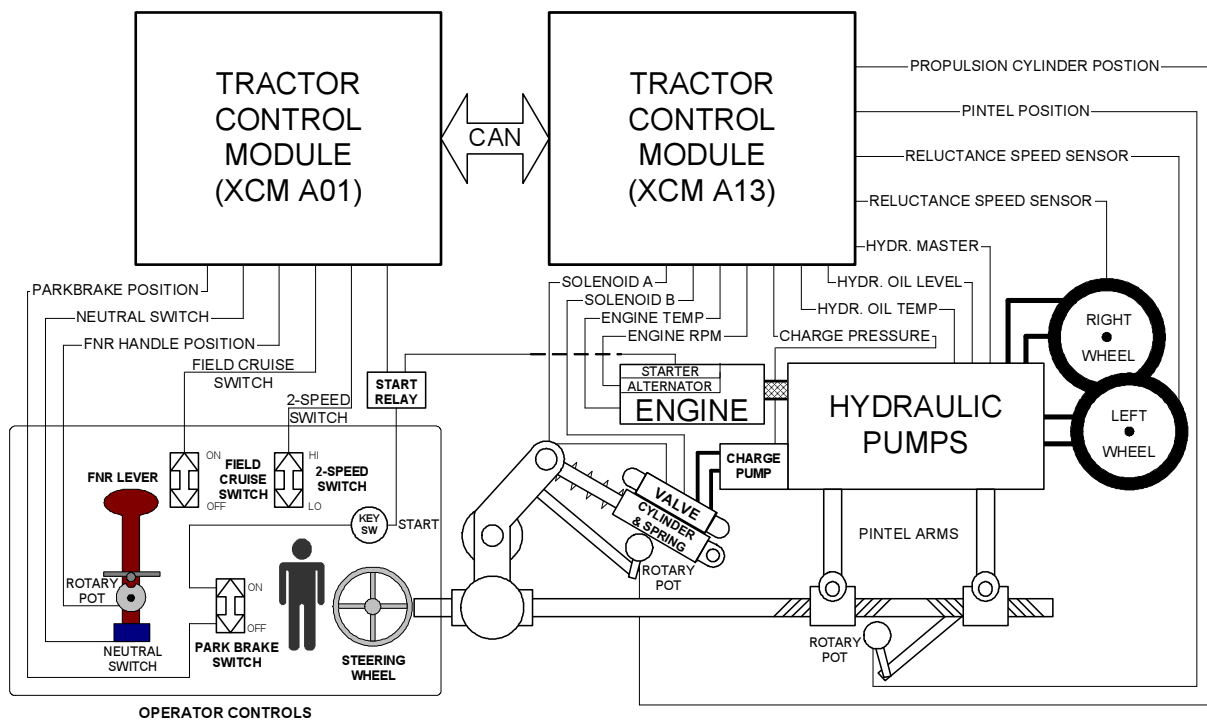


**Figure 1. Schematic of the velocity control hardware. Thick lines represent hydraulic connections and thin lines represent electrical connections. Mechanical components are represented by graphics.**

## CONTROL OBJECTIVES

The objective of the velocity control is to follow the set-point set by the operator. Due to the rough ground conditions in which the vehicle operates, the system must be able to sufficiently reject disturbances. The characteristics of the drive-train also vary in time. The control system needs to be robust enough to compensate for these disturbances and variations. Controls are developed for subsystems required to facilitate velocity control. Figure 2 shows how the velocity control loop encloses the propulsion cylinder position control loop.

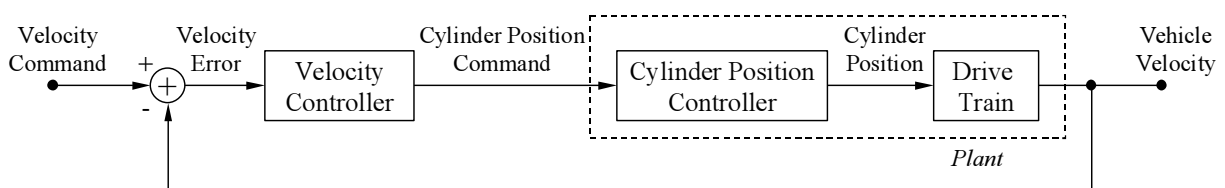


**Figure 2. Block diagram of the velocity control system.**

## CYLINDER POSITION CONTROL DESIGN

The position of the hydraulic cylinder is directly correlated with the angle of the swashplates in the ground drive pumps. The plant input is the current reference, and the plant output is the position of the hydraulic cylinder, as illustrated in figure 3. The spring-centered neutral will be referred to as the zero position. Cylinder position setpoints which extend from the neutral position will be assigned positive values, and setpoints which retract from the neutral position will be assigned negative values.

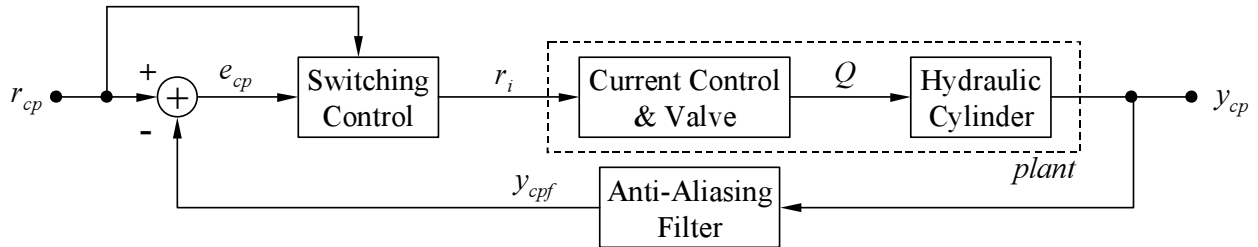


**Figure 3. Block diagram of the gain scheduled control for hydraulic cylinder position:**  $r_{cp}$  is the cylinder position setpoint;  $e_{cp}$  is the tracking error of the cylinder position;  $r_i$  is the valve current setpoint;  $Q$  is the oil flow through the valve;  $y_{cp}$  is the measured cylinder position;  $y_{cpf}$  is the filtered and digitized value of the cylinder position.

The proportional directional solenoid valve used in this work generates a non-linear relationship between electrical current and cylinder position. The nonlinear relationship between valve current and oil flow through the valve is shown in figure 4. The valve has active driving regions (1A and 1B), deadzones (2A and 2B) and a region in which flow is influenced by electrical current and external forces acting on the system (3A and 3B).

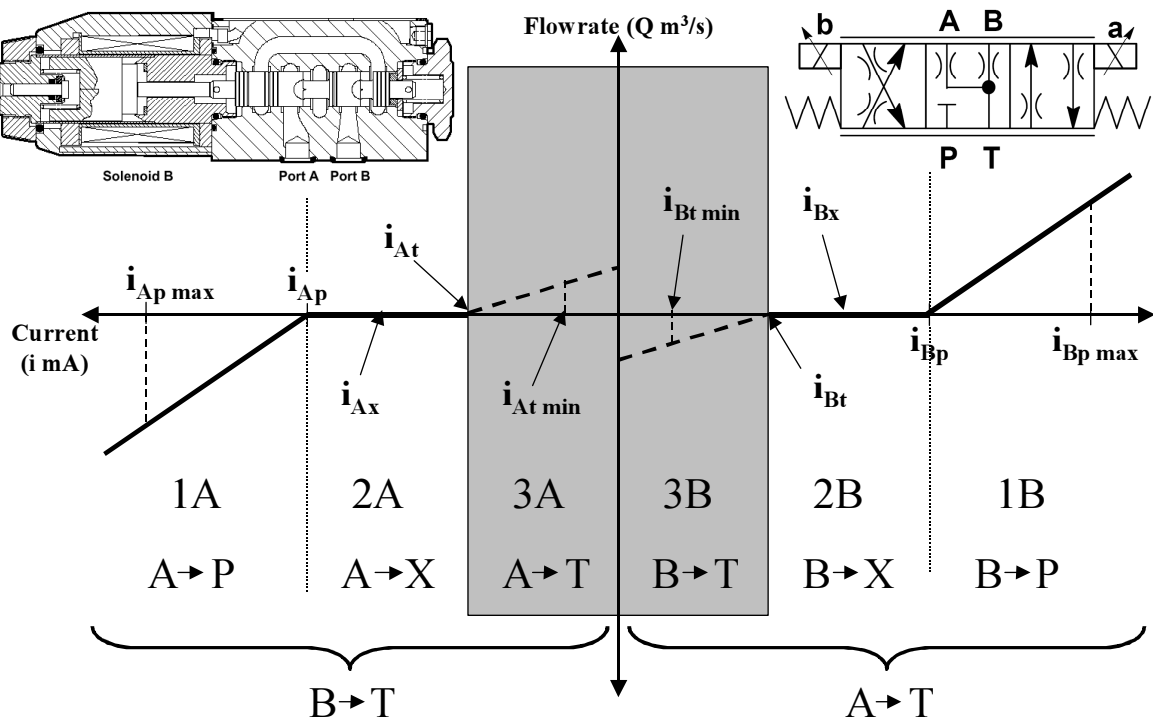


**Figure 4. Flow vs. current characteristics of the electro hydraulic valve:** regions 1A and 1B, proportional flow; regions 2A and 2B, dead zone; regions 3A and 3B, external influence. Letters 'A' and 'B' refer to the ports; P stands for the high pressure supply port; T refers to the tank port at atmospheric pressure; X indicates that the port is blocked;  $i_{BT}$  represents the 'cracking' current when the B port begins to open to T port;  $i_{Bp}$  represents the 'cracking' current when the B port begins to open to P port;  $i_{At}$  represents the 'cracking' current when the A port begins to open to T port;  $i_{Ap}$  represents the 'cracking' current when the A port begins to open to P port. The blocking currents are  $i_{Ax} = (i_{Ap} - i_{At})/2$  and  $i_{Bx} = (i_{Bp} - i_{Bt})/2$ . A double solenoid valve is used but a single solenoid valve shown graphically for improved clarity.

Control specifications include a 1 second 5% settling time, and a damping ratio of 0.707. A digital lag compensator given by

$$C_{cp}(z) = \frac{K_{cp}(z + b_{cp})}{(z + a_{cp})}$$

where  $-1 \leq a_{cp} < b_{cp} \leq 1$ , is considered in the cylinder displacement control. Because of the piecewise nature of the valve response, as shown in figure 4, we propose a switching control strategy combined with a segmented inversion of the deadzones in the valve response curve. The switching parameters are the cylinder position setpoint  $r_{cp}$  and the cylinder position error  $e_{cp}$ .

The switching control is designed in four branches. Each branch is designed for a different combination of regions in the valve response curve. The control for each branch consists of a digital lag compensator, and an inversion of a local hardware deadzone. A switching logic is used to select the set of parameters to be used in the lag compensator and which deadzone inversion to use. The lag compensators used for each branch are tuned slightly differently but retain the structure shown in the equation above.

- Branch 1 is used when  $|e_{cp}| > \delta_l$ . This branch uses an aggressively tuned controller in combination with a deadzone inversion using piecewise linear interpolations of the valve response in regions 1A and 1B to drive the system quickly toward setpoint.
- Branch 2 is used when  $|e_{cp}| < \delta_l$  and  $r_{cp} > 0$ . The controller of this branch is tuned to overdamp the system so that it smoothly approaches the setpoint with no overshoot. The control uses region 1A to push away from neutral and the spring-centering passive action of region 3A to bring the cylinder toward neutral. Region 2A is used to lock the cylinder in position at setpoint.
- Branch 3 is used when  $|e_{cp}| < \delta_l$  and  $r_{cp} < 0$ . This branch is similar to branch 2. It utilises regions 1B, 2B and 3B.
- Branch 4 is used when  $r_{cp} = 0$ . The controller is tuned to bring the vehicle to a halt quickly. A small deadband kills power to the system (for safety reasons) and uses the passive action of the spring to center the cylinder gently as it approaches the neutral position.

## CYLINDER POSITION CONTROL STABILITY ANALYSIS

### Valve Region 1A and 1B

When the valve is operating in regions 1A and 1B the hydraulic cylinder effectively integrates the oil flow coming from the valve. The oil flow can be approximated as a linear function of the valve current minus the ‘cracking’ current ( $i_{Ap}$  or  $i_{Bp}$ ). An approximate model of the plant in these regions is given by,

$$\dot{y}_{cp} \approx K_{A1}u_c$$

where  $K_{A1}$  is a combined gain including the effects of the deadzone inversion, the current control and the cylinder position control. The dot denotes differentiation with respect to time. Branches 1 and 4 cover regions 1A and 1B. Figure 5 shows a root locus plot of the control system in regions 1A and 1B. The system is stable when  $0 < K_{cp} < 808$ . The other branches have minor gain and pole-zero changes in the lag compensator but retain the same basic root locus profile. Hence, the system is stable in regions 1A and 1B.

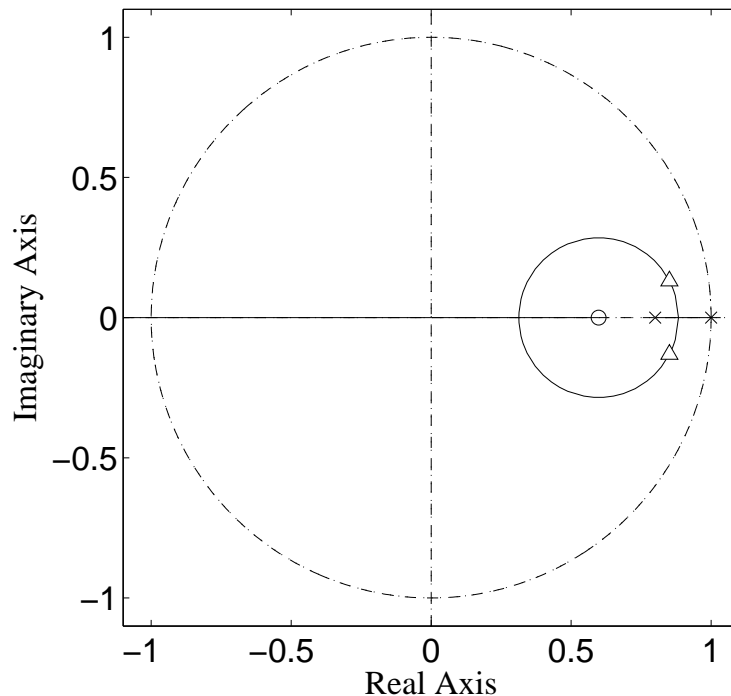


**Figure 5. Root locus of the cylinder position control operating in regions 1A and 1B of Fig. 7: (x) open loop poles; (o) open loop zeros; (Δ) closed loop poles at  $z = 0.85 \pm j0.13$  when  $K = 35.1$ .**

### Valve Region 2A and 2B

In regions 2A and 2B the oil flow is blocked, and the cylinder is locked in position. In this state, we have,

$$\dot{y}_{cp} = 0$$

In other words,  $y_{cp}$  remains constant. The constant value of  $y_{cp}$  is determined by the initial condition upon entering either region 2A or 2B. The system in this state is marginally stable since the hydraulic cylinder has hardware limits that prevent  $y_{cp}$  from becoming unbounded.

### Valve Region 3A and 3B

When the valve is operating in regions 3A and 3B, the valve is ‘cracking’ one of its ports open to tank. The current determines how large the opening to tank will be. The spring force determines the pressure of the oil in the cylinder. The oil flow is therefore a function of both valve current and cylinder position. Due to the passive nature of this action, the spring always pushes the cylinder toward the neutral position. In this region the plant can be approximately modeled by,

$$\dot{y} = K_{A3} y_{cp} u_c$$

where  $K_{A3} > 0$  represents a combined gain of the effects of the valve current, and spring force. When in regions 3A or 3B, the controller operates on either branch 2 or 3. To be in region 3A, the controller must be on branch 2 with  $y_{cp} > 0$ . On branch 2, the controller will be in region 3A only if  $u_c < 0$ . Under these conditions the above equation is stable. A similar argument can be made to prove that the above equation is also stable in region 3B. Hence, the system is stable in regions 3A and 3B.

## VELOCITY CONTROL DESIGN

The basic structure of the velocity control system is shown in figure 2. The input to the single-input-single-output (SISO) plant is the cylinder position reference. The output of the plant is the average ground speed of the vehicle. The plant model incorporates the dynamics of the current control loop, cylinder position control loop and the drive-train.

A first order model with time delay is developed for the velocity control. The input of the model is the cylinder reference position and the output is the filtered velocity of the vehicle. The following plant model is used in the control design.

$$G_v(s) = \frac{6e^{-0.15s}}{0.85s + 1}$$

The Ziegler-Nichols tuning rule is used to generate an initial set of proportional-integral-derivative (PID) control gains. The control gains are tuned further through simulation and again during experimental implementation. It should be noted that the derivative control implemented uses the output derivative only, known as the tachometric derivative, excluding the unwanted derivative of the reference signal, thus allowing non-smooth references. Since the plant model captures the dynamics of the cylinder position and current control loops, the stability of the velocity control loop implies the system as a whole is stable. The control is given by

$$\begin{aligned} u(k) &= u_p(k) + u_i(k) + u_d(k) \\ u_p(k) &= K_p e(k) \\ u_i(k) &= \frac{K_p T_s}{2\tau_i} (e(k) + e(k-1)) + u_i(k-1) \\ u_d(k) &= -\frac{K_p \tau_d}{T_s} (y_v(k) - y_v(k-1)) \end{aligned}$$

where  $e(k)$  represents the error signal,  $y_v(k)$  is the measured averaged velocity,  $T_s$  is the sample time,  $K_p$  is a control gain,  $\tau_i$  is the integral time constant and  $\tau_d$  is the derivative time constant. To prevent integral windup due to actuator saturation, the following conditional integration (CI) algorithm is used.

$$e(k) = \begin{cases} 0, & \text{if } (u_n \neq u_s) \ \& \ [(u_i > u_{i\max}) \ \text{or} \ (u_i < u_{i\min})] \ \& \ [e_v \bullet (u_n < \bar{u}) > 0] \\ e_v(k), & \text{otherwise} \end{cases}$$

where  $e_v(k)$  is the velocity error,  $u_s = \text{sat}(u_n, u_{\min}, u_{\max})$  is the control with the saturation limits  $u_{\min}$  and  $u_{\max}$ ,  $u_n$  is the nominal control,  $u = (u_{\min} + u_{\max})/2$ ,  $u_i$  is the integral control, and  $u_{i\max}$  is the upper limit of the integral control. The closed loop poles of the PID control with tachometric derivative are located at  $z = \{-0.44, 0.96 \pm j0.017\}$  showing that the system is stable. Table 1 lists the implemented control gains.

**Table 1. Implemented velocity control gains.**

Proportional Gain ( $K_p$ )	0.15
Integral Time Constant ( $\tau_i$ )	1.0
Tachometric Derivative Time Constant ( $\tau_d$ )	0.4

## CONTROL SIMULATIONS AND EXPERIMENTS

### Cylinder Position Control

The parameters in the deadzone inversions are carefully identified off-line by following the calibration routine for each valve. Experimental data of hydraulic cylinder displacement control are shown in figures 6 and 7. The system tracks the reference signal with  $\pm 1$ mm steady-state error. The response of the system is smooth. There are no discernible discontinuities in the response as the system transitions from one branch to another. However, figure 7 shows large and sharp changes of the control as the system moves from one branch to another. Recall that the control signal of the cylinder position system is the valve current setpoint. The large and rapid changes of this quantity show the effect of the deadzone inversions.



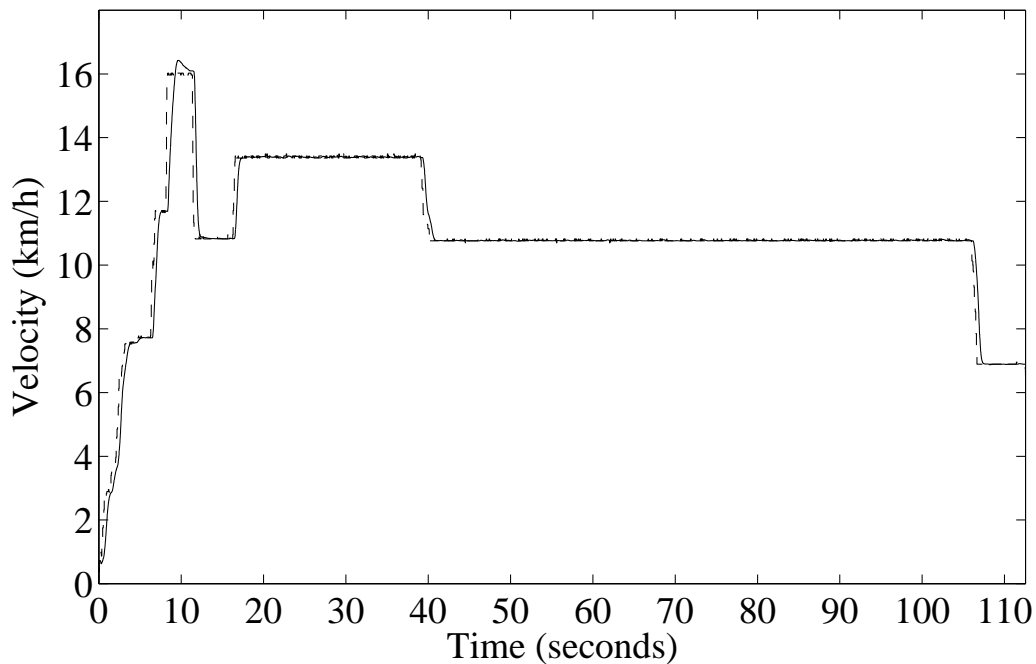


**Figure8. Simulation results of undisturbed PID velocity control of the vehicle. Velocity set point represented by dashed line. Measured velocity represented by solid line.**

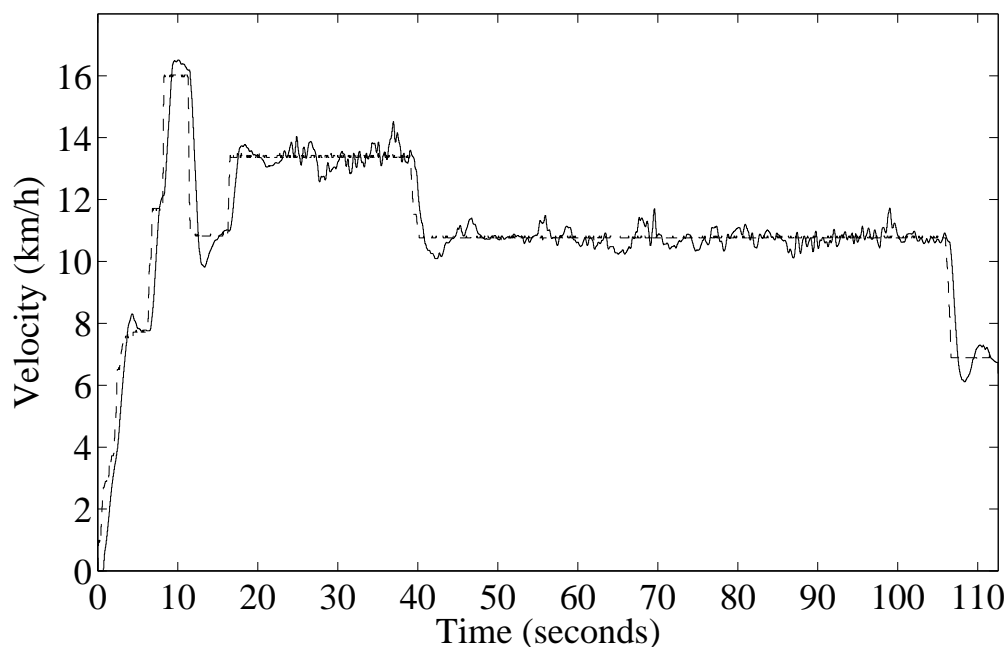


**Figure 9. Experimental results of the velocity control under the influence of disturbances due to unmodeled dynamics and road conditions. The data has been collected from the vehicle on a terrain with transitions from level ground, through a hollow and up a hill. Velocity set point represented by dashed line. Measured velocity represented by solid line.**

The most notable feature of the experimental results when compared with the simulation is the oscillations in the measured velocity. These oscillations can be accounted for by unmodeled dynamics in the plant, external disturbances, and sensor noise. The experimental results show some significant undershoot that is absent in the simulation. This is most likely due to the changes of the system parameters between acceleration and deceleration. Overall, the vehicle tracks a velocity command of 11.3 km/h with an error of approximately  $\pm 0.5$  km/h, or  $\pm 4\%$ . The uncontrolled system with a constant cylinder position providing a velocity of 11.3 km/h on smooth level ground, gives an average tracking error of approximately  $\pm 2.4$  km/h, or  $\pm 21\%$  when following the same path.

## CONCLUSION

This paper has presents an automatic velocity control system for a self-propelled windrower. The control system has a cascade structure involving several subsystems. In particular, the control system includes a hydraulic valve with strongly nonlinear characteristics. A segmented inversion method of the valve nonlinear dynamics such as deadzone has been developed for designing the cylinder position control. Stability of the control system has been proven. The control system has been tested and validated experimentally. The experimental results show that the velocity control system is stable, tracks the reference and rejects disturbances sufficiently well.

### Acknowledgements

This work would not have been possible without the assistance of many people at the CNH Technical Center in New Holland, Pennsylvania, USA.

## REFERENCES

1. Auernhammer, H. 2001, Precision farming -- {The} environmental challenge. *Computers and Electronics in Agriculture*. 30(1-3): p. 31-43.
2. Earl, R., et al. 2000, Potential role of {GIS} in autonomous field operations. *Computers and Electronics in Agriculture*. 25(1): p. 107-120.
3. Fritz, H. 1996, Neural speed control for autonomous road vehicles. *Control Engineering Practice*. 4(4): p. 507-512.
4. Ishida, A., et al. 1992, A self-tuning automotive cruise control system using the time delay controller. *SAE Paper No. 920159*.
5. McMahan, D.H., et al. 1990. *Vehicle modeling and control for automated highway systems*. in *American Controls Conference*. 1990. San Diego, California.
6. Rajamani, R., et al. 2000, Demonstration of integrated longitudinal and lateral control for the operation of automated vehicles in platoons. *IEEE Transactions on Control Systems Technology*. 8(4): p. 695-708.
7. Rajamani, R., et al. 2001, Experimental comparative study of autonomous and co-operative vehicle-follower control systems. *Transportation Research Part C: Emerging Technologies*. 9(1): p. 15-31.
8. Rajamani, R., et al. 2002, Semi-autonomous adaptive cruise control systems. *IEEE Transactions on Vehicular Technology*. 51(5): p. 1186-1192.
9. Rizzoni, G., 1995, *Principles and Applications of Electrical Engineering*. 2nd ed. Burr Ridge, Illinois: McGraw-Hill. 999.
10. Setlur, P., et al. 2003, Nonlinear control of a continuously variable transmission ({CVT}). *IEEE Transactions on Control Systems Technology*. 11(1): p. 101-108.
11. Zhang, N., et al. 2002, Precision agriculture - {A} worldwide overview. *Computers and Electronics in Agriculture*. 36(2-3): p. 113-132.



# AUTONOMOUS UTILITY MOWER

M. A. Zeitzew<sup>1</sup>

## ABSTRACT

Two off-the-shelf John Deere utility mowers were modified for X-by-wire control for the purposes of constructing autonomous vehicles usable in sports-turf mowing applications. The purpose of these mules was to enable the gathering of requirements and customer feedback on such a system. The environment selected initially was that of a baseball stadium. These areas can be characterized as flat, highly controlled and well-groomed, for which precise mowing patterns are necessities.

Typically the operators of these mowers are highly skilled; an autonomous system has the benefits of saving time and labor, permitting the efficient usage of less-skilled employees, and allowing skilled personnel to focus on more complex tasks (such as infield mowing and warning track grooming).

For this application, there are stringent requirements on navigation, path planning and path tracking, while the safeguarding requirements are challenging, but more relaxed than, say, the requirements for golf courses. The calculation of precise position and orientation in this environment requires sensor fusion and is complicated by the fact that frequently the operating area is surrounded by very high walls, limiting sky visibility and preventing the usage of GPS-centric navigation systems. Furthermore, it was desirable to mature the design far enough so that it could be operated regularly by non-technical operators. These results were achieved by developing an accurate local positioning system, making the hardware and software subsystems robust against unexpected failures and constructing a very simple graphical user interface.

This paper will review other relevant existing systems, describe the hardware and software systems utilized, and conclude with descriptions on the performance, customer learning, and description of properties of autonomous systems that enable their integration into a worksite.

**KEYWORDS.** Mowing, Robotic, Stadium, Turf.

## INTRODUCTION

This paper describes a project to fully automate a utility mower for a sports-turf application. The target environment selected is that of a professional baseball stadium. The primary goal for this project is to learn about the durability, performance and value of autonomous systems in real use environments as a means of progressing towards a commercial autonomous machine that meets customer needs and application requirements. Potential customer benefits include saving time and labor, permitting the efficient use of less-skilled employees, and allowing skilled personnel to focus on more complex tasks (such as infield mowing and warning track grooming). As researchers, the benefits of choosing the baseball stadium environment are that they are typically characterized by flat, hard terrain and highly controlled. While the performance requirements are still quite challenging, the aforementioned qualities tend relax them considerably as compared to, say, mowing a public golf course. The overall intent is that this system represents the first generation of a family of autonomous machines with increasing capability and performance levels.

---

<sup>1</sup> NavCom Technology, Inc, A John Deere Company, 20780 Madrona Avenue, Torrance, CA 90503, USA, mzeitzew@navcomtech.com

## Other Systems

In recent times, several autonomous consumer mowers have begun to appear on the market from manufacturers including Friendly Robotics, Toro, Husqvarna, Ambrogio, Zucchetti, Electrolux, and Belrobotics (Plyojump, 2006). None of these machines is near capable of meeting the requirements of a sports-turf application. There has also been a significant amount of research from academia in the area of autonomous mowing, including Carnegie Mellon University (Robotics Institute, 2003) and the University of Florida (Chandler et al., 2000). Also, the Institute of Navigation has been sponsoring a mowing contest for the past two years and this has stirred greater academic interest in the problem domain.

More recently, Self-Guided Systems (Self-Guided Systems, 2006) and McMurtry LTD (McMurtry LTD, 2006) have advertised commercial mowers tailored toward the same application space discussed here. The efforts of these two companies in particular are notable since they have attempted, as we have, to address the issues of highly accurate, precise mowing patterns in areas with sky obstruction, where GPS-centric navigation systems typically degrade beyond system tolerances.

## Overview

First, a brief review of application-specific requirements is given. This is followed by a description of our system hardware and software. Next, a summary of actual performance is presented and then a review of customer learning accomplished during a season of use by two customers. Finally, the conclusion section ends the paper and discusses future work.

## **STADIUM MOWING**

Stadium mowing is considered an art work and generally requires a group of highly skilled groundskeepers working together. While the stadium infield and side line area are usually mowed using a walk-behind mower, the outfield mowing is done using a spinning reel mower, such as the John Deere 2653A (Fig. 1).



**Figure 1. John Deere 2653A utility mower.**

Outfield mowing patterns come in many varieties, but a common feature is that they are constructed by driving straight lines to produce the desired striping effect (Fig. 2). It is imperative that the mowing stripes have uniform width in order to provide a nice look. The striping itself is caused by the blades of grass being pushed in opposing directions and necessitates that adjacent swaths are mowed in opposite directions. Excessive overlap or any gaps between adjacent stripes, and oscillations or other irregularities while driving can ruin the appearance of the field. In our estimation, the composite error in navigation and control (path tracking) needs to stay below 5

centimeters during mowing in order to produce acceptable results; cursory evaluation has shown that expert operators of these machines at normal operating speeds achieve this accuracy.

The outfield mowing task can itself take several hours depending on the desired pattern and may involve more than one mower operating simultaneously. When two mowers operate concurrently, generally they will be mowing in different directions to produce checkered patterns like the one shown in figure 2. In general, each stadium may have different sets of mowing patterns they utilize. Throughout the season, the mowing patterns on the field will change. One reason to change mowing patterns is to prevent excessive turf wear.



**Figure 2. Chase Field, Phoenix, Az. The checkered mowing pattern is produced by mowing the field in the direction from home plate to center field, and also mowing in the direction from foul pole to foul pole. This picture was taken after a day of testing. A side comment is that during this test, the mower was not actually cutting the grass, the reels were lowered while making the passes but were not spinning; the visible striping effect was produced from the rollers on the front of the reels.**

Normal mowing operating speed is around 1.5 - 2.5 meters per second (m/s). At low speeds or when the mower is stationary, the reels are raised to prevent damage to the turf. The reels are also raised any time the vehicle leaves the grass area. Excessive turning on the outfield grass is also frowned upon.

In many cases, the groundskeepers will empty the clippings from the baskets during operation as opposed to letting them fall to the surface. Depending on the length of the grass, this emptying can occur as often as once per pass across the field. This additional task can greatly increase the operation time and either requires coordination with an additional vehicle used to store and haul the clippings or driving the mower itself to a container off the field somewhere.

Particularly on the day of a baseball game, there are many tasks beyond the outfield mowing that must be performed, such as raking and infield mowing. Another motivation for making the mower autonomous is to free the workers to do these other tasks.

### Concept of operation

The current prototype systems are installed by first mounting fixed navigation beacons around the stadium. Next, the field boundaries are surveyed using the navigation system and are input into a map file. The map, together with each set of pattern preferences, is used to create the respective mission plan using an engineering user interface. An example mission plan is shown graphically below (Fig. 3). With our current design, autonomously mowing a checkered pattern requires two separate operations, one for each direction.

Our system is intended to be used in the field by a non-technical operator. As such, it was necessary to not only execute the desired mowing patterns and meet the performance requirements mentioned above, but also provide a simple and intuitive, small, handheld user interface with wireless connectivity to the vehicle.

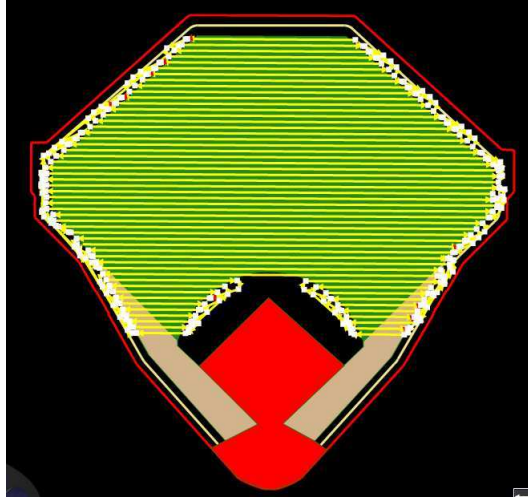


**Figure 3. Foul pole to foul pole pattern.**

The following steps are performed by the operator to execute the autonomous mowing feature:

1. Inspects and adjusts machine (mowing height, reel to bedknife, fluid levels, etc.)
2. Visually inspects mowing area and removes potential obstacles (debris, stuck irrigation heads, etc.)
3. Starts onboard computer system.
4. Starts machine and manually drives onto field.
5. Turns on user interface, ensures proper connection to system and system initialization.
6. Selects pre-computed desired mowing pattern from menu on user interface (Fig. 4).
7. Vehicle begins operation. Operator monitors progress during operation visually and from the user interface, and remains in view of vehicle. Operator has capability of pausing operation at any time (to empty clippings, for example) or exercising remote emergency stop, if necessary (hopefully never).
8. System notifies the operator when the mowing pattern is complete. Operator powers off computer and user interface, or alternatively can select another mowing pattern to execute.

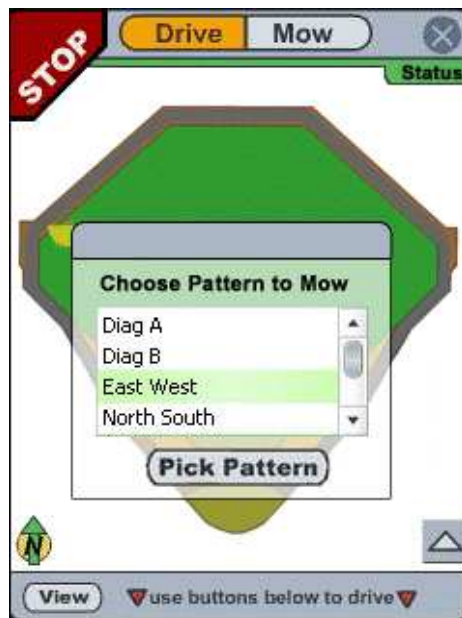


**Figure 4. Screenshot of user interface.**

The system is described in more detail in the next section.

## SYSTEM DESCRIPTION

### Architecture

Most of our software is written using a Model Driven Development tool in C++. Our architecture is such that we can easily adapt to changes in hardware, technology, and application. The same software base has been used successfully on several projects already, with various processors and operating systems, and combinations of sensors and algorithms, vehicles and applications (Fig. 5).

There are five major components that comprise our system: vehicle control unit (VCU), navigation, perception, intelligent vehicle controller (IVC), and user interface. In this application, all five major components reside on separate processors, but in other instances some of the core components reside on the same physical processing unit. Each major component is discussed in more detail below.

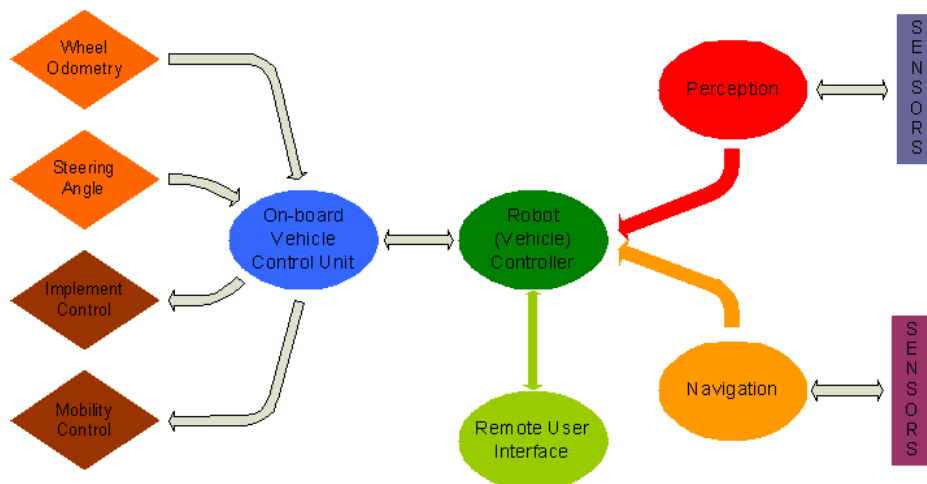


**Figure 5. System architecture. In the figure, "Robot Controller" refers to the Intelligent Vehicle Controller described below.**

### Vehicle and Vehicle Control Unit (VCU)

The vehicle used in this project is a modified version of the John Deere 2653A (Fig. 6). Specifically, the vehicle was converted to X-by-wire control by creating a VCU with a CAN messaging interface to enable control by an external processor. The low-level control algorithms (closed-loop steering and velocity, implement control) were implemented inside the VCU. Command and feedback signals between the VCU and our IVC enabled autonomous operation. At the same time, it is possible to use this machine manually, so that groundskeepers could alternatively use the vehicle as they do the off-the-shelf version of the vehicle available today.

### Navigation

The use of GPS requires good sky visibility. In this application, due to the stringent navigation accuracy requirements, an RTK-GPS solution is required, which requires the use of a base station. Because many of the baseball stadiums have high walls and other obstructions around the field, RTK-GPS is inadequate, even with augmentation by (affordable) inertial sensors and/or odometry sensors. This necessitated the use of alternative technology.

Other earlier prototype systems we made featured local positioning systems (LPS) based on ultrasonic ranging, using time-of-flight measurements from a vehicle to a set of beacons at fixed locations in the environment (Zeitew, 2004). This positioning system had insufficient range to support sports-turf areas, which can involve 100 meter ranges, or more. As a result, we recently developed a new LPS based on radiofrequency signals which exceeds the required range and accuracy requirements. The LPS system requires an antenna on the vehicle and involves RF ranging to battery-operated beacons, typically 6 in this application, mounted on the walls around the stadium. The LPS is part of a larger sensor fusion component that incorporates these ranges together with vehicle odometry information and measurements from inertial sensors (3-axis gyroscope and accelerometers) into an Extended Kalman Filter. Our testing shows the error due to the navigation system is on the order of 2 centimeters RMS (root mean squared) at normal

operating speeds. Moreover, studies indicate that our LPS system has a range of hundreds of meters and can be mass-produced in a cost-effective manner for future products.

Finally, note that the sensor fusion component also admits GPS (or RTK-GPS) instead of or in addition to the LPS; the navigation system was built flexibly to easily allow investigation of different combinations of sensors.



**Figure 6. Modified X-by-wire John Deere 2653A. The RF ranging antenna is at the top of the mast in the front of the vehicle. At the base of the mast is a SICK™ laser used by the perception component, as well as two boxes that house the perception and navigation subsystem computers. The third box just below the facing side of the seat houses the computer with the intelligent vehicle controller. The vehicle control unit is underneath and is not visible in the photo.**

### Perception

Part of our perception research included the investigation of various types of sensors, including ultrasonic, radar and laser, and the usage of differing safeguarding algorithms. Generally, the byproduct of the perception system can be used by other elements for application-specific purposes. In the present case, the only usage of the perception data was to enable vehicle safeguarding.

Because the highest priority in this application is to maintain precise mowing patterns, this alleviated the need to deploy what can generally be a quite complicated obstacle avoidance system. Here, the only acceptable response to obstacles during mowing is to either reduce vehicle speed or stop. Furthermore, since our implementation did not include reverse operation, it allowed us to deploy a greatly simplified safeguarding system onto the fielded system. Specifically, the algorithm relied only on the range scans from a SICK™ laser mounted on the front of the vehicle (Fig. 6). The range scans were combined with vehicle feedback data in order to determine if the current trajectory was clear; if not, the vehicle would reduce its speed as a function of the distance to the nearest obstruction, eventually stopping if necessary.

While this system proved to be reliable and robust against safeguarding humans, walls and other large obstacles, its high cost and inability to detect people approaching the machine from the sides or rear indicate that more work is necessary to provide a comprehensive and marketable safeguarding system.

### Intelligent Vehicle Controller (IVC)

The IVC has several responsibilities in our system, including:

- **Mission Planning.** Ability to construct mission plans based on environment maps and tunable parameters, as well as providing planning services during mission execution. This includes area coverage path planning (Gray, 2006).
- **Mission Execution.** Includes application-specific elements that run during the mission. One such example is the path tracker; the responsibility of the path tracker is to compute steering and velocity commands so that the vehicle follows the desired path. The path

tracking algorithm utilized in this project was a standard PID with feed-forward term to account for path curvature, using the computed path lateral deviation as the error signal.

- User Interface. Gateway to send and receive data from user interface(s).
- VCU Interface. Gateway to the vehicle's actuators and sensors.

### User Interface

Two user interfaces were constructed for this project. The first is best characterized as an engineering user interface, which provided administrative-level access to the functionality of the system. The second user interface was a simplified version that provided only the functionality that was deemed to be useful, usable and desirable. The later user interface ran on a small Pocket PC device and allowed the operator to:

- Select from available maps
- Select from available missions for the selected map
- Start, stop and pause missions
- Monitor progress graphically and other simple feedback signals
- Teleoperate the vehicle if necessary.

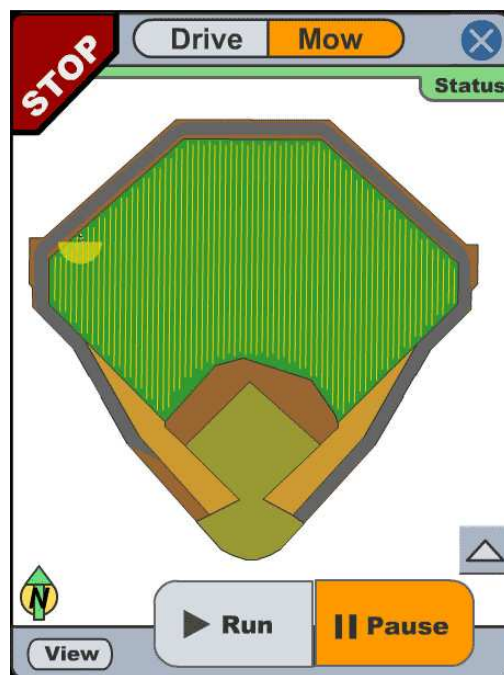


**Figure 7. Screenshot of operator user interface during mowing operation. The mower icon is on left side, shown with a notional hemisphere of coverage by the perception system.**

## **PERFORMANCE**

### Operating in stadiums

Two such vehicles were fielded into professional baseball stadiums, one major league and one minor league. Both of these systems were utilized over the course of several weeks during the spring 2005 baseball season. During the latter portion of the season, the systems were used by the regular groundskeepers as our role migrated to that of occasional observation. The systems were frequently operated without our presence. The groundskeepers were asked to log their comments, and these were collected and later analyzed, the results of which are discussed below in the section on Customer Learning. A third system was used for local testing at a large athletic facility over several fields (mostly soccer fields).

## Path tracking

The table below summarizes typical RMS path tracking performance. The numbers were computed by averaging the RMS errors computed over several missions and the two stadiums. It shows we were able to meet the required subsystem specifications. Note that the total system error is comprised of both the path tracking (how well vehicle tracks reference) and navigation system (how well reference matches ground truth) errors; the latter is not reflected by these numbers and was validated by other means.

**Table 1. Average RMS error for mowing and transport autonomous operation. Transport corresponds to periods where the implement (spinning reels) are disengaged, like during turns between rows.**

Parameter	Initial Specification	Current Performance
Mowing (1.6 m/s)	3.5 cm	2.1 cm
Transport (2.3 m/s)	9.0 cm	3.9 cm

## CUSTOMER LEARNING

The positive feedback from the customers included appreciation for the straightness of mowing stripes and the time savings that allowed employees to focus on other tasks, particularly during baseball team homestands during which the outfield is mowed every day. Having the autonomous machine in regular operation would allow a reduction in the need for highly skilled drivers and potentially allow completion of the required work with a smaller staff.

Other observations we made include:

- The assumptions that operators will be comfortable being a full-time safety rider or that when off-board will give full attention to the machine during autonomous operation are erroneous. Very quickly they become comfortable with the autonomous machine and will ignore it, spending time raking the warning track, painting a logo or other activity, often with their backs toward the machine.
- The need to empty the clippings in some stadiums, and the performance of peripheral tasks such as line painting, present an engineering challenge to further expand the scope stadium automation.
- There would be value in having two (or more) autonomous machines operating simultaneously in order to provide even more time and labor savings, considering that checkered mowing patterns are prevalent in the industry.
- The area bordering the outfield is often cluttered with workers or other equipment. Further progress is needed to safeguard robustly against these hazards.
- The perception system should be upgraded to account for smaller and moving obstacles typically found in the operating environment.
- The ability to detect stuck irrigation heads that fail to retract below surface, which can cause damage to the spinning reels, would also be of value.
- In some cases, a small part of the field is damaged or particularly sensitive and the groundskeeper wishes to avoid mowing or driving over it. The ability to easily adjust the planned mowing pattern from the handheld user interface would be valued.
- The ability to drive in reverse and utilize 3-point turns at the end of rows, rather than always driving forward and turning outside the field, has operational benefit.
- It is worth revisiting the user interface design and form factor, perhaps migrating to a smaller and even simpler design.
- Our system also featured the ability to teleoperate the vehicle, but it turned out to not be sufficiently interesting or useful to anyone other than the engineers who worked on the project.

## CONCLUSION

This paper has described the deployment of two off-the-shelf John Deere utility mowers that were modified for X-by-wire control for the purposes of constructing autonomous vehicles usable in sports-turf applications. It has had two main benefits, first in providing a mechanism for increasing our expertise in autonomous vehicle systems generally and in sports-turf applications in particular and secondly in gaining understanding of the value of such systems to customers. We will continue to improve robustness of vehicle, hardware and software, incrementally improving upon it, and also explore other application spaces. In parallel, we need to build a realistic business model for this type of equipment.

### Acknowledgements

The main sponsor of this project was the Commercial and Consumer Equipment Division of John Deere.

The project team included Mahalalel E. Ahiyya, James C. Beck, Alex D. Foessel, Steven A. Hawkinson, David R. Holm, Boyoon Jung, Mark P. Kaplan, Stewart J. Moorehead, Cameron A. Mott, Andrew J. Norby, Geoffrey M. Phillippe, Jose O. Quan, John F. Reid, Mark A. Schmidt, Scott A. Stephens, Erick C. Velasquez, and Kurt Vander Wiel.

We wish to thank Grant Trenbeath, Scott Strickland, Kyle Waters and their respective crews for both their help and patience in testing and evaluating the system.

## REFERENCES

1. Chandler, R. C. et al. 2000. The Next Generation Autonomous Lawn Mower. In *2000 Florida Conference on Recent Advances in Robotics*. Florida Atlantic University.
2. Gray, S. A. et al. 2006. Path planner and a method for planning a path of a work vehicle. U.S. Patent No. 7010425.
3. Hunt, K. E. 2006, M. A. Schmidt, D. R. Holm, and S. A. Stephens. Method for configuring a local positioning system. U.S. Patent No. 7026992.
4. McMurtry LTD. 2006. Unmanned Mowing Solutions. Available at: [www.mcmurtryltd.co.uk](http://www.mcmurtryltd.co.uk). Accessed 23 June 2006.
5. Plyojump. 2006. Robots that can't jump. Available at: [www.plyojump.com/cant\\_jump\\_yet.html](http://www.plyojump.com/cant_jump_yet.html). Accessed 23 June 2006.
6. Robotics Institute. 2003. Automated Turf Management. Available at: [www.ri.cmu.edu/projects/project\\_422.html/cant\\_jump\\_yet.html](http://www.ri.cmu.edu/projects/project_422.html/cant_jump_yet.html). Accessed 23 June 2006.
7. Self-Guided Systems. 2006. Hybrid Z38. Available at: [www.selfguidedsystems.com/media/literature.pdf](http://www.selfguidedsystems.com/media/literature.pdf). Accessed 23 June 2006.
8. Zeitzew, M. A. 2004. System and method for navigation using two-way ultrasonic positioning. U.S. Patent No. 6674687.



# A BASIC APPROACH TO IMPLEMENT GUIDED TRACTOR CONTROL

R. Freimann<sup>1</sup>

## ABSTRACT

Within a continuous development of mobile agricultural machinery the application and further introduction of electronic controls is offering the fare most potential for working processes optimization. The article gives an introduction to tractor and implement controls, especially targeting implement guided tractor control, underlined with two executed examples for this advanced control design. A structured development model and basic knowledge on safe and robust control loop set-ups were developed. Potential conflict scenarios within the multi master control system of driver, tractor, implement and independently pre-planned task control were identified and solved by arbitrational state strategies. The two exemplarily executed demonstration examples utilize different control commands to functions and interfaces of the tractor. One example is an implement guided headland management; the other is a PTO torque guided tractor speed control. Both automation strategies have been pre-simulated and implemented introducing ISO 11783 communication protocol. Results from final field tests are closing the paper.

**KEYWORDS.** Implement Guided Tractor Control, ISO11783, ISOBUS, Process Optimization.

## INTRODUCTION

The improvement of handling and comfort in general is a prior motivation for the employment of electric and electro-hydraulic systems. In particular the goal of maximum work efficiency along with high precision still remains focus of research and development on mobile machines [1, 2].

In order to enhance functional safety and the efficiency of working processes on mobile agricultural machinery today a multiplicity of networked sensors and controllers are already introduced to modern machine systems of tractors, implements and combines. Although self propelled machines are becoming more and more process optimised, the primary focus within tractor implement combinations is on independent supervision and control of single implements or the tractor and its interfaces separately.

An advanced automation approach that focuses the tractor as a process master would need the implement manufacturers to provide a kind of “driver”-software to be integrated into the tractor ECU. The implement ECU then could be reduced to a smart actuator [3, 4].

The approach of “implement guided tractor control” shifts the process control to the responsibility of specialized implements, which may use existing and mostly standardised energy interfaces on the tractor process-optimally according to their installed functions and strategies [5, 6].

The defined ISOBUS communication protocol (ISO 11783) [7] as a specialized CAN [8] based network protocol for agricultural machinery comes with all the needed definitions to realize such advanced controls. Table 1 shows a rough overview of achievable controls in a closed loop of tractor and implements.

---

<sup>1</sup> IAV GmbH, Rockwellstr. 15, 38518 Gifhorn, Germany, ruediger.freimann@iav.de

**Table 1. Tractor information and external commanded resource access.**

Tractor system	Control Target (tractor resource)	Actual Value	Transmitted target information
<b>Hitches</b>	Rear Hitch Position	Primary or rear hitch status	Hitch and PTO commands
	Front Hitch Position	Secondary or front hitch status	
<b>PTO Speed</b>	Rear PTO rotational Speed	Primary or rear PTO output shaft	
	Front PTO rotational Speed	Secondary or front PTO output shaft	
<b>Hydraulic Valves</b>	Operation Status and Oil Flow of Hydraulic Valves	Auxiliary valve (1-15) measured flow Auxiliary valve (1-15) estimated flow	Auxiliary valve (1-15) command
<b>Power beyond</b>	Hydraulic pump flow	Auxiliary valve 0 measured flow Auxiliary valve 0 estimated flow	Auxiliary valve 0 command
<b>Power train</b>	Theoretical velocity	Wheel based speed and distance	Implement remote control command
	True velocity	Ground based speed and distance	
	Momentary valid velocity target	Implement remote control command tractor response	
	Momentary valid velocity saturation	Implement remote control command tractor response	
<b>Navigation</b>	Front steering angle	Implement remote control command tractor response	Implement remote control command
	GPS Position data	Navigation system message	-

### PROCESS CONSIDERATION

Within the conventional automation approach tractor and implements are operated separately. Even new approaches like teach-in functions are based on men machine interfaces residing on the tractor. System optimisation is divided into “tractor control” and individual implement control as shown in figure 1 (left). The co-ordination of tractor and implements remains operator’s task. The function of the ISOBUS is reduced to an advanced communication system.

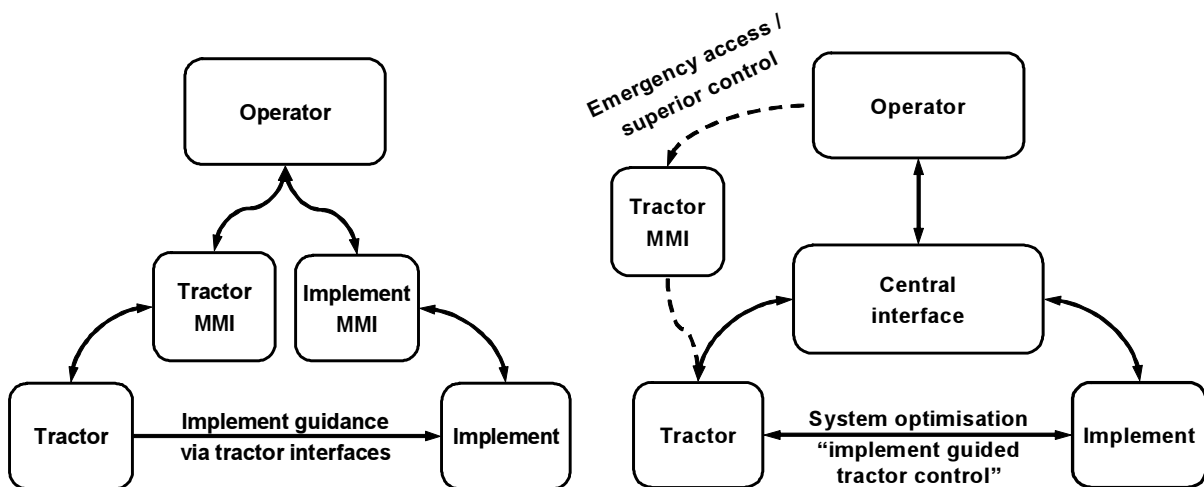


**Figure 1. Conventional (left) and advanced (right) communication structure (MMI = Men-Machine-Interface).**

The right side of figure 1 shows an alternative set-up of the system communication according to the defined possibilities of ISO11783: The top level system co-ordination can be reduced to a process related minimum of driver intended control targets and start/stop commands. A sensor-actor based control algorithm then may be transferred to specialised implements, while direct operation control of the driver could be reduced to emergency access, process specific super control and exception handling.

This communication structure implies that there is a multiple access also to single tractor interfaces at one time possible. Within the standard specification of ISO 11783 these are the operator, attached implements and additionally the task controller. Modern tractors and the

upcoming part 14 of ISO 11783 hold a fourth automatic function accessing the tractor resources. This is the “tractor management” and “teach-in and replay” functions.

To robustly access functional safety and potential conflict scenarios a tailored procedural development model according to the commonly known V-model for software design was applied (Fig. 2). The V-model process details more and more into decomposed function requirements and module design. It starts with a system analysis and fits to the software integration at the very bottom. Following the path up to the complete system validation more and more integrated function models are tested against their prior defined requirements.

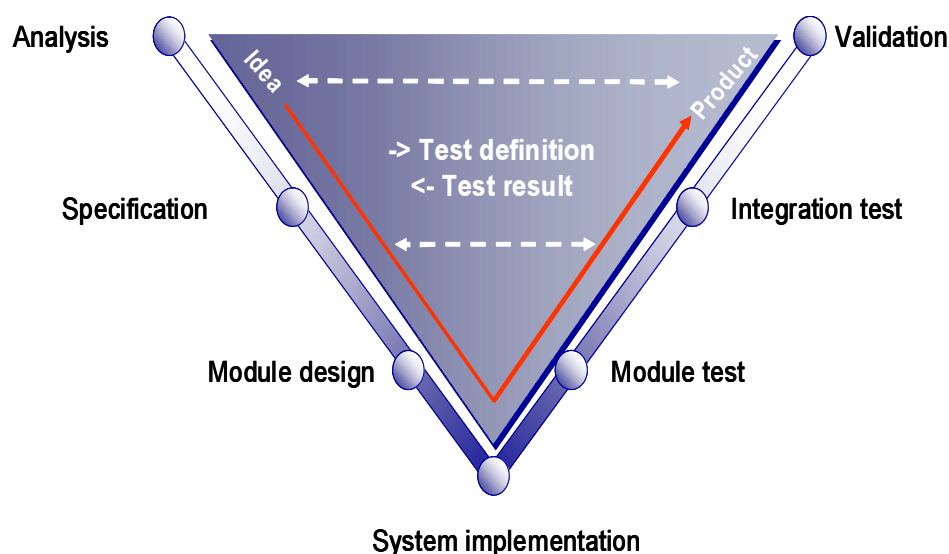


**Figure 2. Procedural development mode; V-model.**

To allow more than one controller to be active at a time, an access conflict could be solved by a distinct as well as resource and configuration specific priority strategy. Within a centralised approach this state control preferably resides within the tractor ECU. This requires the tractor ECU accessing not only the tractor internal functions and the ISOBUS, but also all necessary operator interfaces.

### **REQUIREMENT ANALYSIS AND DEVELOPMENT TARGET**

In order to prove the feasibility of an implement guided tractor control according to ISO11783 the demonstration project had to cover a set of requirements. First of all suitable automations have to be developed targeting partly simultaneously at tractor interfaces like hydraulic valve or speed and hitch commands. In addition also operator interfaces and tractor or the implement internal controls should be included. Also open control loops for precision farming and site-specific applications may be regarded using the defined ISOBUS task controller.

Figure 3 shows the selected tractor implement combination with impactor, rotary tiller and pneumatic seeder. This combination comes closest to the settled requirements and represents also a very common system set-up within modern grain cultivation.

In variance to a today’s standard set-up the seeder is actively hitched up to the tiller and not fix mounted. For the purpose of increasing the complexity of the demonstrator set-up this offers an additional control for a hydraulic valve actuation. To prove the new automation approach the demonstrator combination was subject to two advanced “implement guided tractor controls”.

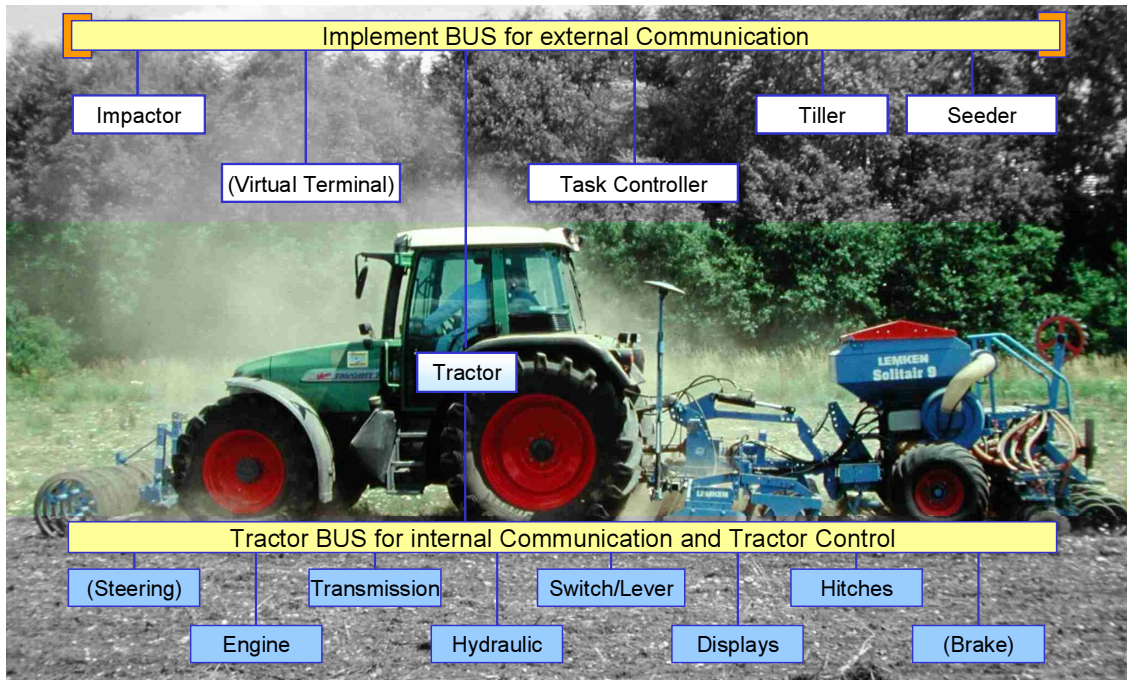


Figure 3. Tractor implement combination with impactor, rotary tiller and pneumatic seeder.

Headland management

The first examined automation was an advanced headland management with a single button engage/disengage control. For operation the driver simply pushes the control button when approaching the headland periphery (Fig. 4). The aiming distance from the drivers' viewpoint can be pre-adjusted via the virtual terminal. Alternatively it would also be possible to feed the task controller from navigational GPS information. Once the button is pushed, all implements individually control their tractor interfaces according to the requested engage/disengage operation. Based on pre defined parameters within the tractor co-ordinate system the implement ECUs calculate their driving distance from the tractor speed information. Each implement commands a maximum velocity to be arbitrated at the tractor ECU (see below). The impactor additionally actuates the front hitch. The tiller commands the rear hitch, the PTO and the hydraulics for the markers. The seeder commands the hydraulics for the additional hitch up and the pneumatic fan power supply.

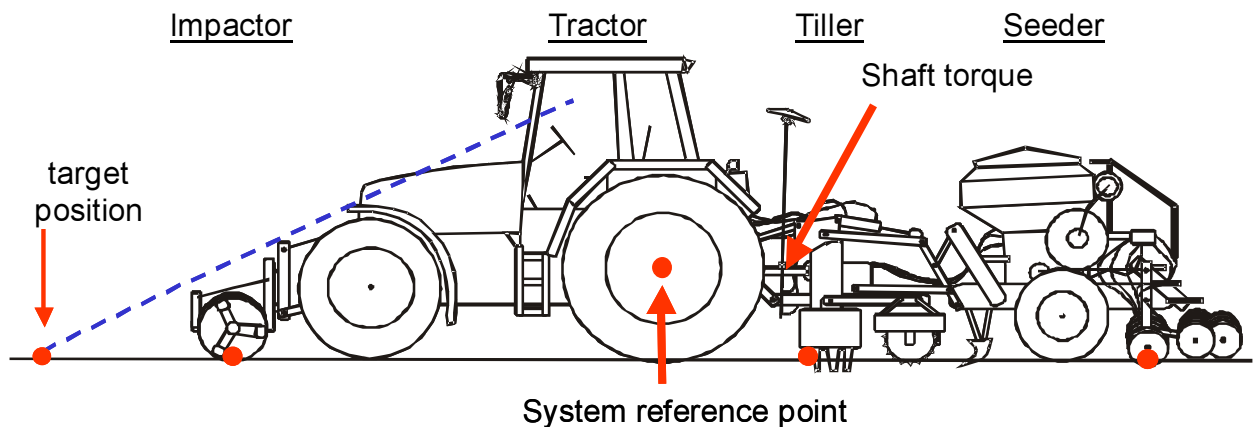


Figure 4. Reference points of the example automation.

Soil cultivation

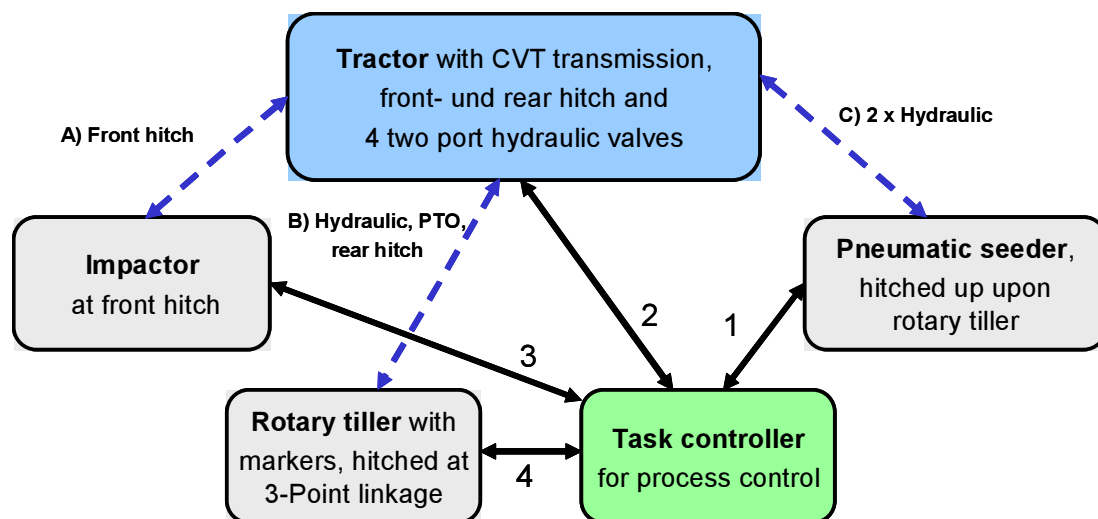
The second examined automatic function was a potential optimisation of the seedbed preparation by target soil treatment. Controlled variable is the tractor velocity guided by a nearly kept constant PTO torque input to the rotary tiller. The idea behind this automation was that for soil preparation quality a site with more compact soil would need more tiller rotations per area than a site with less

compact soil. While the PTO speed - due to the tiller design - was kept constant the driving speed is a possible variable. Agricultural proves of possible benefits were not subject to the investigations.

### AUTOMATION STRATEGY BASED ON ISO 11783

Based on tractor ECU class 3 properties - as defined in ISO 11783 part 9 [9] - the two automation strategies have been realised according to the signal and protocol specification of ISO11783 part 7 (implement BUS). The communication structure in figure 5 shows the sequential process communication within two hierarchical levels. On the top level (1, 2, 3, 4) the task controller is in charge to process the overall system application according to the implement working states (engage/transport/park) and the required application rates (e. g. seeds per acre). On a sublevel of the automation (A, B, C) the implements themselves are controlling the tractor interfaces according to the task controllers' commands. Except manual steering and speed control on turning manoeuvres and manual row guidance the driver interfaces during operation can be reduced to:

- Start/Stop initialisation for the headland management (one button)
- Pre setting of the individual desired view point to the headland periphery (distance)
- Pre setting or on-line adjustment of individual chosen limits for driving velocity and PTO torque as potential variables for the soil preparation quality by tilling intensity.



1 - 4: Process control of system functions via task controller  
A - C: Remote control of tractor functions via implement ECU

Figure 5. Communication structure on the implement-BUS.

### MODULE DESIGN AND SYSTEM SIMULATION

The first function decomposition of the tractor implement combination is on system level, assigning an individual macro software component to the tractor and each implement. The next decomposition step is to separate subsystem internal functions (e. g. application rate control of the seeder) from top-level related functions (e. g. velocity control). Along with the software component decomposition the signal interfaces have to be defined. On top-level level this interfaces are defined by ISO 11783.

To achieve a complete system simulation including the ISO defined communication, a real-time co-simulation of Matlab/Simulink for the functional part and CANoe for the communication part was developed [10].

Simulation set-up

Within Matlab/Simulink a structured model-in-the-loop simulation was developed including modules for each controller software component. The simulative “backbone” of the physical tractor-implement system and the environment was simulated based on energy and force feedback loops from implements and environment to the tractor [11]. CANoe itself is a network design tool including simulation of physical CAN behaviour. Additionally the CANoe option ISO11783 comes with a predefined ISO data base and a build in functionality of a virtual terminal and ISOBUS network management. Co-simulation of both tools, Matlab and CANoe, was done via a commonly accessed variable data base. CANoe was set to simulation timing master in order to prove the correct ISO communication. An additional CAN hardware interface connected the simulated CAN-BUS to a physical CAN communication and allowed to validate the Simulation in an early state. Tests were done among the manufacturer groups that participated to the ISO11783 “plug fests”.

Module design and safety

As an example for an “atomic” (least decomposed) function module figure 6 displays the chosen approach to a tractor ECU safety module related to control access to tractor internal resources. Depending on the system status this module proves the necessary states to grant access to tractor internal function to the requesting source. Within the arbitration priority check the driver access always comes first, followed by the tractor ECU as the energy co-ordinating instance. On third priority are the implement ECUs which are responsible for machine control on a sublevel. The last priorities were “external” target values coming from application control or diagnostic and service functions.

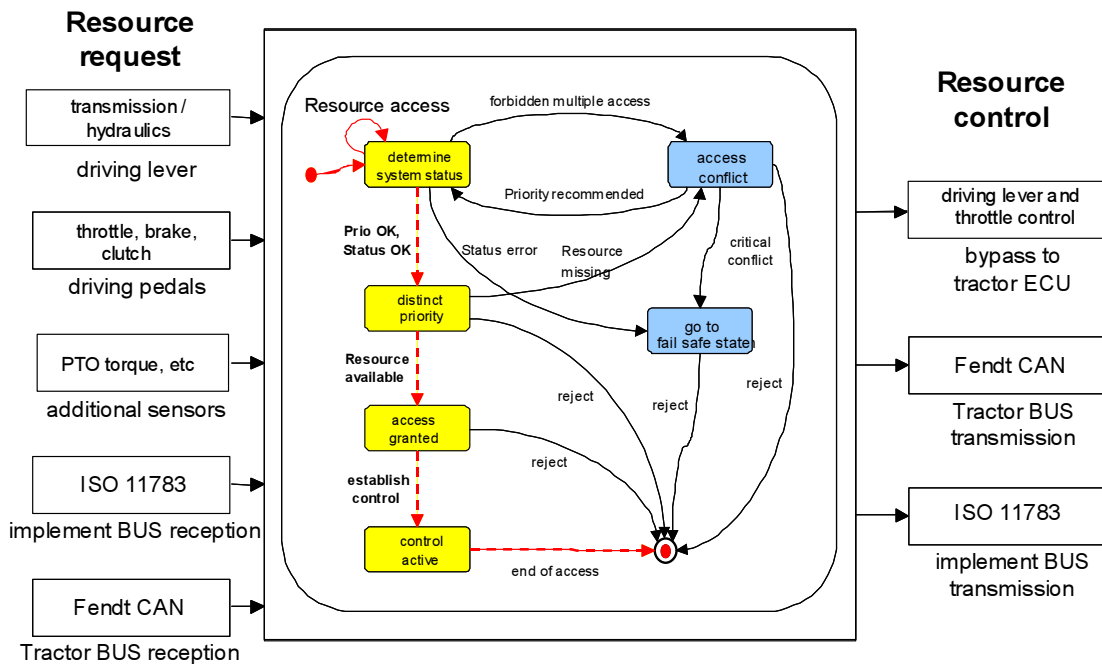


**Figure 6. Approach to a tractor ECU safety module.**

A closer look to the different tractor resource leads to a basic distinction between multiple and single accessible resources. While single accessible resources like the front or rear hitch have to be dedicated to a single requesting controller on system set-up time, a multiple accessible resources like the driving speed can be managed on run time for example by granting the lowest demanded speed [12].

Within the model-in-the-loop simulation it was possible to verify the chosen strategies without the potential risks of damage during a real field test. A second step of testing had been done by integrating the real tractor into the simulation using a CAN hardware interface to CANoe.

## FIELD TEST AND VALIDATION

For the verification of the newly designed functions the technical university of Munich had offered an uncultivated field that could be prepared as needed. The surface was quite plane and homogenous without reasonable differences in the compactness of the soil. In order to achieve reproducible test conditions for the headland management and to prepare significant changes in soil compaction a reference field was designed within the test field. The preparation had been done by cultivating or compacting the soil transversally to the working direction as shown in figure 7.

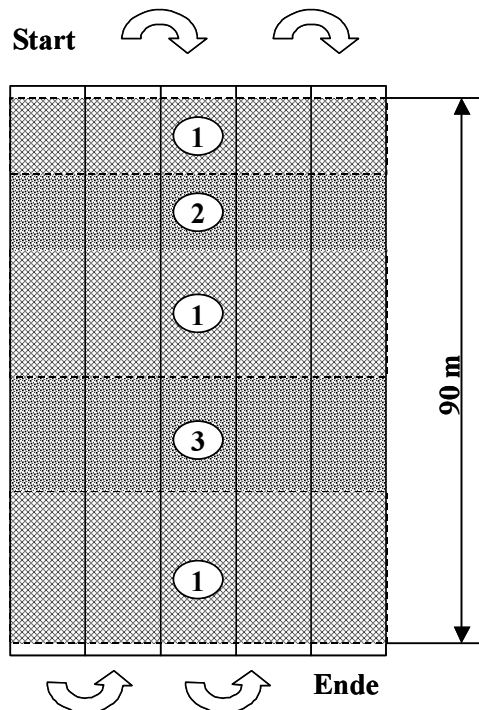


Figure 7. Designed test field.

Examining the PTO torque as a possible control variable for a continuous quality in the seedbed preparation especially the variance of the soil compaction not the absolute value influences the test results. For the control pre-settings the operator only has to set a target torque value, which would equal the desired, working performance - depending on the soil parameters. Setting the target to an expected average value the system would control the velocity accordingly. Setting the target to the maximum scale the system would try to set the velocity as fast as possible until the equalling soil resistances or another speed limit is reached. Individual absolute velocity limits from all connected controllers pretend single system components from overload because the arbitration to tractor velocity is strictly done with a "select low" approach.

A basic dependency between PTO torque and driving speed was proven by preliminary speed variance tests. Also the dependency between working depth and PTO torque was proven as expected. An analysis of the influences of other soil parameters (e. g. water) was not undertaken.

Based on the test results the implement guided velocity control was pre-designed in the simulation set-up. Due to the working forces and the system inertia the best results were achieved by computing big steps to the target speed with even small deviations from the target torque. Big steps within the calculated target velocity are demanding the transmission controller of the tractor to select the maximal acceleration range, thus resulting in an overall sufficient fast response to the actual system velocity.

Figure 8 shows a working trace with an active velocity control guided by the tiller. Under the active control the PTO torque (5) is not constant but still varies around the operator-selected value of 300 Nm. On the other hand the controlled velocity (1) varies very much. The tiller ECU sets target values between 0.75 and 1.5 m/s to the velocity to be processed by the tractor ECU.

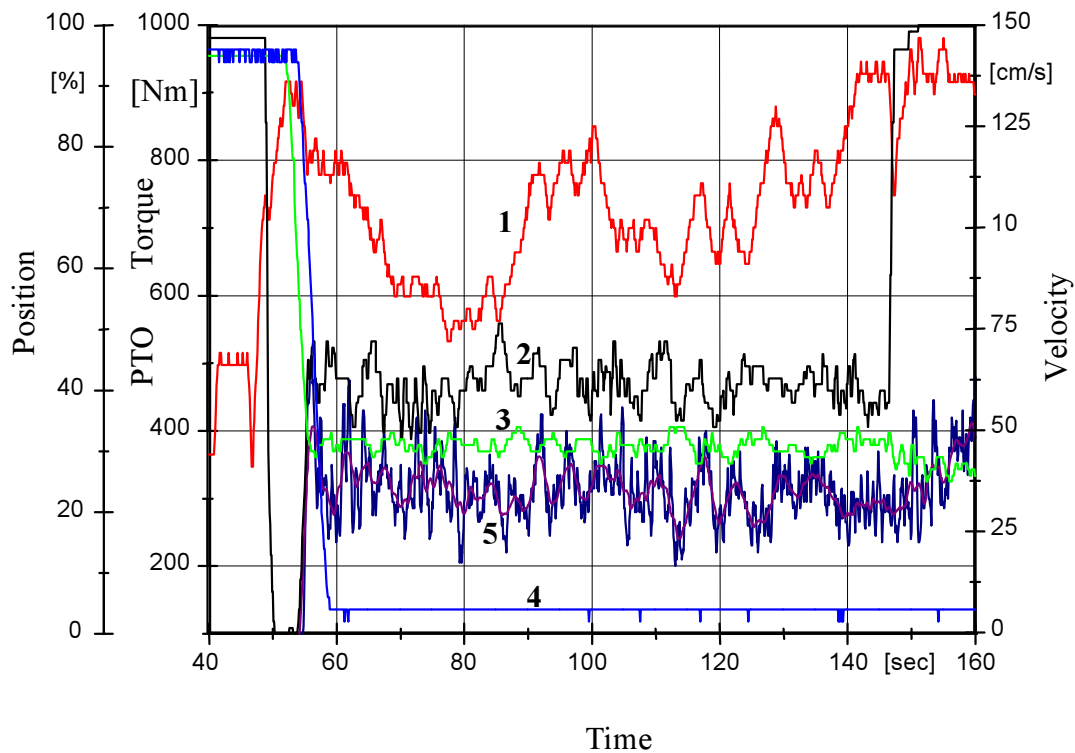


**Figure 8. Trace with PTO torque guided tractor velocity (1 = velocity, 2 = pos front hitch, 3 = pos rear hitch, 4 = pos hitch-up, 5 = PTO torque).**

Target of an optimised headland management is time saving and operator workload release during the turning manoeuvre. While the system engages all velocity controllers within the tractor implement system are active. The implements feed their designed maximum velocity and their actual requested target value to the tractor ECU. Superior to that are a driver selectable maximum and an eventually active tractor management. The starting point of the implement-individual engage procedure is calculated from the actual velocity. Starting with an average value an integrated continuous self-learning algorithm optimises the engagement timing from activation to activation to better hit the target point. Deviations of the implement mass due to seed consumption or collected dirt on the implements therefore could be as well adjusted as deviations in the oil viscosity.

Figure 9 magnifies a trace to a close up of the real engagement procedure. Started with the “one-button” control the tractor accelerates until the impactor ECU sets a first limit to the target velocity (1). The tractor is decelerated only a short time. This allows the impactor to engage at the correct position. At that point both rear implements are still carried in transport status and the unbalanced weight causes the tractor to pitch backwards. The front hitch (2) therefore drops to the tractor indicating 0% front hitch height. Engaging the rear implements the tractor pitches back to the front again and the impactor is released to float on the ground at about 40 % front hitch position. Since the impactor is engaged, the impactor ECU sets the target velocity to “don’t care” and the tractor accelerates again until it is decelerated by the partly parallel engaging tiller and seeder. After the whole combination is engaged, the above described process control of the tiller ECU takes over the velocity control of the tractor.

## CONCLUSION

The applicability of the chosen development process for advanced agricultural field-automations had been approved by realisation and test of two advanced implement guided tractor control functions. Simulated network nodes were used to pre-determine the communication effort and the standard conformity to ISO11783. The simulation based system and controller layout could be optimised by feed back from the test results.

The functional layout was based on a system simulation and did deliver Simulink files as a detailed software design duty book for each network node. Using the dSPACE MicroAutoBox as a

rapid prototyping system for the tractor ECU, the respective Simulink file could be integrated directly into the tractor controller. The implement ECUs of impactor, tiller and seeder were C-coded strict to the duty book. The CAN-BUS simulation has been a substantial support for design and test of the real tractor ECU without the risk of connecting the real implements in the first.

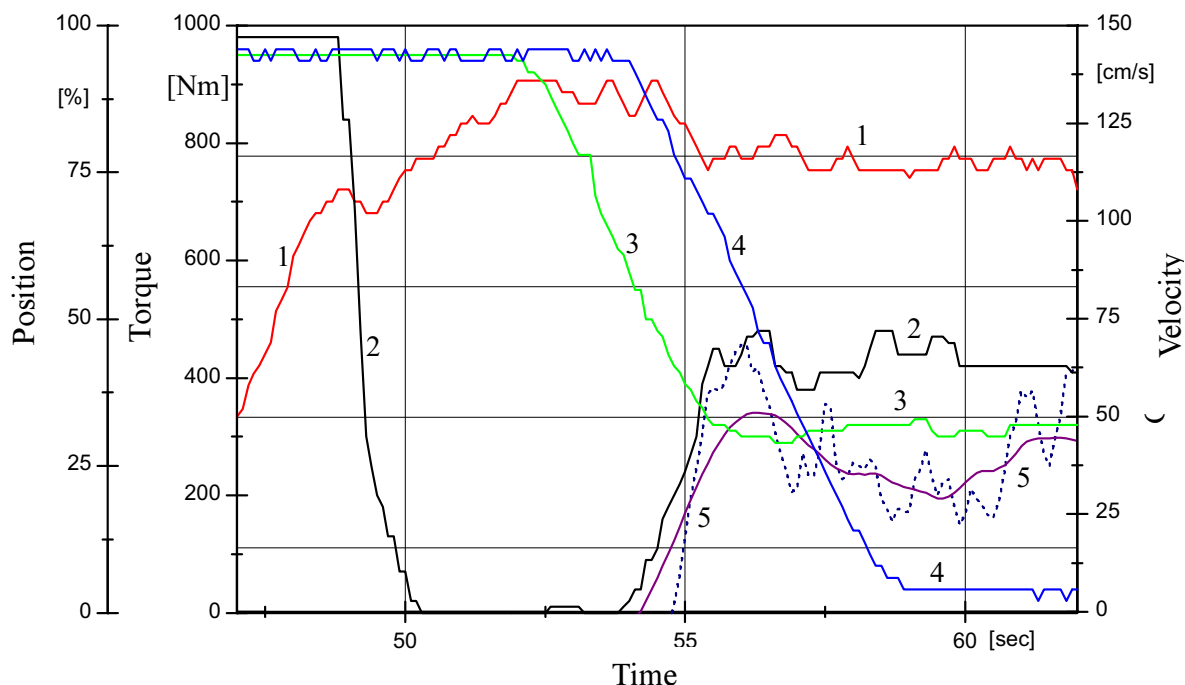


**Figure 9. Trace of implement guided tractor velocity during engagement (1 = velocity, 2 = pos front hitch, 3 = pos rear hitch, 4 = pos hitch-up, 5 = PTO torque).**

The introduced automation and safety strategy for process automation also leads to a potentially general approach for a self-configuring and secured interoperation of tractors and implements of different make - based on ISO11783. The suggested automation and communication structure and the arbitration to tractor resources by priority and resource type are allowing a universal approach to resolve access conflicts within an implement guided tractor control. The chosen automation examples provide an interesting outlook to the possible challenges and benefits to come introducing "implement guided tractor control" to the automation of agricultural off road equipment.

#### Acknowledgements

The author likes to thank the Deutsche Forschungsgemeinschaft (German Research Foundation) and the companies AGCO-Fendt (tractor), Lemken (implements) and Walterscheid (torque sensing drive shaft coupler) for generously supporting and assisting this research project at the Technical University of Munich. Many thanks also to the former colleagues of the standardization working group of ISO TC19/SC23/WG1 and the experts at the VDMA "Fachverband Landtechnik". Very special thanks are going to Prof. Dr.-Ing. Dr. h.c. K.-Th. Renius for supervising the project and to the former colleagues at the institute of agricultural machinery, especially to my workmate Dr.-Ing. Marcus Martinus who focused on the functional safety in this research project [5].

#### **REFERENCES**

1. Auernhammer, H.: Prozesssteuerung und Prozessautomatisierung in der Pflanzenproduktion. In: Agrarinformatik, Hrsg.: Dolusschitz R. und j. Spilke, Eugen Ulmer, Stuttgart, 2002.
2. Renius, K. Th.: Traktorenentwicklung unter besonderer Berücksichtigung der Fahrdynamik und Elektronikanwendung. In: Zaske, S. und H. Ganzelmeier (Hrsg.): Anwendungstechnik in Pflanzenschutz und Traktorentechnik. Fortschritt-Ber. VDI Reihe 14, Nr. 109, S. 1-24. Düsseldorf: VDI-Verlag 2002.

3. Hofmann, R.: Traktorelektronik neue Generation: Konzept und Realisierung am Beispiel des Fendt Favorit 700. Tagung Landtechnik 1999, Braunschweig, VDI-MEG. S. 75-80, Düsseldorf: VDI-Verlag 1999.
4. Seeger, J.: Traktormanagementsystem. In: Jahrbuch Agrartechnik 12 (2000), S. 41-46 u. 339, 340. Münster: Landwirtschaftsverlag 2000.
5. Martinus, M.: Funktionale Sicherheit von mechatronischen Systemen bei mobilen Arbeitsmaschinen. Fortschritt-Berichte VDI Reihe 12, Nr. 586. Düsseldorf: VDI Verlag 2005.
6. Freimann, R.: Automation mobiler Arbeitsmaschinen - Gerät steuert Traktor. Fortschritt-Berichte VDI Reihe 14, Nr. 116. Düsseldorf: VDI-Verlag 2004.
7. -, -: Traktoren und Maschinen für die Land- und Forstwirtschaft - Serielles Kontroll- und Kommunikationsnetzwerk - ISO 11783. Berlin: Beuth Verlag 2002 ff.
8. -, -: ISO/DIS 11898-2 Straßenfahrzeuge – CAN-Protokoll – Teil 2: Ausgabegruppe für hohe Übertragungsgeschwindigkeit (Überarbeitung von ISO 11898: 1993 und deren Änderung 1: 1995) Berlin: Beuth Verlag Ausgabe 2001-09.
9. Freimann, R.: Incorporation of ISO 11783 Data Communication Standard on Agricultural Mobile Equipment, Part 9 Tractor ECU. Continuing Professional Development Workshop CPD #17, ASAE/CSAE-SGCR International Meeting, 18.-22.07.1999 Toronto, Canada (1999).
10. Freimann, R. und P. Fellmeth: Prüfung der Kompatibilität von CAN-Netzwerken zur ISO 11783 durch Simulation. VDI-MEG-Tagung „Landtechnik 2001“, Hannover 9./10.11.2001. In: VDI-Berichte 1636, S. 89-94. Düsseldorf: VDI-Verlag 2001.
11. Meys M.: Mathematisch logische Simulation eines Traktor/Geräte-Gespans. TU München, Lehrstuhl für Landmaschinen, unveröffentlichte Diplomarbeit Januar 2001.
12. Martinus, M. und R. Freimann: Prozesssicherheit Landmaschinenelektronik am Beispiel „Gerät steuert Traktor“. Agrartechnische Forschung Heft 3 Landwirtschaftsverlag Münster Hiltrup 2002.

# NEAR INFRARED SPECTROSCOPY FOR QUALITY MEASUREMENT ON FORAGE SWATHES – FIRST TEST BED EXPERIMENTS

M. Rothmund<sup>1</sup> and M. Strobl<sup>2</sup>

## ABSTRACT

The paper works out a concept to develop a new NIR-based monitoring system for forage quality. It should be discovered, if it is possible to measure quality parameters with a sensor system moving over a forage swath. The influence of environmental parameters caused by unfavorable sample presentation to the sensor on the measured spectra was figured out. For this, a test bed was constructed and repeatable experiments with small hay bales were carried out. The results show that the values of environmental parameters are predictable by the NIR-measurement after creating a sufficient calibration model. This again means, that possible impacts of sample presentation to the measurement have to be considered in the further research work on that monitoring system.

**KEYWORDS.** Forage quality monitoring, Near-infrared Spectroscopy, Process quality.

## INTRODUCTION

Using site specific farming to optimise the cost-value ratio (economical aim) and to increase the environmental sustainability (ecological aim) (Auernhammer, 2001) requires the acquisition of many process parameters. In doing so, it is necessary to measure, process and evaluate these parameters in real-time enhancing the process quality.

To date, systems recording data about the quantity and the quality of materials predominantly were tested and partially implemented on combine and forage harvesters (Demmel et al., 1992 and Isensee et al, 2001). Up to now, quality measurement in forage crops is tested and used on small experimental harvesting systems (Paul and Häusler, 2002). But on regular farms, forage processing chains, sensor-based measurement systems for site specific quality information are not provided, so far. Implementing this technique can help to decrease forage material losses, that are estimated between 5 to 30 percent (for silage and hay) (Rahmann et al., 2003). The knowledge of detailed quality information in all steps of the forage processing chain (mowing, harvest, storage and feeding) can be used to minimise losses and to bring up the efficiency and quality of forage production.

Measuring quality data in lab analysis, Near Infra-Red Spectroscopy (NIRS) is applied increasingly (Hruscka, 1987). Adjusted hard covered and water proof NIRS-sensors are particularly suitable for the installation on mobile harvesters. Thus NIRS sensors were already integrated in combine and forage harvesters (Rademacher, 2003 and Kormann and Auernhammer, 2000) and used especially for field experiments.

On-field analysis can be described as a quasi-continuous measurement with an automatic sample feeding. This way, the analysing method is brought to the material - not vice versa – to get high frequent quality information of many samples in a short time period. An additional benefit of this method is avoiding sampling failures as well as sample aging.

---

<sup>1</sup> Crop Production Engineering, Technische Universitaet Muenchen, Weihenstephan, Germany, matthias.rothmund@wzw.tum.de

<sup>2</sup> Institute for Rural Structural Development, Business Management and Aggroinformatics, Bavarian State Research Center for Agriculture, Muenchen, Germany.

## NEAR INFRARED SPECTROSCOPY (NIRS) AND SAMPLE PRESENTATION

First of all, in-field NIRS-sensors detect diffuse reflection of a sample as spectra information by an opto-electronical measuring method. Using this spectra information in a mathematical model, quality parameters, mainly substance contents, of the material can be estimated. The quality of sample conditioning and the way the sample is presented to the sensor is named sample presentation. It is a central influencing factor on the accuracy of value prediction and for this reason on the measurement error as well.

In labs sample conditioning is done uniformed and regulated by measurement standards. This means that the sample presentation is standardized. Bringing the NIRS method to in-field processes, the foregoing purification, homogenization or drying of the sample material is mostly impossible. In fact, new additional sources of irritation such as variations in the intensity of light, temperature or humidity occur. All these disturbing factors have to be cleared by a real-time standardizing of sample presentation (technical approach while sampling) or by an elimination of influences in the value estimation model (mathematical approach after sampling).

Using mobile NIRS systems on harvesters with bypass pre-conditioning, a higher quality of measurement by a more homogeneous sample presentation is expected. But potentially bypass systems strongly interfere the process technique. A mechanical problem in the bypass-system can endanger the application-reliability of the whole harvesting process. Without a bypass, the NIRS sensor system has to measure at the standing crop or directly at the previously conditioned material flow.

### OBJECTIVES

At nearly all steps of the forage harvesting process (mowing, conditioning, swathing and harvesting) the forage is conditioned as a swath. Consequently, implementing a NIRS sensor system for on-swath quality measurements can be used very effective and flexible. Thus, in this work preparatory investigations on the feasibility of such a NIR-based quality monitoring system for forage swathes should be carried out.

### APPROACH

The implementation of a prototype for geo-referenced online quality data measurement at forage swathes shall be based on a four-step concept:

1. Determining of the general applicability of NIRS acquiring quality information of forage.
2. Analyzing the influence of a varying sample presentation at continuous swath measurements on the measuring results.
3. Adopting estimation models to quantify the substances of content of swathed forage. The aim is to eliminate disturbing environmental effects by mathematical corrections based on additionally measured or calculated parameters.
4. Logical and technical integration of this new measuring method "NIRS on swathes" in the harvest process chain.

The general applicability of the NIRS-method measuring the forage quality (step 1) is already confirmed and well-introduced in labs.

The objective in this paper is observing the migration-effects from lab to varying in-field conditions (step 2). For this, especially the individual influences of separate parameters of the sample presentation (actual state of the forage, material position related to the sensor, light, temperature, humidity and relative speed) were checked, because those influences are not existent in a lab environment and their impact on swath-based measurements is not known. To get a reliable spectra information, a test bed was constructed and reproducible test bed experiments were conducted.

Checking the usability of existing calibration models for forage with this new kind of sample presentation (step 3) is part of the on-going work, but not yet covered in this paper. The

development of an in-field prototype measuring system and the implementation of new calibration models specialised for “mobile NIRS on swathes” (step 4) should be the task for future projects.

## RESULTS

At first, a suitable test bed was developed to ensure the reproducibility and the accuracy of simulated in-field measurements (Fig. 1). In this test environment, a NIRS-sensor (ZEISS CORONA 45 NIR) was guided in repeated experiments over a swath where both the relative speed and the surface pressure were controlled. For these first experiments, the swath was simulated by a set of small hay or straw bales due to easier handling (constant surface texture, only a minimal change of substance of content).

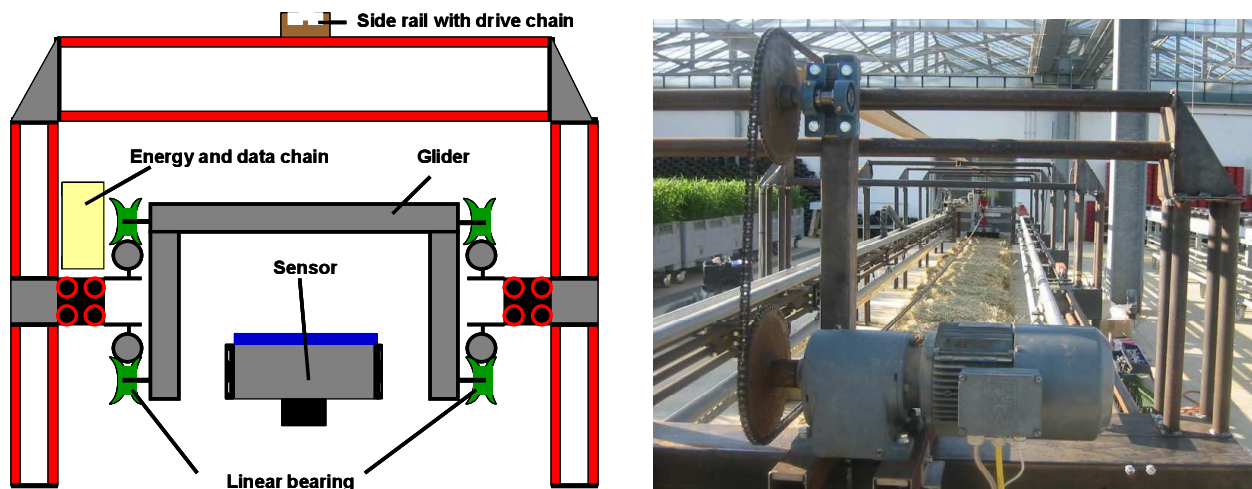


Figure 1. Test bed for NIRS measurements on forage swathes, profile view (left) and picture (right).

Additionally to the spectra, the following six environment parameters of sample presentation were acquired during each run of each trial:

- Relative speed between sample material and sensor unit
- Temperature of the ambient air
- Temperature of the swath surface
- Humidity of the ambient air
- Disturbing light irradiation (sunlight)
- Material type and its exposition to the sensor

The data were analyzed with the software WINISI (InfraSoft International, Version 1.50). On base of the data, six estimation models were generated, each with all spectra data and focussed on calculating the values of one of the six environmental parameters. The significant effect of one environmental parameter is verified, if the estimation model based on its NIRS data is able to forecast the quality and quantity of its effect in a backwards way out of one spectra. In the model, by a multivariate regression method, correlations between the measured environmental parameters (for example the temperature of the ambient air) and the spectra information are searched for. In this case, principal component analysis was chosen for searching the spectral data for wave length reflection information interrelated with the values of environmental parameters. Using the correlations found, those parameters can be predicted by means of the model. For model validation the measured parameters as well as the predicted parameters are compared using the regression coefficient. Figure 2 shows the XY-plots and regression lines of the different predicted and measured parameters with the material “hay bales”. All parameters of sample presentation show a squared correlation coefficient (RSQ) higher than 0.94, excluding the parameter “relative speed of the sensor-unit” (0.89). Thereby, the strength of the dominant water interference specific sections of the spectra correlates with the strength of the parameters “humidity”, “temperature of the

ambient air” and “temperature of the swath surface”. This explains the significant influence of this three parameters of the sample presentation on the spectra.

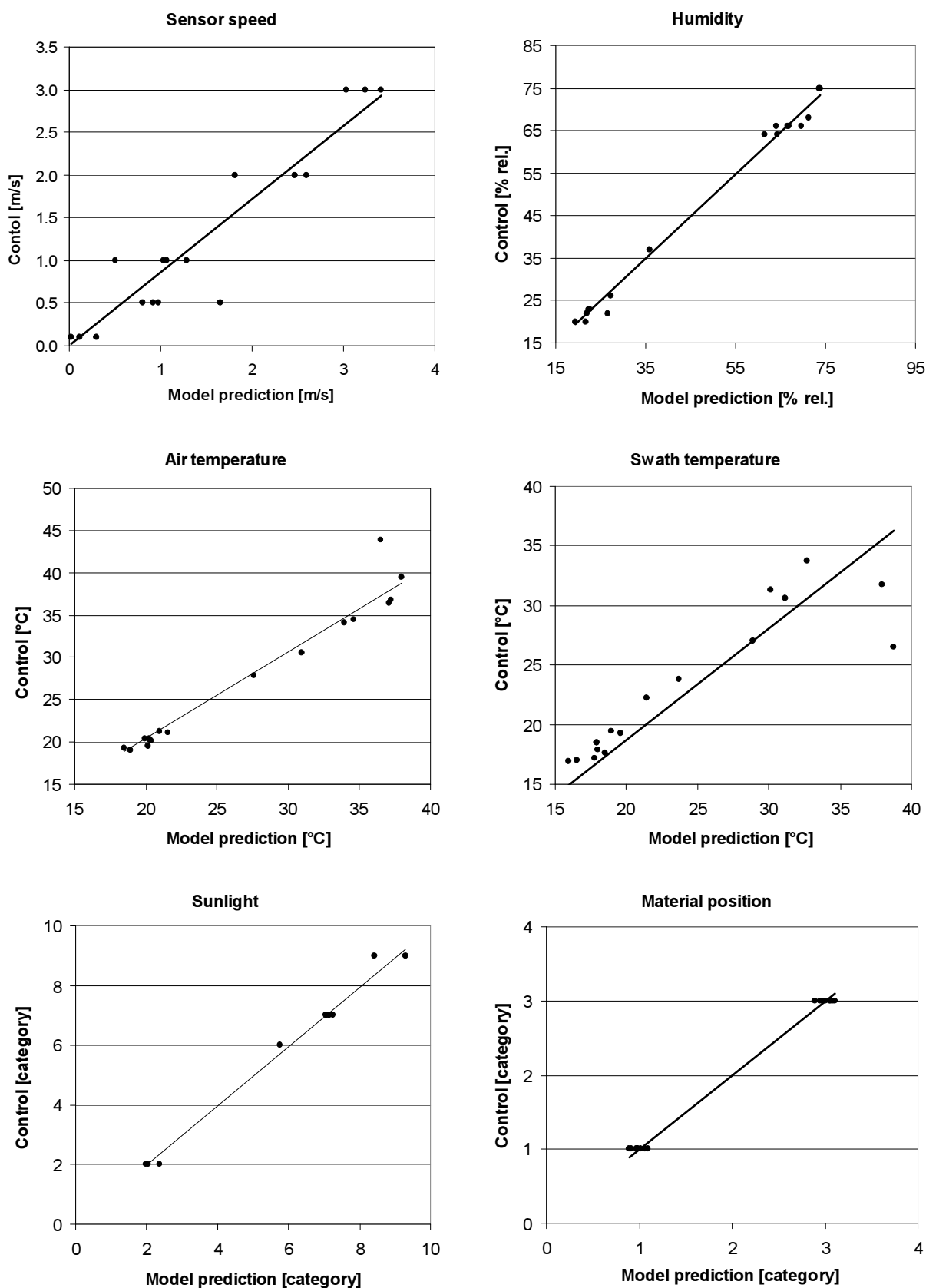


Figure 2. Correlations of estimates by spectral analyses and control values for different parameters.

Although the number of samples as well as the variability of the control values is not sufficient for a final validation so far, the dependence of the resulting spectra information from varying environmental parameters during the NIR-measurement seems to be very high. Indeed, the portability of the created calibration models is limited, because of the insufficient number of

samples. Table 1 shows the significant statistical parameters referring figure 2 calculated from prediction results and control values for the prediction of different varying environmental parameters during the measurement. Here, sensor speed was set at the test bed cruise control. Humidity, air and swath temperature were measured after each test bed run. The intensity of sunlight during the trials was classified in category 1 (sunny, no clouds) up to 6 (night, no moonlight). The material position of the small bales could be top side to the sensor (value 1) or long side to the sensor (value 3).

**Table 1. Statistics of validation of the calibration models for predicting environmental parameters.**

Statistical parameter	Prediction of					
	Sensor speed [m/s]	Humidity [% rel]	Air temperature [°C]	Swath temperature [°C]	Sunlight [category]	Material position [category]
N. of samples	17	17	17	17	11	17
Ave. GH	0.859	0.859	0.859	0.859	1.044	0.859
Ave. NH	0.010	0.010	0.010	0.010	0.014	0.010
Mean Prediction	1.253	47.235	27.335	23.476	5.909	2.059
Mean Control	1.486	47.670	26.845	23.876	5.962	2.060
Bias	-0.233	-0.435	0.460	-0.399	-0.053	-0.001
SEP	0.423	1.976	1.876	1.780	0.262	0.065
SEP(C)	0.365	1.987	1.875	1.788	0.269	0.067
RSQ	0.890	0.993	0.956	0.955	0.990	0.996
Slope	0.893	1.009	1.073	0.863	1.016	0.985

The Neighbor-H(NH)- and Global-H(GH)-values are ratios from the principle component analysis (PCA) of data. The NH-value describes the medial distance between the samples and the GH-value the medial distance of the samples to the center of the PCA. Because both values are referred to the number of samples, their averages for each parameter are equal except for the sunlight parameter. GH-values bigger than 3 indicate outliers. The small values here suggest a homogenous data distribution. The “Mean Prediction” is the average value of all predicted samples using the calibration created with another data set of the same experiment. The “Mean Control” is the average value of the control measurements of the same samples. The bias describes the systematic distortion of the measurement and is the distance between predicted and control values. The standard error of prediction (SEP) is the overall deviation of the prediction from control values and is the most important parameter to assess the quality of the calibration model. Because the control values here are not based on lab analyses but on exact measurements (e.g. temperature), the SEP has to be small. Subtracting the systematic error (bias) from SEP results in the random part of error (SEP(C)). The RSQ is the coefficient of determination of the validation. With RSQ-values between 0.89 and 0.99 the stability of prediction was quite high. The slope-value is the first derivation of the linear regression (Fig. 2). Values far away from 1 would indicate an error caused by a bad distribution in the control data (concentration).

## CONCLUSION

The described experiments show the significant influence of the sample presentation parameters on the measured spectra. But further tests have to ensure the relevance of this significant influence before starting the developing of a suitable in-field calibration model. It has to be verified if this significant influence also has a disturbing effect on the accuracy of model-estimated quality information of a sample. Therefore, further experiments at the existing test bed have to be worked out. At this, in addition to the environmental parameters also quality parameters such as the content of dry matter and other substances of the swath material have to be collected as controls. Validation of existing calibration models for substance of content estimation will show the relevance of varying environment influence during swath measurement.

## REFERENCES

1. Auernhammer, H. 2001. Precision farming – the environmental challenge. *In: Computers and Electronics in Agriculture, Millenium special issue: Past Developments and Future Directions*. Elseviere Science, Amsterdam, Netherlands. pp. 31-42.
2. Demmel, M., T. Muhr, J. Rottmeier, P. v. Perger and H. Auernhammer 1992. Ortung und Ertragsermittlung beim Mähdrusch in den Erntejahren 1990 und 1991. *In: VDI/MEG Kolloquium Agrartechnik, Heft 14: „Ortung und Navigation landwirtschaftlicher Fahrzeuge“*. Düsseldorf. pp. 107-122.
3. Hruscka, W.R. 1987. Data Analysis: Wavelength selections methods. *In: Near infrared technology in the agricultural and food industries (Eds.: Williams, P. and K. Norris)*. American Association of Cereal Chemist, Inc. St. Paul, Minnesota, USA. pp. 35-55.
4. Isensee, E. and S. Krippahl 2001. Online-Vergleich von Ertragsmesssystemen im Mähdrescher. *In: Landtechnik 56, Heft 4*. pp. 274-275.
5. Kormann, G. and H. Auernhammer 2000. Moisture measurement on forage harvesting machines. *Abstracts of AgEng Warwick 2000: Agricultural Engineering into the Third Millenium. Silsoe: Silsoe Research Institute, Part 1*. pp. 309-310.
6. Paul, C., and A. Häeusler 2002. Developing the NIRS Harvest Line concept for forage trials. *In: Multi-function grasslands: quality forages, animal products and landscapes ; proceedings of the 19th General Meeting of the European Grassland Federation, La Rochelle, + France, 27-30 May 2002*.
7. Rademacher, J. 2003. Online measurement of grain-quality with NIR-spectroscopy on combines. *Programme book of the joint conference of ECPA-ECPLF, Berlin, 16.06.-18.06.2003*. pp. 535-536.
8. Rahmann, G. and H. Nieberg 2003. Ressortforschung für den ökologischen Landbau. *Sonderheft Landbauforschung Völkenrode 259, Institut für ökologischen Landbau (OEL) und Institut für Betriebswirtschaft, Agrarstruktur und ländliche Räume (BAL) der Bundesforschungsanstalt für Landwirtschaft (FAL)*. p. 26.

# RESEARCH ON THE AGRICULTURAL DRAINAGE DESIGN USING THERMAL REMOTE SENSING ATTACHED TO AN UNMANNED HELICOPTER

T. Usami<sup>1</sup>, K. Ishii<sup>1</sup> and N. Noguchi<sup>1</sup>

## ABSTRACT

The objective of this research is to obtain the water content of the soil by using thermal remote sensing. On this research, unmanned helicopter was used YH-300 (Yanmar co., ltd). A TH7102MV camera was used as the thermal imaging sensor produced by NEC-Sanei Corporation. This camera is contact less type thermal gauge for ordinary temperature range. This platform can get the picture covered the whole field. Each pixel in thermal picture has 14-bits levels measured temperature. The thermal pictures processed by 3D-transformation can be handled as the map which is useful for precise farming. The parameters used for the affine transformation are recorded by RTK-GPS (real time kinematic global positioning system) and posture sensor attached to the helicopter at the same time. The map temperature of the soil surface and the water content ratio were compared, which were measured on the ground called estimated correlation between field surface temperature and water content ratio.

The highest root mean square was 0.9231 in different flights. Therefore, the thermal remote sensing attached to an unmanned helicopter system is useful to estimate the water content ratio of the field.

**KEYWORDS.** Remote Sensing System, Thermal Camera, Unmanned Helicopter, Water Content of Soil.

## INTRODUCTION

The Vehicle Robotics Laboratory in Hokkaido University, Sapporo, Japan utilized unmanned helicopter for remote sensing such as the GIS (geographic information system). Spatial information is good to use on making a field map. Recent projects conducted were detection of the growth condition of wheat, estimation of the harvesting period, and water content of wheat. This research estimated the water content of the soil by using the thermal remote sensing.

The objective of the research is to generate a map on a specific agricultural area with information on the water content of the soil. The amount of water in the soil influences own specific heat. This will have the correlation between field surface temperature and water content ratio. The research used a thermal camera which is attached on the unmanned helicopter to get the surface temperature of the soil and an unmanned helicopter as the aircraft to survey the agricultural area. Analyzing the surface temperature data obtained by the thermal sensing camera, the lowest temperature corresponds to the high soil water content and vice versa.

In precision farming, the usual ground temperature measurement uses TDR (time domain reflectivity) measurement sensor and thermocouple device. The advantage of using the thermal camera compare the other devices is that, it can obtain large area temperature information's in a lesser period.

---

<sup>1</sup> Vehicle Robotics Laboratory, Hokkaido University, Japan, [usa@bpe.agr.hokudai.ac.jp](mailto:usa@bpe.agr.hokudai.ac.jp)

## MATERIALS

### Unmanned helicopter with different sensors attached

Figure 1 shows an unmanned helicopter YH-300 (Yanmar co., ltd) and its components. YH-300 helicopter was developed for a grain-shaped and liquid pesticide spraying purposes. GPS, thermal imaging camera and laptop PC was attached on the helicopter and became as the platform. GPS works as a RTK-GPS by using the cellular phone to compensate the GPS signal. RTK-GPS acquired the universal transverse Mercator (UTM) coordinate with an error +/- 2cm. The information of body's angle is recorded on time by the posture sensor attached to the helicopter. And it is transferred to laptop PC. The position data from GPS is transferred to laptop PC also. This helicopter and these components can get all parameters needed to generate a map.



Figure 1. Unmanned helicopter YH-300 with equipment (Yanmar co.,ltd.).

TH7101MV (manufactured by NEC San-ei) was used as the thermal imaging sensor. This sensor has a range of -20 °C to 250 °C that can take pictures at the normal temperature with high accuracy. The measurement wavelengths are 8 nm and 14 nm, and these are the wavelengths which an atmospheric influence is hardly taken from. The device image resolution is 320 lines x 240 pixels. Each pixel has the numerical value of 14 bits. A signal is sent to the device from the laptop PC attached on the helicopter, and pictures are directly recorded in its own compact flash memory. The thermal camera was attached on pan head, and an operator can adjust this pan head by using remote controller. The pan head angle is also recorded, with respect to the map projection.

## METHODS

### Mapping algorithm

It is possible to generate the precise map of the field using this information - the information of the helicopter's angle and position, pan-head's angle, and the time of the photography. (R. Sugiura. 2002). That outline is shown in figure 2.

### Verification of ground measurements

The experiment was conducted in the rice field of Hokkaido, Japan. The field area was measured by the RTK-GPS by putting a marker points. At each marker point, the water content of the soil was measured by using a ground measurement value.

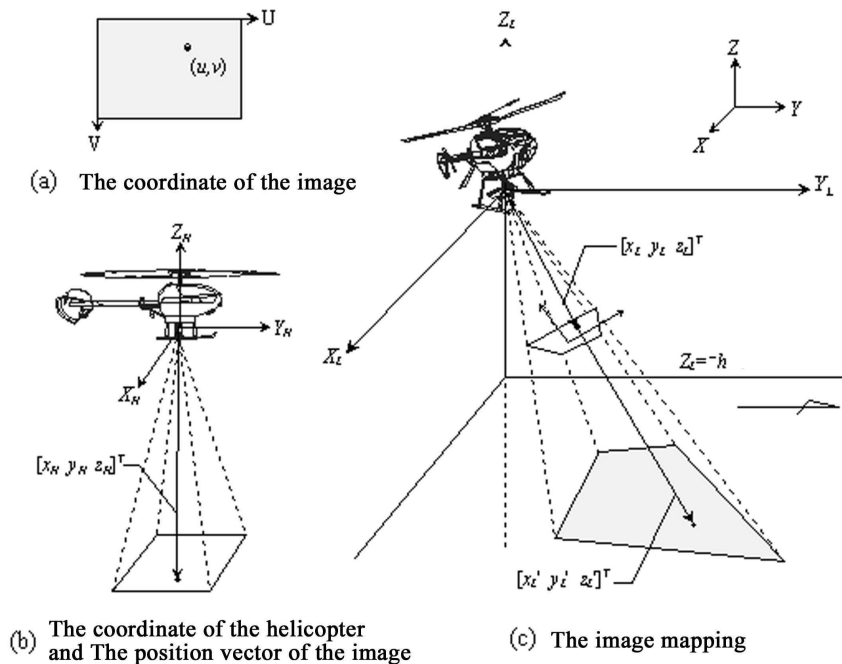


**Figure 2. Outline of map generation using three dimensional coordinate.**

Figure 3 shows the experiment area. SG and HG field's water drainage were good. RB, CB and SB field's water drainage were bad.

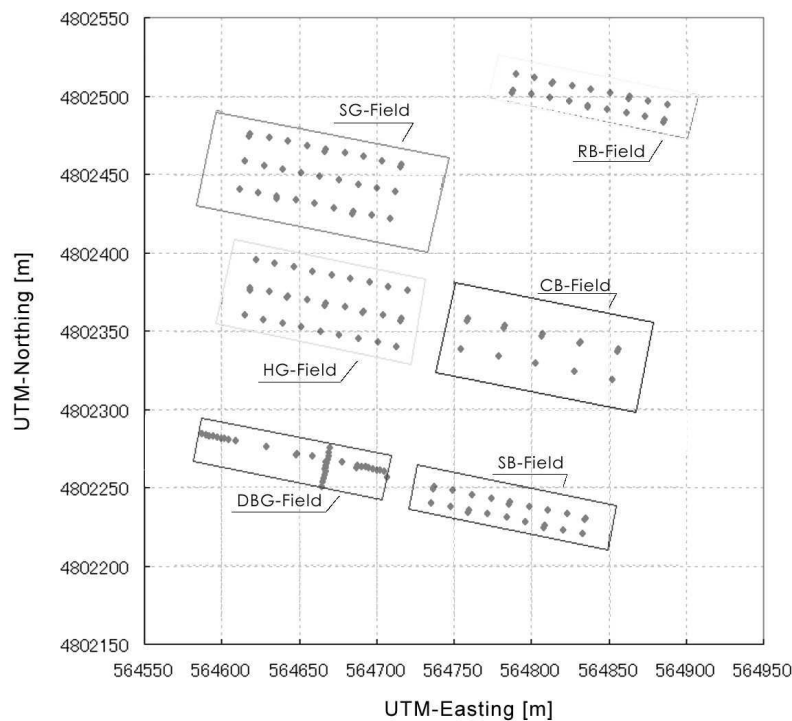


**Figure 3. Experiment field.**

### Outline of remote sensing system

The outline of the remote sensing system is shown in figure 4. Two operators are necessary for application of this system. One operator controls the unmanned helicopter and another operator control the pan-head overlooking the monitor on the ground. By encompassing the whole field in one picture, the time for mapping the field was decrease in getting data points by ground measurements. It took less than 15 minutes to take the pictures of six fields shown in figure 3 by using this remote sensing system.

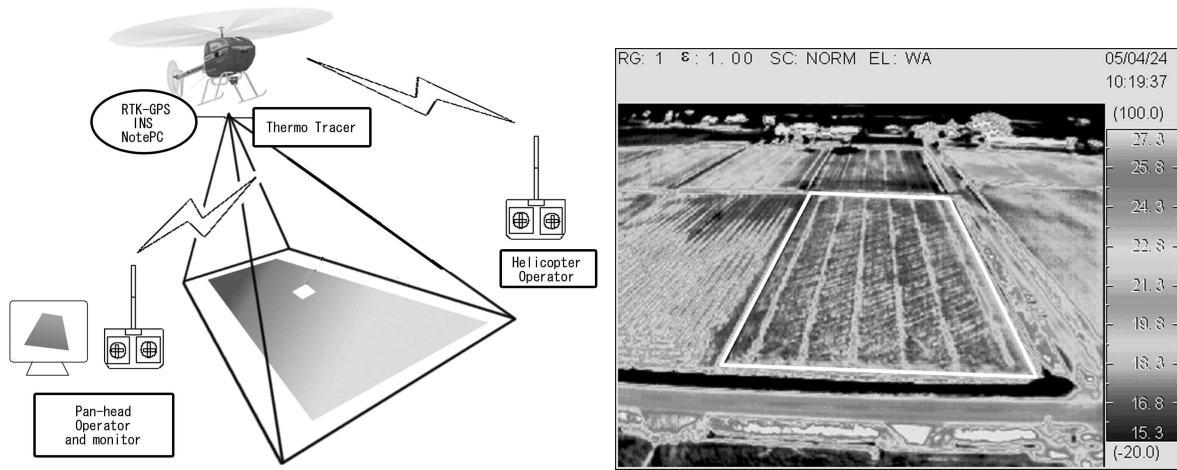


**Figure 4.** The outline of remote sensing system and a picture taken by thermal camera.

### Field image mapping

The images are projected on the map by using the information of GPS, the posture of the helicopter, the pan-head's angle were recorded at the same time. (R. Sugiura et al. 2004). Figure 5 shows the projected map using the developed remote sensing system.

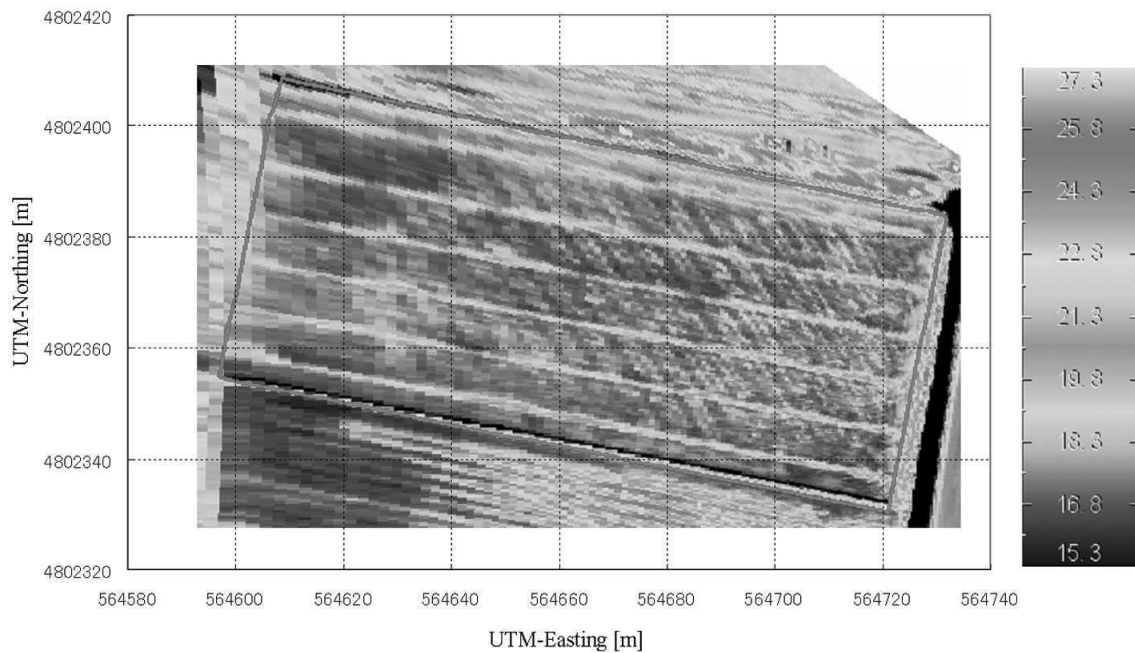


**Figure 5.** Image projected map.

## RESULTS AND DISCUSSION

The values on the ground have great errors due to the conditions of the marker points. The values contain variances in the conditions which a clod and mud were mixed in. When an estimated map was made in the existent method, it is difficult to grasp the variance of the field (Fig. 6).

To solve this problem, average of water content of each marker point was used as a value that shows the whole characteristics of the field (characteristic-value). On the other hand, average temperature of field by remote sensing system was used as a sensing-value. The graph characteristic-value and the sensing-value were shown in figure 7. In the figure, the higher soil surface temperature the lower the water content and vice versa. It causes that water in the soil obstructs rise in temperature. The map of temperature was illustrated in figure 8. The map showed

the actual field condition that can be seen by the naked eyes. But human eyesight has no precision to compare the moisture content of the fields. It is limited only to one field. The thermal remote sensing has an ability of compare the fields by numerical value.

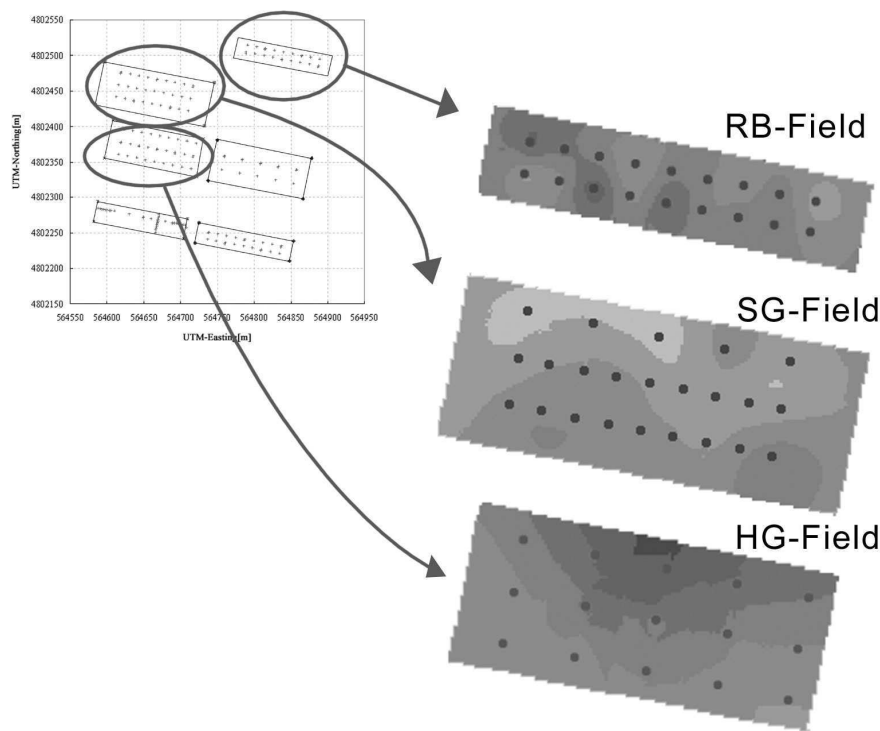


Figure 6. The estimate map using ground measuring data.

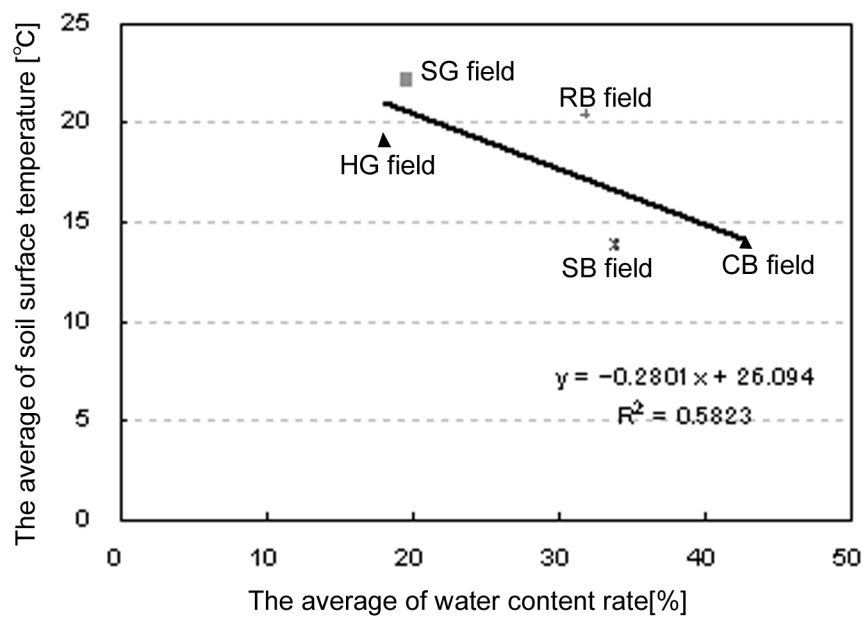


Figure 7. Correlation graph between characteristic-value and sensing-value.

Figure 9 showed the reverse correlation that was taken in the afternoon. This was due to rapid temperature drop from noon to the afternoon. Different experiments were conducted to verify these conditions.

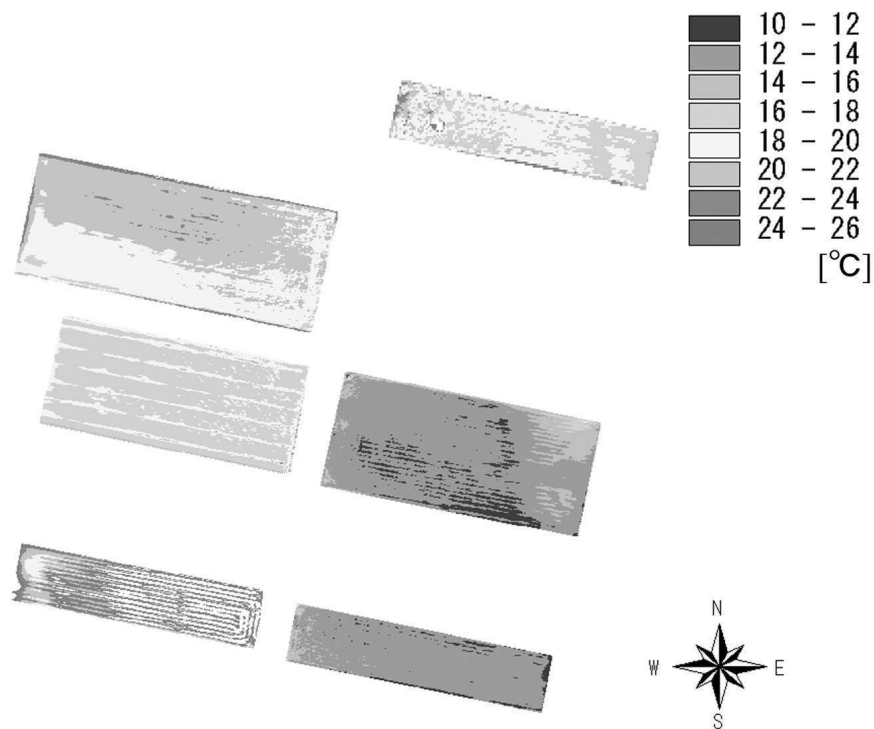


Figure 8. The illustration of temperature map of the field by using remote sensing system.

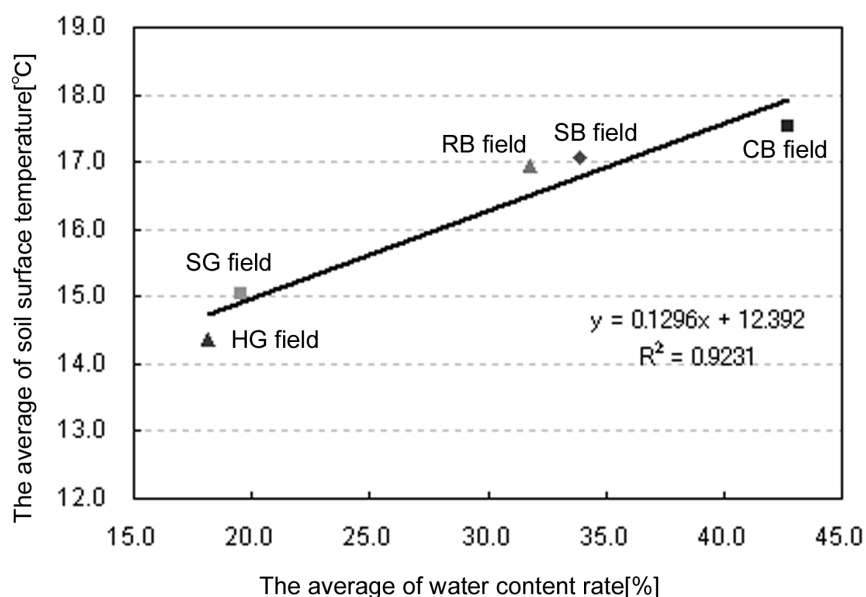


Figure 9. Correlation graph in the afternoon of figure 6.

#### Verification test for temperature changing

The temperature for the whole day and the amount of light were compared and analyzed (Fig. 10). Temperature increase resulted in the increase in the amount of light. It was delayed from the peak of the amount of light for about one hour and a half, and temperature of the soil became peak. It was observed that the reverse of plus and minus of the correlation happened during the temperature drop (Fig. 11). It means that image sensing for the water content was suitable when the soil temperature is high.

A similar experiment was conducted this year yielded the same results. The data taken this year were used in this research.

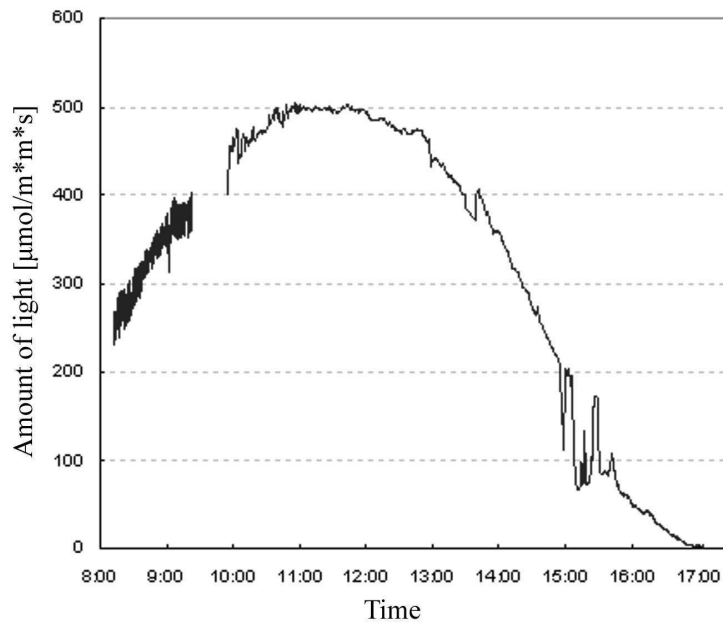


Figure 10. The amount of light.

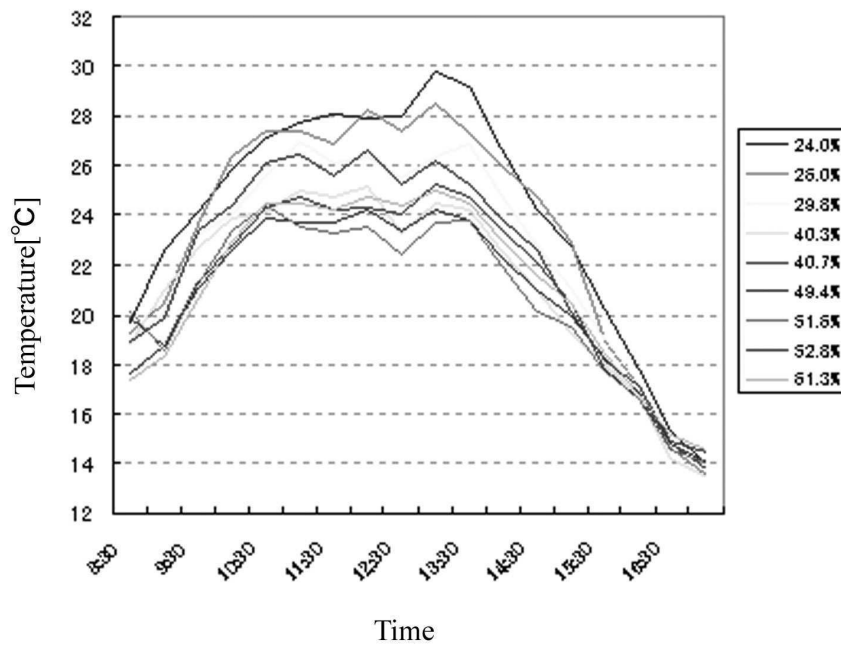


Figure 11. The temperature to the water content with respect to the time.

## CONCLUSION

This paper described the remote sensing system using the thermal camera attached on unmanned helicopter. Using this system, the thermal imaging map was made easier, in a shorter period. It took 15 minutes to get the data for 6-fields by one flight. Different information's were used to generate a thermal imaging map -- information of the helicopter's angle and position, pan-head's angle, and the time of the photography. This information's were obtained using the RTK-GPS and the thermal camera.

In this research, using the developed sensing system the water content of the soil was determined in different fields in a shorter time. The highest correlation marked R.M.S. is 0.9231 in different flights. It is concluded that the suitable time for getting the water content of the filed is when the temperature of the soil is high.

## REFERENCES

1. Sugiura, R., Noguchi, N., Ishii, K., Terao, H. (2002). The Development of Remote Sensing System Using Unmanned Helicopter. Proceedings of ASAE Conference of Automation Technology for Off-road Equipment. 120-128.
2. Sugiura, R., Fukagawa, T., Noguchi, N., Ishii, K., Terao, H., Shibata, Y., Toriyama, K. (2003). Field Information System using an Agricultural Helicopter towards Precision Farming. Proceedings of IEEE/ASME International Conference on Advanced Intelligent Mechatronics. 1073-1078.
3. Sugiura R., Ishii K., Noboru N. (2004). Remote sensing technology for field information using an unmaned helicopter. Proceedings of Automation technology for off-road equipment 2004. 226-231.
4. Iwahori T., Sugiura R., Ishii K., Noboru N. (2004). Remote sensing technology using an unmaned helicopter with a control pan-head. Proceedings of Automation technology for off-road equipment 2004. 220-225.
5. Sugiura R., Fukagawa T., Ishii K., Noboru N. (2006). Crop status sensing system by multi-spectral imaging sensor. Journal of JSAM, 68(2):42-49.

# A REAL-TIME SMART SENSOR ARRAY FOR SCHEDULING IRRIGATION

G. Vellidis<sup>1</sup>, M. Tucker<sup>1</sup> and C. Bednarz<sup>2</sup>

## ABSTRACT

We developed a prototype real-time, smart sensor array for measuring soil moisture and soil temperature that uses off-the-shelf components. The array consists of a centrally located receiver connected to a laptop computer and multiple sensor nodes installed in the field. The sensor nodes consist of sensors (up to 3 Watermark<sup>®</sup> soil moisture sensors and up to 4 thermocouples), a specially designed smart sensor circuit board, and a Radio Frequency IDentification (RFID) tag which transmits data to the receiver. The smart sensor array described in this paper offers real potential for accurately and reliably monitoring soil water status in crops. In production quantities, a system with 20 sensor nodes is anticipated to cost about US\$2400. The relatively low cost of the sensor nodes allows for installation of a dense population of soil moisture sensors that can adequately represent the inherent soil variability present in any field. This paper describes the smart sensor array's performance in a cotton crop.

**KEYWORDS.** Cotton, Irrigation Scheduling, Smart Sensors, Soil Moisture Sensors, Wireless.

## INTRODUCTION

Irrigation is an essential component of cotton production in most areas of the U.S. Cotton Belt. Equally important is the timing of irrigation. Recent studies have shown that delaying irrigation can result in losses of between US\$62/ha to US\$300/ha (Vories et al., 2003). Yet there are few practical technologies that can assist producers with irrigation scheduling. Existing scheduling technologies vary from the water balance or check book method to sophisticated systems like that provided by Adcon Telemetry<sup>®</sup> (Adcon, 2004) and Automata<sup>®</sup> (Automata, 2004). Most wireless technologies now on the market are quite expensive because they require powerful radio transmitters, may still require extensive cabling, and usually require a government license for use of the radio frequency. Furthermore, these products are generally power-hungry and consequently require regular maintenance during the growing season.

Because of this, several research teams have been pursuing alternative means of wireless communications with moisture sensors. Allen (2000a) evaluated an irrigation management system that can provide continuous real-time or near real-time soil water content information to the irrigation system operator. This system used two different data loggers to collect and store data from Watermark<sup>®</sup> soil moisture sensors. The data loggers were installed in the field in close proximity to the sensor and wired to the sensors. This system required the operator to visit the data loggers in order to download the data and thus did not provide a true wireless solution. Shock et al. (1999) used a similar approach but transmitted data from the dataloggers to a central data logging site via radio. This system allowed up to 16 Watermark<sup>®</sup> soil moisture sensors to be wired into a proprietary and expensive transmitting box. These characteristics prevent installation of a dense population of soil moisture sensors that can adequately represent inherent soil variability present in fields. King et al. (2000) and Wall and King (2004) proposed the architecture for a distributed sensor network which includes controls for a variable rate irrigation system. Although this approach may accommodate a large number of sensors, at this point, it is still a theoretical system. Hamrita and Hoffacker (2005) explored Radio Frequency IDentification (RFID) technology as a

---

<sup>1</sup> Biological & Agricultural Engineering Department, University of Georgia, Tifton, Georgia, USA, yiorgos@uga.edu

<sup>2</sup> NESPAL – National Environmentally Sound Production Agriculture Laboratory, University of Georgia, Tifton, Georgia, USA

solution to wireless real-time monitoring of soil properties. In a laboratory setting they demonstrated that RFID technology was feasible for wireless real-time communication with a soil temperature sensor.

The work described in this paper directly addresses these needs. We developed a prototype real-time, smart sensor array for measuring soil moisture and soil temperature that uses off-the-shelf components. The system allows for a large number of sensors to be installed in a field and provide data wirelessly to a centrally located receiver. The data can be used to control a Variable Rate Irrigation (VRI) system, manually schedule irrigation, or provide information to a decision support system such as *Irrigator Pro*<sup>®</sup> for comprehensive crop management. The prototype system was tested successfully in the field under corn during the 2003 growing season.

To be used successfully in the southeastern United States, the smart sensor array also needed to be tested with the region's other important crops – peanuts and cotton. Furthermore, the system required a protocol for scheduling irrigation during the crops' growth cycle. The objectives of this study were to:

1. field test the smart sensor array in cotton,
2. develop a protocol for scheduling irrigation with the smart sensor array and
3. compare the performance of the smart sensor array against conventional cotton irrigation scheduling methods.

## MATERIALS AND METHODS

In its current configuration, the smart sensor array consists of a centrally located receiver or interrogator connected to a laptop computer and multiple sensor nodes installed in the field. The sensor nodes consist of sensors (soil moisture sensors or thermocouples), a sensor circuit board, and a RFID tag which transmits data to the receiver.

### Smart Sensor Circuit Board

The smart sensor circuit board is shown in figure 1. At user-selectable intervals, the smart sensor board acquires sensor values and wirelessly transmits the values to a radio frequency (RF) receiver/data-logging device. The board is capable of reading up to three Watermark<sup>®</sup> granular resistive-type soil moisture sensors and up to four thermocouple temperature sensors. The board was designed to excite the Watermark<sup>®</sup> sensors with a DC voltage rather than the AC voltage recommended by the manufacturer (Allen, 2000a). Analog multiplexers, an instrumentation amplifier, and various other electronic active and passive components condition the sensors' input signals before they are input to a microcontroller. We extensively tested the circuit board's ability to accurately read Watermark<sup>®</sup> sensors and found that it reliably replicated the numbers produced by the Watermark<sup>®</sup> handheld digital meter.

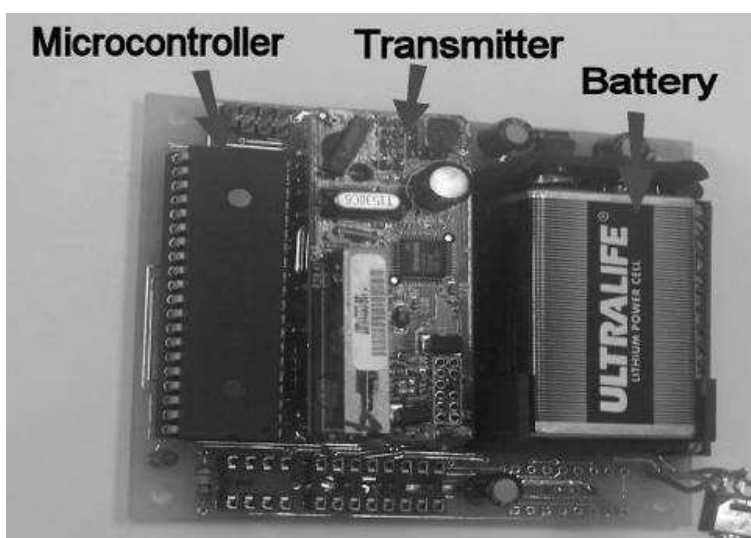


Figure 1. Circuit board used at the smart sensor nodes.

In addition to reading the sensors and making the required conversions to the sensor input values, the microcontroller program properly formats the values and outputs them to the onboard RF transmitter. The smart sensor boards used in the project were powered with single 9 volt lithium batteries. To optimize battery life, the microcontroller was programmed to place itself in a low-current sleep mode between sensor readings and data transmissions. It was also programmed to cycle the sub-circuits on and off as needed when acquiring sensor values. The microcontroller program monitored battery voltage, transmitting an alarm code when the voltage dropped below an acceptable threshold thus eliminating the need for regular inspection. Battery life easily exceeds the duration of the growing season.

An active RFID transmitter, referred to as a tag, was adapted to provide a wireless interface between the field sensor boards and the receiving station. The Wherenet<sup>®</sup> tags transmit in the 2.4 GHz radio frequency range. At each transmission, the tags send a unique identifier code (node ID) and twelve bytes of user data. In our application, the twelve bytes of user data were the sensor values which consisted of three soil moisture values and two temperature values. The tags have a line-of-site transmission range of up to 0.8 km (0.5 miles). Hereafter, the combination of the electronics board, RFID tag, and sensors will be referred to as a “smart sensor node”.

#### Receiver and Data Logging Stations

The Wherenet RF receiver, was installed at the irrigation pivot point at the field site. A notebook computer, housed in a metal enclosure, was used to run the Wherenet acquisition software and to log smart sensor data. The incoming wireless data from the smart sensor nodes to the receiver were transferred to the laptop via an Ethernet connection between the receiver and the laptop. Because the field site is located near the NESPAL building, the sensor data log files stored on the laptop were available remotely via a previously installed wireless Ethernet connection between the irrigation pivot point and the NESPAL building.

#### Field Site

The study was conducted in the 2.3 ha NESPAL field located on the University of Georgia’s Tifton Campus. The field is divided into 8 smaller areas by terraces and berms. Irrigation is applied with a variable rate center pivot irrigation (VRI) system. Unlike conventional center pivot irrigation systems, a VRI system also allows application rates to vary along the length the pivot.

#### Irrigation Scheduling Strategies

One of our objectives was to develop and test an irrigation scheduling protocol for use with the smart sensor array. After a series of consultations with cotton physiologists, a simple protocol was selected. The protocol called for irrigation when soil water tension reached 40 kPa at 0.2 m depth or when soil water tension reached 50 kPa at either 0.4 or 0.6 m depth (Flynn and Barnes, 1998; Thomson et al., 2002). To evaluate the protocol, we established two different irrigation scheduling methods in the NESPAL field. A berm which traverses the field approximately north-to-south (Fig. 2) was used to delineate irrigation scheduling strategies. In the western half of the field, irrigation was scheduled using a traditional qualitative assessment of the crop while in the eastern half, irrigation was scheduled using the smart sensor array and the new irrigation scheduling protocol.

Multiple sources of information including bare soil aerial photographs, soil texture maps, soil electrical conductivity maps, topography maps, and past yield maps were integrated qualitatively to develop four management zones in the eastern half of the NESPAL field (Fig. 2). Irrigation was scheduled in these zones when soil water tension approached the trigger points. The VRI pivot allowed each zone to be irrigated individually if necessary. The soil water tension value used for comparison against the trigger point was determined by averaging of soil water tension readings from each of the smart sensors functioning in that zone. The depth of water applied was determined by the amount of water required to bring the soil profile back to field capacity. This amount varied between 13 mm of water to 25 mm of water.

Ideally, a dense population of sensors would be installed in each zone to properly characterize it. However, funding limitations mandated that only two to three smart sensor nodes be installed in

each of the management zones (Fig. 2). The numbers in figure 2 represent the smart sensor node IDs which were included in each data transmission.

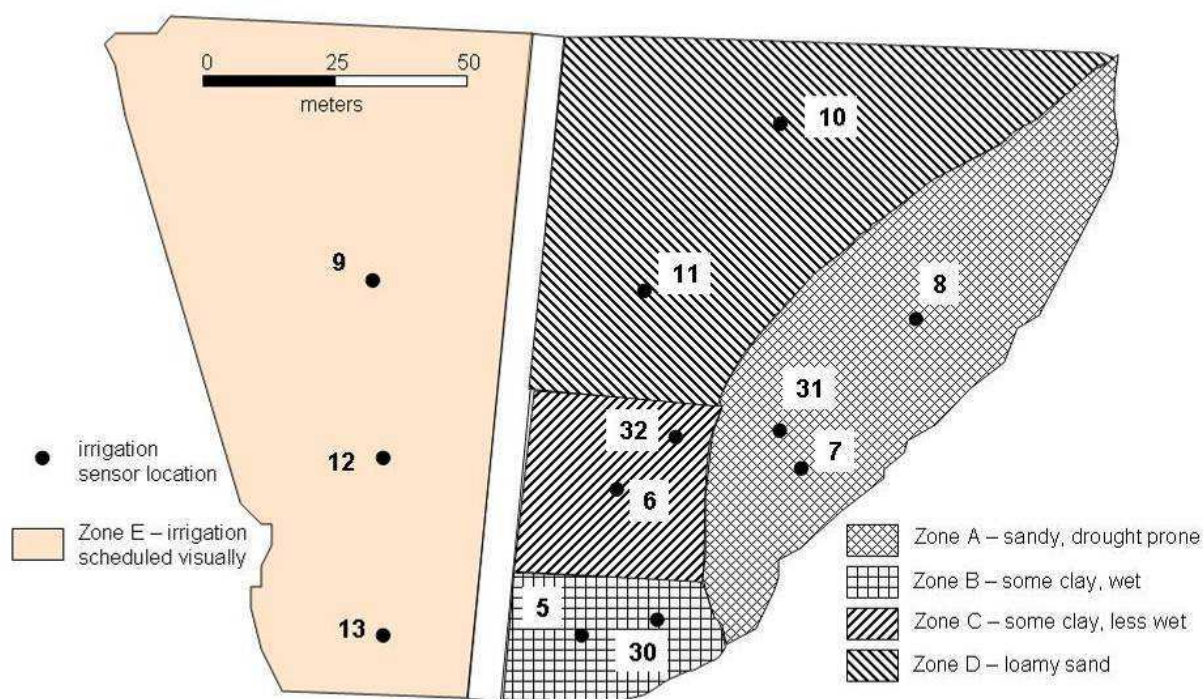


**Figure 2. NESPAL field irrigation management zones.**

Each smart sensor node consisted of three Watermark soil moisture sensors installed within the row at depths of 0.2, 0.4, and 0.6 m and two thermocouples (Fig. 3). One thermocouple was installed to monitor soil temperature at 0.2 m while the other was loosely wrapped around the stem of the nearest cotton plant and monitored ambient temperature.



**Figure 3. A smart sensor node which includes 3 soil Watermark sensors and 2 thermo-couples.**

Irrigation in the west side of the field was scheduled qualitatively by a staff member who has many years of experience growing cotton in a farm setting. His qualitative decision was based on a daily early morning survey of the field and was a function of obvious signs of plant water stress (wilting), days since last irrigation, rainfall, weather forecast, past experience, and other factors. The depth of water applied in the western half of the field was consistently 20 mm of water. Although three smart sensors were installed here, the decision maker did not have access to the sensor readings. They were used only to monitor soil water tension. Rainfall in the field was measured using a tipping bucket rain gauge.

## RESULTS

The NESPAL field was strip-tilled and planted to Round-Up Ready 555 DPL cotton on 27 April 2004. Crop fertility and pest protection was managed by our team's cotton physiologist. Between planting and June 1, regular uniform irrigation applications were applied to ensure proper germination and a good stand. The smart sensor nodes were installed in May and began recording data in June at which time the predetermined irrigation scheduling protocols were initiated. Ample rainfall in June and September obviated the need for irrigation in those months.

Figures 4 and 5 show soil water tension versus time at the three monitored depths in two of the field's five zones. Each tension line on the graphs represents the average of the soil water tension reported by each soil moisture sensor at that depth in the given zone. The vertical bars descending from the upper x-axis of the graphs represent rainfall or irrigation amounts. The cumulative rainfall amounts are time specific while the irrigation amounts are only date specific and indicate the date on which irrigation began and not the date/time during which water was applied to the sensor locations. The graphs illustrate that the smart sensor array was able to successfully monitor soil water tension. Although no alternative method was used to verify soil moisture during the study, Watermark<sup>®</sup> sensors performed well when compared to tensiometers prior to the study. Many researchers have performed similar successful comparisons and have provided calibration curves for Watermark<sup>®</sup> sensors (Thomson and Armstrong, 1987; Eldredge et al., 1993; Thomson et al., 1996; Shock et al., 1998; Allen, 2000b; Thomson et al., 2002). To ensure that the smart sensor array system was properly reading the Watermark<sup>®</sup> sensors during the study, sensors were read with the manufacturer's handheld digital meter on a weekly basis. Without fail, the reported data matched the data collected with the digital meter.

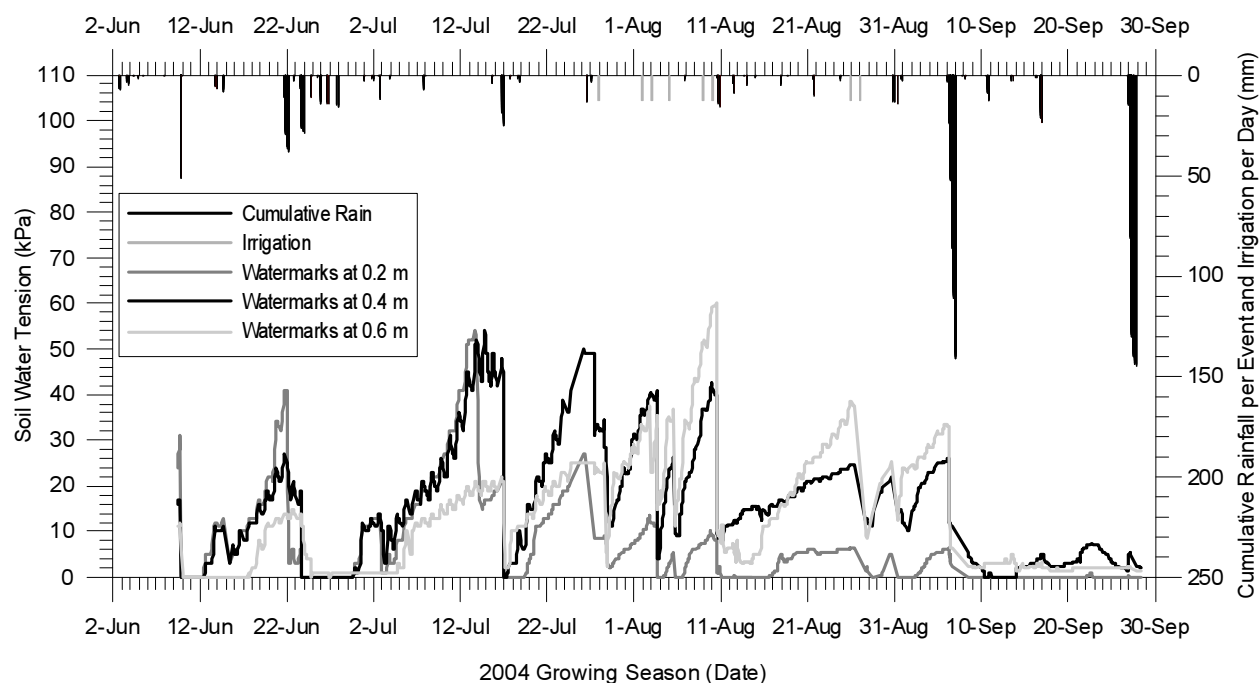


**Figure 4. Soil water tension recorded in Zone C (some clay, less wet). The data are an average of soil water tensions recorded at nodes 6 and 32.**

With a few exceptions, we were able to prevent soil water tension from increasing above our established trigger points. Because it takes many hours for a center pivot irrigation system to apply water to even a small field, we learned from experience that once soil water tension begins to increase sharply and approach the trigger point, irrigation must begin almost immediately or else soil water tension will climb well above the trigger point. It is also clear that the amount of water added during each irrigation event did not bring the entire soil profile back to field capacity. This may have been a function of not adding enough water but also a function of the slow percolation rate of the lower soil profile.

On the west side of the cotton field (Zone E), irrigation was triggered based on visual observations of the crop. This irrigation scheduling strategy resulted in much higher soil water tensions at 0.4 and 0.6 m depth than any observed in the eastern half of the field (Fig. 5). In some instances, measured tension was more than double the trigger points established for the smart sensor scheduling protocol. It is also evident that the amount of irrigation water applied was not enough to bring the soil profile up to field capacity below 0.2 m depth and only served to momentarily reduce soil water tension.

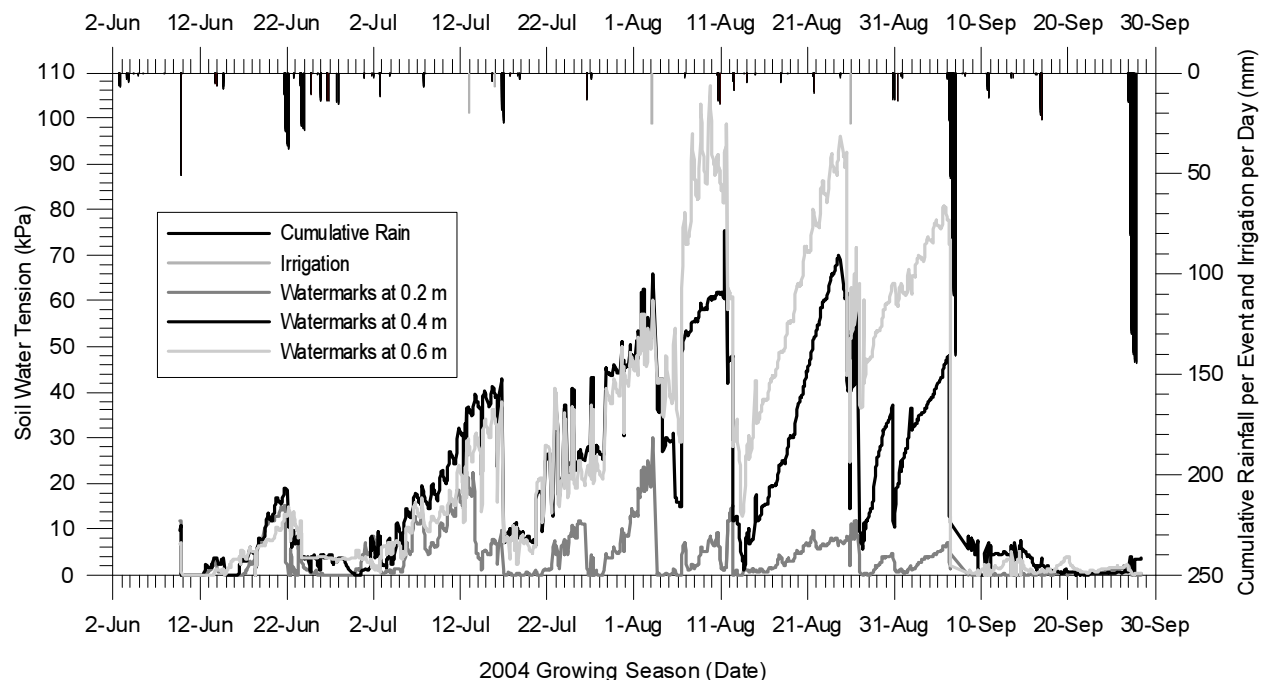


**Figure 5.** Soil water tension recorded in Zone E (west side of NESPAL field). The data are an average of soil water tensions recorded at nodes 9, 12, and 13.

### Thermocouple Response

Although soil and canopy temperature were not used to make management decisions at the NESPAL field, they are important parameters for peanut production and are key input parameters to the *Irrigator Pro* decision support software. Thermocouple response was good for the duration of the study which indicates that the smart sensor array can successfully record three soil moisture values and two thermocouple values at each node. Soil temperature at 0.2 m fluctuated between 24 and 28°C with a gradual decline as the season progressed. In contrast, canopy temperature fluctuated between 20 and 40°C during most of the season and even approached 44°C during mid September.

## DISCUSSION AND CONCLUSIONS

The smart sensor array was able to successfully monitor soil water status and soil and canopy temperature for the entire 2004 growing season with few technical difficulties. The irrigation scheduling protocol appears sound although it will likely need adjustment in response to local conditions. The current low cost design allows for a high population of nodes within a field. At the moment, the cost of a node is primarily a function of the number of Watermark soil moisture sensors used. In small quantities, the Watermarks cost approximately US\$25 each. If purchased in large quantities, the price could be significantly lower. The cost of the other node components is currently about US\$40. In the configuration used for this study, the cost of each node was approximately US\$115. From the soil water tension response curves, it appears that a node with two Watermark sensors installed at 0.2 and 0.5 m depth would adequately characterize the status of the soil at any given location. A dense population of such nodes would be required to adequately characterize the soil water status of an irrigation management zone. It is not unrealistic to expect that in production quantities, a two-sensor node would cost about US\$70. A population

of 20 nodes, which should adequately instrument a 40 ha field with a moderate amount of variability, would then cost about US\$1400. The life of a node is expected to be about 5 years.

More problematic at the moment is the cost of the Wherenet receiver and acquisition software which is approximately \$4500. The current receiver and software are designed for a much more complicated mission than our application. We are currently working with Wherenet company officials and technical staff to simplify the receiver and software with a target price of \$1000 for our application. Simplifying the software will also allow it to operate on a smaller computing platform such as a personal digital assistant (PDA) device. If this objective is achieved, a producer could instrument a large field with a dense population of nodes for approximately \$2700 (including \$300 for a PDA). Planned research will evaluate the potential of transmitting the collected data wirelessly from the field computer/PDA to the home or office computer.

The smart sensor array described in this paper offers real potential for accurately and reliably monitoring soil water status in crops. The relatively low cost of the sensor nodes allows for installation of a dense population of soil moisture sensors that can adequately represent the inherent soil variability present in any field.

#### Acknowledgements

This work was supported by funds from Cotton Inc., the Georgia Research Alliance, the Peanut Foundation, and by Hatch and State funds allocated to the Georgia Agricultural Experiment Stations. Mention of commercially available products is for information only and does not imply endorsement.

#### **REFERENCES**

1. Adcon, 2004. Application information for Adcon telemetry systems. Adcon telemetry, Klosterneuburg, Austria (<http://www.adcon.at>).
2. Allen, R.G. 2000a. Report on AM400 and HOBO loggers. Univ. Idaho, Kimberly, Idaho ([www.kimberly.uidaho.edu/water/swm/](http://www.kimberly.uidaho.edu/water/swm/)).
3. Calibration for the Watermark 200SS soil sater potential sensor to fit the 7-19-96 "Calibration #3" Table from Irrometer. Univ. Idaho, Kimberly, Idaho ([www.kimberly.uidaho.edu/water/swm/](http://www.kimberly.uidaho.edu/water/swm/)).
4. Automata, 2004. Application literature for the Data Lynx IR and radio telemetry systems. Automata, Nevada City, CA ([www.automata-inc.com](http://www.automata-inc.com)).
5. Eldredge, E. P., C. C. Shock, and T.D. Stieber. 1993. Calibration of granular matrix sensors for irrigation management. *Agronomy Journal*. 85:1228-1232.
6. Flynn, R.P., and C.E. Barnes. 1998. Timing first irrigations for cotton productivity and water conservation. *In Proc. 2002 Beltwide Cotton Conference*, National Cotton Council, Memphis, TN. p. 671-673.
7. Hamrita, T.K., and E.C. Hoffacker. 2005. Development of a "smart" wireless soil monitoring sensor prototype using RFID technology. *Applied Engineering in Agriculture* 21(1):139-143.
8. King, B.A., R.W. Wall, and L.R. Wall. 2000. Supervisory control and data acquisition system for closed-loop center pivot irrigation. *ASAE Technical Paper No. 00-2020*. ASAE, St. Joseph, MI. 7 pp.
9. Shock, C.C., J.M. Barnum, and M. Seddigh. 1998. Calibration of Watermark soil moisture sensors for irrigation management. *In Proc. 1998 Irrigation Association Technical Conference*, The Irrigation Association, Falls Church, VA, p.123-129.
10. Shock, C.C., R.J. David, C.A. Shock, and C.A. Kimberling. 1999. Innovative, automatic, low-cost reading of Watermark soil moisture sensors. *In Proc. 1999 Irrigation Association Technical Conference*, The Irrigation Association, Falls Church, VA, p.147-152.
11. Thomson, S. J. and C. F. Armstrong. 1987. Calibration of the Watermark Model 200 soil moisture sensor. *Applied Engineering in Agriculture*. 3(2): 186-189.

12. Thomson, S.J. 1996. Decision support system to interpret soil moisture sensor readings for crop water management. *AI Applications*. 10(1):57-66.
13. Thomson, S.J., D.K. Fisher, and G.F. Sassenrath-Cole. 2002. Use of granular-matrix sensors, models, and evaporation measuring devices for monitoring cotton water use and soil water status in the mississippi delta. *In Proc. 2002 Beltwide Cotton Conference*, National Cotton Council, Memphis, TN. p.623-637.
14. Vellidis, G., C.D. Perry, G. Rains, D.L. Thomas, N. Wells, C.K. Kvien. 2003. Simultaneous assessment of cotton yield monitors. *Applied Engineering in Agriculture* 19(3):259-272.
15. Vories, E.D., R.E. Glover, K.J. Bryant, P.L. Tacker. 2003. Estimating the cost of delaying irrigation for mid-south cotton on clay soil. *In Proc. 2003 Beltwide Cotton Conference*, National Cotton Council, Memphis, TN. p.656-661.
16. Wall, R.W., and B.A King. 2004. Incorporating plug and play technology into measurement and control systems for irrigation management. *ASAE Technical Paper No. 04-2189*. ASAE, St. Joseph, MI. 15 pp.

# A COMPARISON OF THREE STEERING CONTROLLERS FOR OFF-ROAD VEHICLES

Y. Gao<sup>1</sup> and Q. Zhang<sup>2</sup>

## ABSTRACT

Many off-road vehicles use an electrohydraulic (E/H) actuator for implementing steering controls. However, the high nonlinearity of those E/H steering systems often results in a difficult in achieving high performance in steering control, especially when it requires only some small steering corrections. Such feature of E/H steering systems calls for advanced control methods to overcome the nonlinearity problems for achieving a desirable level of steering performance. This paper presents the development and applications of a proportional-integral-derivative (PID) controller, a feedforward-plus-PID (FPID) controller and a fuzzy controller for an E/H steering system typically used on an off-road vehicle. All controllers were implemented on a hardware-in-the-loop E/H steering system simulator for performance comparison. The test tests verified that both the FPID and fuzzy controllers have superior performance on compensating for system deadband and could achieve more sensitive and accurate small steering corrections than a PID controller could.

**KEYWORDS.** Electro-hydraulic Steering Control, Feedforward-plus-PID Control, Fuzzy Control, Off-road vehicles, PID Control.

## INTRODUCTION

Intelligent off-road vehicles are designed to travel and perform various operations on all terrains, and both the research community and the industry have put great efforts on creating apt technologies for intelligent vehicles (Yih and Gerdes 2005). Among all intelligent vehicle functions, the automated path tracking function plays an essential role for supporting many other functions. To implement an accurate path tracking function on an intelligent vehicle, an appropriately designed vehicle steering controller is critical. Because it often needs to overcome varying loads to steer a vehicle traveling on unprepared terrains, hydraulic steering systems are often used on off-road vehicles due to their performance consistency on handling changing loads and their relatively compact size. The integration of electronics with hydraulics makes it possible to implement complicated intelligent control strategies via steering-by-wire for achieving better vehicle maneuvering stability and mobility (Haggag *et al.* 2005). As illustrated in figure 1, in a steering-by-wire E/H steering control system, it uses a rotary potentiometer to sense the steering input from the steering wheel. This steering input will then be fed to a microcomputer-based electronic control unit (ECU) and be converted into a valve control signal in the ECU to drive the steering control valve for implementing the required steering action.

In design a steering controller for an E/H steering system, the response performance of the E/H power control system plays a crucial role. Many researchers have investigated the use of various control schemes for designing sensitive and accurate controllers for off-road vehicle E/H systems. A group of researchers from Lancaster University had successfully developed a series of different forms of PID, including PI, PID and PIP (proportional-integral-plus), controllers for supporting auto-digging functions via controlling the bucket position on an intelligent excavator (Gu *et al.* 2004). Based on the results obtained from an extensive investigation, Dong *et al.* (2002) verified that it is possible to achieve a satisfactory steering control performance on an E/H steered off-road

---

<sup>1</sup> Yanshan University, Qinhuangdao, Hebei, China, yjgao@ysu.edu.cn

<sup>2</sup> University of Illinois at Urbana-Champaign, Urbana, IL 61801, USA

vehicle using a PID controller properly tuned for a specific operation condition. Retuning of the controller is often needed to continuously achieve satisfactory steering performance if the operation condition is changed. To solve this problem, Qiu and Zhang (2003) have successfully designed and implemented a feedforward-plus-PID (FPID) controller for various models of agricultural tractors and combine harvesters, and all achieved a better control performance than a regular PID controller because of its capability on system nonlinearity compensation. Yih and Gerdes (2005) also designed a feedforward-plus-proportional-derivative (FPD) controller by integrating the steering rate and internal friction with the estimated aligning moment to form the feedforward and compensation signals and achieved satisfactory control performance on an E/H steering system of a wheel-type vehicle.

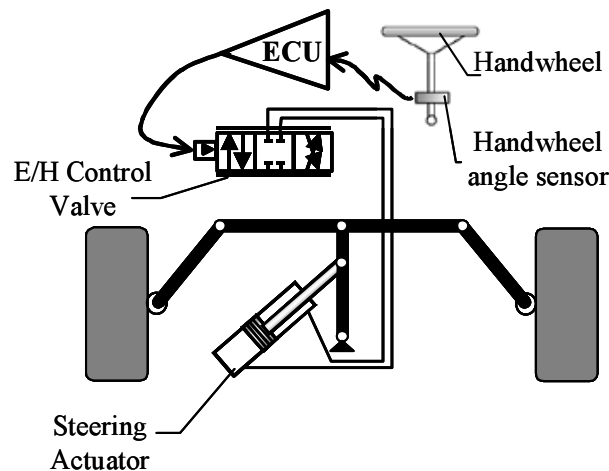


**Figure 1. Illustration of a steering-by-wire system on a wheel-type off-road vehicle.**

Fuzzy logic based controls, for their capabilities on mimicking human operator's behaviors in steering a vehicle to overcome the inherent non-linearity of a hydraulic steering system and the unpredictable disturbances induced by surrounding conditions of a moving vehicle, have been investigated for vehicle steering control applications. For example, Raimondi and Melluso (2005) developed a dynamic fuzzy steering controller to steer a vehicle with two independently driven wheels tracking a desired trajectory accurately. Lin *et al.* (2005) designed a hierarchical fuzzy steering controller for an autonomous wheeled robot to achieve stable, accurate and robust trajectory tracking. Zhang (2003) proposed a generic fuzzy controller design methodology for steering different types of wheel-type vehicles and discovered that a fuzzy steering controller by mimicking human driver's behavior in for steering a vehicle can be used to control all types of vehicles having similar steering mechanisms.

Different control methods using their specific tactics for providing satisfactory steering performance to vehicles with an E/H steering system, and existing literature has provided very well documented steering controller design approaches and corresponding features in terms of the studies conducted on developing and/or implementing a specific type of controllers. This study aimed to obtain a comprehensive appreciation on design methods for PID, feedforward-plus-PID (FPID) and fuzzy controllers, as well as practical tuning methods for those controllers. The expected achievable performances of those controllers in controlling a vehicle E/H steering system were evaluated on a hardware-in-the-loop E/H steering control simulator. The following sections of this article will present the outcomes from this study.

## **DESIGN OF THREE TYPES E/H STEERING CONTROLLERS**

### PID Controllers

PID controller stands for proportional-integral-derivative controller, and is a classical control method with well-developed controller design and tuning technologies. As one of the most commonly applied control methods, PID controllers have been applied in many fields of automation, including vehicle steering controls. Figure 2 illustrates a typical PID controller which

utilizing a feedback signal reflecting the actual operational state of the plant to improve the accuracy in trajectory tracking. While a PID controller receives a control command (often called the set-point), the controller will first compare with the feedback signal to detect the difference (often called error) between the set-point and the actual value of control result, then to make a correction to the plant for minimizing the error. Because of their capabilities on making control adjustments in terms of actual plant outputs, PID controllers can also reduce the undesirable behaviors on plant operation induced by external disturbances.

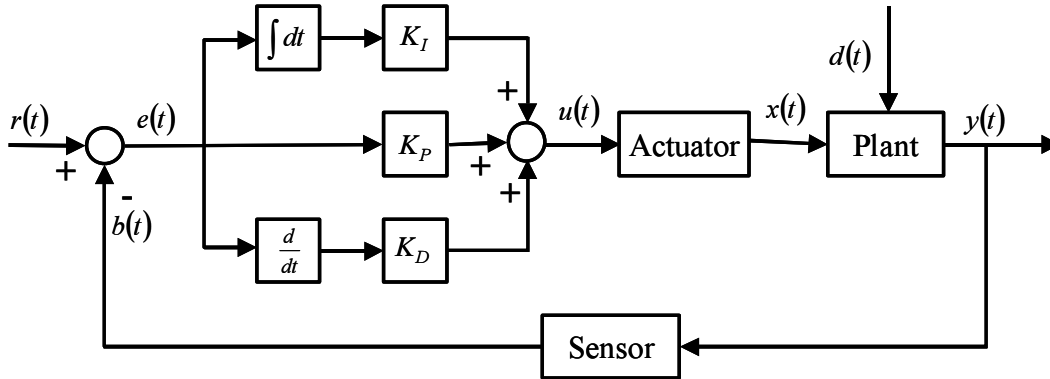


Figure 2. System diagram of a typical PID controller.

The design of a PID controller is mainly to determine the appropriate control gains for correcting the error promptly and accurately. A number of methods have been developed for designing and tuning of PID controllers (Aström and Hagglund 1995; Ang *et al.* 2005). Among those methods, the Ziegler-Nichols straightforward tuning method is one of most commonly used methods for tuning PID controllers (Aström and Hagglund 1995). Based on this method, the PID gains can be determined in the following way that it first sets the set-point value to a typical value for representative uses and turns both the integral and derivative gains to zero as if the controller is a proportional controller. Progressively increase the proportional gain from a reasonable low level slowly until when adjusting the set-point by adding a step (either positive or negative) correction of about 5% of its original value will inducing oscillations of just self-sustaining. Define the proportional gain at this point as the critical gain,  $G_u$ , and the oscillation period at this point as the critical period,  $T_u$ , for the controller. The controller parameters can then be set using the equations listed in Table 1 for different forms of PID controllers using Ziegler-Nichols tuning method.

In this study, a PI controller was designed to be implemented on a hardware-in-the-loop (HIL) electrohydraulic steering simulator for evaluation. To serve for this purpose, the PID controller was closed loop in terms of the actual steering cylinder position corresponding to the commanding position control set point. For implementing the steering controller at the hosting PC, this PID controller was designed in a discrete form as expressed below:

$$u(k) - u(k-1) = K_P(e(k) - e(k-1)) + K_I e(k) T_s + \frac{K_D}{T_s} (e(k) - 2e(k-1) + e(k-2)) \quad (1)$$

where,  $u(k)$  and  $e(k)$  represent an element in control signal and error sequences,  $T_s$  is the sampling interval,  $K_P$ ,  $K_I$  and  $K_D$  are P, I and D gains of the controller, and  $k$  represents the time instant.

As discussed earlier, the Ziegler-Nichols straightforward tuning method was used methods for tuning this PI controller. Due to the constraints of physical parameters of the hardware system on this HIL simulator, the commanding step input should be less than 10 mm for ensuring the system operating within its linear range. Therefore, in tuning this controller, the commanding step a step input of 5 mm was selected as commanding signal. Setting the integral gain to zero, the tuning process started on tuning only the P controller through progressively increasing the proportional gain from a reasonable low level slowly until the controller reached a neutral stability.

Experimentally, It was found that when the  $K_p$  reached a critical value of 0.42, the system reached the neutral stability status. Under this condition, the system response was cycled at 0.192 s. According to Ziegler-Nichols PID controller tuning rules summarized in table 1, the P gain,  $K_p$ , was adjusted to 0.17 and the I gain,  $K_I$ , was adjusted to 1.1. The system performance reached an optimal level with the obtained set of gains. However, this PI controller will always result an offset on the target position with a relatively small commanding position, or in the other words a relatively small steering angle, mainly attribute to the inherent system deadband.

**Table 1. Parameters for different forms of PID controllers determined using Ziegler and Nichols tuning method.**

Controller	$K_P$	$K_I$	$K_D$
P	$0.5K_u$	--	--
PI	$0.4K_u$	$0.5\frac{K_u}{T_u}$	--
PID	$0.6K_u$	$1.25\frac{K_u}{T_u}$	$0.072K_uT_u$

### FPID Controllers

A FPID controller is actual an integration of a conventional PID controller with an open-loop feedforward controller (Fig. 3). In this controller, the feedforward controller forms a base control signal in terms of the input set-point (also called the steering command), and the PID controller formulates a reactive correction signals in respond to the identified error between the input set-point and the controlled plant output. The feedforward controller of E/H steering implement system often uses a look-up table type transform function to support forming the base control signal, which makes it possible to add an initial bias to the steering control signal for compensating for the system deadband and other nonlinearity features inherent to an E/H actuating system. In addition, the open-loop feature of the feedforward controller makes it easier to reject the influence of the external disturbances due to the formation of the base control signal depends only to the input steering command. The PID controller in a FPID controller performs as a fine adjuster to correct the control errors induced by any causes to improve the control accuracy. Because such errors are normally smaller than the desired system output under a certain control command in amplitude, the gains of the PID controller can be therefore reduced for achieving better system stability.

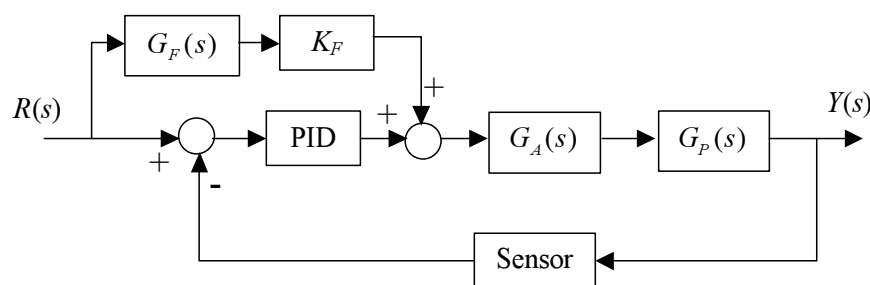


**Figure 3. System diagram of a typical feedforward-plus-PID controller.**

The design of FPID controller normally consists of three steps of feedforward controller design, PID controller design and FPID integration. The major task in design of a feedforward controller focuses on the determination the feedforward function of  $G_F(s)$  and the gain  $K_F$ . For the purpose of compensating for the effects of system internal nonlinearity, an inverse function of the plant dynamics,  $G_P^{-1}(s)$ , is often used as the transfer function for feedforward controllers (Ellis 2000). To eliminate or reduce the effects of external disturbance on the plant dynamics, a feedforward controller can also include an inverse function of the disturbance function acting on the plant

(Levine 1995). Because a feedforward controller sends a control signal directly to a control actuator for implementing, it eliminates the delay caused by feeding the controlled plant states back in a feedback controller and results in a more prompt response to a control command than a feedback controller does. It is also important to point out that the gains in a feedforward controller do not impair the system stability because the determination of those gains are independent to plant dynamics. Normally, the feedforward gain,  $K_F$ , is set equal to or less than 1 (Ellis 2000). The design of the PID controller follows the normal PID controller procedures as discussed the previous section, and a set of reduced gains could be used as appropriate to specific applications. The integration of the feedforward controller and the PID controller is the core for a FPID controller, and a reduced gain for either or both the feedforward controller and the PID controller is often the secret to make the integrated FPID controller stably and accurately in achieving the control goals.

To help eliminate the position offsets hardly to be removed with a PID controller, a FPID controller was designed to remove the system inherent deadband induced offset. As illustrated in figure 3, a FPID controller is actually the integration of a PID controller and a feedforward controller. In this study, the feedforward controller was designed to create an appropriate valve control signal in terms of an inversed function of the velocity control characteristic curve (as shown in figure 4) corresponding to a commanding position control set point. Meanwhile, the PID controller was designed to correct position control errors induced by any disturbance sources, such as the system nonlinearity and environment disturbances. To create a room allowing the PID loop to correct position control errors, a gain of 0.8 was assigned to the feedforward controller to diminish the amplitude of the implementing signal for ensuring the system stability. The PI controller designed in the previous section, with  $K_P$  of 0.17 and  $K_I$  of 1.1, was used to this FPID controller without any modification. This FPID controller could significantly increase the system response by eliminating the control deadband, and improve the control accuracy by compensating for the system nonlinearity.

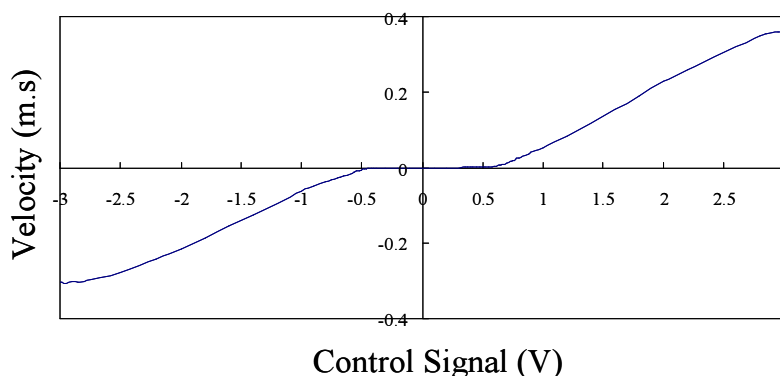


**Figure 4. Velocity control characteristic curve of the E/H steering valves.**

One may notice that the commanding steering set point represents the desired position of the steering actuating cylinder, and the inversed function maps a desired steering rate to the corresponding valve control signal. To make the inversed function workable in this feedforward loop, it is necessary to convert the commanding steering set point to an appropriate steering rate input, and differentiator was applied to perform this task. Because a differentiation operation often generates noises, a first order low-pass digital filter with a cutoff frequency of 10 Hz was designed to attenuate the differentiating induced high frequency noises while still keeping the possible dynamic behaviors may be carried in the steering commanding signal. Since the FPID controller was implemented in a digital form, the discrete form of the differentiator-filter is presented as follows:

$$\dot{x}_f(k) = \omega_c \left\langle x_i(k) - \left\{ x_f(k-1) + \frac{T_s}{1+T_s\omega_c} [\omega_c(x_i(k) - x_i(k-1)) + \dot{x}_f(k-1)] \right\} \right\rangle \quad (2)$$

where,  $x_i$  is the input reference signal,  $x_f$  is the filtered reference signal,  $\omega_c$  is the cut-off frequency of the first order filter, and  $T_i$  is the sampling interval.

### Fuzzy Controllers

A fuzzy controller uses human heuristic knowledge to intuitively create control rules so that the resulting controller can emulate human control behavior to a certain extent. A general scheme of a fuzzy controller is depicted in figure 5. As illustrated, a fuzzy controller consists of an input interface, an inference engine, and an output interface (Lee 1990). The input interface is used to map the system inputs in various forms, such as a real-valued sensor output and an ambiguous human perception, into appropriate word-variables by means of a fuzzification process for supporting word computing (Zadeh 1996). The inference engine, as the core of a fuzzy controller, performs the word computing to identify the suitable control actions for achieving the control goal under different conditions. Those control actions are derived from a set of pre-defined perception-based control rules. The output interface converts the identified control actions presented in word-variables into crisp machine executable control signals using a word-variable defuzzification operation.

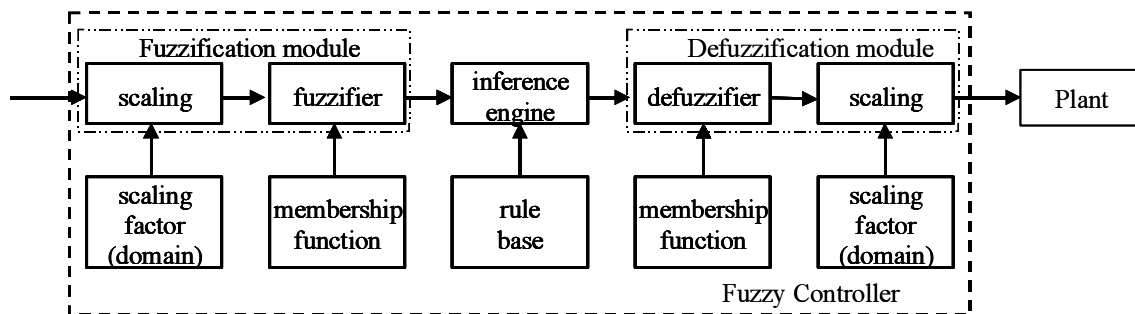


**Figure 5. System diagram of a typical fuzzy controller.**

As a knowledge-based control method capable of mimicking human's way of handling complicated system control, fuzzy steering controller has been successfully developed and applied on electrohydraulically steered off-road vehicles (Zhang 2003). The major challenge in design a reliably and accurately functionable fuzzy controller is the creation of a set of control rules capable of providing consistent control actions for any specific operation conditions and covering all possible operation conditions completely using a minimum number of control rules ([Ying 2000; Norris *et al.* 2006). Normally, the steering control rules are derived based on heuristic knowledge with the specifically defined input variables for the particular system. The hierarchy for determining a control action in terms of which input variable relies on the importance of each input variable in achieving the steering control goal for the situation. A common sense approach is commonly used in this control rule derivation process.

The design of the fuzzy controller consists of three steps of control rules design, input parameters (including both the commanding input and the feedback inputs) fuzzification and control output defuzzification. As an intelligent system, a fuzzy controller mimics human decision process in determining appropriate control actions for different operational conditions. In controlling a hydraulically actuated steering system accurately, one needs to overcome the system deadband for obtaining a prompt response to a steering command by adding a deadband compensation signal to the control output. Meanwhile, to avoid the controller responding to a noise input, it is common to add a no-response zone to the input signal. The fuzzy controller evaluated in this study was designed in terms of the above logic. The deadband compensation addition is  $-0.1$  V and  $0.1$  V for both the retraction and extension action, and the no-response zone was set as  $[-0.5, 0.5]$  mm. All control rules were designed for covering the entire control region for this steering controller. In this study, a most commonly used fuzzy controller, namely a PD-like (also called the error-delta type) fuzzy controller, was designed for base performance comparison analysis. In designing such a controller, all control rules reveal an appropriate control action for a certain combination of the detected error and delta-error between a commanding set point and the actual control output. A table listing approach can be used to create all control rules seamlessly for such a PD-like fuzzy

controller. The determination of the appropriate control actions for each condition is heavily relied on the controller designer's knowledge on controlling the system. The control rules represented in this table can be read as:

$$\begin{aligned} &\text{IF } Error \text{ is } Level\_x \text{ AND } Delta\_Error \text{ is } Level\_y \\ &\text{THEN } Control\_Action \text{ is } Action\_z \end{aligned} \quad (3)$$

In design a fuzzy controller, the variable fuzzification is a critical step. The purpose of the fuzzification is to convert the real-valued input signals into word variables to be used in fuzzy reasoning. Seven levels of error and 11 levels of error rate were defined, and corresponding membership functions were defined for converting between the real-valued inputs to word variables. The eleven word variables of error were negative-full-scale (NF); negative-very-large (NVL); negative-large (NL); negative-medium (NM); negative-small (NS); zero (Z); positive-small (PS); positive-medium (PM); positive-large (PL); positive-very-large (PVL) and positive-full-scale (PF). The domain of the total position error was [-20, 20] mm. When define a triangular membership function for each word error variable (with an exception of zero, for which trapezoidal membership function was defined), the corresponding domains for those variables could be defined using an error characteristic domain ( $CD_{Error}$ ) vector (Lin *et al.* 2005) as follows:

$$CD_{Error} = \{-20 \ -10 \ -7 \ -4 \ -2 \ -1 \ -.5 \ .5 \ 1 \ 2 \ 4 \ 7 \ 10 \ 20\} \quad (4)$$

The seven word variables of error rate were negative-large (NL); negative-medium (NM); negative-small (NS); zero (Z); positive-small (PS); positive-medium (PM); positive-large (PL). The domain of the total error rate was (-2, 2) mm/s. When define a triangular membership function for each word error rate variable, the corresponding characteristic domain vector,  $CD_{d(Error)}$ , can be presented as follows:

$$CD_{d(Error)} = \{-2 \ -.3 \ -.2 \ -.1 \ 0 \ .1 \ .2 \ .3 \ 2\} \quad (5)$$

Defining the characteristic vector for all fuzzy variables is critical in design of the fuzzy steering controller. Properly defined fuzzy variable characteristic vectors for a specific vehicle can achieve prompt, stable, and accurate steering performance. In study, a sufficient number of characteristic points were defined, and those points were used to piece-wisely linearize the nonlinear transfer function of a hydraulic steering plant. Such large number of word levels makes the fuzzy controller require a minimal tuning on the characteristic domains for obtaining satisfactory control performance.

Similarly, it is also necessary to define a fuzzy membership function for each word variable of steering actions for converting the word-valued variables into real-valued control signals for implementation. The fifteen word variables of control actions were defined as negative-full-scale (NF); negative-very-large (NVL); negative-large (NL); negative-medium (NM); negative-medium-small (NMS); negative-small (NS); negative-very-small (NVS); zero (Z); positive-very-small (PVS); positive-small (PS); positive-medium-small (PMS); positive-medium (PM); positive-large (PL); positive-very-large (PVL) and positive-full-scale (PF). For this HIL steering simulator, the domain for the real-valued control signal was [-3, 3] V, and the fuzzy membership functions were defined for this particular range. The defined characteristic domain vector for corresponding triangular membership functions is as below:

$$CD_{Error} = \{-3 \ -2.5 \ -2 \ -1.5 \ -1 \ -.4 \ -.1 \ 0 \ .1 \ .5 \ 1 \ 1.5 \ 2 \ 2.5 \ 3\} \quad (6)$$

To implement the determined fuzzy steering actions on this HIL simulator, it is necessary to convert the obtained word variable steering actions into a real-valued control signal through a defuzzification process which converts two or more word-valued variables to one real-valued control signal. There are many defuzzification strategies available for different applications. This study applied the center of gravity (COG) strategy to calculate the real-valued control signal

because this strategy averages the domains of selected word variable steering actions, and thus it inherently reduces the noise and improves the robustness and accuracy in control (Lin *et al.* 2005). Figure 6 illustrates the fuzzy reasoning process, including appropriate steering actions searching and crisp control signal generating. As illustrated in the figure, when there are four steering actions applicable for the illustrated condition, with the COG approach, the real-valued control signal,  $u$ , is determined by the center of gravities,  $u_i$ , and the memberships of all obtained fuzzy steering actions,  $\mu(u_i)$ , are determined from the following equation

$$u = \frac{\sum_{i=1}^{i=4} u_i \mu(u_i) du_i}{\sum_{i=1}^{i=4} \mu(u_i) du_i} \quad (7)$$

where,  $du_i$  is the fuzzy domain width of corresponding fuzzy action.

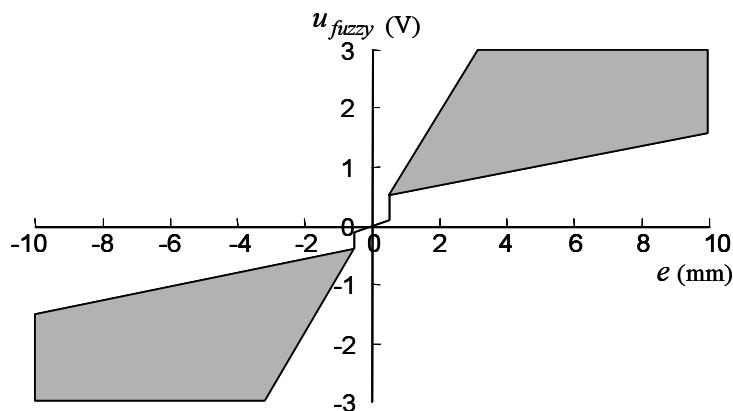


Figure 6. Definition of fuzzy control zone.

## VALIDATION TESTS AND RESULTS ANALYSIS

### General Description of the Laboratory Validation Tests

All three controllers developed in this study were implemented on the hardware-in-loop (HIP) electrohydraulic steering system simulator introduced in section 3.1. The steering control valve used on this HIL simulator was actually a tractor E/H steering control valve used on many agricultural tractors. A series of tests with step, ramp and sine wave inputs of various amplitudes (representing various of commanding steering angles) were conducted to evaluate the performances of three types of developed controllers. Because most of steering control actions in normal off-road vehicle maneuvering is small angle correction for keeping the vehicle traveling on desired paths, a high-performance steering controller should be able to accomplish such small angle correcting actions promptly and accurately. Take this consideration in mind, the commanding input amplitudes in this laboratory evaluation tests were set in the range between 5 and 200 mm in cylinder displacement, with more tests at the low end of the range.

### Hardware-in-the-loop E/H Steering Simulator

To make an unbiased comparison on control performance of three discussed controllers for E/H steering system control, those controllers were designed in terms of a validated E/H hardware-in-loop (HIL) EH steering control simulator and implemented on this HIL simulator. This HIL simulator, consisting of a hydraulic power unit, an E/H proportional steering control valve, a hydraulic steering actuator, a PC computer hosting a vehicle dynamic model and a controller interface, was designed for supporting off-road vehicle steering controllers. The functionality of the HIL simulator has been validated in previous studies (Zhang *et al.* 2000). The E/H steering valve used on the simulator is a Sauer Danfoss (Lincolnshire, IL) proportional valve activated using an electric driver. One function of the controller interface is to convert the steering signal generated by the steering controller hosted in the PC computer to PWM format to implement the

steering control via the electric driver. The controller interface also provides the 12 V DC power supply to actuate the electric driver. By applying a +6 V bias voltage to its input signal range of  $[-3.0, +3.0]$  V, the actual output control signal to the electric driver is between  $[+3.0, +9.0]$  V. Figure 4 shows the velocity control characteristics of the steering control valve corresponding to the input control signal. From this characteristics curve, one may find out that there exist two asymmetric patterns on velocity control gains and on system deadband: the maximum velocities are 0.35 m/s and 0.30 m/s with the corresponding deadbands of 0.52 V and 0.42 V for extending and retracting motions, respectively.

#### Controller performance comparison under ramp steering commands

In performing the evaluation tests, all three controllers were tuned to their optimal status for the specific test platform as described in previous section. The first set of evaluation tests was to investigate the capability of all examined controllers on tracking ramp steering commands of various strokes. Figure 7 shows the frequency response of the optimally tuned PID controller on the HIL steering simulator to sine wave commanding signals of 50 mm stroke. To evaluate and compare the performance of all three developed controller with a minimal influences of the HIL hardware system, the 0.5 Hz cycling time is chosen for all the commanding signals, including the step, ramp and sine wave commands, in conducting the evaluation tests.

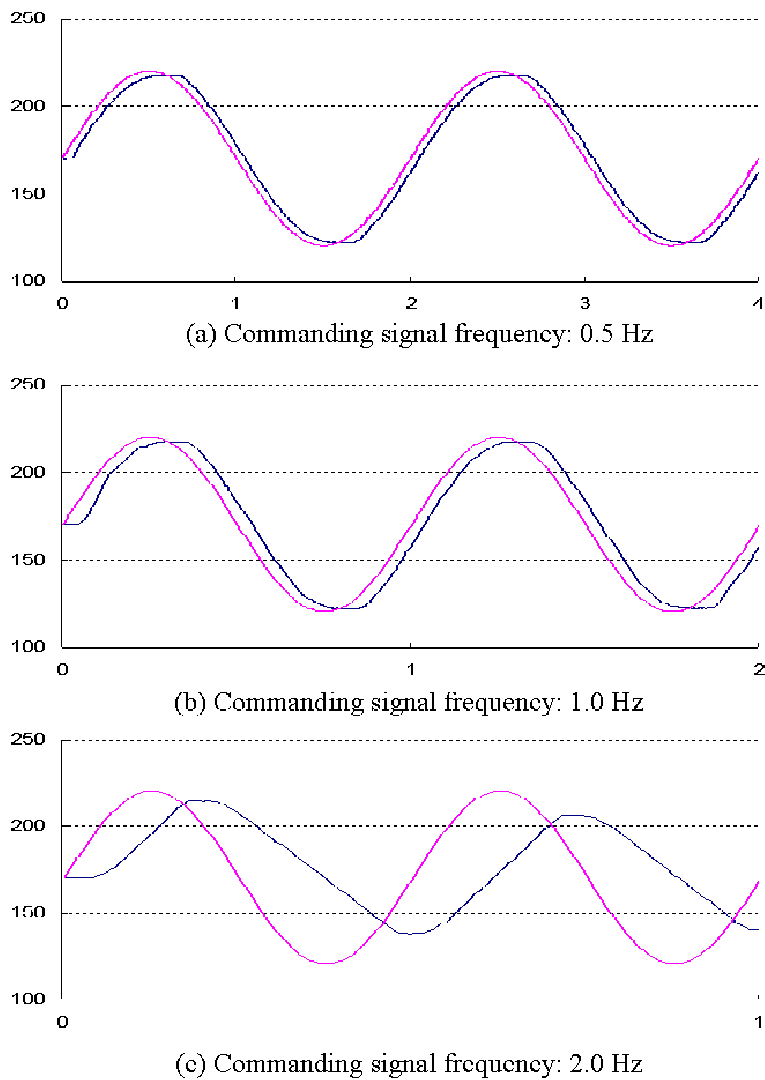


**Figure 7. Frequency response of the optimally tuned PID controller on the HIL steering simulator to sine wave commanding signals of 50 mm stroke.**

Figure 8 shows the response of all three controllers to 5 mm stroke step and ramp commanding steering inputs. From the obtained results, one may find that the PID controller can hardly track a small commanding steering stroke mainly due to the inherent deadband in a hydraulic steering

actuating system. Such poor tracking capability of a PID controller could be improved as the commanding stroke increases.

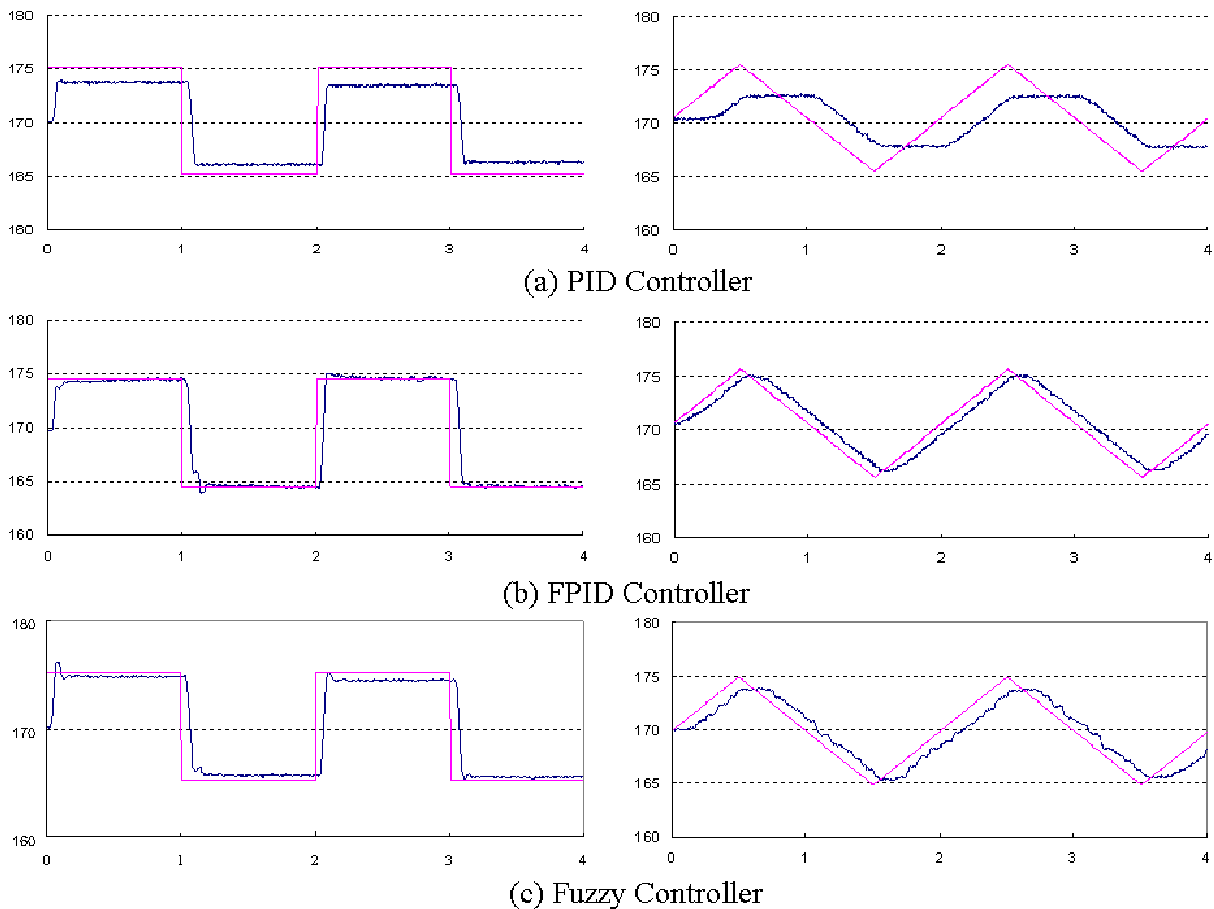


**Figure 8. Steering actuator position control performance comparison under both step and ramp steering commanding of 5 mm stroke for all three evaluated controllers.**

Figure 9 shows the trend of improvement on the trackability of the PID controller to commanding signal as the steering stroke increases. When the commanding stroke increased to 50 mm, it could almost track the commanding stroke completely. It indicates that when the commanding stroke is large enough, the hydraulic steering actuator could respond promptly enough to overcome the system deadband. However, in most cases, the steering corrections for an off-road vehicle traveling on the job site are small angle corrections, and therefore, small commanding strokes would much more likely be implemented. It implies that a PID controller may not provide satisfactory steering control performance for many off-road vehicles in most of the cases.

Comparing the a PID controller, figure 9 reveals that both the FPID controller and the fuzzy controller result in much better commands tracking performance to small steering commands. Such improved performance is mainly attributed to either by adopting a feedforward loop or by defining a zero zone to compensate for the system deadband.

Further evaluation also found that the PID controller resulted in a poor stroke tracking performance responding to a small stroke (5 mm) command, but could satisfactorily tracking the stroke command when it increased to 50 mm (Fig. 10(a)). As comparison, both the FPID and the fuzzy controllers could track the commanding strokes reasonably well, with the former presented a more smooth tracking performance than the later (Fig. 10(b) and 10(c)). That is most likely because the FPID controller integrates a feedforward controller and a PID controller, the feedforward controller can respond to a commanding input promptly and the PID controller can correct control errors effectively which leads to a superior performance on tracking input commands than a fuzzy controller.

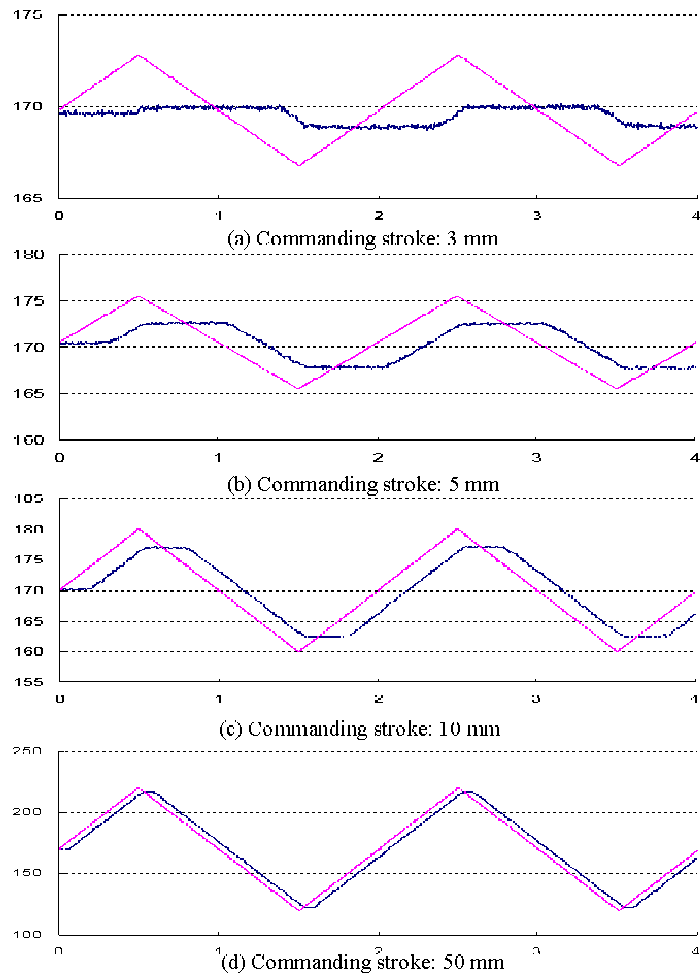


Figure 9. Steering stroke position tracking performance using a PID controller.

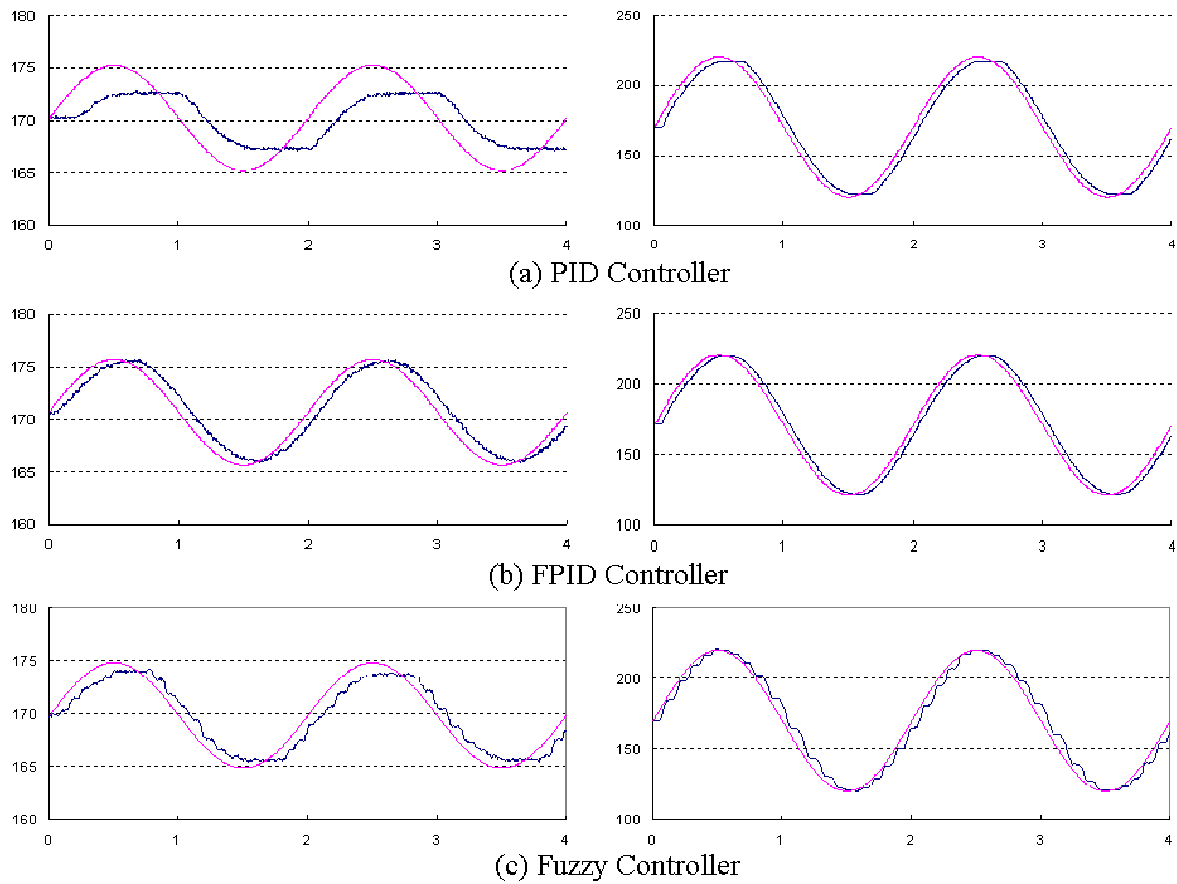


Figure 10. Comparison of steering stroke tracking performance to sine wave steering commands among three controllers.

## CONCLUSION

This study focused on the comparing the response and accuracy performance of three controllers, PID, FPID and fuzzy controllers, on achieving satisfactory steering control for off-road vehicles. While those controllers were designed suitable for any electrohydraulically implemented vehicle steering systems, the specific controller parameters were tuned to an optimal status for each of the controllers against a laboratory scale hardware-in-the-loop electrohydraulic steering simulator. Through analyzing the experimental results obtained from this investigation, it was concluded that the PID controller could not reach a satisfactorily control on the entire range implementation, mainly caused by the inherent system deadband of the hydraulic steering actuator. It always results in large errors both on tracking changing input commands (in the form of either ramp or sine wave) and on accomplishing a commanded steering action (namely with a large stable error). While such a poor performance could be improved with larger stroke of commanding steering input, an off-road vehicle requires making small steering corrections for most of the times in field operations. Therefore, a PID controller has a crucial limitation on achieving satisfactory control performance for an electrohydraulically implemented off-road vehicle steering system. The experimental results also proved that both the FPID controller and the fuzzy controller could offer satisfactory stroke control accuracy for the entire range of steering actuation, with the former could achieve more smooth control than the later. That is because a FPID controller uses an inverse valve transform-based feedforward loop to overcome the system deadband and uses the regular PID loop to correct the tracking error and both can be done in a continuous manner. However, an external disturbance may cause remarkable performance deterioration due to the feedforward loop implements the differentiated input commands and is very sensitive to any disturbance on the input signal, plus its PID loop is heavily relied on the feedback status of the system. In contrast, a fuzzy controller mimics human operator's logic in controlling the steering operation, can robustly handle any irregular behaviors of a hydraulic steering system, including the system deadband and external disturbances. But, its rule-based reasoning process results in a discrete feature in both tracking the commanding inputs and responding to detected tracking errors, which often attributes to less smooth tracking performance in comparing to a FPID controller in ideal cases. Therefore, both FPID and fuzzy controllers could achieve satisfactory steering control performance on off-road vehicles with an electrohydraulic steering system.

### Acknowledgements

This research was funded in partially by USDA Hatch Funds (ILLU-10-352 AE), Midwest Technologies Bruce Cowgur Memorial Funds and Deere & Company. UIUC College of Engineering Yee scholarship provides a scholarship fund to support Dr. Yingjie Gao conducting this research at the University of Illinois at Urbana-Champaign. Any opinions, findings, and conclusions expressed in this publication are those of the authors and do not necessarily reflect the views of USDA, Midwest Technologies Inc., Deere & Company, the University of Illinois, and Yanshan University.

## REFERENCES

1. Ang, K.H., G. Chong and Y. Li, 2005. PID control system analysis, design, and technology. *IEEE Transactions on Control Systems Technology*, 13(4): 559-576.
2. Aström, K.J. and T. Hagglund, 1995. *PID Controllers: Theory, Design and Tuning*. Research triangle park, NC Instrument society of America.
3. Dong, Z., Q. Zhang and S. Han, 2002. Control an electrohydraulic steering system using a PID controller with a nonlinear compensation algorithm. *Proceedings of SPIE, Unmanned Ground Vehicle technology IV*, SPIE Vol. 4715, 87-95: Orlando, FL.
4. Ellis, G., 2000. *Control system design guide (2<sup>nd</sup> Edition)*. Academic press: San Diego, CA.
5. Gu, J., J. Taylor and D. Seward, 2004. Proportional-integral-plus control of an intelligent excavator. *Computer-aided civil and infrastructure engineering*, 19(1): 16-27.

6. Haggag, S., D. Alstrom, S. Cetinkunt and A. Egelja, 2005. Modeling, control, and validation of an electro-hydraulic steer-by-wire system for articulated vehicle applications. *IEEE/ASME Transactions on Mechatronics*, 10(6): 688-692.
7. Lee, C.C., 1990. Fuzzy logic in control systems: fuzzy logic controller–Part I. *IEEE Trans. Syst., Man, and Cybernetics*, 20(2): 404-418.
8. Levine, W.S., 1995. *The control handbook*. Boca Raton, FL: CRC press.
9. Lin, W.S., C.L. Huang and M.K. Chuang, 2005. Hierarchical fuzzy control for autonomous navigation of wheeled robots. *IEE Proceedings of Control Theory Applications*, 152(5): 598-606.
10. Norris, W.R., Q. Zhang, R.S. Sreenivas, 2006. Rule-base reduction for a fuzzy human operator performance model. *Applied Engineering in Agriculture*, (in-press).
11. Qiu, H. and Q. Zhang, 2003. Feedforward-plus-proportional-integral-derivative controller for an off-road vehicle electrohydraulic steering system. *Journal of Automobile Engineering*, 217(5): 375-382.
12. Raimondi, F.M. and M. Melluso, 2005. A new fuzzy robust dynamic controller for autonomous vehicles with nonholonomic constraints. *Robotics and Autonomous Systems*, 52(2-3): 115-131.
13. Yih, P. and J.C. Gerdes, 2005. Modification of vehicle handling characteristics via steer-by-wire. *IEEE Transactions on Control Systems Technology*, 13(6): 965-976.
14. Ying, H. 2000. *Fuzzy Control and Modeling: Analytical Foundations and Applications*. New York, NY: IEEE Press.
15. Zhang, Q., 2003. A generic fuzzy electrohydraulic steering controller for off-road vehicles. *Journal of Automobile Engineering*, 217(D9): 791-799.
16. Zhang, Q., J.F. Reid, D.Wu, 2000. Hardware-in-the-loop simulator of an off-road vehicle electrohydraulic steering system. *Transactions of the ASAE*, 43(6): 1323-1330.
17. Zadeh, L.A., 1996. Fuzzy logic=computing with words. *IEEE Trans. Fuzzy Syst.*, 4(2): 103-111.



# SOFTWARE QUALITY IN DISTRIBUTED EMBEDDED SYSTEMS

J. Lenz<sup>1</sup> and R. Landman<sup>2</sup>

## ABSTRACT

The history of the off-road machine business has been based on proven designs and long times between model updates. However, the world-wide adoption of the ISOBUS standard is poised to change this history. ISOBUS is not only setting an open system for interoperability, it is establishing a sequence of features for diagnostics, sequenced operations, and information management. As customers discover these capabilities, they will expect them to be further advanced and customized for their specific needs. This requires adding agility into the proven durable processes so that manufacturers can respond faster to these growing needs. Electronics, and especially well-planned software systems, offer an agile technology for meeting this coming need. In this paper we will show benchmarking of various embedded software development projects relating project content, project rigor, and quality. From this we gain insights into maintaining quality while including agility into a durable development project.

**KEYWORDS.** Agile, Durable, Electronic, Embedded Systems, ISOBUS, Interoperability, Off-road, Processes, Quality, Rigor, Software.

## THE CHALLENGE BETWEEN DURABILITY AND AGILITY

Traditionally quality in electronics is built through long durability developments (Henning et al.). These long development cycles serve the market need when the market pull for new features changes slowly (Fig. 1). Even this process tends to over-serve the market. Because of the length of time between updates, there is a strategy to go beyond what customers are asking for. Introducing a product that over-serves (provides more performance and features than the customer needs at the time) can produce a negative impression of the product. The concept of a durable process as defined in this paper represents the long time between feature updates. This includes time to define the requirements and validate to these requirements so that the product does not significantly over-serve the market. This durable process is then managed to produce a high quality product where the electronics are primarily performing machine control features.

However, with the coming of ISOBUS standards for sharing controls and interoperability, there is a growing need for features related to machine intelligence instead of just simple machine control. These intelligence features are emerging from many users and suppliers in our industry, fueled by the interoperability of ISOBUS. These features are primarily developed and delivered through software in the electronics.

To keep up with the growing demand, a more agile process is needed (Fig. 2) which can more rapidly deliver when a durable process may mostly under-serve the current market needs. Our industry is being challenged to find a way to produce high quality, i.e. durable software in a faster, i.e. agile process.

---

<sup>1</sup> Deere and Company, Moline, IL, USA, lenzjamese@johndeere.com

<sup>2</sup> Phoenix International Corporation, 1750 Research Park Drive, Fargo, ND 58102 USA

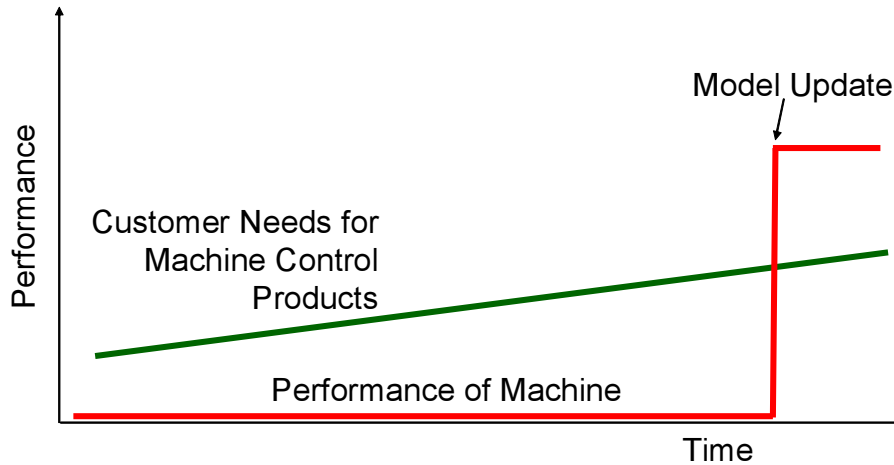


**Figure 1. Durable Approach.** A durable product development approach serves the customer if their need for machine updates increase slowly.

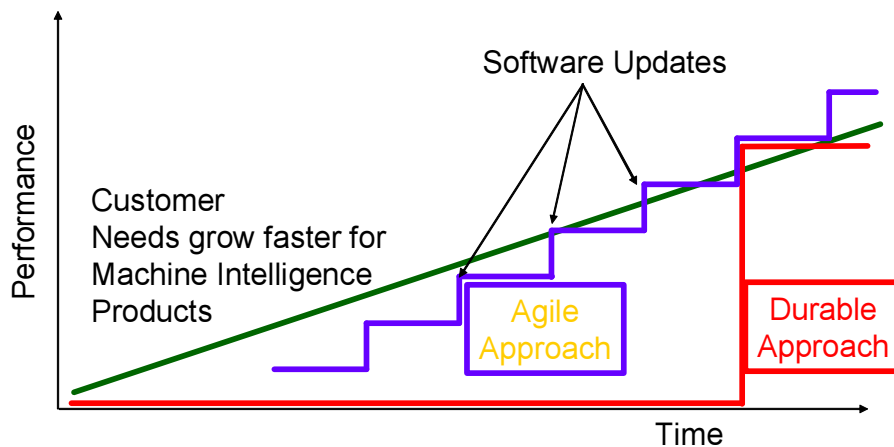


**Figure 2. Agile Approach.** An agile product development approach serves the customer if their needs are growing faster than traditional machine updates can accommodate.

## DEVELOPING SOFTWARE WITH AGILITY FOR DURABILITY

There are two basic foundations to adding agility to a traditional durability development process. The first is highly reliable reusable software components that can be quickly assembled to implement new features or completely new modules. Reuse of components such as vehicle network communications, reprogramming, fault management, user interface and many more give the machine designer a rapid development environment to build their individual module's capabilities (Lenz et al., 2004, 2005).

The second foundation is developer support. Developer support binds together the proven software architecture, standard software modules, and implementation details. Together these reduce development time and eliminate duplication of efforts. This approach is effective in avoiding repetition of costly mistakes that have already been solved. Developer support provides:

1. "Core" software for selected microcontrollers that includes I/O drivers, hardware abstraction and operating system.
2. Re-programming software preconfigured for specific microcontrollers, memory and hardware combinations.
3. In-depth training on the above components.
4. Application integration and debug support available by phone and email to all users.
5. Continuous improvement of "core" software with needed features as determined by a user group.

## SOFTWARE DEVELOPMENT AND QUALITY

A survey of 38 software development projects was performed to gain insight into how agility in the software development process was affecting the quality of the released software. The projects were rated by content, resources, rigor and quality across five different engineering groups. Each of these groups used the re-use software architecture and the support process noted above. Even with this averaging and binning of metrics, the data is still very noisy to compare. Each metric produces a score from 1 to 10 and is defined as follows:

### Content Metric

The Content Metric is computed by multiplying a computation and a code size ranking.

- Computation - ranking 1 for simple interface code, 5 for display-type code and 10 for real-time mathematics calculations.
- Code size - ranking 1 for less than 1,000 lines of code and no special interoperability up to a rank of 10 for greater than 100,000 lines of code with greater than 4 other controller interoperable dependencies.

These two ranking numbers are multiplied to provide a non-linear growth in content from these two factors. The result is then divided by 10 to scale the metric for a range of 1 to 10.

### Resources Metric

The Resources Metric is computed by scaling the total accumulated hours of engineering time involved in the project (across all projects studied) to fit a 1 to 10 scale.

### Rigor Metric

The Rigor Metric is computed by averaging two factors:

- Software development process usage - where full use of the process scores 10 and one point is deducted for each major activity not used.
- Running changes - the level of running changes on the project is measured on a scale from 1 to 10 with 10 equaling no changes to the original requirements down to 1 if the project involves weekly changes coming from marketing, customers, open requirements, etc.

### Quality Metric

The Quality Metric is scored as a 10 with a 1-point deduction for each defect discovered after the software release. All defects were counted. The severity of the defect was not ranked. Defects having no visible impact to the machine performance were still scored against the quality.

The first comparison of the data (Fig. 3) shows how project content varies between various engineering groups. These five groups were selected because they appeared to have different levels of maturity in use of software. One group seemed to have projects where the software was treated and developed as a component. Another seemed to use software to capture its domain knowledge of the systems operation. But as shown, each group covers a wide range of content between various projects. The second comparison of the data (Fig. 4) shows how project resources compare to project content. One would expect a strong correlation but the data shows a general trend and any specific project is not staffed solely based on project content. The third comparison of the data (Fig. 5) shows how project rigor varies between various engineering groups. Each engineering group tailors the development plan for projects.

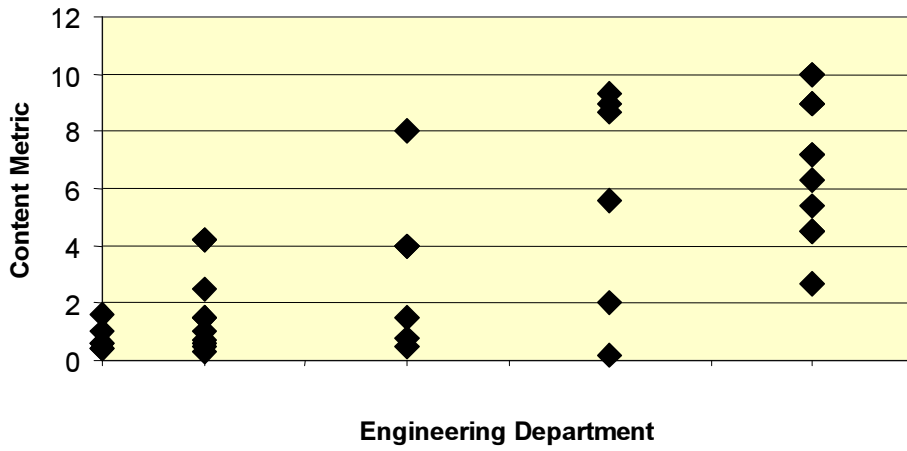


Figure 3. Comparison of project content between various engineering groups. A score of less than 4 indicates the software could be developed as a component versus a system solution.

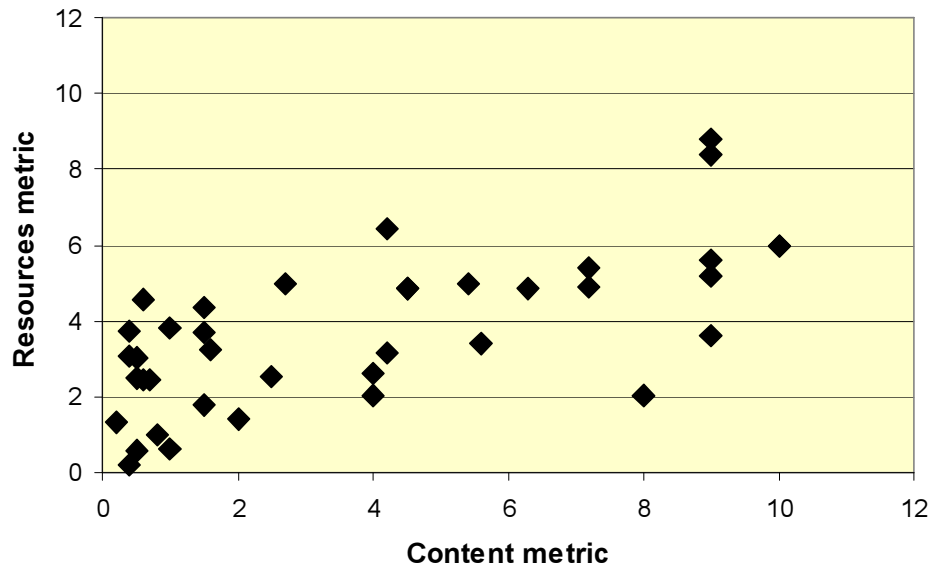


Figure 4. Comparison of project resources and project content. The data is very noisy, but a general trend appears - where there is more content in the project, more resources are needed.

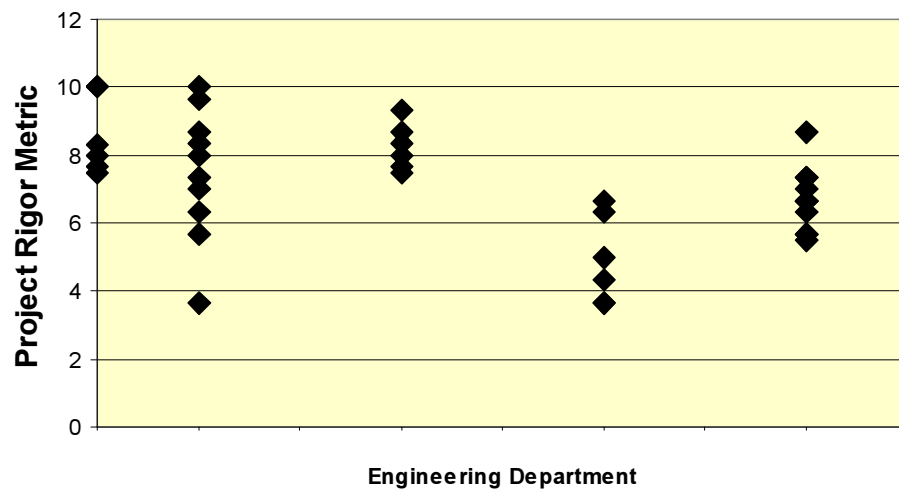


Figure 5. Comparison of project rigor between various engineering groups. A score of less than 10 indicates the software was developed with a tailored version of our process.

The fourth comparison of the data (Fig. 6) shows how project quality relates to the project development rigor in adhering to a software development process. The data is very noisy and there appears to be no measurable affect on quality by project rigor of the development.

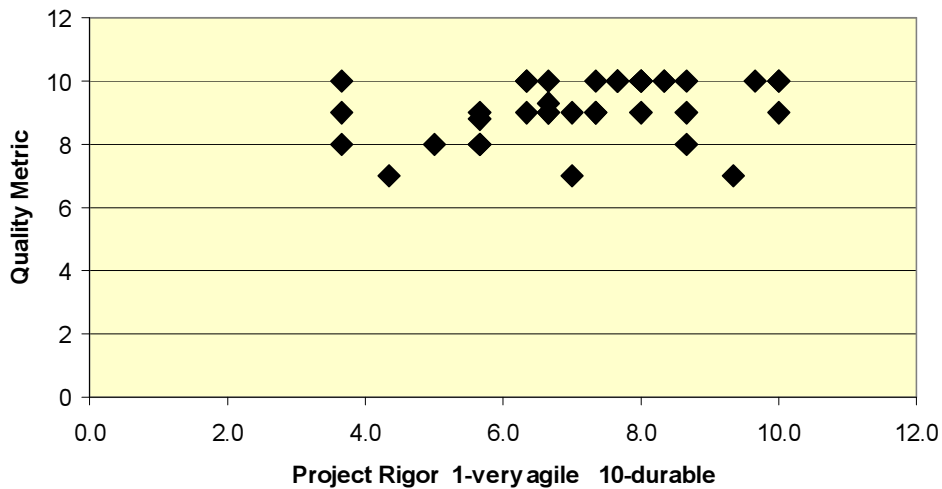


Figure 6. Comparison of Software Quality and the project rigor used for its development. There is no statistically significant measurable effect.

### SUMMARY AND FUTURE DIRECTIONS

Even with 38 projects assessed and generalizing and scaling metrics for scores between 1 and 10, the comparisons are very noisy. It may not be statistically important to draw conclusions, but we will at least attempt to draw some insights. It seems that project content (Fig. 7) is a major driver for tailoring a software project development plan.

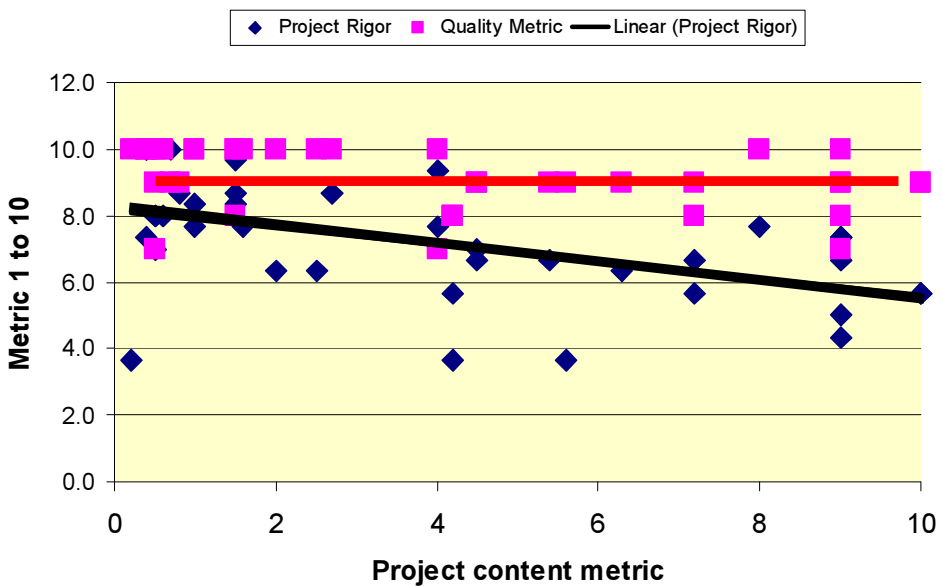


Figure 7. Comparison of project rigor and quality to project content. The use of less project rigor as project content increases should cause concern for quality, but at least in this survey, this agility does not influence software quality. We achieve quality from other factors in addition to project rigor.

The staffing of resources to a project is not strongly related to project content, yet there is some trend to having less project rigor for more complex projects. This would seem like the exact opposite should be encouraged and practiced. However the final quality is not noticeably affected. Including previous discussions, it seems that tailoring of the process is driven between the emerging adoption of electronics, continuous discovery of its capability and value, and a durable schedule for machine updates. High quality is still achieved through four factors: 1) using a

software process, 2) leveraging a high percentage of re-use in the interoperability software, 3) help desk support that gives assistance for the coding details, and 4) experienced staff that specializes in capturing systems domain knowledge in software.

Quality is the motivation for a durable process. As developers face the demand of the schedule there are two options: add inexperienced staff, or tailor the process. In an emerging or 'immature' situation, it appears quality is achieved better by tailoring the process and maintaining a tightly-integrated team. The future goal is always perfect quality. The tailoring of a durable process provides agility which allows for faster turns on ideas. As we grow to more complex systems with still emerging values for electronics, we will need even faster turns on ideas to maintain quality and customer expectations. Modeling and simulations are the next engineering practice to include agility in a durable product development process.

## REFERENCES

1. Henning, Prof. Dr.-Ing. Klaus and Andrea Heide, *Embedded Software Failure Analysis*, Centre for Learning and Knowledge Management and Department of Computer Science in Mechanical Engineering (ZLW/IMA) of the RWTH Aachen University.
2. Lenz, Jim and Robin Jensen. 2004. Customized Software for Distributed Control, VDI Conference, Hanover Germany.
3. Lenz, Jim and Peter Muench. 2005. Software Development for Off-road Machines, VDI Conference, Dresden Germany.

# VEHICLE PATH PLANNING FOR COMPLETE FIELD COVERAGE USING GENETIC ALGORITHMS

A. E. F. Ryerson<sup>1</sup> and Q. Zhang<sup>2</sup>

## ABSTRACT

In farming operations, one of the fundamental issues facing a farmer is the cost of running the farm. If the equipment the farmer is using can be made more efficient, the cost of farming will be reduced. One way of making agricultural equipment more efficient is to develop automated or autonomous functions for the equipment. One of the fundamental tasks for autonomous equipment is to plan the path for the equipment to travel. This paper reports the research on the feasibility of creating an automated method of path planning for autonomous agricultural equipment. Genetic algorithms were chosen to plan the paths with a primary goal of creating an optimal path guiding the equipment to completely cover a field while avoiding all known obstacles. Two example fields were designed for evaluating the feasibility of this concept on simple problems. While simulation results verified the feasibility of this conceptual path planning method, they also indicated that further development would be required before the algorithm could actually be implemented on agricultural equipment for real-world field applications.

**KEYWORDS:** Autonomous Equipment, Genetic Algorithm, Path Planning, Off-road Vehicle.

## INTRODUCTION

As the family farm has grown in size, often giving way to the larger corporate farm operations, many advances in efficiency have developed. Agricultural vehicles have continually grown to meet the ever-increasing demands of farming customers. In order to continue to improve efficiency and profitability, customers have demanded more horsepower, larger capacity, and comfort/convenience items, all allowing the vehicle to work for longer periods. Nevertheless, the ability to continue making improvements in areas such as horsepower and machine capacity is not infinite. Automation of agricultural vehicles has the potential to make farming more efficient (Palmer, 1991). Any automated machine needs a path on which to travel. There are two basic types of paths for automated vehicles. "Off-board" paths are often generated offline, either automatically by a computer or manually by a user. These off-board paths generally can take into account everything known in the operating environment, such as permanent obstacles and boundaries. They do not, however, have the ability to respond to unknown objects. On the other hand, "on-board" paths are those generated by the vehicle controller "on-the-run". On-board paths generally are good at reacting to obstacles or unsafe conditions, handling unexpected situations.

The problem of completely covering an area applies to many of agricultural operations, such as harvesting, mowing, planting, and spraying. The focus of this project is to create an optimal coverage path through a two-dimensional area that could be applied to agricultural applications. Genetic algorithms, combining the natural process of "survival of the fittest" with the power and speed of today's computer algorithms to rapidly find optimized solutions (Goldberg, 1989), have been studied extensively in vehicle path planning. Many researchers have studied using genetic algorithms to generate routes for avoiding obstacles between a "start" and an "end" point. A common approach in attempts was to find the lowest-cost path between "start" and "end" points,

---

<sup>1</sup> John Deere Harvester Works, 158th Street NorthEast Moline, Illinois 61244, USA, RyersonAnneE@JohnDeere.com

<sup>2</sup> Department of Agricultural & Biological Engineering, University of Illinois at Urbana-Champaign, Urbana, IL, 61801, USA

and the cost was often defined as a function of the total length of the path. Some other factors, such as time and obstacle avoidance, are also considered as a factor for cost determination in some of the reported approaches (Kambhampati and Davis, 1986; Lin et al., 1994; Noguchi and Terao, 1997; Hocaoglu and Sanderson, 1998; Gerke, 1999; Capozzi and Vagners, 2002).

The primary goal of this research was to perform a feasibility study on determining if a genetic algorithm approach is an appropriate method for performing dynamic path planning tasks and to develop recommendations for future development if it is a feasible approach. This research focused on evaluating the effectiveness of different components of a standard GA in searching for optimal paths. This research was, therefore, designed to explore a new application for GAs, rather than to create a new GA. To support this goal, several specific objectives were identified. Those research objectives are to investigate the capability of a GA in handling arbitrary obstacle shapes, to study the effectiveness of the GA-based planner on avoiding polygonal-shaped obstacles, and to lay the groundwork for future algorithm development.

## ALGORITHM DESIGN

A genetic algorithm (GA) is just a framework for a problem solution, not a solution in itself. Therefore, a GA must be adapted for each problem. This section describes how the GA-based path-planning problem is customized by making up of five key components to represent the field, the obstacles in that field, the grid of travelable area, the automated vehicle, and the path.

### Representation of Key Components

*Field Representation:* The field is the most important of all the components of this GA because it sets the groundwork for all other components. In this research, a polygonal area was chosen to represent the field of operation. This polygonal area denoted the boundaries of the field in which the automated vehicle will travel. Having an open number of vertices allowed GA to approximate, within the desired small degree of error, any possible area. To represent a polygonal field using a sequence of vertices, it requires at least three of these points to completely cover the area.

*Obstacle Representation:* One of the most important tasks in this project is the representation of obstacles in the field. In terms of the project goal of feasibility study, this project investigated two methods to model obstacles for demonstrating the feasibility. The first method was to model an obstacle as a circle, using a center point and a radius to represent its location and size. The other method was to model an obstacle as a polygon which represents an obstacle using a list of vertices (Lin et al. 1994). The detailed modeling methods will be introduced in the later sections.

*Grid Representation:* Once the field and obstacles were defined, the travelable area was converted into a grid of equally spaced points throughout the area. The grid spacing was defined to be equal to the machine width, and covers all the “travelable area” but not the obstacles. With the grids, the entire to-be-covered area in a field was divided into squares, and a unique index was used to identify the center point of each square in the grid. The rule of assigning the index started with the lower left-hand corner of the grid as index 0 to ensure that the grid numbering was consistent in every case, and that grid “0” was always started at the same place in this algorithm.

*Vehicle Representation:* The representation of an automated vehicle in this algorithm is essential but very simple. An assumption was made that this vehicle had an on-board controller to guide it following a provided path. The only vehicle-specific parameter used in this algorithm was vehicle width which was used to create the grids to represent the path in the field. If the size of a grid were equal to the width of the vehicle, then the machine could pass it, and the area could be considered as being completely covered during the operation.

*Path Representation:* A path in this algorithm was presented as a list of ordered 2D points for performing the functions of a genetic algorithm. A group of these 2D points served as the population in the GA, with each member being assigned a fitness value. This fitness value described the strength of individuals, and was used to determine which individuals were more likely to pass on to future generations. In this research, an ideal path was considered as the one that satisfied the following conditions that it covered 100% of the area (“the coverage measure”); it did not intersect any obstacles (“the obstacle measure”), it did not cross over itself (“the

intersection measure”), and it was as short as possible (“the length measure”). The coverage measure was calculated as the total percentage of the area covered by the selected path. The obstacle measure was a count of the total number of times a path intersected an obstacle. The intersection measure was a count of the total number of times the path crosses itself. And the length measure was the length of the selected path from the start point to the end point.

*Weighting Factors:* The above four parameters were used to define a successful path. However, they do not all hold the same level of importance when determining which path is the best. To solve this problem, each of the parameters was assigned a weighting factor to quantify the impact of those parameters on the fitness value of a path and such fitness values are directly related to the coverage, and inversely related to the obstacle intersections and the length. By tuning weighting factors, the impact of the evaluated parameters can be determined.

### Basic Functions

This GA-based path planning model includes four basic functions of selection, crossover, mutation and reproduction. Selection function is one of the basic functions in a GA system and a weighted roulette-wheel selection approach was used in this model. By this approach, the selection process was designed based on such a rule that the individuals with the highest fitness have a higher probability of being selected. This process simulates a weighted roulette wheel where each individual’s slot on the wheel is sized in proportion to its fitness (Goldberg, 1989).

The crossover is a function simulating the mating of individuals from the population which takes two individuals from the population (the “parents”) to create two “children” from the information in parent individuals. The simplest crossover (Goldberg, 1989) is a basic exchange of information between the two parents. A random point is selected in the parents. The function copies the information before this point from Parent 1 to Child 1, the information in Parent 2 after this point is then copied into Child 1, and the reverse occurs for Child 2. Therefore, each child carries a portion of the information from both parents.

The reproduction function performs the process of creating in a population of individuals in offspring generations (in this case, new paths). The process works in such a way that for a given population of individuals, the function selects individuals based on their fitness, and fill a population of new individuals.

A three-action mutation algorithm was designed to mutate a path as following in this research. The three actions were deleting-a-point, inserting-a-point, and modifying-a-point. One or more actions could be implemented during a particular mutation process for creating new paths. The choice of which of the three actions to implement is random. In this implementation, a random number was applied to determine which of the mutation actions would be implemented. If the action of deleting-a-point is applied, the mutation function will delete a random point in a path to form a new one. Based on this approach, once the delete action is called, the value at a randomly selected location in the path sequence will be deleted which resulted in the new path sequence one point shorter. If the action of inserting-a-point action is applied, the mutation function will insert a new point at a random location in the path sequence, and resulted in a one-point longer new path sequence. If the modifying-a-point action is applied, the mutation function modifies an existing point at a randomly selected location in a path sequence being processed. In this research, the modifying a point mutation function was so designed that it would randomly select a point in the area grid that is not already in the existing path sequence. The selected grid point would be then used to replace an existing point in the path sequence at the selected location.

Other than the four most commonly used functions described above, the GA-based path planner created in this research consisted of three more special functions of swap, record and remove crossing to enhance the performance of these functions. The swap function was used to reorganize the points within a path sequence without completely changing the order or the number of points in the sequence. The swap function was created based on a similar function developed by Lin et al. (1994) which created a new path sequence by swapping a back portion of an existing sequence at a randomly selected point to the beginning of the sequence. The purpose of the swap function is to create a better path while preserving some of the genetic information by retaining the order of the points. The reorder function is used to reorganize the points in a path sequence by completely

changing the order of the points in the sequence. This function was developed based on the work of Capozzi and Vagners (2002). The function took a known path sequence and reordered the points in that sequence in a completely random order. The remove crossings function is used to remove crossings, or places where a path crosses itself, in a path sequence.

One very important and practical function of this GA path planner is to find a location where a path sequence crosses itself and then reorders the points in that area to remove the crossing. This function is unique in that it retains the information and the path that has been generated by the algorithm, but it reverses the direction of travel on that path and swaps two points. The first step in the function was to locate a crossing. The function did this by checking each of the segments of the path against each of the other segments in the path sequence to see if they were intersected. If the intersection point  $(x_i, y_i)$  of these two lines were within the boundary of a grid comprising the X and Y coordinates of the two segments, then those two segments would be classified as intersected. Otherwise the segments were considered not intersected, and the process would continue on to assess the next pair of segments. Once an intersection was found, the next step was to remove the intersection. This was simply done by re-ordering the points around the intersection, to remove the cross. This is best demonstrated using a graphical example. As a path illustrated in figure 1, defined by sequence ABCDEFG, it can simply be reordered to remove the intersection by reversing the order of the points between A and G. The new path is defined as sequence AFEDCBG, and shown in figure 2. After a crossing in a path has been removed, the process will continue through the rest of the path to make sure there are no other crossings. In case it was not possible to remove a crossing without creating a new one, the algorithm would stop after running a finite number of times through the path to avoid an endless loop. After a path was modified, a recalFitness variable would be set to be “True” to signal to the system that the path was changed and should have its fitness value recalculated.

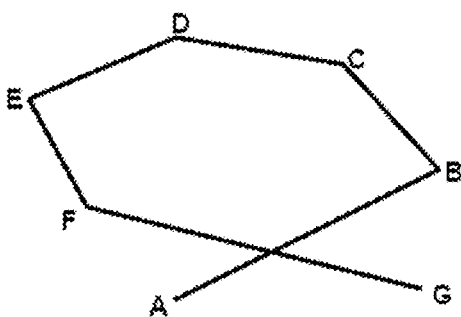


Figure 1. Seven Point Path with Intersection (before removal).

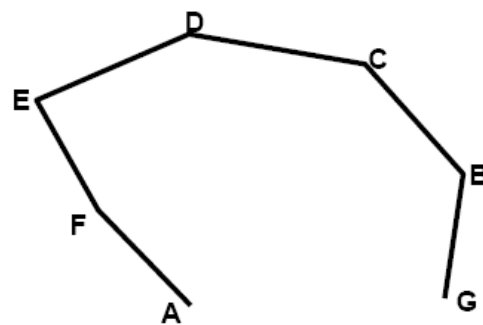


Figure 2. Seven Point Path with Intersection (after removal).

### Integration of Basic Functions

Figure 3 shows a flowchart describing how the basic functions are integrated into the program and how the algorithm works. This research used specialized functions, in addition to the standard genetic algorithm functions, to build the path planner. This approach helps to make the genetic algorithm more problem-specific, by tuning GA functions to specific requirements of the problem. The specialized functions used in this algorithm include the swap and reorder functions, which can create new members in the population while retaining all the points in the original paths. These functions were designed based on the theory that a path might contain all the “correct” points but not in the correct order. By reordering points in a path, the algorithm could find a better path. This concept was based on the work of Capozzi and Vagners (2002) who developed a reorder function. The swap function was based on the work of Lin et al. (1994).

Another function was the remove crossings function. This function allowed the paths to be “corrected” and had those portions of a path that crossed itself to be reordered in order to remove the crossing. This function searches new paths, by retaining the path information and reversing the travel direction on that path. This specially tuned genetic algorithm is able to generate paths through the field meeting the requirements of the application.

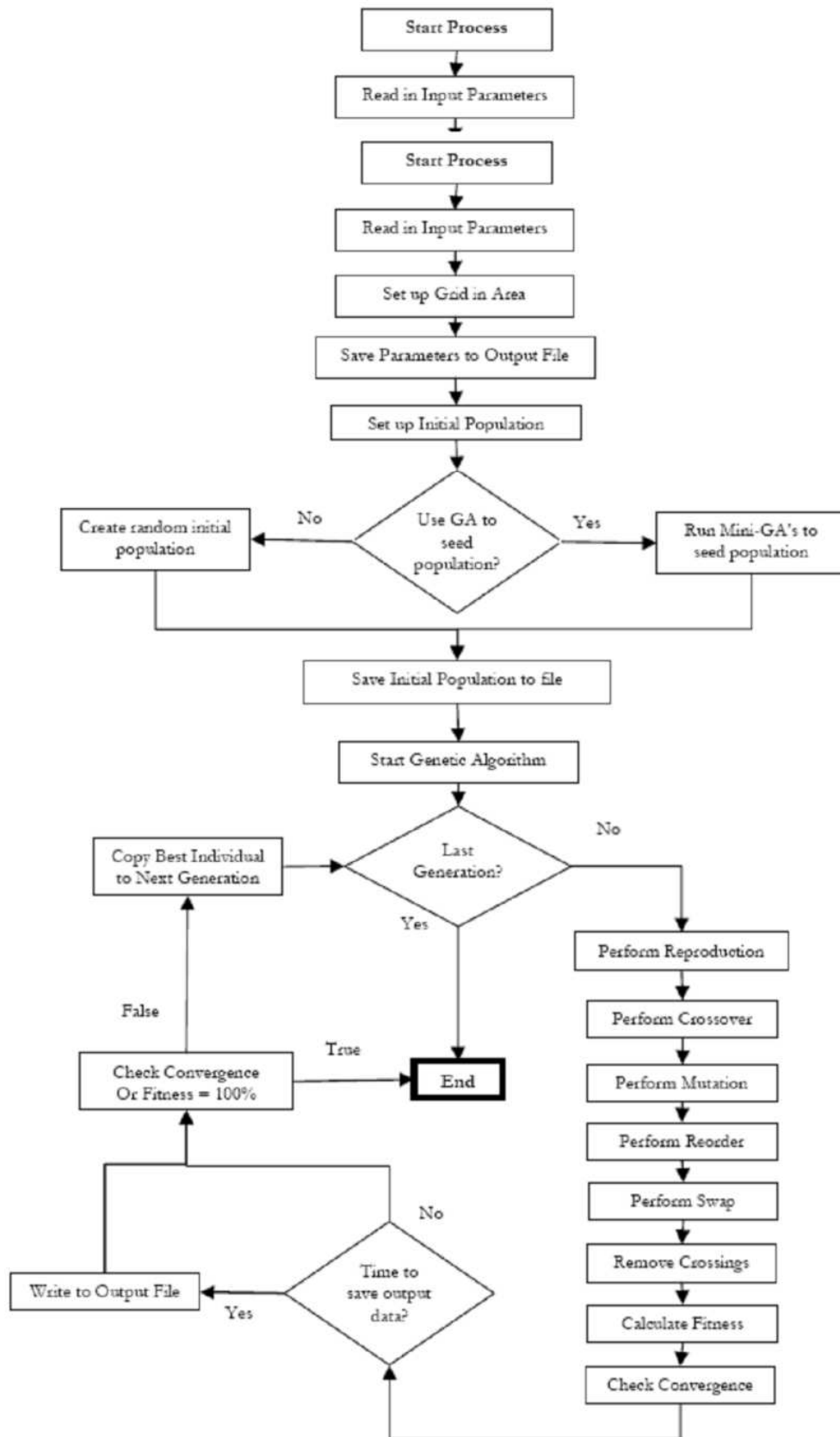
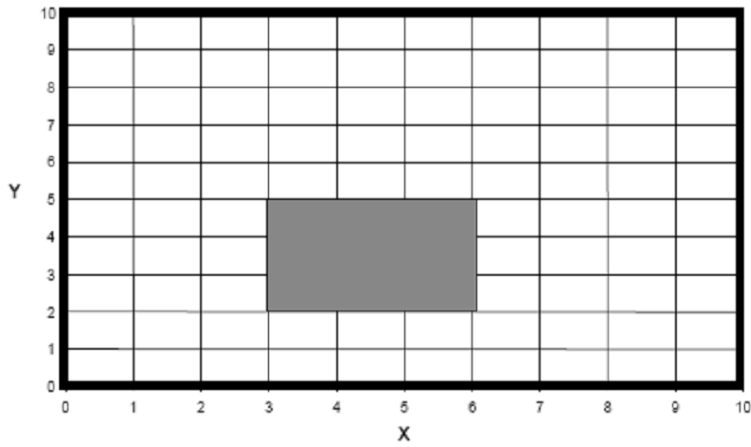


Figure 3. Flowchart of genetic algorithm (GA) based path planner.

## RESULTS AND DISCUSSION

A validation study was conducted based on a test condition of a field with one obstacle and a rectangular area as shown in figure 4. The purpose of the test is to evaluate the algorithm's ability to work on a simple problem and to consistently generate a path with coverage over 90% on this problem.



**Figure 4. Area and obstacles for test condition 1.**

The test settings used for this configuration are in table 1. The settings for the genetic algorithm were the highest-performing settings of 27 different groups of settings. These settings were selected after a series of 135 test runs (27 groups, 5 runs each).

A total eight runs were performed on this test configuration. The results from those runs are shown in table 2, which shows the “best” path, or the path with the highest fitness value. A quick review of this data showed that on four of the eight runs, the total coverage attained was greater than 90%. The average coverage attained was 89%. The top-performer was Run 5, which had a coverage of 97% and a fitness value of 30.95. This path is shown in figure 5. The lowest-performer was Run 7, which had a coverage of 82% and a fitness value of 26.37. The best paths generated by the top runs from this configuration are listed in table 3.

**Table 1. Optimized settings for test condition 1.**

Probability	Optimum Value
Mutation Probability	0.05
Crossover Probability	0.1
Swap Probability	0.01
Reorder Probability	0.01

**Table 2. Results of test configuration 1.**

Run	Coverage	Fitness
1	0.90	28.84
2	0.87	27.78
3	0.89	28.48
4	0.86	27.43
5	0.97	30.95
6	0.91	29.19
7	0.82	26.37
8	0.92	29.54
Avg	0.89	28.57

**Table 3. Top four results from test configuration 1.**

Run	Coverage	Fitness	Figure
1	0.90	28.84	6.4
5	0.97	30.95	6.5
6	0.91	29.19	6.6
8	0.92	29.54	6.7

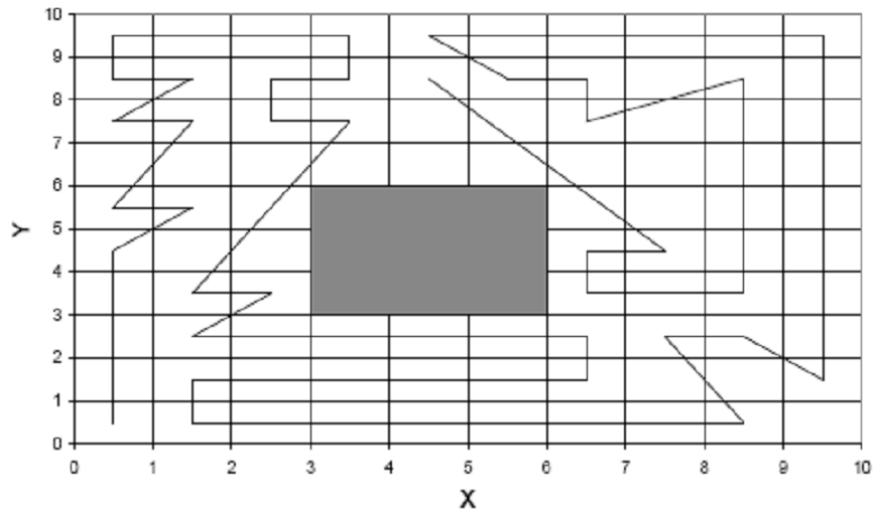


**Figure 5. Results of run 5 for test configuration 1.**

When comparing the results of those four runs, there are a few interesting things to be noticed. First, the path of Run 5 had many sharp edges and turns, which would make it very difficult for a tractor to physically follow. This was because this genetic algorithm could not take turning radius of the machine into account. Such a result implies that a fully developed GA-based path planner for agricultural vehicles must be capable of modifying the path to be “vehicle-specific” in order to be able to physically follow it. Next, in order to attain a higher coverage, the algorithm had a mutation function that added points to the path. Therefore, adding these points caused the path to become more jagged. This means that the algorithm needs to add more points to this path in order to get a higher coverage, however it may result in sharp edges observed in the final path. Last, it is important to remember that a genetic algorithm is still a random process. Each time the genetic algorithm runs, it starts with a completely new random population. Therefore, the results of each run of the genetic algorithm will result in a different solution, and these four solutions are intrinsically different due to the random nature of the genetic algorithm. This is one of the basic characteristics of a genetic algorithm.

Other observations made on the final paths generated by the genetic algorithm indicated that the genetic algorithm could successfully generate paths not intersecting any obstacles. The route a resulting path created remained at least a half-grid away from the obstacle. Since the grid was equivalent to the width of the machine, it could be concluded that the path could successfully avoid the obstacle. Another observation was that the resulting paths were not the “typical” paths as a farmer would traditionally take. That was because the genetic algorithm used in this planner did not have features built in for “encouraging” parallel paths. By adding such a consideration in future GA planner development, it is possible to add such functions into the GA system, and generate paths more like a human operator would normally take.

Similar validation studies were conducted on different field configurations, such as on a non-rectangular field with multiple obstacles. Very similar results were obtained from those studies. Figure 6 shows the results obtained by running these groups of settings. Each data point on this chart corresponds to the average of the best individuals created by the genetic algorithm at the end of each run. Notice that for both the average coverage and the average fitness, the group with the highest performance was Group 1.

How might one be able to improve the performance of the algorithm on this area? There are a few possibilities. One method of improving the results might be to increase the number of generations that the genetic algorithm is allowed to run. This could allow the genetic algorithm more time to create a better solution. Another method of improving the results might be to “seed” the initial population with a set of predefined paths, in effect giving the algorithm a “jump start” on a solution. These methods were not attempted for this project; however, they are interesting possibilities for further development.

### Coverage and Fitness by Group

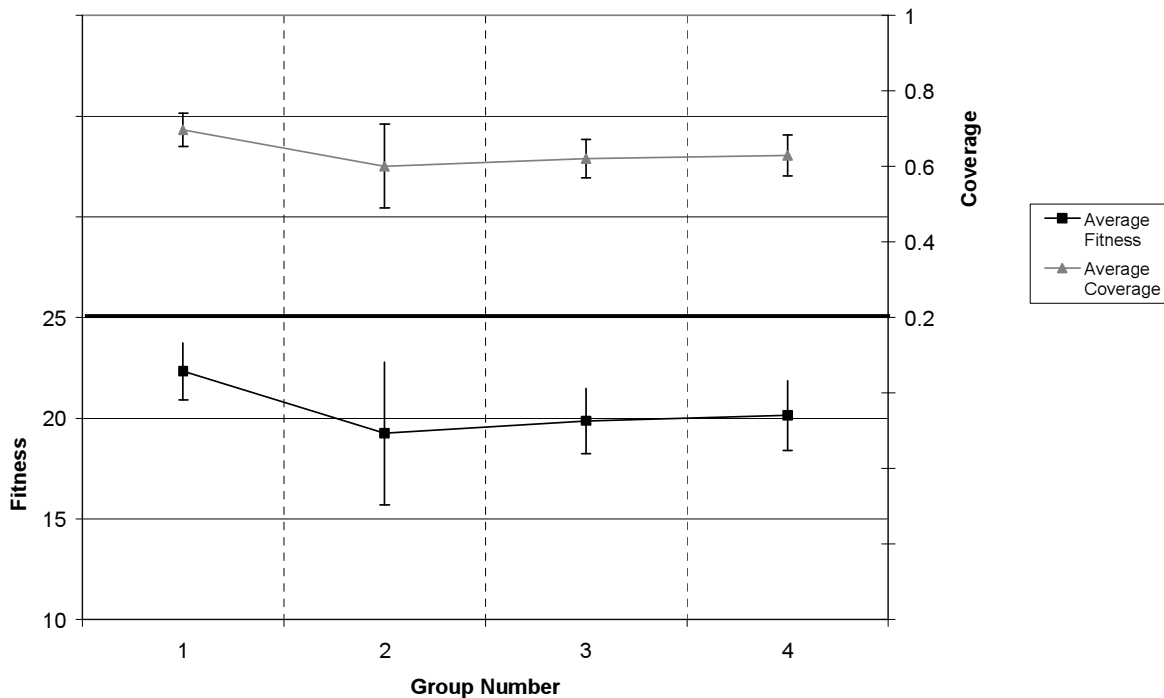


Figure 6. Results obtained from test configuration 2.

### CONCLUSION

This research was intended to conduct a feasibility study on whether it is possible to create a GA-based path planner for machinery operating on agricultural field. It has proven that it is feasible to use a genetic algorithm to create optimized paths through a field. Although this research did not create completely optimized paths, computer simulation analysis demonstrated over 90% coverage on fields of different shapes with various obstacles within the fields.

This research set the foundation for future development by setting up a framework for GA-based path planning system. This research also uncovered a few issues of worthy further investigation. For example, by making the genetic algorithm more intelligent and/or by adding constraints specific to the agricultural problem, it could possibly make the GA-based path planning algorithm capable of planning paths on uneven field terrains by represent the field in a three-dimensional format. An additional enhancement could be to design a “keep out” region around each obstacle, in which the path would not travel, thus ensuring that the vehicle would remain a safe distance from the obstacle. One constraint that was not utilized in this research was the use of vehicle parameters in planning paths. By including the vehicle parameters, such as the vehicle size, the turning radius and the maximum speed, it might help to generate paths more suited to agricultural vehicles to follow.

#### Acknowledgements

The material presented in this paper was based upon work supported partially by USDA Hatch Funds (ILLU-10-352 AE). Deere & Company supports Ms. Ryerson conducting graduate studies at the University of Illinois at Urbana-Champaign. Any opinions, findings, and conclusions expressed in this publication are those of the authors and do not necessarily reflect the views of the University of Illinois, Deere & Company and USDA.

## REFERENCES

1. Capozzi, B.J. and J. Vagners. 2002. Evolution as a guide for autonomous vehicle path planning and coordination. In *Aerospace Conference Proceedings, IEEE* 5: 2527–2536. Piscataway, NJ, USA: IEEE.
2. Gerke, M. 1999. Genetic path planning for mobile robots. In *Proceedings of the 1999 American Control Conference* 4:2424-2429. Piscataway, NJ, USA: IEEE.
3. Goldberg, D. 1989. *Genetic Algorithms in Search, Optimization, and Machine Learning* Reading, MA: Addison-Wesley.
4. Hocaoglu, C. and A.C. Sanderson. 1998. Multi-dimensional path planning using evolutionary computation. In *Proc. IEEE Conference on Evolutionary Computation*, 165-170. Piscataway, NJ, USA: IEEE.
5. Kambhampati, S. and L. Davis. 1996. Multiresolution path planning for mobile robots. *IEEE Journal of Robotics and Automation*, 2(3): 135-145.
6. Lin, H.-S., J. Xiao and Z. Michalewicz. 1994. Evolutionary algorithm for path planning in mobile robot environment. In *Proc. IEEE Conference on Evolutionary Computation*, 1: 211-216. Piscataway, NJ, USA: IEEE.
7. Noguchi, N. and H. Terao. 1997. Path planning of an agricultural mobile robot by neural network and genetic algorithm. *Computers and Electronics in Agriculture* 18: 187-204.
8. Palmer, R.J. 1991. The adoption of automatic field operations. In *Proc. IEEE Western Canada Conference on Computer, Power and Communications Systems in a Rural Environment*, Piscataway, NJ, USA: IEEE.
9. Sugihara, K. 1997. A case study on tuning of genetic algorithms by using performance evaluation based on experimental design. *Technical Report ICS-TR-97-01, Dept. of Information and Computer Sciences*, University of Hawaii at Manoa.



# BE READY FOR THE ISOBUS (ISO 11783) -THE NEW STANDARD FOR AGRICULTURAL MACHINERY

**R. Buschmeier<sup>1</sup>**

**KEYWORDS.** ECU, ISOBUS, Virtual Terminal.

Manufacturers of agricultural equipment increasingly turned to electronics to provide products with improved functionality, productivity, and performance to enhance customer appeal. Electronic content in agricultural equipment has increased; and as a consequence of adding electronic components to agricultural equipment has been realization of the advantages of allowing communication between controllers managing different machine functions.

A hitch controller on a tractor, for example, may communicate with a transmission and engine controller to allow optimized performance. Electronic communications can be used to co-ordinate machine functions and operations, allow information to be shared among different controllers on a machine, this allows control systems to be located closer to the basic function they are controlling on the machine. With the benefits of a reduction in the costs of installation and improves product reliability.

Historically the interface between tractor and implement required significant standardization with development of standardized PTOs, hydraulic connections, and three-point hitches. This standardization enabled equipment designed by various manufacturers to be used together. Addition of electronics to agricultural machines has created a similar requirement and need for additional standardization. A requirement for communications between implements and tractor mounted displays and other tractor mounted controllers, underlines the need for a standardized electronics communication protocol.

ISO 11783 is a new standard for electronics communications protocol for agricultural equipment, which is, named now ISOBUS! This standard has been developed to meet the needs for electronics communication between tractor and implements, between controllers within tractors (based on SAE J1939), within implements, and within other self-propelled machines. Support for precision farming applications has also been built into the standard. Definition and support exists for operator interfaces, and communications with an off-board management information system.

The ISOBUS is supported world wide by well-known tractor and machinery manufacturers and will make it possible to operate and control all types of implements and machines using a single monitor such as the BASIC TERMINAL mounted in the tractor cab. This terminal provides a simple input/output interface for the operator to communicate with the electronic control units (ECU's) participating on the ISOBUS.

The BASIC TERMINAL (Fig. 1) of Müller Elektronik is a real Virtual Terminal according to ISO11783. ISOBUS ECU's are able to present their operator with graphical images on the 320x240 pixel sized graphic LCD screen. The operator can directly take control of the actual connected devices by means of the 5 keys on the left and right hand side of the screen respectively, called softkeys. The conception and design of a successful operator interface is responsibility of the manufacturer of the ISOBUS equipment, and the BASIC TERMINAL provides the basis, of man machine communication. The ISOBUS standard supplies an immense collection of features to create a specific and sophisticated operator interface for any purpose to be displayed on the Virtual Terminal.

---

<sup>1</sup> Müller-Elektronik GmbH & Co., Germany, Buschmeier@mueller-elektronik.de



**Figure 1. BASIC TERMINAL compliant to the ISOBUS.**

The data from a controller, to be displayed on the screen, is always encapsulated in a data mask. Each single element of the data masks might be controlled and modified online by the ECU. By this means for example, static and even animated graphics can be faded in. All elements of data masks are updated cyclically by the appropriate ISOBUS ECU. This enables the operator to be informed about the actual states and working conditions of a machine at any time.

A special area of the screen is reserved as description area for each of the ten softkeys and can be used to display an icon graphic or descriptive text to explain the functional meaning of the keys. These areas are called softkey mask. Softkey masks form a part of a hierarchical design, allowing navigation control between different data masks. By this means the operator can be logically directed to a specific device, even in very complex operator interface structures. The BASIC TERMINAL always assigns the softkeys to the actual displayed ISOBUS ECU's. Furthermore simple and even complex controlling procedures might be activated and controlled by the operator in an easy way by simply pressing some softkeys.

Of course an operator interface is not only related to displaying data and indicating states and conditions. An essential part of any operator interface is the facility of data input. If the terminal detects any input data element inside a data mask the internal input procedure is automatically activated. The BASIC TERMINAL provides navigation control for data input to the operator by an incremental knob on the right hand side of the housing. By pressing the knob the operator enters data input mode. Turning the incremental knob easily does changing values. Once a new value is entered the BASIC TERMINAL sends out the new data to the appropriate ISOBUS ECU.

Furthermore the BASIC TERMINAL offers the operator a menu key. By pressing this key a special menu is displayed and the operator can activate different internal terminal functions or select one of the currently available operator interfaces of the connected ISOBUS ECU's.

A group of ECU's, a so-called Working Set, for example, all ECU's for one implement can use the same set of data masks. One ECU, the Working Set Master, is responsible for communicating with the Virtual Terminal and the operator interface of the whole group.

Another important part of the operator interface is a multifunction grip, shown in figure 2. It allows access to the important operational function of the machine, that are needed while working. The multifunction grip is sited ergonomically for the operator's hand, for ease of use and reduced the operator fatigue. That makes ISOBUS machines very convenient and easy to work with. It is generally possible to share the grip for similar functions on different machines.



**Figure 2. Multifunction grip for the ISOBUS.**

Müller-Elektronik offers also a wide range of ECU's. Engineering for use in the rough environment of the mobile agricultural equipment. Indestructible aluminium housings have been selected, together with a wire harness using AMP single wire sealed connectors (Fig. 3). This also provides high immunity to EMC, voltage overload and short circuit protection are also included.



**Figure 3. 16bit ECU with 3x42pin connectors and wire harness.**

The Tractor ECU controls the tractor power unit management functions, this ECU is able to read these standard tractor signals, then send them via, the ISOBUS to all the connected ECU's. It is equipped with the wire harness and one standardised 9-pin ISOBUS connector to be installed in the rear of the tractor (Fig.4). An optional front connector is available. With this Tractor ECU it is possible to change every tractor into an ISOBUS compliant tractor.



**Figure 4. 9pin ISOBUS connector.**

The general purpose ECU's are available in different hardware levels and with varying scales of functionality.

It starts with small fully podded units with up to 8 outputs and up to 10 inputs that are used for simple solutions or as slave controllers (Fig. 5). The 16 bit microprocessor units are used in a small version as a bridge controller to J1939 networks or for complex control functions with less output capabilities (Fig. 6). The high-end 16-bit units supply up to 55 outputs and 30 inputs and are able to fulfil different complex control functions. For even higher requirements is a 32-bit unit under development.



**Figure 5. 8bit ECU with up to 18 outputs and 8 inputs.**

Each of the ECU's designed by Müller-Elektronik perform the communication with the Virtual Terminal and is responsible for controlling actuators and reading in the signals of connected sensors.

Machine specific application programs are loaded into the memory of these ECU's. They are designed to control and to supervise the complete operation of the machinery. The appropriate operator interface mask is also part of the software and is uploaded into the Virtual Terminal memory, once during the start up period of the network. The operator interface is designed to give the maximum number of screen layouts available with in screen size and the maximum number of ease to operate softkeys. Furthermore different languages are supported and can be selected by the operator.



**Figure 6. 16bit ECU for J1939 bridge.**

Based on the variety of the available ECU hardware there is also an extensive software library available. This enables the manufacturer of machinery to create his specific and proprietary application program and operator interface without too much knowledge about ISOBUS properties. All ISO11783 and also hardware related actions can be executed by the libraries all alone. The manufacturer only has to take care about the machine oriented parts of the solution for

his machine and to become another member in the growing family of providers of ISOBUS based electronic control units for agricultural machines.

With the continuous implementation of compatible ISOBUS-Systems the stage has been set to apply Precision Farming on a wider scale in the future.

With the agricultural software on the farm-PC, tasks for the field work can be planned at all times. Geo-referenced data (e.g. yield maps) can be read and processed to create new application maps (e.g. fertilizing maps). The data transfer to Müller-Elektronik's BASIC-Terminal TOP is carried out with a USB-Stick in the XML-format according to the ISO-Standard 11783.

The operator on the tractor can choose one of the planned tasks at the terminal and put the task to execution, but he can of course modify the task also in the field. He can as well start a simple logging task to fulfill the legal requirements of documenting his plant production work.

Responsible for the execution of the tasks in the field is the „Task Controller,, which is integrated in the terminal. It determines the current GPS-position, sends the respective set points from the application map to the implements and records position specific the current actual values.

Thanks to the ISOBUS-standard one task management is able to work with different implements from different manufacturers.

The farm management information systems of the companies like Agrocom, Helm-Software and Land-Data Eurosoft are currently supporting the ISOBUS XML-interface on the farm-PC side for the task management in the BASIC-Terminal TOP.

The ISOBUS-technology is the basis for the further developments of the agricultural technology in the coming years and decades. Investments in this technology are therefore future-proof. Benefit is the fulfillment of legal requirements to keep records and the automated and error free acquisition of data. Additionally there are the already known ecological and economic advantages of product savings with variable rate applications as a result of this new technology.

A further step of using the already available ISOBUS-terminal and Task Controller is seen with the integration of guidance systems. They start with parallel guidance operated with the VT optionally using a lightbar for steering information. It ends up with RTK high precision automated steering systems showing up on the VT and driving along the planned paths in the field. An additional step of automation is then the switching of sections or the whole implement at the boundaries of the fields. It is available with the COMFORT-Terminal (Fig. 7) of Müller-Elektronik and it is done simply by using the already available information and the available access to the implements.



**Figure 7. COMFORT Terminal.**

The future has begun!



# TTA-GROUP STEER-BY-WIRE WORKING GROUP

M. Plankensteiner<sup>1</sup>, L. Silberbauer<sup>1</sup>, K. Buus-Jensen<sup>2</sup>,  
T. Lovric<sup>3</sup> and C. Seethaler<sup>4</sup>

## ABSTRACT

The development of Steer-by-Wire (SbW) systems for on-road use is a challenging task. In a joint industry effort several companies have teamed up in the TTA-Group SbW Working Group to develop an architectural cookbook for SbW. The working group started with the development of a concept document. It adopts IEC 61508 for the development of a reference SbW architecture for on-road use. The main goal of the working group will be achieved in a second step where electronic architectures will be developed, focusing on three different vehicle classes: Fork-lift, agricultural tractor and wheel loader.

**KEYWORDS.** FleyRay, IEC 61508, Safety, Steer-by-Wire, TTA, TTA-Group, TTCAN, TTP, X-By-Wire.

## INTRODUCTION

Steer-by-Wire (SbW) is an advanced steering concept for adaptable steering and modularity that eliminates the mechanical connection between the steering device and the wheels. Actuators steer the wheels, and an additional steering wheel actuator provides feedback to the driver. SbW promises to improve the vehicle in many ways, from packaging to performance and safety [1].

SbW is a feature that has been discussed for a long time. The EU-funded X-By-Wire project with seven industrial partners from the European automotive industry and two universities started in 1996 [2]. In the meantime the SbW topic has been elaborated in several papers (e.g. [3,4]) and a number of prototypes have been built (e.g. [5,6,7,8]), but so far no larger numbers of vehicles have found their way on public roads.

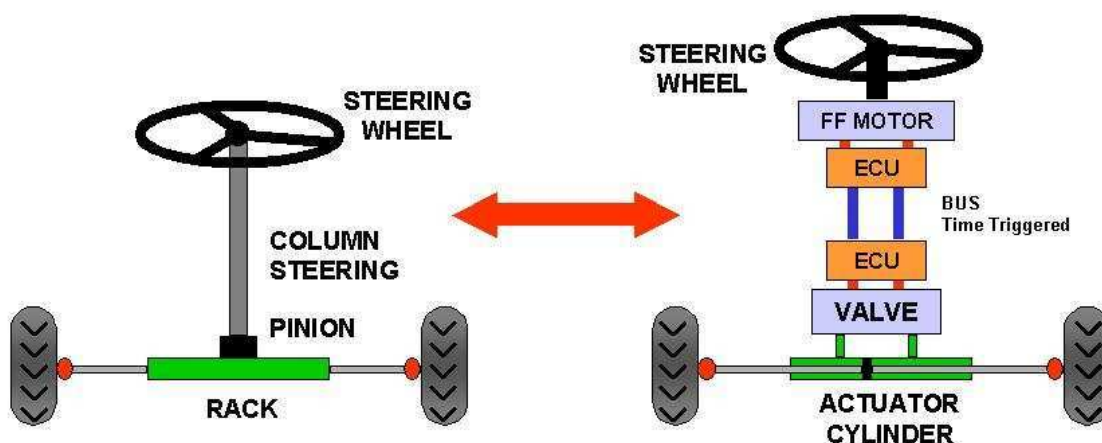


Figure 1. A schematic comparison of a conventional steering system and a Steer-by-Wire System [25].

<sup>1</sup> TTA-Group – The Cross-Industry Consortium for Time-Triggered Systems, Schoenbrunner Strasse 7, A-1040 Vienna, Austria, coordinator@ttagroup.org

<sup>2</sup> Sauer-Danfoss (Nordborg) A/S

<sup>3</sup> TÜV Nord Fahrzeug GmbH

<sup>4</sup> TTControl S.r.l., Kravoglstasse 11, I-39042 Brixen / Bressanone, Italy

## **A STEER-BY-WIRE SYSTEM**

The primary components of a normal steering system are steering input, steering actuator, the link between steering input device and actuator, and a power source. In a steer-by-wire system part of the link between steering input device and actuator is purely electric or electronic. While a mechanical link between steering wheel and the steered wheel in a vehicle is considered safe by mechanical construction, the same level of trust cannot be applied to electronically controlled systems. Programmed electronic control units are complex in their internal structure. Electronic components can fail without previous sign of wear-out.

In case of a steering system the loss of the steering function will lead to a loss of control over the further trajectory of the vehicle. Unless a controlled stop can be considered an alternative control path for vehicles running at low speeds (fail-restrained), the basic characterization of the steering function is fail-operational. In this context it becomes clear that the design of the steering system must meet the functional and safety requirements of a fail-operational control function of the respective criticality.

### **SBW CHALLENGES**

A major reason why there is no general roll out of SbW systems is that a purely electrical and electronic connection between steering input and steering wheel has not been considered by regulations for steering systems. This has changed only recently with the publication of the UN ECE 79 R2 that for the first time provides the basis for the homologation of steer-by-wire for unrestricted use on public roads. This is why the UN ECE 79 R2 will ease the ratification of regulations for restricted on-road use for commercial vehicles. Given the basis for homologation, the development of SbW can be started. Unfortunately, the requirements for homologation are not very precise regarding the development process and the implementation. Many technical questions and also many questions for product liability are still to be answered.

These big technological challenges are hard to solve in highly competitive industries because companies may not be able to clarify all questions and problems themselves without a major evaluation and development investment. Cooperation is necessary between companies and even competitors to address the issues by sharing investments and know-how. TTA-Group offered its support for such an initiative.

### **TTA-GROUP**

TTA-Group was established in 2001 by leading automotive and aerospace companies. Since then several companies from various industries have chosen TTA-Group as a cross-industry consortium to discuss the development and use of Time-Triggered Architecture (TTA) for safety-relevant issues. Today TTA-Group has more than 30 members coming from automotive, aerospace, railway, agricultural tractors, earth moving machinery, and fork lift industries [9].

TTA-Group provides a platform to share knowledge for the development of safety-critical networked applications based on the Time-Triggered Architecture (TTA). TTA is considered a key technology for by-wire systems by leading experts [10, 11]. In their x-by-wire report Frost & Sullivan mention that time-triggered architectures are one of the key solutions for safety-critical applications [12] and in the Allied Business Intelligence report on x-by-wire time-triggered protocols are defined as a prerequisite for the reliable use of safety-critical systems such as x-by-wire [13]. TTA-Group's objective is to share experience and distribute know-how in the area of safety-critical data communication. Members benefit from the successful deployment of data communication systems for safety-critical applications where safety integrity requirements at aerospace level have to be fulfilled at low cost.

Time-Triggered Architecture has been successfully rolled out and is in production since 2002. It is considered a core element for future automotive and aerospace applications. The intention in TTA-Group's SbW Working Group is to leverage this knowledge for commercial vehicles.

## COOPERATION OR COMPETITION?

The focus of the working group is to cooperate at the pre-competitive stage to conduct long term, high risk research and development. Information is shared and common codes, standards, practices, and processes are developed. Prerequisites for cooperation are a mutual confidence in each other and the benefits of the partnership that all involved parties gain. By sharing efforts and know-how cost is reduced and quality is improved. Additionally time-to-market is achieved in a faster and more efficient way. The clear intention is to cooperate on platforms and to compete on functionality at a later stage. Competition follows cooperation but competitive advantage is gained together with the other group members.

## SBW WORKING GROUP MISSION

Manufacturers and suppliers of leading companies of agricultural tractor, forklift, construction and earth moving machinery industries came together with supervising societies to achieve a common goal:

*„Define a certifiable reference architecture for a complete steer-by-wire application without mechanical backup for on-road use“*

This includes a selection of norms and legislations to be compliant with, the derivation of functional and safety requirements and guidelines together with experts of involved companies, the work on concrete implementation of an architecture, and the generation of a technical template. The concept should be approved by a supervising society and aim at a global standard in order to enhance reliability, interoperability, and safety to provide higher cost efficiency for suppliers and manufacturers. Double effort should be avoided and the efficient use of resources should be ensured in order to develop appropriate steering products with a technology for the future. Many basic questions to be answered on the way to a full SbW are common to all participating parties. From the beginning technical supervisory companies are involved in the process. In particular TÜV Nord gave its input at a very early stage of the development and accompanies each step of the group. This helps to size the joint effort and eases the reuse of concept documents for later implementation.

In the meantime 20 companies and organizations have teamed up to accomplish these goals together [14]. Further companies are about to join the initiative to evaluate different options of an electronic architecture.

## SBW – REQUIREMENTS, BENEFITS, ISSUES

SbW in commercial vehicles has very diverse requirements for the implementation of the steering system. Typical steering solutions have 1 or 2 steered axles. Many vehicles have articulated or tracked (tank) steering. The connection between steering input and steered wheels is either mechanical or hydraulic (Fig. 2).

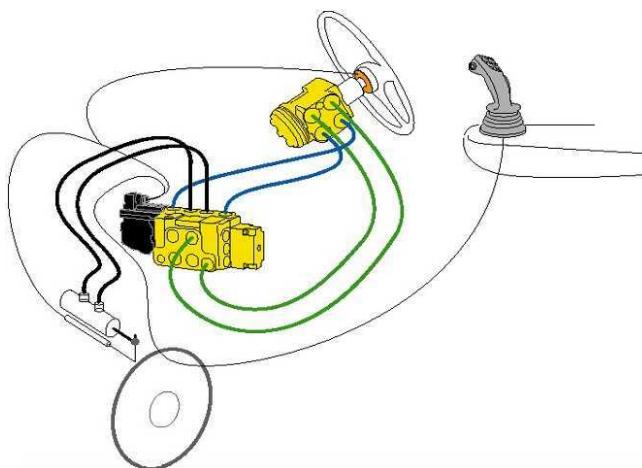


Figure 2. Two channel hydraulic steering system with secondary steering input by joystick [15].

Some commercial vehicles already implement limited SbW like forestry vehicles from Timberjack [16], GPS controlled vehicles [17,18] or vehicles with fast steer functionality from CNH [19].

### Requirements

There are mainly three types of groups interested in a steering function.

1. First of all there is the end user or operator of the vehicle. The operator wants to control and steer the vehicle along a path in an efficient, productive, comfortable, and safe way.
2. The vehicle manufacturer wants to buy steering systems that are cost-effective and enable competition on functional needs.
3. The steering component and system supplier wants to supply products which can be customized for different manufacturers. This means to reuse common technology to minimize investments. Modular components have to be provided that can be reused and put together without high additional efforts.

To satisfy all concerned parties low cost, safety and modularity have to be combined efficiently.

### Benefits

There are many solutions currently available on the market that could profit from SbW. Clear benefits lie in improved productivity and comfort whereas safety issues have to be addressed in a way that SbW systems are safer than or just as safe as conventional systems. Increased productivity is reached through broadening the scope of the vehicle by driving on public roads with enhanced vehicle control and new driver assistance functions. Additional comfort functions can be added. The steering behavior can be defined according to driving conditions and speed. Optimized feed-back from the steered wheels increases the driver comfort. Steering characteristics can be chosen depending on the driver's preferences. The logic next step are automatic driving vehicles without mechanical backup. A better visibility for the driver is achieved by removing the steering column that is no longer necessary. Also the steering effort and the noise and vibrations in the cabin coming from the hydraulic parts are reduced.

New design concepts are possible with SbW such as alternate steering concepts with a joy stick. New vehicle design and aesthetics are possible. Workplace design is no longer subject to geometrical constraints but can be optimized in terms of ergonomics. As the steering unit can be potentially placed wherever it is needed, the driver seat position is variable. Current design heavily depends on the steering assembly. Simplification of the production process is a benefit mainly applying to the vehicle manufacturer. The mechanical connection to the wheels, hydraulic hoses or mechanical backup system is no longer needed. Since the steering unit can be placed wherever it is needed, left-hand and right-hand driver variants can be easily assembled. This also applies to all other steering components and components associated with it, such as the cockpit, the wheel actuators, the control system, and the engine/gearbox combination. The general assembly of the vehicle is eased and simplified by using smaller modules.

Another advantage during the production process is the easy adjustment of a default steering position. The steering column is one of the most disturbing components of the vehicle regarding comfort and production flexibility. Removing this part significantly improves the vehicle design and decreases the total weight. Environmental issues are addressed by omitting hydraulic parts. The fluid disposal and the problems associated with it are no longer troublesome. Moreover, the energy consumption can be optimized because of unit separation.

Modularity and reuse of components was one of the main intentions when the Time-Triggered Architecture was defined and developed. Today the so-called "composability" is a key advantage of TTA and is explained in a variety of specifications and papers [20, 21, 22, 23, 24].

### Issues

One of the biggest challenges in vehicle industry is to have a fail-tolerant SbW system for driving on public road at affordable cost. The current problem is that a SbW system for driving on public road using currently available technologies is too complex and the costs are not acceptable. It is one of the goals of the SbW Working Group to define a reference architecture that demonstrates that SbW is achievable at affordable costs. The target is to make SbW not more expensive than

conventional steering systems. On-road SbW is definitely a safety-critical application without a safe state. The steering must be maintained even in case of an error. Therefore, the system must be fail-operational. This means that the system must stay operational even in case of a serious fault. Fail-operational systems require a fault-tolerant data communication architecture.

The Time-Triggered Architecture (TTA), based on a time-triggered protocol such as TTP, is promoted by TTA-Group and addresses these issues. The use of a time-triggered technology is viewed as state-of-the-art. Only time-triggered communication can ensure that important messages get through on the data bus in worst case scenarios. This is necessary to implement safety-critical dependable applications such as SbW. The reference architecture used in the SbW Working Group is based on the Time-Triggered Architecture (TTA). There is currently a growing interest specially among OEMs and suppliers of special vehicles such as agricultural and construction machinery or fork lifts, in working with this efficient and cost-effective TTA.

## TIME-TRIGGERED ARCHITECTURE

The Time-Triggered Architecture (TTA) establishes a frame for data processing in the area of distributed embedded real-time systems with highly reliable applications. It sets up the computing infrastructure for the implementation of applications and provides mechanisms and guidelines to partition large applications into nearly autonomous subsystems along small and well-defined interfaces so that the complexity of the evolving product can be controlled. Architecture design is thus interface design. By defining an architectural style that is observed at all component interfaces, the architecture avoids property mismatches at the interfaces and eliminates the need for unproductive “glue” code.

A central characteristic of the Time-Triggered Architecture is the handling of (physical) real time as a first-order quantity. The TTA decomposes a large embedded application in nodes (ECUs) and clusters and provides a fault-tolerant global time base of known precision at every node. The TTA takes advantage of the availability of the global time to precisely specify the interfaces among the nodes, to facilitate communication, to guarantee state consistency, to perform prompt error detection, and to support the timeliness of real-time applications.

### Structure of the TTA

The basic building block of the TTA is a node. A node comprises a processor with memory, an input-output subsystem, a time-triggered communication controller, an operating system and the relevant application software all in a self-contained unit (possibly on a single silicon die). Two replicated communication channels connect the nodes to build a cluster. The physical interconnection structure and the communication controllers of all nodes in a cluster form the communication subsystem that is autonomous in the TTA and executes an a priori specified periodic TDMA (Time Division Multiple Access) schedule. The communication subsystem reads a data frame with state information from the communication network interface (CNI) at the a priori known fetch instant and delivers it to the CNIs of all receiving nodes of the cluster at the a priori known delivery instant, overwriting the previous version of this frame. The periodic fetch and delivery instants are contained in a scheduling table within the communication controller called MEDL (Message Descriptor List) consistently known to all communication controllers in a cluster.

At the moment, the TTA is implemented on two different network topologies: on a bus topology (TTA-Bus) and a star topology (TTA-Star). Nodes of the TTA-Bus implementation are equipped with a node-local bus guardian that prevents babbling idiot faults. TTA-Star implements smart central guardians that are shared by all nodes of a cluster. These smart guardians isolate arbitrary nodes failures and support safety-critical applications. As far as the costs are concerned, TTA-Star is very attractive because only one bus guardian per channel is necessary. See figure 3 and 4.

### TTA Design Principles

The following paragraphs discuss briefly the principles that have driven the design of the Time-Triggered Architecture:

**Consistent Distributed Computing Platform.** The main purpose of the TTA is to provide a consistent distributed computing base to all correct nodes in order that reliable distributed

applications can be built with manageable effort. If a node cannot assume that every other correct node works on the same state, then the design of distributed algorithms becomes laborious because the intricate agreement problem has to be solved at the application level. That is why TTP provides consistency support directly at the communication subsystem level.

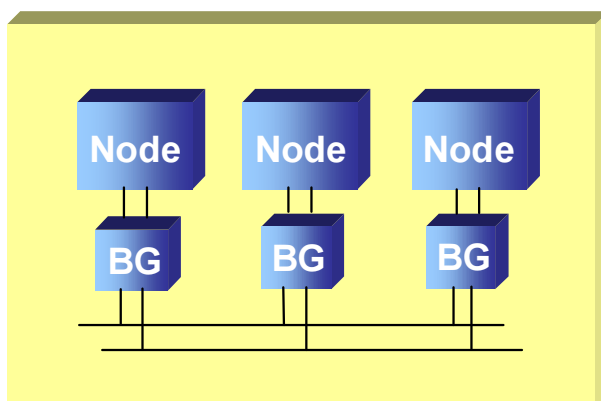


Figure 3. TTP in Dual-Channel topology (TTP-Bus).

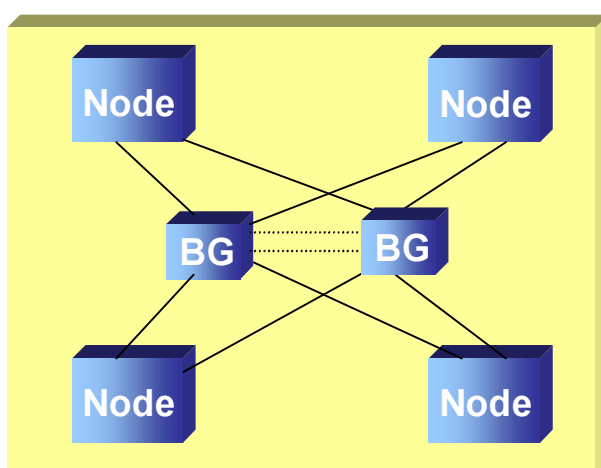


Figure 4. TTP in Star Topology (TTP-Star).

**Unification of Interfaces – Temporal Firewalls.** A good architecture must be based on a small number of orthogonal concepts that are reused in many different situations, thereby reducing the effort needed for understanding complex systems. Driven by its time-triggered schedule, the bus shall be autonomous in carrying data frames from the sender’s communication network interface (CNI) to the receiver’s CNI. According to the push-pull paradigm, the sender can put the information into its local CNI memory while the receiver must get the information out of its local CNI memory. Since no control signals cross the CNI in the TTA (the communication system derives control signals for the fetch and delivery instants from the progress of global time and its local schedule table MEDL), control-error propagation is eliminated by design. We call an interface that prevents control-error propagation by design a temporal firewall.

**Composability.** In a distributed real-time system the nodes interact via the communication system to provide the emerging real-time services. These emerging services depend on the timely provision of the real-time information at the interfaces of the nodes. An architecture is termed composable in the temporal domain if it guarantees the following four principles [24]:

1. Independent development of nodes
2. Stability of services prior to the integration of a new function
3. Constructive integration of the nodes to generate the emerging services
4. Replica determinism

**Scalability.** The TTA is intended for the design of complex distributed real-time applications. A complex system that supports many different functions can be constructed most efficiently if the effort needed to understand a particular system function is independent of the system size. Horizontal layering (abstraction) and vertical layering (partitioning) are the means to master the complexity of large systems. In the TTA the CNIs encapsulate a function and make only those properties of the environment visible that are relevant for its operation.

#### Fault Hypothesis and Fault Handling

Provided that the components of a properly configured TTA-based system are in different fault containment regions, each can fail in an arbitrary way. Under this assumption the probability of two concurrent independent component failures is small enough to be considered a rare event that can be handled by an appropriate never-give-up (NGU) strategy. However, it should be noted that a very prompt error detection mechanism is needed to ensure that two consecutive single faults are not becoming concurrent. As for hardware faults, TTA relies on the underlying time-triggered communication system to isolate and tolerate single node faults. By introducing a bus guardian it is guaranteed that a faulty node cannot prevent correct nodes from exchanging data. The bus guardian ensures that a node can only send once in a TDMA round, thereby eliminating the problem of babbling idiots that monopolize the communication medium. TTA is based on a never-give-up strategy (NGU) for multiple fault scenarios: if a node detects faults that are not covered by the fault hypothesis, it notifies the application. The application may now decide either to shutdown in fail-safe environments or to restart in fail-operational environments with an agreed consistent state among all nodes of the distributed system.

#### Fault Tolerance

The requirements described above ensure fault tolerance at the communication subsystem level. These mechanisms of the communication subsystem guarantee that faulty nodes cannot prevent correct nodes from communicating and serve as communication platform for the application. At the application level fault tolerance needs to be implemented by a fault tolerance layer and an appropriate application design. Fault tolerance can be realized by replicating a software subsystem on two fail-silent nodes. Tolerance of a single arbitrary node failure can be ensured by TMR (Triple Modular Redundancy) voting. Both mechanisms will tolerate single component faults with the respective failure semantics and are thus fit to handle both transient and permanent hardware faults. To re-establish tolerance to single component faults despite the presence of a permanent hardware fault, the time-triggered communication system has to support the implementation of transparent hot-stand-by spares. Fault tolerance is realized by a redundant unit in the network taking over the function of a defective unit, without being noticed at the function level. This is why data consistency is necessary.

For more information on TTA please refer to [20, 21, 22, 23, 24].

### **TIME-TRIGGERED COMMUNICATION SYSTEMS**

The basic building block of TTA is a time-triggered communication system with a synchronization service. There is only one TTA but three communication protocols are currently discussed as potential candidates for safety-critical applications. These protocols have different focuses:

- TTP is a high-speed bus with a strong focus on safety. TTP was developed according to a clearly specified fault hypothesis (single-fault hypothesis).
- FlexRay is a high-speed bus at development stage with focus on high bandwidth.
- TTCAN is based on the CAN protocol. TTCAN expands the capabilities of the CAN bus. Due to the missing redundancy of a second communication channel and the limitations at high speeds TTCAN is currently not in the hotspot.

TTP and FlexRay are similar regarding communication in the static part of TDMA, but they differ regarding the services that they provide for dependable applications. While TTP provides services directly within the protocol, FlexRay protocol generally leaves handling of safety to the application. This includes laborious services such as acknowledgment and check of consistency of

message delivery. The certifiable reference architecture elaborated in the SbW Working Group will be based on a low-cost safe communication protocol that fulfills high safety requirements. Currently this applies to TTP only. FlexRay is probably evolving in this direction. TTA-Group and its members are in close contact with the FlexRay consortium. They will watch the development of FlexRay and will consider it for the definition of the architecture.

### THE SBW WORKING GROUP

The first step in the development of a potentially safety-critical application is the selection or development of an appropriate safety framework. For this purpose the SbW Working Group started out with the identification of relevant standards and regulations. Due to the four industries currently involved this resulted in a large number of standards and norms. Unfortunately, such a survey can hardly cover all national specifics and also many standards and regulations are currently under revision and some are still under development. Fortunately, most new basic standards and regulations are international standards.

The complexity for commercial vehicles is also high due to the ambiguous character of the vehicles depending on their use on-road which is the focus of the working group and their operation off-road in a working environment. A look into the relevant international regulations shows that ECE 79 and technically similar 70/311/EEC are the most relevant regulations for steering systems, as they allow unrestricted on-road use of a vehicle. Recently, UN ECE 79 R2 was released which creates for the first time a basis for on-road type approval for steer-by-wire. For agricultural and forestry tractors regulation 75/321/EEC applies. This regulation is currently under revision for full steer-by-wire. Unfortunately, UN ECE 79 R2 is not very specific regarding the required safety framework (e.g. life cycle, development process). The selection of an appropriate safety framework is left to the OEM considering that industry-specific standards and state of the art are subject to change. Additionally, regulations cover by definition only part of the life cycle. For product liability which has reached a high degree of attention especially in the US the whole life cycle of the vehicle has to be considered (Fig. 5).

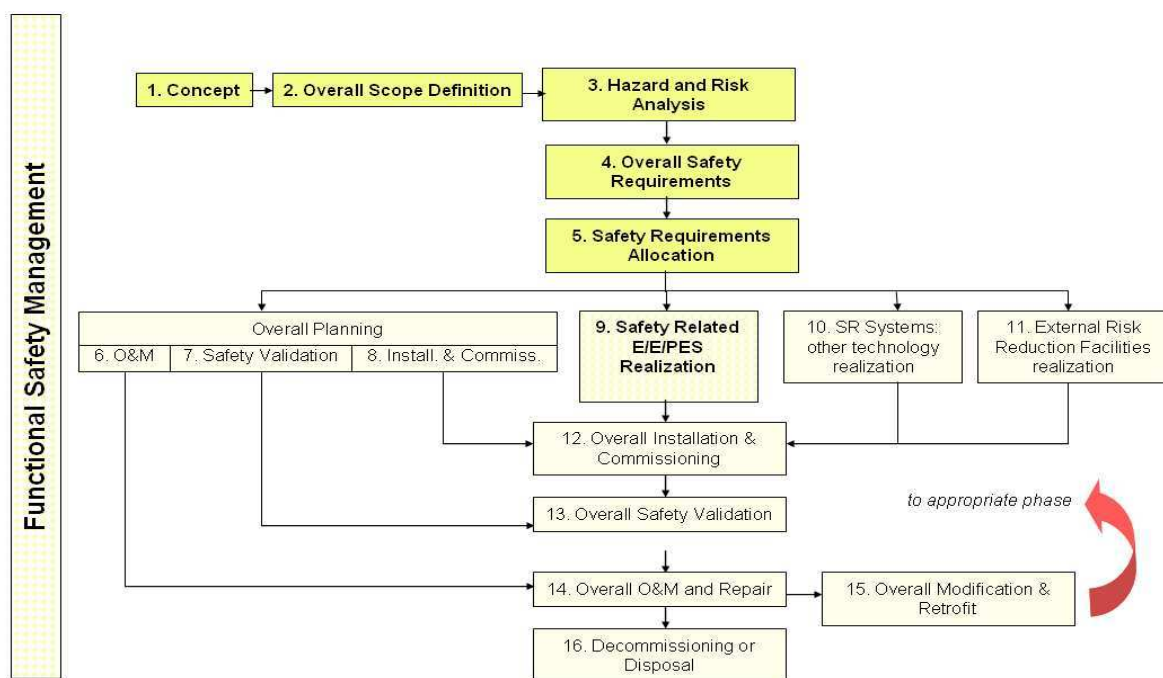


Figure 5. Life cycle IEC 61508.

SbW systems add to the conventional steering system programmed electronic control units which are inherently complex in their design. The state-of-the-art standard for the design of complex electrical, electronic or programmable electronic safety-related systems (E/E/PES) is the IEC 61508. This standard is very generic in its nature, as it was developed originally for pharmaceutical process industry. However, this standard does not cover well the conventional

mechanical and hydraulic parts of the SbW. One intention behind the design of the generic IEC 61508 was that it should serve as basis for the development of industry specific standards. This development of specific standards that are based on the IEC 61508 is currently under way for most of the participating industries. TTA-Group's SbW Working Group seeks to share a common platform between different industries. The life cycle has to consider all relevant overall, E/E/PES and software safety life cycle phases when E/E/PESs are used to perform safety functions. This is, for example, from initial concept, through design, implementation, operation and maintenance to decommissioning.

In the working group a first generic architecture was developed based on functional and safety requirements (Fig. 6). After this initial step, it is necessary to define the criticality of a given architecture. This is done during the hazard and risk analysis. Specific hazards for the industries have to be identified and analyzed (Fig. 7). It was found that a common understanding is necessary especially for the usage of vehicles.

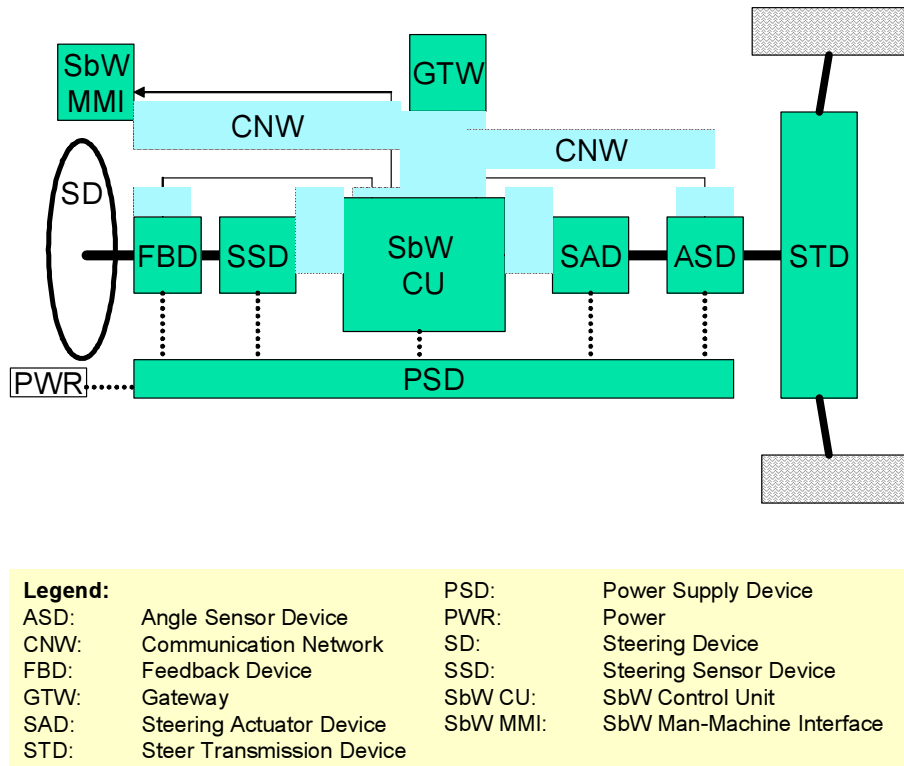


Figure 6. Generic architecture of SbW System.

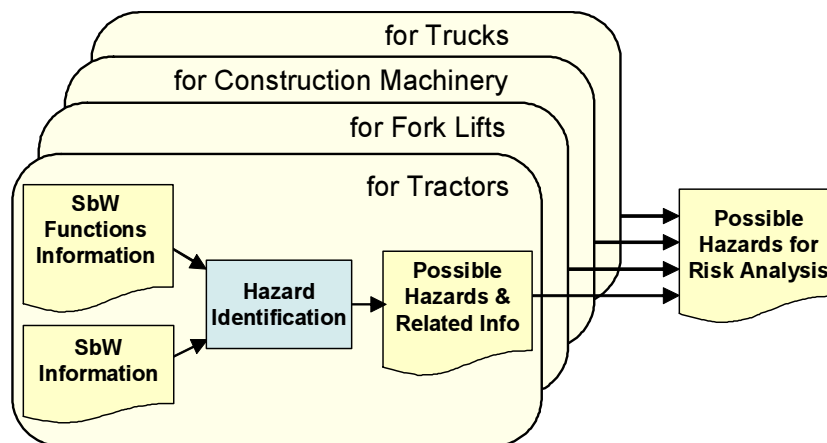


Figure 7. Hazard Identification Process.

Unfortunately, the standards differ in their risk assessments schemes (e.g. they use different risk graphs), although it is possible to combine requirements of different industries. The result of the

hazard and risk analysis is a required Safety Integrity Level (SIL) or Performance Level (PL). Typically a correspondence is given by the standard to relate PL and SIL. Regarding the result SIL and PL imply a recommendation for an acceptable risk. But this acceptable risk should be defined on a larger scale (Fig. 8). A comparison with aerospace industry shows that risk is related to the number of casualties.

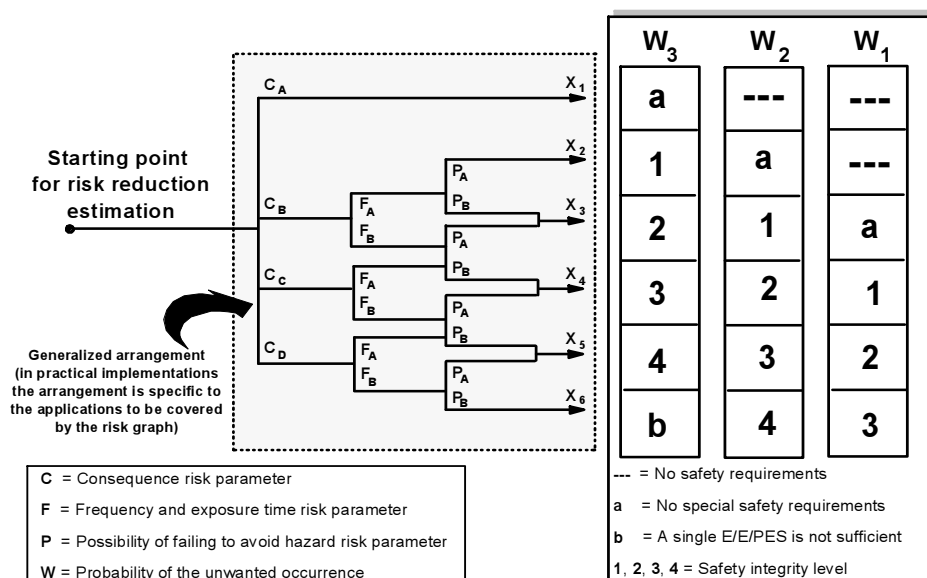


Figure 8. IEC 61508-5 risk graph.

For further refining the developed generic architecture, the group is now focusing mainly on the following three vehicle classes and steering types (Fig. 9):

- Counterbalanced lift trucks (fork-lifts) for a maximum speed of 12kph and rear wheel steering.
- Agricultural tractors for speeds between 40 and 60kph with front wheel steering.
- Wheel loaders for speeds between 25 and 40kph with articulated steering.



Figure 9. Vehicle classes.

## OUTLOOK

The hazard and risk analysis will have to be detailed for each of the three vehicle classes. The outcome of this analysis will determine the required SIL for the respective architecture. Work on the design specification for the three vehicle types has already been started.

## CONCLUSION

TTA-Group initiated a working group to define a certifiable reference architecture for a complete steer-by-wire application without mechanical backup for on-road and off-road use. The costs of

defining such an architecture are shared by the group members. The goal is to split and to minimize research and development costs in the group. There is cooperation at the platform level and, later on, competition in terms of functionality. Because of the common efforts time and costs are saved; over-engineering is avoided. Intelligent architecture and design is developed for all members. Common work on concrete implementations of an architecture and the generation of a technical template and guidelines will allow a smoother homologation process. Upfront investments in setting up the right process and development save cost and unnecessary work.

With the Time-Triggered Architecture (TTA) a proven electronic architecture is available for safety-critical or high-bandwidth applications in the commercial vehicle industry. An example is the use of TTA for the architecture in TTA-Group's Steer-by-Wire Working Group. The advantage of this architecture is the reduction of architectural elements such as gateways, allowing to implement safety applications and other functions in a single network. This approach meets the requirements of commercial vehicle industry. Additionally, the proposed architecture overcomes the complexity challenge and enables further functional growth. Optimized reuse and allocation of functions to control units save cost and wiring and simultaneously enhance system reliability.

## REFERENCES

1. Shaout A., T. Eldos, N. Zaman: Scalable autonic processing systems. International Journal of Computer Applications in Technology, Volume 16, No.1, 2003, pp. 21-32.  
[www.inderscience.com/storage/f219312410687511.pdf](http://www.inderscience.com/storage/f219312410687511.pdf)
2. X-by-Wire Project, Brite-EuRam III Program, X-by-Wire – Safety Fault Tolerant Systems in Vehicles, Final Report, 1998. [www.vmars.tuwien.ac.at/projects/xbywire](http://www.vmars.tuwien.ac.at/projects/xbywire)
3. Amberkar S., F. Bolourchi, J. Demerly, S. Millsap: A Control System Methodology for Steer by Wire Systems. SAE Technical Paper Series, 2004-01-1106, October 2004.
4. Heitzer D., A. Seewald: Development of a Fault Tolerant Steer-by-Wire Steering System. Convergence Transportation Electronics Association, 2004-21-0046, October 2004.
5. Kamp J. v. d.: Electro-Hydraulic Steering in Off Road Vehicles. Automation Technology for Off-Road Equipment, Conference Proceedings, July 2002.
6. Chiappero A., D. Bak: Driving by wire. DesignNews, October 2001.  
[www.designnews.com/article/CA177537.html](http://www.designnews.com/article/CA177537.html)
7. Sirius 2001, [www.cad.luth.se/sirius/Sirius2001\\_eng.pdf](http://www.cad.luth.se/sirius/Sirius2001_eng.pdf)
8. Brown St., E. Holweg: Smart Electro-Mechanical Actuation for Drive-by-Wire Applications. Convergence Transportation Electronics Association, 2004-21-0045, October 2004.
9. [www.ttagroup.org](http://www.ttagroup.org)
10. Pfeifer H.: Formale Analyse für TTA. Presentation at AG Methoden des Software und Systems Engineerings at the Technical University Munich, April 2004.  
[www4.in.tum.de/~streckem/Admin/club2\\_pfeifer04.pdf](http://www4.in.tum.de/~streckem/Admin/club2_pfeifer04.pdf)
11. Rushby J.: A Comparison of Bus Architectures for Safety-Critical Embedded Systems, 2003.  
<http://techreports.larc.nasa.gov/ltrs/PDF/2003/cr/NASA-2003-cr212161.pdf>
12. Frost & Sullivan: European Automotive Market for X-by-wire Technologies, 2001.
13. Allied Business Intelligence: X-By-Wire: A Strategic Analysis of In-Vehicle Multiplexing & Next-Generation Safety-Critical Control Systems, 2003.
14. TTA-Group Press Release: TTA-Group Announces Foundation of Steer-by-Wire Working Group, April 2005. [www.ttagroup.org/news/doc/News\\_2005-04-11-Steer-by-Wire\\_WG.pdf](http://www.ttagroup.org/news/doc/News_2005-04-11-Steer-by-Wire_WG.pdf)
15. Thomsen S., K. Buus Jensen: New ways with electro hydraulic steering concepts. Presentation 3rd Conference of Mobil Hydraulic at the Technical University of Braunschweig, November 2002.

16. Alanen J., M. Hietikko, T. Malm: Safety of Digital Communications in Machines. Espoo 2004, VTT Tiedotteita, Research Notes 2265. [www.vtt.fi/inf/pdf/tiedotteet/2004/T2265.pdf](http://www.vtt.fi/inf/pdf/tiedotteet/2004/T2265.pdf)
17. Coers B.: HarveSTSmart Feedrate Control for Combine Harvesters. Presentation at SAE Commercial Vehicle Engineering, October 2004.
18. Coers B.: AutoTrac Guidance of John Deere Agricultural Equipment. Presentation at SAE Commercial Vehicle Engineering, October 2004.
19. Flamme D.: Fast Steer™ System – A revolution in steering systems. Presentation at SAE Commercial Vehicle Engineering, October 2004.
20. TTA-Group: Time-Triggered Protocol TTP/C – High-Level Specification Document – Protocol Version 1.1, November 2003. [www.ttagroup.org/technology/specification.htm](http://www.ttagroup.org/technology/specification.htm)
21. TTA-Group: TTP – Frequently Asked Questions, 2005, <http://www.ttagroup.org/technology/doc/TTP-FAQ.pdf>
22. Kopetz H., G. Bauer: The Time-Triggered Architecture. Proceedings of the IEEE Special Issue on Modeling and Design of Embedded Software, October 2003. [www.ttech.com/technology/docs/history/HK\\_2002-10-TTA.pdf](http://www.ttech.com/technology/docs/history/HK_2002-10-TTA.pdf)
23. Rech P., M. Plankensteiner, M. Weissengruber: Improved Electronic Architecture for Commercial Vehicles. SAE Commercial Vehicle Engineering, 05CV-187, November 2005.
24. Maier R., G. Bauer, G. Stöger, St. Poledna: Time-Triggered Architecture: A Consistent Computing Platform. IEEE Micro 22(4): 36-45, July 2002. [www.ttech.com/technology/docs/history/IEEE-Micro\\_2002-07-TTA-Consistency.pdf](http://www.ttech.com/technology/docs/history/IEEE-Micro_2002-07-TTA-Consistency.pdf)
25. Università di Modena e Reggio Emilia, [www.dii.unimo.it/steer](http://www.dii.unimo.it/steer)

# LATEST TRENDS IN AUTOMOTIVE ELECTRONIC SYSTEMS, HIGHWAY MEETS OFF-HIGHWAY?

S. Rathmann<sup>1</sup> and R. Fischerkeller<sup>1</sup>

## ABSTRACT

The rapid development of electronic systems in automotive vehicles has been driven for decades by constantly growing requirements of legislation for environmental protection, as well as rising demands of the end-user to improve fuel economy, safety, driving comfort and driving excitement.

The manufacturers of mobile work machines also see themselves increasingly confronted with these requirements. Can we use the technical experiences from automobiles also in this area to efficiently develop high-quality electronic systems, that are future-oriented and able to flexibly adapt the systems to different platforms?

The number of calibration parameters in an engine management system, for example, has risen within the last 20 years from a few hundred to over 7000. Therefore, the engineering effort for software and their calibration has increased dramatically. In the meantime for manufacturers of vehicles with low volumes, the engineering cost are comparable with the actual cost for the system components. Therefore, the future challenge will be the re-use of software functions engineered by manufacturers and suppliers for different vehicles and systems. In the automotive industry this attempt is being undertaken by different companies under the name AUTOSAR. Additionally, the software development is done in compliance to standards like CMMI or SPICE which ensure a consistent, high quality product.

The exchange of information between control units makes the interaction of the systems much more complex and asks for more efficient, faster data communication systems by new standards, such as the bus system FLEXRAY.

When electronic devices are viewed with a holistic approach, a large potential is evident for manufactures and their end-user.

**KEYWORDS.** AUTOSAR, Automotive, Calibration, CMMI, Comfort, Development Process, Driving Excitement, Electronic Systems, Engineering Effort, Engine Management, Environment, FLEXRAY, Fuel Consumption, Legislation, Network BUS Systems, Quality, Safety, Software, SPICE.

## INTRODUCTION

The automobile - a product in a marketplace with a fast technological development – is influenced by different technology drivers. As a recognized supplier and technical expert in this segment, we ask ourselves the question whether there are similar boundary conditions in other high technology markets with similar mechanisms.

Can we learn from experiences in other industries and use synergies while sharing technical knowledge?

---

<sup>1</sup> Bosch Engineering GmbH, Robert Bosch Allee 1, D-74232 Abstatt, Germany, sven.rathmann@de.bosch.com

## DRIVERS FOR DEVELOPMENTS IN THE AUTOMOTIVE INDUSTRY

The electronic systems in motor vehicles have evolved rapidly during the last 25 years, and according to forecasts their proportion of vehicle value will further increase in the next decades. This development was driven from the beginning by three factors, which were also used very early as an advertising slogan by Bosch for their products: Safe - Clean – Economical (Fig. 1).

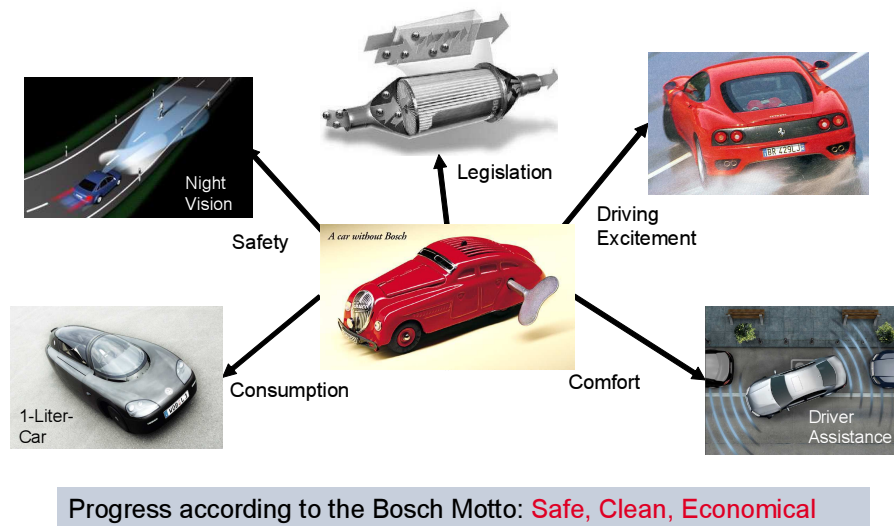


Figure 1. Technology drivers for automotive systems.

**Safe:** The rising consumer demand for safety has led to the fact that airbag, antilock braking systems and electronic stability controls are offered in almost all vehicles in production, at least as an option. While the current systems offer passive safety, the future systems actively work to avoid dangerous situations for the driver and those around him or her. Current innovative systems on the market are predictive safety systems like Brake Assist, Collision Warning and Emergency Braking.

**Clean:** The society and respectively the legislators are challenging the automotive engineers since the seventies with continuously rising requirements for low exhaust emissions. The legal requirements, created and driven by US legislation (EPA, CARB), have reached a high standard also in Europe and in emerging market countries like China. Based on this pressure the reduction of tailpipe emissions, particulate emissions, and the avoidance of other harmful materials has reached a very good state today and therefore, has contributed to the rising quality of life - specifically in densely populated areas.

**Economical:** The lower fuel consumption in modern automobiles is primarily a consequence of the lower tailpipe emissions, avoidance of parasitic engine losses and by the use of lighter materials. The next step is to operate the engine in more efficient areas and also to recuperate brake energy as shown in the hybrid vehicles. Certainly, the direct comparison of today's automobiles with the ones from 15 years ago does not always show a reduction of the absolute fuel consumption, but in the sum of its properties (safety, emissions, comfort, driving excitement) the automobile has become more efficient overall. This view opens two other factors you can see as relevant drivers of the development in the automotive industry.

**Comfort:** The electric operation of windows, seats, mirrors, etc. has been taken for granted in our day. Nearly all customers are opting for air conditioning with a new vehicle purchase. Low interior noise and vibration levels inside the vehicle guarantee relaxing driving conditions over long distances. The vehicle content with electrical motors and electronic devices will continuously increase and new innovations will emerge into smaller vehicle model lines.

**Driving excitement:** The car is not a simple transportation device any more. The customer identifies himself much more with the brand and the image. Providing driving excitement to the customer has become an important unique selling point for the manufacturer - most automotive advertising slogans want to meet this customer demand. The low sales figures of vehicles that

followed the demands of politics and environment groups show that vehicles developed uncompromisingly to the economic market did not reflect the real customer demand. However, the current and future automotive development tries to merge the contrary points of economical and driving excitement closer together. The sales figures of current vehicles with turbo diesel engines, or supercharged gasoline engines designed for downsizing (small engines with high specific power performance) support the development trend. In the chassis area systems can be seen like active suspension and wheel individual torque distribution to improve the agility of the vehicles.

### DRIVERS IN OFF-HIGHWAY APPLICATIONS FROM AN OUTSIDER VIEW-POINT

The technology drivers of the automotive industry are well known to a supplier in this area. However, other markets and other products have other drivers, so an automotive supplier can only look onto the recent developments on the Off-Highway market as an amateur-- How far apart from each other are these industries? Customers of Off-Highway equipment most likely want to have high industrial safety, low running cost, reduced operator fatigue and operator satisfaction. Certainly, these are other words, but actually serve the same basic needs.

From the point of view of an automotive supplier the world of the Off-Highway market is surprisingly complex and the portion of electronics in the modern machines is fairly high. Several control units are communicating with each other and their handling needs quite an amount of software which will rise further in the future. The high diversity of model types with low quantities challenges engineering to deliver a solution with restrained cost targets. Additionally high reliability and life-time durability are to be considered.

In the automobile business there are also products which are not comparable with high volume series production. The manufacturers of these products often use “off the shelf” hardware and software components which are customized from engineering service providers like Bosch Engineering GmbH. Projects with a yearly production volume from less than 10 to several thousand are standard in this case. Here we can observe very similar challenges arise as in the Off-Highway development.

### HISTORY AND EVOLUTION OF ELECTRONIC SYSTEMS IN AUTOMOBILES

A review in the technical development allows good forecasts for the future and provides data to compare the parallel subjects. Today the technical development of vehicle systems is influenced clearly by increasing system complexity. Figures 2 and 3 represent a view about the technical developments in the engine management system area from the first mechanical fuel injection in 1952 up to electronic direct gasoline injection DI-Motronic in 2000 with the most important milestones.

#### Bosch Motronic

<b>1952</b> Mechanical fuel injection for passenger cars	<b>1967</b> Electronic fuel injection with pressure measurement D-Jetronic	<b>1973</b> Air flow controlled injection  L-Jetronic	<b>1976</b> Closed loop controlled injection systems with Bosch-  Oxygen sensor
<b>1979</b> Integrated engine management system with injection and ignition Motronic	<b>1981</b> Electronic fuel injection with air mass measurement  LH-Jetronic	<b>1983</b> Fully electronic distributorless ignition system	<b>1987</b> Low-pressure single-point injection system with $\alpha / n$ control Mono-Jetronic
<b>1993</b> CAN-Motronic with self-diagnostics function OBD	<b>1995</b> Motronic with integrated electronic charge control Electronic throttle	<b>1996</b> Engine mounted control unit  Electronic on the spot	<b>2000</b> Gasoline direct injection system  DI-Motronic

Figure 2. History of engine management.

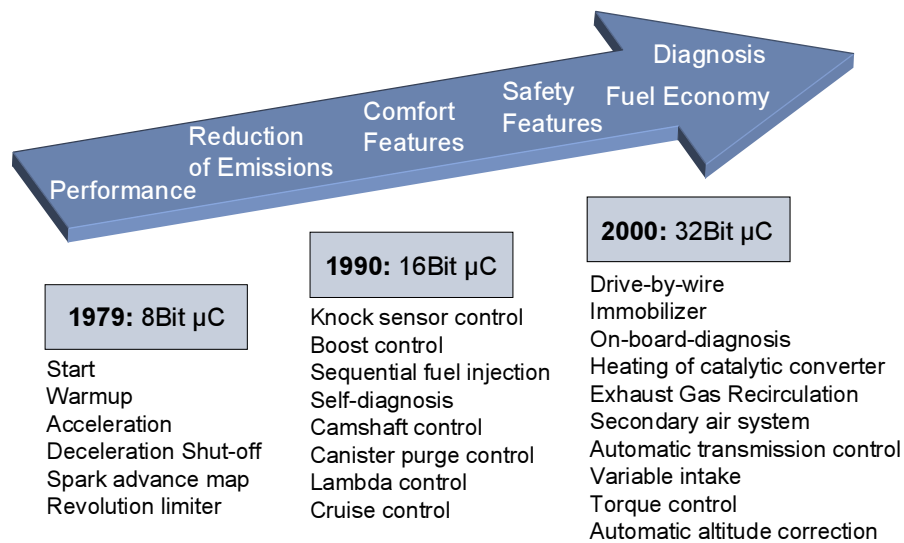


**Figure 3. Technology features – Historical milestones.**

The engine management system software is designed for variable use in different engine configurations. Calibration of the software is performed with changing parameters that influence the activities in the functions. In the early nineties a single engineer was able to calibrate the data of the whole engine management system. In the meantime the functional complexity has risen so high that a full engine calibration of a vehicle variant is executed by about half a dozen specialists each of them responsible for a self-contained subsystem. The number of labels to be calibrated has increased during this time from less than hundred to over 7000. Figure 4 shows the increased system complexity represented by examples of different variables like CPU speed, memory and number of lines of code.

		< 1990	1995	2005
<b>Hardware</b>	<b>Processor</b>	8 Bit	C196, 16 Bit	TriCore, 32 Bit
	<b>Frequency</b>	4 MHz	20 MHz	80-150 MHz
	<b>Flash</b>	10-100 kB	0,25–0,5 MB	1-6 MB
	<b>Sensors</b>	10	17	25
	<b>Actuators</b>	14	22	31
<b>Software</b>	<b>Lines of Code</b>	20.000	44.000	690.000
	<b>Features</b>	1.800	3.100	5.200
<b>Calibration</b>	<b>Calibration Parameters</b>	1.000	1.800	7.200

**Figure 4. Evolution of system complexity in power train.**

### CONTRARY TENDENCIES OF HARDWARE AND SOFTWARE COST

The primary focus of production applications in the past was clearly on the system component cost. In the meantime this has turned around and an increasing amount of the development budget is now allotted to software and calibration cost. The cost of control units, as well as the sensors and actuators have dropped by optimized design, cheaper subcomponents and more efficient production. The development expenses for production software and the calibration of more complex systems shows a rising trend.

This situation leads to a differentiated view and budget planning of automotive manufacturers with different quantities (Fig. 5). A large-volume manufacturer with a platform of several 100.000 pieces per year has its focus clearly on the cost of the components. Certainly, the software and

calibration cost also have an influence, but big saving potentials can be reached with small reduction of component prices. However, a manufacturer with quantities smaller than 1000 yearly has another attempt. The one-time effort for the software and calibration has a stronger effect on its cost per vehicle, than the components themselves. While it makes sense for a high volume manufacturer to invest several months of manpower in the production of software and calibration to save a sensor, it makes sense for a small volume manufacturer to add a sensor in his system if he can keep the software smaller and simpler.

The challenge of a small volume manufacturer is the re-use and adaptation of proven high volume functions. This can still give him a unique selling point on the market accompanied with short development times, but with the same quality targets. This allows him a balanced relation of hardware cost to engineering cost.

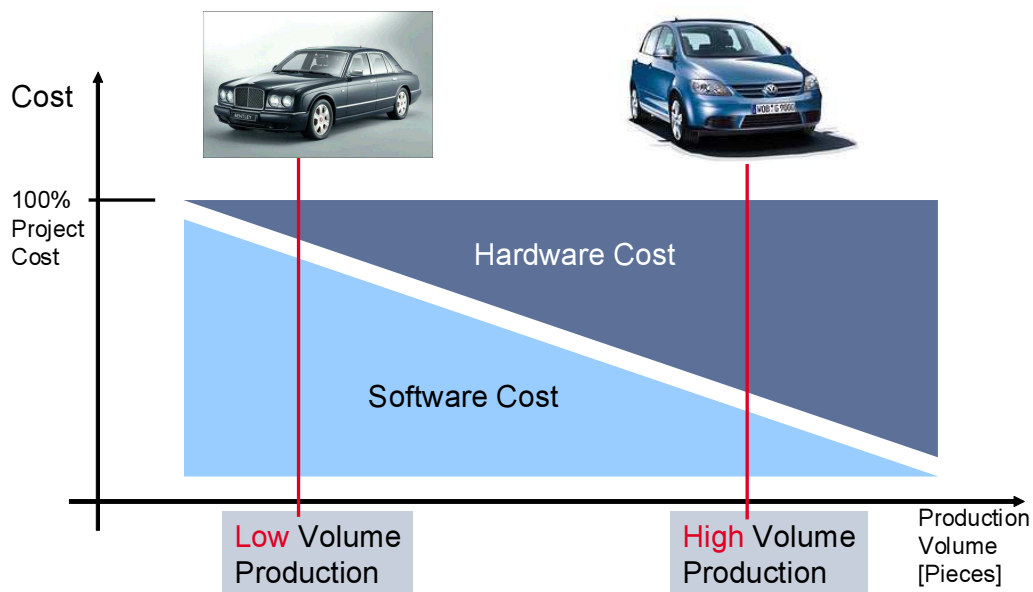


Figure 5. High volume vs. low volume project cost.

## MARKET OVERVIEW AND SHIFT OF ENGINEERING MARKET CONDITIONS

Based on the increased development efforts the supplier market is changing. Studies of independent institutes confirm the aforementioned trends:

- The diversity of vehicle types rises and more niche vehicles are offered.
- The vehicle and engine families decrease, the number of the derivatives increases.
- The complexity and functionalities of the electronic system controllers increases.
- The importance of the driving comfort and driving performance increases.

The external engineering services have increased since the mid-90s, while the OEM's concentrate the resources on their core competence of functional characteristics which can be directly experienced by the end user. This is particularly apparent in the new growing markets like China, for example. The classic component suppliers play a central roll in these markets. They offer their system know-how to the market of the engineering services.

Some representative numbers are shown in figure 6. The market volume of engine engineering for spark-ignition engines and diesel engines world-wide will rise within 5 years from EU 10.100 Mil. in 2003 by 4.3% annually to EU 12.500 Mil. Approximately 2/3 of the volume is still performed within the OEM's and about 15% are performed by Tier1 suppliers and engineering service providers. It is shown that Europe will remain the strongest region for engineering with over 50%; however, the segments in the emerging countries will rise disproportionately.

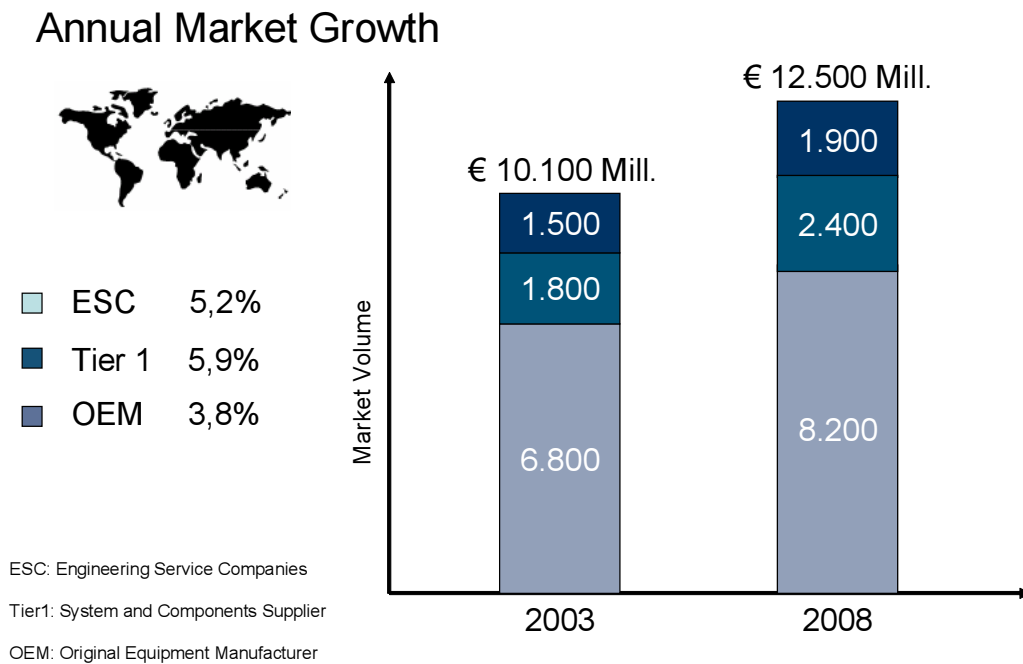


**Figure 6. Worldwide market volume engine engineering.**

### CONSEQUENCES OF SQUEEZED DEVELOPMENT TIMING AND LESSONS LEARNED

The challenge from the engineering viewpoint will be the shortened development time for much more complex systems in order to stay ahead of competition. The result from the networking of different systems is unforeseen defects which are discovered at a late development stage due to late system availability. The root cause analysis and trouble-shooting prove to be very difficult due to poor repeatability of errors in the overall system. High service cost and a negative influence on customer satisfaction are the consequence. Therefore the electric malfunctions are on the top of the list in the vehicle breakdown statistics of the biggest German automobile club “ADAC”.

What are the lessons learned in the automotive industry and what are the measures.

Downsizing of the functions. Even if the number of the functions will increase further, not every imaginable functional variation will be offered to the end user. Only those functions directly perceived and used from the customer will bring an added value.

More simulation in the early phase of engineering. The software and hardware can be tested with designed system models. Even if system modules are still not available in the early stage of development the interaction between the systems can be tested.

The number of tests will be greatly increased, and to keep the cost within budget, the tests have to be executed automatically. The frequency of test runs can be raised with a high degree of automation. This will also improve the repeatability of testing.

Quality processes and development models (for example, CMMI and Spice) help to structure the development so it is predictable and reproducible. Another target of these process models is the unwanted requirement creep, underestimated development resources, as well as the typical increase of change requests right before start of production.

The software structures are designed in a way that re-use of software parts is made easier. With strictly defined and documented interfaces it will be simpler to tie software modules from different vendors together (Fig. 7).

With an integrated consideration of the electronic systems a big potential presents itself to the use of the manufacturers and their end-users.

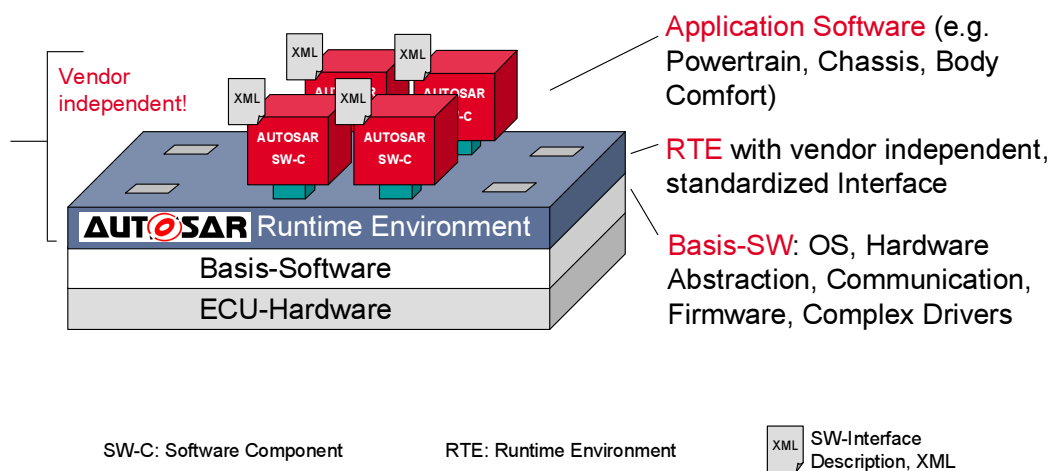


Figure 7. Next generation software platform.

## CONCLUSION

Electronic system developments in the automotive world are driven by the major factors

- Safety
- Environment
- Fuel consumption
- Comfort
- Driving excitement

The electronic value inside the vehicle and system complexity has drastically grown during the last 20 years due to

- Number of controllers and their networking inside one vehicle
- Amount of functionalities and lines of code inside the software
- Hardware memory capacity and speed

For some small volume manufacturers the software engineering effort to develop an electronic system is already higher than the electronic hardware cost over the lifetime of a vehicle production. It will be a challenge also for the large-volume manufacturers to meet future customer demands while keeping the engineering effort to a reasonable amount. Nevertheless the need for electronic engineering will continue to grow worldwide.

An integrated consideration of electronic system development will open big potentials to help the manufacturers creating products with unique selling points for their customers.

With the viewpoint of an automotive-professional, certain aspects of the automotive world are also found in the environment of the Off-Highway developments - what do you think as a specialist?

## REFERENCES

1. Stefan Keller. 2004. Clean – Strong – Efficient and Smart – Bosch Systems for Gasoline Engines. Company Presentation.
2. Elmar Markus, Dr. rer. nat. Helmut Randoll, Martin Knauer. 2006. Aktuelle Entwicklungen bei der Motorsteuerung von Diesel- und Ottomotoren. *ATZ Elektronik* 01/2006. 2-7.
3. ADAC. 04/2006. Informationen aus der Fahrzeugtechnik.



# A METHOD OF EVALUATING THE PERFORMANCE OF RTK GPS RECEIVERS USED IN AGRICULTURE

R. Ehsani<sup>1</sup>, H. Chaoui<sup>1</sup>, D. Grejner-Brzezinska<sup>2</sup> and M. Sullivan<sup>3</sup>

## ABSTRACT

GPS-based auto-steering systems could increase both productivity and efficiency of field operations in agriculture. Auto-steering guidance systems typically use RTK (Real Time Kinematic) GPS receivers, and depend partially on the accuracy of RTK GPS under field conditions. This study introduces a method of evaluating and comparing the accuracy of different RTK GPS receivers in dynamic testing conditions. Two commercially available RTK GPS receivers, John Deere and Trimble 214 were compared to the high accuracy Trimble 4800 RTK and a reference trajectory derived from post processed data, in two field tests. In one of the tests the GPS signal was blocked from the John Deere and Trimble 214 RTK receivers for 30, 60 and 90 meters, to evaluate how the receivers recuperate their accuracy after the signal returns. Receivers were placed on a rover that circumvented a field three times (three replicates) and they were evaluated by calculating their vertical accuracy and the area within their trajectory in each replicate, and their horizontal accuracies. The vertical accuracy of the John Deere and Trimble 214 RTK receivers differed significantly, from each other and the reference trajectory, which was statistically similar to the Trimble 4800 vertical accuracy. The area calculations showed no significant difference among receivers, whether with or without signal blockage. The horizontal accuracy was significantly different among all receivers, in the presence of signal blockage.

**KEYWORDS.** Dynamic Test, Guidance Systems, RTK GPS.

## INTRODUCTION

GPS-based guidance technology is one of the fastest growing precision agriculture advancements. GPS guidance technology has enabled applicators to improve driving accuracy and apply agriculture inputs more efficiently. This technology is currently used for planting, spraying and harvesting. Auto-steering systems could increase both productivity and efficiency of field operations, as well as facilitate the adoption of innovative field practices. Auto-steering can reduce driver fatigue and stress and increase the length of work shifts. It could also allow accurate agricultural operation at night or in poor visibility, the employment of less experienced drivers, and increasing operating speed.

The auto-steering guidance systems have the capability to steer a machine across the field. The driver must then steer the machine to the next pass where the auto-steering system takes over again. Rovira-Más *et al.* (2003) tested a tractor guidance system based on the inputs of a CCD camera, and found that it could guide a tractor along crop rows accurately at traveling speed up to 11 km/h. Kise *et al.*, 2005 successfully tested a row-detection algorithm for stereovision-based auto-guidance designed to localize crop rows, on a weedy soya beans field, including curved crop rows, with missing sections of crop and at normal field operation speeds.

Auto-steering guidance systems usually use RTK (Real Time Kinematic) GPS receivers, a main component of auto steering systems that therefore partially affect their performance. This effect is

---

<sup>1</sup> Department of Agricultural and Biological Engineering, University of Florida, Lake Alfred, FL, USA, ehsani@ufl.edu

<sup>2</sup> Department of Civil and Environmental Engineering and Geodetic Science, Ohio State University, Columbus, OH, USA

<sup>3</sup> Department of Food, Agricultural and Biological Engineering, Ohio State University, Columbus, OH, USA

significant, and is based on the accuracy and performance of RTK GPS under field conditions. The RTK systems available on the market may provide different accuracies for machine guidance, affecting the outcome in the field.

This study introduces a method of evaluating and comparing the accuracy of different RTK GPS receivers in dynamic testing conditions. Similar dynamic tests have been conducted with DGPS (Ehsani *et al.*, 2003). Taylor *et al.* (2003) dynamically tested GPS receivers by setting them up on a rail cart, guided by a short railroad, which was surveyed and referenced to a NGS benchmark.

## OBJECTIVE

The main objective of this study was to introduce a method for dynamic testing RTK GPS receivers used in agriculture and to evaluate the effectiveness of the method by field testing two commonly used RTK GPS receivers used for machine guidance in precision agriculture.

## METHODOLOGY

### GPS receivers field tests

Three commercially available RTK GPS receivers, John Deere, Trimble 214, and a Trimble 4800 RTK receiver were evaluated in a series of field tests. Trimble RTK 4800 was used for comparison purposes, as it is a surveying unit and is not used for auto-steering. The readings from the three receivers were compared to an accurate reference trajectory obtained by post-processing raw GPS data (carrier phase and pseudo range) stored in the memory of a high-accuracy geodetic-grade GPS receiver (Novatel DL4 receiver). The accuracy of the post-processed trajectory is generally superior to the raw GPS data (Fang *et al.*, 1998).

### Deriving the reference trajectory

NovAtel OEM4 GPS receiver was used to collect five datasets at a 10Hz sampling rate, at the same time as the 3 RTK receivers, on July 23, 2004. Stored data was processed using the Trimble Geomatics Office and the OSU kinematic single-baseline software. This process was not completed in real time but was completed after collecting the stored data, which increases accuracy (Fang *et al.*, 1998). The CORS station "COLB" was used as a base station and the 1Hz sampling data was downloaded from the ftp server of CORS. The first GPS software used for post processing, TGO (Trimble Geomatics Office) is a commercial one. The second package is a research software (AmbRes) developed at The Ohio State University Center for Mapping for RTK application based on OTF (On The Fly) GPS ambiguity resolution. All five dataset have TGO solutions and were saved as a text file "TGO.txt" including all the epoch points.

### Location of the receivers and expected accuracy

The reference (base) station used for post process data was less than three kilometers away from the test field. Accuracy at the cm-level is expected for baselines up to 5 km; when the receiver is within 5 km from the base station. The reference receiver and the RTK systems were placed on an in-line rigid platform, each with an individual antenna. The distances between the phase centers of the antennas were measured and used to evaluate the stability of the solutions from the RTK receivers relative to the antennas of the reference receiver.

### Setup for the GPS field test

On July 23<sup>rd</sup> 2004, the test vehicle consisted of a wagon pulled by a tractor at a speed of 4.8 km / h. The testing platform containing the antennas was tightly secured on the wagon. The data from all GPS receivers were simultaneously collected. A C++ program was written to collect the NMEA output from all tested RTK GPS receivers at the same time on a laptop computer and the manufacturer's mobile computer. A USB to RS-232 Serial Interface Adapter (SeaLINK+4/232, Sealevel Systems Inc.) was used to increase the number of RS232 ports on the laptop where the data were collected and stored. The data from the Novatel GPS were stored on a flashcard for post processing. The RTK receiver's base stations for the rover units were located approximately 30 meters away from the test site. The base stations were set up based on the manufacturer instructions for normal GPS location positioning. The base stations were surveyed and their exact

location was determined using a reference point at The Ohio State University. The true position for the John Deere RTK and Trimble 214 RTK receivers was compared to their reported position, to assess the shift in the positions reported by these receivers. In contrast, the base station for the 4,800 auto-corrects for the error in between the reported position and the true position was surveyed from the reference point at The Ohio State University.

#### Repeating the GPS field test twice, with and without signal blockage

Two tests were conducted under normal field conditions; each replicated three times and all were conducted on July 23 2004. In the first test GPS accuracy was evaluated without any signal blockages. In the second test GPS accuracy was evaluated while temporarily covering two of the tested GPS receivers' antennas only: John Deere RTK and Trimble 214 RTK. This allowed an evaluation of these receivers' capability to re-establish the lock after a signal loss. Signal was blocked for 30, 60 or 90 meters, in replicates 1, 2 and 3 respectively. In both tests the design was a completely randomized blocked design with the replicates as blocks. This allowed evaluating the block effect, which is the obstruction time effect in the second test. The spatial configuration of the GPS receivers on top of the vehicle was randomly selected in both tests. The vehicle was driven along a square trajectory to collect data in the N-S and E-W directions. The three replicates consisted of three series of passes along the same trajectory.

#### Data analysis

In the flat area where the test was conducted the following applies; vertical standard deviation in GPS positions is assumed to be roughly equal to twice the horizontal standard deviation; receiver accuracy is expressed in the replicability of the area delimited by its trajectory and in their horizontal standard deviation. Therefore, receivers were evaluated based on these three criteria. To calculate the areas delimited by the receivers' trajectory the three GPS receivers and the reference trajectory data was plotted in ArcGIS 9. The data string of location points was spliced and rearranged to correct for GPS time errors and then the data string was transformed into a polygon. The polygon areas were calculated (Fig. 1) and analyzed using ANOVA, in a Randomized Complete Block Design with the replicates as blocks. Horizontal accuracy was measured as the standard deviation in distances between GPS positions, after projecting the geographic coordinates in a UTM plane.

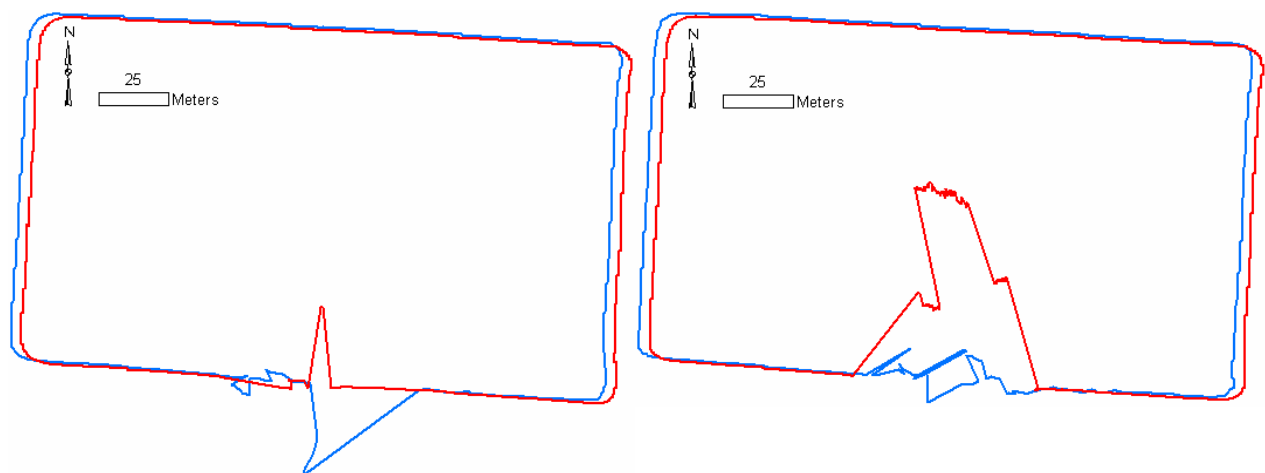


**Figure 1. Maps of the driving paths recorded by the GPS receivers in the first (a) and second (b) replicates, showing the John Deere (blue) and Trimble 214 (red) RTK receivers response to signal blockage.**

## RESULTS

#### Comparing vertical accuracy among receivers

A Complete Random Design was used to evaluate statistical differences in elevation data among GPS receivers. Each location point in the receiver's data string was considered a replicate. In either tests where the GPS signal was either momentarily blocked or not, the John Deere and

Trimble 214 RTK receivers differed from both the reference trajectory and each other ( $p < 0.05$ ) as shown in table 1, while the reference trajectory and the RTK 4800 vertical accuracy did not significantly differ.

#### Comparing area measurements among receivers

The rover equipped with the GPS receivers drove around a field area three times and collected GPS coordinates. After transforming the coordinates from each GPS receiver into a line circumventing the field area three times, these lines were divided into three segments, each circumventing the field area once, and representing one replicate. These treatments were blocked by replicates (time periods of blocking GPS signal) and analyzed for statistical differences using a Randomized Complete Block Design (2 way) ANOVA (Tab. 2). The results showed that total areas did not vary significantly among signal blockage periods (block effect) or GPS receivers / reference trajectory (treatment effect). If alpha is considered to be 20% as opposed to 5%, then there is a significant difference caused by the time period for which the GPS signal is blocked in the John Deere RTK and Trimble 214 RTK receivers, relative to non-blocked receiver (RTK 4800) and the post processed reference trajectory.

**Table 1. Separation of vertical distances means based on LSD = 0.2003 ( $p < 0.05$ ). Standard deviation is shown in m. Significant differences are indicated by different letters.**

	Post Process <sup>a</sup>	RTK4800 <sup>a</sup>	JD no signal block <sup>b</sup>	214 no signal block <sup>c</sup>
Standard Deviation	1.95	1.92	2.09	2.22

In contrast, using the different GPS receivers resulted in a significant difference in elevation accuracy (or standard deviation) as shown in table 1, which indicates a shift in horizontal position man receivers, or a lack of horizontal accuracy among them.

**Table 2. Statistical analysis of area measurements using different GPS receivers (and reference trajectory) with or without signal blockage.**

Type of GPS field test	p value for block effect	p value for treatment effect	Conclusion for block effect	Conclusion for treatment
Results without signal blockage	0.75	0.98	none	None
Results with signal blockage	0.19	0.22	none	None

#### Comparing horizontal accuracy among receivers after signal blockage

In the GPS test where signal was momentarily blocked from the John Deere and Trimble 214 RTK receivers, the distance of the segment between X,Y coordinates at adjacent GPS locations was calculated. Each segment was considered a replicate and an ANOVA was performed. All segments above 10 m (24 out of 10907 data points) and below 0.05 m (identical positions) were considered outliers. The block effect of signal block time was ignored based on the results in table 2. All receivers had significantly different horizontal accuracies (Tab. 3). The reference trajectory had the lowest horizontal standard deviation (horizontal accuracy) and the 4,800 receiver the highest (Tab. 3). Receivers had different sampling rates, which created an error source in measuring distance between adjacent points.

**Table 3. Separation of horizontal distances means based on LSD = 0.0164 ( $p < 0.05$ ). Standard deviation is shown in m. Significant differences are indicated by different letters.**

	Post Process <sup>a</sup>	RTK4800 <sup>b</sup>	John Deere <sup>c</sup>	Trimble 214 <sup>d</sup>
Standard Deviation	0.075	1.174	0.551	0.103

## CONCLUSION

There was no significant difference between two receivers that were tested in terms of horizontal accuracy. The results show a latitudinal and longitudinal position shift among RTK GPS receivers. This position shift was not consistent with the difference in the position of their base station. The shifting in position can potentially become troublesome for a user who uses two different brands of RTK GPS in their operation. The results show that the horizontal accuracy of the two different brands of RTK GPS systems was significantly different when they were exposed to an obstruction. This is particularly important when there are objects such as trees in the field that obstruct the GPS signal.

### Acknowledgements

We would like to thank the John Deere and Trimble companies for providing us the GPS equipment and technical support. Particularly we would like to thank Adam Hart, Jamie Bultermeier, and Scott Azbell. Also we appreciate the help and assistance from Sherrie Buchanon at the University of Florida, Citrus Research and Education Center.

## REFERENCES

1. Ehsani, M. R., M. Sullivan, and T. Zimmerman. 2003. Evaluating the Dynamic Accuracy of Low-Cost GPS Receivers. ASAE Paper No. 031014. St. Joseph, Mich.: ASAE.
2. Fang, P., Bevis, M., Bock, Y., Gutman, S., Wolfe, D. 1998. GPS meteorology: Reducing systematic errors in geodetic estimates for zenith delay. *Geophys. Res. Lett.* Vol. 25, No. 19, p. 3583.
3. Kise, M, Zhang, Q., Rovira-Más, F. 2005. A Stereovision-based Crop Row Detection Method for Tractor-automated Guidance. *Biosystems Engineering*, 90 (4), 357–367.
4. Rovira-Más, F. Zhang, Q., Reid, J.F., Will, J.D. 2003. Machine Vision Based Automated Tractor Guidance. *International Journal of Smart Engineering System Design*, 5(4), 467-480.
5. Taylor, R.K., M.D. Schrock, J. Bloomfield, G. Bora, G. Brockmeier, W. Burton, B. Carlson, J. Gattis, R. Groening, J. Kopriva, N. Oleen, J. Ney, C. Simmelink, and J. Vondracek. 2004. Dynamic testing of GPS receivers. *Transactions of the ASAE* 47(4), 1017-1025.



## Author Index

Andersen, N. ....	41
Ampatzidis, Y. ....	33
Asselt, K. v. ....	51, 201
Auernhammer, H. ....	215, 227
Bakker, T. ....	<b>51</b>
Barawid, Jr. O. C. ....	<b>59</b>
Bednarz, C. ....	281
Bochtis, D. ....	<b>33</b>
Bontsema, J. ....	51, 201
Burks, T. F. ....	71
Buschmeier, R. ....	<b>319</b>
Buus-Jensen, K. ....	325
Chaoui, H. ....	345
Demmel, M. ....	139
Duscher, G. ....	23
Eghbali, H. ....	209
Ehlert, D. ....	23
Ehrl, M. ....	<b>227</b>
Ehsani, R. ....	<b>345</b>
Falke, A. ....	23
Faugno, S. ....	91
Fischerkeller, R. ....	337
Formato, A. ....	<b>91</b>
Foster, C. A. ....	<b>237</b>
Freimann, R. ....	<b>257</b>
Gao, Y. ....	<b>289</b>
Gavrić, M. M. ....	<b>1</b>
Grejner-Brzezinska, D. ....	345
Griepentrog, H. W. ....	41, <b>117</b>
Han, S. ....	171
Han-Ya, I. ....	<b>97</b>
Havn, I. ....	13
Ibarra, J. S. ....	117
Iida, M. ....	<b>125</b>
Inoue, T. ....	7
Ishii, K. ....	7, 59, 97, 103, 273
Jafari, A. ....	<b>201, 209</b>

Jensen, K. ....	13
Jørgensen, R. N.....	<b>13</b>
Kaivosoja, J. ....	145
Kanetani, Y. ....	133
Kang, T. H. ....	<b>103</b>
Kise, M. ....	<b>109</b>
Kitagawa, H.....	133
Kivipelto, J. ....	145
Kokuryu, T.....	133
Landman, R. ....	303
Langner, H. R. ....	<b>23</b>
Lenz, J. E.....	<b>303</b>
Lovric, T. ....	325
Martinov, M. L. ....	1
Matusi, T.....	7
Mejnertsen, A. ....	41
Miettinen, M.....	<b>191</b>
Mizushima, A. ....	59, 133
Mohtasebi, S. S.....	209
Müller, J.....	51
Muhr, T. ....	<b>65</b> , 139
Nagasaka, Y. ....	<b>133</b>
Nielsen, J. ....	117
Niwa, K. ....	97
Noack, P. O.....	65, <b>139</b>
Noerremark, M. ....	117
Noguchi, N. ....	7, 59, 97, 103, 133, 273
Nørremark, M.....	41
Öhman, M.....	191
Oittinen, J. ....	145
Oksanen, T.....	<b>151, 161</b> , 191
Omid, M. ....	209
Ostermeier, R.....	<b>215</b>
Paolillo, G. ....	91
Pedersen, J. M. ....	13
Pesonen, L. ....	145
Peters, J. D.....	237
Plankensteiner, M.....	<b>325</b>
Rathmann, S. ....	<b>337</b>

Ravn, O.....	41
Reid, J. F.....	171
Reske-Nielsen, A.....	<b>41</b>
Rogge, H. I.....	215
Rothmund, M.....	<b>267</b>
Rovira-Más, F.....	<b>171</b>
Ryerson, A. E. F.....	<b>309</b>
Seethaler, C.....	325
Silberbauer, L.....	325
Siramizu, K.....	103
Søgaard, H. T.....	13
Sørensen, C. G.....	13
Sørensen, L. B.....	13
Straten, G. v.....	51, 201
Strobl, M.....	267
Strosser, R. P.....	237
Sullivan, M.....	345
Sun, J. Q.....	237
Suomi, P.....	191
Tsatsarelis, C.....	33
Tucker, M.....	281
Umeda, N.....	133
Usami, T.....	<b>273</b>
Wei, J.....	171
Vellidis, G.....	<b>281</b>
Virolainen, V.....	<b>145</b>
Visala, A.....	151, 161, 191
Vougioukas, S.....	33, <b>183</b>
Yamada, Y.....	125
Yokobori, J.....	97
Younse, P. J.....	<b>71</b>
Yu, Y.....	109
Zeitzev, M. A.....	<b>247</b>
Zhang, Q.....	109, 289, 309





**ISBN: 3-9808234-2-3**